

Integrated Design and Manufacturing in Mechanical Engineering '98

Proceedings of the 2nd IDMME Conference
held in Compiègne, France, 27-29 May 1998

Edited by

Jean-Louis Batoz, Patrick Chedmail, Gerard Cognet and Clément Fortin



Springer-Science+Business Media, B.V.

INTEGRATED DESIGN AND MANUFACTURING IN
MECHANICAL ENGINEERING '98

INTEGRATED DESIGN AND MANUFACTURING IN MECHANICAL ENGINEERING '98

Proceedings of the 2nd IDMME Conference
held in Compiègne, France, 27–29 May 1998

Edited by

JEAN-LOUIS BATOZ

*Département GSM,
Université de Technologie de Compiègne,
France*

PATRICK CHEDMAIL

*Institut de Recherche en Cybernétique de Nantes,
École Centrale de Nantes, France*

GERARD COGNET

E.N.S.A.M., Paris, France

and

CLÉMENT FORTIN

*Department of Mechanical Engineering,
École Polytechnique de Montréal,
Canada*



Springer-Science+Business Media, B.V.

المنارة للاستشارات

A C.I.P. Catalogue record for this book is available from the Library of Congress.

ISBN 978-90-481-5342-8 ISBN 978-94-015-9198-0 (eBook)
DOI 10.1007/978-94-015-9198-0

Printed on acid-free paper

All Rights Reserved

© 1999 Springer Science+Business Media Dordrecht

Originally published by Kluwer Academic Publishers in 1999.

Softcover reprint of the hardcover 1st edition 1999

No part of the material protected by this copyright notice may be reproduced or utilized in any form or by any means, electronic or mechanical, including photocopying, recording or by any information storage and retrieval system, without written permission from the copyright owner.

المنارة للاستشارات

TABLE OF CONTENTS

Preface.....	xiii
Acknowledgements	xv
Introduction	xvii
 Chapter 1 : STRUCTURAL ANALYSIS OF MECHANICAL PARTS	 1
 Helical buckling of an optical fibre composite cable introduced by pushing in a duct	 3
H. BOULHARTS, L. RIVIERRE, J.L. BILLOET, O. POLIT, A. PECOT and J.L. CAMPION	
 Simulation and optimization of thermomechanical sollicitations	 11
V. BOGARD and PH. REVEL	
 Localization of collapse mechanisms for simplified vehicle crash simulation	 19
D. CORNETTE, J.L. THIRION, E. MARKIEWICZ, P. DRAZETIC and Y. RAVALARD	
 Computational code for a simplified analysis of plate structures.....	 27
XIO-LING DENG, C. HOCHARD, G. HUBERT and F. LEBOUVIER	
 Aircraft engine blades-casing contact study.....	 35
GUILLOTEAU, E. ARNOULT, B. PESEUX and M BERTHILLIER	
 Design of a superconducting quadripole prototype : using substructuring to take contact into account	 43
C. BLANZE, L. CHAMPANEY and P. VEDRINE	
 Theoretical and numerical study of a coupler for crashworthy design of a TGV power car.....	 51
JEONG SEO KOO, ZHIGIANG FENG, M. DOMASZEWSKI and F. RENAUDIN	
 Global numerical model of automobile gearboxes.....	 59
A. BOURDON, K YAKHOU and D. PLAY	
 Smart materials design : the Mechatronic approach.....	 67
C. DELEBARRE, P. BLANQUET, T. DEMOL, D. COUTELLIER and E. DELACOURT	

Chapter 2 : COMPUTATIONAL MECHANICS AND OPTIMUM DESIGN OF STRUCTURES	75
Machining optimization of quenched parts	77
A. ABISROR, F. CONGOURDEAU, G. MARIN, J.M. ROËLANDT AND N. VALLINO	
Optimization of a passive safety device by means of the response surface methodology	85
G. BELINGARDI and M. AVALLE	
Optimal design of mechanical components with genetic algorithms	93
L. GIRAUD and P. LAFON	
Design of materials with specific elastic properties using shape optimization method.....	101
SHUTIAN LIU, YUANXIAN GU and GENDONG CHENG	
Shape optimization and adaptativity of axisymmetrical shells undergoing geometric nonlinearities	109
H. NACEUR, S. TRIKI, J.L. BATOZ AND C. KNOPF-LENOIR	
Topological optimization of shells with non uniform thickness	117
E. PAGNACCO and J. E. SOUZA DE CURSI	
Non-deterministic methods for product/process analysis and robust design - the «possibilistic» approach.....	125
V. BRAIBANT, F. DELCROIX , A. OUDSHOORN and C. BOYER	
Design of an automatic topology/geometry optimization software.....	133
S. BEUZIT and A. HABBAL	
Chapter 3 : FINITE ELEMENT SOLVERS. MESHING TECHNIQUES COMPUTER AIDED GEOMETRY	141
Intelligent objects for pre-processing in a mechanical finite element software	143
P. BOMME and TH. ZIMMERMANN	
A message passing paradigm for distributed design and simulation of mechanical systems.....	151
P. BREITKOPF AND Y. ESCAIG	

FEM/CAD system architecture for shape optimization of 3D parts.....	159
A. MERROUCHE and C. KNOPF-LENOIR	
2D Mesh and geometric adaptations using an <i>a priori</i> model of mechanical behavior	167
PH. VERON, L. FINE, F. NOËL and J.C. LEON	
On the automation of non-linear behavioral structural analysis. Guidance and quality control	175
J.P. PELLE and D. RYCKELYNCK	
Computational geometry in the preprocessing of point clouds for surface modeling.....	183
RUIZ OSCAR and POSADA JORGE	
Polyhedron partitioning dedicated to a hierarchical meshing technique.....	191
F. MAZA, F. NOEL AND J.C. LÉON and F. SILLION	
A declarative approach for geometry and topology : a new paradigme for CAD-CAM systems.....	199
A. CLÉMENT, A. RIVIÈRE and PH. SERRÉ	
Piecewise cubic interpolation for reverse engineering.....	207
G. PRADES, J.L. CAENEN, Y. MINEUR and J.M. CASTELAIN	
Chapter 4 : MODELING AND SYNTHESIS OF MECHANISMS	215
Component mode synthesis in the design and the optimisation of mechatronic systems.....	217
P. DE FONSECA, H. VAN BRUSSEL and P. SAS	
The kinematics design of a 3-dof hybrid manipulator.....	225
D. CHABLAT, PH. WENGER and J. ANGELES	
Geometric synthesis of manipulators under kinematic constraints	233
S. GUERRY, B. OUEZDOU and S. RÉGNIER	
A cooperative approach in mechanism design	241
P. CHEDMAIL, T. DAMAY and B. YANNOU	

Study of complex tackles : lifting systems with pulleys and cables.....	249
A. BILLEREY, P. CLOZEL and D. CONSTANT	
Application of a fuzzy logic ordering method to preliminary mechanism design ..	257
J.C. FAUROUX, C. SANCHEZ, M. SARTOR and C. MARTINS	
RVS : a robot visualization software package.....	265
J. DARCOVITCH, J. ANGELES, P. MONTAGNIER AND CHU-JEN WU	
Chapter 5 : ANALYSIS AND OPTIMIZATION OF MATERIAL FORMING PROCESSES	273
Clinch joining modeling with the static explicit method and remeshing	275
V. HAMEL, J.M. ROËLANDT, J.N. GACEL and F. SCHMIT	
Theoretical and practical aspects in modeling of the metal powder compaction process	283
A. GAKWAYA, H. CHTOUROU, and M. GUILLOT	
Study and evaluation of different formulations of the optimization problem applied to the stamping process.....	291
J. PAVIE, E. DI PASQUALE, S. BEN CHAABANE and V. BRAIBANT	
Design optimization of metal forming processes	299
O. GHOUATI and J.C. GELIN	
Modeling and blank optimum design of thin car panels obtained by sheet metal forming	307
Y.Q. GUO, H. NACEUR, J.L. BATOZ, C. KNOPF-LENOIR, O. BARLET, F. MERCIER and S. BOUABDALAH	
Shape and thickness optimization of an aeronautical structure manufactured using age creep forming process	315
J.P. BOURDIN, J.P. BONNAFE, J. DELMOTTE, E. GROSJEAN and J.M. ROËLANDT	
Two component finite element model for the simulation of shaping of prepreg woven fabric	323
A. CHEROUAT, J.L. BILLOET and S. BELHOUS	

A sensitivity analysis for the spring back of the arched tubes.....	331
J.C. DJENI, P. PATOU , H. SHAKOURZADEH and V. BRAIBANT	
Chapter 6 : MODELING FOR CONTROL AND MEASUREMENT TOLERANCING AND ASSEMBLY IN MANUFACTURING	339
Influence of the Machine-Tool defects on the formation of the residual defects on a surface : application to turning	341
A. GOUSKOV and S. TICHKIEWITCH	
Certification of free-form machining : a comprehensive approach from CAD/CAM to measurement	349
D. FEAUTRIER, F. THIEBAUT, G. TIMON and C. LARTIGUE	
Nominal and actual geometry explicit declaration Application to dimensional inspection	357
C. CUBÉLÈS-VALADE and A. RIVIÈRE	
Adaptative digitization of mechanical parts	365
F. BENNIS and F. DANIEL	
Geometric tolerance transfer for manufacturing by an algebraic method	373
F. BENNIS, L. PINO and C. FORTIN	
Modeling dispersions affecting pre-defined functional requirements of mechanical assemblies using jacobian transforms	381
L. LAPERRIERE and PH. LAFOND	
Toward a computer aided tolerancing system for parts and mechanisms	389
E. BALLOT, F. THIEBAUT and P. BOURDET	
Interactions between tolerancing and structural analysis views in design processes	397
S. SAMPER and M. GIORDANO	
Fixturing effects on workpiece quality in milling	405
A D'ACUNTO, J. LEBRUN, P. MARTIN and M. GUEURY	

Chapter 7 : OFF LINE PROGRAMMING AND OPTIMAL PARAMETERS FOR MACHINING, WELDING AND ROBOTICS	413
Subassemblies detection with genetic algorithms	415
P. DE LIT, E. FALKENAUER and A. DELCHAMBRE	
Tool path correction on a numerically controlled machine-tool by characterisation of scattering in relation to type of machining	423
G. DESSEIN, J.M. REDONNET, P. LAGARRIGUE and W. RUBIO	
A ring-shaped mechanical assembly line optimized by a genetic algorithm.....	431
F. FONTANILI, A. VINCENT, T. SORIANO and R. PONSONNET	
Side milling of ruled surfaces-optimum tool radius determination and milling cutter positioning.....	439
J.M. REDONNET, G. DESSEIN, W. RUBIO AND P. LAGARRIGUE	
Optimization of end-mill roughing operation sequence.....	447
F. VILLENEUVE	
A model for the optimization of the relation between product means and product	455
S. TASSEL, F. VILLENEUVE and O. LEGOFF	
Optimal mill positioning in five axis machining on free form surfaces Application at roughing path of moulds.....	463
W. RUBIO, J.M. REDONNET, G. DESSEIN and P. LAGARRIGUE	
Avoiding the need for deburring by analyzing burr formation during product design.....	471
L. BLONDAZ, D. BRISSAUD and D. DORNFELD	
Chapter 8 : INTEGRATED DESIGN METHODOLOGY AND APPLICATIONS. DESIGN AND COMMUNICATIONS.....	479
Engineering design : management of information and uncertainty.....	481
C.A. MCMAHON	
Towards a need satisfaction oriented computer aided design	489
F. LIMAYEM and B. YANNOU	

Aided design of brass musical instruments	497
J.F. PETIOT and J. GILBERT	
Environmentally-conscious design and materials selection	505
ULRIKE G.K. WEGST and M. F. ASHBY	
Design knowledge representation for constrained-based design in CAD systems..	513
C. LENGUIN and P.A. YVARS	
CONCAD Bridging : Managing the integration of technical solutions in a modularized product concept	521
M.W. LANGE	
Mechanical models management in engineering design	529
N. TROUSSIER, F. POURROY, M. TOLLENAERE and B. TRÉBUCQ	
Proposal to control the systems design process Application to manufactured products	537
PH. GIRARD. B. EYNARD AND G. DOUMEINGTS	
Integrated design of mechanical systems by a concurrent engineering approach...	545
P. RAY, M. NIGROWSKY, G. GOGU, C. DEMARQUILLY and A. MALLON	
Contribution to a multi-views, multi-representations design framework applied to a preliminary design phase	553
MG-IT collective noun (Coordinator : J.C. LÉON)	
Proposal of a functional model of logistics for spare parts preservation.....	561
N. BAUD, M. MEKHILEF and J.C. BOCQUET	
A generic model for know-how capitalization	569
J. LE CARDINAL	
Web-based product information visualization through VRML code generation	577
YOONHO SEO	
Collaborative design in education : the TAXIA project.....	585
B. RAMOND	

Chapter 9 : INTEGRATED MANUFACTURING METHODOLOGY AND APPLICATIONS	593
A fast and reliable cost-estimation tool for hot-forged parts..... M. BERLIOZ, PH. MARIN and S. TICHKIEWITCH	595
Cost-based ranking for manufacturing process selection	603
A. ESAWI and M. ASHBY	
Analytical study of multi-agent oriented manufacturing design.....	611
V. PATRITI, K. SCHAFFER, P. CHARPENTIER and P. MARTIN	
Dynamic representation of a manufacturing process	619
B. ANSELMETTI and A. TOUMINE	
Extensions of object formalism for representing the dynamics Application to the integration of viewpoints in the design of a production system	627
M. BIGAND, D. CORBEEL, D. NDIAYE and J.P. BOUREY	
Multidimensional taguchi's model with dependent variables in quality system....	635
C. TARCOLEA, G. DRAGOI, D. DRAGHICESCU and S. TICHKIEWITCH	
An approach to integrate safety at the design stage of numerically controlled woodworking machines	643
D. JOUFFROY, S. DEMOR, J. CICCOTELLI and P. MARTIN	
Virtual manufacturing : set up of a cooperative work in manufacturing.....	651
PH. DEPINCE, H. THOMAS, B. FURET, Y. GRATON and N. RAFII	

PREFACE

This volume contains the selected manuscripts of the papers presented at the Second IDMME Conference on “Integrated Design and Manufacturing in Mechanical Engineering”, held in Compiègne, France, at the University of Technology of Compiègne, May 27-29, 1998.

The purpose of the Conference was to present and discuss topics dealing with the optimization of product design and manufacturing processes with particular attention to (1) the analysis and optimum design of mechanical parts and mechanisms (2) the modeling of forming processes (3) the development of computer aided manufacturing tools (4) the methodological aspects of integrated design and manufacturing in adapted technical and human environments.

The initiative of the conference and the organization thereof is mainly due to the efforts of the french PRIMECA group (Pool of Computer Resources for Mechanics). The international Institution for Production Engineering Research (C.I.R.P.) was helpful to attract international participants.

The conference brought together three hundred and twenty worldwide participants. Hundred and thirty two papers were presented in oral or poster sessions and included in the proceedings in four volumes given to the participants. Four invited lectures were presented:

1. Integrated design and manufacturing applied to aerospace structures
by Didier Guedra-Degeorges from Aerospatiale, Suresnes, France
2. Engineering Design: management of information and uncertainty
by Professor Chris Mac-Mahon, University of Bristol, UK
3. Adaptative topology and shape optimization
by Professor Ekkehard Ramm, University of Stuttgart, Germany
4. The next-generation manufacturing research: a North-American perspective
by Professor Clement Fortin, Ecole Polytechnique, Montreal, Canada

This book contains eighty papers selected by the International Scientific Committee and the PRIMECA Scientific committee :

Chairman: J.L. Batoz (France)
Co-chairmen: P. Chedmail (France) G. Cognet (France)
 D. Dornfeld (USA) C. Fortin (Canada)

International Scientific Members:

J. Angelès (Canada)	H. Hagen H. (Germany)	S.H. Such (Korea)
P. Bettess (UK)	H.I.J. Kals (The Netherlands)	S. Tichkiewitch (France)
J.C. Bocquet (France)	F. Kimura (Japan)	M. Touratier (France)
P. Bourdet (France)	T. Kjellberg (Sweden)	H. Van Brussel (Belgium)
A. Clément (France)	F. Le Maître (France)	M. Véron (France)
Y. Corvez (France)	R. Soenen (France)	

Primeca Scientific Members:

J. C. Bocquet J.C. (EC Paris)	G. Degallaix (EC Lille)	B. Peseux (EC Nantes)
C. Bonthoux C. (IFMA)	H. Gachon (ENSAM)	D. Play (INSA Lyon)
J.L. Caenen (Mines de Douai)	J. Guillot (INSA Toulouse)	G. Ris G. (AIP Nancy)
J.M. Castelain (ENSIMEV)	P. Orsero (UTC)	M. Tollenaere (INPG)
P. Clozel (EC Lyon)	J. P. Pelle (ENS Cachan)	

The above specialists cover a large spectrum in computer science applied to analysis, design and fabrication in mechanical engineering problems.

The third IDMMME Conference will take place in Montreal, Québec, Canada on May 17-19, 2000.

The editors, the scientific and organizing committees hope that they contributed to the development of the challenging research domain of Integrated Design and Manufacturing in Mechanical Engineering.

The editors

J.L. Batoz, P. Chedmail, G. Cognet, C. Fortin

ACKNOWLEDGEMENTS

The Second IDMME Conference held in Compiègne in may 1998 received the scientific support of the M.E.S.R (French Ministry of Higher Education and Research), the C.N.R.S. agency (French National Agency for Scientific Research), the C.I.R.P. (International Institution for Production Engineering Research), the A.U.M. (French University Association of Mechanics), the C.S.M.A. (French Computational Structural Mechanics Association).

The M.E.S.R., the A.U.M. and the C.S.M.A. organizations provided financial support for the Conference and for the edition of this book.

All members of the organizing committee contributed to a successful conference. These members belong to the Department of Mechanical Engineering Systems Department (Laboratoire LG2MS, University of Technology of Compiègne), Laboratoire de Mécanique de Lille), Laboratoire d'Automatique et de Mécanique Industrielles et Humaines (E.N.S.I.M.E.V., Valenciennes). P. Orsero (U.T.C) was chairman of the Organizing Committee and G. Degallaix (E.C.L.) and D. Coutellier (E.N.S.I.M.E.V.) acted as co-chairmen.

INTRODUCTION

This book is devoted to the *optimization of product design and manufacturing*. It contains selected and carefully composed articles based on presentations given at the IDMME conference held in Compiègne University of Technology, France in 1998. Their authors are all involved in cutting-edge research in their respective fields of specialization.

The integration of manufacturing constraints and their optimization in the design process is becoming more and more widespread in the development of mechanical products or systems. There is a clear industrial need for these kinds of methodologies. This class of problems belongs to the problematic of *Concurrent Engineering* which is the object of many academic and industrial projects in Europe (through the ESPRIT and BRITE-EURAM projects particularly) and all over the world.

Important - but still unsolved - problems are related to the definition of design processes, the choice of optimal manufacturing processes and their integration through coherent methodologies in adapted environments. In the same time, different aspects of the problem have to be explored :

- the representation of the products and their properties,
- the modeling of the processes,
- the enhancement of the elementary design activities supported by classical CAD-CAM systems.

Three main topics are addressed in this book:

1. *Analysis and optimization of mechanical parts and products*. In the first chapter, examples dealing with structural analysis of mechanical parts describe the complexity of the activity of concurrent engineering. These examples demonstrate the actual possibilities to simultaneously take into account thermal and mechanical constraints (p. 11), very complex phenomena which are associated to the crash of vehicles (pp. 19 and 51) or to gearboxes functioning (p. 59). The second chapter is devoted to some aspects of the optimal design of mechanical structures. Apart from the classical shape optimization techniques (pp. 101 and 109), it appears clearly that topological optimization techniques (pp. 117 and 133) are an alternative for the research of new solutions. In the same time, global approaches (pp. 85, 93 and 125) are a potential solution when there exist many local minima of the objective function. The third chapter is dedicated to the problem of the integration of the finite element solvers within CAD systems. A key point in this domain is to get a fluent “go-back” process between the numerical mockup of the product and the finite element model (pp. 151, 159 and 167). This goes through the development of efficient automatic meshing algorithms (pp. 143 and 191), new geometric tools for representing complex objects (pp. 167, 183, 199 and 207). The kinematics models are studied in chapter 4 about modeling and synthesis of mechanisms. Out of the classical problem of the analysis of mechanisms (pp. 217 and 265), it becomes

clear that mechanisms synthesis - from a dimensional (pp. 225, 233 and 249) or a topological point of view (pp. 241 and 257) - is a today challenge for industrial purpose. This appears after a long period of academic researches which led to practical limitations due to computers limitations.

2. *Analysis and optimization for production and manufacturing systems.* In this topic, the authors study the complementary aspect of the design process, i.e. the manufacturing and production processes (machining, stamping, clinching, age creep forming, ...). Chapter 5 is related to the optimization of forming processes. Taking into account the complex mechanical phenomena (pp. 275, 283, 323 and 331), it becomes possible to develop some optimization techniques applied to these processes (pp. 299, 307 and 315). The object of chapter 6 is the modeling for control and measurement (pp. 341, 349, 365, 405), and tolerancing (pp. 357, 373, 381 and 389). This last subject clearly interacts with functional and structural views in the design process (p. 397). In chapter 7, design and manufacturing integration goes through off line programming (pp. 415, 431, 455 and 471) and the optimal definition of parameters for machining (pp. 423, 439, 447 and 465).
3. *Methodological aspects of integrated design and manufacturing.* The two above topics are clearly complementary. Moreover they have to be integrated as much as possible. The new methodologies based on the management of fuzzy information (pp. 481) and know-how (p. 569), multi-model (pp. 521, 529, 553 and 569) and constrained-based approaches (p. 513) are presented in chapter 8. Presentations on design with new communication tools (p. 577) and new methodologies (pp. 489, 545 and 561) complete this chapter. Chapter 9 is related to computer aided manufacturing : cost criteria are central in this domain (pp. 595 and 603). Otherwise, modeling of the process becomes possible with multi-agent approach (p. 611). It may include dynamical aspects of the process (pp. 619 and 627). Some training applications are finally presented in the domains of collaborative design or manufacturing (pp. 585 and 651).

By the end, apart from giving a thorough theoretical background, a very important theme is the relation between research and industrial applications.

We hope that this book will be of interest for engineers, researchers and Ph.D. students who are involved in the optimization of design and manufacturing processes. It will be a mine of examples and ideas, and we wish that it will contribute to the improvement and the development of concurrent engineering.

The editors

J.L. Batoz, P. Chedmail, G. Cognet, C. Fortin

Chapter 1
STRUCTURAL ANALYSIS OF MECHANICAL PARTS

Helical buckling of an optical fibre composite cable introduced by pushing in a duct	3
H. BOULHARTS, L. RIVIERRE, J.L. BILLOET, O. POLIT, A. PECOT and J.L. CAMPION	
Simulation and optimization of thermomechanical solicitations	11
V. BOGARD and PH. REVEL	
Localization of collapse mechanisms for simplified vehicle crash simulation	19
D. CORNETTE, J.L. THIRION, E. MARKIEWICZ, P. DRAZETIC and Y. RAVALARD	
Computational code for a simplified analysis of plate structures.....	27
XIO-LING DENG, C. HOCHARD, G. HUBERT and F. LEBOUVIER	
Aircraft engine blades-casing contact study.....	35
GUILLOTEAU, E. ARNOULT, B. PESEUX and M BERTHILLIER	
Design of a superconducting quadripole prototype : using substructuring to take contact into account.....	43
C. BLANZE, L. CHAMPANEY and P. VEDRINE	
Theoretical and numerical study of a coupler for crashworthy design of a TGV power car.....	51
JEONG SEO KOO, ZHIGIANG FENG, M. DOMASZEWSKI and F. RENAUDIN	
Global numerical model of automobile gearboxes.....	59
A. BOURDON, K YAKHOU and D. PLAY	
Smart materials design : the Mechatronic approach.....	67
C. DELEBARRE, P. BLANQUET, T. DEMOL, D. COUTELLIER and E. DELACOURT	

HELICAL BUCKLING OF AN OPTICAL FIBRE COMPOSITE CABLE INTRODUCED BY PUSHING IN A DUCT

H. BOULHARTS^{1,2}, L. RIVIERRE^{1,2}, J.-L. BILLOET¹, O. POLIT¹,
A. PECOT², J.-L. CAMPION²

¹ LM²S /Upres A 8007, ENSAM Paris, 151 boulevard de l'Hôpital, 75013 Paris, France - Tel : 33.1.44.24.64.41, Fax :33.1.44.24.64.68

² FRANCE TELECOM, CNET DTD/IBL, BP 40, 22307 Lannion Cedex, France - Tel : 33.2.96.05.24.60, Fax : 33.2.96.05.27.40

Abstract

Spreading entire optical access networks to connect business customers requires the mechanical properties of composite optical fibre cables to be mastered and their installation in ducts to be optimized. In this context, FRANCE TELECOM is designing new cable-laying tools. One of these techniques, called pushing, consists in applying an axial compressive load to insert cables into underground ducts. However, during this process, the cable can buckle into sinusoidal or helical spatial modes. A life-sized experiment test bench has been produced at the CNET Lannion in order to understand these buckling phenomena. The sinusoidal and helical critical buckling loads and pitches are determined by using an energy approach commonly used in petroleum technologies. Cable buckling is a direct result of bending stiffness, so the influence of this will be studied in the analytical solutions. To complete this study, finite element simulations have been conducted to simulate the pushing process and comparisons made directly between numerical and experiment load values.

1. Introduction

Spreading entire optical access networks to connect the customer requires the mechanical behaviour of the optical fibre cables structure to be mastered in order to optimise the cable laying process. The pushing process consists in applying an axial compressive load to insert the cable into an underground duct. This laying technique is commonly used in urban areas where the maximum length is often less than 300 meters. The major part of FRANCE TELECOM's infrastructure is composed of copper cables and the renewal of such a large network is a difficult task. The fibre cable studied

presents a multilayer cylindrical structure. The diversity of the constitutive materials (PeHD, PVC, Aramid, glass-resin and fibre optical) means that this type of cable can be considered as a composite beam. The analytical constitutive equations have been obtained with homogenisation techniques on multilayer cylindrical beam (Boulharts, 1997). In this study, we will deal only with a homogenised cable submitted to an axial compressive load. Because of friction or the complexity of courses, the cable can buckle when it is being laid by pushing. This phenomena must be taken into account, since, once the cable is buckled, a large friction drag can be created rendering pushing impossible. Increasing the load will damage the fibre optics and increase the cost of laying. In order to understand these phenomena better, the CNET Lannion has manufactured a life-sized experiment bench (Figure 1). The maximum length of the bench is 45 meters. The translucent duct allows the shape formed by the cable during the buckling process to be observed. The presence of different load sensors gives important results that will be compared to the analytical results presented in this paper. The buckling process is obtained by fixing an end stop with a load sensor at the end of the duct.

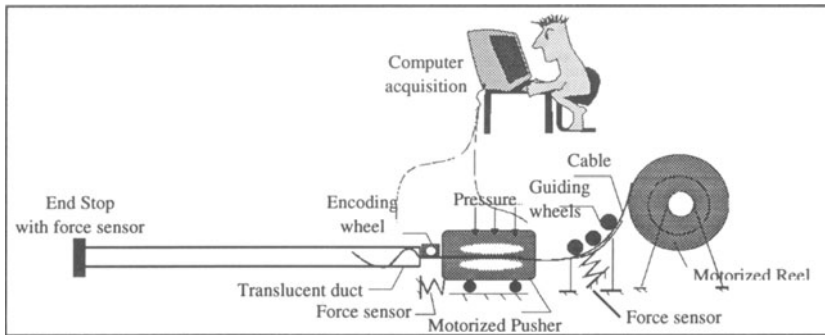


Figure 1. Experiment pushing bench.

The buckling of cable in rigid circular ducts has spatial modes that are called sinusoidal and helical modes, depending on the geometrical configuration taken by the cable. Figure 2 helps explain the process of buckling and post-buckling with an increasing compression load. Since the load is less than a first critical load F_{sin} , the cable is straight in the lower part of the duct. As soon as compression is greater than this, the cable buckles in a sinusoidal configuration, snaking in the lower part. The sinus half-wave grows as soon as a second critical load F_{hel} is attempted. At this instant, a transitory process appears and the cable quickly buckles into a helical shape.

The helical buckling phenomenon was first studied by Lubinski (1950) and sinusoidal buckling by Paslay *et al.* (1964) and Dawson *et al.* (1984). More recently, Wu (1992) re-used some parts of these studies and completed them. All these studies took place in the context of petroleum technologies and presented the same phenomena as ours. Theoretical values such as critical forces and pitches will be compared with experiment results.

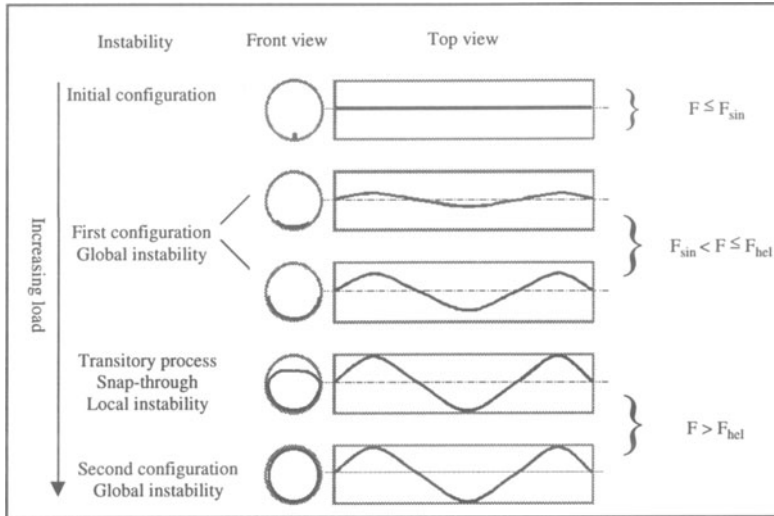


Figure 2. Sinusoidal and helical buckling.

The first part of this study shows the results of experiments, especially for the helical configuration. The second part presents the theoretical study of these phenomena. Thirdly, a finite element simulation of the pushing process, performed with ABAQUS, is described; and finally, comparisons are made between experiment, analytical and numerical results.

2. Buckling study experiment

An example is given for a cable pushed inside a 45 meter long duct. The different loads of interest, which are the pusher effort F_{push} , the reel effort F_{reel} and the end stop effort F_{stop} , are directly recorded by a computer. The real pushing load is obtained by the difference between F_{push} and F_{reel} . Once the pushing experiment stops, the helical pitches are noted by a metric system arranged along the duct.

1. The pushing effort evolution

The pushing speed is fixed at 20 meters per minute to be as close as possible to the real pushing process. The encoding wheel at the entry of the duct denotes the position of the cable head during the experiment. The recording of the experiments can be divided into three distinct parts, according to the compressive load. In part A, the compressive load F_{push} remains nearly constant, the cable is straight in the lower part of the duct, the end stop force is equal to zero. In part B, the cable head reaches the end stop, the pusher load increases in less than 1 second and the cable buckles quickly into a helical configuration. It

can be observed that the end stop effort increases up to 10 daN and tends to be constant. This phenomena is called “lockup” in Wu (1992). Increasing the pushing load has no further influence on the end stop load, as the frictional drag generated by the helical configuration is too great. Part B ends when the pusher load reaches the value 170 daN value, since at this instant the load rapidly decreases due to the break in the cable that buckles in a figure of 8 inside the duct just next to the pusher where the load is at maximum.

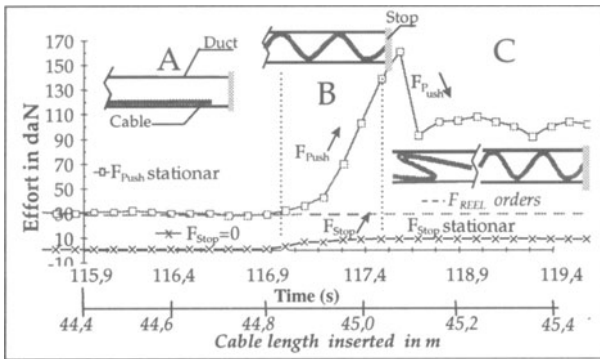


Figure 3. Efforts F_{push} , F_{reel} and F_{stop} recordings

2. Helical configuration study

Once the pushing experiment is finished, the half-pitch P_i of the helix number i is measured with a ruler fixed along the 45 meters of the duct (Figure 4). Pitch length depends on the compressive load applied. As a result of friction, the axial load decreases along the duct and so the helix pitches increase as the end is neared, as shown in Figure 5.

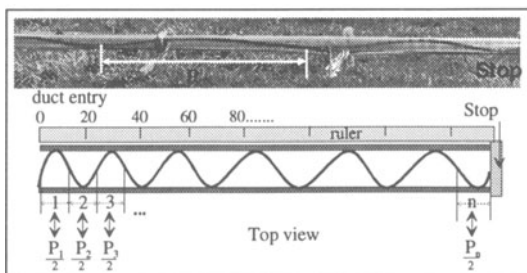


Figure 4. Measurement of helix half-pitches $P_n/2$ along the duct.

Pitches are influenced by the boundary induced by the end stop (Figure 5). The long length used for our experiments here demonstrates its necessity. Some

Some reversal pitches have been observed along the duct. They appear as a result of friction or when snap-through to change from sinusoidal to helical mode does not take place. These reversal pitches induce a large variation in pitches as in Figure 5.

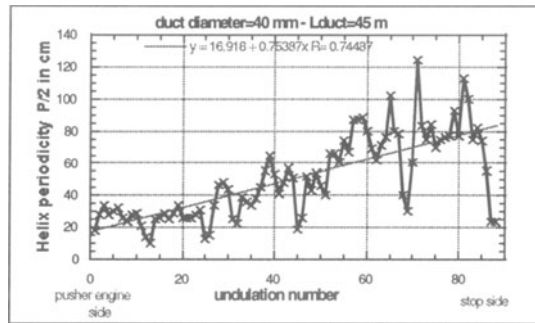


Figure 5. Evolution of experimental cable helix periodicity.

3. Theoretical buckling study

An energy method application developed in petroleum technology (Wu, 1992) is used to determine the critical loads and pitches. Several assumptions must be made: the system is frictionless, the cable has a homogeneous bending rigidity and is always in contact with the duct, which is perfectly circular, rigid and long. An angular perturbation $\eta(x)$, without energy contribution, is applied to the initial straight cable, this perturbation is similar to the sinusoidal or helical buckling modes respectively Eqn. (1) and Eqn. (2).

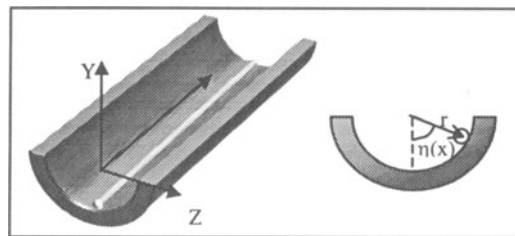


Figure 6. Cartesian reference and angular perturbation

$$\eta(x) = \alpha_0 \sin\left(\frac{n\pi x}{L}\right) \quad (1)$$

$$\eta(x) = \frac{2\pi x}{L} \quad (2)$$

The aim is now to calculate the variation of potential energy between the initial configuration and the new configuration after applying the angular perturbation. The

cable is in a new state of equilibrium if this variation is minimal. The general buckling loads F_s and F_h are obtained (cf. Table 1) in relation to the duct length L , the number of pitches n (with no friction, L/n is exactly the pitch length), the weight w_e , the radius gap r between duct and cable and the bending stiffness EI . These general buckling load values have now to be minimised by $P=L/n$ in order to obtain the critical pitches P_{sin} and P_{hel} which are introduced in the general buckling load to give the critical buckling loads F_{sin} and F_{hel} .

For the transmission of axial load $F(X)$ along the duct, the formulations given by Wu (1992) are used. It is important to notice that $X = 0$ corresponds to the end stop. The cable studied has a low weight (120 g per meter) that allows us to use a force pitch relation for weightless cable. The influence of the cable bending stiffness upon the helix half-pitches is shown in Figure 7.

TABLE 1. Critical buckling load and pitch expressions for each configuration.

Sinusoidal Configuration	Helical Configuration
<p><u>Without friction :</u></p> $F_s = EI \left(\frac{n\pi}{L} \right)^2 + \frac{w_e}{r} \left(\frac{L}{n\pi} \right)^2$ $\frac{\partial F_s}{\partial P} = 0 \Rightarrow P_{sin} = 4 \sqrt{\frac{EI\pi^4 r}{w_e}}$ $F_{sin} = 2\sqrt{\frac{EIw_e}{r}}$ <p><u>With friction :</u></p> $F(X) = \sqrt{\frac{8w_e EI}{r}} \tan \left\{ \mu X \sqrt{\frac{rw_e}{8EI}} + \arctan \left(F_{stop} \sqrt{\frac{r}{8EIw_e}} \right) \right\}$ $\frac{P}{2} = \pi \sqrt{\frac{EI}{F(X)}}$	<p><u>Without friction :</u></p> $F_h = EI \left(\frac{2n\pi}{L} \right)^2 + \frac{w_e}{2r} \left(\frac{L}{n\pi} \right)^2$ $\frac{\partial F_h}{\partial P} = 0 \Rightarrow P_{hel} = 4 \sqrt{\frac{8EI\pi^4 r}{w_e}}$ $F_{hel} = 2\sqrt{2} \sqrt{\frac{EIw_e}{r}}$ <p><u>With friction :</u></p> $F(X) = \sqrt{\frac{4w_e EI}{r}} \tan \left\{ \mu X \sqrt{\frac{rw_e}{4EI}} + \arctan \left(F_{stop} \sqrt{\frac{r}{4EIw_e}} \right) \right\}$ $\frac{P}{2} = \sqrt{2} \pi \sqrt{\frac{EI}{F(X)}}$

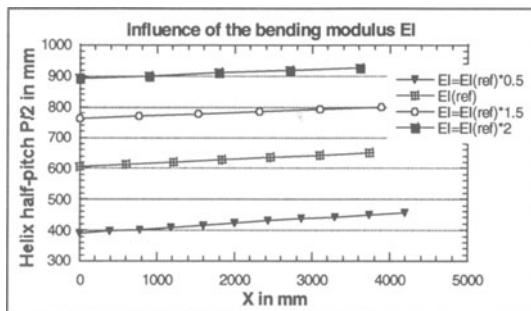


Figure 7. Influence of the bending modulus EI upon helix half-pitches.

4. Numerical buckling study

The 2D finite element simulation of the pushing process is performed with the explicit version of ABAQUS. The pusher is represented by a system of three wheels meshed with rigid elements. The upper wheel, free in axis 2, generates geometrical faults on the cable to initiate the buckling process when the cable reaches the end stop (Figure 8). The cable is meshed by beam elements, the duct and the end stop by rigid elements. The pushing speed is fixed at 30 meters per minute. The evolution of F_{push} (given by the wheels) and F_{stop} is given by Figure 9. As in the simulation experiment, (Figure 3), a large increase of F_{push} in a short time can be noted. F_{stop} also increases and becomes stationary, as in the experiment.

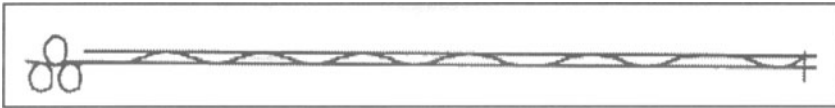


Figure 8 : Deformed cable in 2D numerical simulation.

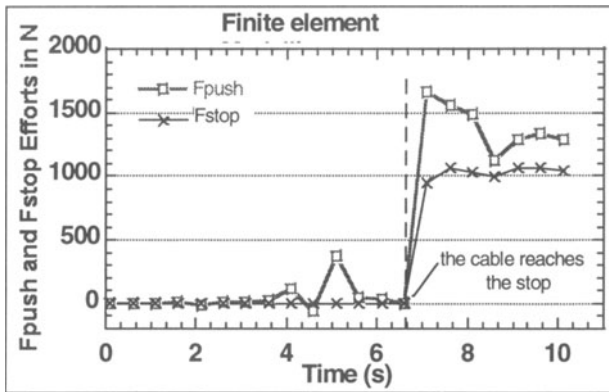


Figure 9 : Effort curves during numerical simulation.

5. Comparison

Table 2 shows the experiment, analytical and numerical values of F_{push} and F_{stop} for a 5-meter duct. The values obtained are consistent; the difference between numerical and experiment values comes from the finite element simulation which is only a 2D simulation.

TABLE 2 : Efforts F_{push} and F_{stop} comparison
($E = 7500 \text{ N.mm}^2$, $r = 28 \text{ mm}$, $w_c = 0.00123 \text{ N.mm}^{-1}$, $\mu=0.3$)

	Experiment	Analytical Model	F.E. Model
F_{push} (N)	980	620	1000
F_{stop} (N)	210	210	750

Figure 10 illustrates a comparison between experiment, analytical and numerical half-pitches. The different pitches along the duct remain within the same, narrow scale [280-420 mm].

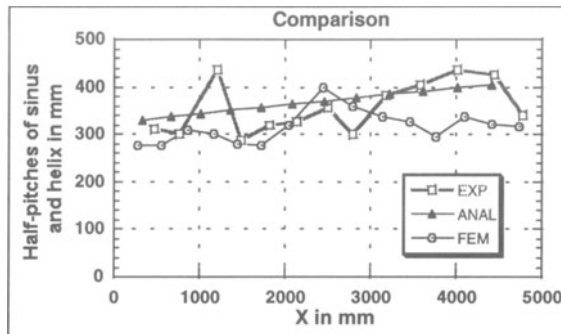


Figure 10. Comparison of buckled cable pitches

Cables present geometrical faults due to their storage on reels. The wheels generate this fault in the numerical analysis, but, in the analytical simulation, the cables are assumed to be perfectly straight, explaining the difference between the analytical and the other two curves.

6. Conclusion

The overall behaviour of cables during the pushing process has been understood well through the experiment bench. The analytical solutions (itches and transmission of axial load) derived from petroleum drilling technology allow us to determine the influence of the different parameters of this process. The 2D finite element simulation of the pushing process, which has never been performed before, gives enough good results compared with the experiment results to forecast 3D modelling for predicting the helical buckling configuration. In conclusion, these three tools together form a helpful approach for cable design and installation by pushing.

7. References

- Boulharts, H., Billoët, J.-L., Le Rouzic, J., Polit, O., Pécot, A., and Campion, J.-L., (1997), *Modeling the pushing installation of an optical fibre in urban area*, proceedings of ICCM-11, Vol. 5, pp. 841-851.
- Dawson, R., Paslay, P.R. (1984) Drillpipe buckling in inclined holes, *Journal of Petroleum Technology*, pp. 1734-1738.
- Lubinski, A. (1950) Helical buckling of rotary drilling Strings, *Drill. And Proc. Prac.*, pp 178-214.
- Paslay, P.R., Bogoy, D.R. (1964) The stability of a circular rod laterally constrained to be in contact with an inclined circular cylinder, *Jour. App. Mech.*, vol.31, pp 605-610.
- J. Wu (1992) *Buckling behavior of pipes in directional and horizontal wells*, PhD, Texas A&M University.

SIMULATION AND OPTIMIZATION OF THERMOMECHANICAL SOLICITATIONS

Virginie BOGARD^{*}, Philippe REVEL^{}**

^{}Laboratoire d'Analyse des Contraintes Mécaniques, Université de Reims-Champagne Ardenne, I.F.T.S, 7 Bd Jean Delautre, 08000 Charleville-Mézières. France.*

*^{**}Laboratoire Systèmes et Machines de Haute Précision, E.A 2224, Université de Technologie de Compiègne, Centre de Recherches de Royallieu (P.G), BP-649, 60206 Compiègne cedex. France.*

ABSTRACT

Some industrial tools are submitted to thermal loading which induces irreversible viscoplastic strains in surface layers, damages them and provokes their failure. The behavior and damage forecast of the structure needs an accurate numerical simulation to evaluate strains and stresses due to the thermal effects. In order to apply a loading which is representative of the experimentation, we propose in this study to use the numerical process of the inverse method to identify and optimize the parameters of constitutive thermal laws.

I. INTRODUCTION

Thermal fatigue, according to the periodicity and the severity of the cycles, induces irreversible strains in surface layers of loaded structures, damages them and provokes their failure [1]. Hot forming tools such as continuous casting cylinders [2] or forging dies and also thermal treatment of metallic alloys such as quenching induce these kinds of solicitations.

We propose in this study to set up a numerical methodology in order to optimize the tooling surface protection (the type of coating material, its thickness, and its treatment, etc.) at less cost.

The numerical simulation consists in modeling the thermomechanical behavior of loaded structures using the finite element method. In order to more accurately simulate thermal loading, an inverse method is used ; it consists in optimizing the parameters of constitutive thermal laws (heat flows and convection parameters).

The optimization and the numerical simulation quality simultaneously depends on : the adequacy between the experimentation and the industrial tooling ; the accuracy

of the experimental measurements ; the numerical conditions such as the mesh and the choice of boundary conditions.

II. OPTIMIZATION AND SIMULATION PROCEDURE

II.1. The inverse method

Fourier laws [3] define the different modes of thermal exchanges. Some of the parameters such as the heat capacity (C_p) and the thermal conductivity coefficient (λ) are well known for each temperature range and each material. However, the convection parameters (h_i) and the heat flow (Q_i) are difficult to quantify by experiment.

An inverse method process makes it possible to numerically estimate a thermal loading which is representative of the experiment process. Therefore, it is necessary to perform experimental tests to measure the thermal evolution in samples.

The optimization procedure is based on the reduction of the difference between the experimental measurements and the numerical results by optimizing the parameters of thermal laws (h_i and Q_i). After the first iteration, the introduction of these optimized parameters in the finite element software using a numerical interface, allows the calculation of a new thermal map and so a decrease of the difference between the experimental and calculated values. After a few iterations, the gap becomes stable at a minimum level. So we consider these parameters as being the best ones to describe the experimental loading with the thermal modeling (Figure 1).

The thermal difference between the experimental and numerical process is calculated at particular points of the structure. At each point, a thermocouple is implanted. And then in the finite element code (ZeBuLoN) [4], a series of nodes of the mesh must be located on these particular positions. The number of measured points and their positions depend on : the dimensions and the geometry of the loaded structure, and also the intensity of spatial gradients.

It must be noticed that a good optimization needs on the one hand, that different values of initial parameters are tested (to avoid the problem of local minima) and on the other hand, that the internal parameters of the numerical process do not affect the final result (the number of iterations, the convergence parameter, etc.). The optimization code used is SiDoLo [5].

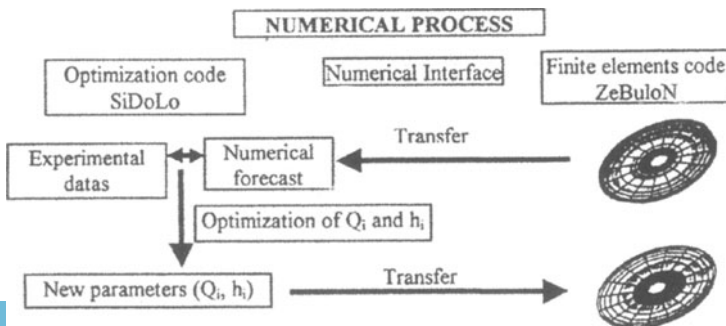


Figure 1 : Numerical procedure of optimization.

II.2. The thermomechanical simulation

After the thermal loading optimization process, the anisothermal mechanical behavior of the structure is calculated using the finite element code where elastoviscoplastic laws [6] were implanted. These laws makes it possible to model the thermoelasticity by elasticity parameters such as the Young modulus and the thermal expansion coefficient. The viscoplasticity is introduced by two kinds of hardening (isotropic and kinematic) and the viscous stress. The twelve parameters of the anisothermal behavior laws of the material are identified in the working temperature range of the thermal cycle. Therefore, it is necessary to set up an experimental database from isothermal mechanical tests such as low cycle fatigue and relaxation or creep tests. All these parameters are identified and optimized for each tested temperature by using a similar numerical process described in the previous part [7].

III. APPLICATIONS

III.1. The continuous casting cylinder

The first application studied here, concerns the hot forming tool used in the continuous casting process. A multilayer coating deposited by a Plasma Transferred Arc protects the cylinder surface. The material used is a stainless martensitic steel (X10Cr13) (with a thickness of 2 mm) and a ferritic steel substrate (25CrMo4). The thermomechanical behavior of each material has been identified and optimized from the numerical procedure described before [8]. The parameter values have been linearly interpolated as a function of the temperature.

III.1.1. Experimental procedure

The rotated cylinder is high frequency heated with a “pancake” inductor type to obtain at its center a maximal surface temperature near 500°C. The cooling sources are performed by compressed air nozzles which are distributed on two generating lines of the cylinder and a lengthwise water circulation at its center. The heating and cooling sources reproduce the same thermal gradients which have been measured on the industrial set up. The thermal evolution is recorded by thermocouples implanted at different depths and by an infrared pyrometer for surface measurements (Figure 2). The experimental database is established for the stabilized cycle which is reached at the fifteenth thermal cycle. Ten measurement points are plotted on the central slice at different depths versus time (Figure 2).

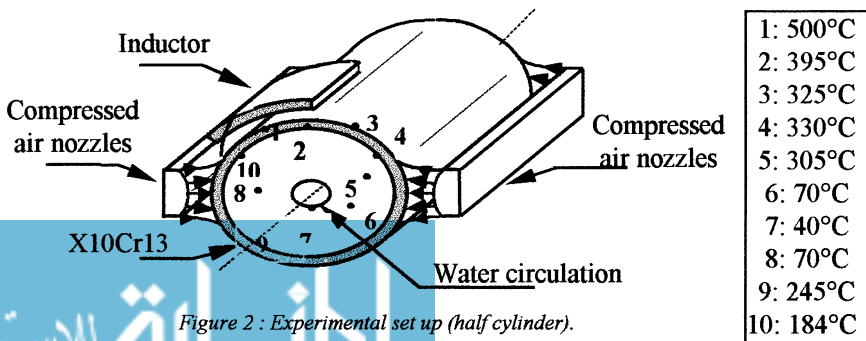


Figure 2 : Experimental set up (half cylinder).

III.1.2. Thermal loading optimization

Finite element calculations are made on a bidimensionnal structure with a thickness of 1 mm which represents the central slice of the cylinder located under the middle of the inductor where thermal gradients are the highest. In order to obtain a best repartition of the thermal exchanges, the slice is divided in sixteen sectors. The heat flows and the convection parameters are distributed on each one of them according to experimental conditions (Figure 3). The mesh is constituted with 8 nodes-quadratic elements and it is composed of 1500 elements. The parameters Q_i and h_i are optimized for the stabilized cycle. The thermal results are obtained after 100 iterations between the optimization software and the finite element code. The optimized temperature values are presented in the table 1.

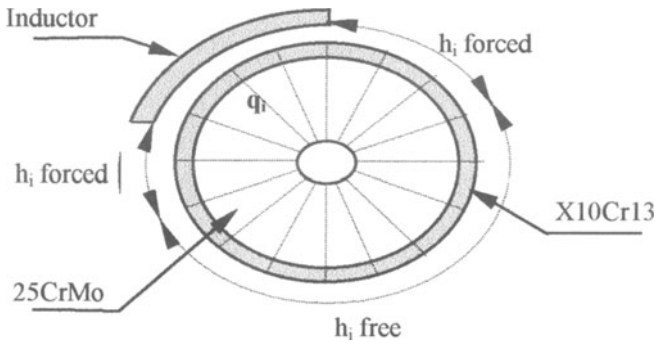


Figure 3 : Thermal exchanges distribution.

Point	Experimental Temperature (°C)	Calculated temperature (°C)
1	500	511
2	395	376
3	325	344
4	330	322
5	305	317
6	70	114
7	40	50
8	70	119
9	245	244
10	184	200

Table 1 : Comparison between the experimental and calculated results.

After the reading of the Table 1, the best results are obtained for the points which are located on the slice surface and also for the ones which are located near the central axis. For the other points, the results are less accurate by reason of the difficulty to simulate the depth of penetration which is induced by the heat flow. However, the

numerical process gives us a good simulation of the experimental test. Before the mechanical calculation of the structure, the complete thermal process is simulated from the initial state (20°C) to the stabilized cycle. Therefore, the cylinder rotation is simulated by the thermal boundary conditions rotation. For the mechanical calculation, the applied thermal loading is composed of the succession of these thermal maps.

III.1.3. Mechanical calculation

One of the two faces of the slice is considered as being the symmetry plane of the cylinder, then the displacements of its nodes are equal to zero in the lengthwise direction and one node which is located at the center is blocked in the three directions. For the other face, we have adopted the hypothesis of the infinite cylinder. A tridimensionnal simulation has been tested to validate this choice of boundary conditions [9].

This applied thermal loading induces low viscoplastic strains ($< 10^{-4}$) in the structure. This low plastification (considered as negligible) predicts a long life to the structure. The numerical results are confirmed by the experiment because after 150 thermal cycles, the cylinder exhibits no crack. The Figure 4 shows that the stress states are always in compression during the thermal cycle, which slows the thermal fatigue crack initiation.

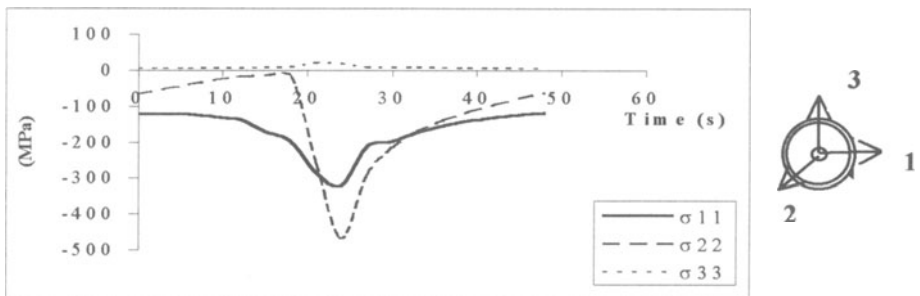


Figure 4 : Evolution of stresses versus time at the stabilized cycle.

III.2. Thermal treatment

The inverse method can also be used for studying thermal treatments and especially superficial quenching of metallic alloys. In order to determine the strain and stress level in the quenched sample, it is indispensable to correctly evaluate its temperature evolution. The simulation makes it possible to define the influence of heating and cooling sources on the thermomechanical evolution of the structure.

III.2.1. Experimental conditions

Quenching tests are realized on cylindrical samples coated by P.T.A process with X10Cr13 steel on a 25CrMo4 substrate. In order to obtain the thermal conditions of a superficial quenching, we apply a temperature gradient to the sample. The cylinder is heated by a three circular spirals inductor and it is cooled by a continuous water

circulation on its basis. The coating is cooled by a compressed air nozzle which is located on the top of the heated surface (Figure 5).

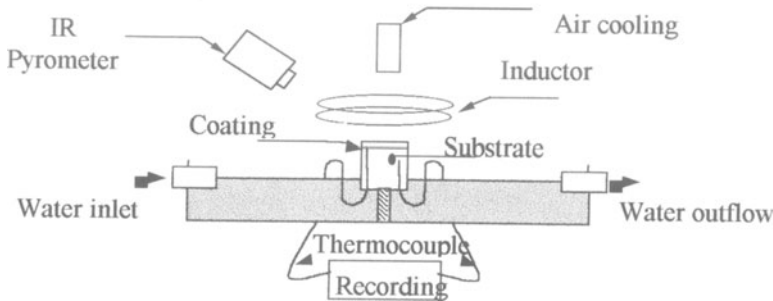


Figure 5 : Experimental set up.

The thermal measurements are recorded versus time by three thermocouples which are implanted at different depths in the sample and by an infrared pyrometer for the surface temperatures. After heating the cylinder surface at 500°C, the inductor is cut off and the air-cooling is activated until the specimen reaches a temperature lower than 50°C.

III.2.2. Cooling optimization

The cylinder is axisymmetrical ; therefore the mesh is bidimensionnal and it is constituted with 8 nodes-quadratic elements and it is composed of 190 elements. The periphery of the sample is more finely meshed because it corresponds to an important thermal exchange area. One node of the mesh is affected to the position of each thermocouple. The optimization procedure is performed on these particular points by minimizing the difference between experimental and calculated values versus time during the cooling. The convection conditions defined for the structure are described on the Figure 6.

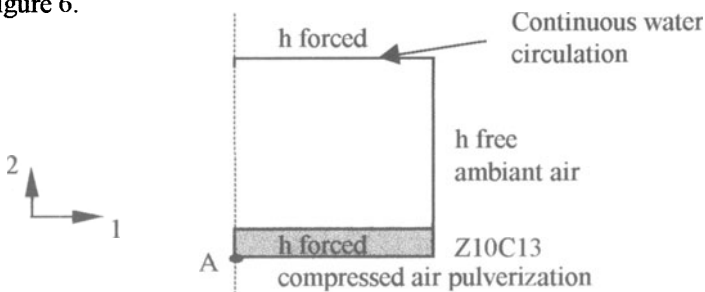


Figure 6: Convection parameters distribution of thermal shock samples.

The results obtained are satisfactory and show a good adequacy between the experimental measurements and the numerical simulation (Figure 7).

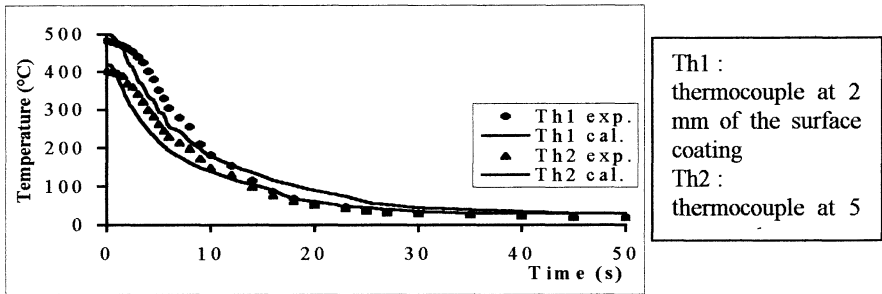


Figure 7: Evolution of temperature at each thermocouple versus time.

After the cooling optimization, we have simulated the complete thermal cycle from the initial gradient (from 500°C to 100°C) to the end of cooling.

III.2.3. Mechanical calculation

The loading is only a thermal loading and it is composed of the succession of thermal maps which have been calculated in the thermal simulation. The mechanical calculation evidences a maximal von Mises stress for the point A located at the center of the cylinder (Figure 5). This applied thermal cycle induces low viscoplastic strains in the structure (Figure 8).

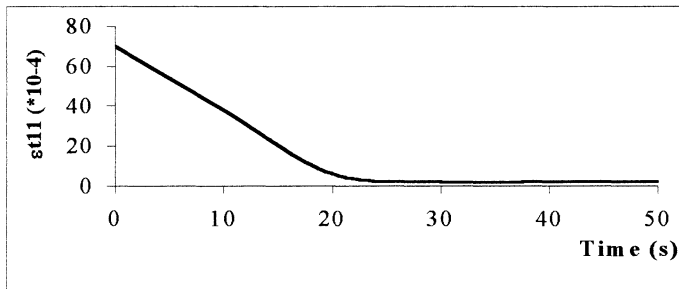


Figure 8: Evolution of the total strain ϵ_{11} versus time at the point A.

IV. CONCLUSION

The inverse method allows us to simulate a thermal loading similar to the one which is applied in the experiment and also to calculate strain and stress levels of the loaded structure. The optimization quality directly depends on the comparison between experimental and calculated thermal values. Therefore, it is indispensable to perform experimental measurements with a maximal accuracy. In the both studies presented here, we have evidenced the no-existence of viscoplastic strain. Now, it would be

interesting to simulate higher thermal loading to reach a viscoplastic strain level and to complete this work by the study of the damage of materials.

In the case of the continuous casting cylinder, we are now going to test different types of coating materials or different thicknesses, in order to observe their thermomechanical effects on the loaded structure.

In the study of superficial quenching tests, we can now approach the notion of residual stresses in order to validate the choice of the behavior model by comparison of numerical forecast and residual stresses measurements.

References

1. D.A. Spera. "What is thermal fatigue", ASTM STP 612 (1976), 3-9.
2. A. Dias, H.P. Lieurade. "La fatigue thermique: Mécanisme: simulation-modélisation", Mécanique-Matériaux-Electricité, n°428, 1988.
3. B. Eyglument. Thermique théorique et pratique, Ed. Hermès, 1994.
4. K. Aazizou. Doctorat de l'Ecole Nationale Supérieure des Mines de Paris, 1990.
5. P. Pilvin. Proceedings of MECAMAT, Besançon (France) (1988), 155-164.
6. J.L. Chaboche. "Sur les lois de comportement des matériaux sous sollicitations monotones ou cycliques", La Recherche Aéronautique, Vol. 5 (1983), 363-375.
7. K. Necib, P. Revel. "Modeling of mechanical behavior of grade 12%Cr steel coating material", Mat. Sci. Eng. A237 (1997), 126-131.
8. P. Revel, K. Necib, G. Beranger, H. Michaud. "Simulation expérimentale de la fatigue thermique d'un cylindre revêtu d'un dépôt en acier inoxydable de nuance Z10C13", Revue de Métallurgie, 95, n°5 (1998), 679-690.
9. V. Bogard, P. Revel. "Simulation numérique de la fatigue thermique d'un cylindre revêtu par un dépôt en acier inoxydable martensitique", Revue de Métallurgie-CIT/SGM, (1999), 227-236.

LOCALIZATION OF COLLAPSE MECHANISMS FOR SIMPLIFIED VEHICLE CRASH SIMULATION

D. CORNETTE*, J.L. THIRION*, E. MARKIEWICZ**,
P. DRAZETIC** and Y. RAVALARD**.

**Research and Development Laboratory for Sheet Products - SOLLAC
17, Avenue des Tilleuls - 57191 Florange Cédex, France*

***Industrial and Human Automatic Control and Mechanical
Engineering Laboratory- Mechanical Engineering Research Group
UMR CNRS 8530 - University of Valenciennes, B.P. 311
59304 Valenciennes Cédex, France (markiewicz@univ-valenciennes.fr)*

An original method is proposed for the localization of collapse mechanisms in axial compression and bending for multibody modelling of simplified vehicle crash simulations. It consists of using a global beam finite element model coupling with results of analytical models for the determination of characteristics in the post-collapse stage. The objective of this paper is to verify, in the context of three dimensional multibody modelling, the localization method with the use of force-displacement and moment-angle relationships obtained from kinematic models. In order to verify the validity of this approach, a study on two thin-walled side bars, such as a double curvature “S” frame subjected to impact a rigid block is performed.

1. Introduction

Numerical simulation of the collision of transport vehicles is currently undertaken using finite element models which can include up to 100 000 shell elements on a supercomputer. While this so-called local approach is altogether feasible and economical when compared to the costs and timings of purely experimental methods, the “fully blown” simulation method must only be used when the structure design is well enough advanced to optimize it. As a matter of fact, during the design phase, the manufacturer wants to have access to a simulation and crash optimization methodology which enables him to have a quick and rough idea about the behaviour of several alternative designs.

2. Multibody Modelling

We have developed a computer-based method CRASH-3D (Cornette *et al.*, 1996), for the formulation of nonlinear dynamical constraints equations of motion for spatial dynamic analysis of mechanical systems. A natural coordinates system, developed by

G. Villalonga *et al.*, with Kane's equations has been used. We have seen that these methods are separately efficient for the modelling of multibody systems and that the combined use developed here allows one to obtain rapidly the spatial dynamic simulation result. We are interested in a method which gives us a minimal system of differential equations and which permits us to model a structure rapidly so as to use it in a mathematical structural optimization. This program uses a super folding element and a super beam element concept in order to characterize plastic deformations during structural collapse (Markiewicz *et al.*, 1996). An analytical method is used to determine the resistance to the collapse of thin-walled structures of a relatively complex geometry when subjected to axial compression and bending.

The use of multibody systems for the numerical simulation of the collision is based on the following concept : the structure we are studying is represented by a set of rigid bodies connected by different joints. Rigid bodies help to characterize on the one hand all the inertial components of the structure and on the other hand, all zones that undergo no or only weak deformations. These different rigid bodies are connected by joints that characterize all the deformation of the structure. These joints are the association of geometrical links with non-linear springs. The axial compression of an element is represented by the superposition of a translation joint (prismatic link) with a rectilinear spring including Force-Displacement characteristics of this element. In the same way, a plastic hinge associates a rotational joint (revolute or spherical link) with a rotational spring so as to characterize the bending of the structure.

Nevertheless, the characteristics of the generalized springs for localized large deformations have to be determined. The response of a typical prismatic column loaded in axial compression or in bending consists of three phases (Figure 1). The pre-collapse phase corresponds to elastic-plastic deformations. In the case of elastic buckling, the point "a" characterizes the critical moment or force of elastic buckling. A second post-buckling stage then takes place in which each plate is subjected to transversal displacements. At the collapse point "b", the moment or force reaches a maximum (or peak). In the case of plastic buckling, for thick plates, plastic deformations appear before reaching peak force or moment. After that, the post-collapse phase leads to a reduction in the moment or force response and large plastic bending deformations. The resistance to collapse of thin-walled structures of a relatively complex geometry when subjected to axial crushing or bending are determined analytically by kinematic models. Pioneering works in this area are due to Abramowicz and Wierzbicki (1989) and Kecman (1979). Present authors have extended it to complex cross-sections profiles (1996) and developed new models (1997, 1999).

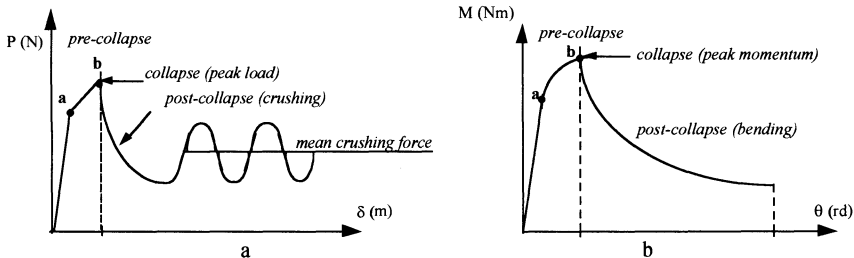


Figure 1. Crushing (a) or bending (b) characteristic of a typical prismatic column.

3. Localization Method

The localization of large plastic deformations is an absolutely necessary tool for the multibody modelling of the structural crash behavior. The localization method has to determine the number and to position the deformation joints so as to optimize the calculation time. An original method based on the comparison between analytical results for the local components and a global beam finite element model is presented. The beam models implemented in PAM-CRASH™ are based on the Belytchko-Schwer (1977) formulation and on the Euler-Bernouilli beam theory. The main feature of this element is its ability to handle efficiently large displacements and rotations.

For axial compression load or purely bending load, this beam describes correctly the pre-collapse stage of thin-walled structures (Figure 2). The use of this beam element in a global beam finite element model allows to obtain the value of peak force or moment. As the beam theory does not represent the post-collapse stage for thin-walled structures, it is taken into account by means of kinematic models in the multibody model. The advantage of a global beam element model is that the pre-collapse curve is obtained for real loading conditions (dynamical inertia and strain rates effects) combining compression and bending. In the case of complex structures, bending moments are calculated for the true moment arm.

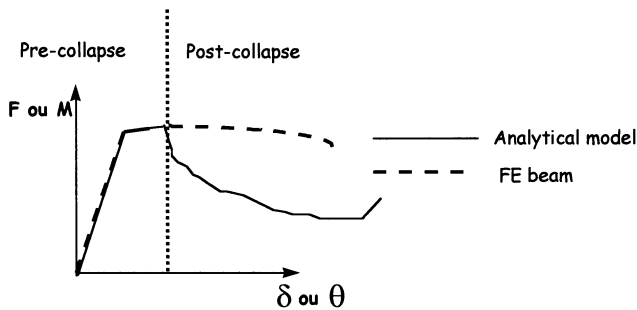


Figure 2. Comparison of force/crushing or moment/folding angle responses for analytical model with the finite element beam model.

In the case of complex structures, for bending load, this beam element allows to obtain the orientation of the bending plane necessary to calculate the post-collapse characteristics with the kinematic model in bending.

This method is summarised by the algorithm on Figure 3. This algorithm is divided into nine parts (0 to 8) which are used in an iterative procedure in the calculation parts.

- *Step 0: A finite element model of the sub-structure or the entire vehicle is made with real loading conditions (initial velocity, rigid wall, added mass and so on).
- *Step 1: Analytical models in axial compression and in purely bending are determined, for each type of beam cross-section of the structure, the peak force P_{xa} and the peak moments M_{ya} and M_{za} for the two principal inertial directions.
- *Step 2: For each calculation time step into each beam element, the maximum compression force P_{xf} and maximum bending moments M_{yef} et M_{zef} for the two principal directions are obtained.
- *Step 3: The norm M_{ef} is calculated by :

$$M_{ef} = \sqrt{M_{yef}^2 + M_{zef}^2} \quad (1)$$

It corresponds to the beam bending moment into the plane oriented with the angle of inclination ϕ to the plane (xOy).

*Step **4**: The angle of inclination of the plane is determined by:

$$\phi = a \tan\left(\frac{M_{zef}}{M_{yef}}\right) \quad (2)$$

*Step **5**: Using an elliptical interpolation, the analytical bending moment for this direction can be predicted by:

$$M_a = \sqrt{(M_{ya} \cos(\phi))^2 + (M_{za} \sin(\phi))^2} \quad (3)$$

*Step **6**: The values **P_{xa}** and **M_a** define localization criteria of the collapse mechanism in axial compression and bending.

*Step **7**: If these peak values are reached by the maximum compression **P_{xef}** or the maximum bending moment **M_{ef}**, the beam element is replaced by an equivalent deformation joint in either axial compression or purely bending. The characteristic of the non-linear spring is obtained by combining the response in pre-collapse stage of the beam element with the response in post-collapse stage of the analytical model in compression or in bending. In the case of a plastic hinge, the bending characteristics are calculated for the post-collapse stage in the bending plane ϕ .

If the peaks are not reached, a new iteration takes place with stage **0**.

*Step **8**: A multibody or hybrid model (multibody/finite element) of the structure is obtained. This step corresponds to the new model for the step **0** of the following iterative procedure until the current time t reaches the final time (t_f) of the study.

This iterative procedure allows to predict all the deformation zones which appear during the simulation. It corresponds to our expectations for an approach in an early design stage because the calculation time is very short.

4. Application to an Impacted Double Curvature Thin-Walled "S" Frame

The structure represented in Figure 4-a is a simplified side member of a vehicle, a double curvature thin-walled "S" beam type. Similar studies have already been undertaken on the same type of structure, but in planar configuration (Drazetic *et al.*, 1993). The vehicle mass was localized at the end of the structure. Consequently, only bending mechanisms were initiated. However, several studies on the crash behavior of transportation vehicles show that compression and bending loading act almost simultaneously. In a previous study by the present authors, the same planar structure was used with some modifications. Load and boundary conditions were used in order to initiate an axial compression collapse, followed by a bending collapse in the curved zones, and to highlight the compression/bending coupling. In the present paper, the same conditions are used for an "S" beam in a three-dimensional behavior. Objectives

are to verify, in the context of three-dimensional multibody modelling, the coupling of the localization method with the use of the force-displacement and moment-angle relationships obtained from kinematic models in compression and bending.

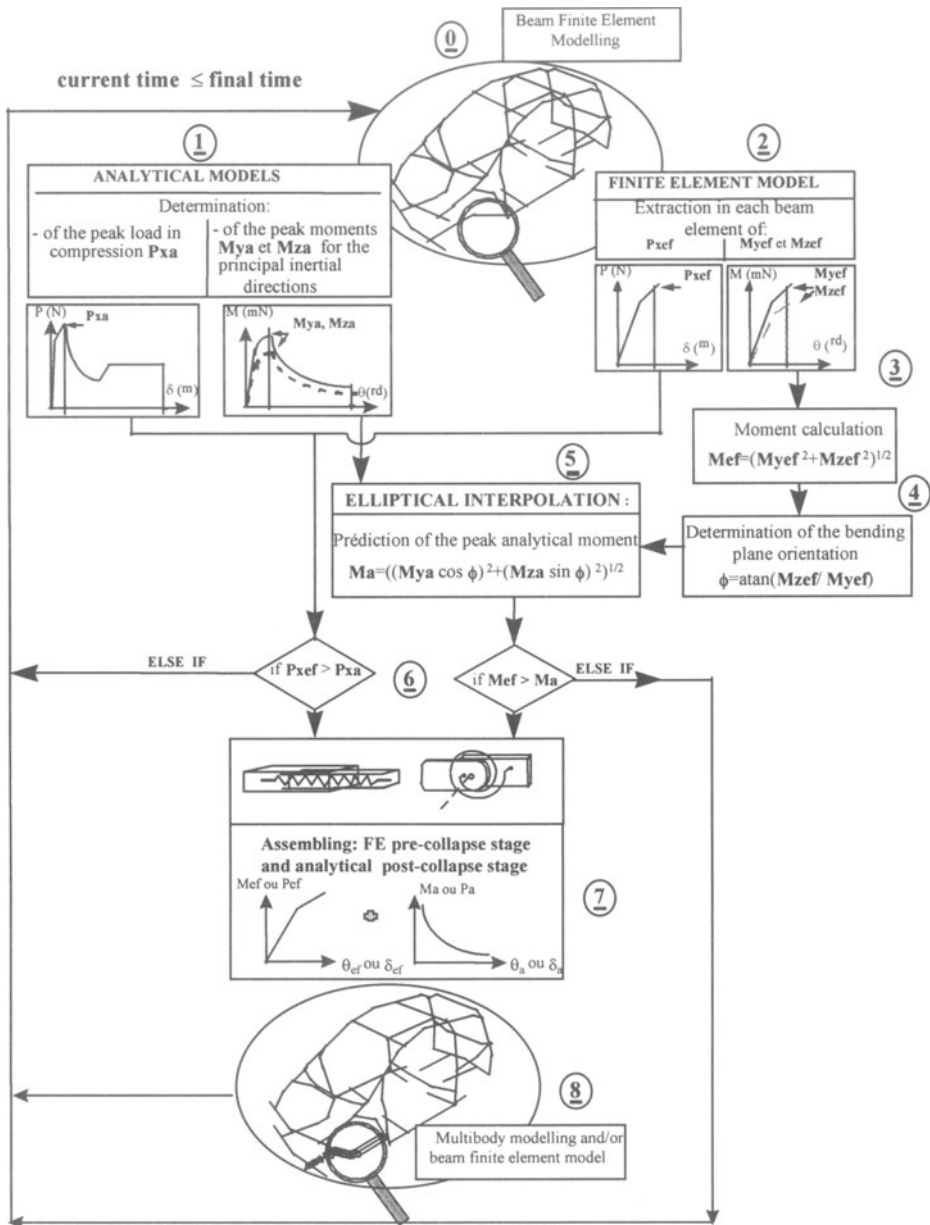


Figure 3. Algorithm of the localization method.

The first objective is to validate with accurate results, the spatial multibody modelling where translational and rotational springs are supplied by the response curves of

compression and bending kinematic models. The second objective is to evaluate the interest of this simplified approach dedicated to the pre-design stage in terms of modelling and CPU time saved.

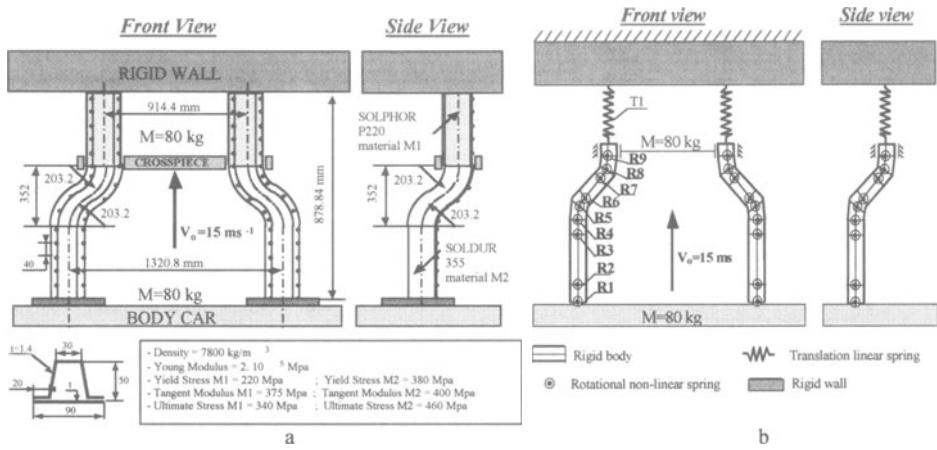


Figure 4. a - Description of the tested structure, b - Multibody model.

To provoke the axial compression collapse and bending collapse in the curved zones one after the other, we have considered a real context which consists of distributing the additional mass into two places according to a ratio 1/2 and 1/2. The energy absorbing capability of two single "S" frames does not allow the use of the total mass of a mean range vehicle of 1200 kg. That is why, from a strictly academic point of view, we have decided to take a total mass corresponding to the kinetic energy dissipation capability of the structure. 80 kg are put on the low extremity that represents the side member / car body link and 80 kg are put on the high extremity that corresponds to the side member / crosspiece link. To avoid the risk that compression and bending mechanisms act in parallel, the double curvature "S" frame is composed of two members made of different steels. These steels are developed by SOLLAC for the car industry in order to improve the energy dissipation capability with the conflicting requirement for weight saving. A SOLPHOR P220 high strength steel is used for the straight part in front of the crosspiece which collapses in compression. A SOLDUR 355 HSLA is used for the rest of the structure which collapses in bending.

The cross-section is of a spot-welded trapezoidal-hat type. The space between two spot-welds, determined by kinematic models and corresponding approximatively to the plastic folding wavelength, is of 35 mm.

4.1 THIN SHELLS FINITE ELEMENT MODELLING

Due to the symmetry only one side member is modelled by 7680 elastic-plastic thin shells. The strain rate material sensitivity is taken into account according to the Cowper-Symonds law. The spot welds are represented by 48 rigid bodies. The impacted zone is modelled by a rigid wall. To simulate the side member / car body link and the side member / crosspiece link where additional masses of 40 kg are added, two rigid bodies are defined and guided in the impact axis. Finally, the initial velocity is applied to the nodes of the whole structure and the calculation is implemented for a study time of 30

ms. At this final calculation time the total kinetic energy is not fully dissipated. There remains about 1.2 kJ, but the energy dissipation capability by plastic folding in the bended zones has reached its maximum.

4.2 SPATIAL RIGID MULTIBODY MODELLING

The localization method with a beam finite element model is tested. We obtain a spatial rigid multibody modelling of the side member with 10 rigid bodies connected to 9 non-linear rotational springs and one non-linear translational spring (Figure 4-b).

The characteristic of non-linear springs is obtained by the combination of the response in pre-collapse stage of the beam element with the response in post-collapse stage of analytical models. In the case of plastic hinges, the bending characteristics are calculated for the post-collapse stage in two bending planes oriented with an angle of 30° (R1,R2,R7-R9) and 58° (R3-R6).

The comparison with FE results has been made qualitatively as well as quantitatively. Table 1 gives the results in terms of crushing distance, velocity, acceleration and dissipated energy at the final time of the simulation for the finite element beam, shell and multibody models. We compare the crushing / times and the velocity / time responses (Figure 5) of the node which corresponds to the side member / car body link. On the PAM-CRASHTM model, this node corresponds to the rear guided rigid body for which the deceleration, velocity and displacement are obtained at the center of gravity. The results obtained by the simulation using the spatial rigid multibody model give satisfactory results when compared to shell finite element results. The results of the beam finite element model are not satisfactory, but the only interest of this approach is its use for the localization method

From the quantitative point of view, in terms of crushing / times and velocity / time curves, the results are similar. The crushing / time comparison shows a good correlation of the history with a final gap of 10.24 mm. In terms of dissipated kinetic energy, the final velocity of the rear end structure is 7.3 ms^{-1} for the shell FE model and 7.39 ms^{-1} for the multibody model. The initial kinetic energy is 9 kJ. By considering that, at time 30 ms only the rear added mass of 40 kg is acting, we deduce an energy dissipation of 7.932 kJ for the shell FE model and 7.906 kJ the multibody model. For the set of results, an acceptable relative difference never exceeds 3.3%.

5. Conclusion

We can conclude that spatial rigid multibody modelling is sufficiently accurate to be used in a pre-design stage. The simulation of the side member crashing over a duration of 30 ms^{-1} requires about 20 hours of CPU time on an HP 9000/770 (J200) workstation in the case of the shell model and only a few minutes for the rigid multibody models. The very quick calculation and modelling times of the multibody approach allow one to highlight zones which undergo large deformations and have a first estimation of the energy dissipation. Coupled with kinematic models which provide the non-linear translational and rotational spring characteristics almost instantly, this approach allows the engineer to implement an iterative design process and retain the first technological solutions before a more accurate but more expensive modelling approach is undertaken.

TABLE 1. Synthesis of results

	shell model (103) R	beam model (213) P	Multibody model M	error P / R	error M / R
total crushing (mm)	308,17	180	297,93	-41,6%	-3,3%
final velocity (m/s)	7,3	0,2	7,39	-97,2%	1,2%
final acceleration (m/s ²)	97,26	0	94,95	100%	-2,4%
dissipated energy(J)	7932	8999	7906	13,5%	0,3%

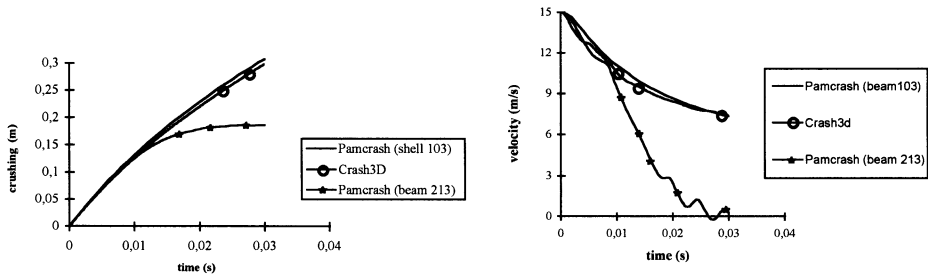


Figure 5. Response curves a- crushing/time b- velocity/time for the 3 approaches.

References

- Abramowicz, W. and Wierzbicki, T. (1989) Axial crushing of multi-corner sheet metal columns, *Journal of Applied Mechanics* **56**, 113-120.
- Belytschko T., Schwer L. and Klein M.J. (1977) Large Displacement Transient Analysis of Space Frames, *J. Numerical methods Engng* **11**, 65-84.
- Cornette D., Drazetic P., Markiewicz E. and Payen F. (1996) Simplified vehicle crash simulation - Part I : spatial multibody modelling with Kane's method in natural coordinates, NATO advanced study institute, crashworthiness of transportation systems, Troia, Portugal.
- Cornette D. (1997) Contribution au développement d'une méthodologie de conception au choc des véhicules automobiles en phase d'avant projet, PhD Thesis, University of Valenciennes, France.
- Drazetic P., Markiewicz E. and Ravalard Y. (1993) Application of kinematic models to compression and bending in simplified crash calculations, *Int. J. Mech. Sci.* **35**, N° 3/4, 179-191.
- Drazetic P., Markiewicz E., Level P. and Ravalard Y. (1995) Application of the generalized mixing kinematic model to the calculation of crushing response for complex prismatic sections, *Int. J. Impact Engng* **16**, N° 2, 217-235.
- Keeman D. (1979) Bending collapse of rectangular section tubes in relation to the bus roll over problem, PhD Thesis, Cranfield Institute of Technology, U.K..
- Markiewicz E., Cornette D., Drazetic P. and Payen F. (1996) Simplified vehicle crash simulation - Part II : Tools for multibody modelling and application to an impacted double curvature "S" Beam", NATO advanced study institute, crashworthiness of transportation systems, Troia, Portugal.
- Markiewicz E., Ducrocq P., Drazetic P. and Ravalard Y. (1996) Calculation of the dynamic axial crushing response of complex prismatic sections, *Int. J. Crashworthiness* **1**, N° 2, 203-224.
- Markiewicz E., Payen F., Cornette D. and Drazetic P. (1999) Calculation of the deep bending collapse response for complex thin-walled columns - II. Post-collapse phase, *Int. J. Thin-Walled Structures* **33**, 177-210.

COMPUTATIONAL CODE FOR A SIMPLIFIED ANALYSIS OF PLATE STRUCTURES

X.-L. DENG*, Ch. HOCHARD**, G. HUBERT*** & F. LÉBOUVIER***
* *RENAULT, 860 Quai de Stalingrad 92105 Boulogne Billancourt*
** *UNIMECA-LMA, 31, chemin Joseph Aiguier, 13402 Marseille cedex 20*
*** *DeltaCAD, Centre de Transfert, R. Guy Deniélou, 60200 Compiègne*

1. Introduction

Product design imposes validations with simulation that are found increasingly upstream of the final product's definitions. The industrialists must thus have simulation software that can be easily and rapidly implemented to compare solutions as from the preliminary design stages.

This paper describes the application of a new simulation technique that can be very rapidly implemented. This approach was initially developed by Renault and LMT at ENS Cachan, France. It is now being industrialised within the framework of a European Brite Euram project entitled "Low Cost Press Tooling - BE 1773". One of the objectives of this project is the development of a software intended to rapidly evaluate the structure of stamping tools to optimise their size, weight and rigidity so as to allow for a cheaper design in terms of manufacture, handling and transport in the future.

Industrial optimisation problems with 3D geometry currently condition the selection of resolution methods. The Finite Element Method (FEM) probably is the most common method for structure calculations, but it can be time consuming in analysing very complex structures. Simplified methods e.g. material resistance or the plate and shell theory are also available; these are efficient but limited to highly specific geometries. Intermediate methods e.g. Trefftz approximations developed from functions observing internal balance can prove very useful during optimisation processes because they help approach the solution satisfactorily with few degrees of freedom.

This paper meets Trefftz methodology to solve structural yield strength problems. This method allows for a quick evaluation of stresses and deformations in structures that may have complex shapes. It can be used at the pre-project stage where it is interesting to rapidly have orders of magnitude as regards rigidity and stresses so as to determine the general shape and size of the structure prior to performing accurate measurements once it has been defined. The edge effects with short variation length that have little effect on the overall rigidity of the structure and impose an accurate definition of the geometry (generally not available in the pre-project phase) prior to calculation can be determined at a later stage.

In the approach presented here, an approximation is designed with polynomials observing the internal balance. A variation formulation suitable for this approximation is used. This choice emphasises the representation of the internal effects. The solution fields do not take the load or displacement continuity into account between the sub-domains that define the

structure. Very few topological constraints thus need to be observed in the definition of geometries for calculation purposes. Likewise, the degree of approximation functions can be different from one sub-domain to the other. This simplicity in the definition of structure and the low number of constraints occurring in the approximation allow for a wide operational flexibility.

A software, designed to be integrated into the CAD software already available on the market, is being developed. This software will allow switching from a volume-related tool CAD model to a digital model ready for calculation. This industrial code imposed a new digital operation based on a conventional numerical integration and resolution performance improvements different from those presented in Hochard (1991).

The calculation code as well as a calculation modelisation example are presented after a brief description of the simplified method.

2. Simplified Method Description

This Trefftz method was originally proposed by P. Ladevèze (1993). In this approach, an approximation is designed from the study of the mathematical structure of the solutions. This study is based on results derived from the St Venant principle as it applies to straight, semi-infinite, homogeneous, constant cross-section beams and was extended to star fields. The approximation evidenced can be considered as a satisfactory representation of the internal effect but may be wrong close to edges where high gradient effects are detected. While taking the nature of the approximation into account, a variational formulation of the problem was suggested to consider any type of boundary conditions. One of the aspects of this definite positive variational formulation is that it is not derived from a minimisation problem or a saddle point because it is not symmetric. In that, it is different from the conventional formulations commonly used (Jirousek, 1986) with Trefftz based functions. The extension to complex structures proceeds by breaking those into sub-domains to which a natural extension of the formulation used for a simple structure with a set of domains (Hochard, 1993) is applied. The method is then applied to the non-zero elastic plates within the framework of the Kirchhoff-Love (Hochard, 1991) theory.

2.1. TREFFTZ APPROXIMATION

The elasticity problem, where body forces are equal to zero, can be written as follows :

To find \mathbf{u} displacement field, such that:

$$\begin{aligned} \operatorname{div} \boldsymbol{\sigma}(\mathbf{u}) &= 0 && \text{in } \Omega, \\ \mathbf{u} &= \mathbf{u}_d && \text{on } \partial_1 \Omega, \\ \boldsymbol{\sigma}(\mathbf{u})\mathbf{n} &= \mathbf{f}_d && \text{on } \partial_2 \Omega, \end{aligned} \quad \text{with } \boldsymbol{\sigma}(\mathbf{u}) = \mathbf{K}\boldsymbol{\varepsilon}(\mathbf{u}) \quad (1)$$

where displacements \mathbf{u}_d and forces \mathbf{f}_d are prescribed on $\partial_1 \Omega$ et $\partial_2 \Omega$ respectively. It can be shown (Hochard, 1993) that, for inner points of the domain, a good approximation of the displacement solution \mathbf{u} is obtained with polynomials belonging to the following finite-dimensional subspace:

$$U_T^p = \{ \mathbf{u} \text{ polynomial of degree } \leq p, \operatorname{div} \mathbf{K}\boldsymbol{\varepsilon}(\mathbf{u}) = 0 \}.$$

These Trefftz functions are representative of the interior effect. Similar results have been obtained for plates in the framework of the Kirchhoff-Love theory (Hochard, 1991).

2.2. VARIATIONAL FORMULATION

A variational formulation, which is consistent with the above approximation and which takes into account the boundary conditions, is then introduced. The initial problem is replaced by an equivalent formulation which can be written as:

$$\begin{aligned} &\text{To find } \mathbf{u} \text{ belonging to } U^p_T \text{ such that:} && \forall \mathbf{u}^* \in U^p_T \\ &\int_{\partial_1 \Omega} \boldsymbol{\sigma}(\mathbf{u}^*) \mathbf{n} \cdot (\mathbf{u} - \mathbf{u}_d) d\Gamma + \int_{\partial_2 \Omega} \mathbf{u}^* \cdot (\boldsymbol{\sigma}(\mathbf{u}) \mathbf{n} - \mathbf{f}_d) d\Gamma = 0 \end{aligned} \quad (2)$$

To extend this method to more complex structures, the whole domain is subdivided into subdomains Ω_i . The problem of elasticity can be written:

$$\begin{aligned} &\text{To find } \mathbf{u}, \text{ with } \mathbf{u}_i \text{ its restriction on } \Omega_i, \text{ such as:} \\ &\text{div } \mathbf{K}\boldsymbol{\varepsilon}(\mathbf{u}_i) = 0 && \text{in } \Omega_i, \\ &\mathbf{u}_i = \mathbf{u}_{di} && \text{on } \partial_1 \Omega_i, \\ &\boldsymbol{\sigma}(\mathbf{u}_i) \mathbf{n} = \mathbf{f}_{di} && \text{on } \partial_2 \Omega_i, \\ &\mathbf{u}_i = \mathbf{u}_j \text{ et } \boldsymbol{\sigma}(\mathbf{u}_i) \mathbf{n}_i + \boldsymbol{\sigma}(\mathbf{u}_j) \mathbf{n}_j = 0 && \text{on } \Gamma_{ij}, \end{aligned} \quad (3)$$

where the last line corresponds to the conditions of continuity between Ω_i and Ω_j along Γ_{ij} ($\mathbf{n}_i + \mathbf{n}_j = 0$ on Γ_{ij}). A generalisation of the simple domain variational formulation can be written (Hochard, 1993):

$$\begin{aligned} &\text{To find } \mathbf{u}, \text{ with } \mathbf{u}_i \in U^p_T \text{ its restriction on } \Omega_i, \text{ such as:} && \forall \mathbf{u}^* \in U^p_T \\ &\int_{\partial_1 \Omega} \boldsymbol{\sigma}(\mathbf{u}^*) \mathbf{n} \cdot (\mathbf{u}_i - \mathbf{u}_{di}) d\Gamma + \int_{\partial_2 \Omega} \mathbf{u}^* \cdot (\boldsymbol{\sigma}(\mathbf{u}_i) \mathbf{n} - \mathbf{f}_{di}) d\Gamma + \\ &\frac{1}{2} \sum_j \int_{\Gamma_{ij}} [\mathbf{u}^* \cdot (\boldsymbol{\sigma}(\mathbf{u}_i) \mathbf{n}_i + \boldsymbol{\sigma}(\mathbf{u}_j) \mathbf{n}_j) + \boldsymbol{\sigma}(\mathbf{u}^*) \mathbf{n} \cdot (\mathbf{u}_i - \mathbf{u}_j)] d\Gamma = 0 \end{aligned} \quad (4)$$

This variational formulation is not-symmetrical but definite positive. This study has been extended to complex assembling of plates.

3. Numerical Implementation of the Method

The first implementation of the software was carried out with a symbolic language for numerical analysis (Macysma). From a set of polynomial interpolation functions in terms of displacement, the deformations, the stresses and the expressions of the various matrices associated with the variational formulation were calculated and automatically translated in Fortran language by Macysma.

This earlier version has shown the potential advantage of the method, but it was not very useful for industrial structures. To answer industrial requirements, a new version has been developed in the framework of Brite Euram « Low Cost Tooling » Project. This new

version, which name is CASSEL (Simplified CA l culation of Elastic Structures), uses several computational techniques well known in the field of the Finite Element Method (Dhatt, 1981):

- Numerical integration rather than explicit integration
- Optimisation of the computer memory usage
- Adding several types of boundary conditions and loads to model the behaviour of industrial structures.

3.1 NUMERICAL INTEGRATION

Using symbolic programming language makes Fortran subroutines very difficult to read and consequently difficult to maintain. Numerical integration, associated with programming rules provides :

- A Fortran code easier to read and more compact.
- Time saving to implement new functionality.
- A better reliability by modular programming (one subroutine for one integral of the variational formulation).
- For further development, the ability to use an adaptive technique to adapt the polynomial basis to the accuracy required

A comparison between explicit integration programming (one term of the 196 terms of the DIO matrix) and numerical integration programming (all terms of the same DIO matrix) is shown Figure 1.

<i>one term of the 196 terms of the DIO matrix</i>	
	$\text{DIO}(13,14) = -12*((3*\text{NU}-1)*\text{NY}^{**3}+(4-2*\text{NU})*\text{NX}^{**2-1}*\text{NY})*\text{Y5}+((6-12$
1	$*\text{NU})*\text{NX}*\text{NY}^{**2}+(-5*\text{NU}-1)*\text{NX}^{**3}+\text{NX})*\text{XY4}+((2*\text{NU}-4)*\text{NX}*\text{NY}^{**2}+(1-3*\text{N}$
2	$\text{U})*\text{NX}^{**3}+\text{NX})*\text{X5}+((5*\text{NU}+1)*\text{NY}^{**3}+((12*\text{NU}-6)*\text{NX}^{**2-1})*\text{NY})*\text{X4Y}+((1$
3	$0*\text{NU}-2)*\text{NX}*\text{NY}^{**2}+(4*\text{NU}+4)*\text{NX}^{**3-6}*\text{NX})*\text{X3Y2}+((-4*\text{NU}-4)*\text{NY}^{**3}+((2$
4	$-10*\text{NU})*\text{NX}^{**2+6})*\text{NY})*\text{X2Y3}$
<i>for all terms of the DIO matrix</i>	
	<pre> DO 30 K = 1, NFBASE DO 40 L = 1, NFBASE OMEGA = -(WDX(L)*NX+WDY(L)*NY) flex = nMn(K)*omega+(DivMn(K)+tMns(K))*W(L) DIO(K,L) = DIO(K,L)+COEF*FLEX 40 CONTINUE 30 CONTINUE </pre>

Figure 1 : Comparison between explicit and numerical integration

3.2 OPTIMISATION

The development of this numerical methods requires to solve a non symmetric system of linear equations (28 equations by plates). In order to save computing memory and to provide a very quick resolution, a skyline matrix storage technique with its associated solver has been implemented.

The figure below (Figure 2) shows how the structure built with plates are connected by their boundary to build the structure. This topology is quite similar to a mesh where nodes are equivalent to plates and elements are the connection between plates. So, it is easier to implement an algorithm of bandwidth (Sloan, 1989) similar to finite element method.

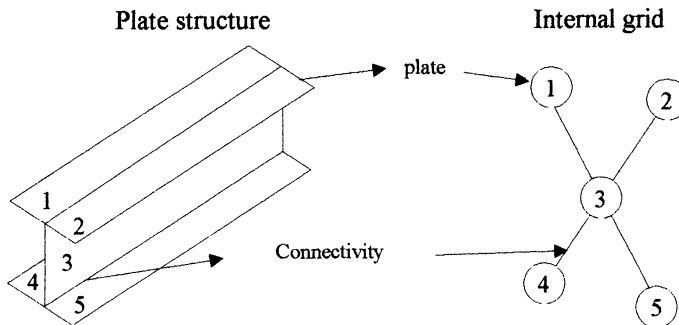


Figure 2 : Topology of the plate structure

4. CAD Integration

For detailed design, usually, stamping tools are defined by a solid modelling method, but in the earlier stage of design, designers think about the tool architecture in terms of plates (walls, ribs, ...). In the earlier stage of design, parametrization (thicknesses, ribs position, ...) can be very useful to evaluate and compare several design solutions.

CASSEL is clearly well adapted to simulation in the earlier stage of design. In order to provide to the designer the necessary geometrical and parametrization tools, it was decided to design the software in a way that it can be connected easily to CAD system available on the market.

Ideas Master Series from SDRC has been chosen for the first integration of CASSEL in a CAD system. Ideas provides a functionality to obtain a mid-surface model with thickness from a solid model (under the condition that volumes are « thin », i.e. with one dimension smaller than the two others). The Figure 3 shows a solid model and the corresponding connected mid surface model with thickness required for CASSEL simulation is represented Figure 4.

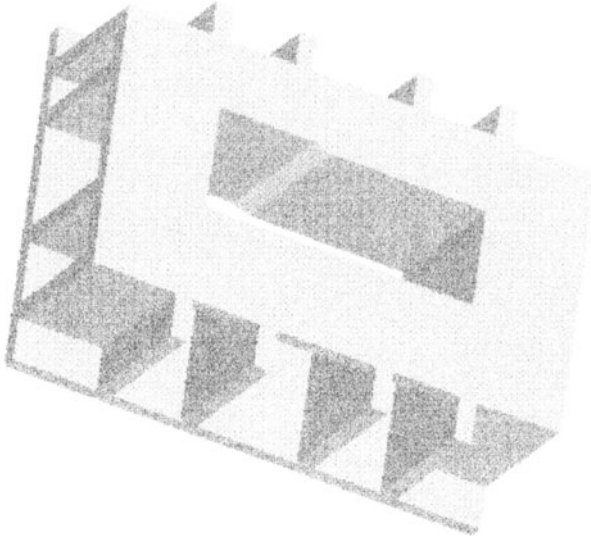


Figure 3 : Solid model

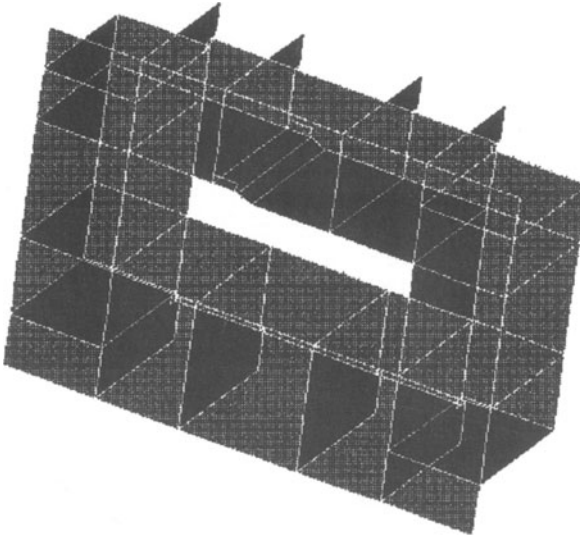


Figure 4 : Connected mid surface model with required for CASSEL simulation

In order to display displacements and stresses in a graphical post-processor, each plate is tessellated and displacements and stresses are approximated at each vertex of the tessellation, using the polynomial interpolation function set.

5. Example

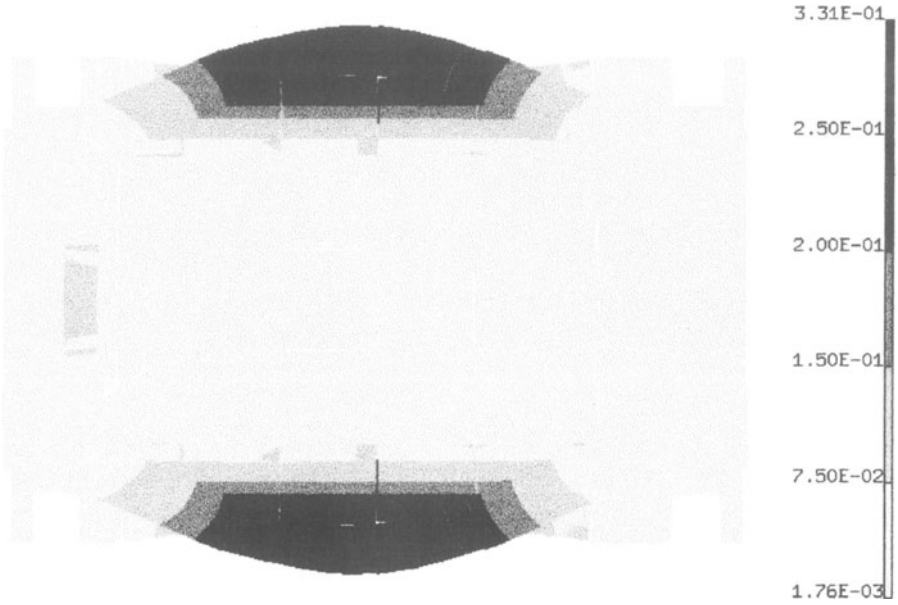


Figure.5 :Displacement magnitude obtained with CASSEL

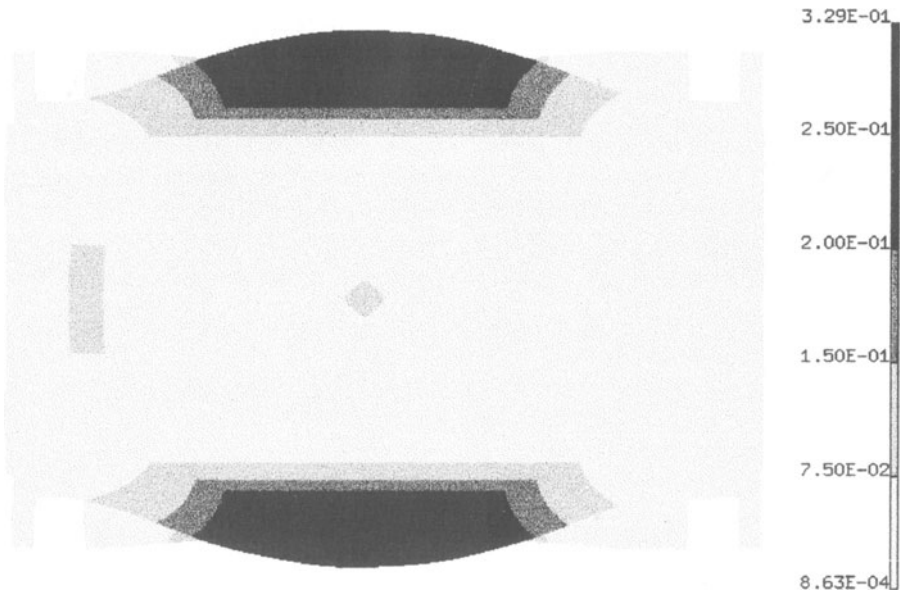


Figure 6 :Displacement magnitude reference results (FEM)

As an example, a mid surface model of a die is considered (Figure 7). The load is prescribed on the entry of the die. The model for CASSEL simulation corresponds to all the plates

represented Figure 7. The displacement magnitude results obtained with CASSEL (Figure 5) are in very good agreement with the reference Finite Element results represented Figure 6.

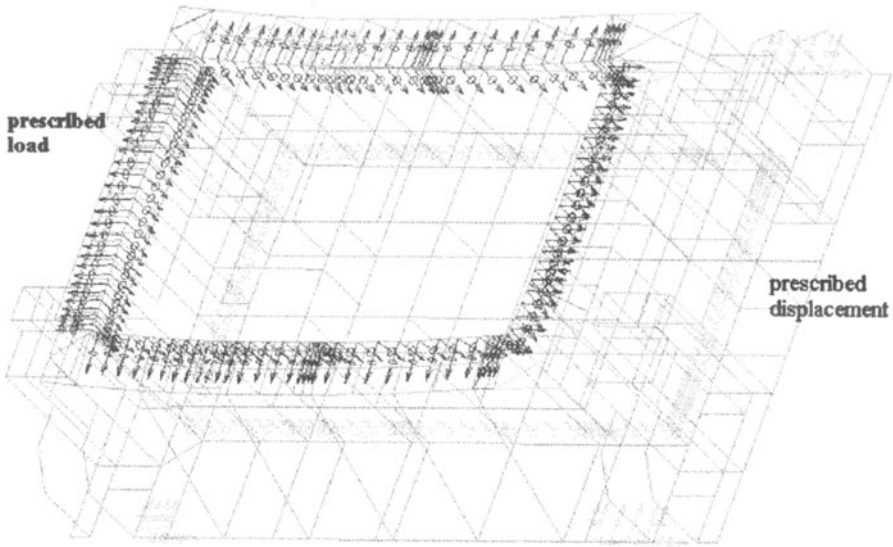


Figure 7 :Mid surface model required for CASSEL simulation

6. References

- Dhatt, G., Touzot, G., (1981) Une présentation de la méthode des éléments finis, Maloine S.A., Editeurs Paris.
- Hochard, Ch., Proslie, L. (1991) A simplified analysis of plate structures using Trefftz functions, *Int. j. numer. methods eng.*, Vol.32.
- Hochard, Ch., Ladevèze, P., Proslie, L. (1993) A simplified analysis of elastic structures, *Eur. J. Mech., A/Solids*, Vol.12, N°4.
- Jirousek, A., Lan Guex, (1986) The Hybrid-Trefftz finite element model and its application to plate bending", *Int. j. numer. methods eng.*, Vol.23.
- Sloan, S.W., (1989) A Fortran program for profile and wavefront reduction", *Int. j. numer. methods eng.*, Vol.23.
- Zielinski, J., Zienkiewicz, O.C., (1985) Generalized finite element analysis T-complete boundary solution functions, *Int. J. Num. Meth. Eng.*, Vol.21.

AIRCRAFT ENGINE BLADES-CASING CONTACT STUDY

I. GUILLOTEAU, E. ARNOULT, B. PESEUX

*Laboratoire de Mécanique et Matériaux, Division Structures,
Ecole Centrale de Nantes, BP 92101, F-44321 NANTES Cedex 3, France*

M. BERTHILLIER

Département YLEA

SNECMA, F-77550 MOISSY-CRAMAYEL, France

Abstract

The present work aims at studying contact phenomena within aircraft engines. These events occur for instance when severe manoeuvrings are operated or when the engine bears a blade-off event. Two approaches are used simultaneously. The former is a numerical one and consists in a fine rotor/stator contact simulation. Various contact-impact algorithms and time integration schemes are tested on elementary cases. The Lagrange multiplier method appears to be the most appropriate one for dynamic studies. The latter approach is an experimental one and consists in a vibratory study of the mechanical coupling between the casing and the fan bladed disk so as to determine what parameters generate interaction. A simplified experimental test rig is used. Interaction is produced with selected casing and blade modes.

1. Industrial Context

During the qualification stage of a civil aircraft engine, a series of tests are carried out. One of these tests is a blade off test that demonstrates the engine capability of containing damage without catching fire and without failure of its mounting attachments when operated for at least 15 seconds, unless the resulting engine damage induces a self shutdown. The engineers need to predict the real loads applied to the engine structure in order to optimize the design stage. For this, a lot of numerical simulations are carried out but current software does not give adequate results, and in particular the finite element simulations involving contact. The aim of our work is to propose simplified models providing accurate results. The first part of this paper deals with the numerical simulation of contact, while the second part is an experimental study.

2. Algorithmic Aspects

In order to build a simplified model of the dynamic contact phenomenon, classical contact-impact methods and time integration operators are studied.

2.1. CONTACT METHODS

Two parameters must be defined to characterize the contact conditions : the gap function g , which represents the distance between the bodies in potential contact, and the contact pressure λ . Thus, the unilateral contact law is expressed as an impenetrability condition ($g \geq 0$), a compressive condition ($\lambda \leq 0$), and a complementary condition ($g\lambda = 0$).

The discretized contact problem consists in finding the displacement vector $U(t)$, so that $M\ddot{U} + F^{int}(U, \dot{U}) - F^{ext} + F^{contact} = 0$ and $G(t) = G^0 + QU$, where M is the mass matrix, F^{int} is the vector of internal forces, F^{ext} is the vector of external forces, $F^{contact}$ is the vector of contact forces, \ddot{U} and \dot{U} are the vectors of nodal accelerations and velocities. The gap functions have been adapted to the finite element method and are noted G and G^0 , vectors of current and initial gaps. Q is a matrix deduced from the discretization of the contact entities.

The contact methods derive from the optimization study with constraints. The first one is the penalty method, adopted by commercial software of dynamic mechanics like LS-DYNA3D, PAMCRASH or RADIOSS. It consists in introducing artificial springs between the contact nodes. This method is easy to implement in a finite element code but admits body penetrations and induces high frequency oscillations. The problem becomes : find U so that

$$M\ddot{U} + F^{int}(U, \dot{U}) + [Q^T \alpha Q]U - F^{ext} + Q^T \alpha G^0 = 0 \quad (1)$$

where the contact force vector is $\Lambda = \alpha G$ and α is the penalty parameter matrix.

The second method is the Lagrange multiplier method, which has the advantage of enforcing the exact geometric contact condition but introduces additional variables, namely the contact forces. The problem is then to find the couple (U, Λ) so that

$$M\ddot{U} + F^{int}(U, \dot{U}) - F^{ext} + Q^T \Lambda = 0 \quad (2)$$

with the condition $G(t) = G^0 + QU = 0$.

Another kind of method is a mix of the penalty functions and the Lagrange multipliers : for example, the augmented Lagrangian or the perturbed Lagrangian methods. We will not deal with these methods in the present paper.

2.2. TIME INTEGRATION SCHEMES

The scheme generally chosen for high velocity impact problems is an explicit one : the second-order accurate central difference method

$$U_{n+1} = U_n + \Delta T \dot{U}_{n+1/2}, \dot{U}_{n+1/2} = \dot{U}_{n-1/2} + \Delta T \ddot{U}_n \quad (3)$$

with $\Delta T = t_{n+1} - t_n = t_{n+1/2} - t_{n-1/2}$.

This scheme is conditionally stable, i.e. the time step must be lower than a limit value, depending on the discretization of the structure : $\Delta T \leq 2/w_{\max}$, where w_{\max} is the highest frequency component in the discretized system.

In the case of low velocities, an implicit scheme can be used. The most common one is the Newmark time integration scheme

$$U_{n+1} = U_n + \Delta T \dot{U}_n + \Delta T^2 \left[\left(\frac{1}{2} - \beta \right) \ddot{U}_n + \beta \ddot{U}_{n+1} \right] \quad (4)$$

$$\dot{U}_{n+1} = \dot{U}_n + \Delta T \left[(1 - \gamma) \ddot{U}_n + \gamma \ddot{U}_{n+1} \right] \quad (5)$$

where β and γ are the Newmark parameters. Integration is globally first-order accurate for $\gamma=1/2$ and a choice of $2\beta \geq \gamma \geq 1/2$ leads to an unconditional stability. If $\beta=0$ and $\gamma=1/2$, the scheme corresponds to the central difference method.

2.3. FORWARD INCREMENT LAGRANGE MULTIPLIER

If the discretized contact problem is resolved using the central difference method for time integration and the Lagrange multiplier for contact, there appears a singularity : the contact forces Λ_{n+1} have no influence on the displacements U_{n+1} ! Carpenter *et al.* [3] propose an alternative formulation compatible with the explicit scheme : $M\ddot{U}_n + F^{int}(U_n, \dot{U}_n) - F_n^{ext} + Q_{n+1}^T \Lambda_n = 0$, $G_{n+1}=0$ (and not $G_n=0$).

The formulation leads to a predictor-corrector process $U_{n+1} = U_{n+1}^* + U_{n+1}^c$, where U_{n+1}^* is the vector of nodal displacements calculated without contact. The vector $U_{n+1}^c = -\Delta T^2 M^{-1} Q_{n+1}^T \Lambda_n$ is a displacement correction due to contact and the force that permits us to impose the contact constraint is

$$\Lambda_n = \left[\Delta T^2 Q_{n+1} M^{-1} Q_{n+1}^T \right]^{-1} \left(Q_{n+1} U_{n+1}^* + G^0 \right). \quad (6)$$

3. Numerical Results

The different methods of dynamic contact are tested on simple examples. The first one is an impact of two identical elastic rods, initially separated, as described in [3]. The methods used to resolve this problem are the penalty and the forward Lagrange multiplier methods, with an explicit time integration scheme. Figure 1 shows that the Lagrange multipliers give very accurate results compared to the penalty method.

If the penalty parameter is increased for a better precision of the results, the nodal penetration decreases but a lot of numerical oscillations appear in the velocity and contact force curves. Theoretically an infinite value must be used for the penalty parameter, but in practice, especially with an explicit time scheme, the contact stiffness should be of the same magnitude as the structure stiffness, otherwise the time step must be widely reduced. That is the reason why the results are not always satisfactory.

With the Lagrange multiplier method, the results are accurate, and the explicit stable time step does not need decreasing [1]. Thus, in order to model the following examples, the Lagrange multiplier method is retained.

The second example deals with the impact of an elastic rod against a rigid wall, resolved using the Lagrange multiplier method with implicit and explicit time integration schemes and LS-DYNA3D, with the default contact values. The Newmark scheme with ($\beta=0.25 ; \gamma=0.55$) does not give satisfactory results ; there appears numerous oscillations in particular in the contact force curve [4]. The ($\beta=0.50 ; \gamma=0.55$) implicit and the explicit schemes, coupled with the Lagrange multiplier method, give similar results, while the explicit-penalty method (LS-DYNA3D) induces a slight nodal penetration.

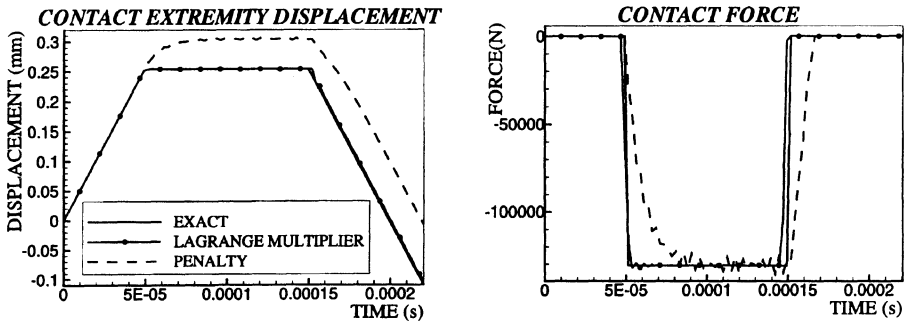


Figure 1. Impact of two identical elastic rods.

The last numerical test is the rebound, without friction, of a 2D rotational elastic beam against a rigid circle (cf. Figure 2). The steel beam describes an eccentric circle with the contact one and is subjected to a torque at its extremity on the hinge.

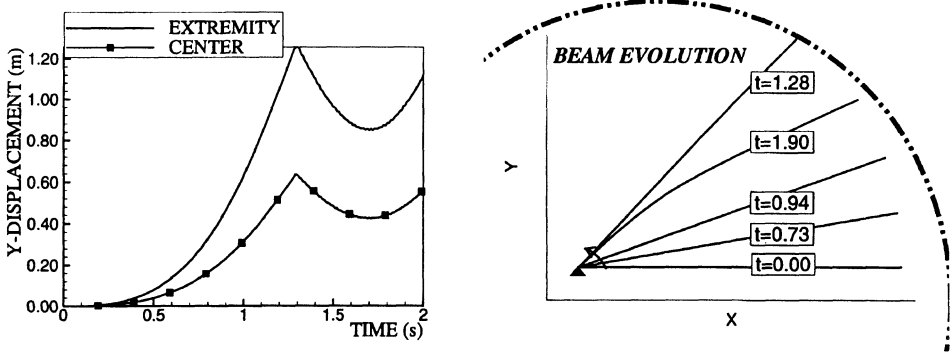


Figure 2. Beam rebound on a circular contact zone.

The next stage of our numerical study consists in modelling contact with a flexible axisymmetric surface.



4. Experimental Aspects

4.1. DYNAMIC INSTABILITY

The experimental part of the study deals with vibratory interaction between the engine and the fan bladed disk. When an aircraft engine bears a blade loss, high unbalanced loads are generated. The bladed disk and the casing come into contact, shocking and rubbing each other. In the meantime the two structures are loaded over a huge frequency spectrum and numerous natural modes of vibration are excited. Some particular conditions are required to make the whole system come into resonance and be submitted to severe stresses. The dynamic instability can lead to the ruin of the engine. Special attention is therefore to be paid on the exact conditions which give rise to the instability.

Both the casing and the bladed disk are supposed to be axisymmetric structures. As a consequence, their natural modal shapes can be represented by the number of their nodal diameters n . If f_c denotes the casing natural frequency for n nodal diameters and f_b the bladed disk natural frequency for the same n diameters mode, if f denotes the rotation frequency of the engine, then a condition for dynamic instability is given by [5]:

$$f_c + f_b = n.f \quad (7)$$

This equation means that waves in opposing directions are travelling both in the casing and the blades.

In order to avoid such a coincidence, engine designers are to respect important frequency constraints which usually lead to increasing the casing stiffness, weighting the engine down and making it clumsy. Other solutions have to be found.

4.2. EXPERIMENTAL TEST RIG

The purpose of the experimental approach is to examine more precisely the behaviour of the blades when rubbing on the casing, and validate numerical simulations. In a second part, the test rig will be used to determine which parameters are involved in the apparition of interaction, in addition to equation (7).

The test rig used is deliberately simplified (see Figure 3). It consists in a part of a casing of an aircraft engine bolted on a steel ring which is fixed on the table of a vertical lathe, and in a blade clamped in the turret. In this configuration, the rotating part is the casing, and no aerodynamic effect due to the rotation of blades has to be taken into account. The use of a single blade instead of a whole set is convenient to get rid of the problem of the direction of the travelling waves through the blades. The contact between the blade and the casing, as well as the lathe rotation, are controlled by the experimenter. The instrumentation is made of classical devices: accelerometers (B&K), amplifiers (B&K), spectral analyzer (HP), and is completed with a Laser Doppler Velocimeter (Polytec), useful for non-contact measurements on the rotating casing.

A first set of measurements was taken to characterize the test rig, especially to determine the natural frequencies and modal shapes of the casing. A finite element model including the casing and the steel ring was established and modified with respect to the experimental results. For a chosen rotation frequency of the lathe, interaction will

be induced with a selected mode of the casing and a corresponding frequency of the blade.

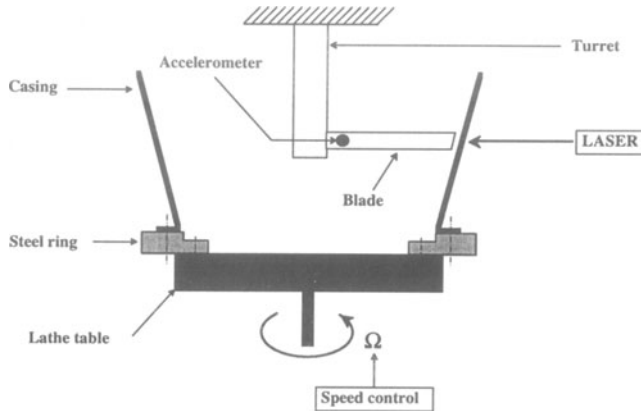


Figure 3. Experimental test rig.

4.3. FINITE ELEMENT MODEL - MODAL ANALYSIS

As a first approximation neglecting geometric and material defaults, the casing which looks like a frustrum of a cone is considered as an axisymmetric structure. The natural modes of this kind of structures have the particularity to be double ones: to each natural frequency correspond two different modal shapes. When the axisymmetry is perfect, and if θ denotes an angular parameter of the structure, the modal shapes in the radial direction are $\cos(n\theta)$ and $\sin(n\theta)$, where n stands for the number of nodal diameters. No special orientation is noticeable. In case of imperfections, the symmetry is broken and the system is said to be mistuned. Each natural frequency splits into two distinct ones, and the modal shapes are modified according to the importance of the unbalancement. Particular orientations appear [8].

The frequency response of the casing was recorded while the lathe was stopped, with a method using a small rotating mirror making the laser spot describe a circle on the inner side of the casing [2]. Once the identification of natural frequencies was complete (see Figure 4), time acquisitions were made to extract the modal shapes (see Figure 5). It appeared that the structure was mistuned both in frequency and time response, the biggest frequency split being obtained for the 4 nodal diameters mode (this is due to the way the steel ring was fixed on the lathe). The lowest modes were the most perturbed ones.

A first finite element model was made with SAMCEF supposing the perfect axisymmetry of the casing. A modal analysis carried out on the model clearly indicated that such an assumption was unacceptable. A fine geometrical study of the casing revealed that for a given altitude, the radius was not constant, the small variation, which never exceeds 1% being significant enough to disturb the modal behaviour. Another finite element model was then made including the geometric alterations.

The new results are compared with the experimental results in Figure 6. The biggest differences are attributed to the imperfections of the casing embedding.

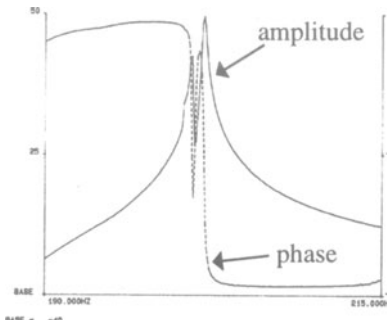


Figure 4. Casing frequency response.

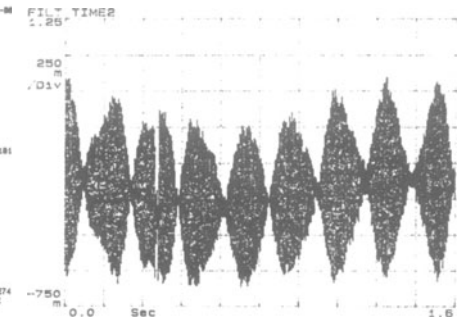


Figure 5. Example of modal shape.

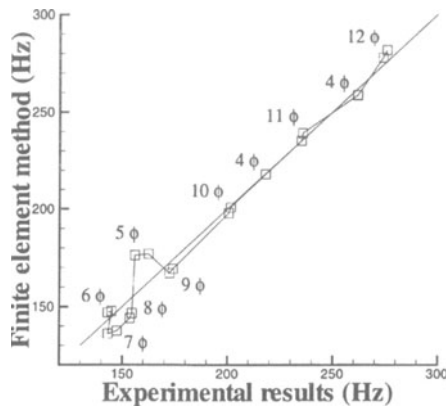


Figure 6. Comparison experimental results - finite element model.

4.4. CREATING INTERACTION

The test rig has been used in its current configuration to make first attempts on the interaction phenomenon. The choice of a mode with regular modal shape is more advisable. Moreover, to avoid the high modal density at the beginning of the spectrum, and because of its weak damping, the 10 nodal diameters mode was finally selected. Using the highest rotation frequency of the lathe (5 Hz), and adapting equation (7) to the situation in which a single blade is implied, the first natural frequency of the blade was set to satisfy the mathematical condition of interaction. The contact was then created on the rotating casing.

The major issue which has to be faced is the lack of symmetry of the casing. The contact is unfortunately not permanent, and the structure is not excited by a constant force. As a result, no significant amplitude in the frequency response is noticeable

neither on the casing nor on the blade. However, it is interesting to remark that for lower rotation frequency, the 10 nodal diameters mode's answer is higher than the others (20 dB). At these rotation speeds, the contact is quite similar to a harmonic excitation. When rotating at 5 Hz, the whole structure experiments impulses whose effect is the excitation of every mode which is confirmed by the frequency response.

In order to suppress the effect of the geometrical default it is considered to fix an abrasive material on the inner side of the casing and to machine it so as to force the blade/casing contact to be permanent.

5. Conclusion and Future Prospects

The interaction phenomena, which have motivated the present work, are of major concern to aircraft designers. The present study is composed of a numerical part dealing with dynamic contact simulations on classical examples, in particular with the Lagrange multiplier method, and an experimental part which consists in identifying the parameters involving modal interaction. The next stage of our work is the simulation and the experimental study of the blade/casing dynamic contact.

6. References

1. Belytschko, T., and Neal, M.O.: Contact-impact by the pinball algorithm with penalty and Lagrangian methods, *International Journal for Numerical Methods in Engineering* **31** (1991), 547-572.
2. Billet, L., and Moreno, J.: Caractérisation des modes de vibration d'une coque de révolution à l'aide d'un vibromètre laser à faisceau tournant, *Bulletin SFM, Revue Française de Mécanique* **1** (1996), 25-32.
3. Carpenter, N.J., Taylor, R.L., and Katona, M.G.: Lagrange constraints for transient finite element surface contact, *International Journal for Numerical Methods in Engineering* **32** (1991), 103-128.
4. Chaudhary, A.B., and Bathe, K.J.: A solution method for static and dynamic analysis of three-dimensional contact problems with friction, *Computers and Structures* **24** (1986), 855-873.
5. Staples, B.C.: Excitation of travelling wave response in axi-symmetric structures, *Proceeding of the 15th seminar on modal analysis, Lewen, Belgium* (19-21 sept 1990), 1339-1354.
6. Schmiechen, P., Ewins, D.J., and Bucher, I.: Excitation of arbitrary displacement / velocity conditions in rotationally periodic structures, *ASME, Design Engineering Technical Conferences* **3B** (1995), 1353-1360.
7. Taylor, R.L., and Papadopoulos, P.: On a finite element method for dynamic contact/impact problems, *International Journal for Numerical Methods in Engineering* **36** (1993), 2133-2140.
8. Tobias, S.A., and Arnold, R.N.: The influence of dynamical imperfections on the vibrations of rotating disks, *Proceedings Institute of Mechanical Engineers* **171** (1957), 669-690.

DESIGN OF A SUPER CONDUCTING QUADRIPOLE PROTOTYPE

Using substructuring to take contact into account

C. BLANZE AND L. CHAMPANEY

*LMT Cachan - 61, Av. du Pt. Wilson
94235 Cachan Cedex - FRANCE*

AND

P. VEDRINE

*CEA Saclay - DSM/DAPNIA/STCM
91191 Gif-sur-Yvette Cedex - FRANCE*

1. Introduction

A superconducting quadrupole constitutes a part of a high-energy accelerator built by the CEA in collaboration with the CERN. Magnetic coils must be adequately prestressed to withstand the magnetic forces without "quenching". The mechanical model of such a complex structural assembly must take into account the frictional contact between the various component elements in order to prevent against both displacement and warm peak.

The behavior of an assembly of three-dimensional elastic structures can be heavily nonlinear when frictional contact is taken into consideration. Classical Finite Element techniques apply an iterative process to the whole problem, an approach that could prove quite expensive, especially when the number of contact zones turns out to be rather high [1]. For this study, we will be using a modular approach which is particularly efficient when the structure is globally linear and the nonlinearities have been localized on the connections. This method is based on two distinct approaches : the first introduces a partitioning of the structure into two mechanical entities - substructures and interfaces - while the second employs an iterative and completely-parallel scheme.

2. Presentation of the problem

2.1. THE L.H.C. (LARGE HADRON COLLIDER)

The L.H.C. is an accelerator which subjects protons to "head-on" collisions at higher levels of energy (14 TeV) than ever attained before. It will be built by the CERN and is

to consist of two "colliding" synchrotrons, able to accelerate protons to 7 on 7 TeV, after which the beams will counter-rotate for several hours, thereby producing collisions at the experimental stage.

High-energy L.H.C. beams require high magnetic bending fields. In order to bend 7 TeV protons around the ring, the L.H.C. dipoles and quadrupoles must be capable of producing fields of 8.2T. Superconductivity has made this achievement possible. The CERN and CEA/Saclay have established a joint program to carry out the design, construction and testing of a superconducting L.H.C. quadrupole prototype.

2.2. MAGNETIC COILS

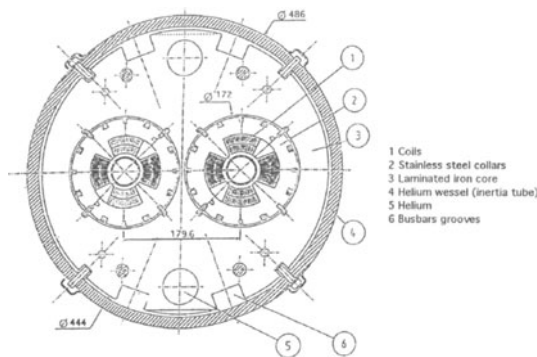


Figure 1. Quadrupole cross-section

Two magnetic channels [2] have been incorporated into a single iron yoke and cryostat and are cooled with a helium superfluid in order to attain the very high guide field required (Fig. 1). The L.H.C. magnet coils will tend to be long, approximately 14 meters, with an inner diameter of 56 mm; they will be made of copper-clad Niobium-Titanium cables. The insulation is to be composed of two layers of Kapton.

The electromagnetic forces in the quadrupoles are contained by the collar structure. The collars are made of austenitic steel laminations of 2 mm in thickness. The pairs of half-collars are alternately turned by 90 degrees and are completed by two separate pole pieces. The keying and prestressing of the assembly is conducted by eight lines of wedge-shaped stainless steel keys, which are progressively inserted into the grooves on the outside of the collars. Once the coil-collar assemblies have been prepared and the coil interconnections completed, the yoke is positioned around the two units. In order to stiffen the entire yoke assembly, a so-called inertia tube is placed around the yoke. This tube also serves as the helium vessel.

2.3. MECHANICAL PROBLEM

The mechanical structure of the quadrupoles has been designed both to withstand the strong forces being generated in the magnet and to limit, to the greatest extent possible,

coil deformation over the entire operating range. The materials used for the most highly-stressed components therefore exhibit a high load-bearing capacity, high elastic moduli, a good level of fatigue endurance and good behavioral characteristics at cryogenic temperatures of as low as $1.9^{\circ}K$. Whenever current is flowing in the cables, the coils must be under compressive stress in order to avoid the appearance of sudden cracks or movements. Coil displacements and deformations must be limited as much as possible. In order to satisfy these conditions, the relative dimensions of the structural components, the choice of materials and the level of prestressing all have to be carefully determined. Furthermore, the peak compressive stress in the coils at room temperature is to be minimized so as to avoid any creep of either the insulation or the copper. The main purpose herein is to optimize the adequate level of azimuthal prestress in order to avoid the appearance of coil movements during the functioning of the magnet. It is thus necessary to take frictional contact into account during the following three load sequences:

- collaring (prestress);
- cooling (from $293^{\circ}K$ to $1.9^{\circ}K$); and
- excitation (at the nominal field).

3. Presentation of the computational strategy

3.1. PURPOSE

For this study, we have used a modular approach which is dedicated to the analysis of such complex situations involving 3D assemblies. It is referred to as the "COFAST3D" (COntact and Friction in Assemblies of 3D STructures) approach. The COFAST3D approach is based on both a formulation and a strategy which have been well-adapted to the use of parallel computers [3]. With respect to the work conducted herein, this parallelism is being applied, above all else, in order to achieve a high level of modularity and flexibility in the problem description. Parallelism also leads to reducing both the size of the models and the numerical costs of their resolution, even when the approach is implemented on sequential computers.

A partitioning of the structure is performed in order to break down the problem from its global formulation; partitioning involves two distinct mechanical entities: substructures and interfaces. Each substructure is considered as a separate structure on its own (in this case, an elastic one) which only communicates with its neighboring interfaces. Interfaces, on the other hand, constitute the key elements to this approach; they are two-dimensional entities with their individual behavior, which can be represented in a mixed manner on the displacement and force fields defined on both sides of the interface [4].

3.2. THE COFAST3D APPROACH

3.2.1. *Decomposition of the structure*

In considering an assembly of various components by linkage elements (bolts, screws, rivets, joints, etc.), a decomposition can be introduced. The components are separated and the interfaces generated serve to model the connections existing between these elements:

contact, friction, . . . Each component can also be separated into substructures in order to reduce the size of the associated model (Fig. 2).

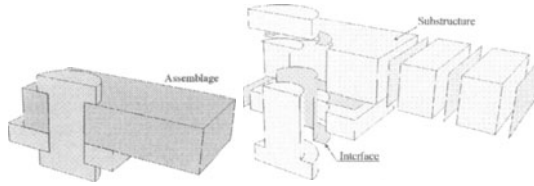


Figure 2. Decomposition of an assembly

The assembly is denoted Ω , the substructures are denoted $\Omega_E, \Omega_{E'}, \dots$, and $\Gamma^{EE'}$ represents the interface existing between Ω_E and $\Omega_{E'}$. A displacement field \underline{W}^E and a field of surface traction density field \underline{F}^E are defined on each side of an interface (\underline{F}^E represents the action of the interface on the substructure Ω_E).

3.2.2. Problem on one substructure

Since a given substructure Ω_E communicates only with interfaces, the problem to be solved consists of finding $(\sigma^E, \underline{U}^E)$, which satisfies:

- Kinematic admissibility with the displacement on the interfaces: $\forall M \in \partial\Omega_E$,

$$\underline{U}^E = \underline{W}^E \quad (1)$$

- Equilibrium equation under the force field on the interfaces: $\forall \underline{U}^*$,

$$\int_{\Omega_E} Tr(\sigma^E \varepsilon(\underline{U}^*)) d\Omega_E - \int_{\Omega_E} \underline{f}_d \underline{U}^* d\Omega - \int_{\partial\Omega_E} \underline{F}^E \underline{U}^* dS = 0 \quad (2)$$

- Constitutive law (linear elasticity): $\forall M \in \Omega_E$,

$$\sigma^E = \mathbf{K}\varepsilon(\underline{U}^E) \quad (3)$$

where \underline{f}_d is the prescribed body forces, \underline{U}^E the displacement field being sought in Ω_E , σ^E the stress field being sought in Ω_E , and $\varepsilon(\underline{U}^*)$ the strain field generated by the displacement \underline{U}^* .

3.2.3. Problem on one interface

The problem to be solved on one interface consists of finding both the force and displacement fields on both sides which satisfy the behavior of the modeled connection. The problem can then be expressed as a constitutive relation:

$$\mathcal{R}(\underline{W}^E, \underline{F}^E, \underline{W}^{E'}, \underline{F}^{E'}) \quad (4)$$

For example, the relation that describes a perfect connection between two substructures Ω_E and $\Omega_{E'}$ is: $\forall M \in \Gamma^{EE'}$,

$$\underline{F}^E + \underline{F}^{E'} = 0 \quad (\text{equilibrium of forces}) \quad (5)$$

$$\underline{W}^E - \underline{W}^{E'} = 0 \quad (\text{continuity of displacement}) \quad (6)$$

3.2.4. Iterative scheme

The iterative resolution scheme employed is based on the LARge Time INcrement method ("LATIN" method) proposed by P. Ladevèze [4]. The case presented herein refers to a degenerate condition of this method where only the final configuration is sought and where time is not taken into consideration. The LATIN method separates out the problem's difficulties; it enables avoiding the simultaneity of both the problem's global and nonlinear aspects. Thus, it takes the mechanical properties of the equations into account in order to divide them into two groups:

- local in space variable, and possibly nonlinear, equations, and
- linear and possibly global in space variable equations.

These groups serve to define two subspaces of elements, s , which denotes the set of unknowns for the entire problem. Since the only nonlinearities being studied are those defined on the interfaces and in order to obtain independent global linear problems on each substructure, the two subspaces are subsequently defined as follows:

$$\begin{aligned} \mathcal{A}_d = \{s, \text{ satisfying } \forall \Omega_E: & \quad \Gamma = \{s, \text{ satisfying } \forall \Gamma^{EE'}: \\ & - \text{ the kinematic admissibility (eqn. 1),} \quad - \text{ the constitutive relation (eqn. 4) } \\ & - \text{ the equilibrium equation (eqn. 2),} \\ & - \text{ the constitutive law on (eqn. 3) } \end{aligned}$$

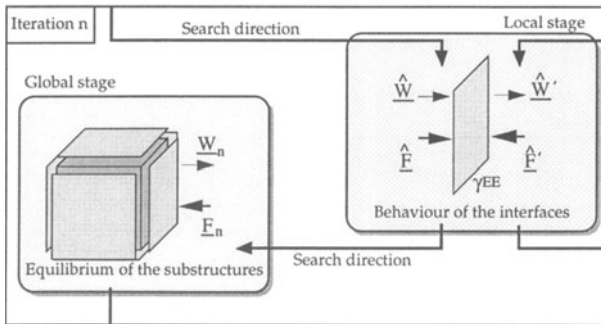


Figure 3. Representation of iteration n

The problem then consists of finding an element s_{ol} that satisfies both the behavior of the substructures ($s \in \mathcal{A}_d$) and the behavior of the interfaces ($s \in \Gamma$). The LATIN method starts with s_0 , an element of \mathcal{A}_d , and builds elements s , which belong to Γ and \mathcal{A}_d , successively up until reaching the solution s_{ol} . Since a substructure communicates only with interfaces, the initial solution $s_0 = 0$ is an element of \mathcal{A}_d .

Each iteration, i.e. the building of a new element s_{n+1} of \mathcal{A}_d from a given one s_n , requires two stages: the local stage and the linear global stage (Fig. 3). The local stage leads to independent nonlinear problems on each point of the interfaces, whereas the linear global stage leads to independent classical linear problems of structural analysis with a density of body forces and a density of surface traction on the substructures. These latter problems are then solved with a finite element discretization of the substructures. The discretized form of equation (10) becomes:

$$[[K^E] + [k^E]\{u_{n+1}^E\} = \{f'\} \quad (7)$$

where $[K^E]$ is the classical FE stiffness matrix and $[k^E]$ is a boundary stiffness matrix. $\{f'\}$ is a force vector expressed by the displacement and force field on the interfaces. It should be pointed out that the stiffness matrix of each substructure remains constant during the iterative process and thus gets factorized only once at the first iteration.

3.2.5. Frictional contact conditions

Frictional contact conditions are to be treated at the local stage. A static formulation of Coulomb's friction law (displacement law, [5]) has been applied for this purpose, i.e. a radial loading assessment is carried out and the solution is sought only at the end of the loading path. For complex loading and unloading conditions, an incremental formulation of the contact law has been used. The increments involved tend to be rather large (one for each loading or unloading step). Since the solution to this problem can be entirely described by the displacement and force field on the interfaces, the only data that need to be transmitted from one step to the next are those fields on the nonlinear interfaces. Thus, a correct representation of the loading path is provided, yet the radial loading assessment does allow for a reduction in the numerical costs

4. Numerical study of the quadripole

4.1. MODEL

The model under study is restricted to 1/8th of the quadripole (Fig. 4). It includes two levels of collars, one key, the coil, one-half of a pole piece and the insulation. Friction is considered on all of the contact zones. A 3D mesh of the structure has been developed.

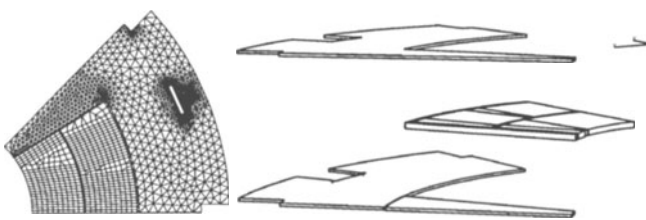


Figure 4. Applied model

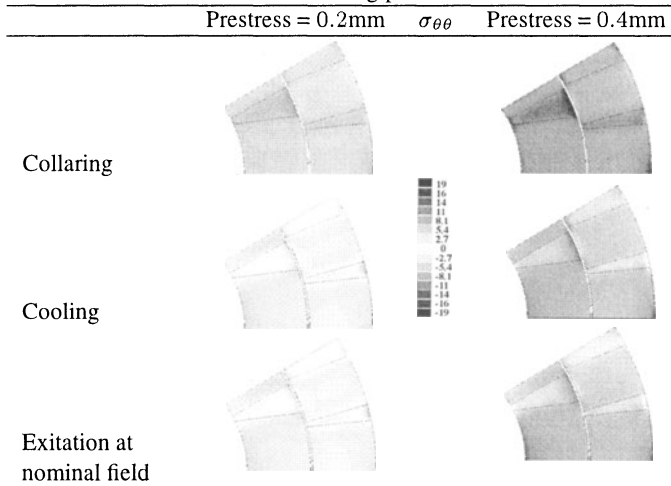
TABLE 1. Comparison with ABAQUS

	ABAQUS	COFAST3D
number of ddl	24, 228	23, 709
problem size	95.4Mb	26Mb
nb of inc./ite.	20 inc.	400 ite.
CPU Time (HP735)	8, 237	718
clock time	4.7h	13mn
reaction force on the lower side of the coil	258daN	252daN

4.2. COMPARISON WITH AN INDUSTRIAL FE CODE

The COFAST3D computational strategy has been compared with an industrial Finite Element code (ABAQUS, [6]). Frictional contact conditions are prescribed in ABAQUS using "master" surfaces and "slave" nodes. The same mesh has been utilized for both computations. Table 1 presents some of the results from the comparison carried out for just the first prestress load case. The ABAQUS number of ddl also includes Lagrange multipliers. The two results turn out to be very close to one another. The significant reduction in numerical costs (with respect to both size and time) provided by the COFAST3D approach is very advantageous for such optimization computations.

4.3. RESULTS FOR THE THREE SUCCESSIVE LOADS

TABLE 2. $\sigma_{\theta\theta}$ (in daN/mm²) at the end of the three loads for two differing pre-loads

The three successive loads have been applied to the structure. The pre-load is then applied by prescribing an artificial gap between the sides of the key and the collars. Cool-

ing from $293^{\circ}K$ to $1.9^{\circ}K$ is modeled by an applied thermal body force over the entire structure. Afterwards, the excitation can be modeled by a pre-computed body force field on the coil. The material properties change during the cooling process. Thus, the stiffness matrices have to be updated between the first and second load cases; however, these matrices remain constant between the second and third load cases. The total computation time is less than 30 minutes on an HP 735 work station. The results for two different pre-loads are presented: 0.2 mm on each side of the key, and then 0.4 mm on each side. The coil's stress state has also been shown. Table 2 indicates the $\sigma_{\theta\theta}$ stress on the coil at the end of the three successive loads for two different pre-loads. For the first preload (0.2 mm on each side of the key), the top of the coil is unloaded when the magnetic field has been applied; opening occurs on the contact surfaces - the prestress is too small. Further computations will be carried out in order to study the influence of the friction coefficient on the stress state of the coil at the end of the third load.

5. Conclusion

We have presented the application of a dedicated strategy to the design of a superconducting quadrupole prototype. The structure includes different materials, a large number of frictional contact zones and complex loading conditions: a mechanical prestress and cooling, followed by magnetic excitation. It is well-known that frictional contact nonlinearities tend to lead to very difficult problems. The dedicated strategy employed herein is based on both a modular decomposition of the structure and a parallel-resolution scheme. Contact nonlinearities get treated locally. A special radial loading assessment has been used to model the complex loading path. The COFAST3D strategy therefore leads to a great reduction in computational costs, a feature which has been demonstrated by means of a comparison with an industrial FE code. This reduction is very significant within the framework of a mechanical design for which many optimization loops can be created.

The initial set of results presented herein are very encouraging and have served to validate the application of such an approach to this type of complex situation. Further computations will be carried out in order to assess the influence of the model's various parameters.

References

1. Raous, M., Jean, M. and Moreau, J.J. (Eds.): *Proc. Second Contact Mechanics International Symposium*, Plenum Press, New York, 1995.
2. Tortschanoff T. et al. (Eds.): *The Short Straight Sections for the LHC, Proceedings from the Particle Accelerator Conference*, Vancouver, 1997.
3. Champaney, L., Cognard, J.Y. and Ladevèze, P.: A modular approach to structure assembly computations: Application to contact problems, *Eng. Comput.* **13** (1996), 15-32.
4. Ladevèze, P.: *Structural nonlinear mechanics: New approach and non-incremental computational method* Hermes, Paris, 2-86601-518-5, 1996.
5. Duvaut, G. and Lions, J.L.: *Inequalities in Mechanics and Physics*, Springer, Berlin, 1972.
6. Hibbitt, Karlsson and Sorensen Inc.: *Abaqus Standard Version 5.6 Manuals*, 1996.

THEORETICAL AND NUMERICAL STUDY OF A COUPLER FOR CRASHWORTHY DESIGN OF A TGV POWER CAR

J.S. Koo¹, Z.Q. Feng², M. Domaszewski² and F. Renaudin³

¹ Korea High Speed Railway, Seoul, Republic of Korea

² MMS - Université de Technologie de Belfort-Montbéliard, 90010 Belfort, France

³ Alstom - Transport, 90018 Belfort, France

Abstract: This paper is devoted to the theoretical and numerical study of a coupler for crashworthy design of a TGV power car. A theoretical model based on the equation of energy conservation is proposed for a basic design of energy absorbers like coupler. The theoretical solution of tube expansion is developed and verified by the finite element solutions using ABAQUS. A parametric sensitivity analysis is performed.

1. Introduction

The energy absorbers in a vehicle play an important role for crashworthy design [1]. Figure 1 shows a conceptual layout of energy absorbing components in the front part of a TGV power car. The crushable front part is composed of three energy absorption zones: retractable coupler, protective headstock and honeycomb structure, as shown in Figure 1.

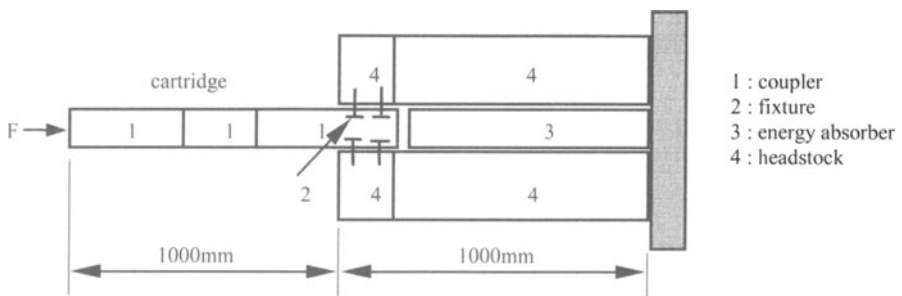


Figure 1. Energy absorbing structures in the front part of a TGV power car

This frontal part must absorb about 80% of the energy that should be realized in a crashworthy design. The conventional TGV can absorb 2mJ impact energy by the frontal end, but 5mJ is the design target for energy absorption in the next generation TGV. To accomplish this design goal, a new concept of design is necessary for energy absorbing components. In this study, we propose a crashworthy design of the retractable

coupler by tube expansion instead of tube buckling collapse [2]. A theoretical and numerical model will be proposed to improve the energy absorbing capacity.

The coupler must be designed to be collapsed at the impact force under 1500kN. Its crush length is estimated to be 600mm. The protective headstock is required to be collapsed at the impact force of 3000kN. This load is applied to the driver's cab at the same time with the impact force on the honeycomb structure. The load applied to the honeycomb structure must be controlled below 2000kN. Therefore, the total load applied to the driver's cab is limited to maximum 5000kN. In this design, the impact velocity of 30m/sec will be used as a typical collision velocity.

To accomplish the impact energy absorption of 5mJ, it can approximately be distributed to the three principal energy absorbing components as follows :

- Coupler = 1.2 mJ as 800mm x 1500kN
- Protective headstock = 2.2 mJ as 730mm x 3000kN
- Honeycomb structure = 1.6 mJ as 800mm x 2000kN

These design specifications are very difficult to be satisfied by conventional energy absorbing components utilizing the tube buckling collapse as shown in Figure 2, even though other components like the cartridge can absorb additional impact energy. The cause is that the buckling collapse has shorter crush length and higher peak force.

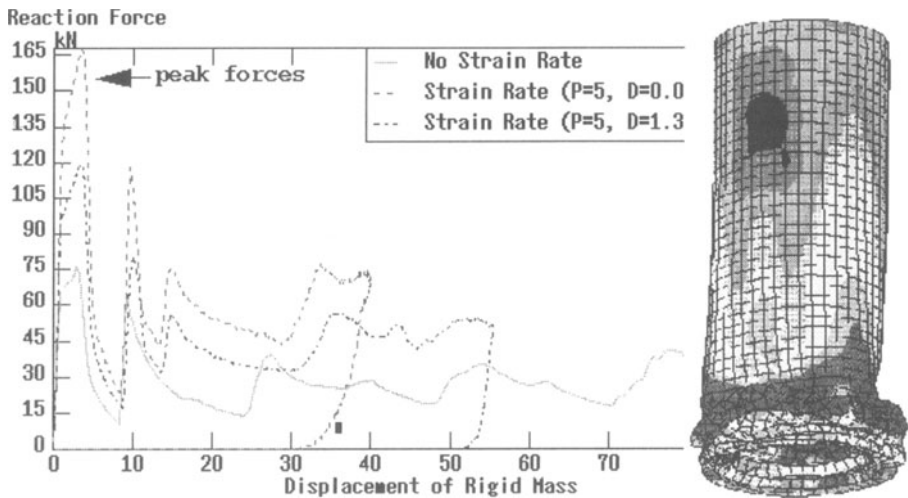


Figure 2. Tube buckling collapse simulated by PAM-CRASH

It is noted that the numerical modeling of tube collapse is performed using the explicit finite element program PAM-CRASH [3]. In case of tube buckling collapse, a flat crushing response and the space efficiency cannot be accomplished. To complement

these shortcomings of conventional energy absorbing components, it is necessary to develop a new kind of energy absorbing components which utilize metal forming technologies such as tube expansion and tube inversion [4].

2. Theoretical Approach for Tube Expansion

A theoretical solution can be obtained approximately using a simplified geometrical and material model (Figure 3).

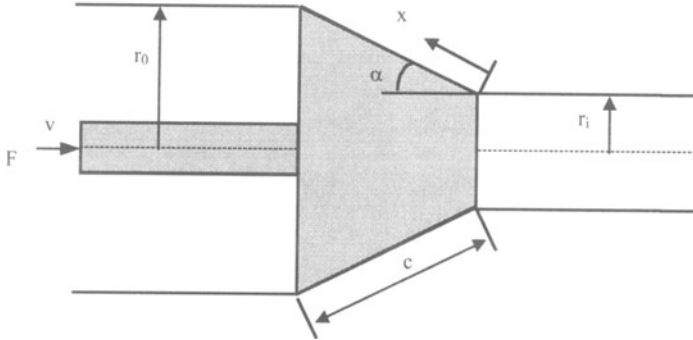


Figure 3. Schematic diagram of the tube expansion process

A kinematic method using the theory of perfect plasticity will be developed with the simplified geometrical model and the following assumptions :

- The material is rigid perfectly plastic and is characterized by the flow stress σ_0 .
- The strain rate sensitivity is considered by the Cowper-Symonds power law.
- The extension rate in the longitudinal direction is neglected.
- The change of curvature in the circumferential direction is not considered.
- The bending deformations near both ends of the die are neglected.
- The tube thickness t is taken as constant.

The compressive force can be calculated from the equality of internal and external rate of energies, as defined in equation (1).

$$F v = \dot{E}_{int} + \dot{E}_{fr} \quad (1)$$

where F and v denote the pushing force and the velocity of the die respectively, \dot{E}_{int} is the internal rate of energy, and \dot{E}_{fr} is the energy rate dissipated by frictional effects. From the energy balance equation (1) and taking into account the assumptions defined above, the pushing force of the die is obtained as :

$$F = F_{int} + F_{fr} \quad (2)$$

where F_{int} and F_{fr} are defined as follows :

$$F_{int} = \frac{2\pi}{\cos \alpha} N_0 r_i \left[\ln \left(\frac{r_o}{r_i} \right) - \frac{p}{2} (r_i \nu \tan \alpha)^{\frac{1}{p}} D^{-\frac{1}{p}} \left(r_o^{-\frac{2}{p}} - r_i^{-\frac{2}{p}} \right) \right] \quad (3)$$

$$\text{and, } F_{fr} = \frac{2\pi}{\cos \alpha} \mu N_0 \left[c + D^{-\frac{1}{p}} (r_i \nu \tan \alpha)^{\frac{1}{p}} \frac{p}{(p-2) \sin \alpha} \left(r_o^{\frac{p-2}{p}} - r_i^{\frac{p-2}{p}} \right) \right] \quad (4)$$

where N_0 comes from the initial yield stress σ_0 ; D and p are material constants in the Cowper-Symonds power law :

$$\sigma = \sigma_0 \left[1 + \left(\frac{\dot{\epsilon}}{D} \right)^{1/p} \right] \quad (5)$$

3. Design and Numerical Evaluation

Because the coupler must move through the expanded tube, the inner radius of the latter can be calculated by the size of the former. The DN300 of TUE220A, a standard tube used in France, chosen after comparison between the size of the coupler and the standard tubes was investigated. The DN300 has the outer diameter of 323.9mm and several different thickness gauges of 7.1mm, 8.0mm, 8.8mm, 10mm, and so on. The TUE220A is made of such material properties as Young's modulus of 210 GPa, Poisson's ratio of 0.3, the yielding stress of 220 MPa, the ultimate strength between 360 MPa and 500 MPa, and the elongation of 23%. A material model is defined from the above material properties for the finite element analysis and the theoretical solution.

The radius of the expanded tube can be calculated using the material elongation and the size of the coupler. In the theoretical model of the tube, the circumferential elongation can be defined as follows :

$$\Lambda = \frac{r_o}{r_i} - 1 \quad (6)$$

In this study, the radius of the expanded tube is designed to be 190.8mm for the circumferential elongation of 20.5%. To reduce the degree of freedom in design, the die angle α is fixed as 30°. From the die angle and the radius of the expanded tube, the die length c is calculated as 64.8mm. The effects of the die angle will be discussed in the next section. The impact velocity is defined as 30m/s. Because the frictional coefficient

is very difficult to define exactly, it is assumed as 0.1 in this study. The frictional effects on pushing load will be discussed in the next section. The design guideline of TGV indicates that a dynamic pushing force is smaller than 1500kN.

With the design variables defined as $\sigma_0=0.36\text{kN/mm}^2$, $v=30\text{m/s}$, $\mu=0.1$, $\alpha=30^\circ$, $F=1500\text{kN}$, $c=64.8\text{mm}$, $r_i=158.4\text{mm}$ and $r_o=190.8\text{mm}$, the wall gauge of the tube is calculated as 7.34mm from the equation (2). Since it is important to use a standard tube in order to reduce the cost of energy absorber, a tube with the thickness of 7.1mm was selected from the DN300. For the designed tube, the theoretical solution gives the pushing load of 1450.9 kN, where the strain rate coefficients are assumed as those of a typical mild steel, $p=5$, $D=0.0404$. To solve the same problem of tube expansion numerically, it is necessary to introduce a moving mass attached to the die and a structural damping coefficient. A mass of 1000kg and a structural damping coefficient of 0.01 are used here. 300 axi-symmetrical solid elements were used for the numerical solution using ABAQUS [5]. Figure 4 shows the ABAQUS result for the relation between the die distance and the reaction force at the fixed end. The small waves in the solution curve are caused by no smooth contact algorithm which uses a searching method from node to surface, that is, one way searching algorithm. It is possible to assume that the smooth solution could be obtained through the points between the peaks and the valleys of the numerical curve. In this study, the averaged values of two extremes are used for numerical evaluation. The numerical solution in Figure 4 has a maximum reaction force of 1635.5kN at about 150mm of the die displacement. This reaction force is about 11.2% higher than the theoretical pushing load. This difference is mainly caused by elastic wave effects of the dynamic problem considered in the numerical analysis but not considered in the theoretical approach. This is the reason that the maximum value of reaction forces should have a higher value than the pushing load of the die. However this result is acceptable for a first basic design step. The equivalent plastic strain is a little high (Figure 4, 29.1%) when compared with the elongation of the material, 23%. In order to obtain a detailed design, this problem must be improved using local stress analyses and experimental tests.

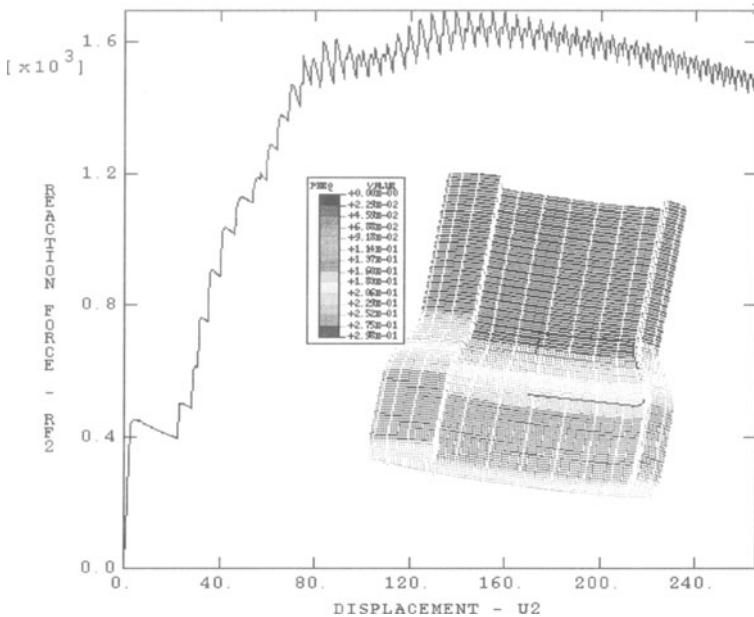


Figure 4. ABAQUS results of tube expansion problem

4. Parametric Study

For optimization and design modifications for the basic design, it is necessary to study the effects of several important design parameters. Furthermore, this parametric study can give useful information about quality control of the energy absorber and tolerance decisions of design parameters. Design parameters which are very sensitive to the energy absorbing performance must be controlled strictly. In this section, several parametric studies are performed for different velocities, frictional coefficients and die angles. Tab.1 summarizes the theoretical solutions and the ABAQUS results (axi-symmetric shell and solid elements) for two different velocities (0, 30m/s), and two different frictional coefficients (0.0, 0.2).

Table 1. ABAQUS results (FE) and comparison to the theoretical solution (Th)

FE model	Ele. #	μ	v (m/s)	F(Th) kN	F(FE) kN	Elong. (Th)	Elong.(FE)
axi-shell	100	0	0	546.65	583.2	0.205	0.21
axi-shell	100	0	30	1189.55	1384.5	0.205	0.21
axi-shell	100	0.2	0	787.0	796.6	0.205	0.21
axi-shell	100	0.2	30	1712.2	1914.0	0.205	0.21
axi-solid	300	0.2	0	-	804.45	0.205	0.295
axi-solid	300	0.2	30	-	1903.5	0.205	0.302

In the static problems, the theoretical solutions and the ABAQUS results are in good agreement within 6% difference. However, in the dynamic problems, the elastic wave due to impact may give some effects on the reaction forces because the impact velocity (30m/s) is not negligible. Two results indicate maximum 14% difference in the dynamic problem. By the way, since the numerical results show a consistent trend that they are higher than the theoretical solutions by about 10% differences, the theoretical approach can be effectively used for a basic design.

With the theoretical solution of the equation (2), the reaction forces can be investigated for changes of impact velocities, frictional coefficients and die angles. The relations between the impact velocities and the reaction forces for different frictional coefficients are displayed in Figure 5. The impact velocity gives a great effect on the reaction force of the fixed end at relatively low speed (0-8m/s). Figure 6 shows the relations between the die angles and the reaction forces for different frictional coefficients. The die angle gives a little influence on the reaction force at low frictional contacts.

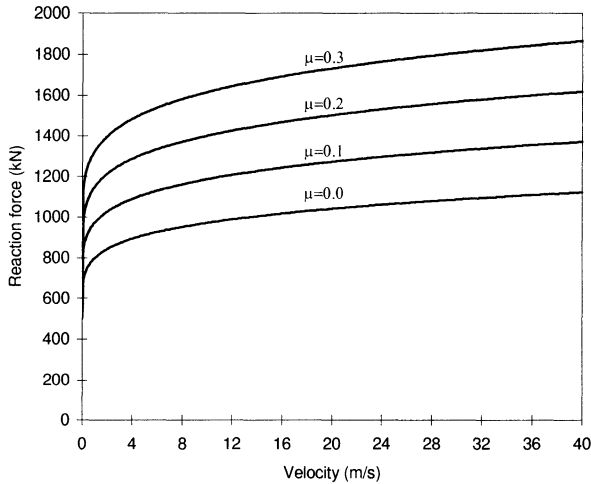


Figure 5. Relations between impact velocities and reaction forces for different frictional coefficients

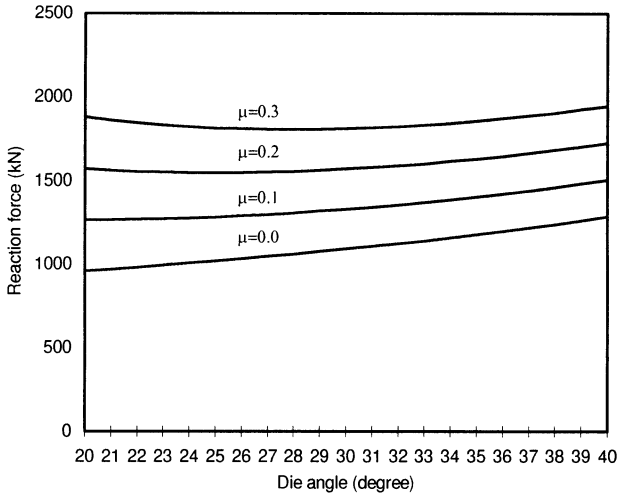


Figure 6. Relations between die angles and reaction forces for different frictional coefficients

5. Conclusions

The theoretical solution of tube expansion has been developed and verified by the finite element solutions using ABAQUS. It is found that reasonable results can be obtained using the theoretical approach. A basic design of energy absorber of the coupler using the concept of tube expansion has been suggested from the theoretical solution, and evaluated by ABAQUS. The suggested design showed a reasonable result as a basic design. However, this design must be improved with the aid of experimental tests in the detailed design step.

References

1. Scholes, D. and Lewis, J. H.: Development of crashworthiness for railway vehicle structures, *Proc. Int. Mech. Engrs.* **207** (1993), 1-16.
2. Thorton, H., Mahmood, H. F. and Magee, C. L.: *Energy absorption by structural collapse*, Structural Crashworthiness edited by N. Jones and T. Wierzbicki, (1983), 96-117.
3. PAM-SYSTEM, *User's Manual*, ESI International, 1996.
4. Al-Hassani, T. S., Johnson, W. W. and Lowe, T.: Characteristics of inversion tubes under axial loading, *J. Mechanical Engineering Science* **14** (1972), 370-381.
5. ABAQUS/Standard, Version 5.7, *User's Manual*, HKS inc., 1997.

GLOBAL NUMERICAL MODEL OF AUTOMOBILE GEARBOXES

A. BOURDON, K. YAKHOU, D. PLAY

Laboratoire de Conception et d'Analyse des Systèmes Mécaniques

INSA de Lyon - Bât 113

20, avenue Albert Einstein,

69621 Villeurbanne Cedex

FRANCE

Abstract

This paper describes a dynamic model for gear transmissions acting around a static working point, and taking into account the complete mechanical components. Gearbox casing behavior is introduced by using substructure analysis, and a tangent stiffness matrix could be defined for each roller body bearing element. This model is used to study the dynamic behaviour of an automobile gearbox. The first studies highlight the influence of the roller bearings on the dynamic behaviour of the kinematic chain and show that the bearings have to be modelled accurately. In a second step, the flexible casing of the gearbox is taken into account and dynamic couplings between deformations of the casing and the kinematic chain are evaluated. As a result of these works, global dynamic behaviour of automobile gearboxes can be provided and consequences of technological choices could be evaluated.

1. Main Principle and Hypothesis

1.1. INTRODUCTION

Mechanical system behaviours have to be defined early in the design process since prototype tests and development times must be reduced. Therefore, numerical models and computation tools have to be developed in view of predicting these global behaviours. Thus, both mechanical behaviour rules and Product Design evolving constraints must be included with the proposed global model. Actually, the matter is to get "downward multileveled" models, which are easily adaptable to geometry enrichments. The aim of this paper is to present such numerical models, allowing both static and dynamic simulations of global gearbox behaviours, in order to improve their performances in terms of power transmissibility and noise levels. Such power transmission mechanisms are made of both "structural elements" – shafts, casing etc – with linear elastic behaviour and "technological linking components" – rolling bearings,

gears, etc – with non-linear behaviour. Thus, numerical models built to study their global behaviour have to take into account those elements as a whole.

In gear transmissions, vibratory studies aim at understanding how vibrations and noise are generated and propagated. It is common to consider the case of small linear perturbations about a static constant load, and to evaluate the vibratory behaviour around the associated equilibrium point -fig.1-. In such models, behaviour of the technological components such as gears and bearings is linearized and meshing acts without contact loss. System components are divided into structural elements modelled by standard finite elements, and linking elements for which specific models were developed.

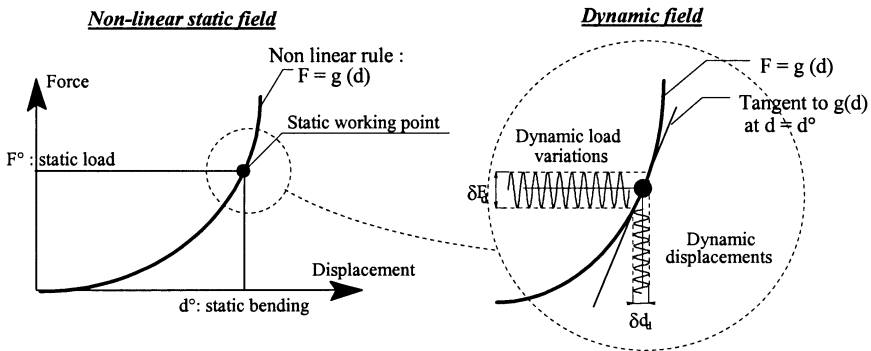


Figure.1 : Static and dynamic field positions.

1.2. DEFINITION OF A STATIC WORKING POINT

Studies performed for several years on complex mechanisms, led to the development of global static models with high performance and which incorporate non-linear components of the gearbox. Particularly, some specific finite elements were developed for modelling static behaviour of rolling bearings [10, 6, 12]. These new elements take into account the non-linear contacts between each rolling body – ball or roller – and inner and outer races [5]. Over and above the static results brought by this model – contact angles under load, casing stress and load distribution ... –, these specific elements allow to associate a tangent stiffness matrix to each rolling element. This matrix is representative of rolling element behaviour around one static working point (Fig.1). Practically, it is a way to "linearize" the non-linear behaviour of the bearings.

1.3. DEFINITION OF DYNAMIC MODELS AND TOOLS FOR ANALYSIS

1.3.1. Structural Elements

Shafts are modelled by standard Timoshenko beams and casing "dynamic flexibility is introduced by "macro-elements" obtained by dynamic substructures analysis [9]. For non-structural elements, mass and inertia effects are introduced by standard condensed elements.

1.3.2. Gear elements

Some previous work [1,2] showed that for global static studies, the mesh interface of the cylindrical helical gears can be modelled by unidirectional springs at the pitch point along the pressure line. The value of this spring depends on the static load, and it can be assessed numerically [1,8,11]. In automobile gearboxes, cylindrical pinions and wheels can be assumed to be rigid bodies except in the contact area. Then specific elements connecting a node of the driving shaft to a node of the driven shaft were developed.

1.3.3. Bearing elements

Bearings are modelled by the tangent stiffness matrices obtained during the static computation step. For each rolling body, the computed 10×10 full matrix connects an outer ring node to the corresponding inner ring node; of course, axial rotational degrees of freedom (d.o.f.) of the bearing are not concerned. This matrix takes into account the bearing geometry, and the flexibility of rings, shafts and housing.

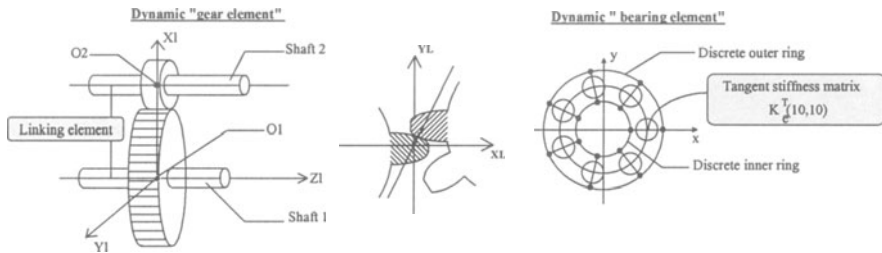


Figure 2 : Dynamic model of linking elements.

1.3.4. Definition of numerical tools for analysis

As a first step, dynamic studies focused on the eigenmodes of the model in order to evaluate the degree of precision to give to each numerical component, and to estimate the influence of the various technological components on the global dynamic behaviour of the gearbox. To do that, appropriate analysis tools and numerical criteria are defined.

The first one is the M.A.C. (Modal Assurance Criterion) matrix, also called modal correlation matrix. It is often used to compare two sets of eigenvectors Y_1 and Y_2 – for instance in numerical and experimental updating procedures –. This matrix allows to quantify the correlation between two vectors with a single percentage number.

Let : $Y^1 = [y_1^1 \dots y_k^1 \dots y_{N_1}^1]$ be the first set of eigenvectors
 and $Y^2 = [y_1^2 \dots y_k^2 \dots y_{N_2}^2]$ be the second set of eigenvectors

The MAC matrix associated to the former set of vectors is defined by :

$$(MA C)_{i,j} = \frac{|^T(y_i^1) \cdot (y_j^2)|^2}{\|y_i^1\|^2 \|y_j^2\|^2} \quad (1)$$

In order to make them more legible and easier to interpret, the MAC matrices are subsequently figured in a two dimension form with a color map scale.

The second numerical tool used is the modal energy analysis of eigenmodes. This energy sharing gives an evaluation of the various elements influences on modal shapes of the system [9, 7, 3].

2. Studies of the gearbox kinematic chain

2.1. MODEL

The following dynamic analysis were performed on a five speed medium size automobile gearbox. The technological arrangement and details of this gearbox are shown in figure 3. The input power is applied on the right end of the primary shaft supported by two tapered roller bearings noted B₁₁ and B₁₂. This shaft transmits power to the intermediate shaft through one of the 5 cylindrical gears labelled G₁ to G₅ which act independently according to the desired speed ratio. The reverse speed gear is not considered in this presentation. The intermediate shaft is supported by a ball bearing labelled B₂₁ and a cylindrical roller bearing noted B₂₂. Power is transmitted to the output shaft through cylindrical gear G_{out}, which is always in mesh. This shaft is supported by two taper rolling bearings labelled B₃₁ and B₃₂. The output shaft is constituted by a differential system which is not active in this study, and so is ignored.

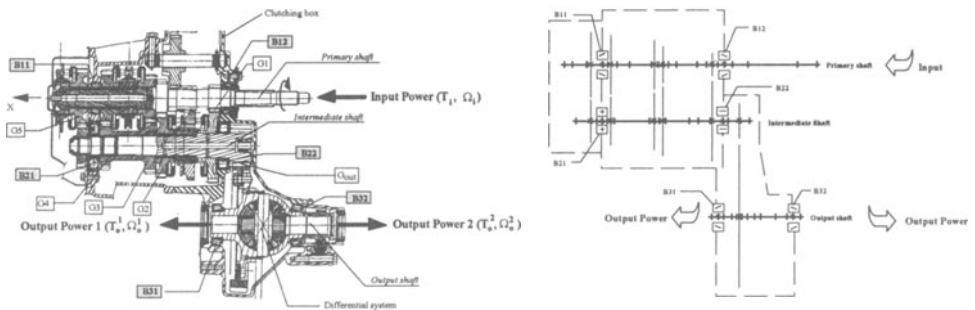


Figure. 3 : Technological arrangement and kinematic chain model of the studied gearbox.

In a first step, the casing dynamic behaviour is not considered and the outer rings of rolling bearings are fixed. The static working point is calculated for a given gear ratio and a given loading torque applied on the "right side" of the primary shaft. The axial rotational degree of freedom of the end nodes of the output shaft are fixed.

2.2. INFLUENCE OF THE ROLLING BEARINGS

Earlier work has revealed the importance of rolling bearings in the global dynamic behaviour of gear transmission [1,10]. The following diagram shows the percentage of potential modal energy in the rolling bearings for the first 19 eigenmodes <math>< 2600\text{ Hz}</math> - of the kinematic chain of the gearbox described above.

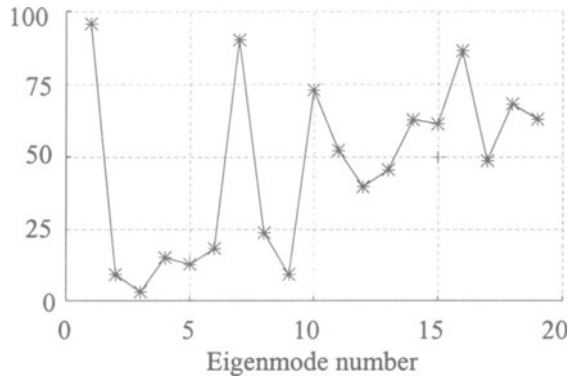


Figure.4 : Percentage of potential modal energy in bearing elements for the third speed ratio.

For the largest part of the eigenmodes, at least 45% of the strain energy is located in the rolling bearings (Fig. 4.). This large contribution of the bearings to the deformation of the kinematics chain implies that the bearings are properly modelled. In order to quantify the degree of precision to give to this modelling, comparative studies were performed with various modelling choices. It appeared that the use of purely unidirectional stiffness elements (model n°2) is insufficient to describe properly the global dynamic behaviour of the mechanical system. Indeed, the eigenmodes computed with scalar stiffnesses (model 2) are different from those computed with full tangent stiffness matrices (model1) : the frequency distributions are quite different (Fig.5a) and the eigenvectors are not collinear (Fig.5b).

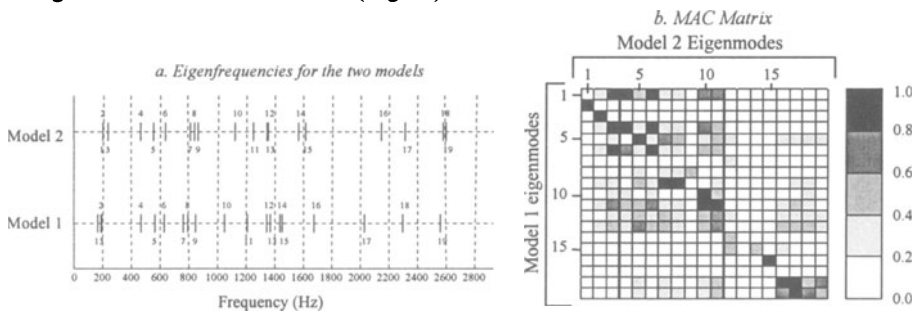


Fig.5 : Comparison of the eigenmodes computed for two numerical models of bearing

These differences can be explained by the fact that the couplings between the 5 d.o.f. of the rolling bearings are not taken into consideration by scalar stiffness elements. From the strain energy point of view, the eigenmodes which are energetic for the bearings

have lower frequencies in model 2 than in model 1. All these noteworthy differences could make the use of modal or pseudo-modal methods inconvenient for computing mechanism dynamic responses if the bearings are not accurately modelled.

An earlier work [5] has shown the influence of the real static environment of the bearing on the static results. It appears here, that the use of global static models to compute the tangent stiffness matrices rather than local models with rigid environment, changes significantly the dynamic results.

2.3. INFLUENCE OF THE MEAN VALUE OF THE MESHING STIFFNESS

As mentioned previously, the meshing is modelled by a scalar constant spring whose value corresponds to the mean meshing stiffness which can be accurately estimated with finite element methods [11, 7]. Some previous work – not detailed here – has shown that, for values in the range of $5 \cdot 10^8$ N.m to 10^{13} N.m, the modal results remain unchanged: frequency variations lower than 5% and MAC criterion very close to 1. The use of lower values leads to a significant decrease of eigenfrequencies and to the modification of eigenvectors. From the energy point of view, the decreasing of meshing stiffness leads to the appearing of modes energetic for the gears. However, the global behaviour of the model is less sensitive to the mean meshing stiffness value than it is to the rolling bearing modelling options discussed above.

3. Dynamic Influence of the Casing

3.1. PRINCIPLE

The dynamic influence of the casing is introduced into the earlier model by mass and stiffness matrices obtained by dynamic substructures analysis [9]. A large casing dynamic model – about 100 000 d.o.f - is reduced and only 672 d.o.f. are kept. The first 19 eigenmodes of the casing with fixed junction d.o.f. are used to reduce the initial casing model to a smaller one. The former kinematic chain is assembled to the reduced casing model by using the rolling body stiffness matrices defined earlier.

3.2. DYNAMIC COUPLINGS BETWEEN CASING AND KINEMATIC CHAIN

Computation of the eigenmodes of the complete model shows that modal density is important such as there are 30 modes with eigenfrequencies below 1.400 Hz. The modal energy analysis performed on these eigenmodes – Fig.6 –, consists of computing, for each one, the percentage of strain energy located in the casing and in the kinematic chain.

This analysis shows the couplings between the modal deformations of kinematic chain and casing. Indeed, for each eigenmodes at least 10% of the strain energy are located in the casing, and there is no eigenmode of the kinematic chain alone. On the other hand, there are some "casing modes" where the whole strain energy is located in the casing as mode 3 for instance.

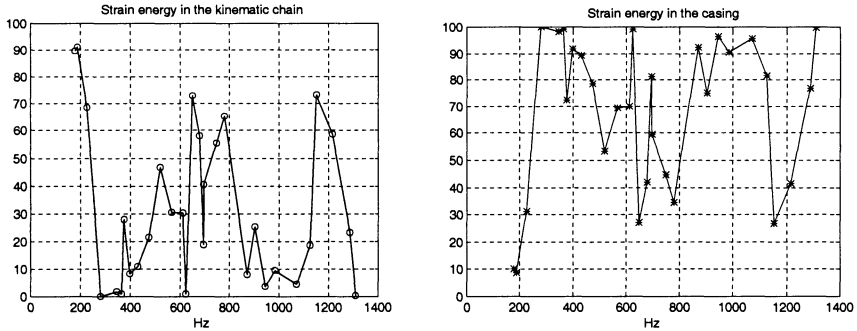


Figure.6 : Percentage of strain energy in function of the frequency in the kinematic chain and in the casing.

4. Conclusion

The aim of this paper, was to present a global numerical dynamic model of automobile gearboxes in a CAD environment. This model was performed in order to reduce noise and define dynamic transmission conditions. The dynamic behaviour is evaluated around of a static working point, defined for a given static load, where non-linear behaviour of the technological linking components can be linearized. Practically, the proposed model is based on the finite element method (F.E.M.) for small displacements. Structural elements are modelled by usual finite elements and several specific finite elements were developed to introduce the behaviour of the technological linking components. A particular attention was brought to rolling bearing behaviour. This model allows to determine eigenmodes and dynamic responses of the complete gearbox and appropriated analysis tools and numerical criterion were defined.

The first studies presented are achieved on the kinematic chain of the gearbox. They highlight the influence of the roller bearing on the global behaviour, and so how important it is to model them accurately. In a second step, casing dynamic flexibility is introduced and dynamic couplings between casing and kinematic chain are evaluated. At the end of this work, which is validating by experimental studies, global dynamic behaviour of automobile gearboxes can be provided and consequences of technological choices could be evaluated.

Acknowledgments

Part of this work has been financed by contracts with PSA Peugeot Citroën. The authors wish to thank their industrial collaborators for their numerous helpful comments, and the researcher of the CASM Laboratory at INSA Lyon (France) for their valuable contribution to this work.

References

1. C. BARD. "Modélisation du comportement dynamique des transmissions par engrenages", Thèse de doctorat en mécanique, INSA de Lyon, 1995.
2. Blankenship, G., Singh, R., 1992, "A comparative study of selected gear mesh interface dynamic models," Proceeding *International Power Transmission and Gearing Conference*, DE-Vol. 43-1 A.S.M.E, Phoenix, 1992, Vol. 1 pp137-146.
3. A. BOURDON, J.F. RIGAL, D. PLAY. "Numerical Modal Result Processing using CAD, for analysing the global vibrating behavior of gearboxes". International Congress Gear Transmissions '95, Iftomm-Europeans, Sophia, 1995, pp. 104-110.
4. A. BOURDON. "Modélisation dynamique globale des boîtes de vitesses automobile", Thèse de Doctorat en mécanique, INSA de Lyon, 1997.
5. A. BOURDON, J. F. RIGAL, D. PLAY. "Static rolling bearing models in C.A.D. environment for the study of complex mechanisms, Part I - Rolling bearing model, Part II - Complete assembly model". *Transaction of ASME Journal of Tribology*", April 99, vol. 121, pp205-214, pp215-223
6. I.S. CHOI. "Simulation des mécanismes complexes en C.M.A.O. Etude des non-linéarités de comportement", Thèse de doctorat en mécanique, INSA de Lyon, 1993.
7. A. GIRARD, J. CHATELAIN, J. ROY. "Efficient sensitivity analysis of frequency response function", Intespace, IMAC, San Diego (USA), 1993.
8. M. GUINGAND, J.P. de VAUJANY, D. PLAY, "Conception, optimisation et représentation C.A.O. d'engrenages cylindriques. Integrated Design and Manufacturing in Mechanical Engineering.", I.D.M.M.E.'96, Nantes (France), April 1996, pp. 15-17.
9. J.F. IMBERT. "Analyse des structures par éléments finis", Ecole Nationale Supérieure de l'Aéronautique et de l'Espace, Cepadues Editions, Toulouse, 1979, p 480.
10. T.C. LIM, R. SINGH. "Vibration transmission through rolling element bearings. Part I : Bearing stiffness formulation; Part II : System studies; Part III : Gear rotor system studies.", *Journal of Sound and Vibrations*, , Vol. 139, n° 2, pp. 179-199; pp. 201-225, 1990. Vol. 151, n° 2, pp. 31-54, 1991.
11. A.A. OLAKOREDE, D. PLAY. "Development of the finite prism method in computer aided design of spur gear.", Proceedings of the fourth SAS world Conf. FEMCAD, Paris, Oct 1988, pp. 17-79. IITT-International, Vol. 1, 1988, pp.384-391.
12. J.F. RIGAL "Le comportement global des mécanismes en Conception Assistée par ordinateurs", Habilitation à diriger des recherches en sciences, spécialité mécanique, INSA de Lyon, 1994.
13. J.F. RIGAL, A. KARAM, D. PLAY, G. LENEVEU. "Analysis of a complex mechanical system in Computer Aided Design. Application to an automobile gearbox", International Gearing Conference University of Newcastle upon Tyne, England, 1994, pp. 207-211.

SMART MATERIALS DESIGN: THE MECHATRONIC APPROACH.

C.DELEBARRE*, D.COUELLIER and E.DELACOURT***.**

* IEMN-DOAE UMR CNRS N° 9929

** LAMIH-GM URA CNRS 1775

*** ENSIMEV

Université de Valenciennes- le Mont Houy - BP 311 - 59304 Valenciennes Cedex. France.
christophe.delebarre@univ-valenciennes.fr

1. INTRODUCTION.

In order to increase security, to reduce delays of airplane maintenance and to lower the repair costs, integrated monitoring could be envisaged in a permanent or semi-permanent way, for the evaluation of the degradation state of composite structures. This could furnish information about damage state.

The embedment of sensors within composite structures gives the opportunity to develop Smart Materials for Health and Usage Monitoring Systems (HUMS).

The choice of the monitoring system must be guided by the respect of the material integrity through its ability to receive sensitive sensors. In particular, the loss of mechanical properties and/or failure strength due to the presence of the insert must be minimized. Another selection criterion of the system is the reduction of the sensor number for different imperatives: cost, connectors reduction and complexity of the electronic equipment. Because they can propagate over long distances, Lamb waves are totally adapted to the inspection of large, thin plates with a very small number of transducers. These waves are usually generated by mode conversion at the interface using an angled transducer. This method of excitation, generally known as the "wedge method", requires a transducer with a plastic or perspex body providing the suitable angle of incidence. This body makes it impossible to significantly reduce the height of the transducer. The interest in Smart Materials, especially health monitoring and impact damage detection on composite laminates using Lamb waves, justifies the development of a thin transducer which may be integrated into the structure. Hence, the priority is to reduce the height of the transducer, and the use of a comb-like array of piezoelectric elements makes it feasible.[DEM.95]

Longitudinal, transverse and Rayleigh waves are the solution of the waves propagation equation in infinite solid elastic media. On the contrary, Lamb waves are the solution of this equation for limited media, and they must verify the limit conditions fixed by the medium dimensions.

These waves may propagate in plates with a thickness value nearly equivalent to the wavelength, and are generated under oblique incidence using a conversion mode. There are mainly two kinds of waves, antisymmetrical and symmetrical, with a propagation direction parallel to the surface of the plate. Their associated displacement presents a longitudinal and transverse components. Two zero modes, A_0 and S_0 , exist at all frequencies, but higher modes had switch frequencies f_c given by the following formulae:

for symmetrical modes:

$$f_c = n v_l / 2 e \quad \text{where } n = 1,3,5,\dots$$

$$\text{and } f_c = n v_t / 2 e \quad \text{where } n = 2, 4, 6,\dots$$

for antisymmetrical modes :

$$f_c = n v_l / 2 e \quad \text{where } n = 1,3,5,\dots$$

$$\text{and } f_c = n v_t / 2 e \quad \text{where } n=2,4,\dots$$

where v_l is the longitudinal velocity, v_t the transverse velocity and e the sample thickness. As the velocity of the different modes depends on the frequency, Lamb waves have a dispersive feature. The usual method of generation relying on a transducer that cannot be reduced to a low thickness (oblique incidence transducer), so the development of a thin transducer using a comb-like array of piezoelectric elements has been investigated.

The integrated design process of Smart Materials needs first of all a good understanding of the Lamb waves propagation conditions inside the plate structures as a function of their thickness. From these conditions it is possible to define the working frequency. This parameter, thus defined, it is then possible to study the optimal dimensions of the piezoelectric element to embed in order to generate non dispersive waves.

The study of the sensor dimensions involves constraints on the embedded PZT element which induce a mechanical behaviour of the structure with the insert which must be optimized. So three different tools have been used in this work to optimize the final performances in terms of sensibility to impact detection of the demonstrator. The following paragraphs give, after a short description of the design methodology, the different results leading to the definition of a composite structure with embedded actuators for impact detection.

2. DESIGN METHODOLOGY.

The development of miniaturized actuators for defect and impact detection involves an integrated design methodology taking into account the study of :

- the Lamb waves propagation,
- the insert vibration modes,
- the mechanical behaviour of the structure with embedded insert.

The following figure (fig 1) describes the different studies realized in order to perform a demonstrator proving the feasibility of a Health and Usage Monitoring System.

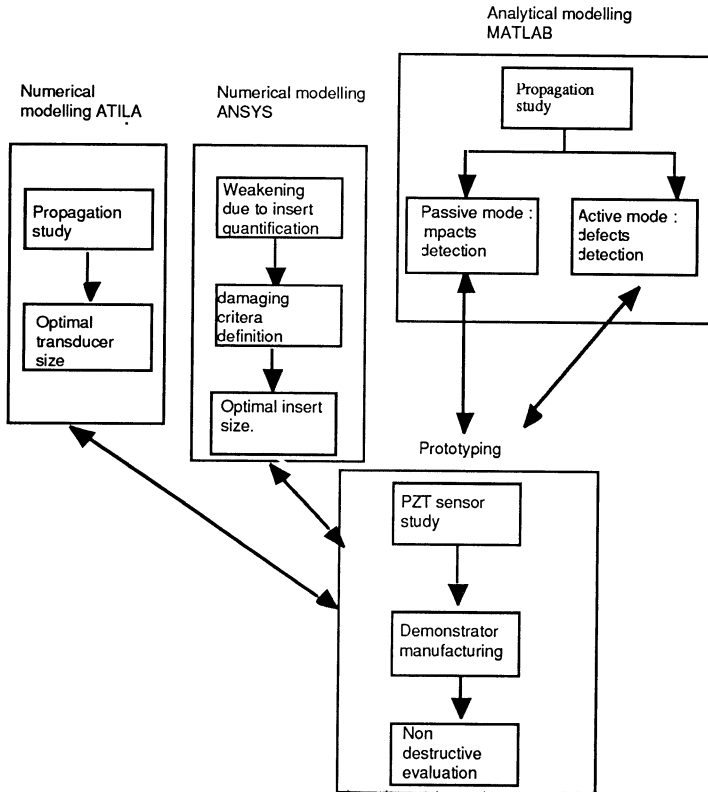


Fig.1: integrated design methodology for Smart Materials.

Three kinds of modeling have been investigated: an analytical one for Lamb waves propagation study (MATLAB®), and numerical ones (Finite Element Codes) for the study of mechanical behaviour of the structure (ANSYS®), and for the study of the insert (ATILA®). The theoretical results lead to the definition of geometrical parameters for the demonstrator prototyping.

Lamb waves propagation requires a deep understanding of the dispersion relations in the material, in order to determine the geometrical parameters of the insert for a set of frequencies, the following paragraph gives the main results concerning this study.

2.1 ANALYTICAL MODELING.

The first method of excitation, already described by Viktorov [VIK.67] as the comb structure method, consists in generating a set of normal perturbations, distributed periodically over the surface of the plate with a spatial period equal to the excited Lamb wavelength. To determine the geometrical parameters of the sensor, the first task to complete is to calculate the appropriate wavelength, corresponding to the less dispersive mode in the material at the working frequency.

The carbon-epoxy composite plates used in this study have 16 and 32 layers. The ply lay-ups for these laminates are $[0_{32}]$, $[0_2/90_2/0_2/90_2]_S$, $[45_2/0_2/-45_2/90_2]_{2S}$ and $[45/0/-45/90]_{4S}$.

An extensive literature on methods to calculate the dispersion relations in anisotropic media is available (Nayfeh [NAY.89a], Nayfeh and Chimenti [NAY.89b], Datta, Shah, Bratton and Chakraborty [DAT.88], Lowe [LOW.95],...). But few papers take the disparities in mechanical properties between layers into account and develop the calculations for every lay-up.

This study relies on the classical method, i.e. the resolution of a matrix equation which describes stresses and displacements in each layer of the laminate and the transfer relations between them. This equation leads to characteristic functions whose roots bring the results. Discussions of the different methods may be found in [LOW.95].

The standard dispersion curves (phase velocities as a function of the frequency-thickness product) show the less dispersive mode likely to be generated in a frequency range. Figure 2 shows these curves for the same sample.

These curves allow the determination of the frequency for the generation of Lamb waves in a specific plate. As soon as the frequency range is imposed by the piezoelectric element, the following modeling will permit to define the transducer's geometrical parameters.

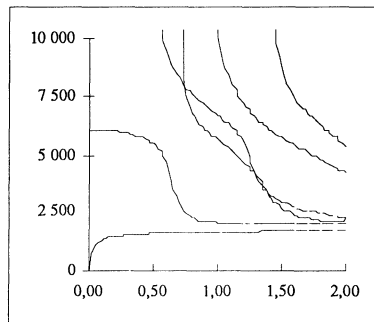


Fig 2: phase velocity as a function of frequency for a laminate

2.2 NUMERICAL MODELING.

2.2.1 Brief description of the Finite Element Modeling (FEM) approach.

In order to determine the optimal dimensions of the insert for Lamb waves generation, the linear FEM has been used here with the help of the ATILA code. The FEM is a very powerful tool for modeling complex structures. It is able to provide the electrical impedance and the displacement field, as a function of the excitation frequency.

The general formulation of finite element transducer modeling is described in many papers [ASS.93,ASS96] and only the main equations are briefly recalled here. With standard notations :

$$\begin{bmatrix} [K_{uu} - \omega^2 [M]] & [K_{u\phi}] \\ [K_{u\phi}]^T & [K_{\phi\phi}]^T \end{bmatrix} \begin{bmatrix} \underline{U} \\ \underline{\Phi} \end{bmatrix} = \begin{bmatrix} \underline{F} \\ -\underline{Q} \end{bmatrix} \quad (1)$$

where \underline{U} , $\underline{\Phi}$, \underline{F} and \underline{Q} are vectors which contain the nodal values of the mechanical displacement, the electrical potential, the applied forces and the electrical charges, respectively. $[K_{uu}]$, $[K_{u\phi}]$ and $[K_{\phi\phi}]$ are the electroelastic stiffness matrices, while $[M]$ is the consistent mass matrix and ω is the angular frequency ($\omega = 2\pi f$, f being the frequency). The upper index T indicates matrix transposition.

From this matrix, the displacement field \underline{U} can be computed as follows:

$$[[\bar{K}_{uu}] - \omega^2 [M]] \underline{U} = -\bar{K}_{u\phi} \Phi_0 \quad (2)$$

Then using the second line together with Eq. (2) the electrical impedance (Z) can be deduced from the following relation :

$$\frac{1}{Z} = -j\omega \left(\bar{K}_{\phi\phi} - \bar{K}_{u\phi}^T [[\bar{K}_{uu}] - \omega^2 [M]]^{-1} \bar{K}_{u\phi} \right) \quad (3)$$

Minima and maxima of this impedance correspond respectively to resonance and antiresonance frequencies (f_r and f_a) of the successive vibration modes. The electromechanical coupling coefficient k_e is then defined for each mode as :²⁰

$$k_e = \sqrt{1 - (f_r/f_a)^2} \quad (4)$$

Finally, it can be noticed that it is possible to take into account losses in the material, by introducing complex material coefficients such as : $s = s' - j s''$, $d = d' - j d''$, $\epsilon = \epsilon' - j \epsilon''$, where s , d and ϵ are the complex elastic compliance tensor, the complex piezoelectric tensor and the complex dielectric tensor, respectively.

2.2.2 Embedded transducer characterization.

A general rule of ultrasound emission is to excite the emitting element at its natural resonances rather than at any frequency. This method enables a very efficient conversion from electric to mechanical energy. Electrical impedance as a function of frequency is a suitable indicator of those resonance modes.

It is now supposed that a transducer is embedded into a composite plate. This plate is a 32-ply [0₄, 45₄, 90₄, -45₄]_S 'T300-914' composite plate with a 3.85 mm thickness. The transducer is shown in Fig. 3(a). It is a 'P7-62' (a classical 'Quartz & Silice' piezoelectric ceramic) PZT cylinder with radius to thickness ratio R/T equal to 1.25 and $T = 2$ mm. As its polarization direction is assumed to correspond to the Z-axis, this one is a revolution axis, as it is well known for PZT materials (equivalent to 6mm crystalline class). Thus only a two-dimensional finite element mesh of the ABA'B' section may be used [Fig. 3(b)].

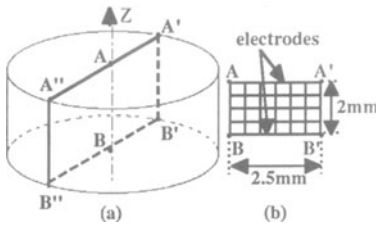


Fig. 3: Transducer

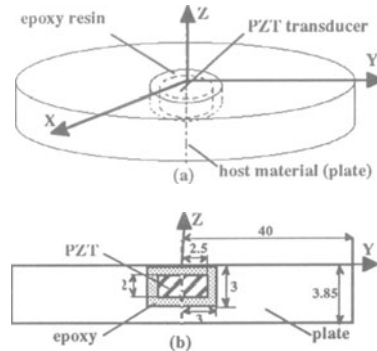


Fig. 4: Modeled configuration.

Figure 4 shows the modeled configuration. The PZT transducer is placed inside a hole machined in the plate and surrounded by epoxy resin.

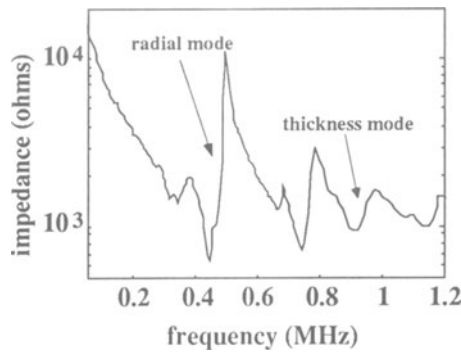


Fig. 5: electrical impedance.

Using Eq. (3), the electrical impedance of the transducer is computed and shown in Fig. 5. From this figure, it is evident that there are three main resonance modes. The resonance frequencies correspond to natural vibration modes of the transducer, but modified by the influence of the acoustical loading conditions (embedding). It is noticeable that, according to the computed strain field in the piezo-element, the resonance which occurs around 435 kHz appears to remain a radial vibration, with the highest coupling coefficient yet ($k_e = 47\%$). Thus the effect of embedding on the radial eigenmode of the piezo-ceramic does not seem to be a change in its nature, but only a slight frequency shift and a variation in the electrical impedance modulus, due to the non-zero acoustical impedances of the surrounding media.

2.2.3 Modes identification

The deformed shape of the structure, that the FEM is able to display in post-processing treatment, clearly puts in evidence the presence of plate vibration modes at various frequencies. As an example, the real part of the normalized displacement fields computed at the three main resonance frequencies (435 kHz, 735 kHz and 910 kHz) are given in Fig. 6 (for convenience, only the displacement fields in the plate are represented). It is clear that Fig. 6(a) corresponds to a “purely” symmetrical displacement field, whereas Figs. 6(b) and 6(c) correspond practically to antisymmetrical displacement fields, but with slight interactions between several Lamb modes. Moreover, the amplitude of the displacement field for the first resonance (435 kHz) is greater than the other ones.

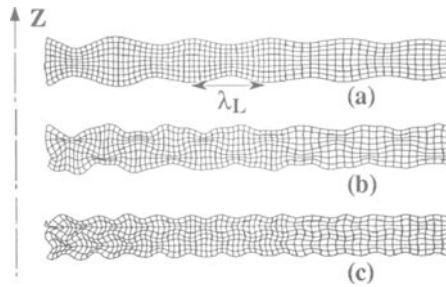


Fig. 6: Displacement field.

By the inspection of these computed displacement fields, it is possible to pick out the wavelength l_L of the corresponding Lamb waves. Then knowing the frequency, the phase velocity c_L can be determined, according to the relation : $c_L = l_L f$. Several finite element computations have been performed, varying the excitation frequency, and thus the corresponding phase velocities c_L are reported in the dispersion curves of the host material. A remarkable agreement is shown, allowing an unambiguous identification of modes present in the plate.

In this part a particular transducer has been considered, but it is interesting to note that other specimens having the same dimension ratios $2R/T$ and d/T (d is the host plate thickness) would generate the same Lamb waves (same phase velocities) at the same values of fd .

2.2.4 Mechanical behaviour modeling.

Due to the manufacturing cost of a composite plate, the mechanical behaviour of structure with embedded transducer will be studied using finite elements. Two models will be developed: The first corresponds to a plate without any embedded transducer and the second will represent a plate with embedded piezo-electric elements. In both cases, the numerical results obtained during a three point bending will be compared with experimental data. The model (Fig 7) represents the plate using a specific element for multilayer geometry. The element has been designed to represent multilayered materials (up to 100 layers with different mechanical features). A single element can represent the different layers of composite materials and the piezo-electric element.

The study has been carried out on the models of instrumented and non-instrumented plates during a three-point bending.

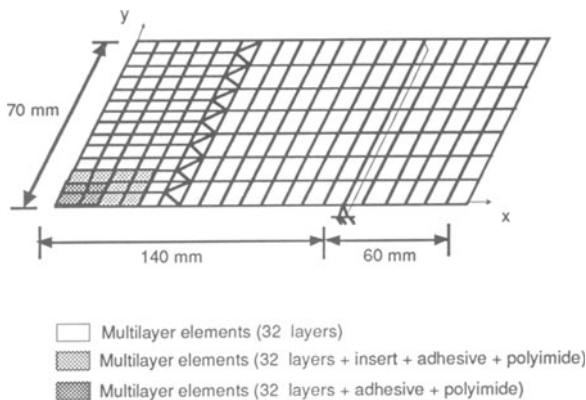


Fig.7: Numerical model of the plate with insert

The same load was applied onto the models of both instrumented and non-instrumented plates. A comparison between the different results highlights the fact that the built-in piezo-electric element does not influence the deformation of the plate. The results are described and discussed in [BLA.98].

The previous models have led to the definition of an innovative demonstrator prototyping. The next paragraph gives the experimental results obtained with an embedded PZT element inside a Carbon-Epoxy composite.

3. EXPERIMENTAL STUDY

3.1 CARBON-EPOXY COMPOSITE DEMONSTRATOR.

The demonstrator has been made in a classical way : a 130 μm -thick element has been embedded in the middle of the plate. It has however the advantage of putting the piezoelectric insert in acoustic load conditions which are close to those of an inter-ply integrated element. Moreover it allows easier experimentation while validating our approach.

The embedded transducer being used is a 10 mm square piezo-electric 130 μm -thick element . Two polyamide films (Fig 8) are stuck onto the element. Those films allow the electric connection with the outer media of the plate.

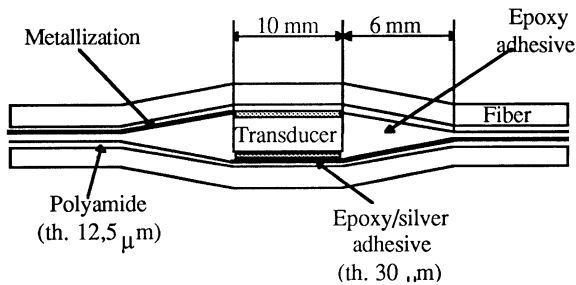


Fig. 8: Schematic description of the sensor

The dimensions of the considered piezoelectric transducer had been chosen as satisfying the following criteria. First of all, to have a good electromechanically coupling for vibration mode at 400 kHz, the corresponding radius is 2.5 mm for the P7-62 material (radial mode). Then a thickness of 2 mm has appeared to imply no interaction between the radial mode and the other vibration modes (thickness and harmonic modes) ; it is easy to embed in a 3.85 mm thick plate as well. In addition, the FEM has demonstrated that these transducer dimensions are suited to a good generation of Lamb waves in the host material. Therefore the same dimensions have been used to build the specimen studied in this section.

As it has been previously said, the composite plate of this instrumented specimen can be macroscopically considered as a quasi-isotropic material in the X-Y plane. Thus the surrounding conditions of the piezo-element are expected to be relatively close in both the experimental and the numerically modeled configurations. So this specimen aims both at confirming the results obtained with the FEM study, as well as checking the practical feasibility of using embedded transducers for generating exploitable Lamb waves in a relatively realistic composite structure.

4. CONCLUSION.

This work has demonstrated the feasibility of generating and detecting Lamb waves in a composite plate, with bulk-embedded piezoelectric transducers. Moreover, with the help of the FEM, the identification of modes has been obtained. By selecting the vibration mode of the embedded transducer, it seems to be possible to selectively privilege the propagation of various Lamb modes.

Future work will consist in the integration of the different theoretical results in a larger model describing both, the insert vibration modes and the Lamb waves propagation. The use of an Analog Hardware Description Language (AHDL) will allow the creation of mixed signal models, modeling both electrical and non-electrical components in complex systems as Smart Materials. The Mechatronics approach will permit quite an integrated design methodology.

The authors would like to thank Mr BALAGEAS from ONERA for helpful and precious advices.

REFERENCES

- [DEM.95] T.Demol, P.Blanquet and C.Delebarre, « *Lamb waves generation using a flat multi-element array device* ». 1995 IEEE International Ultrasonics symposium, 7-10 Nov 95, Seattle.
- [VIK.67] I.A. Viktorov, *Rayleigh an Lamb Waves*, New-York: Plenum Press, 1967
- [NAY.89a] A.H. Nayfeh, "The propagation of horizontally polarized shear waves in multilayered media", J. Acoust. Soc. Am., vol. 89, pp. 2007-2012, November 1989
- [NAY.89b] A.H. Nayfeh and D.E. Chimenti, "Free Wave Propagation in Plates of General Anisotropic Media", Journal of Applied Mechanics, vol. 56, pp. 881-886, December 1989
- [DAT.88] S.K. Datta, A.H. Shah, R.L. Bratton and T. Chakraborty, "Wave propagation in laminated composite plates", J. Acoust. Soc. Am., vol. 83, pp. 2020-2026, June 1988
- [LOW.95] M.J.S. Lowe, "Matrix Techniques for Modeling Ultrasonic Waves in Multilayered Media", IEEE Transactions on Ultrasonics, Ferroelectrics, and Frequency Control, vol. 42, pp. 525-542, July 1995
- [ASS.93] J. Assaad, C. Bruneel, J-N. Decarpigny and B. Nongaillard, "Electromechanical coupling coefficients and far-field radiation patterns of lithium niobate bars (Y-cut) used in high-frequency acoustical imaging and nondestructive testing", J. Acoust. Soc. Am., **94**, pp 2969-2978, (1993).
- [ASS.96] J. Assaad and C. Bruneel, "A physical interpretation of the far-field directivity pattern of lithium niobate bars (LiNbO₃)", J. Appl. Phys., **80**, pp 5489-5493, (1996).
- [BLA.98] Blanquet P, Delebarre C, Coutellier D, « *Development of numerical tools for the optimal design of a Smart Composite Structure* ». IDMMME98, May 27-29, Compiègne, France.

Chapter 2
COMPUTATIONAL MECHANICS AND OPTIMUM
DESIGN OF STRUCTURES

Machining optimization of quenched parts	77
A. ABISROR, F. CONGOURDEAU, G. MARIN, J.M. ROËLANDT AND N. VALLINO	
Optimization of a passive safety device by means of the response surface methodology	85
G. BELINGARDI and M. AVALLE	
Optimal design of mechanical components with genetic algorithms	93
L. GIRAUD and P. LAFON	
Design of materials with specific elastic properties using shape optimization method.....	101
SHUTIAN LIU, YUANXIAN GU and GENDONG CHENG	
Shape optimization and adaptativity of axisymmetrical shells undergoing geometric nonlinearities	109
H. NACEUR, S. TRIKI, J.L. BATOZ AND C. KNOPF-LENOIR	
Topological optimization of shells with non uniform thickness	117
E. PAGNACCO and J. E. SOUZA DE CURSI	
Non-deterministic methods for product/process analysis and robust design - the «possibilistic» approach.....	125
V. BRAIBANT, F. DELCROIX , A. OUDSHOORN and C. BOYER	
Design of an automatic topology/geometry optimization software.....	133
S. BEUZIT and A. HABBAL	

MACHINING OPTIMIZATION OF QUENCHED PARTS

Albert ABISROR*, Fabrice CONGOURDEAU*,
Gilles MARIN**, Jean-Marc ROELANDT**,
Nicolas VALLINO**

**AEROSPATIALE, Centre de Recherches Louis Blériot, 12 rue Pasteur, B.P. 76,
92152 Suresnes Cédex, France
e-mail: dcrml@siege.aerospatiale.fr*

***Département Génie des Systèmes Mécaniques, Université de Technologie de
Compiègne, LG2MS, UPRES A 6066, B.P. 20529,
60205 Compiègne Cédex France*

ABSTRACT

During machining of aluminium alloy made structural parts, the state of stress due to quenching may result in non-acceptable deformations. Besides calculating the post-quenching residual stresses, we develop a numerical method in order to simulate machining by using the mapped stress from the drop forging onto the final part mesh.

We then develop a 2D optimization program in order to minimize deformation during machining, depending on the final part position in the drop forging part.

Comparison between experimental and numerical results show a good correlation.

1. INTRODUCTION.

It is desirable that the heat treatment of aluminium alloy made parts should result in high strength and low residual stresses. However, during machining, these stresses may give rise to non-acceptable deformations.

In this work, a finite element method is used to simulate quenching and stress releasing during machining. Besides, we are developing a program in order to optimize the final part position during machining.

2. QUENCHING OF THE DROP FORGING PART.

In addition to structural transformations, stresses develop in the part during quenching. They result from the temperature gradient between center and surface. When they become higher than yield stress, residual stresses occur after heat treatment.

2. 1. Quenching modelisation.

The finite element modelisation of quenching is carried out in two stages:

- a/ simulation of heat conduction in the part during the quench cooling,
- b/ resolution of the elastic-plastic problem created by the change of temperature.

Figure 1 shows a 2D section of a drop forging part for which we have calculated quenching and machining. The 2D mesh, made with I-DEAS code, contains 612 four-node elements, and 711 nodes.

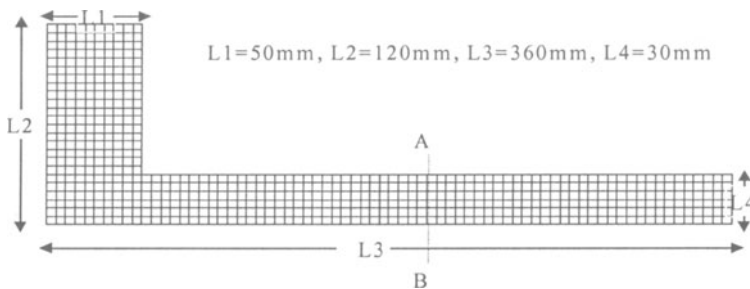


Figure 1 : Drop-forging mesh

2. 2. Thermal calculation.

The material is an aluminium alloy. The thermal conductivity and specific heat variations with temperature are shown in figures 2 and 3. For heat conduction calculations, we use DC2D4 elements from ABAQUS code. The initial temperature is about 400°C. A temperature versus time curve is prescribed on the mesh surface. The final temperature is about 60°C. At each time step, the temperature distribution is used as initial condition for the elastic-plastic computation.

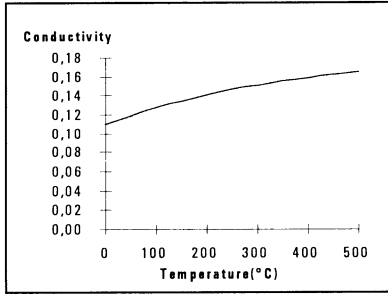


Figure 2 : Conductivity (W/mm.C°)

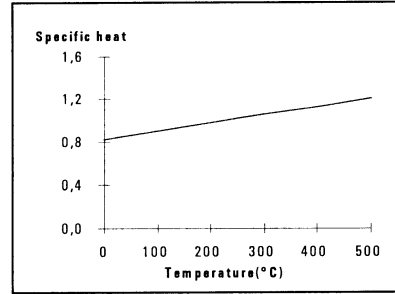


Figure 3 : Specific heat (J/g.°C)

2. 3. Mechanical calculation

We use CGPE6R generalized plane strain elements with reduced integration. The variations of mechanical parameters with temperature are taken into account: Young's modulus, plastic slope, yield stress [ARC. 80] (figures 4 to 6). The expansion coefficient evolution has been measured by AEROSPATIALE (figure 7).

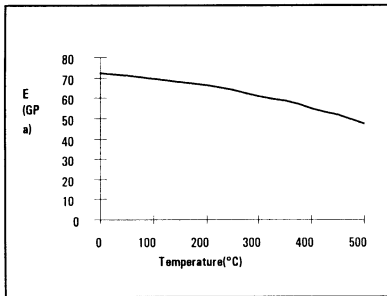


Figure 4 : Young's modulus

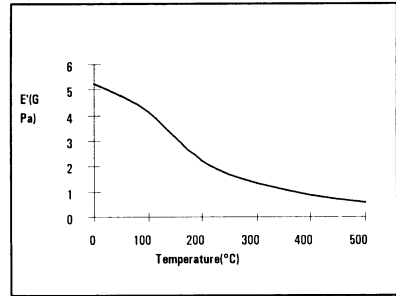


Figure 5 : Plastic slope

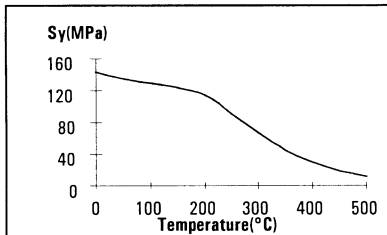


Figure 6 : Yield stress

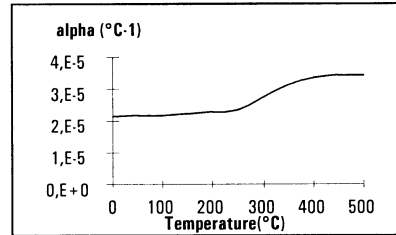


Figure 7 : Expansion coefficient

Comparison between X-ray measured residual stresses and finite elements calculations has shown a very good correlation. We can see in figure 8 that, at the beginning of cooling, stresses are tensile on the surface and compressive in the

center of the part. At the end of cooling, this is reversed; figure 9 shows the residual stress distribution across the thickness.

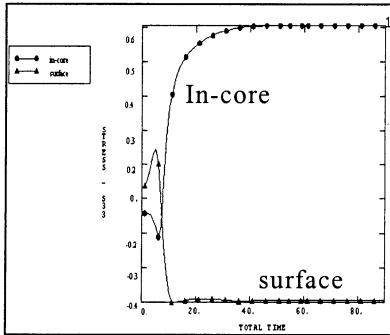


Figure 8 : In-core and surface stress S33

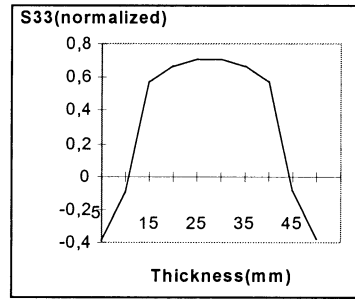


Figure 9 : S11 after quenching in section AB

3. STRESS FIELD MAPPING AND MACHINING.

During machining of the drop forging part, the state of stress due to quenching may give rise to deformations which have to be rectified in order to fit the dimensional tolerances.

We then developed 2D and 3D numerical modelization of machining which only needs to know the final part mesh position in the drop forging part mesh.

3. 1. Machining modelization.

We make a stress field mapping from the quenched drop forging part mesh (E) onto the final part mesh (P), which we want to obtain after machining (figure 10).

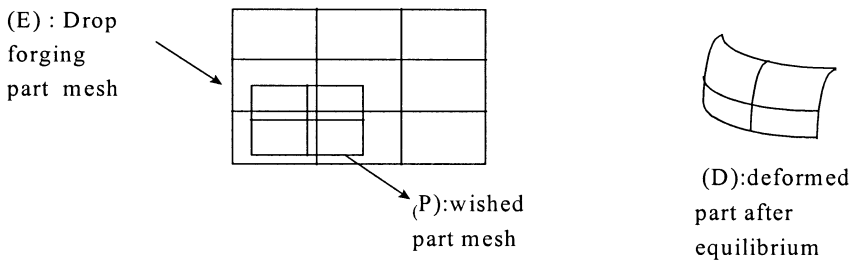


Figure 10 : Machining simulation method

Reactions F_i , equivalent to the action of (E) on (P), are calculated on the boundary of (P). We then calculate an equilibrium by canceling F_i .

We suppose here that the material remains elastic with small displacements during machining. We then get the deformed machined part geometry and stresses.

This method allows to easily estimate the influence of (P) part position in (E).

3. 2. Stress field mapping formulation.

This mapping is carried out between Gauss points of both meshes. We have used a weighted average method, which is easy to perform. For every M' Gauss point in the final mesh (P), we calculate the N nearest Gauss points in the initial mesh (E). For each M' point, we calculate the weighting coefficient $f(d_i)$ depending on the distance $d_i=d(M_i'M)$.

The stress value at point M' is a weighted average of the M_i stress values:

$$\sigma (M') = \frac{\sum_{i=1}^N f(d_i) \cdot \sigma (M_i)}{\sum_{i=1}^N f(d_i)}$$

We have used a Gaussian weighting function: $f(d_i)=\text{Exp}(-kd_i^2)$

where k coefficient is calibrated on the farthest neighbour distance:

$\text{Exp}(-kd_{\max}^2)=\varepsilon$, with for example, $\varepsilon =10^{-2}$

Another field mapping which can also be used is the diffuse approximation method [NAY. 92]:

If $X=(x,y,z)$ is the point coordinates vector where we have to calculate the stress field σ , we approximate this field as:

$$\sigma (X)=\langle p(X) \rangle \{a\}$$

where $p(X)$ (for example $\langle 1,x,y,xy \rangle$) is the chosen polynomial base, $\{a\}$ the coefficient vector of the polynomial to be determined. Polynomial $p(X)$ is an approximation of $\sigma (X)$ in the neighbourhood of X , by the least square method.

The $\{a\}$ vector solution is given by minimizing the following function with respect to a_i :

$$\sum_{i=1}^N W(X_i) [\langle p(X_i) \rangle \{a\} - \sigma_i]^2$$

where:

- X_i are the N nearest neighbours of X ,

- $W(X_i) = \text{Exp}(-kd_i^2)$, $d_i = d(X,X_i)$, with $W(X_{\max}) = \varepsilon$

Minimization is equivalent to solving the linear system:

$$[A] \{a\} = \{b\}, \text{ with:}$$

$$[A] = \sum_{i=1}^N W(X_i) \{p(X_i)\} \langle p(X_i) \rangle, \{b\} = \sum_{i=1}^N W(X_i) \{p(X_i)\} \sigma_i$$

3. 3. Machined part equilibrium.

After stress field mapping, each Gauss point of the final part mesh is assigned with an extrapolated stress field. This forms an initial condition for an elastic calculation in ABAQUS code. We thus get the final part deformed shape and the stress field after machining.

3. 4. Application.

The part geometry that we want to get after machining is given on figure 11. The calculated deformed shape is shown in figure 12.

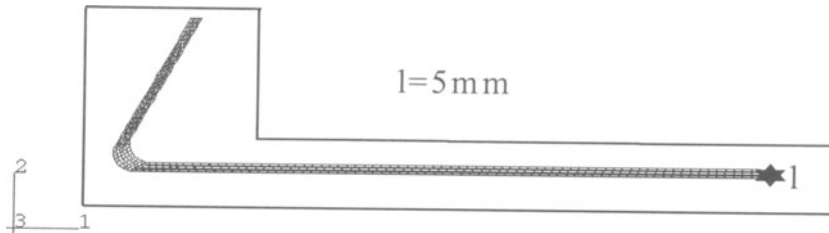


Figure 11 : Machined part mesh in the drop forging part

The machined part deformations are measured with respect to a shape rigging template.

These measurements have shown that experimental displacements are in a good agreement with calculated ones. Stress field distribution is similar to the drop forging one after quenching but stress values are lower.

4. MACHINED PART POSITION OPTIMIZATION IN THE DROP FORGING PART.

Experimental and numerical investigations have shown that the machined part deformations depend on its position in the drop forging part (figure 11) [ABI. 96]. We have then developed a 2D computer program in order to calculate the machining position which minimizes the final part deformations.

4. 1. Method.

The optimization problem is posed as follows:

- the drop forging part geometry being fixed, with a 2D calculated residual stress field,
- under the constraints related to the drop forging part contour (the final part mesh must remain in this contour),
- minimize the following U function (global displacement):

$$U(dx, dy) = \frac{1}{N} \sum_{i=1}^N \sqrt{u_{ix}^2 + u_{iy}^2}$$

where :- N is the number of nodes on machined part contour,

- u_{ix} and u_{iy} are these nodes displacements after a machining simulation.

The optimization parameters are the increments dx and dy on the final part center of gravity position. For each increment (dx, dy) , we calculate the final mesh nodes coordinates, with respect to the drop forging part mesh. Then we carry out a machining simulation and evaluate U .

U minimization is made using the SiDoLo parameters identification code [PIL. 91]

4. 2. Application.

We have applied this optimization algorithm to the part shown in figure 11.

The initial stress field results from the quenching simulation described in section 2.

3. The deformed part for the initial machining position is given in figure 12.

Optimization calculation results are given in figures 14 to 16 which show respectively dx and dy parameters evolution and U function during iterations. The algorithm allowed a convergence towards the minimum U in 19 iterations.

NU value for the initial machining position is $NU=75.30\text{mm}$. After optimization, we have $NU=30.45\text{mm}$, which represents a decrease of 56.70%. Figure 13 shows the deformed machined part mesh after optimization.

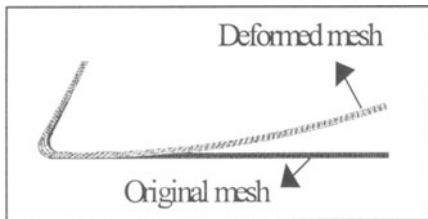


Figure 12 : Deformed mesh before optimization

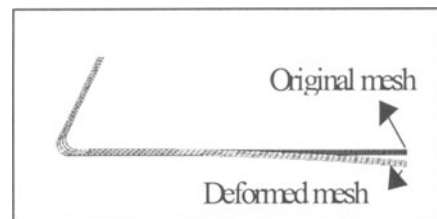


Figure 13 : Deformed mesh after optimization

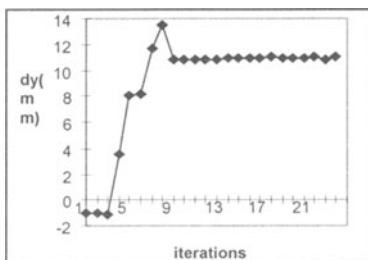


Figure 14 : dx evolution during optimization

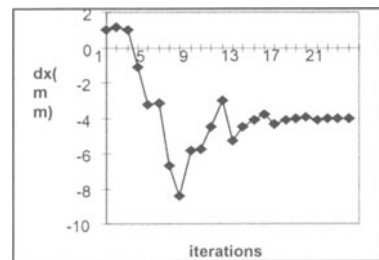


Figure 15 : dy evolution during optimization

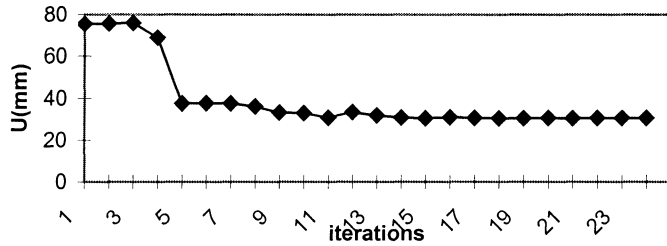


Figure 16 : NU function evolution during optimization

5. CONCLUSION.

Quenching modelisation in 3D or 2D-generalized plane strains allows the computation of residual stresses in agreement with X-ray diffraction experiments.

The numerical modelisation of machining only needs to know the final part mesh position in the drop forging part mesh. Application to an industrial part has shown a good agreement between calculated and measured deformations.

We have developed a 2D optimization program which enables to calculate the machining position which minimizes the final part deformations. This integrated modelling system will help understanding the residual stresses influence on distortion and improve the design of industrial parts.

References

- ABISORR, A., CONGOURDEAU, F., MASSE, C., ROELANDT, J.M. (1996) Approche numérique de l'usinage des grandes pièces en alliage d'aluminium, Paris, Congrès STRUCOME. [ABI.96]
- ARCHAMBAULT, P., CHEVRIER, J.C., BECK, G., BOUVAIST, J. (1980) A contribution to the optimization of a 7075 heat treatment, Materials, Science and Engineering, 43. [ARC. 80]
- NAYROLLES, B., TOUZOT, G., VILLON, P., RICARD, A. (1992) Diffuse approximation and diffuse elements, New Advances in Computational Structural Mechanics, Elsevier Ed. [NAY. 92]
- PILVIN, P., SAÏ, K., CAILLETAUD, G. (1991) Optimal design against creep and fatigue, Proc. of 4th Int. Conf. On Nonlinear engineering computations, 731-740, Swansea (Pays de Galles). [PIL. 91]

OPTIMIZATION OF A PASSIVE SAFETY DEVICE BY MEANS OF THE RESPONSE SURFACE METHODOLOGY

G. BELINGARDI, M. AVALLE

*Department of Mechanics, II Faculty of Engineering
Politecnico di Torino, Corso Duca degli Abruzzi, 24
I-10129 Torino, Italy*

1. Abstract

The design of new cars requires the satisfaction of ever stricter safety standards defined by certification regulations and to match the continuously growing attention of the customer for safety. Hence, it is necessary to improve every component of the vehicle to achieve better performance. An effective component in reducing loads transmitted to the driver chest in frontal crashes is the deformable steering wheel column, capable of collapsing with high energy absorption while reacting with little axial loads. The controlled collapse of the column can be achieved by inserting a corrugated tube. To achieve optimum performance it is necessary to find the proper value of its geometrical parameters. Aim of the work is to show how the use of the structural optimization approach based on the response surface methodology is an effective strategy to optimize such a component.

2. Introduction

Structural crashworthiness design of vehicles has two main goals: to obtain a strong, undeformable survivability cell for the passenger compartment and to provide a series of parts able to deform while absorbing and dissipating energy in a stable and controlled manner. In this second group of passive safety devices, some should dissipate the kinetic energy of the vehicle reducing quickly but gradually its initial speed and others should collapse, thereby reducing the loads transmitted to the passengers.

One of the main problems for driver safety is the impact of his chest with the steering column. Seat belts and airbags strongly help to this end but in some occasions are not sufficient to avoid a severe impact. Furthermore, even if the impact with the inflated airbag is light, it is desirable that the airbag does not transmit excessive loads. In order to limit the force transmitted through the airbag from the steering wheel or by the steering wheel itself to the driver's chest, it is necessary to use a collapsible steering wheel column. This effect can be obtained by introducing in the steering column an

intermediate component able to collapse with limited loads but with a torsional strength and stiffness appropriate for the steering system task in normal use conditions. Such a component can be a simple tubular member, which is known to be an efficient energy absorber [1, 2, 3]. In addition, to limit the maximum load without reducing the energy absorption capability, the tube can be suitably shaped.

A simple and effective method proposed to obtain such a behavior is to pre-deform the tube with a series of axisymmetric enlargements (bulges) similar to the axisymmetric folds that occur in the axial collapse of tubes [4]. This element is known as “corrugated tube” or “bellows”. The bulges are usually obtained by plastic deformation of a simple circular tube in a die under internal pressure applied with water or other liquids (hydroforming).

Once the overall length of the bellows, its base diameter and material are fixed, the design parameters are the length of the bulges, the external diameter of the enlargements and, consequently, the number of enlargements (which is in turn related to the total length and to the length of the folds). These geometrical parameters influence the global behavior that is evaluated in terms of the energy that the component can dissipate in its axial collapse and of the maximum sustained axial load. These two structural indexes can be combined in one further parameter, ratio of the previous two, known as the load uniformity parameter (LU).

This work shows the analysis of a corrugated steel tube when changing the geometrical parameter with the objective of obtaining a component with the minimum load uniformity parameter (the ideal value being one). Structural analysis is performed using an explicit finite element code.

The aim of the work is twofold: first, to design an optimized component for energy absorption and, second, to show the usefulness and efficiency of an optimization algorithm. The optimization procedure used in the work is a steepest descent algorithm based on the response surface methodology that has proved to be very efficient in the case of highly non-linear problems [8, 9].

3. The corrugated tube used as an energy absorbing device

The subject of this work is the so-called “corrugated” tube or bellows shown in Figure 1. The tube is defined by external radius r_e , internal radius r_i , total length l , length of each bulge p , number of bulges n and wall thickness t . It's worth noting that the bellows internal radius r_i is equal to the outer radius of the two cylindrical ends of the tube, whereas the internal radius of the tube at the ends is equal to $r_i - t$. The base values for these dimensions were 30 mm for internal radius r_i , 35 mm for external radius r_e , 150 mm for total length l , 7.5 mm for bulge length p . The base number of bulges was 12.

Changing design parameters during the optimization process, there is a certain number of constraints linking the number of bulges to their length. In particular the number of bulges was determined by the condition that the total length of the “corrugated” part does not exceed the initial length, equal to $(l - 2 l_b)$. Hence, to ensure

that the number of bulges is an integer number, the length of the straight ends can change during optimization.

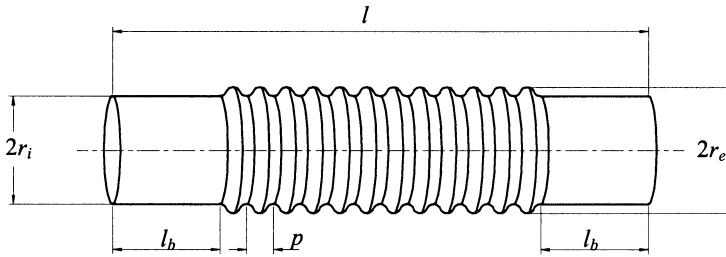


Figure 1. Scheme of the corrugated tube

The next problem deals with the bulges' profile. The more obvious choice would be to use circular arcs as generating curves (so the bulges are formed by portions of circular toroidal surfaces). When considering surfaces of revolution obtained from circular arcs connecting each other, three cases may occur as shown in Figure 2. If $(r_e - r_i) > p/2$ the profile of one bulge is formed by four arcs, comprising a 90° angle, connected by a straight line (left diagram of Figure 2). The radius of the arcs defining the bulge is thus equal to $p/4$. When $(r_e - r_i)$ is equal to $p/2$ the length of these connecting lines falls to zero, that is the bulge profile is formed by four arcs of $p/4$ radius each comprising a 90° angle. When $(r_e - r_i) < p/2$ to have a smooth profile with tangent curves the included angle must be less than 90° (right diagram of Figure 2). Hence, angle α and radius r are obtained from the following relations:

$$\alpha = 2 \arctan \frac{2(r_e - r_i)}{p} \quad (1)$$

$$r = \frac{p^2}{16(r_e - r_i)} + \frac{r_e - r_i}{4} \quad (2)$$

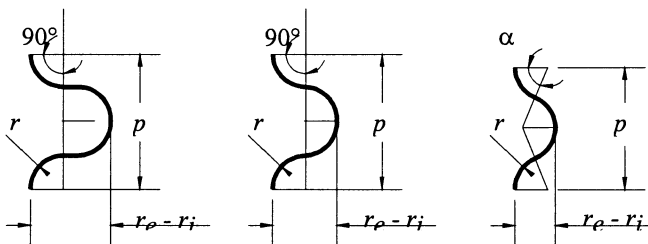


Figure 2. Bulge profile

The structure was studied using a simplified finite element model, taking advantage of the axial symmetry of the problem. The simplified finite element mesh models a single axial strip of the surface with four-node shell elements (axisymmetric shells are not a feature of the DYNA3D code). Proper constraints coerce the mesh nodes to move only in the axial and radial directions. The load was applied by two rigid walls, one fixed and the other moving against the structure with an initial speed of 13.89 m/s (50 km/h). Figure 3 shows the finite element mesh of the base bellows configuration together with a sequence of plots taken at different times during the crush and a diagram showing the force-displacement characteristic.

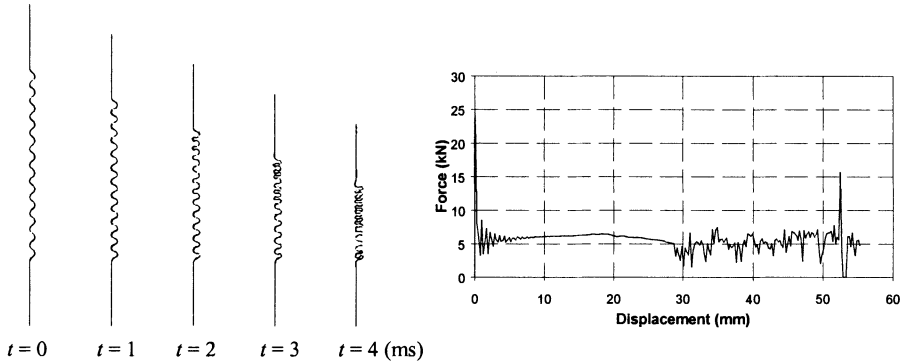


Figure 3. Finite element mesh of the base configuration with collapse

4. The optimization algorithm

The optimization algorithm used in the work is based on a steepest descent procedure [5] and uses the response surface methodology [6, 7] to establish the search direction [8, 9].

In the algorithm [9] the initial step consists of a complete plan of experiments (two levels for each design variable) plus a central point. According to the results of the response function evaluations, a regression plane is computed and the direction opposite to the gradient of the plane is used as the search direction (if the value of the objective function at the central point of the plan of experiments is less than the values obtained at the other four points, a new plan centered on the same central point but of half the original size is used). New points are evaluated along the search direction until the objective function value does not increase again. In this case a half size plan of experiments centered in the last point evaluated before the objective function increase is studied and the algorithm restarts with a half length step.

The search algorithm stops when either the variation of the objective function between two consecutive steps is less than a predetermined value ϵ_f , or the variation in the variables (the size of the plan of the experiments) is less than a predetermined value ϵ_x , or the number of function evaluation exceeds a limit number.

The algorithm as previously described is an unconstrained search procedure. Constraints to the values of the design variables are therefore taken into account using penalty functions. Penalty functions used in this problem add to the objective function a quantity proportional to the cube of the distance of the point outside the admissible region from the boundary of the domain.

5. Results

In order to better understand the problem, a first evaluation of the structure behavior as a result of changing the geometrical parameters was done (Figure 4). The two variable parameters were fold length p and external radius r_e . The results of this parametric study are the maps of the three structural parameters, load uniformity LU , maximum force F_{max} , and average force F_{mean} respectively. The fold length p was let to vary from 2 to 20 mm and the external radius r_e from 15 to 25 mm (when r_e is equal to 15 mm the bellows is a straight circular tube and the structural parameters are obviously unaffected by length p).

A plain observation of the plots of Figure 4 shows that the maximum load is roughly constant everywhere except in the region where p is minimum and r_e maximum. The maximum load shows a “valley” when r_e is between 17 and 19 mm. The average load is minimum when p is 17 mm and r_e is equal to 25 mm. The surface representing load uniformity is somewhat complicated. It is possible to observe a global decrease of the load uniformity parameter with decreasing external radius r_e . However, in the region of greater external radius ($r_e = 22 \div 23$ mm) the influence of the length of the folds is not regular and there are many local minima. The region with r_e from 16 to 18 mm is roughly flat with a local minimum at $p = 10.5$ mm, $r_e = 16.5$ mm and a global minimum in $p = 4.5$ mm, $r_e = 16.5$ mm. All these local minima are very “dangerous” when using an optimization algorithm (especially in the region of greater external radii) because it is necessary to avoid their “attraction”: the algorithm should not fall in this point and must be able to go further.

Figure 5. shows the results of numerical optimization. The starting point was in $p = 10$ mm $r_e = 21$ mm and the size of the first plan of experiments was 16 mm for the length of the folds and 8 mm for the external radius. The starting point and the size of the plan of the experiments were chosen in order to explore an adequately large region of the search domain. The risk of using a smaller plan is that of falling into a local minimum region. With a larger plan there is a greater probability of avoiding this problem. Actually, a new point is examined in $(p, r_e) = (5.66, 17.08)$ mm. The next point in the search direction is outside the admissible region (that is, it would correspond to an external radius lower than the internal radius of 15 mm). Hence, the algorithm moves back and examines a new plan with size equal to half the size of the initial plan. Afterwards, as it is not possible to reduce the objective function value in this way, a new reduced plan of experiments is analyzed. The algorithm stops because the final point (the solution) in $(p, r_e) = (3.75, 16.30)$ mm (with $LU = 1.778$) decreases the objective function value by less than the required tolerance with respect to a

previous point in $(p, r_e) = (3.66, 16.33)$ mm (with $LU = 1.796$). The objective is reached in 21 steps.

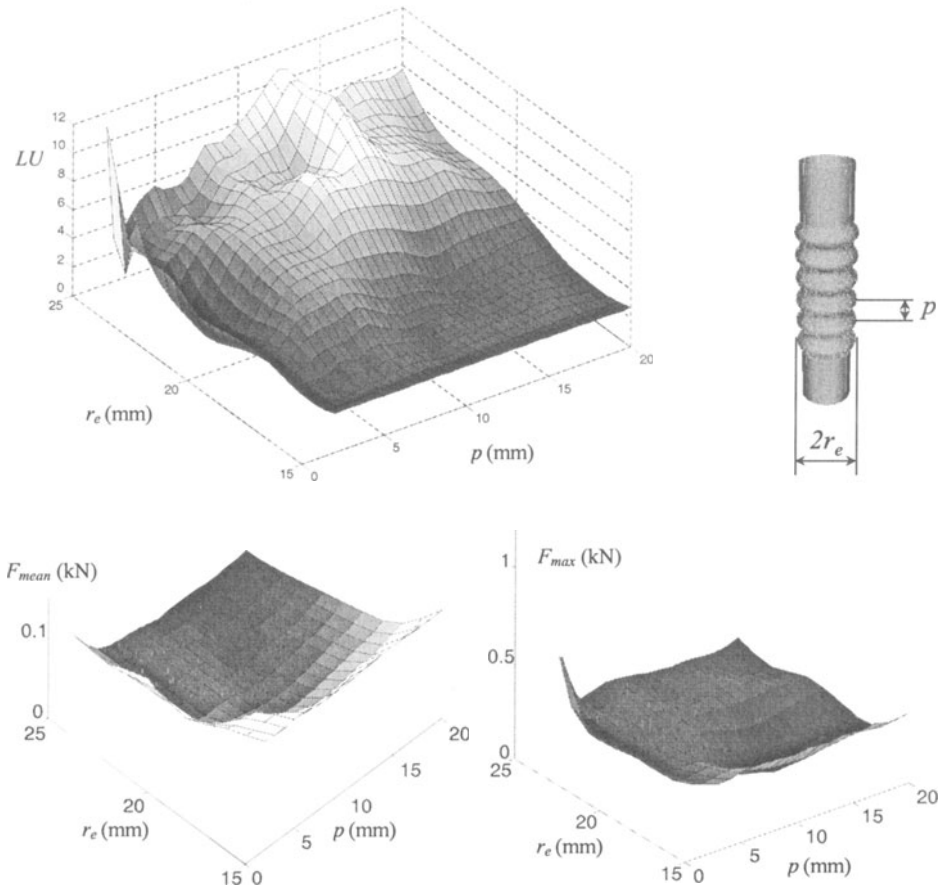


Figure 4. Influence of the geometry on the structural behavior of the bellows

It should be pointed out that the algorithm does not ensure a proper solution if incorrect starting parameters are chosen. In particular, it is important to use a sufficiently large initial plan of the experiments able to find data about the global shape of the surface. It has been verified, for example, that with a smaller initial plan centered in $(p, r_e) = (6, 24)$ mm with a variation of 6 mm for the length of the folds and of 2 mm for the external radius, the algorithm converges to the local minimum in $(p, r_e) = (2.40, 23.39)$ mm. The same result is obtained by starting the algorithm search in $(p, r_e) = (10, 22)$ mm and with the same initial variation of the design parameters.

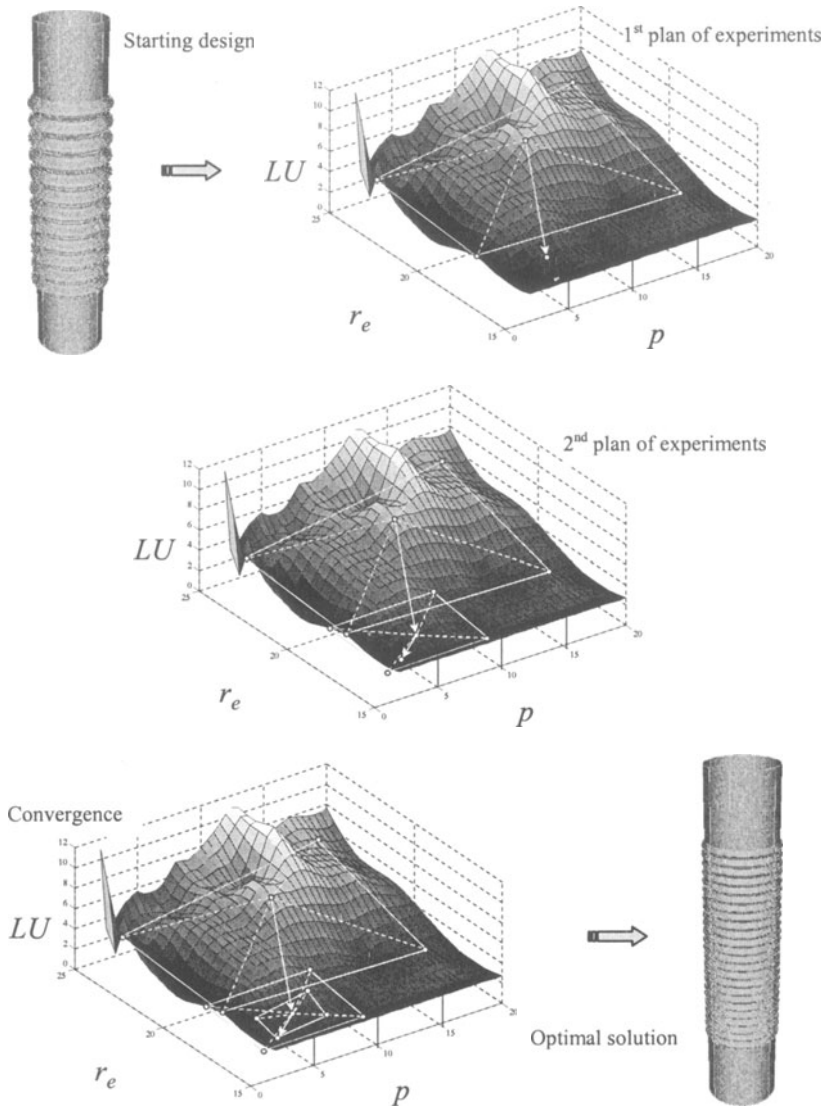


Figure 5. Results of the optimization

6. Conclusions

The passive safety of a car driver can be improved by introducing in the steering wheel column a deformable part able to reduce the loads transmitted to the chest during a frontal crash. A feasible and effective element able to achieve this goal is a simple thin

tube. The behavior of a tube for this aim can be improved by suitably pre-deforming it in the shape of a corrugated tube.

The geometrical parameters of the corrugated tube strongly influence its structural behavior especially for what concerns the load uniformity. In fact, load uniformity in fact can vary from a minimum of about two to a maximum of ten and more. The geometrical configuration corresponding to the minimum load uniformity parameter has been obtained from a parametric study of the component. This investigation showed that efficient sizing comes with a length of the folds about one third of the diameter of the extremities and an external diameter 1.1 times the diameter of the extremities. Furthermore structural behavior is scarcely affected by the fold length but highly sensitive to the increase of external radius. This result is, however, valid for the current thickness over diameter ratio.

The same result can be obtained through the use of an efficient optimization algorithm. The response surface of the problem is very irregular and a classical minimization procedure would presumably fall into a local minimum. If a complete parametric study requires scores of structural analyses, which are in this case non-linear dynamic simulations, the optimization algorithm proposed herein can achieve nearly the same result in about twenty evaluations of the structural behavior.

7. Acknowledgments

The financial support of the Italian National Research Council CNR through the 97.01789.CT11 contribution is gratefully acknowledged.

8. References

1. Johnson, W., Reid, S.R.: Metallic energy dissipating systems, *Applied Mechanics Review* **31** (1978), 277–288.
2. Jones, N.: *Structural impact*, Cambridge University Press, Cambridge, 1989.
3. Avalle, M.: *Collasso Plastico Progressivo di Strutture Metalliche: Sviluppo di Modelli Teorici e Analisi Sperimentale*, Ph.D. Thesis, Dipartimento di Meccanica, Politecnico di Torino, Torino, 1995.
4. Singace, A.A., El-Sobky, H.: Behaviour of axially crushed corrugated tubes, *Int. J. Mechanical Sciences* **39** (1997), 249–268.
5. Vanderplaats, G.N.: *Numerical optimization techniques for engineering design*, Mc Graw Hill Inc., New York, 1984.
6. Chiandussi, G.: *Metodologie di Ottimizzazione in Campo Lineare e non Lineare*, Ph.D. Thesis, Dipartimento di Meccanica, Politecnico di Torino, Torino, 1996.
7. Khuri, A.I., Cornell, J.A.: *Response Surfaces*, ASQC Quality Press, New York, 1987.
8. Avalle, M., Belingardi, G., Chiandussi, G., Vadori, R.: Structural Optimisation of the axial crushing behaviour of thin walled tapered columns, in D.R.J. Owen, E. Oñate and E. Hinton (eds.), *Computational Plasticity*, CIMNE, Barcelona (1997), 1959–1864.
9. Avalle, M., Belingardi, G.: Confronto fra Strategie di Ottimizzazione in Campo Non Lineare nell'Applicazione a un Problema di Collasso Strutturale, in P. Conti and C. Braccesi (eds.), *Atti del XXVII Convegno Nazionale dell'Associazione Italiana per l'Analisi delle Sollecitazioni*, Catania (1997), 467–474.

OPTIMAL DESIGN OF MECHANICAL COMPONENTS WITH GENETIC ALGORITHM

LAURENCE GIRAUD AND PASCAL LAFON

Université de Technologie de Troyes

12 rue marie curie BP 2060

F 10010 TROYES Cédex

laurence.giraud@univ-troyes.fr

1. Introduction

Our aim is to propose design-making tools, which can be introduced in Computer Aided Design software. Thank to the analysis of the design process of a known mechanical system, we can formulate the mechanical design problem as an optimization problem, called problem of optimal design. The latter contains non-linear equations, inequality constraints and mixed variables that are continuous and discrete. There are also interdependent discrete parameters whose values may be taken in normalized tables and which directly depend on the choice of one of the discrete variables. Some problems of optimal design have been solved with a method using the augmented Lagrange multipliers, combined with a branch and bound algorithm [5]. In order to calculate the functions gradients, interpolation functions have been used to bind the discrete parameters to the discrete variable, on which they depend. Good results have been obtained for many design problems. However, for some complex structures, we can not obtain a simple analytical expression relating the different parameters to a discrete variable. The functions gradients can not be calculated so that classical methods can not be used. In this paper, we propose to use genetic algorithms (GAs) to solve these difficult problems of optimal design. The genetic algorithm is a recently emerged heuristic optimization technique, based on concepts from natural genetic and guided by the model of Darwin. The algorithm differs from traditional optimization methods by the fact that it does not require derivative information. It just requires the value of the functions at different points. This method is not sensitive to problem non-linearity, non-convexities, and it can solve problems with mixed variables.

We are able to directly use the tables with the normalized values of the secondary discrete values. First, we present GAs, the classic genetic operators and other genetic operators which can enhance their performance. Then, problems of optimal design are presented and the computational results are given. Finally genetic operators, different representations are presented and conclusions are stated.

2. Genetic algorithms

Early implementations and theoretical analysis of the genetic search method are credited to Holland in 1975 [4]. Genetic algorithms were originally developed to simulate adaptation as in natural systems. A good review on GAs can be found in [3],[7] .

2.1. REPRESENTATION

Contrary to the other methods, GAs do not use a single point but a population of points called individuals. Genetic algorithms use a binary representation of individuals as fixed-length strings over the alphabet 0, 1, which are analogous to chromosomes in biological systems. Each string represents a solution point in the search space. A multivariable coding is constructed by concatenating individual single variable coding into a complete string. The strong preference for using binary representations of solutions in genetic algorithms is derived from schema theorem [4], on which the algorithm is based. All the design variables are then coded into fixed-length digit strings. A continuous variable is treated as a discrete variable with small values of increment.

2.2. FITNESS FUNCTION

In GAs, the fitness value represents the “performance” of each individual. Individuals with better fitness value will have higher a probability of being selected as parents. In order to solve our optimal design problems with many inequality constraints, we have chosen to use an exterior penalty method because we just have to choose the value of the penalty coefficient. This coefficient will increase during the optimization process in order to initially keep a slow exploration of the design space and then force a greater exploitation of promising designs as the number of trials increases [8].

2.3. GENETIC OPERATORS

Figure 1 shows the main step of genetic algorithms. They start with the creation of an initial population of designs, usually at random. Each in-

dividual is evaluated and is assigned a fitness value. A new population is reproduced on the basis of these evaluations through genetic operators, selection, crossover and mutation. Thereafter, a newly generated population replaces the old one and enters the evaluation stage again as the cycle of evaluation and reproduction continues. The population improves from generation to generation. We will now detail the genetic operators, giving traditional operators [3] and other methods found in the literature.

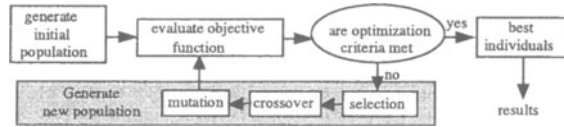


Figure 1. The genetic algorithm

Selection determines which individuals are chosen for the reproduction. Classical selection is implemented as a probabilistic operator, using the relative fitness $p(a_i) = \frac{F(a_i)}{\sum_{i=1}^p F(a_i)}$ to determine the selection probability of the individual a_i , where p is the number of individuals in the population and $F(a_i)$ the fitness of the individual a_i . Rank-based selection methods are often used rather than using absolute fitness values [6], [7]. The population is now sorted according to the fitness. The probability assigned to each individual depends only on its position in the individuals rank. In the application, we will study the classical selection and two different linear rank-based selection methods ([6], [9]). Crossover is the primary operator in the GAs. The traditional one-point crossover is achieved by swapping partial chromosomal materials above a randomly chosen crossing site to reproduce new offspring. Numerous extensions of this operator, such as increasing the number of crossover points, uniform crossover (each bit is chosen randomly from the corresponding parental bits)... have been proposed [7]. We will test the classical one-point crossover, a two-point crossover and the uniform crossover. Mutation in genetic algorithms was introduced as a “background operator” of small importance [2]. Mutation alters a gene value according to a predetermined probability, usually very small. With the classical mutation, a bit of the chromosome is chosen uniformly at random. This bit value is then flipped from 1 to 0 or vice versa. With the uniform mutation, the mutation is applied on a bit-by-bit basis. This means that many bits of the chromosome can be altered. We have chosen an elitist model of GAs [6], where the two best individuals (the best feasible individual and the individual with the best fitness) are kept from one

population to the next, so that the best individual never disappears at the change of generation.

3. Application and results

The previously described genetic algorithms have been applied to three design problems. The first two problems are not detailed, as their equations can be found in the literature. The first problem (prob1) is the design of a pressure vessel [9]. This problem contains 2 discrete variables, 2 continuous variables and 7 inequality constraints. The second problem (prob2) is a coupling with bolted rim [5], formulated with one discrete variable, one integer variable, 3 inequality constraints and 5 discrete bolt parameters. The last problem (prob3) is a ball bearing pivot link (see fig.2). The aim is to find the lengths x_1 , x_2 and the two ball bearings R_1 and R_2 in order to minimize the weight of the assembly composed of a shaft and two ball bearings. The formulation of the optimization problem requires to list all functional relations and conditions to describe the behaviour of this linkage. We have geometrical conditions, stress conditions on the shaft and conditions on the bearings life span. In order to simplify the formulation, we deal with a numerical example. We want to transmit a power of 23.5kw at 970t/mn for a nominal life span of 1800 hours. We obtain a problem with 4 variables, 2 continuous (x_1, x_2), 2 integer (R_1, R_2) variables, 12 discrete parameters and 10 inequality constraints. In order to solve this problem with the genetic algorithm, we have numbered the ball bearings from 1 to 28, as they are ordered in the normalized table. The parameters of the 2 ball bearings are $(C_1, d_1, D_1, b_1, ba_1, m_1)$ and $(C_2, d_2, D_2, b_2, da_2, m_2)$ respectively, depending on the choice of the ball bearing. Thus, we have the following formulation, with $X = \{R_1, R_2, x_1, x_2\}$:

Minimize the function :

$$F(X) = \frac{\pi \rho}{4} (x_1 d_1^2 + 0.5(b_0 d_1^2 - b_2 da_2^2 + b_1 d_1^2)) + b_3 da_1^2 + x_2 da_2^2 - b_3 da_2^2 + b_2 d_2^2 + d_2^2) + m_1 + m_2$$

Subject to the constraints :

$$\begin{aligned} G_1(X) &= 0.5b_1 - x_1 + (0.5b_0 + e_1) \leq 0 & G_2(X) &= D_2 - D_1 \leq 0 \\ G_3(X) &= 29216(1 + x_1/x_2) - C_1 \leq 0 & G_4(X) &= d_0 - d_1 \leq 0 \\ G_5(X) &= 29216(x_1/x_2) - C_2 \leq 0 & G_6(X) &= d_5 - d_2 \leq 0 \\ G_7(X) &= (615.51x_1 + 3930)^{1/3} - d_1 \leq 0 & G_8(X) &= D_1 - D_M \leq 0 \\ G_9(X) &= 0.5b_1 + 0.5b_2 - x_2 + e_4 + b_3 \leq 0 & G_{10}(X) &= x_2 + x_1 - 177 \leq 0 \end{aligned}$$

Data: $\{b_0, b_3, e_1, e_4, e_2, D_M, L_M, b_5, d_0, \rho\}$

From the different selection, crossover and mutation operators, described in the previous chapter, we have created 18 sets of tests in order to compare all these operators on our three problems. Each continuous variable is represented with a 20 bits length string. The population contains 200 indi-

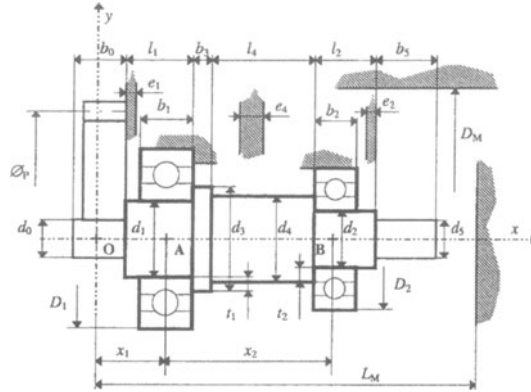


Figure 2. Ball bearing pivot link

viduals. To obtain statistically significant data, one hundred independent runs have been performed for each combination of operators.

3.1. RESULTS

The average error between the theoretical optimal solution and the solution given by GAs is always smaller than 1.4% and the error for the best run is always smaller than 0.01%. Finally, for the 3 design problems for which we know solution, we have obtained results of good reliability.

From the tests made on our three design problems, we can draw the following remarks about the genetic operators. The classical selection gives the worth results because it causes a premature convergence for the three problems. With the two rank-based selection methods, we obtain good results because we avoid the domination of the best individual. In fact, by using the classical selection method, we can have an individual in the population, which is much better than the average fitness of the population. Such individual has a large number of offspring and prevents other individuals from contributing to the next generations. That causes a rapid convergence to a local optimum. The difference between our two rank-based methods is the selective pressure. As the first method has a bigger selective pressure, it has a better convergence velocity.

For the crossover methods, the traditional one-point crossover performs worse than the two-point crossover. With the two-point crossover, we have higher convergence velocity and higher convergence reliability. The reason is that one-point crossover has a very high probability of separating bits that are located at the extremes of the chromosome. On the figure 3, we

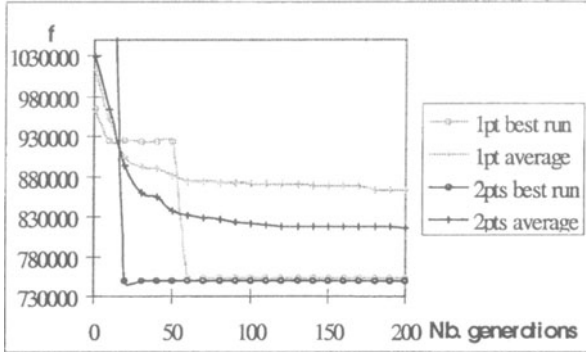


Figure 3. Comparison between 1 point crossover and 2 point crossover (prob3)

compare for the prob3 these two crossovers, by showing for each method the evolution of the objective function corresponding to the best execution, and the average of the executions. Some recent empirical studies [10] have shown that crossover operator having higher number of crossover points may be more effective at times but uniform crossover does not always give for our design problems the best results. Results depend on the problem treated. We prefer not to keep this method. However, the actual standard used in implementations is a two-points crossover but according to Bäck [2], no generally recipe for the choice of a recombination operator can be given.

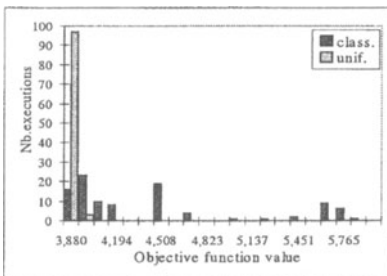


Figure 4. Histogram for prob2

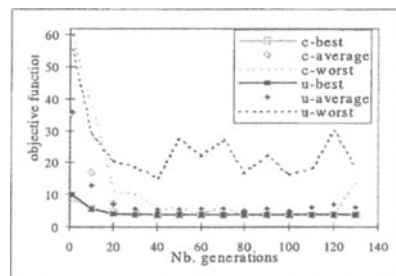


Figure 5. Diversity of the population

Concerning the mutation, uniform mutation performs better than classical mutation for the 3 problems (see histogram on fig.4 for prob2 for which the known optimal value is 3.88). We have a clearly better reliability with the uniform mutation and more runs converge. By analysing our graph-

ics and watching the population evolution, we have noticed that with the classical mutation, the population converges too rapidly around a single point, this being the cause of the premature convergence. With more mutations (uniform mutation), we have more diversity in the population and this can prevent premature convergence. We had chosen a mutation rate p_m of 0.02, $p_m = 1/l$ (l : chromosomes length) being, according to Mühlenbein [1] the optimal mutation rate. Figure 5 presents the evolution of the objective function for the best individual, the worst individual and average of the population, showing the population diversity in the course of the generations, for the best run of prob2 with classical (c) and uniform (u) mutation.

3.2. DISCUSSION ABOUT THE REPRESENTATION

During the analysis of the histograms, we had noticed that many runs identify exactly the same local optimum. This phenomenon is represented by peaks on the histograms (fig.5). It seems to be interesting to analyse the chromosomes strings, which correspond to this local optima, in order to find the cause of these repeated premature convergence. We also compare the theoretical optimal binary string with the string corresponding to each local optima. This comparison shows that for all the problems, there is an error in the string associated to one of the continuous variable of the local optimum. The theoretical string, corresponding to each theoretical variable, generally contains an alternation of many 0 and 1. But the string, corresponding to each local optimum, contains a succession of 0. The values of these decoded strings are generally not very different but in the coding space, they are very far. If the algorithm converges too rapidly, the individuals are almost identical and it becomes very difficult to obtain the theoretical string. This explains that we have better results when we have more mutation, more diversity in the population. This study shows that the standard binary coding is not suitable for continuous variables. The major drawback of standard binary coding is that the Hamming distance between consecutive numbers is usually greater than 1. In the worst case, with a 20 bits string, all 20 bits have to be changed simultaneously. Other practical experiences have noted that the binary encoding has some disadvantages [1].

In order to enhance performances, we solve again our design problems, by using the binary Gray coding instead of the standard coding. The advantage of the Gray coding is that consecutive numbers have always Hamming distance of 1, then we obtain results with a better reliability. For example, the average error between theoretical solution and the calculated one decrease from 0.58% to 0.0003% for prob2.

4. conclusions

GAs are very interesting basic methods for solving complex problems of optimal design. For our three design problems, we obtain results with a good reliability. One of the principal advantage of this algorithm is that it does not require derivative information. Moreover it can provide number of potential solutions, which can let a choice to the user. GAs have the disadvantage of having a high computational cost. When gradient-based algorithms are not applicable, GAs are powerful stochastic method but when deterministic methods are applicable, we do not advise GAs. The schema theorem advises a standard binary representation but our study has shown that this representation is not suitable for continuous variables. Moreover, the mutation operator was presented as a background operator of small importance. On the contrary, we have found that this operator, by introducing diversity, improves convergence greatly. By using a binary Gray coding, we have obtained better results than with a standard binary coding. A binary representation does not seem the best method for the continuous variables. This mechanism implies that in continuous space of the original problem, only a search on grid points is performed. The reliability will always be limited by the increment value. Our next research will then be on the use of a real valued vectors for the continuous variables, with genetic algorithms or other evolutionary methods.

References

1. Bäck, T.(1996) *Evolutionary algorithms in theory and practice*, Oxford University Press, New York.
2. Bäck, T., Hammel, U., Schwefel, H-P. (1997) Evolutionary computation: comments on the history and current state, *IEEE Transactions on evolutionary computation*, Vol. no. 1.
3. Goldberg, D-E. (1989) *Genetic algorithms in search, optimization and machine learning*, Addison Wesley publishing compagny.
4. Holland, J-H. (1975) (1975) *Adaptation in natural and artificial systems*, The University of Michigan Press, Ann. Arbor, MI.
5. Lafon, P. (1994) Conception optimale de systèmes mécaniques: Optimisation en variables mixtes, Thèse 3ème cycle, no. d'ordre 273, Institut National des Sciences Appliquées de Toulouse.
6. Le riche, R. (1994) Optimisation de structures composites par algorithmes génétiques, Thèse 3ème cycle, Université de Technologie de Compiègne.
7. Michalewicz, Z. (1996) *Genetic Algorithms + Data Structures = Evolution Programs*, Springer, Berlin.
8. Powell, D., Skolnick, M-M. (1993) Using genetic algorithms in engineering design optimization with non linear constraints, Proceeding of the fifth international conference on genetic algorithms, pp. 424-431.
9. Wu, S-J., Chow, P.-T. (1994) Genetic Algorithms for solving mixed-discrete optimization problems", The Franklin Institute, Vol 331B. no. 4, pp. 381-401.
10. Wu, S-J., Chow, P.-T. (1995) Steady-state genetic algorithms for discrete optimization of trusses, Computer and structures, Vol. 56. no. 6, pp. 979-991.

DESIGN OF MATERIALS WITH SPECIFIC ELASTIC PROPERTIES USING SHAPE OPTIMIZATION METHOD*

SHUTIAN LIU, YUANXIAN GU AND GENG DONG CHENG

*State Key Laboratory of Structural Analysis of Industrial Equipment
Dalian University of Technology, Dalian, 116024, P.R. China*

Abstract

In this paper, we use a shape optimization method to determine the microstructure shape of composite materials composed of two phases (a material phase and a void phase) in order to design composite materials with specific elastic properties, such as with zero Poisson's ratio. Microstructure topology is limited to honey-combed skeleton structure in a unit cell as this is most easily manufactured. The microstructural parameter is the angles between two sides, the length of sides and the thickness of skeletons. The optimal goal is to minimize the differences between the components of effective elastic tensor and the desired (given) value of these components. The effective behavior of composite materials is found by use of a finite element based numerical homogenization procedure. As an example, the design of materials with zero Poisson's ratio shows the procedure.

Key words: material design, optimization, homogenization.

1. Introduction

Development of high technology leads to a number of special structures. These structures often need to meet the special requirement for structural performance. For example, the different regions or different surfaces of the structure may need different physical properties. In some cases, the materials may need to have specific properties, such as with zero thermal expansion coefficients, or with negative or zero Poisson's ratio. The traditional way to improve the performance of a structure is to optimize its size, geometry, and/or topology with the assumption that the structure is made of the given materials. Composites have the potential to be easily designed. By changing their composition, the fiber orientation or the microstructure topology and shape, they can exhibit different mechanical properties [2, 5]. Optimization of material selection and material composition provides a new era for structural engineers.

From the mechanical point of view, the aim of design of materials is to determine

* The project was supported by the National Natural Science Foundation of China (19602007)

the topology and shape of microstructure composed of material and void phases in a unit cell to realize a technical requirement. This aim is analogous to that of topology and shape optimization for continuous medium. This observation bridges the gap between material design and optimal shape and topology design and initialize a novel method for material design, i.e., shape optimization method.

In this paper, we use a shape optimization method to determine the microstructure shape of composite materials composed of two phases (a material phase and a void phase) in order to design composites with specific elastic properties, such as with zero Poisson's ratio. Microstructure topology is limited to honey-combed skeleton structure in a unit cell as this is most easily manufacturable. The microstructural parameters include the angles between two sides, the length of sides and the thickness of skeletons. The optimal goal is to minimize the differences between the components of effective elastic tensor and the components of specific (given) elastic tensor. The optimization problem is solved using programming techniques, such as Sequential Linear/Square Programming Method, Golden Division Search Method.

The shape optimization procedure proposed here, essentially follows the steps of conventional shape optimization procedures. The design problem is initialized by defining a design microstructural topology (a honey-combed skeleton structure) discretized by a number of finite elements. The optimization procedure then consists in solving a sequential finite element problem followed by changes in shape representative parameters.

At each step of the shape design optimization procedure, we have to determine the effective elastic properties of the composites. Because of the homogenization method is mathematically rigorous and effective in predicting the elastic properties of composites, we use a finite element based numerical homogenization procedure to determine the effective elastic properties.

2. Shape Optimization Procedure

Composite properties are dependent on the microstructure of materials, which is depicted with a unit cell. The parameters for representing the microstructure should include the shape parameters of unit cell and the parameters used to describe the distribution of materials in the unit cell. The goal of material design optimization is to find these parameters to make the materials with desired properties. In this work, a shape optimization procedure is used to determine the distribution parameters on the bases of a given topology of a unit cell. By selecting parameters, the effect of the shape of a unit cell on the overall properties is also considered.

2.1. OBJECTIVE FUNCTION

The objective function $f(E_{ijkl}^H)$ can be any combination of the elastic properties E_{ijkl}^H .

The concerned example in this paper will be the case where we want to design a material microstructure with specific Poisson's ratio in some one direction. In this case,

the objective function f will be the square of the difference between the value of Poisson's ratio, ν_{12}^H , and the given value, $f = (\nu_{12}^H - \nu_{12}^0)^2$, where, ν_{12}^0 is the desired poisson's ratio of the materials.

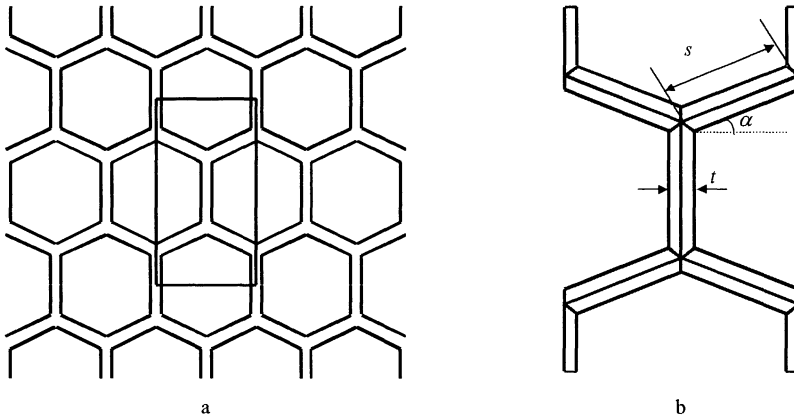


Figure 1. Periodic structure of materials and a unit cell

2.2. DESIGN VARIABLES

Consider a two-phase material which is combined by a material phase and a void phase. If the topology of solid material phase is given, e.g. a honey-combed skeleton structure, the parameter of the shape of unit cell and the parameters which depict the shape of the solid structure in unit cell domain will be the design variables. The unit cell shape parameters will be chosen as the length scales of the rectangular domain of the unit cell. The shape parameters of the material phase may be the characteristic point's coordinates. For a honey-combed skeleton structure shown in Figure 1, these parameters may be the thickness and length of the bars, $\mathbf{x} = (t_1, t_2, t_3, \Lambda, s_1, s_2, s_3, \Lambda)^T$. In the case where the skeleton structure is an equal side length polygon, the thickness t and the angle α determine the shape of the solid structure and the shape of the unit cell.

2.3. CONSTRAINTS

For the purpose of design materials either with orthotropic, square symmetric or with isotropic parameters, such constrains must to be implemented in the optimization problem. These constrains are equality ones and are difficult to implement in an optimization problem because of the starting guess may be infeasible. One approach to overcome this difficulty is to choose constrains as a penalty function added to the cost function, such as taken by Sigmund in [5]. In this paper, two symmetric lines are specified to obtain orthotropic properties, although only one symmetric line is needed to obtain this nature [5].

Another type constrains are the boundary limits on design variables. The thickness is required great than zero and the variation of the angle is limited to the region of 0 Degree to 90 Degree.

2.4. FINAL OPTIMIZATION PROBLEM

An optimization problem including the above mentioned features can now be written as

$$\begin{aligned} \text{Min}_{\mathbf{x}} f(\mathbf{x}) &= (v_{12}^H - v_{12}^0), \mathbf{x} = (s_1, s_2, \Lambda, s_n, t_1, t_2, \Lambda, t_n) \\ \text{s.t. } s_i &\geq \underline{s}_i, s_i \leq \bar{s}_i \\ t_i &\geq \underline{t}_i, t_i \leq \bar{t}_i (i = 1, 2, \Lambda, n) \end{aligned} \quad (1)$$

where s_i and t_i represent the length and thickness of the polygon sides respectively. For equal side polygon problem, the optimization problem becomes

$$\begin{aligned} \text{Min}_{\mathbf{x}} f(\mathbf{x}) &= (v_{12}^H - v_{12}^0), \mathbf{x} = (t, \alpha) \\ \text{s.t. } t &\geq 0 \\ \alpha &\leq 90^\circ \\ -\alpha &\leq 0^\circ \end{aligned} \quad (2)$$

This optimization problem will be solved using Golden-division method for a series of thickness parameters t . The iteration procedure will end when the change in the angle or the objective function from step to step is lower enough, for example less than 10^{-4} .

3. Homogenization Method

Assuming two-dimensional linear elasticity, the overall elastic behavior of a porous materials can be described by the constitutive relations expressed as:

$$\bar{\sigma}_{ij} = E_{ijkl}^H \bar{\epsilon}_{kl} \quad (3)$$

Where over bar denotes the volume average. The effective elastic properties E_{ijkl}^H of porous materials are computed using a numerical homogenization method as described in the following. The effective Poisson's ratio is

$$\nu_{12}^H = \frac{E_{1122}^H}{E_{1111}^H}, \quad \nu_{21}^H = \frac{E_{1122}^H}{E_{2222}^H} \quad (4)$$

In the followings, the important equations of the homogenization theory are summarized. The detail of this theory may be found in the literatures [1, 3, 4].

The effective elastic properties is determined by the equation

$$E_{ijkl}^H = \frac{1}{|Y|} \int_Y (E_{ijkl} - E_{ijmn} \frac{\partial \Psi_n^{kl}}{\partial y_m}) dy \quad (5)$$

Where the displacement fields $\Psi_i^{mn}(y)$ are the periodic solutions of the following cell problem

$$\int_Y (E_{ijmn} - E_{ijkl} \frac{\partial \Psi_k^{mn}}{\partial y_l}) \frac{\partial v_i}{\partial y_j} dy = 0, \quad \forall \mathbf{v} \in V_Y = \{\mathbf{v}: \mathbf{v} \text{ is } Y\text{-periodic}\} \quad (6)$$

The above problem is usually solved by finite element method. The base cell is discretized by finite elements and solving equation (6) means solving a finite element problem with periodic boundary conditions for three different prestrain problem.

4. Examples

Let's consider an Aluminium with uniformly distributed pores. The solid structure of Aluminium is a 6-sides polygon skeleton type one. The periodic microstructure and the unit cell are shown in Fig.1. The Yang's modulus and Poisson's ratio are 6.958×10^4 Mpa and 0.3148, respectively.

TABLE 1. microstructure parameter and properties of materials with zero Poisson's ratio for various thickness.

t	α /Degree	Fraction	E_1 /Mpa	E_2 /Mpa	G_{12} / Mpa
10	-0.3038	0.1458	7087.03	103.81	41.3
20	-0.9977	0.2848	14462.00	645.08	275.96
30	-2.4270	0.2848	22456.00	1905.70	934.38
40	-5.1850	0.5696	31842.00	3955.00	2306.10

For a series of variable thickness values, the angles which make the materials exist zero effective Poisson's ratio are determined. When $t = 20$, the microstructure of materials with zero Poisson's ratio is expressed in Figure 2. In this case, the angle is 0.9977 degree. The other parameters of properties of materials are listed in Table 1. Figure 3 shows the variation of Poisson's ration with angle degrees. For different thicknesses, the angle may be different, but this difference is small, see Table 1.

5. Conclusion

From a skeleton type microstructure of composites with a material phase and a void phase, designing the shape of the structure of the material phase can make the materials

have a specific overall behavior, zero Poisson's ratio. The example shows that the shape optimization method is effective.

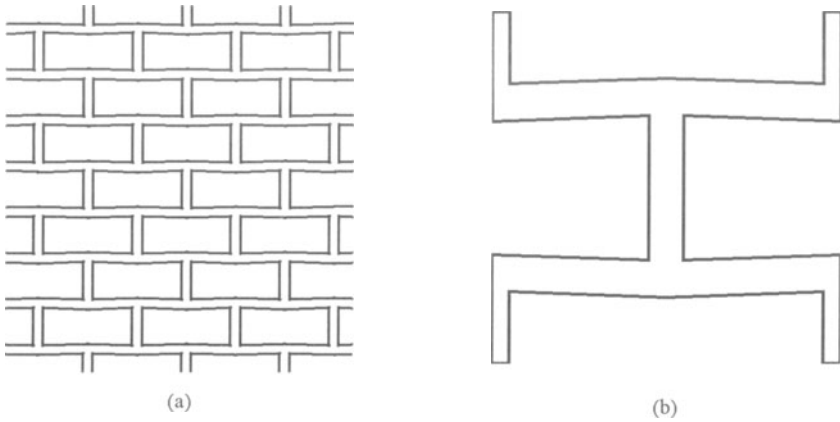


Figure 2. The periodic structure(a) and unit cell(b) of materials with zero Poisson's ratio

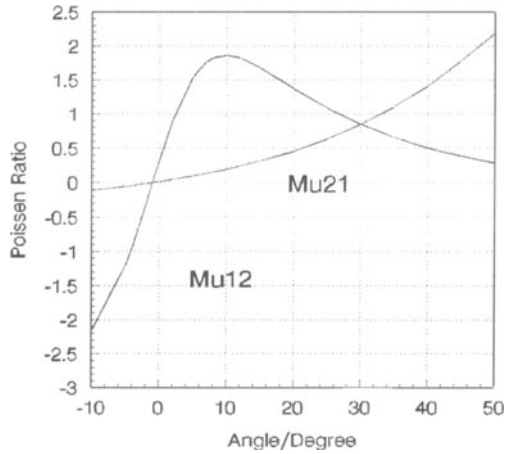


Figure 3. Variation of Poisson's ratio with angle

6. References

1. Guedes and Kikuchi, N.: Preprocessing and postprocessing for materials based on the homogenization method with adaptive finite element methods, *Computer method in applied mechanical engineering*, **83** (1991), 143-198
2. Lakes, R. : Foam structures with negative Poisson's ratio, *Science*, **235**, (1987), 1038-1040

3. Liu, S.T., Cheng, G.D.: Homogenization-based method for predicting thermal expansion coefficients of composite materials, *Journal of Dalian University of Technology (In Chinese)*, **35** (1995), 451-457
4. Liu, S.T., Cheng, G.D.: Prediction of coefficients of thermal expansion for unidirectional composites using homogenization method, *Acta Materiae Compositae Sinica (In Chinese)*, **14** (1997), 76-82
5. Sigmund O. and Torquato, S.: Design of materials with extreme thermal expansion using a three-phase topology optimization method, *Dannish Center for applied mathematics and mechanics*, Report No. 525 (1996), Technical University of Denmark

SHAPE OPTIMIZATION AND ADAPTIVITY OF AXISYMMETRICAL SHELLS UNDERGOING GEOMETRIC NONLINEARITIES

H. NACEUR, S. TRIKI, J.L. BATOZ, C.KNOPF-LENOIR
*Université de Technologie de Compiègne, Lab. LG2mS
Département GSM, B.P. 20529, 60205 Compiègne Cedex, France*

ABSTRACT: In this paper a general methodology to perform shape optimization of geometrically non-linear shells of revolution including automatic mesh generation, error estimation technique and adaptivity, is proposed. The optimization process is carried out by coupling non-linear FE analysis, B-Spline shape parametrization, sensitivity analysis, mathematical programming and automatic adaptive mesh refinement. An efficient sensitivity analysis is used to determine the gradients of the objective function and constraints. An example of shell optimization is considered to illustrate the application of the proposed approach

1. Introduction

Shape optimization process for geometrically non-linear shells of revolution involve several computational aspects [1-3]. The first is the structural response analysis, which consist of solving the governing equilibrium equations for a given geometry using efficient finite element formulations such as those presented in [4,5]. The second is the shape parametrization and the selection of a relevant number of design variables. This is a crucial step since different curve parametrizations [7] have a great influence upon the quality of the design results and can sometimes lead to optimal shapes which are not practicable from the engineering point of view. The third phase is the discretization error estimator, adaptivity and the automatic mesh generation. Without it, one cannot assure the accuracy of the structural analysis as the shape changes during the optimization cycles. The last phase includes the design sensitivity analysis and the non-linear constrained optimization package based on the sequential quadratic programming method [8]. The values of the objective function, constraints and their

gradients provide a new geometry. In this paper we will present an efficient approach to shape optimization of axisymmetrical shells undergoing large displacements and rotations.

2. Shape optimization problem

Here we adopt the approach of shape optimization based on *design element technique*, in order to minimize the number of design variables [6,7]. The problem is to find the shape of each design element. The structure is subjected to a given set of external loads, while minimizing an objective function which is an integral of the Von Mises stress criterion.

$$J = \sum_{e=1}^{nelt} \int_{v^e} \left(\frac{\sigma_{vm}}{\sigma_e} \right)^{2p} dv^e = \sum_{e=1}^{nelt} \int_{v^e} \left(\frac{\sigma_s^2 + \sigma_\theta^2 - \sigma_s \sigma_\theta + 3\sigma_{sz}^2}{\sigma_e^2} \right)^p dv^e \quad (1)$$

Where v^e is the finite element volume, σ_e is the elastic limit of the material and p is a exponent which takes values 0, 1, 2, When $p = 0$ we minimize the weight of the structure and when p becomes greater than 2 we try to minimize the maximum of Von Mises criterion. The shape optimization problem of the axisymmetrical shell structure is stated mathematically as:

$$\begin{aligned} \min J(\vec{v}), \quad \vec{v} \in R^n \\ \text{subject to } g_j(\vec{v}) \leq 0 \quad j = 1, m \\ v_{il} \leq v_i \leq v_{iu} \quad i = 1, n \end{aligned} \quad (2)$$

where $J(\vec{v})$ is the objective function, \vec{v} is the design variable vector, $g_j(\vec{v})$ are equality and inequality constraints. v_{il} and v_{iu} are the lower and upper bounds of the i th component of \vec{v} . The optimization algorithm we have used is coded in an SQP subroutine available from the IMSL/MATH library (Powell 1978) [8].

3. Shape parametrization

In our approach cubic B-Splines are used to represent the shape of the structure. They allow a C^2 continuity which is well sufficient for our applications. The geometry of the structure is divided into a few subregions, named "*design elements*", each one is described by two end *control points*. Connected together they give a good approximation of the geometry of the structure. Each design element consists of several finite elements, with

geometrical, material properties, supported loads and boundary conditions extracted directly from those of the design element they belong to. Thus, with this definition our structural parametrization presents a quite general form. The shape design parameters are some or all *control points* coordinates. The optimization constraints such as displacements or stresses limitations can also be imposed at these *control points*.

4. Axisymmetric non-linear F.E. formulation

For our non-linear analysis we consider a Total Lagrangian Formulation (TLF) valid for large displacements, large rotations and small elastic strains. A simple Reissner-Mindlin conical shell element with two nodes and three degrees of freedom per node U , V , and β is developed. The displacement gradient tensor $[F]$ defined such that $d\vec{x}_q = [F] d\vec{x}_q^0$ can be expressed as [4]:

$$[F] = \begin{bmatrix} 1 + u_{p,s} + z \cos\beta \beta_{,s} & 0 & \sin\beta \\ 0 & 1 + \frac{1}{r}(u_q \cos\varphi - w_q \sin\varphi) & 0 \\ w_{p,s} - z \sin\beta \beta_{,s} & 0 & \cos\beta \end{bmatrix} \quad (3)$$

For small strains we can consider the following approximate expressions for the G-L strains:

$$E_{ss} = e_s + z \chi_s, \quad E_{\theta\theta} = e_\theta + z \chi_\theta, \quad 2E_{sz} = \gamma_s \quad (4)$$

with

$$\begin{cases} e_s = u_{p,s} + \frac{1}{2}(u_{p,s}^2 + w_{p,s}^2) \\ e_\theta = \frac{U}{r} + \frac{U^2}{2r^2} \\ \chi_s = [(1 + u_{p,s}) \cos\beta - w_{p,s} \sin\beta] \beta_{,s} \\ \chi_\theta = \frac{1}{r} [\sin\beta \cos\varphi + (1 - \cos\beta) \sin\varphi] \left(1 + \frac{U}{r}\right) \\ \gamma_s = (1 + u_{p,s}) \sin\beta + w_{p,s} \cos\beta \end{cases} \quad (5)$$

For small strains, but large displacements and large rotations a linear material behaviour law can be considered between the second Piola Kirchhoff (PK2) stresses and the Green-Lagrange strains. After integration through the shell thickness we can obtain:

$$\{N\} = [H] \{E\} \quad (6)$$

where $\langle N \rangle = \langle N_s \ N_\theta \ M_s \ M_\theta \ T_s \rangle$ and $\langle E \rangle = \langle e_s \ e_\theta \ \chi_s \ \chi_\theta \ \gamma_s \rangle$. By considering a single Gauss point for integration, the internal force vector can be defined in the global coordinate system as:

$$\{F_{int}\} = 2\pi r L [T]^T [B]^T \{N\} \quad (7)$$

Then the problem is to solve the system of nonlinear equations:

$$\{R\} = \{F_{int}\} - \{F_{ext}\} = \{0\} \quad (8)$$

5. Mesh generation and adaptive refinement

At each iteration of the optimization process, a new design model is created. Then a uniform mesh inside each design element is generated. After imposing the applied loads and the boundary conditions, a first and complete non-linear finite element analysis is carried out. According to the results obtained, the discretization error estimator provides indications on how and where the mesh has to be modified. Following this instruction, a procedure updates the mesh. Once again the applied loads and the boundary conditions are imposed on the new mesh. Instead of carrying a complete non-linear finite element analysis, the last finite element solution is transferred on the new mesh and taken as an initial solution to the new mesh. The procedure is repeated until the percentage error on the finite element results is less or equal to a fixed value defined by the user.

For each element, the strains are evaluated at the middle of the element and provide discontinuous distribution. The errors can be defined as:

$$e_E = E - E_h \quad (9)$$

where E are the exact values for strains, E_h are those obtained by the finite element model. The unknown exact values are replaced by "smoothed" ones and denoted by \hat{E} :

$$\hat{E}(s) = N_k(s) \hat{E}_{hk} \quad (10)$$

where \hat{E}_{hk} is the value obtained at Gauss point, in the element k , $N_k(s)$ is a quadratic shape function in the element k . So the smoothed values obtained using equation (10) can be substituted effectively to the exact solution to estimate the error i.e:

$$\hat{e}_E = \hat{E} - E_h \quad (11)$$

The strain energy norm, expressed in terms of the generalized strains can be written as:

$$\| \hat{e} \|^2 = \sum_k 2\pi \int_0^L \langle \hat{e}_E \rangle [H] \{ \hat{e}_E \} r ds = \sum_k \| \hat{e}_k \|^2 \quad (12)$$

The elementary contribution $\| \hat{e}_k \|$ is integrated numerically by using two Gauss points. The global relative error which represent the percentage error is defined by:

$$\eta = \frac{\| \hat{e} \|}{\| \hat{W} \|} \quad (13)$$

$$\text{with } \| \hat{W} \|^2 = \sum_k 2\pi \int_0^L \langle \hat{E} \rangle [H] \{ \hat{E} \} r ds = \sum_k \| \hat{W}_k \|^2$$

For the refinement procedure, we define the acceptable elementary error as:

$$\bar{\rho} = \bar{\eta} \left(\frac{\| \hat{W} \|^2}{n} \right)^{1/2} \quad (14)$$

where n is the number of elements and $\bar{\eta}$ is the percentage error requested by the user. It is possible to evaluate coefficients which define the size change of the elements by $\xi_k = \frac{\| \hat{e}_k \|}{\bar{\rho}}$, Thus the new size \bar{l}_k of the element k is given by $\bar{l}_k = C_k l_k (\xi_k)^{-1/p}$, where l_k is the actual size, C_k is a correction coefficient and p is the element convergence rate. For the present two nodes shell element we consider $C_k = 1$ and $p = 1$.

6. Sensitivity analysis

Let the objective function be represented as :

$$F = F(\vec{v}, \vec{U}) \quad (15)$$

The problem of design sensitivity analysis is to calculate the total derivative of F at (\vec{v}, \vec{U}) as:

$$\frac{dF}{dv_i} = \frac{\partial F}{\partial v_i} + \left\langle \frac{\partial F}{\partial U} \right\rangle \left\{ \frac{\partial U}{\partial v_i} \right\} \quad i = 1, n \quad (16)$$

The differentiation of equation (8) with respect to a design variable, leads to :

$$[K_T] \left\{ \frac{\partial U}{\partial v_i} \right\} = - \left\{ \frac{\partial R}{\partial v_i} \right\} \quad i = 1, n \quad (17)$$

where $[K_T]$ is the tangent stiffness matrix and $\{R\}$ the residual vector. By introducing an adjoint variable vector $\{P\}$ solution of $[K_T]^T \{P\} = -\{\frac{\partial F}{\partial U}\}$, then equation (16) and equation (17) give :

$$\frac{dF}{dv_i} = \frac{\partial F}{\partial v_i} + \langle P \rangle \left\{ \frac{\partial R}{\partial v_i} \right\} \quad i = 1, n. \quad (18)$$

The total derivatives of all constraints, can be calculated in the same manner, by replacing F with g_j where g_j is the j th constraint function. For any choice of the objective function the terms $\{\frac{\partial F_{int}}{\partial v_i}\}$ and $\{\frac{\partial F_{ext}}{\partial v_i}\}$ will be unchanged because they do not depend on the objective function.

7. Numerical application

The structure to be optimized is (in its initial geometry) a simply supported circular plate subjected to a circonfential load at the edge. The mechanical properties used are: $E = 1.2E6$, $\nu = 0.3$ and the total circonfential load is $P = -1.0E6$.

The shape is described by six definition points (five design elements) which are the control knots of B-Spline curves. The chosen design variables are the coordinates z_1, z_2, z_3, z_4, z_5 and z_6 of definition points (Figure 1.). The shape optimization problem consists in finding the best shape of the middle shell surface which minimizes the Von-Mises stress, with the geometrical constraints allowing variations of the design variables inside the interval $[-1, +1]$, and an equality constraint on the displacement of the center of the plate $W_1 = +2 \text{ cm}$. The objective function is given by equation (1), with $p = 2$.

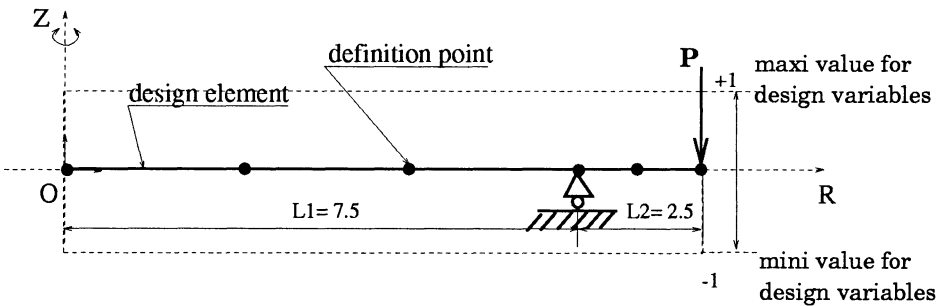


Figure 1. Shape optimization design model

For numerical study of the optimization problem we use the geometrical parameters given in Figure 1 which represent the design model. We note that for 3% discretization error 29 elements are needed. Figure 2 shows the geometrically non-linear behaviour of both, the initial flat plate and

the optimum shell. The displacement at the center of the flat plate is $w = 1.32 \text{ cm}$ for $P = -1.E + 06$.

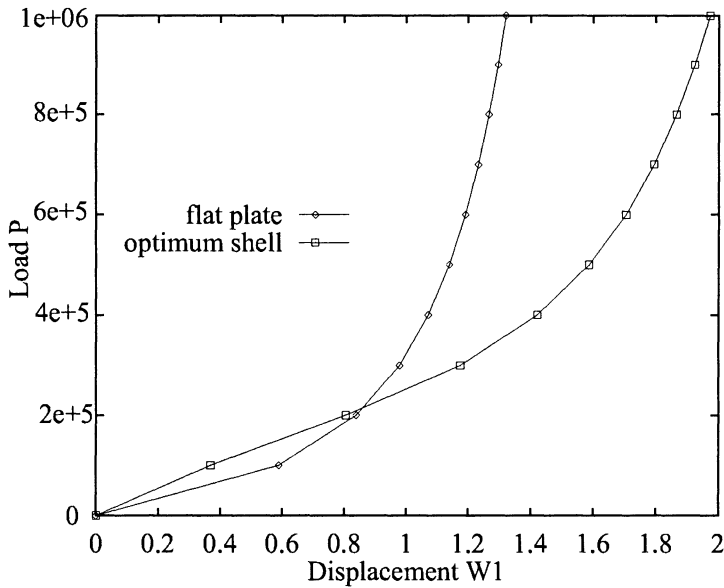


Figure 2. Load displacement curves at the center of the structure

The optimization algorithm converges after 19 iterations. The optimized shell structure leads to a reduction of 43.76% of the objective function. The number of elements for the optimal structure is about 42 for a discretization error fixed at 3%. Figure 3 represents the FE model of the optimal shell structure and its deformed configuration. The displacement at the center of the shell is about $W_1 = +1.973 \text{ cm}$ and very close to $+2 \text{ cm}$ (Figure 3).

8. Conclusion

A general methodology to optimize the shape of shells of revolution taking into account the large displacements, large rotations and small elastic strains. Our formulation includes a general shape parametrization to approximate the geometry, a discretization error estimation and mesh adaptivity for an automatic control of the accuracy of the F.E. results during the optimization process preventing mesh distortions. An explicit method is used to evaluate the sensitivities to reduce the CPU time by a large amount.

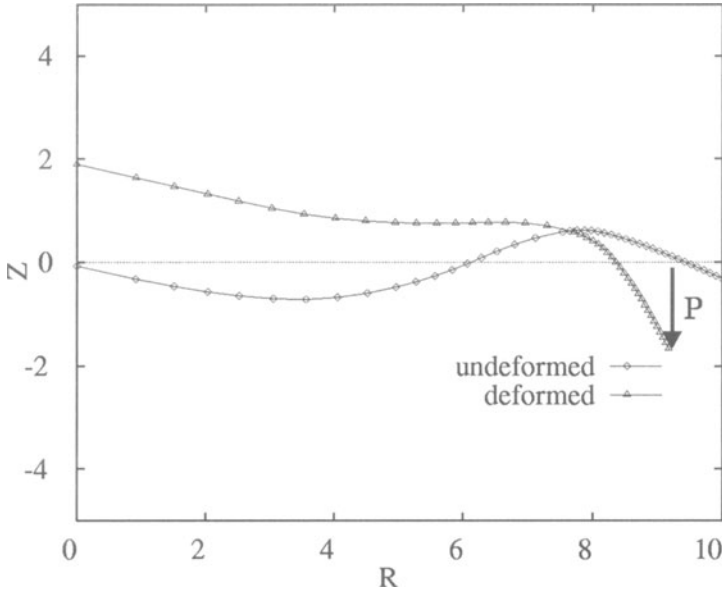


Figure 3. Meshes on the optimum shell

9. References

1. A.A. Polynkine, F. Van Keulen and V.V. Toropov, "Optimization of geometrically non-linear structures based on a multi-point approximation method and adaptivity", Eng. Comput., Vol 13, No. 2/3/4, 76-97, (1996).
2. K.M. Okstad and K.M. Mathisen, "Towards automatic adaptive geometrically non-linear shell analysis, Part I: Implementation of an h-adaptive mesh refinement procedure", Int. J. Meth. Eng., 37, 2657-2678 (1994).
3. G. Bugeda and J. Oliver, "A general methodology for structural shape optimization problems using automatic adaptive remeshing", Int. J. Num. Meth. Eng., 36, 3161-3185 (1993).
4. S. Triki, "Analyse linéaire et nonlinéaire auto-adaptative des coques de révolution par éléments finis", Thèse de Doctorat, UTC, (1996).
5. W. Wagner, "A finite element model for non-linear shells of revolution with finite rotations", Int. J. Num. Meth. Eng., 29, 1455-1471 (1990).
6. E. Ramm, K. U. Bletzinger and S. Kimmich, "Strategies in shape optimization of free form shells", Festschrift Erwin Stein, Nonlinear Computational Mechanics, Springer, Berlin, Heidelberg, (1991).
7. V. Braibant and C. Fleury, "Shape optimal design using B-Splines", Comput. Methods Appl. Mech. Eng., 44, 247-267 (1984).
8. M.J.D. Powell, "A fast algorithm for nonlinearly constrained optimization calculations", G.A. Watson (ed.), 630, New-York, (1978).

TOPOLOGICAL OPTIMIZATION OF SHELLS WITH NON UNIFORM THICKNESSES

Vibration Case

E. PAGNACCO and E. J. SOUZA de CURSI
*Laboratoire de Mécanique de Rouen,
UPRES-A CNRS 6104 & INSA de Rouen, B.P. 8,
76801 Saint-Etienne du Rouvray Cédex, France.*

This work concerns the automatic design of minimum weight spare parts, under geometrical and frequencies constraints. We propose a method of rapid topological optimization which has successfully solved industrial situations involving about 3,000 unknowns. In the considered approach, the topology of the structure is characterized by an unknown thickness distribution and the frequency constraint is treated by a dual method.

1. Introduction

One of the main design problem for the car industry is to rapidly find the morphology of the lightest elastic homogeneous spare part required for a specific task. Geometrical constraints exist as a result of space limitations and casting production processes and vibration analysis introduces lower bounds on eigenfrequencies of a particular mode shape.

This kind of problem has often been treated by describing the morphology as a parametric model in CAD systems (shape optimization). However, these approaches implicitly introduce preliminary assumptions on the topology of the spare part: the number of holes and connectivity are imposed.

Other approaches that permit varying topologies have been proposed: for instance the spare part may be characterized by a density of matter and the holes correspond to regions where the density is equal to zero. This approach leads to numerical and mathematical difficulties that are only partially solved by homogenization methods (see for example [1]). Moreover the first design steps need to be completed in a short time, whereas homogenization leads to computationally expensive methods.

An efficient approach is proposed here to optimize the topology of shell structures (given the constraint of the design space available). The topology is characterized by a mean surface and a thickness distribution ρ (holes correspond to regions where ρ is equal

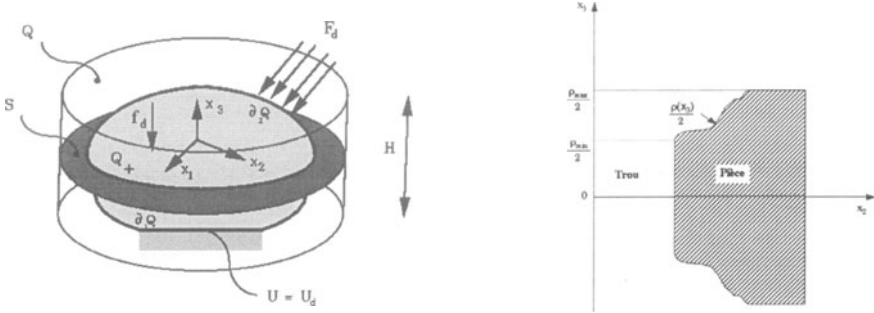


Figure 1. a) Problem description, and b) a view of the thickness near a hole.

to zero) [2]. The combination of this surface assumption, and advanced analysis and optimization strategies offer an efficient pre-design tool.

In this work, we assume that the mean surface is determined or imposed, thus only the thickness map has to be determined. After introduction of the mathematical model, a solving technique is proposed for the optimization problem. The optimization process is based on solving the Lagrangian stability equations with a particular linearization of the vibration constraint. This approach is suggested by physical considerations, which show that the mechanically consistent solutions must satisfy such stability conditions. Finally, an application to a car distribution hood is presented.

2. Shell Model

The spare parts are considered as shells (Fig. 1a). Shells are defined by a mean surface $S \subset R^3$, assumed regular and bounded. Its boundary is denoted ∂S and is decomposed into two parts Γ_1 and Γ_2 : $\partial S = \Gamma_1 \cup \Gamma_2$. S is described by curvilinear coordinates $a = (a_1, a_2) \in \Omega \subset R^2$

$$S = x(\Omega) = \{x = (x_1, x_2, x_3) \in R^3 \mid x = x(a), a \in \Omega\} \quad (1)$$

The intrinsic basis on S is generated by $e_1 = \frac{\partial x}{\partial a_1}$, $e_2 = \frac{\partial x}{\partial a_2}$ and $e_3 = \frac{e_1 \wedge e_2}{|e_1 \wedge e_2|}$. The region Q occupied by the spare part is defined by a thickness distribution $\rho : \Omega \rightarrow R$:

$$Q = \{x + re_3 \in R^3 \mid x \in S, -\frac{\rho(x)}{2} < r < \frac{\rho(x)}{2}\} \quad (2)$$

Thus, the parameter ρ defines the topology of the spare part: the holes are the regions where $\rho = 0$. The lateral boundary of Q is denoted by $\partial Q_{lat} = \{x + re_3 \in Q \mid x \in \partial S\}$. In the sequel, we consider, for $i = 1, 2$,

$$\partial Q_i = \{x + re_3 \in Q \mid x \in \Gamma_i\} \quad (3)$$

We can split Q in two sub-regions $Q_0 = \{x \in Q \mid \rho = 0\}$ and $Q_+ = \{x \in Q \mid \rho > 0\}$: $Q_+ \cup Q_0 = Q$. The holes correspond to Q_0 and the spare part to Q_+ . In addition, we

shall also consider $Q(\alpha+) = \{x \in Q \mid \rho \geq \alpha\}$ in which α is an inferior bound on ρ (Fig. 1b). In this case $Q_+ = Q(\alpha+)$. The geometrical constraint is implicitly treated by providing S and the maximal thickness $H > 0$ (the results can be extended to the situation where $H : \Omega \rightarrow R$ is a function). The region of S corresponding to the holes is $S_0 = \{x \in S \mid \rho(x) = 0\}$ and the region of S corresponding to the spare part is $S_+ = \{x \in S \mid \rho(x) > 0\}$. Thus, the determination of the topology is equivalent to the determination of S_0 or its complementary S_+ : these two sets are entirely characterized by the thickness distribution ρ . In the following, we consider the determination of the thickness distribution problem.

The material constituting part Q is assumed to be elastic and homogeneous. The stationarity of the discrete energy functional for such a linear undamped structure leads to the discrete time invariant linear equation for free vibrating structures written in the frequency domain: $(K - \omega_j^2 M)\Phi_j = 0$ where K and M are the discrete global rigidity and mass matrices and ω_j and Φ_j are the j -th pulsation and j -th eigenmode.

3. Optimization Problem

The standard discretized formulation is given by:

$$\begin{cases} \min(f(h_i) = \sum_i a_i h_i) & i = 1, \dots, n \\ g = \omega_j^2 - \varpi_j^2 \geq 0 \\ h_i = 0 \quad \text{for} \quad \rho_{min} \leq h_i \leq \rho_{max} \end{cases} \quad (4)$$

The cost function f represents the mass of the spare part. The first constraint is an *imposed* mode j with a pulsation ω_j higher than a threshold pulsation ϖ . The second one introduces geometrical limitations: ρ_{min} is a threshold of matter below which a hole is assumed and ρ_{max} is a maximum value of the thickness. Surface S is defined by the mesh for the space available to design. The optimization parameter is the thickness distribution ρ of the shell discretized by the element thickness h in n elements. Thus, the same discretization is used for the mesh of the mean surface and for the discretized thickness distribution. This is an interesting feature since the mesh can be easily refined in order to approximate conveniently the thickness distribution. That ensures consistency for the approximations used for both the finite element model and thickness distribution. Moreover, such a discretization is sufficient because in the first design steps, we only need a rough idea of the overall shape.

Difficult mathematical questions concerning this problem are still with us, such as the existence of solutions and Lagrange multipliers which are closely connected to the topological properties of the set of admissible configurations (for example, its closure or the existence of an interior). These questions will not be evoked here since this work is mainly concerned with the numerical aspects of the problem. We point out that a particular treatment has to be considered when multiple eigenvalues are involved: this point will be not developed in the sequel, due to length limitation.

3.1. RESIZING RULE

Due to the non-linear nature of the eigenvalue constraint, problem (4) requires sequences of solutions of more simple approximate problems. Currently, calculating second sensitivity derivatives of eigenvalue constraints with respect to n design variables is still too expensive in terms of computational cost and storage. Thus, sequential quadratic programming methods are not practical for large problems and it has been advised to use a sequence of linearized sub-problems [3]. In addition, shell behaviour in vibration is known to be governed by inertial effects (themselves being thickness dependent). This mechanical knowledge is taken into account by sub-problems obtained from a Taylor series expansion about $h^{1-\eta}$ (for $\eta = 2$ linearization is obtained about reciprocal variables of h)

$$\left\{ \begin{array}{l} \min (f = \sum_i a_i h_i) \quad i = 1, n \\ g = g(h_{0i}) + \sum_{i|h_{0i} \neq 0} \left[\left(\frac{h_i}{h_{0i}} \right)^{1-\eta} - 1 \right] \left(\frac{h_{0i}}{1-\eta} \right) \frac{\partial g(h_{0i})}{\partial h_i} \geq 0 \quad \text{for } \eta \neq 1 \\ \rho_{min} \leq h_{li} \leq h_i \leq h_{ui} \leq \rho_{max} \quad \text{or } h_i = 0 \text{ for } h_i < \rho_{min} \end{array} \right. \quad (5)$$

The last set of equations introduces additional constraints (move limits) with h_{li} and h_{ui} used to reduce the domain of variation of the variables. These bounds must be chosen to guarantee a good approximation of the problem within the move limits.

Because there exists only one constraint (except side constraints) it is recommended to treat the dual problem of (5). The h -stationarity of the Lagrange functional associated to the dual sub-problems leads directly to the iterative scheme (denote by superscript k) for the thickness variable

$$h_i^{k+1} = \text{proj}_{[h_{li}, h_{ui}]} \left[h_i^k \cdot \left(\alpha + (1-\alpha) \cdot \left(\lambda \cdot \frac{\partial g / \partial h_i}{\partial f / \partial h_i} \right)_k^{1/\eta} \right) \right] \quad i = 1, \dots, n \quad (6)$$

with a relaxation factor $0 < \alpha \leq 1$. The Lagrange multiplier λ is obtained by assuming that it corresponds to an extremum of L :

$$\lambda = \left[\left((\eta - 1)g + \sum_{i \in I_a} \frac{\partial g}{\partial h_i} h_i^k \right)^{-1} \times \sum_{i \in I_a} h_i^k \frac{\partial g}{\partial h_i} \left(\frac{\partial f / \partial h_i}{\partial g / \partial h_i} \right)^{-\frac{1-\eta}{\eta}} \right]^{-\frac{\eta}{1-\eta}} \quad (7)$$

with I_a the set of variables within h_{li} and h_{ui} . Numerical efficiency is due to the fact that no matrix inversion is required in this scheme.

3.2. RESTORATION MOVE

One difficulty caused by the nonlinearity of the constraint is that this search moves away from the constraint boundary (search is done in the tangent subspace that no longer follows exactly the constraint boundary). So, a restoration move is performed to bring h back to the constraint boundaries. In this case, a small correction $\Delta h = h^{k+1} - h^k$ in the

perpendicular subspace must be found so that constraint g is exactly satisfied. The form of this new sub-problem is:

$$\begin{cases} \min_{\Delta h} (\frac{1}{2} \Delta h^T \Delta h) \\ g = 0 \end{cases} \Rightarrow \Delta h = -N (N^T N)^{-1} C \quad (8)$$

with a first-order approximation of $g = N^T \Delta h + C$. Such an approximation was suggested in [4] for one variable design. It is based on the integration of the differential equation of g

$$\frac{\partial g}{\partial h_i} = \frac{\Phi_j^T \left(\frac{\partial K}{\partial h_i} - \omega_j^2 \frac{\partial M}{\partial h_i} \right) \Phi_j}{\Phi_j^T M \Phi_j} \quad (9)$$

By considering that the gradients $\frac{\partial \bullet}{\partial h_i}$ finite element matrices are constant, one obtains:

$$N = \{dM_i\}, \quad C = -\ln \left(\frac{\omega_j^2 - \frac{\{dK_i\}^T \{dK_i\}}{\{dK_i\}^T \{dM_i\}}}{\varpi^2 - \frac{\{dK_i\}^T \{dK_i\}}{\{dK_i\}^T \{dM_i\}}} \right) \quad \text{with} \quad d\bullet_i = \frac{\Phi_j^T \frac{\partial \bullet}{\partial h_i} \Phi_j}{\Phi_j^T M \Phi_j} \quad (10)$$

First, this correction must be applied before optimization until g is small enough because, for practical applications, the first design of shell structures (given without stiffeners) is generally non-admissible. Next, during the optimization iterations, the restoration move is combined with improvement step (6) to give:

$$h^{k+1} = \text{proj}_{[h_{li}, h_{ui}]} \left[h^k \cdot \left(\alpha + (1 - \alpha) \cdot \left(\lambda \cdot \frac{\partial g / \partial h}{\partial f / \partial h} \right)_k^{1/\eta} \right) - N (N^T N)^{-1} C \right] \quad (11)$$

3.3. MODE TRACKING STRATEGY

The spare part is modified during optimization, so the eigenvalues can change from iteration k to iteration $k + 1$. If the frequency constraint concerns the eigenvalue associated to a given normal mode, special attention must be given to the possible modification of the ordering of this mode: frequencies can be modified in such a way that mode Φ_i (corresponding to the i -th eigenvalue) at iteration k becomes Φ_j at step $k + 1$. In this case, the method must be able to follow the target optimization mode, and find index j : we must ensure that the optimization concerns the same mode at each step. It can be performed by evaluating a Modal Assurance Criterion (MAC),

$$MAC = \frac{(\Phi_j^T \Phi_i)^2}{(\Phi_j^T \Phi_j) (\Phi_i^T \Phi_i)} * 100 \quad (12)$$

which is expected to be maximum when the same mode is considered ($\Phi_i = \Phi_j$).

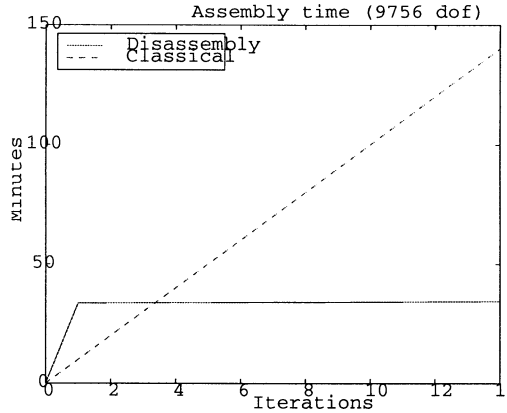


Figure 2. Cpu-time comparison between disassembly method and classical assembly.

4. Model Updating

The optimization technique is efficient because no large matrix is inverted, but the finite element analysis is still time consuming when the number of finite elements is important. First, a constant mesh is kept during optimization for efficiency purposes. Only nodes freed during the formation of holes need particular attention. Time and problems involved in remeshing are eliminated. Second, a part of the cpu-time is spent in assembling finite element matrices. Mass and stiffness matrices must be re-assembled after each correction of the thicknesses. Third, another part of the cpu-time is spent in calculating frequencies and modes shapes. The last part of the cpu-time is devoted to sensitivity calculation.

The disassembly technique explained below permits to save time during the assembly and sensitivity calculations, and the preconditioned conjugate gradient algorithm saves time during the eigenproblem. Note that these two improvements are not fast reanalysis techniques which involve structural response error.

4.1. THE DISASSEMBLY TECHNIQUE

In fact, design parameters impact exclusively the constitutive relation. This leads to the idea of using a representation of finite element matrices where the contribution of unchanged data (such as nodes coordinates, connectivity, ...) is disconnected from constitutive equations. Such a representation may be formulated as $K(h) = QW(h)Q^T$, using the stiffness matrix as an example. The same decomposition may be written with the mass matrix. In this decomposition mesh informations are stored in matrix Q while matrix W is diagonal and depends on the updated design variables h . Hence, any updating of the model only involves re-assembly of the diagonal matrix W . Evaluation of Q is more expensive than a classical evaluation of $K(h)$, but needs to be done once for all. As shown in fig. 2 for the example treated below, the disassembly technique pays off in subsequent analyses. The same decomposition is used to efficiently compute sensitivity derivatives of finite element matrices with respect to design variables ($\frac{\partial K}{\partial h_i} = Q \frac{\partial W}{\partial h_i} Q^T$).

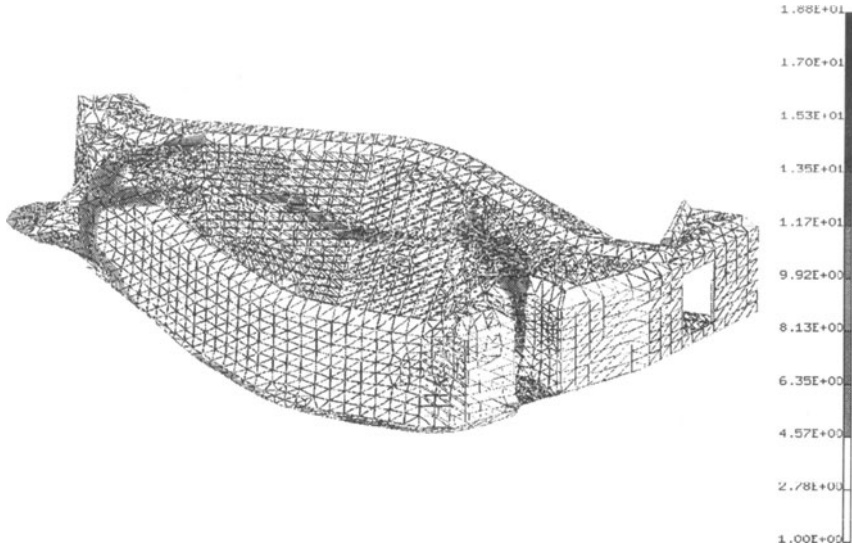


Figure 3. Optimal stiffening distribution on the hood mesh.

4.2. THE EIGENVALUE PROBLEM

For the eigenproblem, a subspace inverse iteration method is used. The main step of this method is to solve the equation $K\Phi^{k+1} = M\Phi^k$ until Φ -convergence. The conventional implementation is to use a Cholesky factorization of K at each optimization step for solving the eigenproblem. It is known that this Cholesky factorization is computationally expensive. The use of an iterative method based on the preconditioned conjugate gradient algorithm becomes advantageous in the context of structural optimization. The main idea is to use the Cholesky factorization of K as a preconditioned matrix for the first optimization step. Until large modifications in K occur, this preconditioned matrix remains meaningful. Therefore, only one Cholesky factorization can be computed for several optimization steps.

5. An Industrial Case

The result presented below has been obtained using a DKT18 shell element [5], which involves a Kirchhoff model of 6 degrees of freedom (dof) per node. The method has been implemented with MATLAB.

The optimal distribution and topology of stiffeners is determined for a car hood. The first global mode with a frequency above 250Hz is imposed. Material is polymer with properties of $E = 1000 \text{ mN/mm}^3$, $\nu = 0.42$, and $\mu = 1.36 \times 10^{-9} \text{ Kg/mm}^3$. The mesh has 9756 dof and 3078 design variables. Bounds on thicknesses are 1mm and 25mm . By specifying a strictly positive lower bound for the thickness, the overall shape is found without holes.

The initial shell has a mass of $0.106Kg$ and the frequency associated to the first mode is 90 Hz. An admissible configuration is first determined which may not be optimal: this leads to a part having a higher mass of $0.153Kg$, but which satisfies the frequency constraint. It is used to start the optimization. The final topology gives an admissible piece of $0.069Kg$. Figure 3 shows the distribution of thicknesses on the hood mesh. Regions in dark represent the topology of stiffeners.

Note that if a more precise optimized CAD model is sought after, a parameterized model can be defined from the knowledge of the overall shape stiffeners, then this shape can be optimized.

6. Conclusions

Structural topological optimization suffers from the curse of computational complexity which prevents its application to large-size dynamic finite element models. A numerical approach for the case of linear, undamped shells has been proposed. Emphasis has been put throughout this work to develop computationally efficient algorithms, for example, by using an assembly technique adapted to multiple reanalysis. The dual approach combined with a parameterized resizing rule is implemented in the Matlab environment. This procedure is illustrated successfully with a large-size structural model where about 3,000 design variables are optimized simultaneously on a workstation. Moreover, our particular choice of design variables and optimization method enables us to deal with structural and topological optimization within the same framework.

Developments presented here could be found in Reference [2] where the parameter η is adjusted to extend the range of validity of the approximation, and an extension to multiple frequency constraints with upper and lower bounds is given.

References

- [1] Diaz, A. and Kikuchi, N. (1992) Solutions to Shape and Topology Eigenvalue Optimization Problems using a Homogenization Method, *Int. J. Num. Meth. Eng.* **35**, 1487-1502.
- [2] Pagnacco, E. (1998) *Optimisation Topologique des Structures de Type Coques*, Ph. D. Thesis, Laboratoire de Mécanique de Rouen, UPRES-A CNRS 6104 & INSA de Rouen, Rouen.
- [3] Haftka, R.T. and Gürdal, Z. (1993) *Elements of Structural Optimization*, Kluwer Academic Publishers, Dordrecht.
- [4] Pritchard, J. I. and Adelman, H. M. (1990) Differential Equation Based Method for Accurate Approximation in Optimization, *AIAA/ASME/ASCE/AHS/ASC 31st Structures, Structural Dynamics and Materials Conference*, 414-424.
- [5] Batoz, J.L. and Dhatt, G. (1993) *Modélisation des Structures Par Eléments Finis*, Ed. Hermes, Paris.

NON-DETERMINISTIC METHODS FOR PRODUCT/PROCESS ANALYSIS AND ROBUST DESIGN – THE “POSSIBILISTIC” APPROACH

V. BRAIBANT*, F. DELCROIX**, A. OUDSHOORN*, C. BOYER*

* *Faculté Léonard de Vinci, Département Mécanique des Systèmes
92916 Paris La Défense Cedex, France*

** *Université Pierre et Marie Curie
LM2S, Tour 66, 5^{ème} étage, 75256 Paris Cedex*

Abstract

The development of methods to take into account uncertainties in structural analysis computations and in design optimisation procedures is attracting a fast growing interest from both the scientific and the industrial communities. *Possibilistic* methods in which uncertainties are represented by fuzzy numbers appear as an alternative to the classical *probabilistic* methods like the Monte-Carlo methods or the Statistical Finite Element Method. The principal difficulty of *possibilistic* methods is that they lead to the solutions of systems of equations whose coefficients are defined by intervals. The following paper presents several approaches for the solution of such systems, some of them original, taking the Vertex engineers' method as reference. Extension of these methods to inverse design problems is considered.

1. Introduction

As computational methods for structural analysis are now mature and more and more widely recognised, a new challenge is clearly to make possible estimation of effects of uncertainties. Uncertainties have different origins. Most of the time, they will be more or less directly related to product manufacturing and assembly processes. From the computational point of view, uncertainties lead to the scattering of analysis data like geometrical dimensions, material and physical properties, applied loads and boundary conditions and, in turn, scattering of structural responses.

When dealing with data uncertainties, several objectives are possible. The first one is clearly to get sensitivity information and quantify how structural responses will be influenced. Another objective is related to reliability and estimation of failure probabilities. However, the main benefit from non-deterministic computational methods is perhaps for design, either in helping the designer in fine tuning process parameters so as to achieve prescribed level of reliability, or to design structures as insensitive as possible to uncertainties. The latter is usually known as robust design.

There exist today several techniques to compute the statistical distributions of structural responses. The best knowns are the now classical Monte-Carlo Simulations (MCS) and the Stochastic Finite Element Method (SFEM). A third class of methods, which uses the concept of fuzzy numbers to represent uncertainties and arithmetic of intervals for computing structural responses, is considered in this paper. The latter differ from the classical “probabilistic” approaches such as MCS or SFEM in the sense that, instead of computing statistical distributions of structural responses, “distributions of possibilities” are obtained. For that reason, they are known as “possibilistic” approaches.

The idea to represent a distributed parameter by a fuzzy number is not new. The use of fuzzy logic to formulate a design problem can be found in literature [6], as well as the use of fuzzy arithmetic and arithmetic of intervals [1]. A fuzzy number can be seen as representing a distribution of possibilities, which describes the degree of membership of an uncertain parameter on a given range. In practice, the fuzzy response of a structure is computed in three steps. First, the fuzzy numbers describing the parameter uncertainties are sampled for different levels of degree of membership, resulting for each of them in the possible intervals of variation of the parameters. This is known as “fuzzification” (figure 1) :

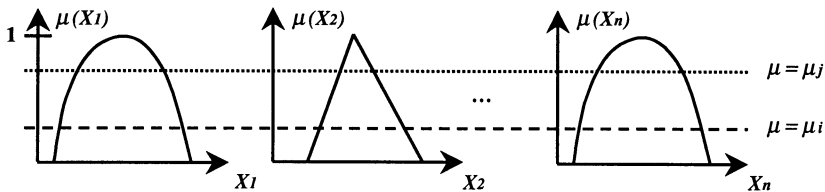


Figure 1 : Fuzzification

Second, the finite element equilibrium equations are solved for each level, leading to the corresponding intervals of variation of the structural responses (figure 2) :

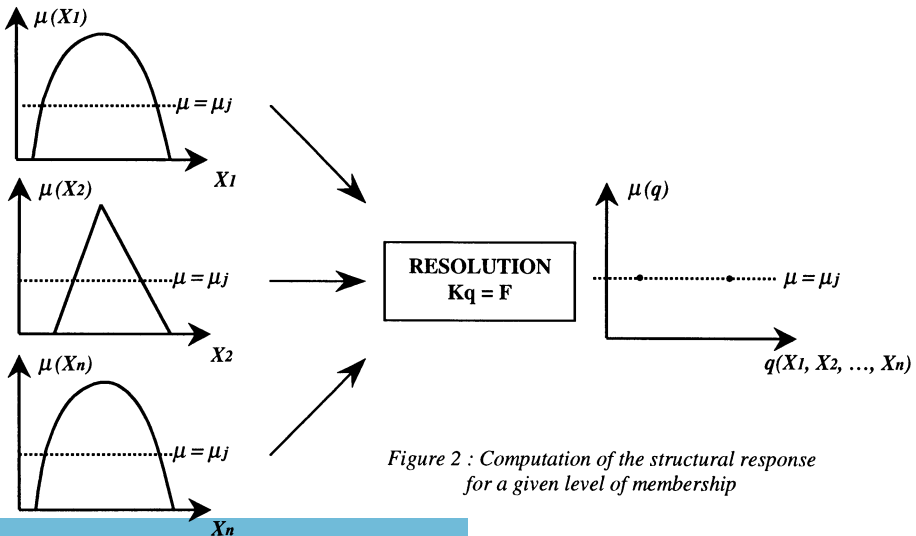


Figure 2 : Computation of the structural response for a given level of membership

Finally, putting together for each structural response the intervals related to the different degrees of membership allows to re-build the fuzzy response (figure 3) :

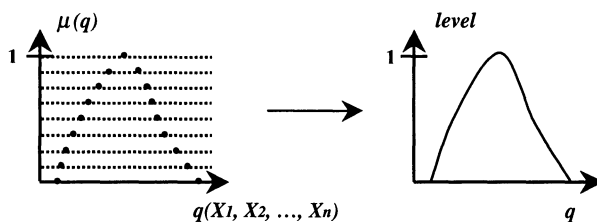


Figure 3 : De-fuzzification

As far as problem-solving for a given level of membership is concerned, and that uncertainties do not only affect the boundary conditions but also geometrical dimensions or material and physical properties, the difficulty is clearly to solve discretized equilibrium equations in which, first, all terms are replaced by *mathematical intervals*, and second, the arithmetic of intervals takes the place of the classical arithmetic rules. Defining an interval linear system of equations $\hat{A}\hat{x} = \hat{b}$ as the family of equations :

$$Ax = b \quad (1)$$

with $A \in \hat{A}$ ($R^{n \times n}$ intervals matrix) and $b \in \hat{b}$ (R^n interval vector), the solutions set will be defined as :

$$\Sigma(\hat{A}, \hat{b}) = \{ x \in R^n / Ax = b \text{ where } \tilde{A} \in \hat{A} \text{ and } \tilde{b} \in \hat{b} \} \quad (2)$$

It can be shown that the structure of $\Sigma(\hat{A}, \hat{b})$ is complex. In practice, it will not be possible to compute the exact solutions set and only bounding estimations will be obtained, either *optimistic* or *pessimistic*. The paper will be first devoted to the review of different possible direct algorithms to compute approximations of the set of solutions. Original methods will be proposed. The Vertex method [3], which requires for each level of membership 2^n analyses, with n the number of uncertain parameters, will be used as reference. Second, under the assumption of static linear analysis, application of these methods to inverse design problems will be considered.

2. Implicit Formulation

The implicit formulation corresponds to the *optimistic* approximation of the solutions set. The interval linear system of equations $\hat{A}\hat{x} = \hat{b}$ is considered in the following way :

$$\begin{pmatrix} [a_{11}, \bar{a}_{11}] & \cdots & [a_{1n}, \bar{a}_{1n}] \\ [a_{21}, \bar{a}_{21}] & \cdots & [a_{2n}, \bar{a}_{2n}] \\ \vdots & \ddots & \vdots \\ [a_{n1}, \bar{a}_{n1}] & \cdots & [a_{nn}, \bar{a}_{nn}] \end{pmatrix} \begin{pmatrix} [x_1, \bar{x}_1] \\ [x_2, \bar{x}_2] \\ \vdots \\ [x_n, \bar{x}_n] \end{pmatrix} = \begin{pmatrix} [b_1, \bar{b}_1] \\ [b_2, \bar{b}_2] \\ \vdots \\ [b_n, \bar{b}_n] \end{pmatrix} \quad (3)$$

An approximation of the solutions set is sought as the interval vector \hat{x} , which allows matching the uncertainties of the left-hand side of the equations to the uncertainties on

the right hand side \hat{b} . Provided that the system is compatible, i.e. uncertainties on \hat{b} are greater or equal to the uncertainties resulting from the product of \hat{A} and \hat{x} (in the sense of the arithmetic of intervals), the solutions are known as *optimistic* as the intervals of \hat{x} components can be *under-estimated*.

To compute an *optimistic* solution, an original formulation consists in solving the following large sparse linear mathematical programming problem :

$$\begin{aligned} \max \min (\bar{x}_i - \underline{x}_i) \quad s.t. : \\ \underline{x}_i \leq \bar{x}_i \quad \left[\begin{array}{l} \sum_i \underline{u}_{ij} = \underline{b}_j \\ \sum_i \bar{u}_{ij} = \bar{b}_j \end{array} \right] \quad \left[\begin{array}{ll} \underline{u}_{ij} \leq \underline{a}_{ij} \underline{x}_i & \bar{u}_{ij} \geq \underline{a}_{ij} \underline{x}_i \\ \underline{u}_{ij} \leq \underline{a}_{ij} \bar{x}_i & \bar{u}_{ij} \geq \underline{a}_{ij} \bar{x}_i \\ \underline{u}_{ij} \leq \bar{a}_{ij} \underline{x}_i & \bar{u}_{ij} \geq \bar{a}_{ij} \underline{x}_i \\ \underline{u}_{ij} \leq \bar{a}_{ij} \bar{x}_i & \bar{u}_{ij} \geq \bar{a}_{ij} \bar{x}_i \end{array} \right] \quad (4) \\ i=1,n \quad j=1,n \quad i,j=1,n \end{aligned}$$

where the slack variables u_{ij} are introduced to enforce the arithmetic of intervals multiplication rule. Additionally, a perturbation strategy consisting in solving the perturbation of the initial system around mean values is used to cope with *compatibility* problem [2] :

$$\hat{A} = \tilde{A} + \Delta\hat{A}, \quad \hat{x} = \tilde{x} + \Delta\hat{x}, \quad \hat{b} = \tilde{b} + \Delta\hat{b} \quad (5)$$

$$\hat{A}\Delta\hat{x} \subseteq \Delta\hat{b} - \Delta\hat{A}\tilde{x} \quad (6)$$

with respectively \hat{A} , \tilde{A} and $\Delta\hat{A}$ the $R^{n \times n}$ intervals matrix, the mean value and the perturbation.

3. Explicit Formulation

The explicit formulation of the intervals linear equations system $\hat{x} = \hat{A}^{-1}\hat{b}$ will lead to a *pessimistic* approximation of the solutions set, as computing \hat{x} can be seen as an error propagation process. An *over-estimation* of the interval components of \hat{x} is obtained, sometimes *unbounded*.

3.1. THE HANSEN ALGORITHM

One of the most important features of the arithmetic of intervals is that the zero value cannot be contained in the interval at the denominator of a division. As a result, iterative algorithms of the Gauss-Seidel or Jacobi family will be used as a basis to the solution of intervals linear equations system. Iterates in the Gauss-Seidel algorithm are given by :

$$\hat{x}_i^{(k+1)} = \frac{1}{\hat{a}_{ii}} \left(\hat{b}_i - \sum_{j=1}^{i-1} \hat{a}_{ij} \hat{x}_j^{(k+1)} + \sum_{j=i+1}^n \hat{a}_{ij} \hat{x}_j^{(k)} \right) \quad (7)$$

where, contrary to the Gauss algorithm, the \hat{a}_{ii} are known and positive if \hat{A} corresponds to the stiffness matrix. It should be pointed out that all terms in the preceding equation are intervals. The two specific features of the Hansen algorithm are first a mid-point inverse preconditioning of the system and second an intersection strategy between two successive iterates to limit occurrence of unbounded solutions.

3.1.1. Mid-point inverse pre-conditioning

Hansen's algorithm [4] solves the preconditioned system :

$$\hat{M}\hat{x} = \hat{r} \quad (8)$$

with :

$$\hat{M} = \tilde{A}^{-1}\hat{A}, \hat{r} = \tilde{A}^{-1}\hat{b}, \tilde{A} = (\overline{A} + \underline{A})/2 \quad (9)$$

3.1.2. Intersections

Using the Gauss-Seidel's algorithm for the solution of the system $\hat{M}\hat{x} = \hat{r}$, one will have at iteration k :

$$\hat{x}_i^{(k+1)} = \frac{1}{\hat{m}_{ii}} \left(\hat{r}_i - \sum_{j=1}^{i-1} \hat{m}_{ij} \hat{x}_j^{(k+1)} + \sum_{j=i+1}^n \hat{m}_{ij} \hat{x}_j^{(k)} \right) \quad (10)$$

with : $\hat{x}_i^{(k+1)} = \hat{x}_i^{(k)} \cap \hat{y}_i^{(k+1)}$, $\hat{y}_i^{(k+1)} = \frac{1}{\hat{m}_{ii}} \left(\hat{r}_i - \sum_{j=1}^{i-1} \hat{m}_{ij} \hat{x}_j^{(k+1)} + \sum_{j=i+1}^n \hat{m}_{ij} \hat{x}_j^{(k)} \right)$ (11)

According to a *pessimistic* approximation of the solutions set, the intersection strategy will help in minimising error accumulation and avoiding unbounded solutions. Rohn's algorithm [5] gives further extensions of the Hansen's algorithm.

3.2. THE VERTEX METHOD

For all the problems considered in the experimental phase, and when possible, the Vertex method was used as reference. The Vertex method consists in successively exploring the 2^n combinations of the extreme values of the design variables and taking the corresponding extreme values of the structural response. It should also be pointed out that the Vertex method implicitly assumes that the x_s are monotonic functions of the design variables.

4. A Simple 2D Example

A simple example taken from Hansen's works will help fix ideas. Considering the system :

$$\begin{bmatrix} [2;3] & [0;1] \\ [1;2] & [2;3] \end{bmatrix} \begin{Bmatrix} x_1 \\ x_2 \end{Bmatrix} = \begin{Bmatrix} [0;120] \\ [60;240] \end{Bmatrix}$$

Tables 1 and 2 give values of the unknowns x and the recomputed right hand side for four direct methods, Vertex method, Hansen's algorithm, classical Gauss-Seidel's algorithm and finally implicit formulation (respectively subscript v , h , g and s).

	x_1	x_2
q_v	[-120;90]	[-60;240]
q_g	[-120;90]	[-60;240]
q_h	[-130.2;167.7]	[-104.4;267.2]
q_s	[0;22.5]	[30;52.5]

Table 1 : Unknown intervals x

	b_1	B_2
q_v	[-420;510]	[-420;900]
q_g	[-420;510]	[-420;900]
q_h	[-495;770.3]	[-537.7;1137.1]
q_s	[0;120]	[60;202.5]

Table 2 : Recomputed right hand sides

Figure 4 represents the different sets of solutions with respect to the exact set of solutions.

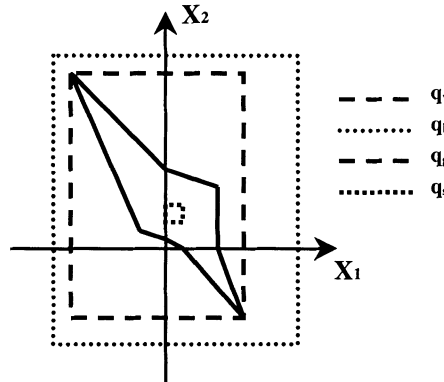


Figure 4 : Comparison of the different solutions sets

From the solution of different small to medium sized problems, it comes the following conclusions :

- Perturbation and pre-conditioning enlarge the approximations of the solutions set.
- The implicit method enforces the left-hand side of the system of equations to the (perturbed) right hand side, what is not the case in the explicit approaches where the recomputed right hand sides are larger than the prescribed ones.
- The perturbation strategy is essential to *ensure feasibility* in the *optimistic* formulation.
- The preconditioning strategy is essential to ensure *robustness* in the *pessimistic* algorithms.
- The Vertex solution always appears to be the reference solution.
- Hansen's algorithm and its Rohn's variant provide solutions sets greater or equal to those provided by the Vertex method, with a quite good robustness.

Finally, emphasis will be place on the fact that prior to the solution of intervals equations systems, extreme values of systems coefficients have to be computed.

5. Vertex Solution Using Neumann Series Expansion

As the Vertex method remains the more robust approach, and as it leads most of the time to the best approximation to the solutions set, a way was searched to improve its

efficiency. In this section, the solution of the Vertex problem is built using Neumann series expansion. Assuming a linear static analysis problem, and that uncertainties affect the stiffness matrix K only, one can write :

$$\hat{K} = [\underline{K}; \overline{K}] = \tilde{K} + \sum_{i=1}^{n_i} \mu_i \Delta K_i \quad (12)$$

so that one will have successively :

$$\hat{K}\hat{q} = g, \quad q = \left(\tilde{K} + \sum_{i=1}^n \mu_i \Delta K_i \right)^{-1} g, \quad q_0 = \tilde{K}^{-1} g, \quad q = \sum_{r=0}^{\infty} \left(- \sum_{i=1}^n \mu_i \tilde{K}^{-1} \Delta K_i \right)^r q_0 \quad (13)$$

or recursively :

$$q^{(k+1)} = q_0 + \sum_{i=1}^n \mu_i \tilde{K}^{-1} \Delta K_i q^{(k)} \quad (14)$$

K^0 is the “mean” stiffness matrix. The ΔK_i ’s are the n perturbations of the stiffness matrix, either the i^{th} term in $\Delta K = (\overline{K} - \underline{K})/2$ with \underline{K} the lower bound of the interval for the stiffness matrix, \overline{K} the upper bound. The extreme values of the different terms of K have to be *a priori* computed, or :

$$\Delta K_i = \partial K / \partial d_i \Big|_0 \delta d_i \quad (15)$$

if the stiffness matrix is linear in the design variables d_i . The μ_i ’s are scalar values equal to (-1) or (+1) according to \underline{K} or \overline{K} . Considering now a design criteria $c(q)$, e.g. :

$$c = b^T q \quad (16)$$

the signs of the μ_i ’s in (*) will be selected so as to minimise or maximise c , whether \underline{c} or \overline{c} is searched. Closed form solutions are most of the time possible.

6. Inverse Design Problems

Now that methods are available to compute uncertainties on structural design criteria according to uncertainties on the design variables, an industrial frequent question is which tolerances should be specified on the design variables so as to achieve prescribed uncertainties on the design criteria. Let us once more consider an example to help fix idea. In the design of a flange joint for instance, the designer will have to maintain pressure on the leak joint between extreme values to avoid leakage. As the pressure on the leak joint depends on design parameters, the problem will be to find for the latter, which intervals of variation will make sure that the pressure on the leak joint is in the prescribed interval. Such a problem can be mathematically formulated as an inverse optimisation problem:

$$\begin{aligned} & \max (\min \delta d_i) \text{ or } \max (\min \Delta K_i) \\ & \text{s.t.:} \\ & \begin{cases} \max(c(q)) = \bar{c} \\ \min(c(q)) = \underline{c} \end{cases} \end{aligned} \quad (17)$$

where $\max(c(q))$, $\min(c(q))$ and their derivatives are computed according to section 5. It should also be pointed out that, under the monotonic assumptions of sections 4 and 5, the confidence on the design variables can be transferred on the design criteria.

7. Conclusions

In this paper, uncertainties in structural analysis are considered through *possibilistic* formulations. Representing uncertainties on the design parameters by fuzzy numbers, different algorithms have been presented to compute intervals of variation of design criteria. The respective performances of the algorithms have been discussed. Putting aside the cost criteria, it appears that the Vertex engineers' method remains the most robust and gives most of the time the best approximations to the solutions set. An iterative approach has been proposed for building Vertex solutions, using Neumann series expansion and sensitivity analysis information. Using these results and defuzzification techniques, *possibilistic* distributions of design criteria can be built. Another possibility is to use these informations to set through the solution of inverse design problems specifications on design parameters.

References

1. CHEN, R., WARD, A.C.: Generalizing interval matrix operations for design, ASME of Mech. Eng. **119** (1997), 65-72.
2. DELCROIX, F., BRAIBANT, V.: De l'utilisation des intervalles en mécanique des structures - Application à la prise en compte des incertitude de données, Mechanical Engineering Department, Pôle Universitaire Léonard de Vinci, Paris La Défense.
3. DONG, W.M., WONG, F.S.: Fuzzy weighted averages and implementation of the extension principle, Fuzzy sets and systems **24** (1987), 65-78.
4. KEARFOTT, R.B.: Interval computations, Introduction, Uses and Resources, Department of Mathematics, University of South Westem Louisiana, Lafayette, LA, USA.
5. NING, S., KEARFO'IT, R.B.: A comparison of some methods for solving linear interval equations, Department of Mathematics, University of South Western Louisiana, Lafayette, LA. To appear in the SIAM Journal on Numerical Analysis.
6. WOOD, K.L., OTTO, K.: Engineering design calculations with fuzzy parameters, Fuzzy sets and Systems **52** (1992), 1-20.

DESIGN OF AN AUTOMATIC TOPOLOGY/GEOMETRY OPTIMIZATION SOFTWARE

S. BEUZIT, A. HABBAL

*Laboratoire J.A. Dieudonné – UMR CNRS 6621
Université de Nice – Sophia-Antipolis
BP 71, PARC VALROSE
06108 Nice Cedex 2
France*

Abstract

Within the structural optimization framework, the so-called topology methods are well-suited in order to find the best general layout. Their main disadvantage is that they generally lead to structures which are difficult to manufacture because they own composite materials, sometimes with intermediate densities. On the other hand, when the layout is fixed, the geometry optimization methods can lead to a good-looking optimum, but cannot change the layout.

The presented approach consists in a coupling between these two methods. First, the optimal layout is found by means of any generic topology optimization method; then, using simple image processing algorithms, a good-looking structure is extracted from the topology result, and then the geometry of the latter is optimized. Some numerical results are presented which clearly illustrate the fully automatic process.

1. Introduction

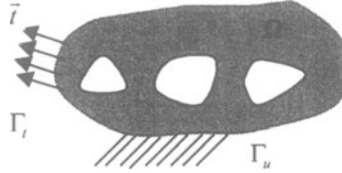
Structural optimization can be conceived as a search for the optimal distribution of material within an initial domain with given loading and boundary conditions. The standard design optimization systems generally implement shape–thickness or geometry-optimization for a fixed topology, while new emerging topology-based codes address the optimal layout finding problem, leaving to the engineers the heavy task of interfacing the two methods.

The interest of an automatic tool which achieves the coupling between these two optimization methods is then obvious.

Based on this idea, a fully automatic program has been developed. In the following, the main conceptual steps are presented, and some illustrating numerical experiments are given.

2. The problem

Within the linear elasticity framework, the problem is to find an optimal design for given boundary conditions and loading.



The equations are :

$$\begin{cases} -\operatorname{div}\sigma &= \bar{f} & \text{in } \Omega \\ \sigma\bar{n} &= \bar{t} & \text{on } \Gamma_t \\ u &= 0 & \text{on } \Gamma_u \end{cases} \quad (1)$$

where σ is the stress tensor, \bar{f} a volume force, \bar{t} the tension and \bar{u} the displacement.

We minimize an objective function, for instance the compliance :

$$J(\Omega, u) = \int_{\Gamma_t} (\bar{t} \cdot \bar{u}) d\Gamma + \int_{\Omega} (\bar{f} \cdot \bar{u}) d\Omega \quad (2)$$

This problem is equivalent, for a linear elastic structure, to the maximization of the potential energy :

$$\Pi(\Omega, u) = \frac{1}{2} a_{\Omega}(u, u) - l_{\Omega}(u) \quad (3)$$

where

$$a_{\Omega}(u, v) = \int_{\Omega} \sigma(u) : \varepsilon(v) d\Omega \quad \text{and} \quad l_{\Omega}(v) = \int_{\Omega} \bar{f} \cdot \bar{v} d\Omega + \int_{\Gamma_t} \bar{t} \cdot \bar{v} d\Gamma$$

and $u \in V_u$ is the solution of the state equation:

$$a_{\Omega}(u, v) = l_{\Omega}(v) \quad (4)$$

for any v in $V_u = \{v \in H^1(\Omega), v = 0 \text{ on } \Gamma_u\}$.

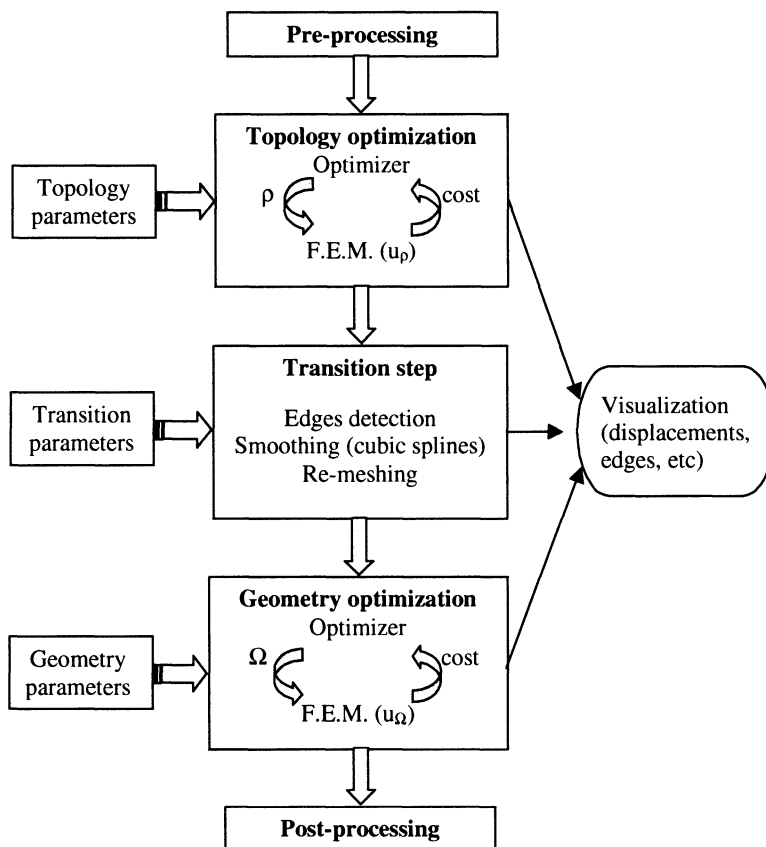
Taking into account classical constraints on the total volume, the problem is the following :

$$\sup_{\substack{\Omega \text{ admissible} \\ |\Omega| \leq \bar{V}}} \Pi(\Omega, u) \quad \begin{array}{l} u \in V_u \text{ solution of} \\ a_{\Omega}(u, v) = l_{\Omega}(v) \text{ for any } v \in V_u \end{array} \quad (5)$$

3. The main steps of our approach

3.1. OVERVIEW OF THE SOFTWARE ORGANISATION

There are mainly three modules which are independent : topology, transition and geometry modules. Each of them is configurable using a parameter file.



3.2. TOPOLOGY OPTIMIZATION

3.2.1. *The goal*

The goal of this step is, starting with an initial domain (ground structure) with given loading and boundary conditions, to find an optimal topology (i.e. an optimal distribution of density) according to a prescribed criteria, for instance the compliance of the structure.

Unfortunately, this problem is known to be ill-posed because it is generally possible to obtain a more rigid structure for the same volume of material with more smaller holes (this leads to « chattering » designs with microscopic perforations) [CHE.81]. There are two methods to obtain a well-posed problem and achieve topology optimization.

The first one consists in including, in the design space, solutions with microscopic holes (relaxation) using for example periodic perforated microstructures and then compute their properties using the homogenization theory [BEN.94]. The advantage of this method is to guarantee the existence of solutions for the relaxed problem [ALL.94] and to suppress almost all the local extrema [KOH.86]. A drawback is that the generated structure often contains perforated microstructures and hence is difficult, if not impossible, to manufacture. An explicit penalty or some restrictions on the microstructure (square holes in square cells) can be used to eliminate intermediate values of the density but if they are totally suppressed we are back to the original ill-posed design problem. The existence of a continuum solution is not assured and the solution does not converge by grid refinement.

A more recent approach consists in excluding any structure with microscopic holes by bounding the perimeter [JOG.94] and [HAB.96] : an additional constraint is added to the problem in order to ensure that the perimeter, computed as the total variation of the density (i.e. the density jump between each element of the mesh), does not exceed a fixed value. The advantage of this method is the control of the complexity of the optimal structure and therefore of the difficulty of its manufacturing. It also ensures the existence of a solution [AMB.93] -but not the uniqueness-, and we can numerically observe the convergence with respect to the grid refinement. Moreover, this method is not restricted to compliance optimization and can be used with any design objective and non-linear constraints. The topology module implements this method.

3.2.2. *Mathematical formulation of the perimeter method*

The optimization problem is the following :

$$\begin{array}{l} \sup \\ \text{for } \Omega \text{ admissible} \\ \left\{ \begin{array}{l} |\Omega| \leq \bar{V} \\ |\partial\Omega| \leq \bar{P} \end{array} \right. \end{array} \quad \begin{array}{l} \Pi(\Omega, u) \\ u \in V_u \text{ solution of} \\ \alpha_{\Omega}(u, v) = l_{\Omega}(v) \text{ for any } v \in V_u \end{array} \quad (6)$$

The admissible domains, which are described by their elasticity tensor, are only composed of void and of plain material, but in order to solve the optimization problem, a continuous model for this tensor was considered. For instance, the model presented in [HAB.96] where the tensor depends on the density of the material ρ and on the displacement field u_{ρ} was used, but any other consistent model could fit as well. The design variable is then the density of material. To eliminate intermediate values of this density we add a penalization function. The optimization problem is then stated as follows :

$$\begin{array}{l} \sup \\ \rho \in V_{\rho} \\ \left\{ \begin{array}{l} |\Omega| \leq \bar{V} \\ |\partial\Omega| \leq \bar{P} \end{array} \right. \end{array} \quad \begin{array}{l} \Pi(\Omega, u) \\ u_{\rho} \in V_u \text{ solution of} \\ \alpha_{\Omega_{\rho}}(u_{\rho}, v) = l_{\Omega_{\rho}}(v) \text{ for any } v \in V_u \end{array} \quad + \quad S(\rho) \quad (7)$$

where $V_\rho = \left\{ \rho \in L^\infty(\Omega) / \rho \in H^1(\Omega_\alpha), 0 < \rho_{\min} \leq \rho \leq 1 \forall x \in \Omega \right\}$ with Ω_α a partition of Ω and $S(\rho)$ is the penalization function.

3.2.3. Implementation

A large scale optimization code [TIT.97] was used in order to solve the problem (7). The main difficulty is to find an efficient optimizer to solve the large scale non linear constrained problem within the topology phase, since every element of the mesh is taken as design variable.

Based on triangular mesh, the linear elasticity state problems were solved by means of a modified version of the Modulef (INRIA) finite element library.

3.3. TRANSITION BETWEEN TOPOLOGY AND GEOMETRY OPTIMIZATION

3.3.1. Edge detection

Using the optimal topology layout, i.e. the optimal distribution of density found during the first step, the problem is to extract the edges which will be used as a starting point for the geometry optimization. To this end, a threshold for the density is set and we consider the equivalent picture¹ as binary : below this threshold there is no material, above there is material. For the edge detection itself, it is not necessary to use a gradient method because we have an artificial binary picture without noise [TOU 87] and [DER.94].

3.3.2. Edge smoothing

After locating the material zone by edge detection, one obtains an oscillating boundary. Then, a smoothing by means of cubic periodic splines is applied. Non-design parts of the boundary can be specified by the user, which are then not modified by the interpolating splines.

3.3.3. Domain re-meshing

After obtaining oriented and smoothed edges which are the new boundaries of the domain, we generate new data (new mesh, boundary conditions, loading) that are used as pre-processing data file for the geometry optimization task.

3.4. GEOMETRY OPTIMIZATION

3.4.1. The goal

The goal is now to finalize the shape of the structure which has an optimal layout, using eventually new optimization criteria (new objective functions, additional constraints).

The method used here is the classical transport method [SIM.76], [ROU.82] and [SOK.92]. The competing domains are the images through topology-preserving mappings of a reference one. The application of this method to the elasticity can be found in [MAS.87]. The optimal design variable reduces to the coordinates of the spline interpolating nodes. A general numerical implementation is described in [HABB.96].

¹ In fact, the edge detection is directly based on the mesh in order to preserve the information related to the boundary conditions, the loading, etc.

3.4.2. Mathematical formulation

The third and final problem is to minimize an objective function, not necessarily the compliance, which is defined as classical, depending on the state of the system, which is the solution of the equilibrium equation introduced in (4).

$$\inf_{w \in D_{\Omega}} \begin{matrix} J_w(u_w) \\ u_w \in V_u \text{ solution of} \\ a_w(u, v) = l_w(v) \text{ for each } v \in V_u \end{matrix} \quad (8)$$

where D_{Ω} is the set of the admissible domains.

4. Numerical results

We present some numerical results for the wheel problem (see Figure 1. which represents the initial domain with loading and boundary conditions).

The Table 1 presents the cost (compliance) at each step of the optimization process. The Figure 2 is the result of the topology optimization with the perimeter method. The Figure 3 is obtained from the optimal topology by edges detection. The Figure 4 illustrates the application of cubic splines interpolation to smooth the boundary and the Figure 5 shows the final optimal geometry. The Table 2 shows that the gradient components are already quite small at the starting of the geometry optimization, when the topology and geometry costs are the same (compliance).

	Ground structure	Optimal topology	Edge Detection	Smoothed domain	Final optimal geometry
Value of The compliance	0.012	0.032	0.030	0.035	0.029

Table 1. Value of the compliance at each iteration

Master nodes	Value of the gradient
1	0.0048188041
2	-0.0003015747
3	-0.0034778551
4	-0.0103603724
5	-0.0016344769
6	-0.0028007630
7	-0.0010873297
8	0.0007015557
9	0.0027923416
10	0.0018784474

Table 2. Gradient components at the start of geometry optimization

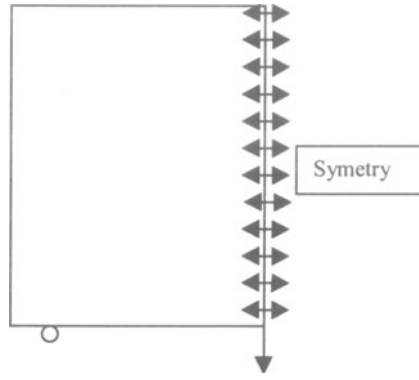


Figure 1. Ground structure



Figure 2. Optimal topology

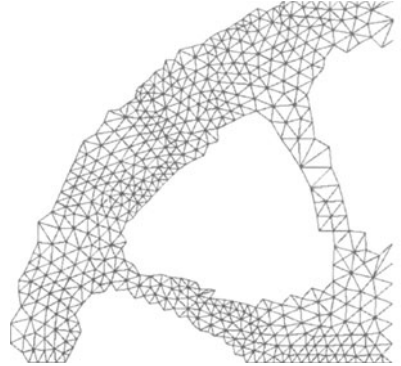


Figure 3. Edges detection

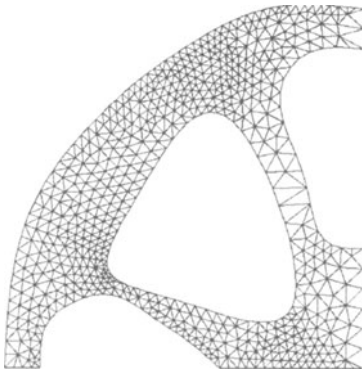


Figure 4. Smoothed edges

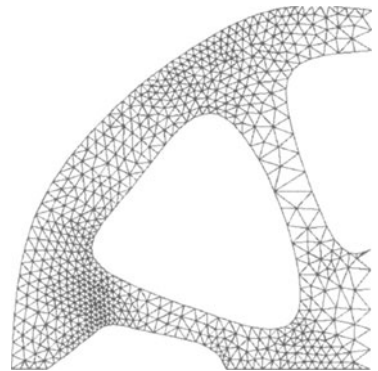


Figure 5. Optimal geometry

5. Conclusion

Efficient Product and Process Improvement tools naturally require as a prerequisite a good Integrated Optimal Design approach. To this end, we considered the combination of the topology-based methods with the geometry classical optimization. The interface between these approaches requires simple image processing techniques.

Based on these considerations, within the framework of the two-dimensional linear elasticity, a fully automated integrated optimizer was developed and successfully exploited to illustrate the integrated cycle of optimum design.

References

- [ALL.94] G. ALLAIRE, R.V. KOHN. "Topology optimization and optimal shape design using homogenization", Topology design of structures, M.P. BENDSOE, C.A. MOTA SOARES, Kluwer - Dordrecht , 1994, pp. 207-218.
- [AMB.93] L. AMBROSIO, G. BUTTAZO. "An optimal design problem with perimeter penalization", Calculus of Variations and Partial Differential Equations 1, 1993, pp. 55-69.
- [BEN.94] M.P. BENDSOE, A. DIAZ, N. KIKUCHI. "Topology and generalized layout optimization of elastic structures", Topology design of structures, M.P. BENDSOE, C.A. MOTA SOARES, Kluwer - Dordrecht , 1994, pp. 159-205.
- [CHE.81] K.T. CHENG, N. OLHOFF. "An investigation concerning optimal design of solid elastic plates", Int. J. Solids and Struct., Vol. 17, 1981, pp. 305-323.
- [DER.94] R. DERICHE. "Techniques d'extraction de contours", Cours de D.E.A. , 1994.
- [HABB.96] A. HABBAL. "Some basics in optimal control of domains", Control and Cybernetics, Vol. 25, 1996, No.5.
- [HAB.96] R.B. HABER, C.S. JOG, M.P. BENDSOE. "A new approach to variable-topology shape design using a constraint on perimeter", Structural Optimization, Vol. 11, 1996, pp. 1-12.
- [JOG.94] C.S. JOG, R.B. HABER, M.P. BENDSOE. "Topology design with optimized, self-adaptive materials", International journal for numerical methods in engineering, Vol. 37, 1994, pp. 1323-1350.
- [KOH.86] R.V. KOHN, G. STRANG. "Optimal design and relaxation of variational problems", Comm. Pure Appl. Math., Vol. 39, 1986, pp. 1-25 (part I), pp. 139-182 (part II), pp. 353-377 (part III).
- [MAS.87] M. MASMOUDI. "Outils pour la conception optimale de formes", PhD thesis, Université de Nice – Sophia-Antipolis (France), 1987.
- [ROU.82] B. ROUSSELET. "Quelques résultats en optimisation de domaines", PhD thesis, Université de Nice – Sophia-Antipolis (France), 1982.
- [SIM.76] J. SIMON, F. MURAT. "Sur le Contrôle par un Domaine Géométrique", PhD thesis, Paris.
- [SOK.92] J. SOKOLOWSKI, J.P. ZOLESIO. "Introduction to Shape Optimization, Shape Sensitivity", Springer-Verlag, 1992.
- [TIT.97] A.L. TITS, C. LAWRENCE, J.L. ZHOU. "User's Guide for CFSQP Version 2.5", University of Maryland, 1997.
- [TOU 87] J.J. TOUMAZET. "Traitement de l'image sur micro-ordinateur", Sybex, 1987.

Chapter 3
FINITE ELEMENT SOLVERS. MESHING TECHNIQUES
COMPUTER AIDED GEOMETRY

Intelligent objects for pre-processing in a mechanical finite element software	143
P. BOMME and TH. ZIMMERMANN	
A message passing paradigm for distributed design and simulation of mechanical systems.....	151
P. BREITKOPF AND Y. ESCAIG	
FEM/CAD system architecture for shape optimization of 3D parts.....	159
A. MERROUCHE and C. KNOPF-LENOIR	
2D Mesh and geometric adaptations using an <i>a priori</i> model of mechanical behavior	167
PH. VERON, L. FINE, F. NOËL and J.C. LEON	
On the automation of non-linear behavioral structural analysis. Guidance and quality control	175
J.P. PELLE and D. RYCKELYNCK	
Computational geometry in the preprocessing of point clouds for surface modeling.....	183
RUIZ OSCAR and POSADA JORGE	
Polyhedron partitioning dedicated to a hierarchical meshing technique.....	191
F. MAZA, F. NOEL AND J.C. LÉON and F. SILLION	
A declarative approach for geometry and topology : a new paradigm for CAD-CAM systems.....	199
A. CLÉMENT, A. RIVIÈRE and PH. SERRÉ	
Piecewise cubic interpolation for reverse engineering.....	207
G. PRADES, J.L. CAENEN, Y. MINEUR and J.M. CASTELAIN	

INTELLIGENT OBJECTS FOR PRE-PROCESSING IN A MECHANICAL FINITE ELEMENT SOFTWARE

P. BOMME and Th. ZIMMERMANN
Laboratory of structural and continuum mechanics (LSC)
Civil Engineering Department (DGC),
Swiss Federal Institute of Technology (EPFL)
CH-1015 Lausanne, Switzerland

Abstract

The purpose of this paper is to describe an intelligent-object concept for the integration of rules in objects. It is proposed to design an intelligent object as a usual object with data and methods to which an expert object consisting of rules and reasoning capabilities is added. The main interest is that associating rules with objects organises knowledge in a hierarchy identical to the hierarchy of objects without any additional artefact. Such intelligent objects control the activation of their knowledge. Therefore, knowledge processing becomes a local and temporary process that can be activated only when needed. Actually, the intelligent-object concept generates intelligent object-oriented applications within which the knowledge is distributed over the objects of the application, and knowledge processing is decentralised. This new concept is particularly well adapted for numerical simulation tools, typically in engineering applications that mainly require pure numerical behaviour, and sometimes locally intelligent behaviour. The proposed approach is illustrated in a simple example.

1. Introduction

The purpose of this paper is to describe an intelligent-object concept. Before describing those intelligent objects, the need for assistance within finite element software is discussed. Then, the intelligent-object concept is described; defining the intelligent objects, their associated knowledge, and finally how such objects process their own knowledge. An intelligent user interface managing its own options follows as an illustration of the proposed approach. Lastly, conclusions are drawn.

1.1. NEED FOR ASSISTANCE IN FINITE ELEMENT CODES

Finite element codes are complex tools dedicated to numerical simulation of difficult problems. So, it may take a user a year or more to learn effectively and efficiently how to use the various options and capabilities of a large FEA program [1], for instance.

However, inexperienced engineers are often told to analyse structure without having the proper knowledge of the underlying mechanics governing their behaviour. Often, this leads to inappropriate structure modelling and interpretation of results. Consequently, modelling assistants may be useful to novices who are not familiar with all modelling details, and often not in a position to evaluate the adequacy of the various models they must build. Furthermore, finite element assistants can reduce the number of tasks delegated to the user, allowing a short turn-around time for analysis. Different types of knowledge-based systems can help the user of finite element packages: intelligent modules helping to find particular program options, data entry procedure, suitable solutions, etc.; specification and modelling aids helping to translate appropriate element types, material models, boundary conditions, mesh density; results evaluation and design change proposals.

1.2. HISTORICAL OUTLINE OF FINITE ELEMENT ASSISTANTS

The pioneer of finite element assistants is SACON [2], standing for Structural Analysis CONSULTANT. It helped the user of a commercial package with the selection of an appropriate analysis strategy. This research showed the feasibility and the potential of using knowledge-based system coupled with FE software. Among this literature, Cagan's [3] and Fink's [4] work deserve the most attention; they report on developments that combine object-oriented and rule-based programming with finite element programs. Although as not broad as SACON, PLASHTRAN (PLate And SHell sTRuctural ANalysis) [3] has the advantage of providing a more user-friendly interaction resulting from its design, that follows the logic of the expert instead of following the logic of the shells. PLASHTRAN enables the user to take shortcuts, which force the system to make the appropriate assumptions in order to preserve consistency within the system. But, unfortunately, its conclusions pointed out the difficulty of integrating expert systems and FE packages essentially due to incompatible development tools.

2. Intelligent-object concept

1.3. DISTRIBUTED OBJECT-ORIENTED ARCHITECTURE

Failure in using numerical simulation tools with knowledge-based systems is due to the lack of interoperability that mainly results from the design of usual AI environments, as well as their language of implementation. Most commercial AI environments are written in LISP, which is a widespread language in AI community, but not in the scientific one. Furthermore, AI environments provide a centralised reasoning process with a single inference engine working on a single knowledge base (set of rules). This means that the expert system is always activated whatever action is to be performed; therefore the computational efficiency which is of great importance in numerical simulation tools, is highly penalised. Even though in such systems, knowledge can be organised in order to eliminate irrelevant rules from knowledge processing, this approach is not appropriate for finite element codes.

The proposed concept is based on the object-oriented approach that provides a common paradigm for the development of numerical simulation tools coupled with AI tools. It renders possible the integration of multiple rule-based expert systems into a given application, instead of developing an application within a prescribed environment, as illustrated in Figure 1. Knowledge bases (sets of rules) are distributed over the application and knowledge processing (inference engines) is decentralised. The main advantage of this approach is that only a limited amount of knowledge is activated simultaneously, i.e. that related to the action to be carried out. Resulting numerical simulation applications are able of behaving as pure numerical packages ignoring knowledge, or as hybrid applications capable of activating some knowledge when needed. Therefore, a good level of efficiency is achieved.

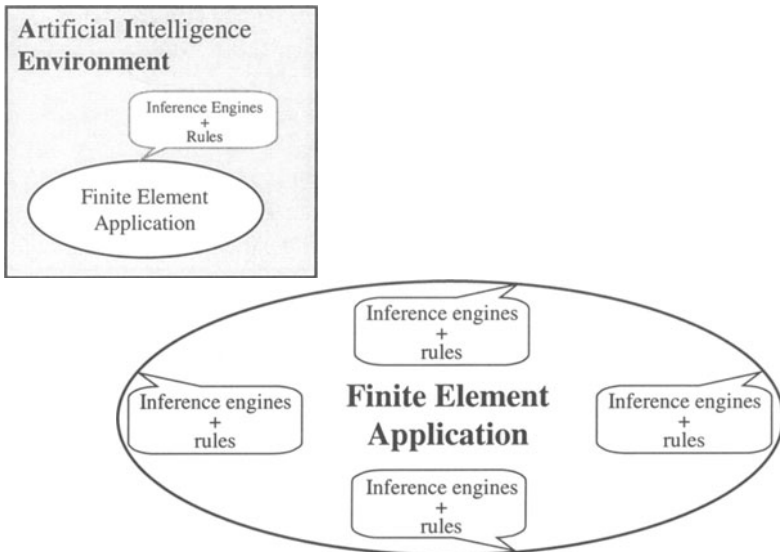


Figure 1. Centralised Vs Distributed object-oriented intelligent architecture

1.4. DEFINITION OF AN INTELLIGENT OBJECT

The intelligent-object concept relies on a hybrid definition of objects integrating declarative knowledge and reasoning capabilities within a simple blackboard architecture [5]. Such a hybrid object consists of data and methods that represent a usual object, and rules and inference engines that represent an expert object.

These objects communicate through messages and share knowledge through the blackboard. Intelligent behaviours of these objects result from the action of knowledge, and can be invoked within usual methods as well as in rules. Intelligent objects provide their hosted application with an architecture in which knowledge is distributed and knowledge processing decentralised.

1.5. RULES OF AN INTELLIGENT OBJECT

Associating rules with objects endows them with the same status as the usual methods [6]. So, in the proposed approach, rules are considered as pseudo-methods working on the state of an object. Thus, like in any method, the internal data of an object can be directly accessed in its rules, while encapsulated data (variables of other objects) are accessed by message passing. Consequently, such a definition fully respects the state encapsulation of the object with which rules are associated. The following kinds of rules are distinguished:

- *rules of instances*, which are activated by every instance of a class;
- *private rules*, which are rules of instances with a scope limited to the instances of class with which they are linked;
- *identity rules*, which are associated with a single object, and dedicated to reinforcing the identity of that object. Such rules are very useful to distinguish exceptional behaviour of a particular instance of a class;
- *inherited rules*, which are rules of instances of superclasses from which private rules of superclasses have been excluded;
- *polymorphic rules*, which override inherited rules.

Rules are defined as follows:

```

RULENAME: name
CLASS_LINK: classname or OBJECT_LINK: objectname
ACCESS: Public or Private
IF premises THEN conclusions [SHARED or NOTSHARED]
COMMENT: [optionnal]
  
```

in which

- a *name* represents the name of the rule.
- a *member* (*classname* or *objectname*) identifies a class or an object, with which this rule is associated.
- a *keyword* (*public* or *private*) facilitates rule hiding and defines the inheritance scheme. A *public* rule is a rule that can be inherited, whereas a *private* one has influence restricted to the specific object or to the class with which it is associated.
- *IF... THEN...* is the body of the rule consisting of premises and conclusions. Two kind of conclusions can be distinguished; the ones that the owner of the rules shares with other intelligent objects through the blackboard. Hidden conclusions represent local information limited to the knowledge base of the owner.
- and some optional comments.

The contents of rules are analysed as the contents of methods, so rules may be considered as particular methods called *pseudo-methods*. Notice that these pseudo-methods have no arguments. If external data is needed in conclusions or premises, it can be acquired by interrogating the blackboard or by sending messages to other intelligent objects.

Associating rules with objects provides a natural way of organising knowledge hierarchically. Since rules are like methods, rules and methods are organised in the same way. This means that the resulting hierarchy of rules is identical to the one of the application as shown in Figure 2. Additionally, modifying the hierarchy of the

application automatically changes the organisation of rule in the same manner. Therefore, both hierarchies always remain consistent, meaning that the hierarchy of rules does not require specific management.

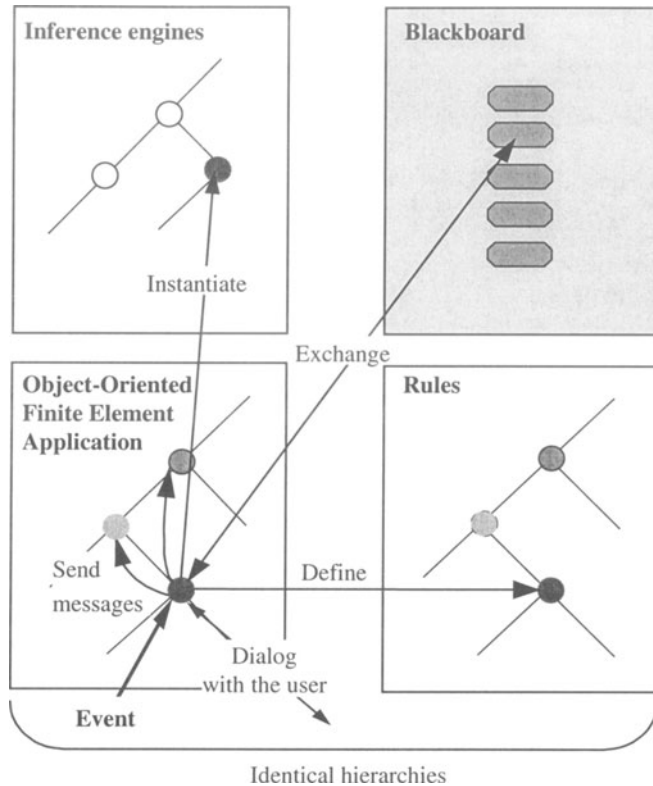


Figure 2. Hierarchy of intelligent object-oriented application

Any intelligent object is capable of constructing its own set of rules with respect to object-oriented features such as identity, inheritance, and polymorphism. Therefore, the set of rules that can be applied to an object consists of: (i) the rules inherited from superclasses of the object's class, (ii) rules associated with the object's class, and (ii) rules characterising the object's identity. Notice that polymorphism is taken into account automatically by collecting rules in this order, since a rule of a subclass overrides the rule of one of its superclasses having the same name.

1.6. EMBEDDED REASONING

Knowledge processing is kept under the control of an object, that instantiates an inference engine in order to process its knowledge. This instantiated process dies when its task is over. Thus, reasoning mechanisms are local concepts implemented by temporary objects created only when needed. This decentralised knowledge processing

reinforces data encapsulation and forces objects to communicate by sending messages in order to exchange knowledge. A simple blackboard architecture introduces more flexibility, by providing a common area that can be freely accessed by objects for writing and reading knowledge [7,8].

Every intelligent object has its own set of rules on which it activates reasoning as shown in Figure 2. When an object receives a message requiring activation of knowledge, it instantiates first a reasoning process on its own rules; then, if needed, it interacts with its environment during the reasoning. The object's environment consists of a privileged partner, the blackboard, to which the requests are sent in priority, and of other intelligent objects, with which co-operation may occur, and finally of the user. Such reasoning modes enable an object to activate purely local reasoning processes, or completely co-operative ones involving other objects and the user.

The hierarchy of the inference engines shown in Figure 2 is an object-oriented implementation of search algorithms, and therefore is independent of the hierarchy of the application.

3. Illustration

The simple example that follows is extracted from Bomme's thesis [5]. In this work, the intelligent-object concept was developed in C++ from scratch, meaning that the implementation required the development of an object-oriented propositional expert system (rule parser and inference engines) and of a class providing the capabilities of a generic intelligent object (class **IntelligentObject**). This generic object provides its subclasses with capabilities of activating inference engines on rules. In this illustration, class **IntelligentUserInterface** was created as a subclass of **IntelligentObject** in order to maintain the consistency of data in non-linear finite element software for rock and soil mechanics. The main issue is first to provide the user with the minimal user interface options for objects such as materials and numerical algorithms according to the existing input, and also to be capable of recovering data consistency whatever changes are carried out. Hereafter, it is described how a simple object, i.e. an elastic soil material manages its user interface.

Let us assume that the adopted formulation for elastic soil materials accommodates two-phase problems and integrates creep, heat, and humidity migration phenomena. Figure 3 shows an elastic soil material defined by three parameters (Young modulus, Poisson ratio, and Unit weight), some material properties (geometry, initial state, creep, heat, and humidity), and a button to check the consistency of the object.

This object is an instance of class **ElasticSoil** located in the hierarchy given in Figure 4. All classes of this hierarchy are derived from class **IntelligentUserInterface** that takes into account the specificity of the application and provides the appropriate reasoning capabilities and knowledge management.

Figure 5 shows how rules can be associated with classes. *NoGeometry* is associated with class **ElasticSoil**, and hides the *Geometry* button when the analysis is a deformation one. *ShowResource(...)* is a method of class **IntelligentUserInterface**, the argument of which identifies the resource, i.e. the button to be hidden. This method is inherited by the subclasses of **IntelligentUserInterface**, i.e. by **ElasticSoil**. *NoFlow* is

associated with class **AbstractMaterial** and hides the *Seepage* button. As a subclass of **AbstractMaterial**, **ElasticSoil** inherits *NoFlow*.

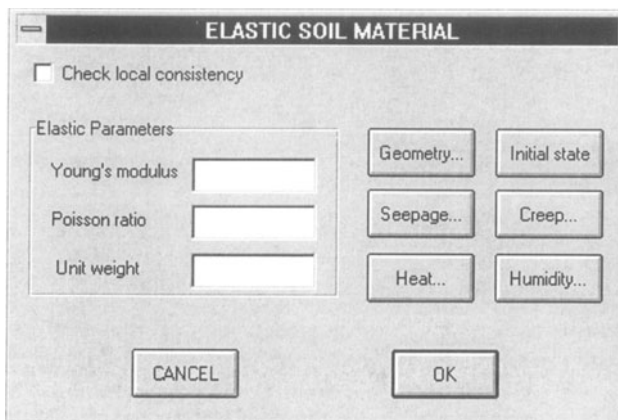


Figure 3. User interface for an elastic soil material

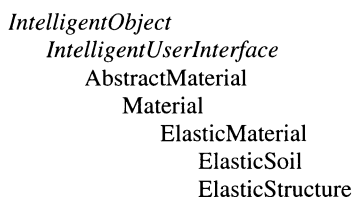


Figure 4. Partial hierarchy of materials

RULENAME: NoGeometry	RULENAME: NoFlow
CLASS_LINK: ElasticSoil	CLASS_LINK: AbstractMaterial
ACCESS: Public	ACCESS: Public
IF AnalysisType = "Deformation"	IF AnalysisType = "Deformation"
THEN @HideResource(IDC_GEOMETRY)	THEN @HideResource(IDC_SEEPAGE)

Figure 5. Example of rules associated with an **ElasticSoil** object

Figure 6 illustrates how an object can activate its rules within methods. Here, an elastic soil processes its set of rules to update the options of its user interface when it is created. The options that are consistent with the current user's input, are displayed by the method *OnInit()* shown in Figure 6.

ShowModelState() initialises the variables depending on the internal state of the object: here the elastic parameters. Then, a forward reasoning is carried out on the object's rules in order to take into account the influence of the environment. In the present illustration, this will determine which of the *material properties* buttons are consistent with the existing knowledge. Furthermore, the *checking local consistency*

button visible is hidden. This button allows the user to recover the consistency of the object when inconsistency is detected. When an object is created, consistency is always achieved.

```

Void ElasticSoil::OnInit() {
    ShowModelState()           Show the internal state
    Deduce()                   Update the user interface
}

```

Figure 6. Source code of method *OnInit()*

4. Illustration

This paper proposed a new approach for the integration of rules into objects. This leads to the development of an intelligent-object concept, in which objects have a hybrid definition consisting of data and methods with rules and reasoning processes. Associating rules with objects automatically distributes the knowledge over objects, and leads to a natural way of organising knowledge, which is induced from the hierarchy of implementation of the application. Additionally, these objects control the activation of their own knowledge. Reasoning processes are decentralised, and this approach allows multiplicity of reasoning mechanisms. To conclude, the described model is well adapted for numerical simulation tools, which mainly require computational power, and occasionally local reasoning. Obviously, this methodology can be used in any type of object-oriented applications. The feasibility of the approach is demonstrated on a simple example of management of user interface in finite element software.

References

1. Fenves, J (1985) A framework for a knowledge-based finite element analysis assistant. *Applications of knowledge-based system in structural design*. Dym, C.L. (ed.), pp. 1-7.
2. Bennett, J. Creary, L. Engelmores, R. and Melosh, R. (1978) "SACON: A knowledge-based consultant for structural analysis", Technical Report STAN-CS-78-699, Stanford University, September.
3. Cagan, J. and Genberg, V (1987) PLASHTRAN: an expert consultant on two-dimensional finite element modeling techniques. *Engineering with Computers*, Vol. 28, pp. 199-208.
4. Fink, R.K. Callow, R.A. Larson, T.K. and Ramson, V.H. (1988) An intelligent modeling environment for large engineering analysis code: Design issues and developments experience. *Engineering with Computers*, Vol. 3, pp. 167-179.
5. Bomme, P. (1998) "Intelligent objects in object-oriented environments", PhD thesis report no 1763, Swiss Federal Institute of Technology (EPFL).
6. Graham, I. (1994) SOMA method: Adding rules to classes. *Object Development Methods*. Carmichael (ed.) SIGS Book, pp. 199-210.
7. Hallam, J. (1990) Blackboard architectures and systems. *Artificial Intelligence: Concepts and Applications in Engineering*. Mirzai, A. (ed.), p35-64.
8. Nii, H.P. (1989) Chapter 1: Introduction. *Blackboard architectures and applications*. Jagannathan, V. Dohiawala, R. and Baum, L.S. (eds.), Academic Press, pp. xix-xxix.

A MESSAGE PASSING PARADIGM FOR DISTRIBUTED DESIGN AND SIMULATION OF MECHANICAL SYSTEMS

PIOTR BREITKOPF*, YVES ESCAIG**

**Codiciel, UPS CNRS 856*

BP 511 – P.A.T. de la Vatine, 32, rue Raymond Aron

76824 Mont-Saint-Aignan CEDEX, Piotr.Breitkopf@codiciel.fr

***INSA de Rouen*

Laboratoire de Mécanique de Rouen

Place Emile Blondel, BP 8, 76131 Mont-Saint-Aignan

1. Abstract

We present an application of object-oriented approach in the context of distributed computing in the field of structural engineering problems. In this work, conducted in the frame of a general purpose finite element code, we consider two types of distributed algorithms: the cooperation of heterogeneous computing systems and an algorithm for distributing the resolution of the finite element problem. In the first case, the major issue is the transparent distribution of the data base involving data structures and algorithms. In the first part of the present work, we present DDSM (Distributed Data Structures Manager) dealing with this first issue. The second case addressed is that of solution of linear systems by a domain decomposition direct method.

2. Introduction

The maturity of the field of computational engineering is such that the user has to deal with a growing complexity of individual software components. The simulation process involves a number specialized tools such as pre- and post-processors, linear, non linear and dynamic solvers or auto-adaptive mesh generators. On the hardware side, multiple architectures are available: networks of RISC processor systems, vector processor systems, shared memory multiprocessor systems, massively parallel systems, networks of workstations and arrays (or clusters) of shared memory systems.

These two aspects put to evidence the need for new programming paradigms. An object oriented approach permits one to partition programs into manageable pieces that closely match the concepts of computational engineering. Objects interact and

communicate with each other by exchanging messages. The interesting aspect of the object oriented approach is that objects do not need to be in the same process or even on the same machine to send and receive messages back and forth to each other. In this sense, objects match well with distributed computing. Adoption of an object oriented methodology may therefore lead to the distribution of the current centralized numerical simulation's process, limiting at the same time its complexity and increasing the overall performance.

The work presented in this paper has been conducted in the frame of the project SIC (Système Interactif de Conception) [BRE 92]. The aim is to conceive a general platform for various kinds of finite element simulations (structural mechanics, heat transfer, fluid mechanics, electromagnetism and any kind of coupled problems involving concurrent simulations of different aspects of a complex phenomenon). This platform allows tight cooperation between different development teams through sharing and reusing common software modules (data manager, solver, pre- and post processing, finite elements,...).

The distribution of the computations may be achieved in one of the two following ways:

- either by distributing the computational algorithms on a certain number of processing elements (usually identical) to reduce the elapsed execution time of the program ,
- or by performing different phases of the simulation process possibly using different software concurrently on different computing systems, in order to optimize the use of available ressources.

In the first case, a SPMD (Single Program Multiple Data) programming model is often used, meaning that each processor executes the same program but operates on different data. In the latter case, the main issue is the distribution of the data base. In the present paper, we present a project of a simulation software, based on the finite element method, that implements both types of distribution previously mentioned. A key issue in this project is the control of remote process and the communication of data between heterogeneous processing elements.

The paper is organized in the following way. In the first section, we present our « object manager » along with a run time system for the distribution of objects. The next section concerns performance aspects and a distributed implementation of the finite element method using a domain decomposition strategy.

3. Design of the Object Manager

While designing the data base for the SIC project we tried to find a compromise between the following constraints:

- simplicity, reusability, flexibility

- high performance - because of intensive calculations involved in the finite element method, the data has to be accessed in a very efficient way, ideally as fast as a simple memory access
- compatibility with the extensive range of existing libraries and modules written mainly in Fortran
- support for parallel processing
- provide both compiled and interactive interfaces

The design of GO (Gestionnaire d'Objets) [AUN 90], the data manager of the project SIC. GO permits us to implement a number of features commonly found in object-oriented languages such as data abstraction, inheritance, encapsulation. We have to stress that GO is not an object oriented language. Its programming interface is at a relatively low level as it relies on libraries rather than on syntactic constructs. GO may be seen as a research vehicle that permits us to experiment with object oriented concepts being applied to computationally intensive tasks.

4. Distributing the data base

In this section, we present the run time system DDSM (Distributed Data Structure Manager) which allows an easy and efficient displacement of previously described objects between local memories of distributed processing elements. Chaos++ system [SAL 95] proposes an alternative approach applied to objects of the C++ programming language.

There are four major issues in the design of DDSM: remote data access, maintaining pointers across the network, support of heterogeneous computing environments and efficiency considerations.

4.1. REMOTE DATA ACCESS

In order to reduce the number of messages exchanged, an access to a remote object is replaced by a local copy of the entire remote object. This principle is equivalent to that of "ghost objects" of the Chaos++ run time system. In our approach however, the objects are accessed directly in the memory rather than through an access function. This compromise, due to the performance considerations implies that there is no run time system to supervise the remote data access. Therefore, it is the application's responsibility to validate the objects it will use. If the objects are local, the usual consistency validations take place. If the object exists in a remote memory, then the run time system gets a copy of it before resuming execution. Because a single object can have multiple copies, it is necessary to ensure the coherence of these copies. Again, as we do not use a function to access objects, we assume that the coherence is supervised by the application.

4.2. DISTRIBUTION OF OBJECTS CONTAINING POINTERS

This issue concerns the distribution of objects containing pointers (in our case identifiers) to other objects. Suppose, that an object points to another one in a local

memory. The run time system must preserve this relation for the remote copies of the two objects. One solution consists in copying the two objects together and in recreating the relation when allocating objects in the remote memory. This is the solution implemented in Chaos++. However, this approach is not always acceptable when dealing with large graphs of objects. Our solution consists in introducing the notion of “universal identifier” (which contains the local identifier of an object and a processor number) and in maintaining in each memory the correspondence between local and universal identifiers. When transferring an object to another memory, a generic function scans its content and replaces each local identifier by a universal one. The opposite operation takes place at the reception of the object, just before putting it into the local object base. If the universal identifier does not correspond yet to a local object, then a new local virtual object appears. If later an object with the same universal identifier arrives, then it will take the local identifier of the placeholder object. Therefore, the relation between the two objects is restored.

4.3. SUPPORT OF HETEROGENEOUS COMPUTING ENVIRONMENTS

For basic data types, the XDR (eXternal Data Representation) library [KOP 95] ensures the consistency of coding between different binary representations. PVM [GAI 95], for example, uses XDR to support heterogeneous networks. This feature is not sufficient when handling complex data types like C language structures. This is also the case of our objects that can contain fields of different basic data types as well as variable length fields. Therefore, in our system, an XDR encoding takes place at the DDSM level rather than at the PVM level. This is done by a generic function and is transparent to the application.

5. Applications

Two classes of distributed finite element applications may be implemented using DDSM. The first class of applications aims at using optimally a set of computing resources: a network involving several processors and a 3D graphic workstation running the user interface. There are many different scenarios for such applications. One of them concerns the analysis of loosely coupled systems. In this case, two models of one problem are executed concurrently and an exchange of data takes place at fixed time intervals. The data transfer must be transparent to the user and very efficient. In this scenario, there is a different process and a different object base on each machine. Communication of objects among these bases is achieved using DDSM.

The second class of applications concerns Single Program Multiple Data (SPMD) programming models. We apply this approach for the distribution of a single finite element model over a network of processing elements. In the following section, we describe a distributed domain decomposition method. All the data of a finite element problem are represented by a graph of objects. The graph representing the finite element problem is partitioned into subdomains and distributed to different processing elements.

5.1. DISTRIBUTED DOMAIN DECOMPOSITION DIRECT METHOD

In this application, we aim at using a certain number of processing elements, usually identical, to reduce the elapsed execution time of the program. When using distributed memory systems, the privileged approach for parallelizing the finite element method is the use of domain decomposition methods. The domain decomposition methods solve first the initial problem independently on each subdomain, and then they add constraints to fit the local solutions on the boundaries between the subdomains. For example, in the Schur Complement method, the constraint is the equality of forces at the interfaces between subdomains. Detailed references can be found in [FAH 94]. For the Schur complement method, the decomposition algorithm can be written in the case of two subdomains:

1. renumber equations so that the internal degrees of freedom (dof) of each subdomain appear first

$$[k][u] = \{f\} \Leftrightarrow \begin{bmatrix} k_{11} & 0 & k_{13} \\ 0 & k_{22} & k_{23} \\ k_{31} & k_{32} & k_{33} \end{bmatrix} \begin{Bmatrix} u_1 \\ u_2 \\ u_3 \end{Bmatrix} = \begin{Bmatrix} f_1 \\ f_2 \\ f_3 \end{Bmatrix}$$

2. eliminate all internal dof

$$\begin{bmatrix} k_{11} & 0 & k_{13} \\ 0 & k_{22} & k_{23} \\ 0 & 0 & \bar{k}_{33} \end{bmatrix} \begin{Bmatrix} u_1 \\ u_2 \\ u_3 \end{Bmatrix} = \begin{Bmatrix} f_1 \\ f_2 \\ \bar{f}_3 \end{Bmatrix}$$

where

$$\begin{aligned} \bar{k}_{33} &= k_{33} - k_{31}k_{11}^{-1}k_{13} - k_{32}k_{22}^{-1}k_{23} \\ \bar{f}_3 &= f_3 - k_{31}k_{11}^{-1}f_1 - k_{32}k_{22}^{-1}f_2 \end{aligned}$$

3. solve the interface problem

$$[k_{33} - k_{31}k_{11}^{-1}k_{13} - k_{32}k_{22}^{-1}k_{23}][u_3] = f_3 - k_{31}k_{11}^{-1}f_1 - k_{32}k_{22}^{-1}f_2$$

4. back-substitute interface solution on internal degrees of freedom

$$\begin{Bmatrix} u_1 \\ u_2 \\ u_3 \end{Bmatrix} = \begin{Bmatrix} k_{11}^{-1}f_1 + k_{11}^{-1}k_{13}u_3 \\ k_{22}^{-1}f_2 + k_{22}^{-1}k_{23}u_3 \\ u_3 \end{Bmatrix}$$

The conditioning of structural mechanics problems implies the choice of direct rather than iterative methods for eliminating internal dof and for solving the interface problem [ESC 94].

Steps 2 and 3 of the algorithm are the most time consuming ones. Step 2 involves only calculations local to subdomains. Internal unknowns for each subdomain can be eliminated concurrently. For step 3, the interface problem matrix is distributed over the local memories of the processing elements and it is factorized and solved in parallel. The main issue for this parallelization is the relation between the number of subdomains and the number of processors. The analysis of the sequential execution times shows that:

- total execution time depends on the number of subdomains,
- execution time of step 2 is dominant for a small number of subdomains (up to 8) and tends to decrease as the number of subdomains increases,
- execution time of step 3 increases with the number of subdomains, and becomes dominant from about 16 to 32 subdomains.

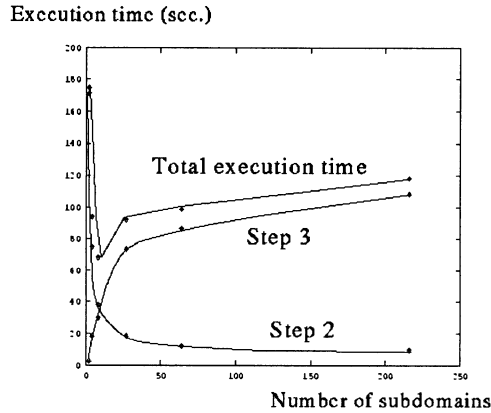


Figure 1. Sequential performance of a 3D test case with 6591 dof

Typical execution times are shown in Figure 1. A straightforward choice is to assign one processor per subdomain. For large numbers of processors, most of the execution time is spent in step 3, which requires large amount of communication and does not lead to high efficiency. Therefore, it could be more interesting to assign several processors per subdomain. On the other hand, load balancing problems occur in the cases when the computing times of step 2 for each subdomain are not constant. To reduce these problems, it would be necessary to have more tasks and consequently more subdomains than processors. This is in contradiction with the previous remark. In the rest of the paper, the choice of one processor per subdomain will be assumed.

The implementation of the domain decomposition method on a distributed memory system can be described as follows:

- (S1) distribute the data of the finite element problem (nodes, elements, boundary condition, material characteristics, ...) of the subdomains to the processors using DDSM;
- (S2) for each subdomain concurrently, eliminate all internal dof;
- (S3) for each processor:
 - allocate one part of the interface problem matrix,
 - send the locally condensed matrix (matrices) k_{33} to all other processors,
 - receive the other condensed matrices and assemble the elements which belong to the local part of the interface problem matrix;
- (S4) factorize the interface problem matrix (eventually in parallel!);
- (S5) solve the lower and upper triangular systems of the interface problem matrix;
- (S6) for each subdomain concurrently, back substitute the solution of the interface problem on internal dof.

This algorithm is currently being implemented on a Cray T3D system. Performance analysis of the algorithm raises the following issues: there is no possible direct comparison with sequential execution time because the problems solved in parallel do not fit into the memory of a single processor. A comparison with a sequential machine (with a sufficient memory) having a different processor should take into account the relative performances of the processors that are difficult to evaluate (non linear behavior). For these reasons, the performances presented concentrate on the elapsed (wall clock) execution time for different number of processing elements (PE). These execution times are compared to those obtained sequentially on a Cray J916. As mentioned before, the size of the problem solved depends on the number of PEs.

The test problem considered is a 3D cube partitioned regularly into 4, 8, 16 and 32 subdomains. The execution times obtained are given in Figure 2

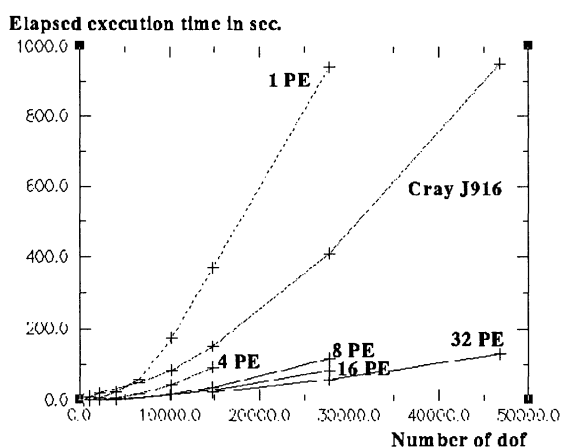


Figure 2. Elapsed execution times for different numbers of PE

Following remarks can be drawn from these results :

- for small numbers of PEs (4 and 8), efficiency approaches 100%
- for larger numbers of PEs (16 and 32), at fixed problem size the efficiency drops rapidly
- for the same numbers of PEs (16 and 32), the efficiency increases with the problem size.

The above conclusions mean that the proposed parallel algorithm is not well scalable at fixed problem size, but is scalable if the problem size increases with the number of processors.

6. Conclusion

We have presented different aspects of distributed computing in the context of structural engineering problems. Distributed computing was applied for optimizing the use of heterogeneous computing resources. A runtime system for communicating objects between distributed object bases has been developed. Next, we demonstrated the use of distributed parallel systems to reduce significantly the execution time of finite element simulations. A domain decomposition direct method was applied. The same communication system could be used for these different classes of applications for a wide range of computing systems: networks of heterogeneous workstations, vector supercomputers, massively parallel systems.

The actual work forms a basis for future research aiming at optimization of all the steps of direct domain decomposition methods: communication and assembly of condensed matrices, factorization and resolution of the interface problem, using several processors per subdomain, load balancing problems.

7. References

- [AUN 90] S. Aunay, *Architecture de logiciels de modélisation et traitements distribués*, thèse UTC, Université de Technologie de Compiègne, 1990
- [BRE 92] P. Breikopf, G. Touzot, *Architecture des logiciels et langages de modélisation*, Révue Européenne des Eléments Finis, 1(3) :333-368, 1992
- [ESC 94] Y. Escaig, M. Vayssade, G. Touzot, *Une méthode de décomposition de domaines multifrontale multiniveaux*, Révue Européenne des Eléments Finis, 3(3) , 1994
- [FAH 94] C. Fahrat, F.X. Roux, *Implicit parallel processing in structural mechanics*, Monograph, Computational Mechanics Advances, 1994
- [GEI 95] A. Geist, J. Dongarra, W. Jiang, R. Manchek, V. Sundream, *PVM : Parallel Virtual Machine ; A User's Guide and Tutorial for Networked Parallel Computing*, MIT Press, 1995
- [SAL 95] J. Saitz, R. Ponnusammy, S. Sharma, B. Moon, Y-S Hwang, M. Uysal, R. Das, *A manual for the CHAOS runtime library*, Technical Report CS-TR-3437, University of Maryland, 1995
- [KOP 95] C. Kopp, *Introduction to NFS Performance, Part 1*, Open Systems Review, September 1995

FEM/CAD SYSTEM ARCHITECTURE FOR SHAPE OPTIMIZATION OF 3D PARTS.

Ahmed MERROUCHE*, Catherine KNOPF-LENOIR*, Olivier STAB**

** LG2mS, Pôle Régional de Modélisation, Université de Compiègne, BP 20529, 60205 Compiègne Cedex, France - cklv@utc.fr*

*** CGES, Ecole Nationale Supérieure des Mines de Paris, 35, rue Saint-Honoré, 77305 Fontainebleau Cedex, France - stab@cges.ensmp.fr*

A new system architecture for optimum design is presented. The objective of the present work is to contribute to automatize the procedure of shape optimization of 3D parts : the optimization process is described as tasks operating in a distributed network and coordinated by a pilot system. The principle consists in exploiting the efficiency of specific tools dedicated to the different applications involved : a solid modeler, an adaptive mesh generator, a finite-element code and a mathematical programming module. An example of 3D part optimization is presented to validate the system and demonstrate its capacities.

1. Introduction

Today CAD/CAM systems are performant and allow a considerable productivity gain by integrating several steps of the design and manufacturing process of industrial products. Tools such as IDEAS, Pro-Engineer, Euclid, CATIA, etc. reduce in a significant way the difficulties related to the design of a product and they allow the automatization of a number of operations. Therefore the engineer's role remains of the utmost importance, because he is in charge of the design and he has to choose the most appropriate one .

This task corresponds to a creation of a set of different models (local, global, taking into account different physical phenomena) and the synthesis of their results : this is called multidisciplinary optimization. Assistance tools for helping the use of these various softwares and for decision making are especially needed as they are complex and computer resource consuming.

Recent works have been devoted to study new system architectures adapted to optimum design, they take into account the multidisciplinary aspect of the optimization e.g. [2],[1], and particularly [5], which concerns the Boss-Quattro system commercialized by SAMTECH. The originality of our approach is on one hand the use of a « pilot »

system to handle all interactions between the applications, and on the other hand to allow a distributed tasks management.

2. Basis of the proposed architecture.

The present study introduces an architecture dedicated to drive the shape optimization process, which is an example of situation where various independant applications have to be coupled : a geometric modeler, an adaptive mesh generator, a finite-element program, an error estimator and mathematical programming codes. First, the shape optimization process is decomposed into several tasks distributed on a network of computers and coordinated by a pilot system ; a general method to manage this process is based on a collaborative approach. The required functionalities and information exchange in the used tools environment are specified for each application (Figure 1). These specifications have led to definition of functional interfaces which are available in a general framework and which have been used in the construction of the prototype. The pilot system and the functional interfaces are presented.

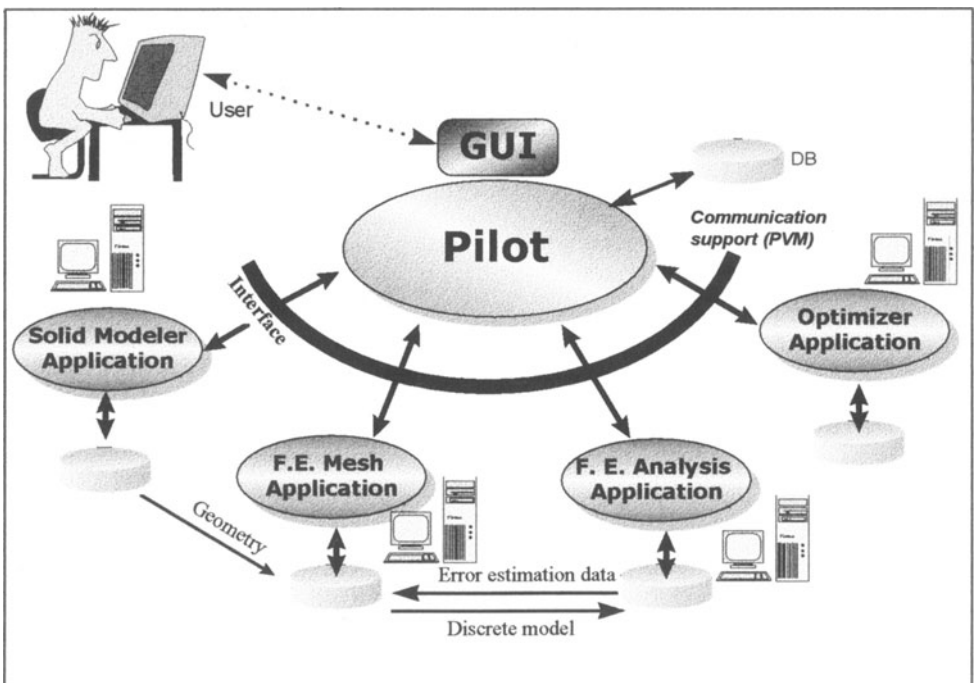


Figure 1 Principle of the system architecture

The figure 2 shows the main steps in the shape optimization process of a mechanical part: the problem is first formulated : the design variables, the objective functions and the constraints are defined. A geometrical model (parametric) of the object to optimize

is then built and the design variables are associated with geometric parameters. A discrete model is created by the mesh generator and the various mechanical characteristics such as loading and boundary conditions are affected to the mesh entities. This mesh is adapted by successive finite element analysis, error estimations and refinements ; when the required precision is reached, the results are used to evaluate the objective function, the constraints and their gradients. The design variables are modified by the mathematical programming algorithm and the geometry is updated . The problem is solved iteratively.

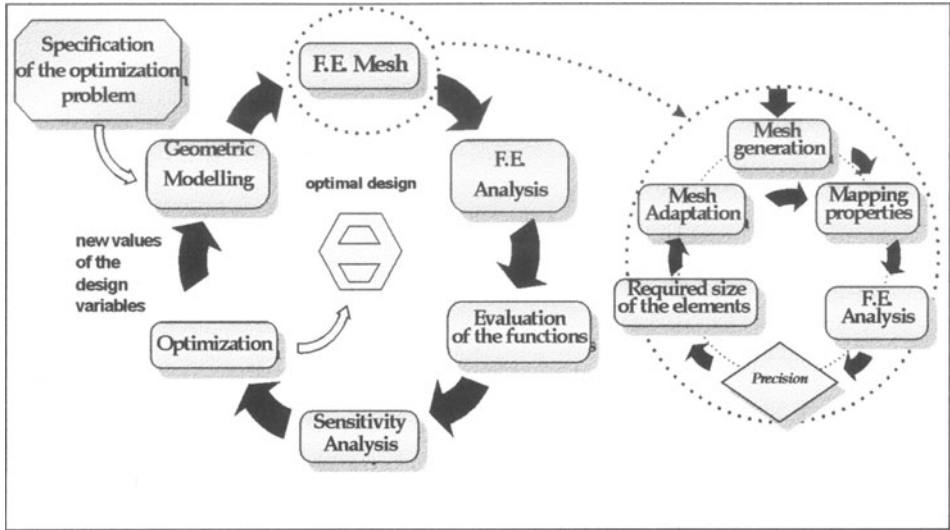


Figure 2 The optimum shape design process

3. Architecture of the proposed system

3.1 THE FUNCTIONAL INTERFACES

The main interest for separating the tasks implied in the process is a flexible and open architecture allowing the replacement of one tool by another one. To make this effective, the applications in the architecture must provide normalized functionalities and also support data exchanges between them. These specifications have been given in details in [3]. The Table 1 gives some examples of functions used by the tasks to access and to modify the data. The data are exchanged through the normalized interfaces, either by messages or by files, depending on the nature and of the amount of information to handle.

GET/SET	can be applied to a design variable value, to a node position of a mesh, ...
COMPUTE/UPDATE	can be applied to the geometric model, the mesh or the discrete model.
READ/WRITE	read or write a file in the specified format for external exchanges.

Table 1. Some functions of the normalized interfaces.

3.2 THE PILOT SYSTEM

The pilot has the following functions :

- definition of the optimisation data : choice of the design variables, criteria, constraints,
- process control : management of the tasks (execution/stop/interrupts), tests,data flows management (transfer and naming of files)
- choice of options : sensitivity analysis method, mesh adaptator, ...
- overview : choice of driving mode (step by step, automatic, ...) viewing of results, state of the tasks , machines, execution times, ...

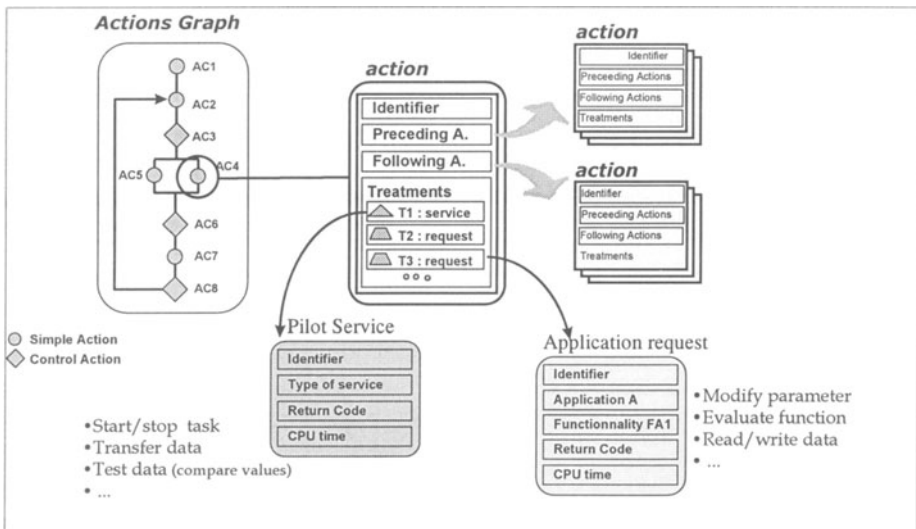


Figure3 Graph of actions defining the optimization process.

The scenario describing the process can be defined by a graph of actions (Figure 3). An action defines the elementary executive unit which cannot be interrupted ; it is defined by a sequence of parallel or sequential operations which are either commands or quests which are related to an application or to the pilot. Each quest specifies the elementary function, the task doing it, the CPU resources required and some information describing the success or failure of the treatment (return code, value of a variable, a constraint or data specific to the status of the applications : waiting, executing or inexistent application..

4. The prototype system worked out

We started with five tools : a solid modeler (DIMAT, C.S.G. parametric modeler of GIAT-Industries), a 3D automatic mesh generator (XMAILLE, [7]), a finite element program (SIC, [4]), an error estimator (ESTIM3D, [6]) and an optimization module. Each tool has been initially designed to be used independantly on different UNIX plateforms, without collaborating with other tools.

At the beginning of our work, these pre-existing tools have been modified to satisfy the requirements of the architecture and the communication functionalities. New tools have been developed, mainly for adaptive meshing, in order to assure the missing fonctionnalities for optimization. A model of the pilot system has been worked out (XPILOTE). The messages between applications are exchanged by the PVM interface (*Parallel Virtual Machine*)

5 Example : shape optimisation of a 3D component.

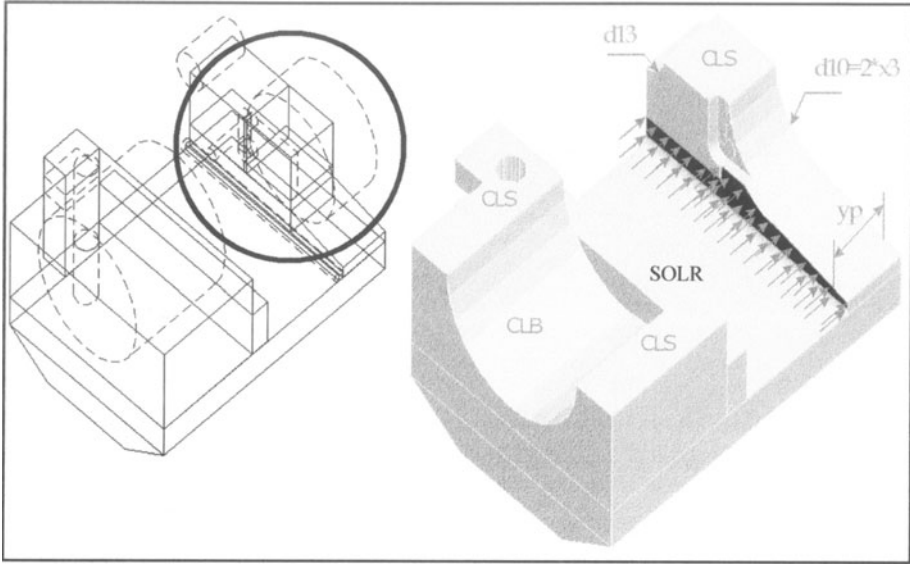
This example is proposed by GIAT Industries (Figure 4). Only one half of the component is studied, with symmetric conditions on the middle plane ; the structure is submitted to a uniform pressure due to another part which is not represented here. The problem is to optimize the shape of the circled area on Figure 4. We have defined a region (a box, pointed out as ZONE) which is automatically located on the mesh when a new geometry is defined. This area is described on the geometrical model by using the primitives of the CSG model.

First, the system is used to carry out various studies of this piece : the pilot computes the values of the objective function, constraints and their gradients on a grid of design variables values. At the end of these pre-studies, several optimization problems have been stated. For example, we consider the minimization of a L4 norm of the von Mises stresses, integrated on the ZONE region, and submitted to a weight constraint:

$$\left\{ \begin{array}{l} \text{Min} \left(\frac{1}{\Omega^4} \sqrt{\int_{\Omega} \sigma^4 d\Omega} \right) \\ \text{Weight} < 1.443 \text{Kg} \\ 16\text{mm} \leq y_p \leq 26\text{mm} \\ 18\text{mm} \leq x_3 \leq 25\text{mm} \\ 8\text{mm} \leq d_{13} \leq 16\text{mm} \end{array} \right. \quad \text{with initial values} \quad \left\{ \begin{array}{l} y_p^0 = 18.6\text{mm} \\ x_3^0 = 17.5\text{mm} \\ d_{13}^0 = 14.9\text{mm} \end{array} \right.$$

The problem is treated with only one adaptive meshing iteration in the optimization process. The mesh has about 7000 elements and 1600 nodes and the error is approximately 35%. Convergence is obtained after only 7 iterations. The weight constraint is satisfied, reducing the weight of the variable area by 50%, and at the same

time, the maximum von Mises stress has a 5% decrease (Figure 5). For this solution, the bound $x_3 > 17$ is active. The initial and final shapes are shown in Figure 6.



Mechanical data

Linear elastic analysis, tetrahedral elements (TH4)

$E = 210000 \text{ MPa}$, $\nu = 0.3$ $\rho = 7.8 \text{ Kg/dm}^3$

SOLR : uniform loading 600N/mm^2 on the underlined part

CLS : symmetric boundary conditions ($w=0$) on the top of the part.

CLB : all the cylindric part CLB is fixed

Figure 4. Geometry and design variables of the GIAT component.

6 Conclusions

In this paper, we are concerned with the general process of shape optimization of 3D components, and with the problems related to its implementation.

A new system architecture, based on the concept of the « Pilot » has been developed; it has been shown that existing tools as different as a CAD solid modeler, a mesh generator, a finite element program and an optimizer can be carried to normalized interfaces and integrated in this architecture. A model of the whole system has been worked out and validated by several academic and practical examples. The pilot software handles 8 applications distributed on 5 machines. The advantages of this approach are the following :

- a full assistance for the automatic implementation of the optimization problem : after the data definition, the intervention of the user is restricted to the overseeing task only. The execution of the tasks and the associated data exchanges are done by the pilot.

- flexibility : due to the notion of functional interfaces, the user can replace any application of the architecture by another one, more suitable for its problem on two conditions : it must have the same functional interface and it must support the communication mechanism used by the pilot. The distributed management of the tasks is another aspect of this flexibility : codes specific of given machines can be exploited through the architecture and thus optimized applications can be used.

- the open character of the pilot : the use of an action graph to describe the process and the concept of normalized interfaces are general features that permit to consider the extension of the system to other processes than optimization.

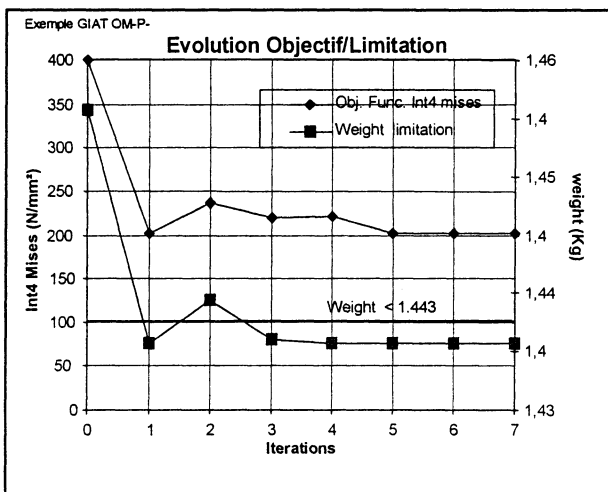


Figure 5. Convergence of the functions (weight and L4 norm of the von Misès stresses).

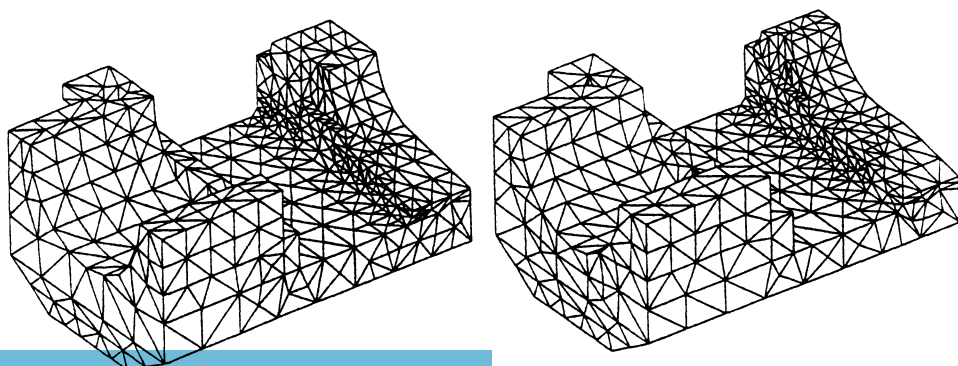


Figure 6. Mesh of the initial and optimized shapes

7. Références

1. T. M. EIDSON, J. C. TOWNSEND, R. P. WESTON, *A programming Environment for Distributed Complex Computing. An Overview of the Framework for Interdisciplinary Design Optimization (FIDO) Project*, NASA TM 109058, Dec. 1994
2. B. ESPING, D. HOLM, F. CAMPION, P. CLARIN, L. LJUNGGREN, O. ROMMELL, *Integrated Modular Software for Design Optimization with Structural and Multidisciplinary Objectives*, OPTI'93, 3rd Int. Conference on Computer Aided Design of Structures, Zaragoza, Spain, July 1993
3. A. MEROUCHE, *Vers une mise en œuvre automatique de la conception optimale : architecture de système et outils logiciels pour l'optimisation de forme de pièces 3D*, Thèse de doctorat, UTC, Sept. 1997
4. L. MORANCAY, *Représentation paramétrée et modélisation de système physique pour la conception optimale*, Thèse de doctorat, UTC, Juin 1993
5. P. MORELLE, J. J. MAISONNEUVE, *Multidisciplinary optimization through the Boss-Quattro architecture : an Integrated Parametric Design methodology*, First International Conference: IDMM'E'96, Nantes, France, April 1996
6. A. SELMAN, *ESTIM3D, logiciel 3D d'estimation d'erreurs et calcul de densités de maillage*, rapport interne, UTC, Octobre 1993.
7. O. STAB, *Maillage automatique 3D par opérations booléennes*, Thèse de Doctorat, Ecole Nationale Supérieure des Mines de Paris, Déc. 1992.

2D MESH AND GEOMETRIC ADAPTIONS USING AN A PRIORI MODEL OF MECHANICAL BEHAVIOUR

Ph. VERON*

* Centre d'Etudes et de Recherches de l'Ecole Nationale Supérieure des Arts et Métiers, 2, Cours des Arts et Métiers, 13617 Aix en Provence, France

E-mail : Philippe.Veron@aix.ensam.fr

L. FINE**, F. NOËL**, J-C. LEON**

**Laboratoire des Sols, Solides, Structures UMR-CNRS 5521, BP 53, 38041 Grenoble Cedex, France

E-mail : [Lionel.Fine| Frederic.Noel| Jean-Claude.Leon]@hmg.inpg.fr

Abstract. So far, the generation of meshes adapted to mechanical part analysis requires an iterative process which implies a large computation time. The aim of this paper is to present a method of computing an *a priori* map of element sizes to generate the mesh for a studied case, i.e. without a complete computation of the analysis. This method is based on the *a priori* approximation of the stress field in the structure. The present approximation is both performed from the identification and the characterisation of the over stressed areas close to geometric features of the studied part and from the boundary conditions applied to its geometric domain. This approximated field allows to deduce, at each point of the structure, the element size of a mesh able to respect a prescribed value of energy deviation. This map is used during the generation process of an adapted mesh. It also provides useful data to geometry adaption in order to generate a simplified geometric model.

1. Introduction

In the field of Finite Element Analysis (F.E.A), the generation of meshes adapted to each analysis requirements is still a critical step to obtain significant numerical results. Until now, adapted mesh generation is carried out mainly from a *posteriori* optimisation methods [6, 2]. Such methods incorporate a process which requires to solve a complete F.E. problem at each iteration of the adaption. During each iteration, the analysis of the F.E. solution helps locate the areas of the mesh which need to be refined [11]. In this case, the analysis criterion is based on an energy error estimated from the current mesh elements. Thus, each additional iteration allows to improve the

optimality¹ of the mesh. Although they can be used by current F.E.A. software, such techniques usually lead to rather large calculation times which reduce the use of F.E.A as a decision making tool during design processes rather than a design tool (F.E.A is still widely used for validation steps rather than for structural dimensioning purposes).

Conversely, the aim of the current approach consists in generating an element sizes map from an *a priori* analysis both of the geometry and of the boundary conditions of the part studied [3]. The goal of this *a priori* analysis is not to determine very accurate values of the stress field throughout the part like a F.E.A. software could do it, but rather to get an approximation of it through functions which would express the stress field behaviour throughout the part and especially near geometric and mechanical singularities. These singularities, also called specifications, characterise potentially over stressed areas for the given analysis (fillets, welded joints, areas where boundary conditions are applied and so on).

Both approaches, i.e. *a posteriori* and *a priori* methods, are illustrated in Figure 1. Their main difference stems from the fact that *a priori* methods use the physical model properties to generate an adapted mesh before the computation of the F.E. solution whereas *a posteriori* methods generate the adapted mesh after a preliminary F.E. solution was computed. Moreover, this *a posteriori* adaption process is often iterative. Using *a priori* adaption methods, the first mesh generated readily integrate the mechanical behaviour of the case studied.

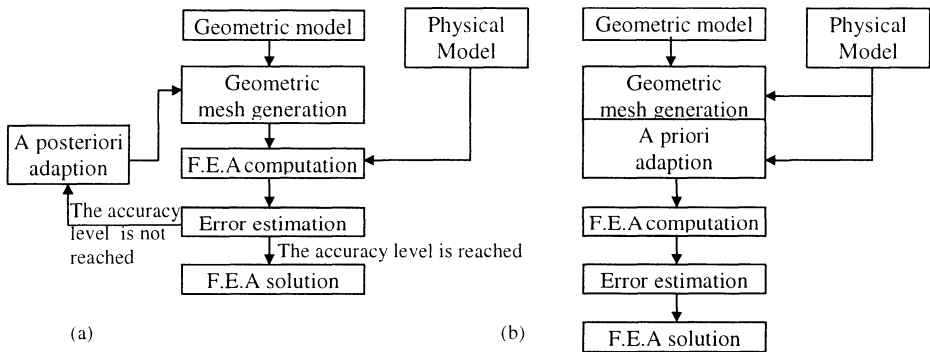


Figure 1: General description of the a posteriori (a) and a priori (b) mesh adaption processes.

The map of element sizes estimated from the *a priori* analysis forms the basic information used either to generate an adapted mesh from the initial one or to compute a simplified (or abstracted) geometry of the part in order to optimise (see footnote 1) the given F.E.A. problem.

2. A priori generation of the element sizes maps

The present method is currently dedicated to 2D problems. The element sizes generation process can be divided into four steps :

¹ Here, the term optimality characterises the ability of a mesh to produce accurate F.E. solutions with a minimum number of elements. When this objective is reached, the F.E. problem solved incorporates a minimum number of degrees of freedom.

- the first one consists in analysing the data attached to the configuration studied in order to identify all the potential specifications (both mechanical and geometric ones) (see Figure 1 (a) and (b)). The mechanical specifications are defined by the user during the creation of the analysis model. Therefore, their location and their type are known. Conversely, the geometric specifications (fillets, holes, ...) are contained into the geometric representation of the part. Thus, a geometric analysis is necessary to identify and to locate high radii of curvature areas, holes and so on. Currently, this task is still carried out manually by the analyst. These specifications being identified, a database allows him/her to select the adaption function that each of them induces within the stress field. This function, which expresses the over stresses generated, decreases according to the distance from the related specification location. Each of these functions is parametrized and its coefficients are closely linked with the shape geometry of the part around this specification,
- at the second step, the specifications which significantly modify the stress field are identified. Then, the geometric representation of the part is used as a basis for the construction of an elastic bar network. The main characteristic of this bar network is its ability to represent the geometry of the case studied as well as possible using a minimum number of bars (see Figure 2). The mechanical specifications (boundary conditions, loads, ...) are applied to this bar network and the analysis of the strains in each bar helps locate and quantify approximately the relative influence of each specification over the stress field of the initial structure. As a result, it is possible to estimate for each specification a coefficient which characterises its influence on the stress field of the initial structure. Thus, it is possible to estimate a coefficient which characterises its prominence on the stress field around each specification,



Figure 3 : Mesh with a minimum number of bars.

- at the third step, the results of the two previous steps are combined to define the stress gradients into the structure. The method consists in taking into account the effects of the specifications located into the highly stressed areas only. To this end, their influences are adjusted using a coefficient representing the intensity of the associated loads (force, momentum, pressure) (cf. step 2),
- finally, the last step leads to the generation of the element sizes map. To this end, a set of points uniformly distributed over the geometric model, like a rectangular grid, is used to ease the map generation. It is also assumed that all the adapted mesh elements use a linear approximation of the stresses. Thus, the ideal element size is estimated at each point of the map in order to minimise the stress error (see Section 3 for map examples). To monitor the map size generation process, a maximum acceptable error is set by the user. In such a map, small element sizes are located in the areas characterised by large stress gradient variations. At the

opposite, large element sizes are located in the areas characterised by weak variations of the stress gradients.

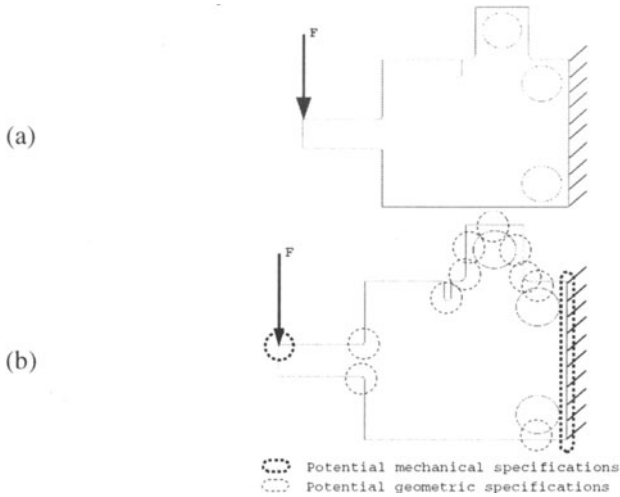


Figure 2: (a) Geometry and boundary conditions. (b) Potential specifications.

In addition to the fact that this map represent the target element sizes for an adapted mesh generation process, it also allows to locate the geometric features which have no or only a weak influence on the target F.E.A. (areas where large element sizes are estimated are weakly stressed areas).

Such a map can be used for the optimisation of F.E.A. calculations at two different levels :

- the generation of an adapted mesh from the initial geometric representation of the part (see Section 3),
- the simplification of the initial geometric representation of a part by removing geometric details which do not have a significant influence on the F.E.A. solution (see Section 4).

3. Adapted mesh generation

An element sizes map generated with the previous method represents a first action level. Element sizes computed from this first map (rough map) only takes estimated constraints distribution into account, they are neither compatible with geometric requirements (necessity of an adapted discretisation for the part outline when element sizes are larger than the local size of the part, ...) nor with computational requirements (necessity of a bounded gradient of element sizes to ensure the validity of the computed results). Therefore it is necessary to modify this size map to preserve the coherence with the geometric domain being meshed. This process is performed in order to minimize the size of the elements that must be created, hence error criteria are always satisfied.

Various processes for mesh adaption have been developed [1, 4, 10]. Here, the adapted mesh generation is obtained from an approach proposed by Noël [5]. The

strategy chosen consists in modifying an initial mesh to create a new one which is compatible with the size map. This is obtained through two stages :

- mesh refinement in the areas where the mesh is too coarse. All the initial mesh edges are scanned. Those which have their length larger than the local element size prescribed by the map are selected and subdivided,
- coarsening of the areas where the mesh is too dense. Vertices linked by edges which have a length shorter than the local size defined by the map, are removed.

These two operations are incorporated into an iterative process until there is no more refinement or deletion to perform. Between each iteration, mesh vertices are automatically repositioned with an algorithm based on the Force Density Method (FDM) [7, 5], in order to generate elements with a good aspect ratio, i.e. as equilateral as possible.

3.1. ADAPTED MESH APPLICATIONS

Figures 3(a) and (b) show the specifications identified from two different sets of boundary conditions applied to the same geometric shape. Using these sets, two different size maps are computed (see Figure 5(a) and (b)).

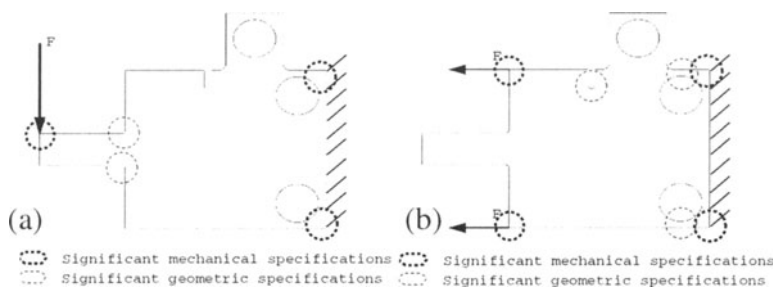


Figure 4 (a) and (b): Mechanical specifications identified for two sets of different boundary conditions.

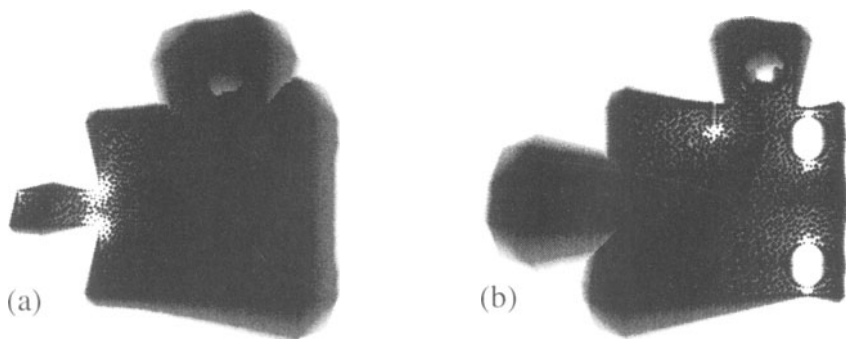


Figure 5 (a) and (b): Size maps computed from conditions defined in the figure 4 (sets of spheres with radius reflecting the element size).

To evaluate the efficiency of these maps, a mesh has been generated from the map of Figure 5 (a) (see Figure 6). This mesh is composed of 486 elements and has been used as input for a F.E.A computation. To get a reference result, another F.E.A

computation has been performed from an accurate mesh (1880 small elements with a regular size). As shown on Figure 7, the results of these two computations are very close to each other into over stressed areas. The global stress distribution also stays unchanged. Thus, the adapted mesh generated provides an efficient discretisation of the studied case.



Figure 6: Example of mesh generated from the map size shown on figure 3(a).

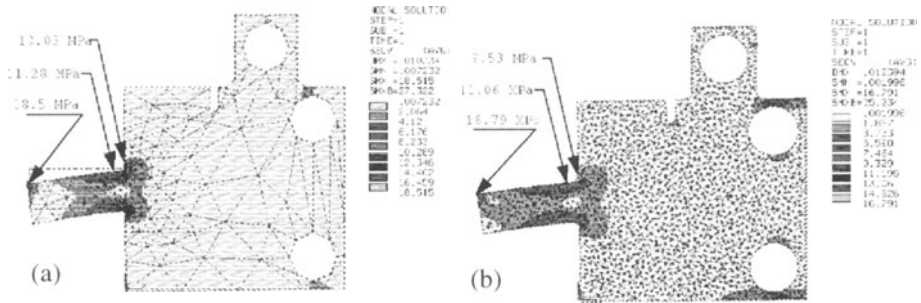


Figure 7(a) and (b): Maps of Von Mises Equivalent stress from F.E.A computations.

3.2. CONCLUSIONS

Meshes obtained from the method described (*a priori* map definition and adapted mesh generation) cannot be considered as the optimum meshes of the studied cases. Rather, the meshes generated stand for a first mesh generation step (compared with iterative methods) which is compatible with a target error and uses a reduced number of elements. Hence, the meshes generated produce efficient numerical models. Similarly, the next section introduces a method of geometric simplification which reduces meshes complexity through geometric transformations of the shape of the domain.

4. Geometric simplifications

Here, they characterise the second action level. The element sizes produced by the size map are used to monitor the simplification process of the initial geometry of the studied case. Indeed, the areas of the part where large element sizes have been estimated are areas of the part which are either not or weakly loaded with respect to the mechanical analysis considered. Nevertheless, these areas can incorporate geometric details (small holes for example) which generate unnecessary constraints during the generation of an adapted F.E. mesh (see Section 3). The goal of the initial

geometry adaptation process consists in removing these details or some features of the part shape which are not relevant for the current analysis. Consequently, the generation of an adapted mesh based on the simplified geometry produced is eased and less elements are needed.

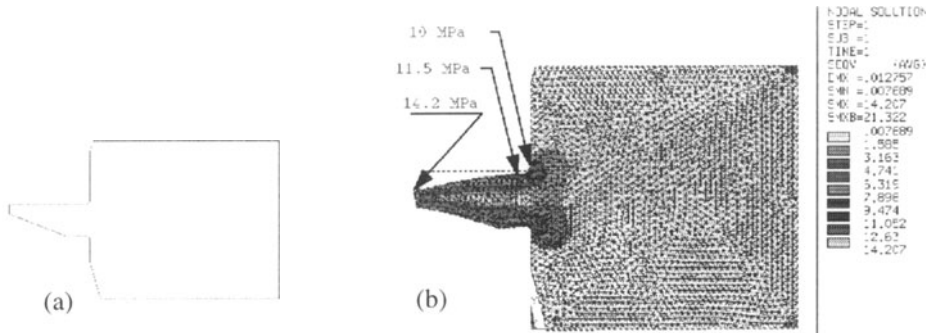


Figure 8: (a) Adapted geometry, (b) Map of Von Mises Equivalent stress from F.E.A computation.

The geometric simplification process used here is based on the approach previously developed by Véron [8, 9]. The geometric restoration of the initial geometry during the simplification process is achieved through an error zone concept. A spherical error zone is assigned to each vertex of the initial polygonal model which describes the initial contour of the case studied. All the error zones define a discrete envelope around the initial geometry where the simplified geometry must lie. An iterative vertex removal algorithm is used to produce the simplified geometry. The simplification stops when no more vertex can be removed. During the simplification process topologic and manifold changes may occur because of the size of the error zones specified. This ability of the approach is essential to be able to remove some details of the part, like holes for example. To produce the adapted geometry, error zone values are set up from the element sizes estimations produced by the map previously generated. A selection criterion is used to monitor the simplification process. It allows to select the best candidate vertex for removal. In this case, the vertices are sorted in accordance to the size of their error zone. They are ordered from the largest error zone to the smallest one. Thus, the areas of the part with large element sizes estimations are simplified first. Then, the areas characterised by smaller element sizes are processed but the probability to remove vertices in such areas decreases. Such a selection process allows to preserve the areas of interest.

4.1. APPLICATION OF THE GEOMETRIC SIMPLIFICATION PROCESS

The size map (Figure 5(a)) computed from the case studied of Figure 2(a) is used during the geometric simplification process defined above. The result of the simplification is shown in Figure 8(a).

Compared to the initial geometric model, the one has lost all the features which don't significantly modify the stress field (the three holes and the notch). The map of Von Mises stresses of the F.E.A computation from an accurate mesh of the adapted geometry (Figure 8(b)) show that stress values in highly stressed areas stay close to those of the reference map (Figure 7(b)) whereas the complexity of the contour mesh

has been largely decreased. Hence, the generation of an adapted mesh based on a simplified geometry allows to generate a reduced numerical model (with a smaller number of degrees of freedom) which is very important from a computing time and mesh generation criteria.

5. Conclusion

An approach has been presented in this article to generate an efficient numerical model for F.E.A. computation. Therefore, techniques of *a priori* mesh adaption and geometry simplification are processes which lead to reduce F.E.A. time by reducing the time required to generate an adequate mesh. For complex analyses, a time reduction of the pre-processing and computation phases could add flexibility to F.E.A. tools to improve their integration into the design process and increase their interactivity. Future work will focus on the extension of the current approach to 3D structures and idealisation techniques where manifold transformations are required.

6. References

1. Chinnaswamy, C., Amadei, B., Illangasekare, T.H., "A new method for finite element transitional mesh generation", Int. J. for Num. Meth. in Eng., **31**, 1991, 1253-1270.
2. Dumeau, J.P., "Contrôle et adaptation des maillages 3D : application à l'automatisation des calculs", Ph.D. thesis, Ecole Normale Supérieure de Cachan, 1995.
3. Fine, L. "Adaptation de maillages surfaciques basée sur l'analyse a priori de spécifications mécaniques", DEA de l'Université Joseph Fourier, September, 1996.
4. George, P.L., Borouchaki, H., "Triangulation de Delaunay et maillage", HERMES, Paris, 1997.
5. Noël, F., "Mailleur auto-adaptatif pour des surfaces gauches en vue de la conception intégrée", Ph.D. thesis, l'Institut National Polytechnique de Grenoble, October, 1994.
6. Pelle, J.P., "Contrôle de paramètres des calculs éléments finis. Application au 3D et au non-linéaire", Journée d'Etudes CSMA, INRIA, Rocquencourt, France, 1994.
7. Schek, H.J., "The force density method for form finding and computation of general networks", Comp. Meth. in Applied Mech. and Eng., **3**, 1974, 115-134.
8. Véron, P., Léon, J-C., "Static polyhedron simplification using error measurements", CAD, **29**, n°4, 1997, 287-298.
9. Véron, P., Léon, J-C., "Geometric tools dedicated to the adaption and idealization of 3D models for F.E. Analysis", Proc. of the DETC'97, ASME paper DETC97CIE4457, Sacramento, 1997.
10. Zienkiewicz, O.C., Zhu, J.C., "A simple error estimator and adaptive procedure for practical engineering analysis", Int. J. For Num. Meth. in Eng., **24**, 1987, 337-354.
11. Zienkiewicz, O.C., Zhu, J.C., "Adaptivity and mesh generation", Int. J. For Num. Meth. in Eng., **32**, 1991, 783-810.

ON THE AUTOMATION OF NON-LINEAR BEHAVIORAL STRUCTURAL ANALYSIS. GUIDANCE AND QUALITY CONTROL

J.P. PELLE, D. RYCKELYNCK
*Laboratoire de Mécanique et Technologie,
ENS de Cachan / C.N.R.S. / Université Paris 6
61, avenue du Président Wilson 94 235 Cachan Cedex
Ryckelynck@lmt.ens-cachan.fr*

Abstract

Controlling the numerical quality of non-linear simulations allows automating the discretization choices. Within the framework of time-dependent problems, this quality depends on the errors introduced in the calculation of the transformation history. Generally, before obtaining a calculation of satisfactory quality, it is necessary to carry out an evaluation of the numerical approximations to use by utilizing all of the history of the approximate solution flaws. We propose a strategy which naturally includes this evaluation. The solution sought is built iteratively, improving the entire history at each iteration thanks to the LA.T.IN. method. The simulation is initialized with a coarse model. Then, all of the approximations are adapted during the subsequent iterations in order to obtain the prescribed quality. This quality is estimated by a global dissipation error. Thanks to an approximation classification, we are able to identify the nature of the different contributions to the global error. We use, in particular, a space indicator to characterize the mesh, and another indicator to characterize the time discretization.

1. Introduction

When designing complex systems, it is increasingly necessary, even essential, to take into account the non-linear phenomena (non-linear material behavior, large deformations, contacts) because only in doing so does it become possible to build representative numerical models of physical realities. However, we have to admit that the simulation of such non-linear phenomena is very costly with respect to calculation time, memory size and data time preparation. For example, the simulation of a mechanical part that takes into account only one plastic or viscoplastic behavior in small deformations can, according to the type of loading applied, cost 100 to 1,000 times as much as a simple linear analysis. Indeed, these problems are generally solved by the incremental method, which is based on a fine partition of the time interval over which the loading is defined, in addition to the space discretization of the studied structure.

This is why, nowadays, this kind of simulation is very seldom used during the design stage. In most cases, it is used as a checking computation when the structure is designed. If we wish to compute a complete manufacturing process, such a task is obviously more difficult.

Over the past few years, various approaches have been suggested, in non-linear

cases, to adapt the mesh and the size of the time steps during the computation in order to reduce the cost while maintaining a reasonable level of quality [1], [2], [3]. These approaches are based on the incremental method as well as on error estimators or indicators. The structural behavior at moment t is naturally dependent on the history since the beginning of the loading. If the discretization errors associated with the history part are too large, no adaptation can improve the computation during the following moments. To better the simulation, it is generally necessary to carry out at least two resolutions for the whole history. An initial stage, which we could call an expert stage, consists of defining the significant aspects of the solution over the whole time interval and provides an error estimation of discretization used. The second stage leads to the required quality resolution thanks to adapted time and space parameters. In complex cases, the first stage involves more than one resolution followed by an adaptation, which does not help reduce costs.

The objective of this paper is to propose, within the framework of non-linear behavior in small perturbations, a methodology which includes the expert's stage and an adaptive control during the resolution. It is based on:

- a non-incremental method of resolution for non-linear problems [4] which, at each iteration, builds an approximate solution (displacements, stresses, ect.) defined on both the structure and the entire time interval;
- a constitutive error estimator adapted to non-linear behavior [4] which allows evaluating discretization errors globally;
- error indicators to separate the different kinds of errors into the global error, according to space, time and other discretizations; and
- an automatic guidance strategy for the main parameters of the algorithm, such as the mesh and the time discretization, during the computation.

Our strategy consists of adapting the numerical effort during the iterative resolution, using a real error control. For example, the mesh and the time representation are coarse for the first iterations. According to the indications provided by our error estimator, these are refined as the non-linearities are better taken into account. Since the algorithm yields a complete solution in time and space, once the solution quality is sufficient, the algorithm is stopped. If the solution quality is not sufficient, the computation is continued. No return is generated, like the one used with the incremental method; the whole history is improved with the non-incremental approach.

An important point is that the user only has to describe the geometry and mechanical data of the problem (loading, constitutive coefficients); the rest of the simulation is entirely automated. Thus, the user is no longer responsible for the often difficult choice of the non-incremental method parameters and the choice of time and space discretization. We then obtain a decrease in computation costs (saving of time, saving of memory) but also a saving user data preparation time, which is a very important consideration from an industrial point of view.

The method is presented here for viscoplastic problems with small perturbations, but it can be extended to a variety of other situations.

This procedure has been programmed in the finite element software CASTEM 2000 environment and uses the automatic mesh generator ARAIGNEE and an error estimator software developed at the LMT. The use of another Finite Element code or another automatic mesh generator is entirely possible with a few minor modifications.

2. Reference Problem and Dissipation Error

The viscoplastic constitutive law studied is a standard [5] and normal [4] version of a Chaboche model which is often used, for example, to compute turbine paddles [6]. The internal variables are: the plastic strain ε^p , a tensor α associated with the kinematic hardening β and a scalar p associated with the isotropic hardening R .

When using the simplified notations $\mathbb{X} = (\alpha, p)$, $\mathbb{Y} = (\beta, R)$ and $s = (\varepsilon^p, \mathbb{X}, \mathbb{Y})$ for which each quantity is defined over $[0, T] \times \Omega$, the constitutive equations are:

- state laws:

$$\varepsilon^e = K^{-1}\sigma; \mathbb{X} = \Lambda\mathbb{Y} \quad (1)$$

where K and Λ are characteristic operators,

- evolution laws:

$$\dot{\varepsilon}^p = \partial_{\sigma}\varphi^* \text{ and } -\dot{\mathbb{X}} = \partial_{\mathbb{Y}}\varphi^* \text{ with } \varphi^*(\sigma, \mathbb{Y}) = \frac{k}{m+1}\langle z \rangle_+^{m+1} \quad (2)$$

where: $z = \|\sigma_D - \beta\| + \frac{1}{2c}\|\beta\|^2 - \ell(R) - R_0$; $\|\bullet\|^2 = \text{Tr}[(\bullet)^2]$; σ_D is the deviatoric part of σ ; and:

$$\ell(R) = Q \frac{R}{R_s} \left(2 - \frac{R}{R_s} \right) \text{ for } R \leq R_s; \ell(R) = -\infty \text{ for } R > R_s \quad (3)$$

The exact solution to the reference problem s_{ex} must satisfy not only these constitutive equations but also the kinematic equations, initial conditions and equilibrium equations. s is said to be *admissible* if and only if it satisfies all of the linear equations in the reference problem, which is all of the equations except the *evolution laws*. We can then note: $s \in A_d$. If s confirms the non-linear evolution laws, we note: $s \in \Gamma$. We therefore obtain :

$$s_{ex} = \Gamma \cap A_d \quad (4)$$

If $s \in A_d$ the dissipation error [4] $e(s)$ is defined by:

$$e(s) = \int_0^T \int_{\Omega} \{ \varphi(\dot{\varepsilon}^p, -\dot{\mathbb{X}}) + \varphi^*(\sigma, \mathbb{Y}) - \text{Tr}[\sigma \dot{\varepsilon}^p] + \mathbb{Y} \circ \dot{\mathbb{X}} \} d\Omega dt \quad (5)$$

where the local dissipation is: $\text{Tr}[\sigma \dot{\varepsilon}^p] - \mathbb{Y} \circ \dot{\mathbb{X}}$. Thanks to this definition, we obtain: $e(s) \geq 0$ and ($s \in A_d$ and $e(s) = 0$) if and only if $s = s_{ex}$. This quantity enables us to quantify the quality of $s \in A_d$ in terms of the approximation of s_{ex} .

3. Applied Non-incremental Method

The non-incremental method applied is a version of the LA.T.IN. method introduced by Ladevèze [4]. At each iteration, we build an approximate solution in A_d and then an approximate solution in Γ (see Figure 1).



Figure 1. LA.T.IN. iteration diagram.

If $s_n \in A_d$ et $\hat{s}_n \in \Gamma$ are known, the iteration n consists of determining s_{n+1} and \hat{s}_{n+1} by solving the two following problems:

- *Global but linear stage* : find $s_{n+1} \in A_d$ such that:

$$\forall (t,M) \in [0,T] \times \Omega, \begin{bmatrix} \dot{\mathbb{S}}_{n+1}^p \\ -\dot{\mathbb{X}}_{n+1} \end{bmatrix} = \begin{bmatrix} \hat{\mathbb{S}}_n^p \\ -\hat{\mathbb{X}}_n \end{bmatrix} + H \begin{bmatrix} \mathbb{C}_{n+1} - \hat{\mathbb{C}}_n \\ \mathbb{Y}_{n+1} - \hat{\mathbb{Y}}_n \end{bmatrix} \tag{6}$$

- *Non-linear but global stage* : find $\hat{s}_{n+1} \in \Gamma$ such that:

$$\forall (t,M) \in [0,T] \times \Omega, \left(\hat{\mathbb{C}}_{n+1}, \hat{\mathbb{Y}}_{n+1} \right) = \left(\mathbb{C}_{n+1}, \mathbb{Y}_{n+1} \right) \tag{7}$$

The operator H is associated with φ^* through the real tangent subspace in $(\hat{\mathbb{C}}_n, \hat{\mathbb{Y}}_n)$. An elastic computation followed by a local stage enables initializing the algorithm with (s_0, \hat{s}_0) .

For the numerical implementation of the global problem, the quantity $s_{n+1} \in A_d$, a function defined on $[0, T] \times \Omega$, is searched as the sum of the products of a scalar time function by a space function with the space functions being similar to a base. Such a base, represented by the classical finite element method, is built during the computation. If necessary, at the beginning of iteration n , the base of all known space functions is upgraded by new functions. The time function determination leads to the resolution of a first-order time differential system, which is integrated on $[0, T]$ by the θ -method, according to a time discretization.

It must be noted that this implementation provides s_{n+1} in A_{dh} which is an approximation of A_d . In order to estimate the error at the end of the iteration, we have to rebuild an element $s_{n+1}^* \in A_d$ on the base of s_{n+1} . This construction is performed through techniques developed at Cachan over the past 15 years [7].

4. Adaptive Strategy

At the end of a current iteration, the computation of $e(s_{n+1}^*)$ enables evaluating the global quality of the approximate solution obtained. If the prescribed quality level e_0 is not obtained, the computation has to be continued in order to better the solution. To obtain this improved result, we can adapt either the mesh or the time discretization, or increase the dimension of the space function base.

In order to develop an adaptive strategy, we have defined error indicators which



enable separating the various sources of error within the global error :

I_{esp} : space indicator which characterizes the quality of the mesh,

I_{tem} : indicator which considers all other sources of error.

In addition, we have defined the following indicators :

I_{int} : indicator to characterize the quality of the time discretization,

I_{bas} : indicator to characterize the quality of the space function base,

which allows sorting error sources evaluated by I_{tem} . We succeeded in building these various indicators, as well as the global error, from the concept of error in the constitutive relation and by defining hierarchical reference sub-problems [8].

Using these indicators, some simple guidance criteria can be defined. They essentially consist of obtaining a balanced distribution of the various levels of error during the computation. For example: as long as $I_{esp} < 1.5 I_{tem}$, the mesh is not modified. But if $I_{esp} > 1.5 I_{tem}$ at the end of an iteration, then a new mesh is built. Of course, the various finite element type fields are then projected onto this new mesh in order to pursue the computation (see Figure 2).

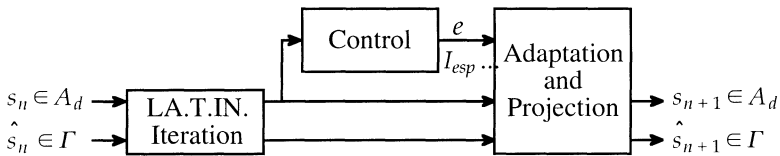


Figure 2. Adaptive iteration of the strategy

The two following rules are added to these criteria:

- R1: after the initialization, if plasticity is not negligible (in practice, we choose the criterion: $2 I_{tem} > e_0$), then an iteration is performed with the coarse mesh. If such is not the case, the mesh is automatically refined in order to obtain a better initialization.
- R2: after each mesh adaptation, at least one iteration is carried out before a subsequent mesh modification.

Other rules should also be added to reduce the quality control number.

5. Example

We consider the evolution of the iterations on the base of a test sample. The computation is performed with the following data: $E = 200000$ MPa, $\nu = 0.3$, $R_0 = 150$ MPa, $Q = 80$ MPa, $R_s = 50$ MPa, $c = 24800$ MPa, $a = 300$, $m = 2$, $k = 4$. 10^{-5} MPa $^{-2}$ s $^{-1}$, $F_d(t) = F t/T$, $F = 25$ MPa. The interval $[0, T]$ is divided into 4 time steps. The loaded part, as well as the plastic zones, are presented in Figure 3. The goal is to obtain $e_0 = 5$ percent.

The evolution of the global error e and of the indicator I_{esp} during the iterations is presented in Figure 4. During the resolution, the mesh is adapted 3 times. The meshes are called M1, M2, M3 and M4 (see Figure 5). The analysis is conducted with 6-node triangular elements.

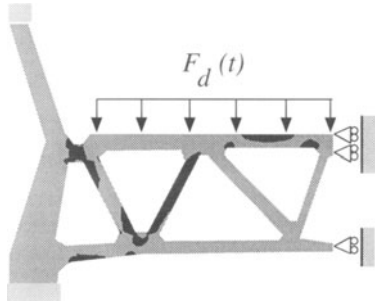


Figure 3. Loading and plastic zones in black

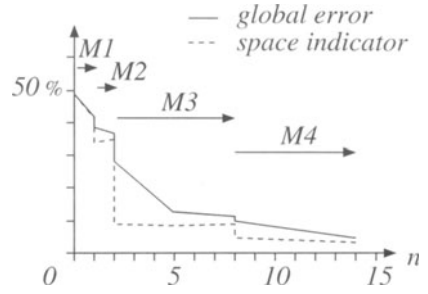
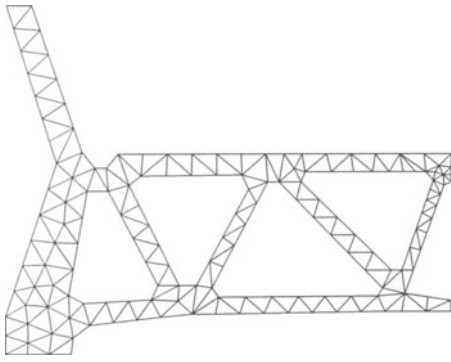
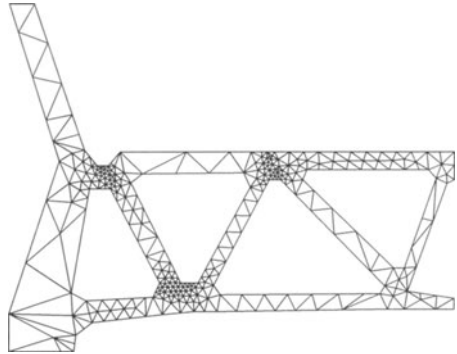


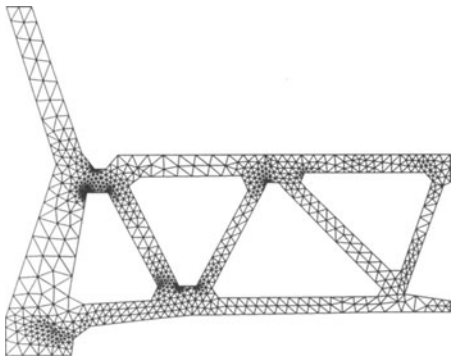
Figure 4. Error evolution during the iterative computation



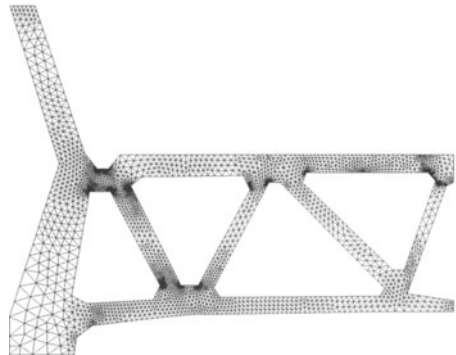
Mesh M1 (186 elements)



Mesh M2 (453 elements)



Mesh M3 (1,360 elements)



Mesh M4 (5,268 elements)

Figure 5. Meshes used during the computation

An elastic computation with the coarse mesh M1 (186 elements) allows initializing the resolution with an admissible solution s_0 . Using this approximation, the global error computed is $e(s_0) = 49$ percent, the space error indicator is $I_{esp} = 49$ percent, and $I_{tem} = 5$ percent. Plasticity is not negligible ($I_{tem} > 2.5$ percent). An initial iteration is then carried out with the coarse mesh (rule R1) to take better account of plasticity in the admissible solution. Thus, the error computation gives: $e = 41$ percent, $I_{esp} = 41$ percent, $I_{tem} = 4$ percent. Thus, at the end of this first iteration the space error is great with respect to the other error sources ($I_{esp} > 1.5 I_{tem}$). Thanks to the local contribution to I_{esp} , a new mesh M2 (453 elements) is automatically built to reduce the space error. Data are then transferred from mesh M1 to mesh M2, and an error control is introduced. We can notice that the global and space errors have strongly decreased ($e = 37$ percent, $I_{esp} = 34$ percent), and error sharing has been modified ($I_{tem} = 8$ percent $\approx 0.25 I_{esp}$). A second iteration is performed before a new mesh adaptation (rule R2). The new adapted mesh is M3 (1,360 elements). The different error levels are now balanced ($e = 27$ percent, $I_{esp} = 9$ percent, $I_{tem} = 16$ percent). The subsequent iterations improve the integration of the non-linear finite element problem: I_{tem} decreases. At the end of the 8th iteration, the mesh has to be changed ($I_{esp} > 1.5 I_{tem}$). The mesh M4 is then built (5,268 elements). At the end of the 14th iteration, the global error equals 5.3 percent. The objective has been reached.

The time representation has been adapted once, at the end of the first iteration. The space function base has been completed at each iteration.

It should be noted that the majority of the iterations have been performed on coarse meshes, which leads to a very low numerical cost. To assess the adaptive strategy performance, we use the last mesh (M4) and the time discretization built by the strategy to conduct a new resolution without any adaptation. This resolution is carried out with the same non-incremental algorithm. We then obtain a reference computation similar to that of an expert who, a priori, knows the appropriate parameters to obtain the prescribed quality. We note that the CPU time (on an hp700) needed by the reference computation is almost twice as high as the one needed by our adaptive strategy. Moreover, since our procedure is entirely automated, it considerably reduces the time necessary to prepare the computation (especially the meshing of complex structures).

References

1. Peric, D., Yu, J. and Owen, D.R.J. (1994) On error estimates and adaptivity in elasto-plastic solids : applications to the numerical simulation of strain localisation in classical and Cosserat continua, *Int. Jour. for Num. Meth. in Engrg.* **37**, 1351-1379.
2. Gallimard, L., Ladevèze, P. and Pelle, J.P. (1996) Error estimation and adaptivity in elastoplasticity, *Int. J. for Num. Meth. in Engrg.* **39**, 189-217.
3. Barthod, F-J., Schmidt, M., and Stein, E. (1997) Error estimation mesh adaptivity for elastoplastic deformations, *Complas V, Computational Plasticity: Fundamentals and applications*, Owen - Oñate - Hinton Editors, CIMNE, Barcelona, 597-602.
4. Ladevèze, P. (1996) *Mécanique non linéaire des structures. Nouvelle approche et méthodes de calcul non incrémentales*, Hermès, Paris.
5. Halphen, B. and Nguyen, Q.S. (1975) Sur les matériaux standards généralisés,

Journal de Mécanique **14**, 39-63.

6. Lesne P.M. and Savalle, S. (1989) An efficient cycle jump technique for viscoplastic structure calculations involving large numbers of cycles, *2nd Int. Conf. on Computational Plasticity : Models Software and Applications*, Owen - Oñate - Hinton Editors, CIMNE, Barcelona, 591-602.
7. Ladevèze, P., Pelle, J.P. and Rougeot, P. (1991) Error estimation and mesh optimization for classical finite elements, *Engrg. Computation* **8**, 69-80.
8. Ryckelynck, D. (1998) *Sur l'analyse des structures viscoplastiques : stratégie adaptative et contrôle de qualité*, thesis, ENS de Cachan (France).

COMPUTATIONAL GEOMETRY IN THE PREPROCESSING OF POINT CLOUDS FOR SURFACE MODELING

O E. RUIZ (Associate Professor), J. L. POSADA (Student)
Center for Interdisciplinary Research (CII) in CAD / CAM / CG
EAFIT University
A.A. (P.O. Box) 3300, Medellin, COLOMBIA

ABSTRACT

In Computer Aided Geometric Design (CAGD) the automated fitting of surfaces to massive series of data points presents several difficulties: (i) even the formal definition of the problem is ambiguous because the mathematical characteristics (continuity, for example) of the surface fit are dependent on non-geometric considerations, (ii) the data has a stochastic sampling component that cannot be taken as literal, and, (iii) digitization characteristics, such as sampling interval and directions are not constant, etc. In response, this investigation presents a set of computational tools to reduce, organize and re-sample the data set to fit the surface. The routines have been implemented to be portable across modeling or CAD servers. A case study is presented from the footwear industry, successfully allowing the preparation of a foreign, neutral laser digitization of a last for fitting a B-spline surface to it. Such a result was in the past attainable only by using proprietary software, produced by the same maker of the digitizing hardware.

1. Introduction

In CAD / CAM massive point data sets from digitized objects must be approached by data structures and / or formulae that organize and represent them. This process, called surfacing, is needed for purposes of data reduction, object edition, analysis, visualization and manufacturing. Several problems are present in this endeavor: (i) given a raw set of points, discrimination of functional subsets is needed to preserve the design intent, (ii) given a functionally coherent point set, the mathematical form of the surface fit to it is the designer's choice; (iii) given a mathematical form of the surface, the topological organization of the points is to be decided, and (iv) boundary conditions (C^0 , C^1 , C^2 continuity) are to be enforced, or waived, depending on functional characteristics of the local neighborhood. Therefore, *automated* fitting of surfaces has proven to be a difficult problem in industry and academy. A traditional solution is to write programs specifically oriented to a family of digitized objects and to lump together digitizing hardware, software and CAD / CAM into one package. This solution

usually rises the prices of this technology, since the software and hardware only function with each other, thus producing a closed product.

This investigation has aimed to produce and apply a set of open geometric reasoning tools, which take advantage of characteristics of digitizations and data sets to produce surface models. Such characteristics include locking of axis, convex object cross sections or with non empty kernel (Preparata, 1985), oversampling, character lines as curvature discontinuities, etc. To test the tools, a laser digitization was loaded, preprocessed and fit a surface using popular, open CAD systems (Saldarriaga, 1997, Posada, 1997). Originally this could be done only by using vendor's proprietary software operating on data from its own digitizer.

The code for the described tools was implemented to be Application Interface Specification (AIS)-compliant. AIS (Ranyak, 1994, Posada, 1997, Saldarriaga, 1997) describes in functional, generic form the services that a geometric modeler should provide. As a result, the AIS-compatible code written runs transparently on AutoCAD® and MicroStation®.

This article is organized as follows: Section 2 surveys the relevant literature. Section 3 discusses the geometric reasoning tools devised. Section 4 presents a case study while Section 5 concludes the paper. Last section contains the bibliographic references.

2. Literature Review and Background

Surface fitting has been attacked from two different points of view: (i) mathematical and (ii) algorithmic. In (i) mathematical formulae are proposed and fit to the data by parameter identification. Among formulations independent on the order of the data there are interpolations and statistical fittings. Polynomial interpolations present large oscillations and large computational expenses as the set grows. Statistical techniques fit equations which are the most likely to represent the sampled points. These techniques are used for tolerance assessment in which hypotheses of planarity, cylindricity, perpendicularity, etc, are evaluated by sampling points of the tested feature, and finding their correlation factors with the desired geometry (ANSI, 1993, Carr, 1995).

Order dependent approaches use parametric surfaces, attracted by a subset of the sampled points (the control points): Bezier, B-splines, NURBS, etc (Farin, 1990, Mortenson, 1985). One of the most common errors in automated surface fitting is the trend to smooth all the blends, even in regions in which the real object was not intended to be smooth. The issue of intelligent automated enforcement of continuity is still an open problem in Computer Aided Geometric Design (CAGD).

The algorithmic approach places the emphasis on classification and partition of the point set. It is most needed in industrial applications, since it is preparatory for mathematical methods. For example, fitting of Bezier or B-spline curves renders completely different results as different *orderings* in the control points are used.

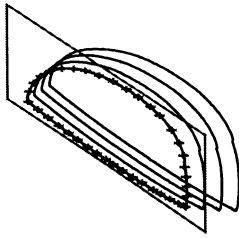


Figure 1: Point classification in coplanar subsets.

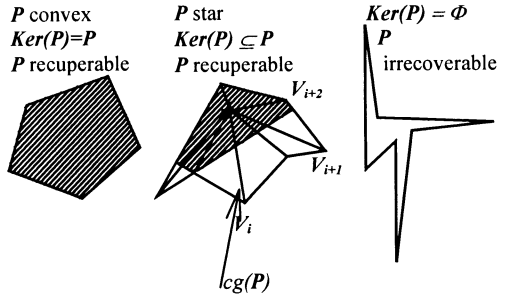


Figure 2. Recovery of polygon P according to convexity type.

Alpha shapes (Edelsbrunner, 1994) help to reconstruct surface and volume for a given point cloud, according to the selected alpha parameter. Since they present only C^0 continuity among them, some investigators (Guo, 1997) use alpha shapes as an intermediate step for smooth surfacing. In contrast, this investigation will focus on direct, selectively (C^1 and C^2) continuous surfacing, supported by geometric reasoning tools (Preparata, 1985, Posada, 1997, Ruiz, 1995) to preprocess the point data set to fit as few as possible parametric surfaces to the data. Therefore, it can be seen as an hybrid application of the mathematical and algorithmic approaches. The geometric reasoning tasks are implemented on top of modeling engines as reported in (Ruiz, 1994, Ruiz, 1995).

3. Geometric Reasoning Tools

Along the following discussion it must be stressed that neighboring points *on the object* may appear as scattered samples *in the point set*. Therefore, algorithms to recover the neighborhood information have to be implemented. In the following discussion notation $\{ \}$ represents an unstructured set of elements, $[]$ corresponds to an ordered list and $\{ \{ \}$ denotes a set of sets of objects

3.1 POINT - SURFACE CLASSIFICATION

Since many digitizations are performed in pre-defined trajectories (for example by locking one degree of freedom of the digitizer), the points lie on parallel planes (Fig.1). The function *planar classification* takes an unstructured set S of points in E^3 (*point*) and a family of N digitizing planes, defined by the vector (\hat{u}) normal to all planes. It returns a partition P of the initial set, formed by subsets Π_i of S :

$$\Pi = \{ \Pi_1, \Pi_2, \Pi_3, \dots, \Pi_N \}, \text{ with } \Phi = \Pi_j \cap \Pi_k \text{ for all } j \neq k, \text{ and } S = \bigcup_{j=1}^{j=N} \Pi_j \quad (1)$$



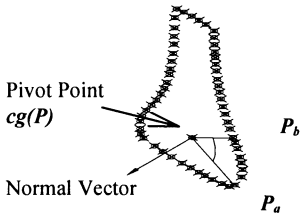


Figure 3. Recovery of a cross section P of the last.

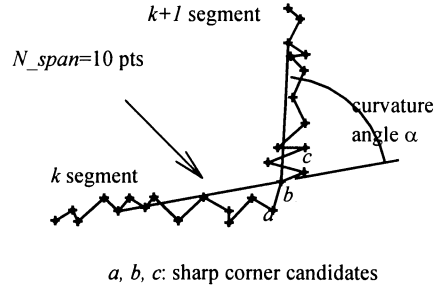


Figure 4. Parameters for corner detection algorithm.

The type of the partition is $\{\{point\}\}$. Each set Π_i in the partition is formed by the points contained in the i^{th} plane of digitization, each specific plane being fixed by its pivot point. The common normal of the digitization planes is (Preparata, 1985):

$$\hat{u} = (n_x, n_y, n_z) / \|(n_x, n_y, n_z)\| \tag{2}$$

$$n_x = \sum_{i=0}^{i=N} (y_i - y_{i+1})(z_i + z_{i+1}) ;$$

$$n_y = \sum_{i=0}^{i=N} (z_i - z_{i+1})(x_i + x_{i+1}) ;$$

$$n_z = \sum_{i=0}^{i=N} (x_i - x_{i+1})(y_i + y_{i+1})$$

Points are considered coplanar if they are within an ϵ normal distance from the plane. Allowing a coplanarity deviation is a common practice in tolerancing, where planarity of a surface is a statistical rather than deterministic quality (ANSI, 1993, Carr, 1995).

3.2 POLYGON RECOVERY. ANGULAR SORTING ABOUT THE KERNEL

From a set of (coplanar) points Q randomly sampled on a cross section of an object, it is required to recover the ordered list P (f point f) which represents the cross section. It is immediately clear that, as stated, this problem has no solution. However, if the cross section P of the object has the properties mentioned below (Preparata, 1985, Posada, 1997), the problem becomes tractable.

Definition: Given a planar, ordered set of points representing a polygon $P = \{p_0, p_1, p_2, \dots, p_n\}$, its kernel, $Ker(P)$, is the locus of the points a inside P such that for all points b in the boundary of P , the segment ab lies inside P (all points a from which the boundary of P is visible).



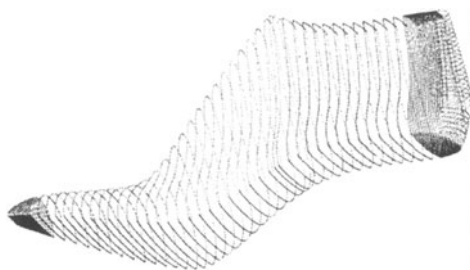


Figure 5. Initial data set from digitization.

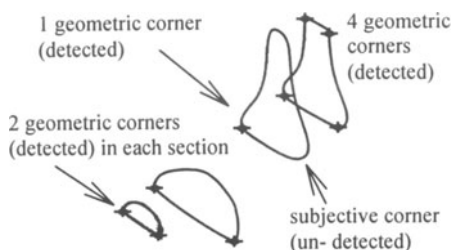


Figure 6. Results of corner detection algorithm.

Corollaries: For all P , $Ker(P)$ is convex and $Ker(P) \subseteq P$. If P is convex, then $Ker(P) = P$. If $Ker(P)$ is not empty, any point q inside $Ker(P)$ can be used (along with \hat{u} , the normal to the plane) as polar origin to angularly sort Q . The sequence so obtained is P , with a possibly different starting point.

A heuristic approach can be used to recover a polygon P from a random enumeration of its vertices Q if two hypotheses are assumed: (i) the cross section of the sampled object has non empty kernel, (ii) the center of gravity of P , $cg(Q)=cg(P)$ lies inside $Ker(P)$. As shown in Fig.2 and Fig.3, in such cases the angular sort about $cg(Q)$ enables the recovery of P . The hypotheses just mentioned hold in many engineering applications: objects frequently have sections P which are either convex or have non empty kernel $Ker(P)$. If $cg(P)$ is not inside $Ker(P)$, the designer may be prompted for a point within it. The treatment of the cases in which the cross section has empty kernel are not considered in this work.

3.3 CORNER DETECTION

Detection of sharp corners of polygon P is required to avoid enforcement of non-existent C^1 or C^2 continuity conditions on such corners. Since a digitization is a discrete process, every point of P is, in strict sense, a sharp corner because in each one C^1 continuity is lost. Corner detection algorithm takes a point list (J point J) of digitized data, and two parameters, displayed in Fig.4: (a) an angle α , the threshold of tangent discontinuity, above which a sharp edge is recognized, and (b) a re-sampling interval or span N_span , which isolates the estimation of tangent discontinuity from accidental irregularities of the digitization process. Notice that the detected corner could have been a , b or c since there is no additional argument to chose one of the three points.

3.4 RE-SAMPLING

Resampling can be used to generate an “artificial” digitization with different sampling parameters than the original one. Different cases are: (a) **Re-sampling by distance:** Given a polygon P in E^3 , and a distance d , it returns a polygon P' resulting from

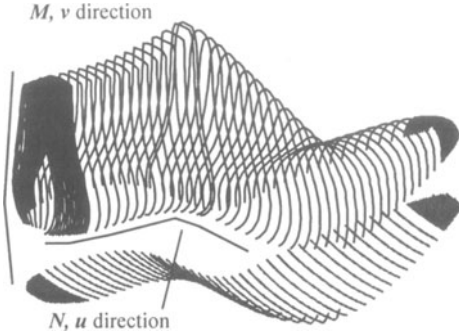


Figure 7. Control polyhedra with $N_u \times M_v$ points.

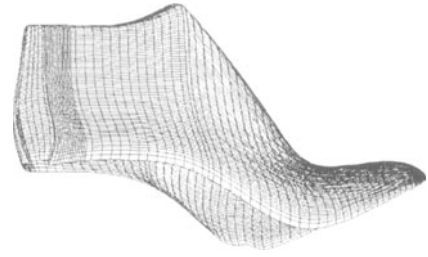


Figure 8. B-spline surface fit for upper part of the last.

resampling the boundary of P in segments of length d . (b) **Re-sampling by number of points**: Given a polygon P in E^3 , and an integer N , it returns a polygon P' , formed by the vertices of P sampled every N points. (c) **Re-sampling by entity intersection**: Given a polygon P in E^3 , and a list of entities $L=[e_0, e_1, \dots, e_m]$, this procedure returns a polygon P' , formed by the intersections of P against entities e_0, e_1, \dots etc. Currently, this operation is implemented with L being a family of planes with common normal and different pivot points.

3.5 FILTERING

Filtering is the process by which a function $f(\)$ is applied to a subsequence $S=[p_i, p_{i+1}, p_{i+2}, \dots, p_{i+W-1}]$ of W vertices of a polygon P , returning vertex q_i , to form the sequence $S'=[q_m, q_{m+1}, q_{m+2}, \dots, q_n]$. The points of S' are not necessarily in S , and S' may be smaller in size than S depending on how the window W is managed. The filter mask used calculates a new point as:

$$\bar{q}_i = f(\bar{p}_i \dots \bar{p}_{i+W-1}) = \sum_{j=1}^{j=W} \alpha_j \cdot \bar{p}_{j+i-1} \quad (3)$$

$$\text{where } \sum_{j=1}^{j=W} \alpha_j = 1.0, \alpha_j \geq 0, j=1..W$$

with $\alpha_1 = \alpha_2 = \dots = \alpha_N = 1/W$ for averaging, and $\alpha_1 = 1, \alpha_2 = \alpha_3 = \dots = \alpha_W = 0$ for resampling.

4. Case Study

The original data set from a last digitization (Fig.5) contains 33000 points. Notice that: (i) the last was sampled with three different digitization patterns, and (ii) curvature discontinuity between the sole and the upper part requires to fit separate surfaces to them. Therefore, in this case automated surfacing would have immediate limitations. In

contrast, with the tools proposed the designer is able to identify, separate and process several point sets, to respond to the above considerations, as follows:

Point - Surface Classification. An initial partition of the point set classifies the points into subsets of coplanar points. Based on the point set, the normal vector \hat{u} is determined, which is common to all the digitizing planes. Fig.1 shows the plane of digitization found by formula (1) (the trajectories shown are very tightly sampled point sets).

Polygon Recovery. Figs. 2 and 3 display polygon recovery. The (non convex) polygon shown: (i) has non-empty kernel, and (ii) its center of gravity is inside the kernel of the polygon. Under those conditions the algorithm for angular sort can be applied. The normal vector \hat{u} is used to enforce an order on the points, according to the right hand rule.

Corner Detection. Fig.6 shows the recognition of sharp edges for different regions of the last. It is found that corner detection works very efficiently for the front and back part of the last. In the central part (foot arc) the algorithm is unable to identify the inner sharp edges of the sole, since they do not exist in the geometric sense. Corner detection was used for removal of the sole (see Fig.7).

Re-sampling. In the present example, re-sampling by number of points was applied with two purposes: (i) to diminish the size of the data set, and (ii) to provide a $N_u \times M_v$, rectangular array of (x,y,z) points as the control polyhedra for a B-spline surface covering the upper part of the last. Each polygon was then resampled to 50 points (Fig.7).

Surface Fitting. The previous tools built 51 planar polylines with 50 points each. A parametric B-spline surface was fit with $N_u \times M_v = 51 \times 50$ control points, with order 3 in u (N_u) direction, order 4 in v (M_v) direction and standard knot vectors in both directions (Mortenson, 1985). Fig.8 shows a rendering of the B-spline surface obtained. Notice that the heel region required the generation of an artificial digitization resampled by entity intersection from the original one.

5. Conclusions

This article has presented a set of generic tools which take advantage of geometric properties of digitized data in helping a designer in surface fitting tasks. Geometric reasoning allows the separation and sorting of parts of the point data set to conform to functional and geometrical criteria. The software described has allowed to start from raw digitization data to arrive to the surface without using the proprietary tools of the hardware - software maker. Comparing the initial data set of 33.000 points with the 2.550 control points of the surface being fit, significant data reductions can be assessed. The fact that the tools have been written as AIS compatible client software makes them portable across other geometric modeling servers.

6. References

- ANSI Y14.5.1M-Draft (1993) *Mathematical Definition of Dimensioning and Tolerancing Principles*, American Society of Mechanical Engineers. New York.
- Carr, K. (1995) *Modeling and verification methods for the inspection of geometric tolerances using point data*, Ph.D. Dissertation, University of Illinois at Urbana-Champaign.
- Edelsbrunner, H., Mücke, E. (1994) Three Dimensional Alpha Shapes. *ACM Transactions on Graphics*, Vol. 13, No. 1, pp. 43-72.
- Farin, G. (1990) *Curves and Surfaces for Computer Aided Geometric Design. A Practical Guide* Academic Press. Boston.
- Guo, B. (1997) Surface Reconstruction: from Points to Splines. *Computer Aided Design*. Vol. 29, No. 4, pp. 269-277.
- Mortenson, M. (1985) *Geometric Modeling*, John Wiley and Sons. New York.
- Posada, J. (1997) *An Implementation of the AIS Interface on MicroStation*, B.Sc. Thesis, EAFIT University Medellin, Colombia.
- Preparata, F., Shamos, M. I. (1985) *Computational Geometry. An Introduction*, Springer Verlag. New York.
- Ranyak, P. (1994) *Application Interface Specification (AIS) Version 2.1*. Consortium for Advanced Manufacturing International (CAM-I). Integrity Systems, USA.
- Ruiz, O., Marin, R. and Ferreira, P. (1994) *A Geometric Reasoning Server with Applications to Geometric Constraint Satisfaction and Reconfigurable Feature Extraction*. Proceedings, 3rd Luso-German Workshop on Graphics and Modeling in Science and Technology, Coimbra, Portugal.
- Ruiz, O. (1995) *Geometric Reasoning in Computer Aided Design, Manufacturing and Process Planning*, Ph.D. Dissertation, University of Illinois at Urbana-Champaign.
- Saldarriaga, J. and Isaza D. (1997) *An Implementation of the AIS Interface on AutoCAD*, B.Sc. Thesis, EAFIT University Medellin, Colombia.

ACKNOWLEDGMENTS

This investigation was supported by Colciencias (Colombian National Council for Science and Technology) grant 152-96 and EAFIT University. The authors wish to thank Professor Placid Ferreira of the Large Scale Flexible Automation of the University of Illinois at Urbana - Champaign and Dr. Charles Wu from Ford Motor Company for their support in the years 1993-1995 for early works on surface fitting for stamping engineering.

POLYHEDRON PARTITIONING DEDICATED TO A HIERARCHICAL MESHING TECHNIQUE.

Stéphane MAZA[†], Frédérique NOEL[†],
Jean Claude LEON[†], François SILLION^{*},
[†]*Laboratoire Sols, Solides, Structures / Projet Conception intégrée*
BP 53 X, 38041 Grenoble cedex 9
^{*}*Laboratoire iMAGIS/IMAG*
BP 53 X, 38041 Grenoble cedex 9
Email : Stephane.Maza@hmg.inpg.fr - Frederic.Noel@hmg.inpg.fr
Jean-Claude.Leon@hmg.inpg.fr - Francois.Sillion@imag.fr

1 Abstract

In the last few years, polyhedral representations have been widely used for geometric modelling. Handling this type of model is quite complex and it is often necessary to adjust the polyhedron to the purpose of its future uses. A lot of treatments have been developed in the recent years in order to ease their manipulation. The aim of this paper is to present a new method of polyhedron partitioning. This treatment is used in an approach for the generation of hierarchical polyhedral representations. This method uses an arbitrary polyhedron which is subdivided into several parts with respect to its geometric features. The first stage of this method simplifies the initial polyhedral representation of the object. Then, thanks to a concept of inheritance and dependency lists built during the simplification process, a first draft of the partitions is obtained. The last stage introduces some optimisation tools to improve the boundaries and the shape of partitions. The partitions thus created can be easily incorporated into a hierarchical mesh generation process.

2 Introduction

Polyhedron representations are frequently used to model geometry in reverse engineering applications and visualisation processes. The accuracy of the 3D scanning techniques produces large sets of points which can contain several hundreds of thousands of points. These digitised points are input into a triangulation process in order to generate a polyhedral representation of the object. Then, the obtained polyhedron can be used to generate new models based on a parametric or an implicit description of surfaces. The same polyhedron may act as a reference model for manufacturing or visualisation purposes.

The use of these polyhedra becomes very difficult and complex because of their size (hundreds of thousands of points) and the incoherences generated by digitising and triangulation processes (hole, double points and edges,...). Many simplification algorithms have been recently developed to reduce the number of nodes of a polyhedron. These algorithms have made possible an easier handling of polyhedra. These methods are controlled only through geometric criteria which do not take into account specific criteria related to subsequent applications. Therefore, the result of the simplification process may not be adequate for different application software. Hence, each application requires specific corrections and adaptations of the polyhedron to their boundary conditions and analysis model.

To simplify the polyhedron re-meshing schemes, a decomposition of the initial polyhedron into smaller sets of faces is performed. A lot of decomposition methods are developed for parallel treatments to reduce inter-processor communications. Unfortunately, the criteria of these methods have no geometric meaning, the only purpose is to decompose the initial polyhedron in k partitions (where k is the number of processors) and to minimise the number of edges at the boundary shared by two partitions. This techniques are usually based on the optimisation of a graph decomposition [1,3].

The polyhedron partitioning method described in this paper is controlled through geometric characteristics of the object. A simplified version of the polyhedron helps to determine these characteristics. Then, links between faces resulting from the simplification and the initial entities (nodes and faces) are created thanks to an inheritance concept. When every initial face is located into a partition, optimisation treatments are applied to improve the boundary of the partitions.

3 Polyhedron re-meshing techniques

The re-meshing methods used are based on a mapping of the initial 3D polyhedron into a 2D convex hull [4]. The 3D representation is mapped in a 2D parametric space in order to handle this domain rather than the 3D one. This process creates a bijection between the 3D polyhedron and a 2D convex hull. To perform this mapping, some nodes of the 3D polyhedron boundary are selected according to geometric criteria and are positioned around a unit circle in 2D space. Their coordinates are calculated in such a way that the arc length between two successive nodes is proportional to the 3D length of the boundary edges. Those nodes are called "fixed nodes" and hold for the 2D convex polygon vertices. The other boundary nodes (called "line nodes") are located onto their corresponding side according to an equidistant distribution. Then, a polyhedron with the same topology than the initial one is generated and the interior nodes are located using the Force Density Method [6,7].

Since each 3D face of the initial polyhedron is mapped on a 2D face, a bijective transformation is set up between the 2D representation and the 3D polyhedron ; any point, P , located onto a face, f_{2D} , of the 2D polyhedron can be mapped in 3D using its barycentric coefficients (p , q and r). The face f_{2D} is associated with a 3D face f_{3D} . The point P is projected in the 3D space as the point of the face f_{3D} with barycentric coefficients (p , q and r). Within this transformation, the same barycentric coefficients as in 2D are applied onto the corresponding 3D face and the 3D coordinates of the image

point are calculated. When a new mesh in the same 2D convex hull with the same "fixed nodes" is generated it can be mapped on the 3D initial polyhedron by projected any node of the mesh into the 3D space through the previous projection.

The Figure 1 (a) shows the initial polyhedron and its mapping in the 2D space with three "fixed nodes" (b). On Figure 1 (c), a new mesh is generated in the same 2D polygon and (d) shows the mapping of this mesh in 3D space.

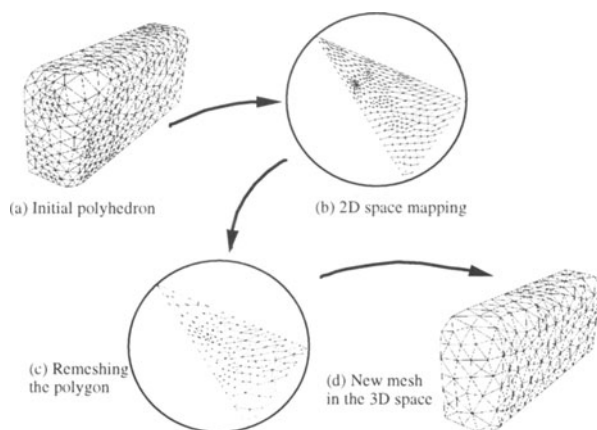


Fig.1 : Polyhedron mapping and remeshing techniques

In this approach, the initial polyhedron must be bounded by a single boundary to create the 2D polygon. If it has more than one boundary, the Force Density Method used to place the interior nodes may produce non conform 2D polyhedra. Moreover, many polyhedra are closed ones and no boundary can be found. Thus, to exploit this method with any polyhedron, it is necessary to use a partitioning technique in order to get a set of 2D spaces corresponding to a set of mesh partitions.

4 Polyhedron Partitioning

The aim of the polyhedron partitioning method is to divide the initial polyhedron into a set of smaller ones when the initial polyhedron is closed or when it has more than one boundary. To reduce the re-meshing constraints, the number of partitions must be as small as possible [5]. To reduce the distortion between 3D and 2D spaces, the partitions must cover areas which are compatible with the geometric characteristics of the object. The method presented here is split into several steps. The first simplifies the initial polyhedron to highlight the overall shape of the object. Then, every node and every face from the initial polyhedron which are removed during the simplification process are identified and associated with a face of the final polyhedron in order to generate every partitions. The final step, is used to optimise the boundaries of partitions.

4.1. POLYHEDRON SIMPLIFICATION

The method of polyhedron partitioning presented in this paper is based on a polyhedron simplification process [8]. The simplification preserves the geometry and topology of the initial polyhedron in accordance with an error criterion. To start the simplification process, an error tolerance is associated with each node. At each face, a list is set up according to the three error zones associated with the three nodes of the face. Similarly, for each boundary edge a list of two errors is generated. The simplification process is carried out in two steps : at first some surface nodes are removed, and in a second step some boundary nodes are removed. The error criterion ensures that each new re-meshed area intersects every error zone attached to the node and the faces removed. The node selection is gained through geometric properties of the initial polyhedron. For each surface node, a discrete gaussian curvature [2] is evaluated, and for each boundary node, an evaluation of the angle defined by its two adjacent boundaries edges is performed. The candidate node is the one which has the smallest absolute value of discrete gaussian curvature, or the node which is located along straight lines. The absolute value is employed to determine nodes from shapes close to either planes or cylinders. Then, the node is removed if the new mesh of its 3D contour polygon (i.e. : the polygon built with the edges surrounding the node) verifies the following criteria :

- the new mesh is conform, there is no overlapping face and no intersection,
- each error zone attached to the candidate node and to the faces removed must intersect at least one of the new faces,
- the topology of the mesh is preserved.

After each node removal, the error zones that intersect a new face are added to the list of that face. Hence, a new face has a list with the three error zones associated with its nodes and some error zones of previously removed nodes. Therefore, when the simplification process goes up, faces and nodes are more and more constrained. The simplification process stops when no more node can be removed.

To find the final polyhedral model which will be used to determine the partitions, several simplifications are carried out successively. The size of the error zones for each iteration is defined by the length of the smallest edge of the polyhedron at the previous iteration. This error holds for the size of the smallest detail which will be removed. This process converges toward a polyhedron with a small number of faces, and this model cannot be simplified anymore. When convergence is reached, the removal of a node would generate too many transformations and the criterion used to mesh the polygon around this node could not be verified. This method guarantees the mesh conformity and the final polyhedron preserves the main characteristics shape of the initial one. Figure 2 represents an example involving 4 stages of a polyhedron simplification.

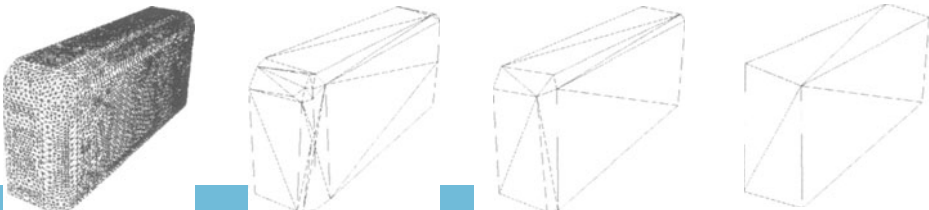


Fig.2 : Various stages of a polyhedron simplification.

4.2. DETERMINATION OF THE PARTITION

The previous section has described a method to simplify a polyhedron. This process produces a polyhedron with a small number of faces. These faces and the list of error zones are used to identify the partitions of the initial polyhedron. This process is decomposed into three steps :

- the faces of the final polyhedron are merged according to a geometric criterion to form subsets covering the whole polyhedron,
- for each subset, the nodes and faces of the initial polyhedron which are close enough to this subset are identified,
- the last step places the faces left after the second one into an appropriate partition.

Firstly faces of the final polyhedron must be merged into several groups. Indeed, the result of a rectangular plane simplification is two faces, but the best partition which characterises the shape is composed of both faces. Then, some faces of the final polyhedron are merged together thanks to an angle criterion. This process is based on a frontal method. First of all, an initial face is selected and a subset is generated around it by selecting the adjacent faces. This initial face is the face whose average of the discrete gaussian curvature assigned to its nodes has the minimum absolute value. The face clustering starts with the previous criterion and stops when the following condition is false :

$$\overbrace{\vec{n}_f, \vec{n}_{f.adj}} < \alpha_{max}$$

where \vec{n}_f is the normal of the initial face and $\vec{n}_{f.adj}$ is the normal of the face just added to the cluster. α_{max} is chosen to be equal to 45° .

When the clustering phase is completed, the faces and nodes of the initial polyhedron forming the partitions must be determined. Thanks to the list of error zones used during the simplification process, the nodes of the initial polyhedron used to create the final faces, are identified. Indeed, each error zone corresponds to an initial node. The nodes of each subset of final faces may not be significant. Some of them belong to several subsets. Hence, it is necessary to keep only the significant ones. The node selection process uses the scalar product between the normal vector of the initial node (average of the normal of its adjacent faces) and the normal vector of the final face. If this scalar product is positive then the node is a significant node, on the other hand the node is removed from the subset. After the node selection, faces which constitute the partitions must be chosen. Through the node treatment, a face is selected if its three nodes belong to the list of error zones of a final subset. This selection process is performed for each subset and if an initial face belongs to more than one partition, it will be removed from this process and its final partition will be determined at the optimization stage.

4.3. PARTITION OPTIMIZATION

The optimization stage is used in two configurations :

- to determine the partition of the faces left after the previous step,
- to improve the boundary polygon of each partition.

The remaining faces are assigned to the partition whose normal of the partition forms a minimum angle with the face normal. The normal of a partition is defined as the average of the normal of all its faces.

The shape optimization process is based on a modification of the boundary of the partitions by exchanging their boundary faces. The treatment dedicated to the remaining faces can also be used to improve the shape of the partitions. Each face with an edge belonging to a boundary of a partition changes of partition if the angle between its normal and the normal of the adjacent partition is minimum. Another tool to modify the boundary of the partition tries to exchange faces which have two edges on two partitions outlined like on figure 3 (the face F1 is exchanged between partition 1 and partition 2).

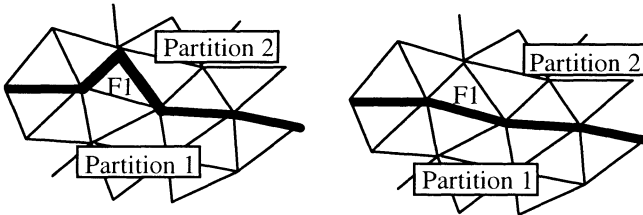


Fig 3. Face with two edges on a common boundary

The remeshing process described in the second part of this article requires partitions without several boundaries. Therefore, two operators are created, the first one is used when a partition is made up from two parts (figure 4 b)), and the second one divides in two partitions a partition which has a hole (figure 4 a)).

These two operators perform the separation through an advancing frontal method. For the operator illustrated on the figure 4 b), fronts are built from the two faces around N1. Two sets of faces are determined and they can be transformed either in two partitions or in one partition and the remaining set is spread over the other partitions using the first operator. For the operator figure 4 a), the smallest edge path between two boundaries is searched and fronts are initiated by two sets of faces which belong to each side of the edge path. Then, two partitions are generated. If a partition has more than two boundaries, the process is reiterated until the partition has only one boundary.

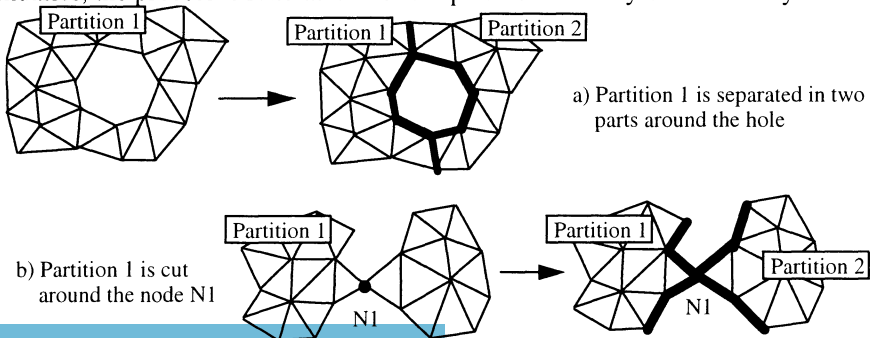


Fig 4. Operators for partitions with several boundaries

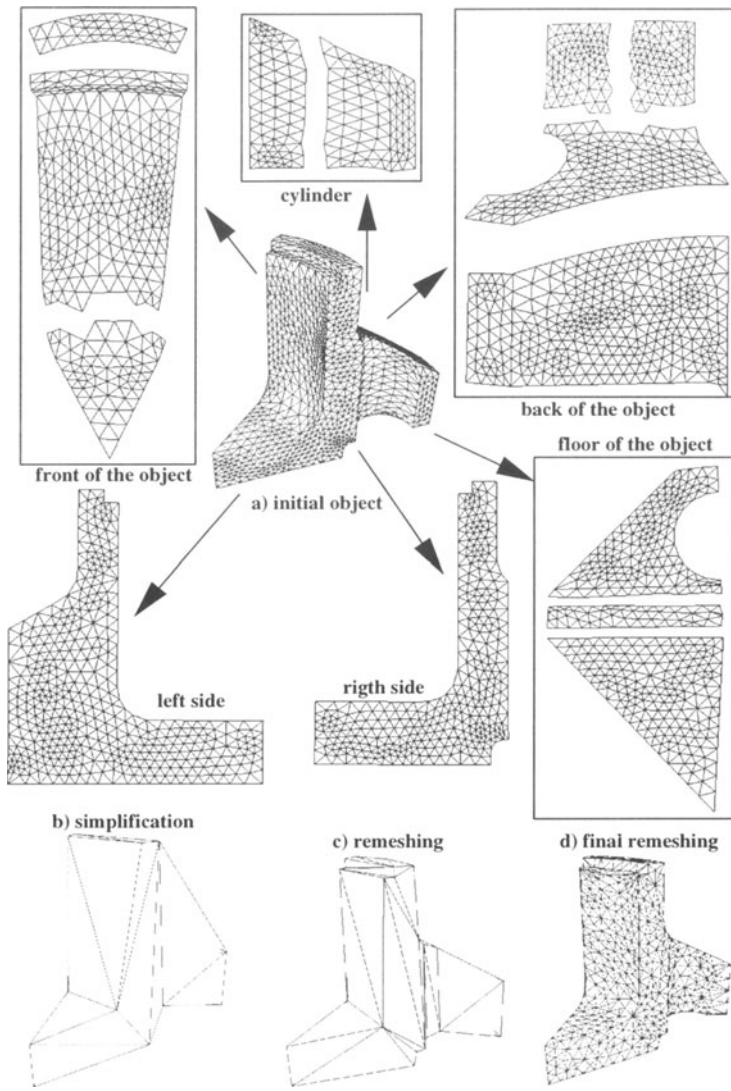


Fig 5. An example of mesh partitioning and re-meshing of a polyhedral model

Figure 5 shows an example of this method. The initial polyhedron is positioned in the middle of the page a). Figure 5 b) represents the result of the simplification algorithm and all the partitions (14 altogether) are placed around the initial polyhedron. Some of them are grouped to represent the front and back faces, the floor and the sides of the object. Figure 5 c) illustrates the first remeshing step generated and d) a denser mesh.

5 CONCLUSION

This paper has introduced a new method for partitioning a polyhedron using its own geometric characteristics. The initial polyhedron may be an arbitrary polyhedron (closed or open polyhedron, with or without holes). At the first stage of this method, the use of a polyhedron simplification process preserves as much as possible the shape and the topology of the initial polyhedron. This method allows to identify the final faces of a simple polyhedron thanks to the list of errors. Thus, a first set of partitions can be found. Some operators have been developed in order to optimise the shape and the boundaries of each partition. Then, the final result gives partitions incorporating the geometric characteristics of the object. At present, the order of these operators has not been defined yet. It will be studied in future work together with the integration of a criterion which could take into account developable surfaces corresponding to a set of partitions in order to reduce the number of partitions.

6 References

1. Chazelle B., Dodkin D. P., Shouraboura , Tal A. (1997). "Strategies for polyhedral surface decomposition : An experimental", Computational Geometry, Vol. 7, pp 327-342.
2. Boix E.(1995). "Approximation linéaire des surfaces de R^3 et applications", Ph D Thesis, Polytechnique.
3. Diekmann R., Lülling R, Monien B., Spräner C.(1995). "A parallel local search algorithm for the k-partitioning problem", 28th Hawaii International Conference on System Science.
4. Maza S, Noël F.(1997). "Mesh construction dedicated to a multi-representation for structure analysis based on an initial polyhedral representation", ASME 97, Sacramento (California), Detc97/Cie-4445.
5. Noël F, Léon J.-C, Trompette P (1995). "A new approach to free-form surface mesh control in a CAD environment", International Journal For Numerical Methods In Engineering, Vol. 38, pp. 3121-3142.
6. Rémondini L, Trompette P, Léon J.-C, Noël F (1994). "A new concept in two dimensional auto-adaptative mesh generation", International Journal for Numerical Methods in Engineering, Vol. 37, pp. 2841-2855.
7. Schek.H.J (1974) "The force Density method for form finding and computation of general network", Computer methods applied mechanics and engineering, Vol. 3, pp. 115-134.
8. Véron P., Léon J.-C.. "Static polyhedron simplification using error measurements", Computer Aided Design, Vol. 29, n° 4, 1997, pp. 287-298.

A DECLARATIVE APPROACH FOR GEOMETRY AND TOPOLOGY: A NEW PARADIGM FOR CAD-CAM SYSTEMS

André CLEMENT
Dassault Systèmes
9, quai Marcel Dassault, 92156 Suresnes Cedex, France
email: andre_clement@ds-fr.com

Alain RIVIERE and Philippe SERRE
Institut Supérieur des Matériaux et de la Construction Mécanique
3, rue Fernand Hainaut, 93407 SAINT-OUEN Cedex, FRANCE
email: ariviere@ismcm-cesti.fr
email : philippe.serre@ismcm-cesti.fr

1. Introduction

The geometric models currently used in CAD-CAM modellers are chiefly based on a procedural approach. Over the past few years, the appearance of parametric and, above all, variational modellers, has opened up the way to a more declarative approach. It is true to say that parametric design is efficient, but it requires knowledge of a design chronology whose flexibility is thus diminished. On the other hand, variational design is very general and flexible but does need the use of solvers to simultaneously solve a large number of non-linear equations.

Generally speaking, several solutions are found to one given problem ; this is because not enough constraints are specified - we then talk about a problem of constraint insufficiency - and the majority of specialised solvers have been developed to deal with this type of problem.

In this article, we are presenting another approach. In fact, the various specifications expressed by the designer when elaborating a geometric form are not limited to purely dimensional constraints. We will present the other 2 types of constraint - topological and chiral - required to specify a geometric shape. A totally declarative approach to geometry for CAD-CAM then becomes possible.

2. Analysis of the Problem

In a geometric figure, the dimensions and angles between each element of which the object is composed have to be stipulated. These dimensional constraints are expressed by non-linear mathematical equations. It is then possible to construct a discrete number of geometric objects which observe all the imposed dimensional constraints. However,

a designer will reject a certain number of the objects that are generated. This point underlines the fact that the full scope of dimensional constraints specified by the designer is not sufficient.

In point of fact, in order to describe the geometry of an object using constraints, a designer will generally make a drawing on which he will put the dimensional constraints and it is by means of this drawing that the operator implicitly specifies other constraints. For example, he will mark in a point to the left of a straight line, a line above a plane, etc.

There will be an initial phase to solving this problem, consisting of the analysis of the sketch in order to enrich the set of constraints which are purely dimensional, by other constraints.

At the present time, the solutions normally used are as follows: [BOU.95], [CAP.96] and [SHP.97].

- the adding of a sign to the dimensional parameter associated with each dimensional constraint;
- the generation of an additional constraint of a cross product type. Take the example of a triangle composed of three vertexes, A, B and C. The cross product $\vec{AB} \wedge \vec{BC}$ must have the same sign on the drawing and on the new object generated;
- the generation of an additional constraint of a scalar product type. Take the example of two segments [AB] and [CD], the scalar product $\vec{AB} \cdot \vec{CD}$ has the same sign on the drawing and on the new object generated.

Once these additional constraints have been added, they will enable the solver to eliminate any solutions generated that do not respect the initial implicit topology of the drawing.

The consequences of this approach are as follows:

1. the generation of these new constraints is transparent for the designer. In this case, it is difficult to analyse the result obtained. What should he do if the system does not find any solutions? Why is the solution generated by the system not what he requires?
2. it is currently impossible to declare a geometric shape with constraints without having an initial drawing describing its topology
3. at present, the use of specialised solvers is mandatory to solve these variational geometry problems.

Our work is related to the formalisation of all these constraints so as to be able to specify them in the same way as dimensional constraints.

3. Elements of solution

In this paragraph, we present the geometric constraints which we have classified into three types. We will give the mathematical expression of each of these constraints using distance between points parameters. The conditioning of the basic geometric

elements is as follows: a point is defined by a Point, a straight line by two Points which do not meet and a plane by three Points not in a straight line. All the constraints are thus expressed by means of the distances between each of these points.

3.1. DIMENSIONAL CONSTRAINTS

Dimensional constraints correspond to the distance and angle parameters that exist between the basic geometric elements which are: the point, the straight line and the plane. We have identified 13 constraints using the TTRS theory. These 13 constraints are presented in [CLÉ.96] and [CLÉ.97].

It should be noted that, for these 13 constraints, the distance parameter is represented by a positive real number or zero and the angle parameter is represented by a real number between 0 and π .

We have chosen to give the expression of the required dimensional constraints to the solving of plane problems. That is to say, constraints C1, C2, C4, C5, C11, C12 and C13.

3.1.1. Constraint C1: Point-Point, coincidence

Given two points A_1 and A_2 , constraint C1 is expressed as: $A_1 \equiv A_2$

3.1.2. Constraint C2: Point-Point, distance

Given two points A_1 and A_2 , constraint C2 is expressed as:

$$\text{Dist}(A_1, A_2) = L_{A_1A_2}$$

where $L_{A_1A_2}$ represents the length of the segment joining points A_1 and A_2 .

3.1.3. Constraint C4: Point-Straight line, coincidence

Given a point A and a straight line $[BC]$, constraint C4 is expressed as follows:

$$S_{ABC} = 0$$

where S_{ABC} represents the plane surface encompassed by points A , B and C .

3.1.4. Constraint C5: Point-Straight line, distance

Given a point A and a straight line $[BC]$, constraint C5 is expressed as follows:

$$\text{Dist}(A, [BC]) = 2 \cdot \frac{S_{ABC}}{L_{BC}}$$

where S_{ABC} represents the plane surface encompassed by points A , B et C , and L_{BC} represents the length of the segment joining points B and C .

3.1.5. Constraint C11: Straight line-Straight line, coincidence

Given two straight lines $[B_1C_1]$ and $[B_2C_2]$, constraint C11 is expressed as follows:

$$4 \cdot L_{B_1C_1}^2 \cdot L_{B_2C_2}^2 = \left((L_{B_1B_2} + L_{C_1C_2}) - (L_{B_1C_2} + L_{B_2C_1}) \right)^2$$

AND

$$S_{B_1C_1B_2} = 0 \text{ or } S_{B_1C_1C_2} = 0 \text{ or } S_{B_1B_2C_2} = 0 \text{ or } S_{C_1B_2C_2} = 0$$

where S_{ABC} represents the plane surface encompassed by points A, B and C, and L_{BC} represents the length of the segment joining points B and C.

3.1.6. *Constraint C12: Straight line-Straight line, parallelism, distance*
 Given two straight lines $[B_1C_1]$ and $[B_2C_2]$, constraint C12 is expressed as follows:

$$4 \cdot L_{B_1C_1}^2 \cdot L_{B_2C_2}^2 = \left((L_{B_1B_2} + L_{C_1C_2}) - (L_{B_1C_2} + L_{B_2C_1}) \right)^2$$

AND

$$Dist([B_1C_1],[B_2C_2]) = Dist_{12} = 2 \cdot \frac{S_{B_1C_1B_2}}{L_{B_1C_1}} \text{ or } Dist_{12} = 2 \cdot \frac{S_{B_1B_2C_2}}{L_{B_2C_2}} \text{ or } Dist_{12} = 2 \cdot \frac{S_{C_1B_2C_2}}{L_{B_2C_2}} \text{ or } Dist_{12} = 2 \cdot \frac{S_{B_1C_1C_2}}{L_{B_1C_1}}$$

where S_{ABC} represents the plane surface encompassed by points A, B and C, and L_{BC} represents the length of the segment joining points B and C.

3.1.7. *Constraint C13: Straight line-Straight line, angle and distance*
 In the particular case of the two straight lines belonging to the same plane, when the straight lines are not parallel (constraint C12) then the distance between them is nil. Given two straight lines $[B_1C_1]$ and $[B_2C_2]$, constraint C13 is expressed as follows:

$$V_{B_1C_1B_2C_2} = 0 \text{ and } \cos \alpha = \frac{(L_{B_1B_2} + L_{C_1C_2}) - (L_{B_1C_2} + L_{B_2C_1})}{2 \cdot L_{B_1C_1} \cdot L_{B_2C_2}}$$

OR

$$V_{B_1C_1B_2C_2} = 0 \text{ and } \sin \alpha = \frac{\sqrt{4 \cdot L_{B_1C_1}^2 \cdot L_{B_2C_2}^2 - \left((L_{B_1B_2} + L_{C_1C_2}) - (L_{B_1C_2} + L_{B_2C_1}) \right)^2}}{2 \cdot L_{B_1C_1} \cdot L_{B_2C_2}}$$

where V_{ABCD} represents the volume encompassed by points A, B, C and D, L_{AB} represents the length of the segment joining points A et B and α represents angle($[B_1C_1],[B_2C_2]$).

3.2. TOPOLOGICAL CONSTRAINTS

The topological constraints correspond to constraints belonging to a geometric element in a zone of space. This zone can be defined by intersections and/or unions of element zones.

Problem in one dimension: positioning of a point C in relation to two points A and B.

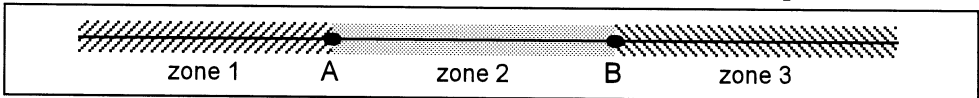


Fig. 1 : division of a line

Given three distances L_{AB} , L_{AC} and L_{BC} .

Our proposal is based on the fact that a point belonging to a zone is evidenced by writing a relation of consistency between the three dimensional parameters indicated above.

We will write that a point C belongs to zone 1, or zone 2, or zone 3, or any of the zones described by a Boolean operation of these three zones, as follows.

$$\text{Point C belongs to (zone 1) : } L_{AB} + L_{AC} - L_{BC} = 0$$

$$\text{Point C belongs to (zone 2) : } -L_{AB} + L_{AC} + L_{BC} = 0$$

$$\text{Point C belongs to (zone 3) : } L_{AB} - L_{AC} + L_{BC} = 0$$

$$\text{Point C belongs to (zone 1} \cup \text{zone 2) : } (L_{AB} + L_{AC} - L_{BC}) \cdot (-L_{AB} + L_{AC} + L_{BC}) = 0$$

We can, therefore express the topological constraints by using a dimensional parameter which may seem superfluous **AND** by declaring an additional consistency relation.

Writing previous relations implies writing that the triangular surface encompassed by the three points A, B and C is nil. In point of fact, the surface of a triangle ABC may be written as follows:

$$S_{ABC} = \frac{1}{4} \cdot \sqrt{(L_{AB} + L_{AC} + L_{BC}) \cdot (-L_{AB} + L_{AC} + L_{BC}) \cdot (L_{AB} - L_{AC} + L_{BC}) \cdot (L_{AB} + L_{AC} - L_{BC})}$$

It can be noted that this expression cancels itself out when at least one of these four terms is nil.

Thus, finding the expression of topological constraints in the plane involves finding a factorised form of the volume of a tetrahedron encompassed by four points A, B, C and D. This work has been achieved with the help of [ROU.97], and the conclusions are as follows:

- There are 6 factorised forms of the volume of a tetrahedron, one of which is presented below (α represents the angle between segments [AB] and [CD]):

$$V_{ABCD} = \frac{1}{3 \cdot L_{AB}} \cdot \sqrt{\left(\frac{1}{2} \cdot L_{AB} \cdot L_{CD} \cdot \sin \alpha + S_{ABC} + S_{ABD}\right) \cdot \left(-\frac{1}{2} \cdot L_{AB} \cdot L_{CD} \cdot \sin \alpha + S_{ABC} + S_{ABD}\right) \cdot \left(\frac{1}{2} \cdot L_{AB} \cdot L_{CD} \cdot \sin \alpha - S_{ABC} + S_{ABD}\right) \cdot \left(\frac{1}{2} \cdot L_{AB} \cdot L_{CD} \cdot \sin \alpha + S_{ABC} - S_{ABD}\right)}$$

- Each of these forms comprises four terms;
- Of these four terms, only three can cancel one another out.

We can thus divide up the plane space in six different ways, each of these divisions splitting the plane space into three zones.

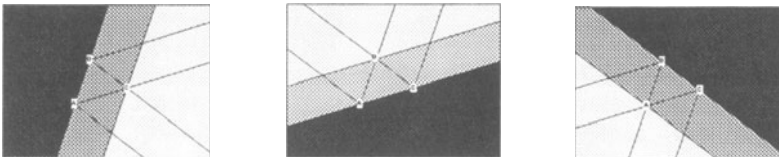


Fig. 2 : division of a plane into 3 bands

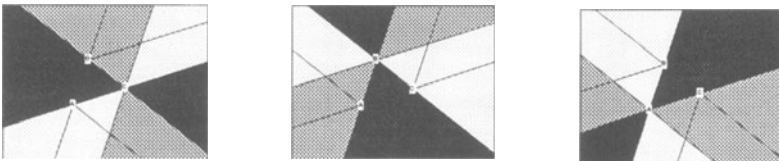


Fig. 3 : division of a plane into 3 angular sectors

3.3. CHIRAL CONSTRAINT

In industry, it is frequently useful to manufacture parts in pairs. The first part being called the « right-hand part » and the second the « left-hand part ». Among a number of examples from industry, we can quote: aircraft wings, automobile headlights, the fascia for left or right-hand drive, apartment doors, etc.

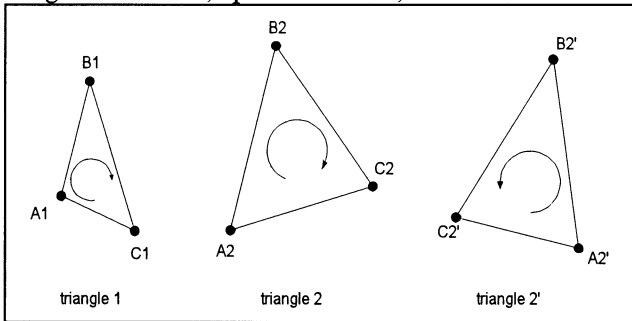


Fig. 4 : Demonstrating the chiral constraint

Given the three triangles shown above. Without declaring any dimensional constraints, it is necessary to declare the fact that the order of the three vertexes A_1 , B_1 and C_1 of the triangle 1 is:

1. the **same** as that of vertexes A_2 , B_2 and of triangle 2 ;
2. the **opposite** of that of vertexes A_2' , B_2' and C_2' of triangle 2'.

We will call this constraint the 'chiral' constraint which, mathematically speaking is evidenced by this expression:

$$L_{A_2B_2} \cdot \cos([A_1B_1],[A_2B_2]) \cdot L_{A_2C_2} \cdot \cos([A_1B_1],[A_2C_2]) - L_{A_2B_2} \cdot \cos([A_1C_1],[A_2B_2]) \cdot L_{A_2B_2} \cdot \cos([A_1B_1],[A_2C_2])$$

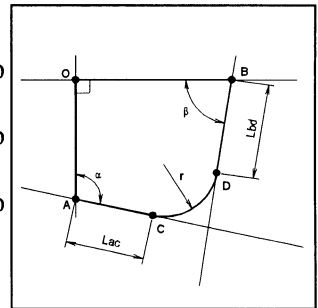
which will be positive when the two triangles $A_1B_1C_1$ and $A_2B_2C_2$ have the same chirality and negative if the contrary is true.

4. Illustration

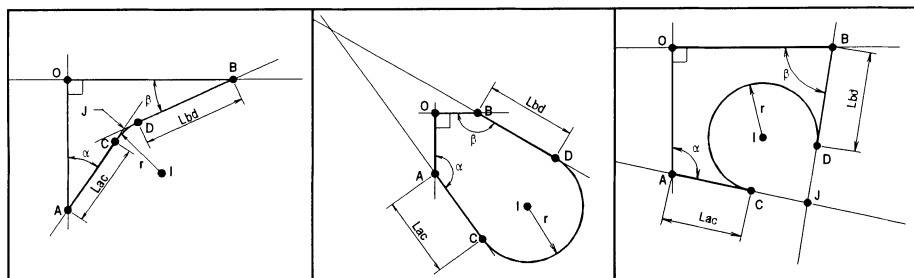
We are presenting an example in which all the geometric constraints of a plane figure have been declared. This figure has been taken from [BOU.95].

The dimensional constraints are as follows:

1. segments [OA] and [OB] are perpendicular;
2. the angle between segment [AO] and [AC] is equal to « α » ;
3. the angle between segment [BO] and [BD] is equal to « β » ;
4. the distance between points A and C is equal to « L_{ac} »;
5. the distance between points B et D is equal to « L_{bd} »;
6. the radius of the arc of the circle CD is equal to « r ».



The author demonstrates that it is possible to generate at least three topologically different solutions which respect the dimensional constraints imposed.



We can, of course, devise other solutions apart from those presented above. However, our aim is to prove that, with the previously defined geometric constraints, we are able to unequivocally declare the initial geometric figure.

The solution we propose is as follows:

Declaration of geometric entities:

- 4 segments [OA], [OB], [AC] and [BD]
- the arc of the circle [CD], with a centre I and running point M
- point J, intersection of segments [AC] and [BD]

Dimensional constraints:

- $\text{angle}([OA],[OB]) = 90^\circ$
- $\text{angle}([AO],[AC]) = \alpha$
- $\text{angle}([BO],[BD]) = \beta$
- $\text{distance}(A,C) = L_{ac}$
- $\text{distance}(B,D) = L_{bd}$
- $\text{distance}([AC],I) = \text{radius}$
- $\text{distance}([BD],I) = \text{radius}$
- $\text{distance}(M,I) = \text{radius}$

Topological constraints:

- point C belongs to the plane zone defined as the intersection between angular sector OAB and the plane band parallel to [AB], on the opposite side to O:

$$2 \cdot S_{ABO} + 2 \cdot S_{ABC} - L_{AB} \cdot L_{OC} \cdot \sin([AB],[OC]) = 0 \quad \text{and} \quad 2 \cdot S_{AOC} + 2 \cdot S_{BOC} - L_{AB} \cdot L_{OC} \cdot \sin([AB],[OC]) = 0$$

- point D belongs to the plane zone defined as the intersection between angular sector OAB and the plane band parallel to [AB], on the opposite side to O

$$2 \cdot S_{ABO} + 2 \cdot S_{ABD} - L_{AB} \cdot L_{OD} \cdot \sin([AB],[OD]) = 0 \quad \text{and} \quad 2 \cdot S_{AOD} + 2 \cdot S_{BOD} - L_{AB} \cdot L_{OD} \cdot \sin([AB],[OD]) = 0$$

- point J belongs to segment [AC] and the C side

$$-L_{AC} + L_{AJ} + L_{CJ} = 0$$

- point J belongs to segment [BD] and the D side

$$-L_{BD} + L_{BJ} + L_{DJ} = 0$$

- running point M belongs to the plane band parallel to [CD] and the opposite side to I

$$2 \cdot S_{CDM} + 2 \cdot S_{CDI} - L_{CD} \cdot L_{MI} \cdot \sin([CD],[MI]) = 0$$

This set of constraints is necessary and suffices to generate the initial figure without any ambiguity, whilst eliminating the various figures presented at the beginning of this paragraph.

To totally complete the declaration, we need to specify whether we require a « right-hand » or « left-hand » materialisation of the figure. For this, a chiral constraint has to be added between our figure and another triangle which will define the « right-hand » or « left-hand » concept.

5. Conclusion

Three types of constraints have been described and illustrated in this article: dimensional, topological and chiral. It should be noted that all these constraints are expressed in a consistent manner, due to the use of the distance between two points parameter. Furthermore, expression of these constraints is local since it is independent of a reference frame which is often arbitrarily defined by the CAD-CAM system. In our opinion, declaration of these geometric constraints is necessary and is sufficient to define iso-constraint problems from a geometric and topological point of view.

The study presented here is limited to two-dimensional geometry but we are in the process of generalising this approach to real three-dimensional problems. However, the delicate problem of substantiating such a declaration still remains.

We do feel that a new community more specifically devoted to declarative or variational geometry needs to develop alongside the scientific community involved in algorithmic geometry.

6. References

- [BOU.95] BOUMA W., FUDOS I., HOFFMANN C. M., CAI J., PAIGE R., « Geometric constraint solver », *Computer-Aided Design*, Vol. 27, N°6, pp. 487-501, 1995.
- [CAP.96] CAPOYLEAS V., CHEN X., HOFFMANN C. M., « Generic Naming in Generative, Constraint-Based Design », *Computer-Aided Design*, Vol. 28, N°1, pp. 17-26, 1996.
- [CLÉ.97] CLÉMENT A., RIVIÈRE A., SERRE P., VALADE C., « The TTRS : 13 Constraints for Dimensioning and Tolerancing », 5th CIRP Seminar on Computer Aided Tolerancing, The University of Toronto, Canada, April 27-29, 1997.
- [CLÉ.96] CLÉMENT A., RIVIERE A., SERRE P., « The TTRS : a Common Declarative Model for Relative Positioning, Tolerancing and Assembly », *MICAD proceedings, Revue de CAD-CAM et d'informatique graphique*¹, Volume 11 - n°1-2/1996, Hermès, p. 149-164, February 1996.
- [ROU.97] ROUCHÉ E., De COMBEROUSSE C., « *Traité de géométrie*² », Jacques Gabay, Paris (France), ISBN 2-87647-136-1, 1997.
- [SHP.97] SHPITALNI M., LIPSON H., « Automatic Reasoning for Design under Geometrical Constraints », *Annals of the CIRP*, Volume 46(1), p. 85-88, 1997.

¹ CAD-CAM and computer graphics

² Geometry paper

PIECEWISE CUBIC INTERPOLATION FOR REVERSE ENGINEERING

G. PRADES*, Y. MINEUR**, J.L. CAENEN*, J.M. CASTELAIN**
LAMIH, Conception des Systèmes Mécaniques et Energétiques.

* *Ecole des Mines de Douai, 941 rue Charles Bourseul, F-59508 Douai.*

** *ENSIMEV, B.P. 311, F-59304 Valenciennes.*

Abstract. This paper presents a new fitting method with cubic Bézier curves with a monotone curvature. The slopes at the endpoints are imposed, which allows to generate G^1 -connected curves. The proposed method is based on a parametrization free interpolation scheme, whose study leads to the determination of areas for the intermediate interpolating points, so that the generated curve is convex, close to the data points, with a monotone curvature. Examples of application are presented and discussed.

1. Introduction

The 1990s give time and quality an essential importance in the marketing of a new product. Reverse engineering is one of the technologies developed today to achieve these goals. Its main purpose is to generate a CAD model from a part or a prototype, in order to update its design or to manufacture it using CAM techniques. The process consists in digitizing a shape and then in converting the obtained discrete data set into a continuous piecewise smooth model [13]. A classical way to achieve this modelization is to generate curves from which surfaces are then constructed. Several curve fitting methods have been developed for this purpose. However, as they operate on all the data points with the same ponderation, they produce curves which tend more or less to reproduce the measurement errors, and which present extraneous oscillations. Thus, in most cases, these curves need to be modified in an interactive and empirical manner, until the achievement of a result satisfying accuracy and geometric quality. Some previous works propose fitting principles imposing accuracy constraints [10], convexity constraints [5] or smoothness constraints [7]. Most of them use optimization methods that do not guarantee to converge on a satisfying solution.

In this paper, we present a new fitting method with cubic Bézier curves, defined by interpolation and tangency conditions at endpoints, and by two intermediate interpolating points. The curve extremities correspond to the endpoints of the data set to be fitted ; imposing the slopes at these points allows a G^1 -continuity between two curves connected end to end. The proposed approach selects two intermediate interpolating points within the set to be fitted, according to their ability to generate a convex curve,

with a monotone curvature, close to the data points. These characteristics are determined according to the intermediate points positions.

Thus, our fitting method is based on a new piecewise cubic G^1 interpolation scheme that we present in section 2. It is defined by its endpoints positions associated with two unit tangent vectors (slopes), and by two intermediate interpolating points. Unlike classical cubic interpolation methods derived from Hermite interpolation which define a curve segment between each point [2], our scheme generates a curve every four points and allows to reduce the amount of information to be stored for the representation of the data. Moreover, our modelization does not require any parametrization and thus gets released from the influence of this process on the resulting curve [3]. In section 2, we also present conditions on the positions of the two intermediate interpolating points for generating a convex curve. The fitting method is implemented in section 3, and it consists in choosing two intermediate interpolating points within the set to be fitted. The choice of these two points is controlled by analytical criteria, translating their ability to generate a curve close to the data set, with a monotone curvature. In section 4, the proposed approach is tested and compared to classical fitting methods. The results show that both the curve accuracy and quality are drastically improved.

2. Cubic interpolation and theoretical backgrounds

The fitting method that we propose is based on an interpolation scheme with planar cubic Bézier curves. It is described in this section.

2.1. PRESENTATION OF THE INTERPOLATION PROBLEM

The problem we define here is to generate a planar cubic Bézier curve about which we possess position and tangency direction at extremities, and which interpolates two imposed points. The general expression of a cubic Bézier curve P defined by its control polygon $\{S_i = (X_i, Y_i), i = 0..3\}$ is given by the parametric equation :

$$P(t) = (X(t), Y(t)) = \sum_{i=0}^3 S_i \binom{3}{i} t^i (1-t)^{3-i} \quad \text{with} \quad t \in [0,1]. \quad (2.1)$$

Given in the plane two points P_a and P_b , two corresponding unit vectors d_a and d_b , and two interpolating points P_1 and P_2 , we can then state our problem as follows; generate a planar cubic Bézier curve P , so that for parameter values $t \in [0,1]$, we have :

$$\begin{cases} S_0 = P(0) = P_a, & S_3 = P(1) = P_b, \\ d_a = \frac{P'(0)}{\|P'(0)\|}, & d_b = \frac{P'(1)}{\|P'(1)\|}, \\ P(t_1) = P_1, & P(t_2) = P_2, \\ P \text{ is a convex curve.} \end{cases} \quad (2.2)$$

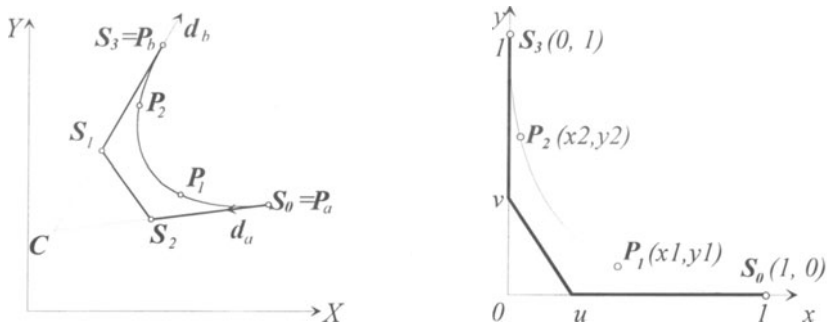


Figure 1. Cubic Bézier curve and passage from initial to local coordinate system.

The problem consists in searching (Fig.1) the positions of the control points S_1 and S_2 of the Bézier curve satisfying the conditions (2.2). It is important to notice that such a problem cannot be solved with classical interpolation methods [1] which require either tangent vectors at endpoints to be known in norm and direction, or points P_1 and P_2 to be assigned a parameter value. In order to find the positions of S_1 and S_2 , we transpose the problem in a local coordinate system (O, x, y) , with orthogonal unit vectors, and linked to the curve endpoints (Fig.1). In this coordinate system, the cubic Bézier curve is defined by :

$$p(t) = \begin{cases} x = (1-t)^3 + 3u(1-t)^2t \\ y = 3v(1-t)t^2 + t^3 \end{cases} \quad \text{with} \quad t \in [0,1], \quad (2.3)$$

where we have stated :

$$u = \frac{\|CS_1\|}{\|CP_a\|}, \quad \text{and} \quad v = \frac{\|CS_2\|}{\|CP_b\|}.$$

Put into form (2.3), the problem consists in searching the values u and v , corresponding to the positions of the intermediate control points S_1 and S_2 in the local coordinate system. To do this, we rewrite relation (2.3) as :

$$\begin{cases} u = \frac{x - (1-t)^3}{3(1-t)^2t} \\ v = \frac{y - t^3}{3(1-t)t^2} \end{cases} \quad t \in]0,1[, \quad (2.4)$$

which defines a parametric curve that we denote by q . Then the values u and v correspond to the intersection (Fig.2) of two parametric curves q_1 and q_2 defined by :

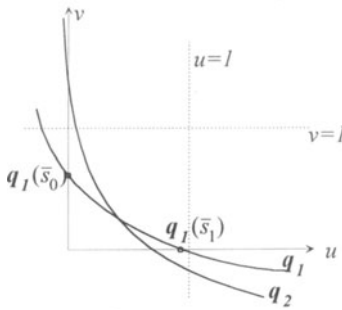


Figure 2. Intersection problem.

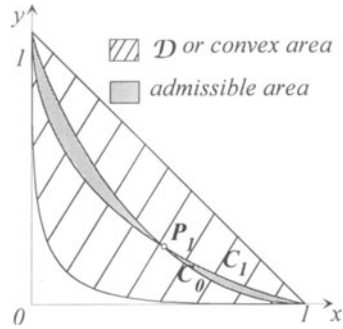


Figure 3. Convex and admissible areas.

$$q_1(s) = \begin{cases} u(s) = \frac{x_1 - (1-s)^3}{3(1-s)^2 s} \\ v(s) = \frac{y_1 - s^3}{3(1-s)s^2} \end{cases} \text{ and } q_2(t) = \begin{cases} u(t) = \frac{x_2 - (1-t)^3}{3(1-t)^2 t} \\ v(t) = \frac{y_2 - t^3}{3(1-t)t^2} \end{cases}, \quad (2.5)$$

where x_1, y_1, x_2 and y_2 are the coordinates of the two interpolating points P_1 and P_2 in the local coordinate system. Among the three currently used algorithms for the research of intersections (nonlinear techniques, subdivision techniques and algebraic techniques), it is shown in [11] that those based on an algebraic approach are the most performant for parametric curves of degree less or equal to 4. Therefore it is the one we have retained to solve our problem. Without describing it, we just precise that this approach allows to express one of the two curves in an implicit form, and that the intersection problem is thereafter reduced to solving a single polynomial equation.

2.2. GENERATION OF A CONVEX CUBIC BEZIER CURVE

In the previous paragraph we have described the general interpolation scheme that we propose. The purpose of what follows is to define the conditions on the interpolating points $P_1(x_1, y_1)$ and $P_2(x_2, y_2)$, so that the generated curve is convex, that is [11], so that the intermediate control points satisfy $(u, v) \in]0,1[\times]0,1[$. The demonstration of these conditions is omitted here, but a discussion of this subject is made in [8].

The first condition operates on the two points $P_1(x_1, y_1)$ and $P_2(x_2, y_2)$, and translates the fact that (u, v) belongs to $]0,1[\times]0,1[$. It can be written as follows :

$$\begin{cases} (1-t)^3 < x_i < (1-t)^3 + 3t(1-t)^2 \\ t^3 < y_i < 3(1-t)t^2 + t^3 \end{cases} \quad i = 1,2, \quad \text{with } t \in]0,1[, \quad (2.6)$$

and defines a convex area \mathcal{D} , to which $P_1(x_1, y_1)$ and $P_2(x_2, y_2)$ have to belong.

The second condition operates on the relative position of $P_2(x_2, y_2)$ with respect to the position of a point $P_1(x_1, y_1)$, fixed in \mathcal{D} . It defines a parametric area we call admissible area, denoted by $adm(P_2 / P_1)$, and satisfying :

$$\left\{ \begin{array}{l} x_2 = \frac{x_1 - (1 - \tilde{s})^3}{(1 - \tilde{s})^2 \tilde{s}} (1 - t)^2 t + (1 - t)^3 \\ y_2 = \frac{y_1 - \tilde{s}^3}{(1 - \tilde{s}) \tilde{s}^2} (1 - t) t^2 + t^3 \end{array} \right. \quad \text{with } \tilde{s} \in]\bar{s}_0, \bar{s}_1[, \text{ and } t \in]0, 1[, \quad (2.7)$$

where $\bar{s}_0(x_1, y_1)$ and $\bar{s}_1(x_1, y_1)$ are shown in Fig.2. This area is enclosed between two parametric curves C_θ and C_I (Fig.3). It defines both the admissible positions of $P_2(x_2, y_2)$ and all the convex cubic Bézier curves we can generate from $P_1(x_1, y_1)$.

3. Interpolation based fitting method

This section is dedicated to the application of our interpolation scheme to a fitting problem. Our objective is to minimize the number of useful points for the generation of a curve, and to state identification criteria on these points. These criteria must be first independant of any parametrization. They also have to reflect demands inherent to reverse engineering problems, such as the curve accuracy in terms of distance from the data points, and the curve quality in terms of smoothness or monotony of its curvature. Taking into account these criteria allows to generate a satisfying curve straight away, and therefore to get released from the different processings intended to take up defects correction.

Fig.4 shows a set of data we wish to approximate with a convex cubic Bézier curve. The fitting problem consists in choosing two intermediate interpolating points within this set. In opposition to classical fitting methods, our approach proposes a large number of solutions, and instead of testing each of them [6], we first propose a rapid estimation *a priori* of the average deviations between the curves we can generate and the data points. This estimation leads to the selection of the first interpolating point. In a second step, we generate several convex curves passing through this point and another point within the data set. Among these curves, we finally retain the closest to the data set, which also presents a monotone curvature.

3.1. ESTIMATION OF THE FITTING ERROR

The objective of what follows is to provide an estimation of the average deviation $\bar{\varepsilon}$ from a cubic convex Bézier curve interpolating a point P_I , to the data points $Q_{i,i=1..n}$. This estimation comes from the properties of the curves C_θ and C_I to enclose all the convex cubic Bézier curves passing through P_I .

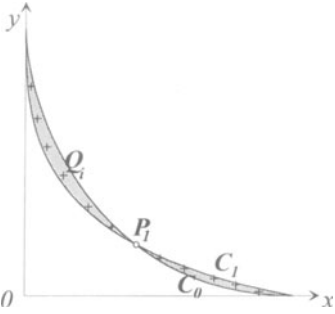


Figure 4. Local representation of the data.

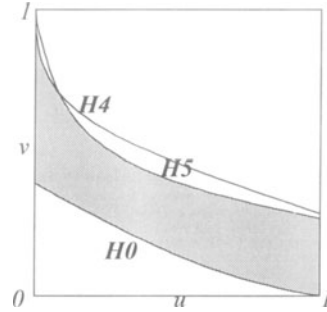


Figure 5. Monotone curvature area.

If we denote respectively by ε_0 and ε_1 , the deviations from the curves C_0 and C_1 to the data points, then we have necessarily :

$$\varepsilon < \max(\varepsilon_0, \varepsilon_1), \tag{3.1}$$

which is a significant estimation when the data points are sparse. If it is not the case (Fig.4), it is less significant, and we can then verify that we have :

$$\varepsilon < \min(\varepsilon_0, \varepsilon_1), \tag{3.2}$$

which leads to a better estimation of the curve accuracy.

Even though relations (3.1) and (3.2) do not allow to find the best curve, they provide an efficient way to choose *a priori* a first interpolating point that will lead to the construction of a curve close to the data points.

3.2. GENERATION OF A CURVE WITH A MONOTONE CURVATURE

Besides the accuracy of the approximating curve, demands in reverse engineering concern the curves quality. This quality is often expressed in terms of monotony [9] or smoothness [4] of the curvature. Smoothness being too restrictive as far as the shapes of the curves that can be generated are concerned, we will only be interested in the monotony.

We have determined (Fig.5) the monotone curvature areas for the two intermediate control points of a cubic Bézier curve. These areas are enclosed between three implicit curves representing some coefficients of the mathematical expression of the curvature variation [9]. As for the admissible areas, these areas can be translated to impose conditions on the positions of $P_1(x_1, y_1)$ and $P_2(x_2, y_2)$.

All the areas we have determined are now used to choose *a priori* two intermediate interpolating points that will generate a convex curve, with a monotone curvature, and close to the data points. At last, it is important to notice that the curves enclosing these different areas can be expressed implicitly, and thereafter that the location of a point with respect to these areas is determined easily.

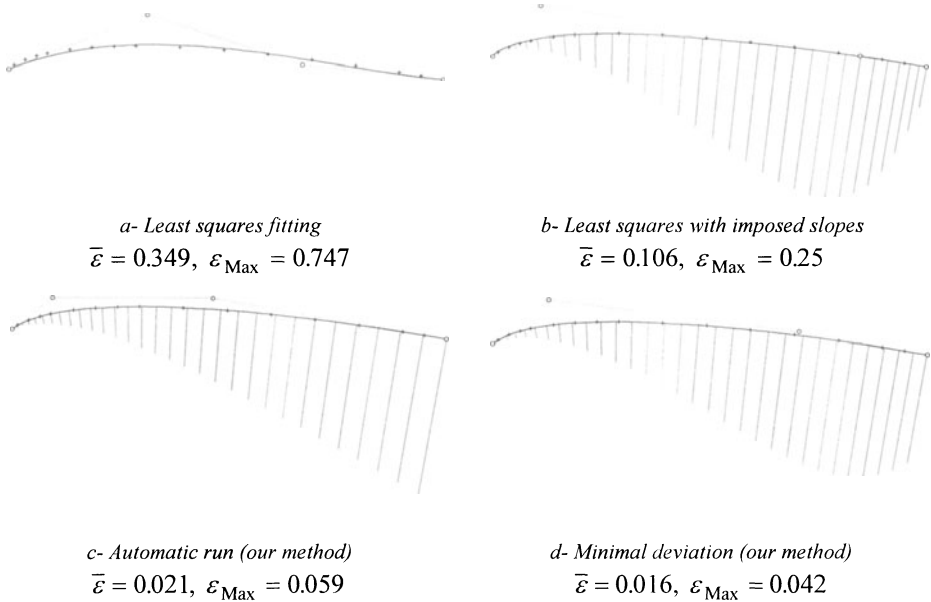


Figure 6. Curve fits from a set of digitized data points.

4. Examples and experimental results

The fitting method was implemented on MapleV. In this section we compare it to classical methods such as least squares fitting with endpoints interpolation, and least squares fitting with imposed tangent directions at endpoints. For a reverse engineering problem, we assume that by means of a process we are studying, the set of data is decomposed into subsets on each of which we can generate a convex cubic Bézier curve. In such a case, the different curves are connected according to a G^1 continuity. Fig.6 shows several curve fits from a set of 17 data points measured on a turbine blade profile. For the least squares approximations, a chord length parametrization was used to perform the curve determination. For our fitting method, we first retain the second interpolating points capable of generating a curve with a monotone curvature, and then we select those that may generate a curve with a deviation as small as possible. The areas determined in the previous section allow to choose these points very quickly, and the fitting procedure is ran automatically. In this case, the retained interpolating points are P_4 and P_6 , and the resulting curve is shown on Fig.6c. In order to compare this result to other fits obtained with our method, we have tested all the convex curves we could generate; the best fit in terms of average deviation is shown on Fig.6d for P_3 and P_{12} , and the worst is $\bar{\varepsilon} = 0.034$ for P_6 and P_7 . The average deviations are given in millimeter, given that the curve arc length is approximately 100mm.

By viewing these different results, we can first note that our method allows to improve drastically the curves accuracy (even in the worst case). The main reason for

that is we do not need any parametrization for the curves generation. The second advantage is that besides the accuracy, the generated curves most of the time present a monotone curvature. This characteristics however depends on the data configuration, but was achieved for all the examples we have tested.

5. Conclusion

A new method for data fitting with cubic Bézier curves is presented. Its originality lies in the use of a parametrization free interpolation scheme, operating from the curve endpoints, tangent directions at these points, and two intermediate points. The choice of these two points within the set to be fitted, is based on a characterization of the resulting curve in terms of accuracy and curvature variation. These characteristics are related to the intermediate points positions in an analytical way.

The fact that no parametrization is required for the modelization, allows to significantly improve the accuracy of the approximating model compared to classical fitting methods.

The fact that only two significant intermediate points are used for the curve generation, provides in a sense the modelization with immunity from local measurement errors.

References

- [1] Bézier P. (1987). *Courbes et surfaces*, Mathématiques et CAO tome 4, Hermès, Paris.
- [2] De Boor C., Höllig K., Sabin M. (1987) High accuracy geometric Hermite interpolation, *Computer Aided Geometric Design* **4**, 269-278.
- [3] Epstein M.P. (1976) On the influence of parametrization in parametric interpolation, *SIAM Journal of Numerical Analysis* **13**, 261-268.
- [4] Higashi M., Kaneko K., Hosaka M. (1988) Generation of high quality curve and surface with smoothing varying curvature. *Eurographics'88*, in D.A. Duce and P. Jansene (Eds), Elsevier Science, 79-92.
- [5] Léon J.C. Trites J.B. (1988) Constrained optimization applied to geometric modeling, *FEMCAD*, Paris (France), 17-19 Octobre 1988, 179-191.
- [6] Limaiem A., Nassef A., El Maraghy H.A. (1996) Data fitting using dual kriging and genetic algorithms, *Annals of the CIRP* **45**, 129-134.
- [7] Nowacki H., Liu D., Lü X. (1990) Fairing Bézier curves with constraints, *Computer Aided Geometric Design* **7**, 43-55.
- [8] Prades G., Mineur Y., Caenen J.L., Castelain J.M. (1998). A non parametric interpolation based fitting method with fair cubic Bézier curves, submitted for publication in *Computer Aided Geometric Design*.
- [9] Roulier J.A., Rando T., Piper B. (1990) Fairness and monotone curvature, *Approximation Theory and functional Analysis*, in C.K. Chui (ed), Academic Press, 177-199.
- [10] Sarkar B., Menq C.H. (1991) Smooth surface approximation and reverse engineering, *Computer Aided Design* **23**, 623-628.
- [11] Sederberg T.W., Parry S.R. (1986) Comparison of three curves intersection algorithms, *Computer Aided Design* **18**, 139-159.
- [12] Stone M.C., DeRose T.D. (1989) A geometric characterization of parametric cubic curves, *ACM Transactions on Graphics* **8**, 147-163.
- [13] Varady T., Martin R.R., Cox J. (1997) Reverse engineering of geometric models - an introduction, *Computer Aided Design* **29**, 255-268.

Chapter 4
MODELING AND SYNTHESIS OF MECHANISMS

Component mode synthesis in the design and the optimisation of mechatronic systems.....	217
P. DE FONSECA, H. VAN BRUSSEL and P. SAS	
The kinematics design of a 3-dof hybrid manipulator.....	225
D. CHABLAT, PH. WENGER and J. ANGELES	
Geometric synthesis of manipulators under kinematic constraints	233
S. GUERRY, B. OUEZDOU and S. RÉGNIER	
A cooperative approach in mechanism design	241
P. CHEDMAIL, T. DAMAY and B. YANNOU	
Study of complex tackles : lifting systems with pulleys and cables.....	249
A. BILLEREY, P. CLOZEL and D. CONSTANT	
Application of a fuzzy logic ordering method to preliminary mechanism design ..	257
J.C. FAUROUX, C. SANCHEZ, M. SARTOR and C. MARTINS	
RVS : a robot visualization software package.....	265
J. DARCOVITCH, J. ANGELES, P. MONTAGNIER AND CHU-JEN WU	

COMPONENT MODE SYNTHESIS IN THE DESIGN AND OPTIMISATION OF MECHATRONIC SYSTEMS

P. DE FONSECA, H. VAN BRUSSEL, P. SAS
*Katholieke Universiteit van Leuven,
Dept. Mechanical Engineering, Division PMA,
Celestijnenlaan 300B, B-3001 Heverlee, Belgium*

Abstract

The present paper discusses the numerical condensation of a finite element model of a three-axis high speed milling machine to a low-order state-space model suitable for control system design. In order to analyse the dynamic characteristics of the machine within the whole working domain, the dynamics of the machine in different spatial configurations should be investigated without the time consuming complete recalculation of the machine dynamics. The paper shows that a multi-stage component mode reduction and synthesis procedure provides a solution to that problem, because it allows a cheap analysis of different configurations. Substructures with known dynamic characteristics are described by their respective component modes. They are combined in the appropriate relative positions, and the system is solved through a reduced set of equations for each configuration. A well-considered selection of the types of component modes improves the quality of the reduced model.

1. Introduction

Mechatronics can be defined as the science of motion control [1]. Essentially, motion control comprises the control of desired motion, or tracking control, and the control of undesired motion, or vibration cancellation. Nowadays, performance levels, imposed on mechatronic systems in terms of tracking error and residual vibration level, require the use of complex control algorithms and high bandwidth drive systems in order to improve the deficiencies in the dynamic behaviour of the mechanical subsystem. These high bandwidth control systems interact with the structural dynamics of the mechanical subsystem. An optimal design can only be achieved by taking into account this interaction in an early design phase of a mechatronic system. This explains the necessity of developing a Virtual Concurrent Engineering or a Virtual Prototyping environment for mechatronic systems design [1,2], where the mechanical and the control design problem are tackled simultaneously. An adequate description of the dynamic behaviour of the mechanical structure is based on a finite element model, usually with a very large number of degrees-of-freedom. The reduction of this finite element model into a model of much smaller dimensions, suitable for control system design, forms a necessary step in the development of such a Virtual Engineering environment. It is advocated here that

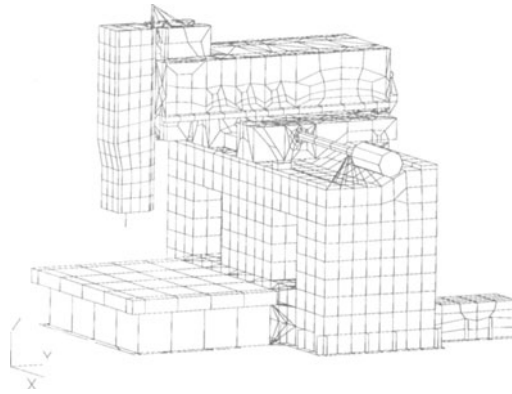


Figure 1 : Finite element model of the machine tool

the component mode synthesis (CMS) techniques [3] provide an appropriate solution for the reduction of the finite element model.

An important class of mechatronic systems, like machine tools, robots, flexible space structures, ... have a large number of different operation positions. Their dynamic behaviour, described by their eigenfrequencies and modeshapes, will change with changing working configuration. This will inevitably affect the performance and the robust stability of the control system [4], and should therefore be taken into account during controller design. In a next step, the mechanical system model, assembled in different working configurations, has to be reduced to a set of state-space models suitable for control system design. Finally, a control algorithm is designed, which yields a good performance and robust stability, in all operation positions of the system being considered. This controller synthesis problem is beyond the focus of this paper.

The present study focuses on the design of a three-axis high speed milling machine for the super-finishing of dies and moulds, as a representative example of a complex mechatronic system. As this is a very time-consuming operation, a faster machine, which proceeds at higher speeds, while keeping the required accuracy, would yield a significant reduction in production costs. The machine analysed here is represented by its finite element model in figure 1. The motion along the X-axis of the machine is the lateral motion of the tool, the motion along the Y-axis of the machine is the frontal motion of the tool, and the motion along the Z-axis of the machine is the vertical motion of the tool. This machine has been developed in the frame of the Brite-Euram project KERNEL II [5]. The model used here represents an intermediate design of the final machine tool with substantial differences in eigenfrequencies and static stiffness.

The discussion in this paper focuses on the three-axis milling machine, but the methodology can be readily applied to other (flexible) multibody structures. The proposed reduction method makes use of two standard engineering software packages. All finite element calculations are performed within MSC/Nastran. The Matlab environment is used to coordinate the assembly of the machine in the desired spatial configuration, to convert the modal machine model, obtained from MSC/Nastran, into a state-space model, and to perform the subsequent control system synthesis and analysis. Figure 2 shows the different steps in the method.

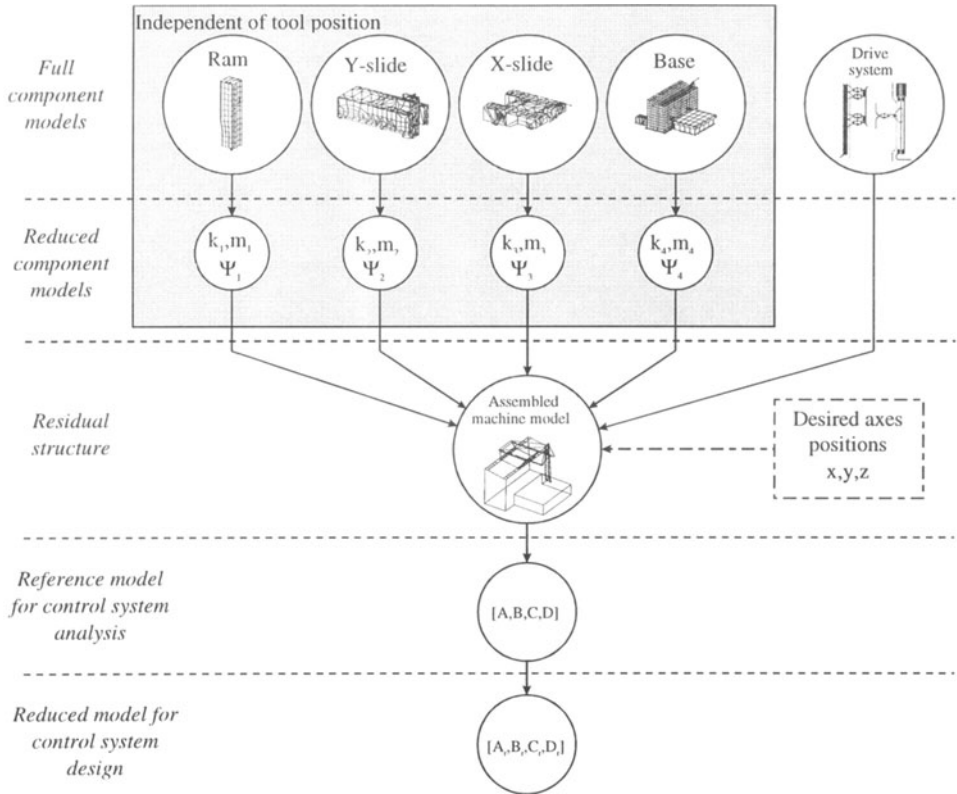


Figure 2 : Overview of the proposed reduction method

2. First component mode reduction and synthesis step

The construction of the three-axis milling machine allows a natural definition of the components as the ram (machine Z-axis), the Y-axis slide, the X-axis slide, and the base. These components are represented in figure 2 by their finite element models in the upper part of the grey box. The modal models of the four components of the milling machine are obtained from a standard component mode reduction, and are stored on hard disk as four separate MSC/Nastran databases. They are represented in the lower part of the grey box in figure 2 by their respective component modal stiffness and mass matrices, k_i and m_i , and by their component mode vectors Ψ_i .

The residual structure, on the third level in figure 2, is the finite element machine model after numerical condensation of the components. This residual structure consists of the reduced component models and the full drive chain models. In the assembly phase, the reduced component models are attached to the residual structure as “external superelements”, each defined in a different relative coordinate system. These relative coordinate systems allow the assembly of the components in the appropriate relative positions. The locations of these relative coordinate systems, which actually determine

the location of the tool tip in the operation space of the milling machine, are defined from within Matlab.

The component modal models should be independent of the spatial configuration of the milling machine, and may, therefore, not contain any element of the drive chains. These drive chains for the three slides, represented on the right of the grey box, belong to the residual structure as their dynamic properties depend on the relative positions of the two slides to which they are connected. For example, when considering a ballscrew drive, the dynamics of the drive depend on the position of the nut on the screw.

3. Comparison of different CMS methods in the first reduction step

The performances of three different CMS methods are evaluated in this section in terms of accuracy of the calculated eigenmodes. Three correlation measures are used to compare the eigenmodes, calculated from the residual structure after numerical condensation, with the '*exact*' eigenmodes, calculated with the full model with 30598 degrees of freedom : the relative eigenfrequency difference for the ten lowest modes of the full structure, the MAC-value [6] between the lowest ten corresponding eigenmodes, and the COMAC-values [6] for all degrees of freedom of the full model.

In the first method, ten fixed-interface normal modes are used in each component modal transformation matrix, together with the constraint and the rigid-body modes (if any). This method is the so-called Craig-Bampton method [3]. The left-hand column of figure 3 summarises the performance of this method as estimated by the three above mentioned correlation measures for the first ten eigenmodes of the finite element model of the high speed milling machine. These results indicate that the correlation between the actual mode shapes and those calculated with the Craig-Bampton method is sometimes not so good. As appearing from the lower left-hand part of the figure, there are a considerable number of degrees of freedom whose COMAC-value is far from unity.

In the second method, ten free-interface normal modes are used in each component modal transformation matrix, together with the constraint and the rigid-body modes (if any). The central column of figure 3 shows the performance of this method as estimated by the three above mentioned correlation measures for the first ten eigenmodes of the finite element model of the high speed milling machine. The results indicate that the correlation between the actual mode shapes and those calculated with this second CMS method is already somewhat better than for the Craig-Bampton method. The reason for this improvement is that a major part of the boundary nodes of the slides in the assembled model are free, while only the boundary conditions of the nodes to which an adjacent slide is connected, are closer to a clamping. Of course, this distinction in boundary conditions between those two types of nodes cannot be made in the proposed method, because different nodes are connected to adjacent components for different spatial configurations of the machine, and the component modal models must be independent from the spatial configuration in which the machine is assembled.

In the last method, four free-interface normal modes and six inertia-relief modes are combined with the constraint and the rigid-body modes (if any). Inertia-relief modes

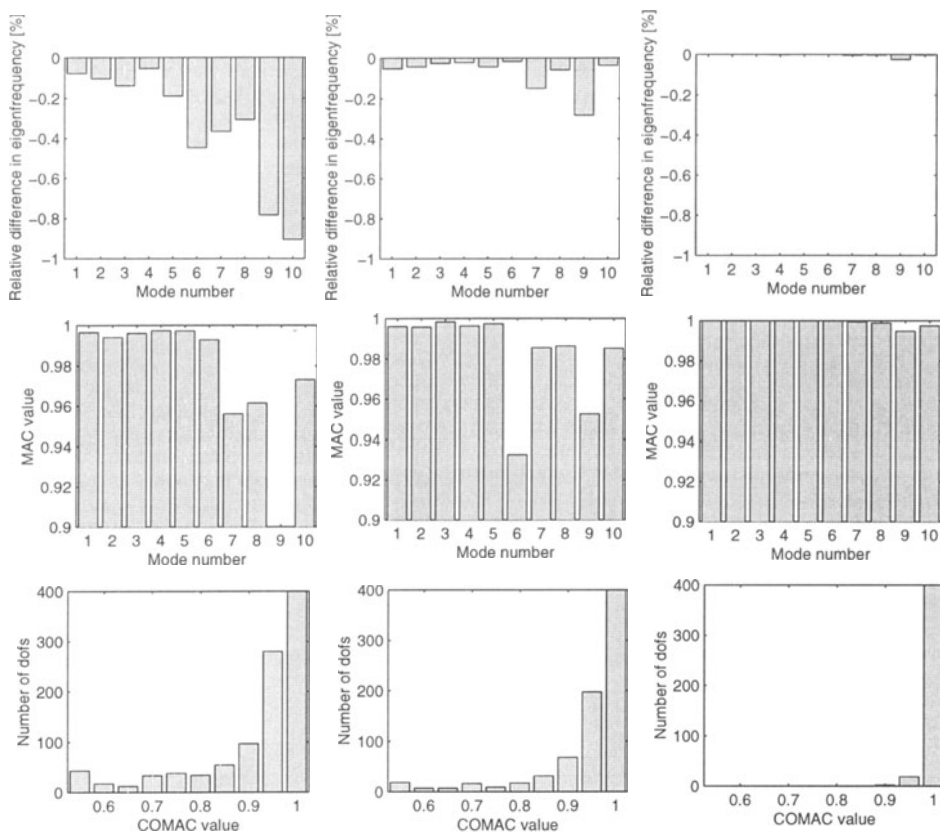


Figure 3 : Performance evaluation and comparison of the three CMS methods

describe the deformation of the component, loaded by d'Alembert inertial forces due to rigid-body motion, and supported such that the stiffness matrix is not singular. This method is comparable to Hintz' method of constraint modes [7], supplemented with a small number of free-interface normal modes.

The right-hand column of figure 3 shows the performance of this method as estimated by the three above mentioned correlation measures, also for the first ten eigenmodes. The results indicate that the correlation between the actual mode shapes and those calculated with this last CMS method is almost perfect. The relative eigenfrequency difference has been reduced by a factor 30 compared to the first method, and by a factor 10 compared to the second method, and amounts now to no more than 0.025 % ! The same holds for the spatial correlation of the mode shapes : not more than 20 degrees of freedom, out of more than 30000, have a COMAC-value below 97.5%. The time required for a modal analysis of the reduced model is a factor 12 smaller than for the analysis of the full model. The reason for this nearly perfect correlation is the fact that the inertia-relief modes account for the residual effects of the omitted high-frequency normal modes at zero frequency. This means that this third component mode set can

represent exactly the static deformation of the component, loaded by the inertial forces due to a uniform acceleration. Analogously, the static deformation due to concentrated forces in the exterior nodes, is exactly represented by the constraint modes [7].

4. Second component mode reduction step

This assembled residual structure is then further considered in the second reduction step as a single component. It has only nine external degrees of freedom, being, on the one hand, the rotations around the three motor axes, on which the torque input for generating the desired trajectory is applied, and, on the other hand, the six degrees of freedom of the tool, on which possible external disturbance forces, originating from the cutting process or from a spindle unbalance, apply. The component mode reduction projects the degrees of freedom of the residual structure (i.e. the assembled machine model on the third level in figure 2) on a modal base consisting of the 9 constraint modes, 36 fixed-interface normal modes and 6 inertia-relief modes. The number and type of component modes in this modal base have again been selected such that the correlation with the original full model is almost perfect in the frequency band of interest and for all possible tool positions in the operation space. This second component mode reduction is performed with a dedicated MSC/Nastran DMAP-alter [8] that writes the reduced mass, stiffness and damping matrix and the modal transformation matrices to an ASCII-file. These matrices are then converted into a state-space model in Matlab. This state-space model, represented by the matrices $[A,B,C,D]$ in figure 2, forms a reference model for the design of a control system for the motors of the machine axes. A major part of this second reduction step is based on the work reported by Bianchi et al. [2].

5. Controller design issues

The order of the reference model $[A,B,C,D]$ is still considerably high. In the case of the milling machine, this reference model is obtained from a component modal model with 51 modal degrees of freedom, resulting in a state-space representation with 102 states. Prior to the control system synthesis, this reference model is again reduced to a state-space model of much lower order, represented by $[A_r, B_r, C_r, D_r]$ in figure 2. Different methods, including, for example, singular value-based truncation methods or (non-linear) least-squares identification methods are available for performing this third reduction step. This third reduction step is typically related to the control system design. Generally, modern motion control algorithms for machine tool axes are developed using a state-space representation of the dynamic behaviour of the machine being considered. Such a state-space model is unavoidably extracted from an experimental or analytical model of the machine in one specific working configuration. Control engineers then employ robust control methods to ensure the stability of the closed-loop system in the presence of uncertainties or variations in the state-space model [4]. The robust control methods, however, require to estimate a certain level of uncertainty which is expected

not to be exceeded. When this uncertainty level is set too conservatively, the performance of the resulting control algorithm will be poor, but when it is set too low, the control system might become unstable. This uncertainty level accounts for discrepancies between the finite element model and the real machine, and for changes in the machine model due to a varying spatial configuration. The use of CMS techniques allows to cheaply analyse the dynamic behaviour of the machine in different spatial configurations, and, hence, to estimate more accurately the uncertainty levels to be used in robust control design. Of course, the problem of assessing the uncertainty due to finite element model inaccuracies, is still not solved with this approach.

Figure 4 shows a frequency response of the tool displacement in X-direction, when a unit torque is applied at the X-axis motor, for four different positions of the tool in its operation space. Obviously, the dynamics of the machine tool are strongly affected by its spatial configuration. The largest relative difference between these curves can, for example, serve as an estimate of the upper bound on some unknown multiplicative model uncertainty in an H_∞ controller design [4].

6. Conclusions

This paper deals with the use of component mode synthesis techniques in the design and the optimisation of mechatronic systems. They offer a viable solution for performing multiple dynamic analyses of a complex mechanical structure in an iterative optimisation process. They also provide the possibility to efficiently study the dynamic behaviour of complex structures in multiple spatial configurations. A modern high speed milling machine is used as a representative example of a complex mechatronic system throughout this text. Machine tools, robots, space structures, and a lot of other mechatronic systems have a number (often an infinite number) of different working positions. Generally, the dynamic behaviour of these structures changes significantly from one spatial configuration to another. Such an analysis forms the basis for a more founded treatment of “uncertainty” in the design of robust motion and vibration controllers for these machines.

The performances of these CMS methods for a normal mode analysis are also discussed. The resulting eigenfrequencies and eigenmodes are compared with those of the full model by means of the MAC and the COMAC correlation criteria. The main conclusion is that the third method, employing rigid-body modes, constraint modes, inertia-relief modes and free-interface normal modes, significantly increases the accuracy of the reduced model in comparison with the Craig-Bampton method.

The further reduction of the reduced finite element model of the machine tool into a state-space model, which is well-suited for control system design, forms the second step in the proposed procedure. The choice of the modes taken into account in this second reduction again determines the accuracy of the resulting state-space model. The use of some well-chosen static deformation vectors yields, also in this case, an additional improvement compared to the usual approach with only normal modes.

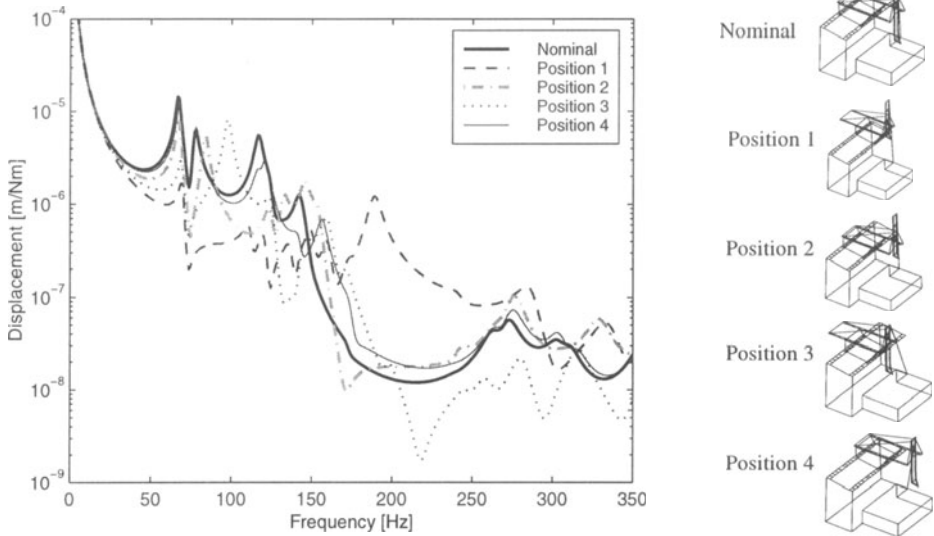


Figure 4 : Transfer function from the X-axis motor torque to the X-displacement of the tool for five different spatial configurations of the machine tool.

Thereafter, a robust motion and vibration control system can be designed by exploiting the knowledge of the changing dynamic behaviour of the machine in different operation positions. Finally, some structural and some control parameters can be optimised in an integrated structure/control design optimisation procedure with respect to some objective function, which adequately describes the desired quality of the resulting machine tool.

References

1. H. Van Brussel, *Mechatronics - A powerful concurrent engineering framework*, *IEEE/ASME Transactions on mechatronics*, **1**, pp. 127-136, 1996.
2. G. Bianchi, F. Paolucci, P. Van den Braembussche and H. Van Brussel, *Toward Virtual engineering in machine tool design*, *Ann. CIRP* **45**, 1996.
3. R.R. Craig, *Structural dynamics - An introduction to computer methods*, John Wiley & Sons, New York, 1981.
4. K. Zhou, J.C. Doyle, and K. Glover, *Robust and optimal control*, Prentice Hall, Englewood Cliffs, New Jersey, 1997.
5. N., *Technical Annex, Brite-Euram II project KERNEL II*, Contract #BE 7423, 1995.
6. W. Heylen, S. Lammens and P. Sas, *Modal analysis : theory and testing*, K.U.Leuven, Belgium, 1995.
7. R.M. Hintz, *Analytical methods in component modal synthesis*, *AIAA J.* **13**, pp.1007-1016, 1975.
8. T. Rose, *Component modal synthesis for coupled dynamic analysis using superelements (using version 68.2 of MSC/Nastran)*, MacNeal-Schwendler Corporation, MSC Internal paper, 1996.

THE KINEMATIC DESIGN OF A 3-DOF HYBRID MANIPULATOR

D. CHABLAT, P. WENGER, J. ANGELES*

Institut de Recherche en Cybernétique de Nantes (IRCyN)

1, Rue de la Noë - BP 92101 - 44321 Nantes Cedex 3 - France

Damien.Chablat@ircyn.ec-nantes.fr

** McGill University,*

817 Sherbrooke Street West, Montreal, Quebec, Canada H3A 2K6

Abstract

This paper focuses on the kinematic properties of a new three-degree-of-freedom hybrid manipulator. This manipulator is obtained by adding in series to a five-bar planar mechanism (similar to the one studied by Bajpai and Roth [1]) a third revolute passing through the line of centers of the two actuated revolute joints of the above linkage (Figures 2 & 3). The resulting architecture is hybrid in that it has both serial and parallel links. Fully-parallel manipulators are known for the existence of particularly undesirable singularities (referred to as parallel singularities) where control is lost [4] and [6]. On the other hand, due to their cantilever type of kinematic arrangement, fully serial manipulators suffer from a lack of stiffness and from relatively large positioning errors. The hybrid manipulator studied is intrinsically stiffer and more accurate. Furthermore, since all actuators are located on the first axis, the inertial effects are considerably reduced. In addition, it is shown that the special kinematic structure of our manipulator has the potential of avoiding parallel singularities by a suitable choice of the « working mode », thus leading to larger workspaces. The influence of the different structural dimensions (e.g. the link lengths) on the kinematic and mechanical properties are analysed in view of the optimal design of such hybrid manipulators.

1. Introduction

It is worth noting that most industrial manipulators have a serial kinematic architecture, that is, their links are arranged serially, resulting in a cantilever type structure. The serial kinematic arrangement of links produces large workspaces but suffers from high positioning errors and poor stiffness. Another well known but far less widespread kinematic architecture is the fully-parallel one for which the output link is connected to the ground through several « legs ». Fully-parallel kinematic architectures are known for their high stiffness and low positioning errors but suffer for relative small workspace. They had been used for a long time in flight simulators and, more recently, in robotic and machine tool applications. The idea of mixing the above two kinds of kinematic arrangement in a single « hybrid » architecture is more recent and still too poorly exploited, despite of the potential benefits which can be gained with such architecture.

This paper focuses on the kinematic properties of a new three-degree-of-freedom hybrid manipulator. This manipulator is obtained by adding in series to a five-bar planar mechanism a third revolute passing through the line of centers of the two actuated revolute joints of the above linkage (Figures 2 & 3). The resulting architecture is hybrid in that it has both serial and parallel links. The hybrid manipulator studied is intrinsically stiffer and more accurate than the classical 3-revolute-jointed 3-DOF fully serial « elbow » manipulator (Figure 1). Furthermore, since all actuators are located on the first

axis, the inertial effects are considerably reduced. In addition, it is shown that the special kinematic structure of our manipulator has the potential of avoiding parallel singularities by a suitable choice of the « working mode », thus leading to larger workspaces.

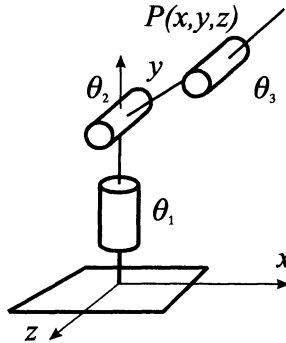


Figure 1. The « elbow » manipulator Robot anthropomorphe

The main kinematic equations of the hybrid manipulator are derived. Two Jacobian matrices appear in the kinematic relations between the joint-rate and the Cartesian-velocity vectors, which are called the « inverse-kinematics » and the « direct-kinematics matrices ». These matrices enable the determination of the serial and parallel singularities, which govern the global behavior of the manipulator and define the topological structure of the workspace in Cartesian and joint spaces. The influence of the different structural dimensions (e.g. the link lengths) on the kinematic and mechanical properties are analyzed in view of the optimal design of such hybrid manipulators.

2. Preliminaries

2.1 A TWO-DOF CLOSED-CHAIN MANIPULATOR

The closed-chain manipulator which constitutes the parallel array of the hybrid manipulator is a five-bar, revolute (R)-coupled linkage, as displayed in figure 2. The actuated joint variables are θ_1 and θ_2 , while the Cartesian variables are the (x, y) coordinates of the revolute center P . To decrease the inertia effects of moving bodies, we place actuated joints of the closed-chain onto pivots A and B . Lengths L_0, L_1, L_2, L_3 , and L_4 define the geometry of this manipulator entirely. However, in this paper we focus on a symmetrical manipulators, with $L_1 = L_3$ and $L_2 = L_4$. The symmetrical architecture of the manipulator at hand is justified for general tasks. In manipulator design, then, one is interested in obtaining values of L_0, L_1 , and L_2 that optimize a given objective function under some prescribed constraints.

2.2 A THREE-DOF HYBRID MANIPULATOR

Now we add one degree of freedom to the manipulator of figure 2. We do this by allowing the overall two-dof manipulator to rotate about line AB by means of a revolute coupling the fixed link of the above manipulator with the base of the new manipulator. We thus obtain the manipulator of figure 3.

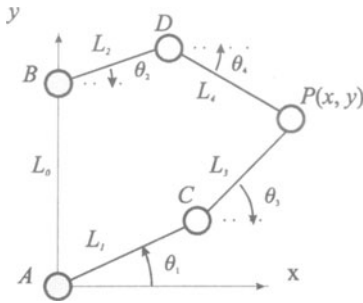


Figure 2. A two-dof closed-chain manipulator

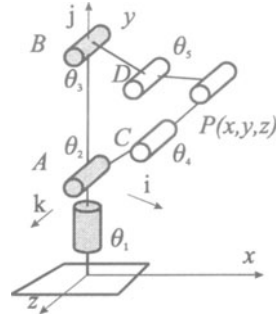


Figure 3. The three-dof hybrid manipulator

2.3 KINEMATIC RELATIONS

The velocity $\dot{\mathbf{p}}$ of point P can be obtained in two different forms, depending on the direction in which the loop is traversed, namely,

$$\dot{\mathbf{p}} = \dot{\mathbf{c}} + (\dot{\theta}_1 \mathbf{j} + \dot{\theta}_4 \mathbf{k}) \times (\mathbf{p} - \mathbf{c}) \quad (1a)$$

and

$$\dot{\mathbf{p}} = \dot{\mathbf{d}} + (\dot{\theta}_1 \mathbf{j} + \dot{\theta}_5 \mathbf{k}) \times (\mathbf{p} - \mathbf{d}) \quad (1b)$$

The equations (1a & b) can be shown to lead to the following 3-dimensional vector equation relating joint and Cartesian velocities [3],

$$\mathbf{A}\dot{\mathbf{p}} = \mathbf{B}\dot{\boldsymbol{\theta}} \quad (2)$$

where

$$\mathbf{A} \equiv \begin{bmatrix} L_2 \mathbf{k}^T \\ (\mathbf{p} - \mathbf{c})^T \\ (\mathbf{p} - \mathbf{d})^T \end{bmatrix} \quad (3)$$

$$\mathbf{B} \equiv L_1 L_2 \begin{bmatrix} \sin(\theta_2) + \lambda_1 \sin(\theta_4) & 0 & 0 \\ 0 & \sin(\theta_2 - \theta_4) & 0 \\ 0 & 0 & \sin(\theta_3 - \theta_5) \end{bmatrix} \quad (4)$$

with λ_1 defined as $\lambda_1 \equiv L_2 / L_1$, while vectors $\dot{\boldsymbol{\theta}}$ and $\dot{\mathbf{p}}$ are given by

$$\dot{\boldsymbol{\theta}} = [\dot{\theta}_1; \dot{\theta}_2; \dot{\theta}_3]^T, \quad \dot{\mathbf{p}} = [\dot{x}; \dot{y}; \dot{z}]^T \quad (5)$$

2.4 THE WORKING MODE

The manipulator under study has a diagonal inverse-kinematics matrix \mathbf{B} , as shown in eq. (4), the vanishing of one of its diagonal entries thus indicating the occurrence of a *serial singularity*. The set of manipulator postures free of this kind of singularity is termed a *working mode*. The different working modes are thus separated by a serial singularity, with a set of postures in different working modes corresponding to an inverse kinematic solution. The formal definition of the working mode is detailed in [2]. For the manipulator at hand, the closed chain admits eight working modes, four of which are

depicted in figure 4, the remaining four being the mirror image of the first ones about line *AB*.

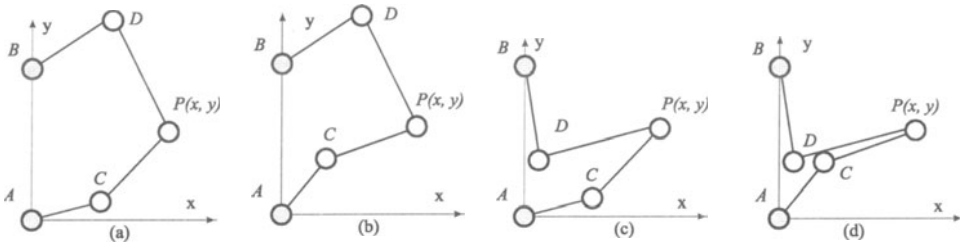


Figure 4. The four working modes

2.5 THE PARALLEL SINGULARITIES

Parallel singularities occur when the determinant of the direct kinematics matrix **A** vanishes, the corresponding singular configurations occurring inside the workspace. They are particularly undesirable because the manipulator can not resist efforts in some direction(s). To interpret these singularities, we calculate $\mathbf{A} \mathbf{A}^T$:

$$\mathbf{A} \mathbf{A}^T \equiv L_2^2 \begin{bmatrix} 1 & 0 & 0 \\ 0 & 1 & \cos(\theta_4 - \theta_5) \\ 0 & \cos(\theta_4 - \theta_5) & 1 \end{bmatrix} \quad (6)$$

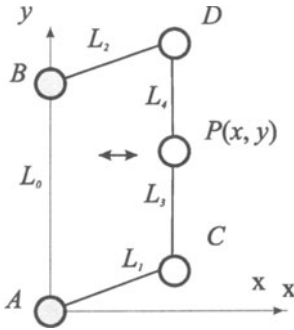


Figure 5. Parallel singularity

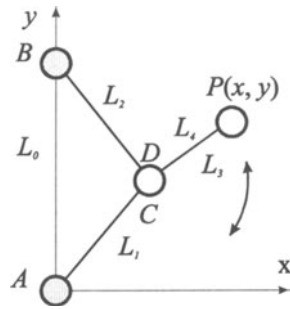


Figure 6. Parallel singularity

whence it is apparent that these singularities occur whenever $\theta_4 - \theta_5 = k (\pi / 2)$, for an integer *k*, i.e., when the points *C*, *D* and *P* are aligned. In such configurations, the manipulator can not resist an effort in the orthogonal direction of *DC* (Figure 5). Besides, when the points *C* and *D* coincide, the position of *P* is no longer controllable since *P* can rotate freely around *D* even if the actuated joints are locked (Figure 6). It will be shown in § 3.2 and § 3.3 that parallel singularities can be avoided either by design or by path-planning.

2.6 THE SERIAL SINGULARITIES

Serial singularities occur when the determinant of the inverse kinematics matrix **B** vanishes. When the manipulator is in such a singularity there exists a direction along which no Cartesian velocity can be produced (Figure 7). Such singularities are reached at



the boundary of the workspace when BD and DP or AC and CP are aligned. They cannot be avoided.

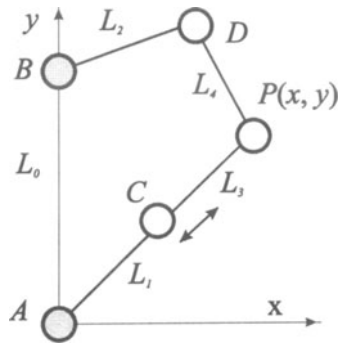


Figure 7. Serial singularity

3. Kinematic analysis and design

3.1 WORKSPACE

A possible design of the manipulator at hand is obtained upon maximizing its workspace volume, which is given by the intersection of two hollow spheres, where radii are $L_1 + L_2$ and $L_1 - L_2$, the distance between the centers of these spheres being L_0 . Therefore, the workspace is maximum when L_0 is equal to 0 and, by extrapolating the results from [7], when L_1 is equal to L_2 . A cross section of the workspace of such an optimized manipulator is displayed in both Cartesian and joint spaces in figures 8 and 9.

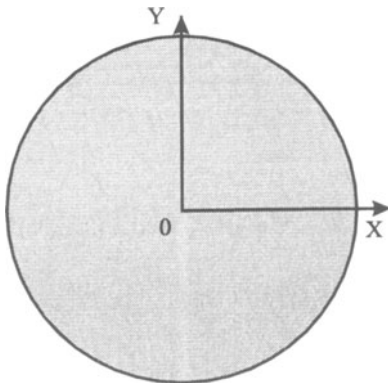


Figure 8. A cross section of the Cartesian workspace for $L_0 = 0$

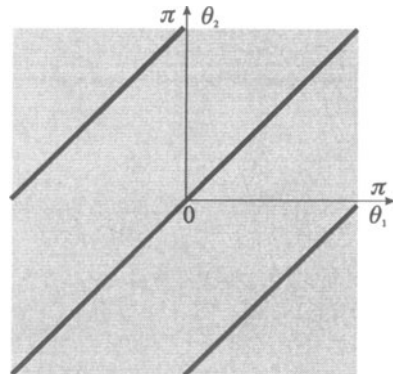


Figure 9. A cross section of the joint space

We notice that the optimum manipulator has only two operative working mode because the other two working modes lie in parallel singular configurations (see figures 4 b & c when $L_0 = 0$ and $L_1 = L_2$). Thus, all singularities of this mechanism lie at the border of the workspace.

3.2 AVOIDING PARALLEL SINGULARITIES BY PROPER DESIGN

We choose lengths allowing to avoid this configurations for which points C and D coincide. If the sum of lengths $L_1 + L_1$ is greater than the distance between the two pivots A and B , i.e. L_0 , we eliminate a parallel singularity type. In the same way, we can eliminate all parallel singularities if the condition below is imposed:

$$2L_2 - 2L_1 > L_0$$

In using this property, the mechanism has no parallel singularity (Figures 10 & 11).

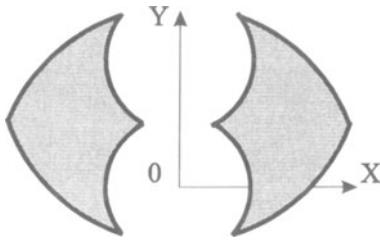


Figure 10. Cross-section of the workspace free of parallel singularities

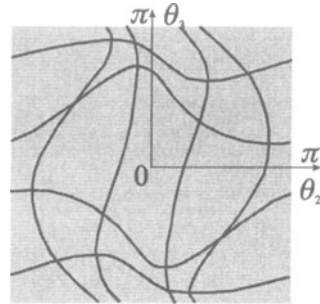


Figure 11. Cross-section of the joint space free of parallel singularities

3.3 AVOIDING PARALLEL SINGULARITIES BY A CHANGE OF WORKING MODE

According to the working mode chosen, the parallel-singularity posture changes inside the workspace, as displayed in figure 12.

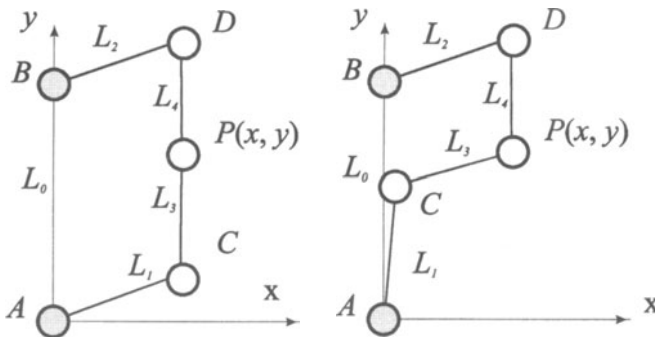


Figure 12. Working mode and parallel singularity

In the «convex working mode» (Figure 12 left), the manipulator is in parallel singularity, while it is in a regular configuration in the non-convex working mode (Figure 12 right). Also, to execute operations in a highly constrained environment, it can be desirable to change working mode. It is possible, by means of a change of working mode, to reach points inside the two workspace sections displayed in figures 13 and 14. To change working mode, it is necessary to pass through a serial singularity, located at the boundary of the Cartesian workspace. By doing so, we can reach a workspace that is twice as large as each of those displayed in figures 13 and 14. In fact, parallel singularities not being avoidable, the workspace of a parallel manipulator is always smaller than that of its serial counterpart of the same size. Also, according to the working

mode, the condition numbers of the direct- and the inverse-kinematics matrices are different. Thus, according to the task to execute, requiring either a precise motion or a fast motion, we can choose one suitable working mode.

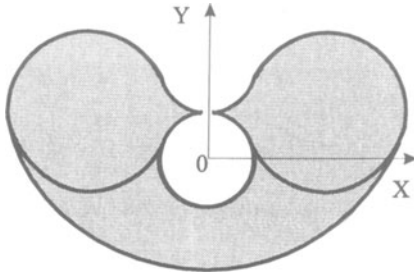


Figure 13. Workspace of the convex working mode

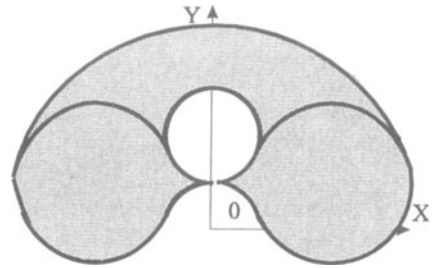


Figure 14. Workspace of the nonconvex working mode

3.4 THE ISOCONDITIONING CURVES

Another interesting design criteria is the isoconditioning curves in the workspace ([5] and [3]).

We derive below the loci of equal condition number of the direct-kinematics matrices. To do this, we first recall the definition of *condition number* of an $m \times n$ matrix \mathbf{M} , with $m \leq n$, $\kappa(\mathbf{M})$. This number can be defined in various ways; for our purposes, we define $\kappa(\mathbf{M})$ as the ratio of the largest, σ_1 , to the smallest σ_s , singular values of \mathbf{M} , namely,

$$\kappa(\mathbf{M}) = \frac{\sigma_1}{\sigma_s} \quad (7)$$

The singular values $\{\sigma_k\}_1^m$ of matrix \mathbf{M} are defined, in turn, as the square roots of the nonnegative eigenvalues of the positive-semidefinite $m \times m$ matrix $\mathbf{M} \mathbf{M}^T$. The eigenvalues of the matrix $\mathbf{A} \mathbf{A}^T$ (6) are, $\alpha_1 = 1 - |\cos(\theta_4 - \theta_5)|$, $\alpha_2 = 1$, and $\alpha_3 = 1 + |\cos(\theta_4 - \theta_5)|$ [3], the foregoing eigenvalues having been ordered as

$$\alpha_1 \leq \alpha_2 \leq \alpha_3$$

The condition number of matrix \mathbf{A} is thus

$$\kappa(\mathbf{A}) = \frac{1}{|\tan((\theta_4 - \theta_5) / 2)|} \quad (8)$$

These loci are, in fact, surfaces of revolution generated by the isoconditioning curves of the 2-dof manipulator, when these are rotated about the axis of the first revolute.

In light of expression (8) for the condition number of the Jacobian matrix \mathbf{A} , it is apparent that $\kappa(\mathbf{A})$ attains its minimum of 1 when $|\theta_3 - \theta_4| = \pi / 2$, the equality being understood *modulo* π . At the other end of the spectrum, $\kappa(\mathbf{A})$ tends to infinity when $\theta_3 - \theta_4 = k\pi$, for $k = 1, 2, \dots$. When matrix \mathbf{A} attains a condition number of unity, it is termed *isotropic*, its inversion being performed without any roundoff-error amplification. Manipulator postures for which condition $\theta_3 - \theta_4 = \pi / 2$ holds are thus the most accurate for purposes of the direct kinematics of the manipulator. Correspondingly, the locus of points whereby matrix \mathbf{A} is isotropic is called the *isotropy locus* in the Cartesian workspace.

On the other hand, manipulator postures whereby $\theta_3 - \theta_4 = k\pi$ denote a singular matrix \mathbf{A} , and hence, define the boundary of the Cartesian workspace of the manipulator. Such singularities occur at the boundary of the Cartesian workspace of the manipulator, and hence, the locus of P whereby these singularities occur, namely, the *singularity locus* in the Cartesian space, defines this boundary.

Interestingly, isotropy can be obtained regardless of the dimensions of the manipulator, as long as *i)* it is symmetric and *ii)* $L_2 \neq 0$. For the two working modes, the position of the isotropic configurations are different (Figure 15).

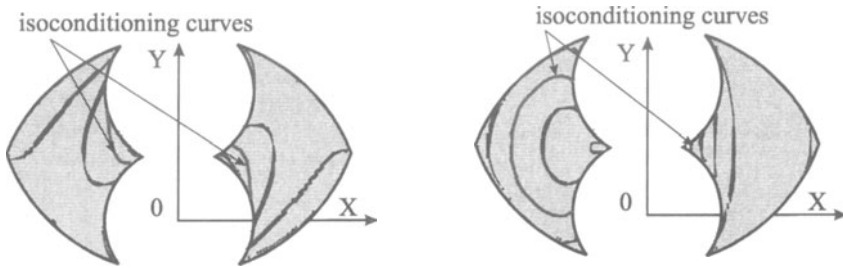


Figure 15. Isoconditioning curves for two working modes

The isoconditioning curves are, by definition, the sets of points which are at equal distance from the singularities and, in turn, can be used as a criterion for designing and/or placing the manipulator in such a way that the working trajectories be in a region of the workspace where a minimum stiffness is guaranteed.

4. Conclusions

We have defined a novel architecture of hybrid manipulators and produced design and path-planning guidelines for the implementation of these manipulators. Two Jacobian matrices were identified in the mapping of joint rates into Cartesian velocities, namely, the direct-kinematics and the inverse-kinematics matrices.

The hybrid manipulators studied were optimized for maximum Cartesian workspace volume and iso-conditioning. Further research work is being conducted by the authors on such hybrid manipulators with regard to their optimal design.

5. Acknowledgments

The third author acknowledges the support from the Natural Sciences and Engineering Research Council, of Canada, the Fonds pour la formation de chercheurs et l'aide à la recherche, of Quebec, and École Centrale de Nantes (ECN). The research reported here was conducted during a sojourn that this author spent at ECN's Institut de Recherche en Cybernétique de Nantes.

References

- [1] Bajpai A., Roth B. : Workspace and mobility of a closed-loop manipulator, *The International Journal of Robotics Research*, Vol. 5, No. 2, 1986.
- [2] Chablat D., Wenger Ph. : Domaines d'unicité des manipulateurs parallèles : Cas général, *IRCyN Internal Report*, No. 97.7, École Centrale de Nantes, Nantes, 1997.
- [3] Chablat D., Wenger Ph., Angeles J. : The isoconditioning Loci of A Class of Closed-Chain Manipulators, *Proc. IEEE International Conference of Robotic and Automation*, pp. 1970-1976, Mai 1998.
- [4] Gosselin C., Angeles J. : Singularity analysis of closed-loop kinematic chains, *Proc. IEEE Transactions On Robotics And Automation*, Vol. 6, No. 3, June 1990.
- [5] Gosselin C. : Stiffness Mapping for Parallel Manipulators, *Proc. IEEE Transactions On Robotics And Automation*, Vol. 6, No. 3, June 1990.
- [6] Merlet J-P. : Les robots parallèles, HERMES, seconde édition, Paris, 1997.
- [7] Paden B., Sastry S. : Optimum kinematic design of 6R manipulators, *The International Journal of Robotic Research*, Vol. 7, 1988, No. 2, pp. 43-61.

Chapter 1

GEOMETRIC SYNTHESIS OF MANIPULATORS UNDER KINEMATIC CONSTRAINTS

S. Guerry, F. B. Ouezdou, S. Régnier

Laboratoire de Robotique de Paris, CNRS-UPMC-UVSQ.

10-12 Avenue de l'Europe, 78140 Vélizy, France.

guerry@robot.uvsq.fr

Abstract In this paper the improvement of a preliminary design process based on an iterative and interactive synthesis procedure is proposed. The problem deals with the determination of dimensional parameters of a manipulator able to manage a set of elementary geometrical tasks defined by the position and the orientation of the tool frame under kinematic performance constraints. The kinematic constraints (requested velocity at end-effector level) are included as a penalty function. The approach is validated with a planar robot manipulator (i.e. with three revolute joints) where we show that the solution obtained for geometrical synthesis solving problem has to be modified in order to take into account the actuators capabilities with regard to maximum joint velocity.

1. INTRODUCTION

Designing functional, robust and interactive tools to assist preliminary design is a wide and emerging research field, boosted by the increased computer processing power. Such tools may be based on the determination of architectural parameters of a manipulator or a mechanism able to manage a set of given tasks [CHE90], [REG96]. Constraints may be imposed either on joint parameters, or on implicit or explicit functions of these parameters. Solutions of these problems are far from being unique. In a hope to decrease the number of possible solutions, the manipulator is required to fulfill additional performance criteria.

These performances may be of geometrical nature but also of kinematic and dynamic one. Miscellaneous criteria, such as isotropy or dynamic manipulability, were proposed [ANG95], [YOS85]. The aim of the present work is to determine the influence of actuation capabilities of the manipulator on its archi-

ture while respecting kinematic or dynamic constraints. Thus, architectural parameters must be changed in order to allow the manipulator end-effector to reach a set of frames (position and orientation) while achieving kinematic wrenches at these points for a set of given actuators. To solve this problem, Matone et al.[MAT97], consider an approach which consists of performing a geometric synthesis under performance indices. In the proposed approach, we consider that the manipulator end-effector must reach a set of points while respecting a given velocity law, so the desired kinematic wrench appears like a constraint which must be satisfied.

The synthesis process used and the task modeling are detailed in the next section. The objective function allowing a geometric synthesis under kinematic constraint is given in section 3. Finally, results from the synthesis of a planar 3R manipulator able to reach a set of points with the guarantee of end-effector velocity is presented.

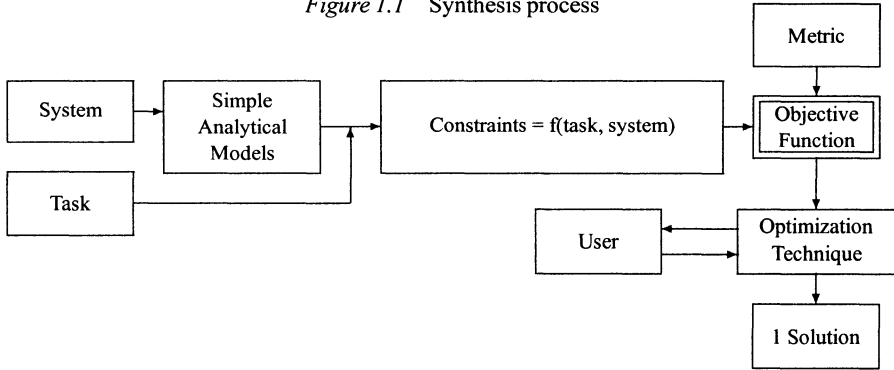
2. SYNTHESIS PROCESS

The synthesis process used is given by figure 1.1 where the first step consists of modeling the task and the robot. The task is defined by a set of k elementary tasks. Each elementary task is defined by a goal frame (position and orientation) to be reached by the end-effector and the kinematic wrench the end-effector must develop. The robot model is built in an analytical way from an elementary model of each of its parts (body, joints, actuators, . . .). This modular approach enables us to deal with much realistic modeling of the manipulator such as joint and/or body flexibilities. Manipulator parameterization is based on the modified Denavit-Hartenberg parameters proposed by Khalil and Kleinfinger [KLE86]. This leads to consider $(3*n)$ dimensional parameters and $(k*n)$ joint parameters, where n is the number of joints. Actuators velocity characteristics are also considered to be known and are added to the robot model. Requested kinematic constraints are expressed as a penalty function built from the robot and task models.

A metric (i.e. Frobenius norm or biquaternions decomposition [ETZ96]) should be used to measure the distance between the current solution performances and the desired performances. This metric has to deal with a combination of linear and angular quantities. Thus, homogeneous and comparable measures based on dimensionless models have to be carried out [WAM91], [REG96]. Then an objective function including constraints is built based on this metric.

The synthesis process can be viewed as looking for the robot's parameters which minimize the objective function value. Due to the high dimension of the search space and the strong non-linearity of the problem, it is not possible to find an analytical solution in the general case. To overcome this difficulty,

Figure 1.1 Synthesis process



we suggest the use of numerical optimization method. Different optimization techniques were used to solve the geometric synthesis problem, such as genetic algorithms [CHE96], [CHO97] or distributed method [REG96]. The selected method is based on a simulated annealing algorithm [SCH95]. It is a probabilistic heuristic technique able to statistically find a global optimum, while being fast enough for a high dimension search space [LES98].

The problem addressed in this work is to carry out the synthesis of a manipulator able to reach a set of points while providing a given end-effector velocity. So, the synthesis takes into account *geometric and kinematic* characteristics.

3. OBJECTIVE FUNCTION

Let \mathcal{S} be the set of dimensional parameters, \mathcal{Q} be the set of joints parameters, and $\mathcal{X} = \mathcal{S} \times \mathcal{Q}^k$ the set of design parameters. The objective function taking into account geometric and kinematic constraints has the following expression:

$$F_o(x) = F_{geo}(x) + P_{kin}(x) \quad (1.1)$$

where $x \in \mathcal{X}$ is the vector of unknown variables, $F_{geo}(x)$ is built from geometric constraints and $P_{kin}(x)$ is a penalty built from kinematic constraints. As a task is a set of k elementary tasks in position, orientation and velocity, the objective function $F_{geo}(x)$ and the penalty $P_{kin}(x)$ are written as a sum of distances and elementary penalties.

3.1 GEOMETRICAL PART

The function $F_{geo}(x)$ dealing with geometric constraints is defined by:

$$F_{geo}(x) = \sum_{j=1}^k d(T_0^{eff}(x), T_0^h) \quad (1.2)$$

where d is a distance based on the chosen metric, $T_0^{effj}(x)$ is an homogeneous matrix which binds the end-effector position and orientation to a reference frame, T_0^hj is an homogeneous matrix which describes the j -th elementary task goal frame (position and orientation) with respect to the reference frame.

The previous homogeneous matrices $T_0^{effj}(x)$ and T_0^hj can be expressed as following:

$$T_0^{effj}(x) = \begin{pmatrix} R_1 & | & U_1 \\ 0 & | & 1 \end{pmatrix} \quad et \quad T_0^hj = \begin{pmatrix} R_2 & | & U_2 \\ 0 & | & 1 \end{pmatrix} \quad (1.3)$$

where R_1 and R_2 are 3×3 rotation matrix and U_1 and U_2 are the end-effector and goal frame origin. Distance d is defined by using a manipulator characteristic length L as defined by Wampler et al. [WAM91] in order to get dimensionless elements.

Frobenius norm leads to the following distance expression:

$$d(T_0^{effj}(x), T_0^hj) = \sum_{k=1}^3 \sum_{l=1}^3 (R_{2,kl} - R_{1,kl})^2 + \frac{1}{L^2} \sum_{l=1}^3 (U_{2,l} - U_{1,l})^2 \quad (1.4)$$

where $R_{i,kl}$ is the (k, l) -th element of matrix R_i and $U_{i,l}$ the l -th element of vector U_i .

3.2 KINEMATIC PART

Kinematic constraints are determined from the end-effector velocity $\dot{X}^j = [V^j, \Omega^j]^t$ which is imposed for each elementary task. Linear (V^j) and angular (Ω^j) velocities are written as:

$$V^j = [V_1^j, V_2^j, V_3^j]^t \quad \Omega^j = [V_4^j, V_5^j, V_6^j]^t \quad (1.5)$$

where V_i^j , ($i = 1, 2, 3$) is the desired linear velocity of the origin of the tool frame and V_i^j , ($i = 4, 5, 6$) is its desired angular velocity.

Kinematic penalty is then written as:

$$P_{kin}(x) = \sum_{j=1}^k P_{kin}^j(x) \quad (1.6)$$

where $P_{kin}^j(x)$ is the elementary kinematic penalty. In this approach, the kinematic constraint is satisfied if the maximal possible end-effector velocity is greater or equal to the desired velocity. Otherwise, the penalty should be

proportional to the difference between the desired velocity and the obtained one.

The maximum possible end-effector velocity for the j -th task \dot{X}_{max}^j is determined using the direct kinematic manipulator model. Let $\dot{X}_{max}^j = (V_{1\ max}^j, \dots, V_{6\ max}^j)^t$. Assuming symmetric actuators, $V_{i\ max}^j$ can be defined as:

$$V_{i\ max}^j = \sum_{m=1}^n |J_{im}^j \cdot \dot{q}_m^{max}| \quad 1 < i < 6 \quad (1.7)$$

where J_{im}^j is the (i, m) -th element of the jacobian matrix when the manipulator is in the configuration corresponding to the j -th elementary task, \dot{q}_m^{max} is the maximum velocity of the m -th actuator. Thus, the joint velocity has to verify the following relations:

$$|\dot{q}_m| \leq \dot{q}_m^{max} \quad 1 \leq m \leq n \quad (1.8)$$

The elementary penalty function build from kinematic constraints is defined as follows:

$$P_{kin}^j(x) = \sum_{i=1}^6 \epsilon_i \begin{cases} |V_i^j| - |V_{i\ max}^j| & \text{if } |V_{i\ max}^j| < |V_i^j| \\ 0 & \text{otherwise} \end{cases} \quad (1.9)$$

$$\text{with } \epsilon_i = \begin{cases} \frac{1}{L} & \text{if } (i = 1, 2, 3) \\ 1 & \text{if } (i = 4, 5, 6) \end{cases} .$$

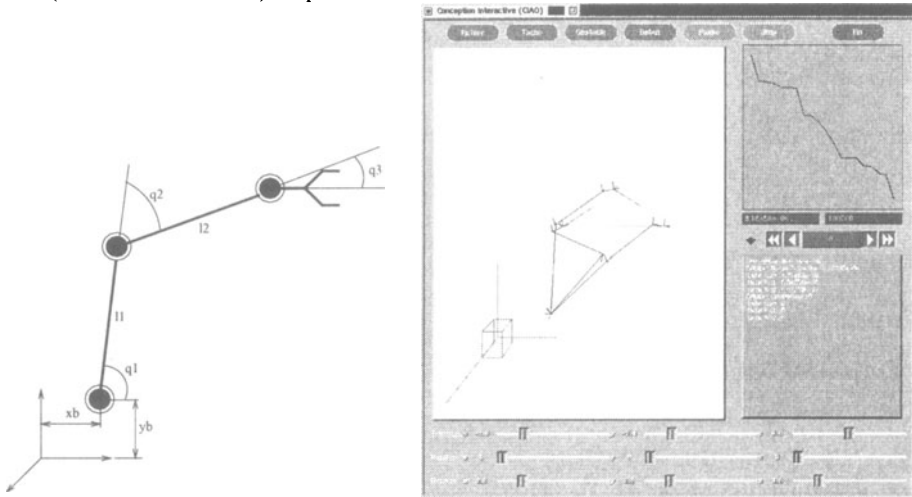
4. OPTIMIZATION TECHNIQUE

The objective function evaluates a given manipulator with respect to the task to accomplish. As it is the sum of distances and penalty functions, the lower the objective function value, the better the manipulator. An optimization technique samples the search space \mathcal{X} and provides a point $x \in \mathcal{X}$ corresponding to a manipulator which has the lowest objective function value.

Even with kinematic constraints, the number of solutions is still huge. Furthermore, the high dimension of the search space leads to long computation time. In order to address these problems, it will be convenient to allow a user interaction with the optimization technique. During the optimization process, the optimization technique provides the user with data about its progress. The user may decide to interrupt it, change some parameters value and resume the search. As the user has better knowledge of the domain, he may orient the search to a particular area of the search space parameters.

The optimization technique used in this paper is an Adaptative Simulated Annealing algorithm based on the bounce of a "ball" on a surface represented by the cost-function. A parameter, named temperature T , controls how far

Figure 1.2 Studied manipulator and ICADM: Interactive Computer Aided Design of Manipulators (home made software) snapshot



the ball bounces from its previous point. As the annealing-time k progress, T decreases, so the ball tends to go to the lowest point. In order to avoid local minima, T is periodically raised according to a some probabilistic function. Further details can be found in [LES89] and [LES98].

5. RESULTS

The proposed approach has been validated for the 3R planar manipulator shown in figure (1.2).

We need to find the limb length l_1, l_2 , the base position (x_b, y_b) with respect to the reference frame, and the joints parameters (q_1, q_2, q_3) for each of the three elementary tasks (T_0^1, T_0^2, T_0^3) defined on table (1.1). At each point T_0^j , the manipulator should be able to provide the end-effector kinematic wrenches given by table (1.2).

In order to emphasize the influence of kinematic constraints, the first stage consists in a geometrical synthesis with the objective function limited to the only term $F_{geo}(x)$. Initial variables values are: $x_b = y_b = 0.0$, $l_1 = l_2 = 1.0$, $q_1 = q_2 = q_3 = 0.0$ for all elementary tasks. The solution of this synthesis is used as an initial guess for a second synthesis process which considers geometrical and kinematic constraints. In both cases, parameters x_b and y_b are restricted to the interval $[0, 1]$, lengths l_1 and l_2 to the interval $[0.5, 2.0]$, all angles to the interval $[-\pi, \pi]$ and the maximum actuators velocities are $0.6rd/s$.

Table 1.1 Geometrical description of tasks

$${}^1T_0^h = \begin{bmatrix} 0.984808 & -0.173648 & 0 & 2 \\ 0.173648 & 0.984808 & 0 & 2 \\ 0 & 0 & 1 & 0 \\ 0 & 0 & 0 & 1 \end{bmatrix} \quad {}^2T_0^h = \begin{bmatrix} 0.996195 & 0.0871557 & 0 & 2.86603 \\ -0.0871557 & 0.996195 & 0 & 1.5 \\ 0 & 0 & 1 & 0 \\ 0 & 0 & 0 & 1 \end{bmatrix} \\
 {}^3T_0^h = \begin{bmatrix} 0.939693 & -0.34202 & 0 & 1.13397 \\ 0.34202 & 0.939693 & 0 & 1.5 \\ 0 & 0 & 1 & 0 \\ 0 & 0 & 0 & 1 \end{bmatrix}$$

Table 1.2 Required end-effector kinematic wrenches

$$V^1 = [0.5, -0.25, 0, 0, 0, 0]^t \quad V^2 = [-1, 0, 0, 0, 0, 0]^t \quad V^3 = [0.5, 0.25, 0, 0, 0, 0.6]^t$$

Results are given on tables (1.3) and (1.4). The first solution allows to reach the geometrical part of each elementary task, but the kinematic part is not satisfied because of the low maximum actuators velocity. The second solution solves this problem by modifying the dimensional parameters. As the actuators remain unchanged, the only way is to increase the limb lengths in order to increase the end-effector linear velocity. The dimensional parameters changes imply a changes in the base position and joint parameters.

Table 1.3 Structural parameters

parameters	x_b	y_b	l_1	l_2
geometrical synth.	1.00	0.77	1.04	0.80
kinematic constraints	0.91	0.32	1.21	0.92

Table 1.4 Joint parameters (in degrees)

		Geometrical synthesis	Kinematic constraints
task 1	q_1	88.46	86.14
	q_2	-76.92	-57.56
	q_3	-1.53	-18.57
task 2	q_1	26.94	36.44
	q_2	-6.35	-4.74
	q_3	-25.60	-36.71
task 3	q_1	44.39	41.94
	q_2	140.13	118.69
	q_3	164.68	-140.78

6. CONCLUSION

A process performing a geometric synthesis under kinematic constraints was defined allowing us to determine the dimensional parameters of a serial

manipulator able to move its end-effector at a desired velocity, with given actuators. The kinematic constraint formulation allows us to carry out an actuator sizing procedure in an easy manner. Indeed, in this case, one need to find the manipulator able to reach a set of frames with a given velocity while minimizing at the same time the maximum joint velocity. This problem can be addressed by solving the following cost function: $\min \sum_i (\dot{q}_i^{max})^2$.

Futher development of the proposed approach will focus on the involvement of dynamic effects in the system while generating force and movement in order to perform actuator sizing.

References

- [ANG95] F. Ranjbaran, J. Angeles and M. A. Gonzales-Palacios “*The mechanical design of a seven-axes manipulator with kinematic isotropy*” *Journal of Intelligent and Robotic Systems*, 14: 21–41, 1995
- [CHE90] P. Chedmail, “*Synthèse de Robots et de Sites Robotisés modélisation de Robots Souples*”. Thèse d'état, Université de Nantes, Janvier 1990.
- [CHE96] P. Chedmail et E. Ramstein “*Robot mechanism synthesis and genetic algorithm*” *IEEE Conference on Robotics and Automation*, pp 3466–3471, 1996
- [CHO97] O. Chocron and P. Bidaud “*Evolutionary Algorithms in Kinematic Design Of Robotic Systems*”, *International Conference on Intelligent Robots and Systems*, September 7–11, 1997, Grenoble, France, Vol 2, pp 1111–1117
- [ETZ96] K. R. Etzel, J. M. McCarthy. “*A metric for Spatial Displacements using Biquaternions on SO(4)*”. *Proceedings of the 1996 IEEE, International Conference on Robotics and Automation*, Minneapolis, Minnesota, April 1996, pp 3185–3190
- [KLE86] J. F. Kleinfinger, “*Modélisation dynamique de robots à chaines cinématiques simples, arborescente ou fermée en vue de leur commande*”. Thèse de Doctorat, Université de Nantes, Mai 1986.
- [LES89] L. Ingber. “*Very Fast Simulated Re-Annealing*”. *Math. Comput. Modelling*, Vol. 12, pp 967–973, 1989.
- [LES98] Lester Ingber. “*Adaptive Simulated Annealing (ASA)*”. URL <http://www.ingber.com> the 4–15–99. Lester Ingber Research, P.O. Box 857, McLean, VA 22101-0857 USA
- [MAT97] R. Matone et B. Roth, “*The Effects of Actuation Schemes on the Kinematic Performance of Manipulators*”. *Transaction of the ASME, Journal of Mechanical Design*, Vol 119, June 1997, pp. 212–217.
- [PAR93] C. Paredis et P. Khosla, “*Kinematic design of serial link manipulators from task specifications*”. *International Journal of robotics research*, vol 3, n 12, 1993, pp. 274–287.
- [REG96] Stéphane Régnier, “*Une méthodologie distribuée et interactive pour l'aide à la conception de systèmes robotiques*” Thèse Université Pierre et Marie Curie, Juillet 1996.
- [SCH95] L. Schmidt et J. Cagan, “*A computational model for a machine desgin*”. *Research in Engineering Design*, vol 7, 1995. pp. 102–125.
- [WAM86] C. Wampler “*Manipulator inverse kinematic solutions based on vector formulations and damped least-squared methods*” *IEEE Transactions on Systems, Man and Cybernetics*, 16 (1), 1986, pp. 93–101.
- [WAM91] C. W. Wampler and A. P. Morgan “*Solving the 6r inverse position problem usinga generic case solution methodology*” *Journal of Mechanism and Machine Theory*, vol 26, n1, 1991, pp 91–106
- [YOS85] T. Yoshikawa “*Manipulability of robotic mechanisms*” *International Journal of Robotics Research*, Vol 4, n2, 1985, pp 3–9

A COOPERATIVE APPROACH IN MECHANISM DESIGN

Patrick CHEDMAIL*, **Thomas DAMAY*** and **Bernard YANNOU****

**IRCyN/ECN, 1 rue de la Noë, 44321 Nantes, France*

***LPL/ECP, Grande Voie Des Vignes, 92295 ChatenayMalabry, France*

Abstract

In the present paper, we intend to propose special configurations of coupling between distributed agents, to achieve an optimal dimensional synthesis of a fourbar mechanism. As any conventional optimisation problem, this one often fails in local minima because of its nine variables characterisation. A distribution (Bond et al, 1988), (Ferber, 1995), (Garro et al, 1995), (Sichman et al, 1992) of the study allows a cooperation between actors (reactive agents as optimisers and constraint agents, or cognitive agents as a designer) working towards different goals, with different criteria. This cooperation leads to a global convergence for a given priority set. Thus our solution is to propose a timebased priority that keeps the independence of the agents. No supervisor agent is introduced. Results show the existence of a set of configurations for the agent priorities, ensuring a good global convergence.

1. Introduction

The purpose of the paper is to propose a new approach in mechanism synthesis by simultaneously integrating designer skills and algorithmic techniques in the designing loop of a mechanism. The design process presents two different aspects:

- description of objects and knowledge representation,
- concurrent (or parallel) actions of different cooperative designers or agents during the design process.

In the present paper, we are focusing on the second point of view. More precisely, we look into the problem of sharing decisionmaking between designers and computer aided design systems. Due to technical considerations, a crucial problem stems from the time scheduling of the different actions, their priorities, their possible integration and their coupling level. In current industrial practice, the interactions are managed by the designer. The question is whether it is possible to formalise and optimise this interaction.

The designer and the artificial decision making systems (i.e. the algorithms) are considered as simple agents that are not able to achieve the design of a mechanism

alone. The hypothesis of such an approach is that a sound cooperative process should be more efficient than any specific design process. This general idea has been already proposed in (Chedmail et al, 1996). It was applied to a conventional path planning problem in robotics. We intend here to demonstrate the validity of this approach in the case of the 4bars mechanism synthesis.

The 4bars mechanism synthesis problem is a basic issue in mechanics. In spite of its apparent simplicity it remains a challenge to define an optimal process for designing such a mechanical system. Different methods have been proposed in the literature (Vasiliu, 1997), (Chedmail, 1997). We propose here a new methodology where different complementary agents simultaneously and independently contribute to the solution improvement with different time priority levels. The performance of the global process is measured with an index. We evaluate the influence of each agent priority on the global performance index.

2. Problem Description

We consider here fourbars planar mechanisms composed of four rotational joints. The four bars are AB, BC, CD and DA of respective lengths L_1 , L_2 , L_3 , L_4 (see fig 1). Their configuration is entirely determined by the crank (bar AB) position. This mechanism may be used as a *path generator*, the path is described with effector point E of coupler bar 2. The objective of a path generator dimensional synthesis is to determine the best intrinsic dimensions of the mechanism and the best positioning of E and of the mechanism in order to superimpose, as much as possible, the desired path and the generated path of the current mechanism solution. An optimisation process has the advantage, compared with an analytical method (Freudenstein et al, 1979), that it can find a satisfactory mechanism even for high degree paths, since a four bar mechanism generates a six degrees paths. Moreover, no complete atlas currently exists which points out precise dimensions for a specific desired path.

A fourbar mechanism is characterised by 9 parameters. We choose a parameterisation which decomposes the global vector X in the mechanism intrinsic shape (the design vector X_{sh}) and its positioning and size (the design vector X_{po}). The intrinsic shape is given for a normalised mechanism with $L_4=100$. The shape is defined by the initial position (before simulation) of the mechanism for which $y_B > 0$. The other parameters are absolute cartesian parameters of points C and E (x_C, y_C, x_E, y_E) may have negative values); the advantage, comparatively to the bar lengths parametrisation, is the ability to give the assembly of the mechanism in the initial position.

During a kinematic simulation, the mechanism can reach a blocking configuration: when bar 1 can (resp. can not) achieve a complete revolution, the mechanism is called a crank (resp. rocker). In the same way, bar 3 (CD) may or may not achieve a complete revolution. Four global behavior modes exist: crankcrank, crankrocker, rockerrocker and rockercrank depending on the complete revolution or not of bar 1 (our crank) and,

respectively, bar 3. A remarkable property of the fourbars mechanism is given by the *Grashov conditions* which fixes the behavior mode only with the bars lengths. In our case, we require the bar 1 to be able to achieve a complete revolution (modes crankcrank or crankrocker). Then, the generated path is a closed curve. The Grashov agent (see 3.1) is in charge of this constraint. It must act as a "repulser" but it does not "reenter" in a straightforward way in the valid design space (where no blocking configuration exists) that allows the simulation to avoid local minima. In brief, we get $X_{sh}=(y_B, x_C, y_C, x_E, y_E)$.

The positioning and size design vector X_{po} characterizes the affine transformations which can be applied to both mechanism and its generated path, i.e. a translation (x_A, y_A), a rotation around point A (α), a zoom centered on point A (z). We will use the property that a mechanism and its generated path are invariant by affine transformations. An artificial tenth parameter would have to be taken into account because of our mechanism positive normalisation ($L4=100$); this is the vertical symmetry Oy noted (s). One can notice that parameter (s) is a discrete parameter which allows us to switch to another mechanism morphology. In short, we get $X_{po}=(x_A, y_A, \alpha, z, s)$.

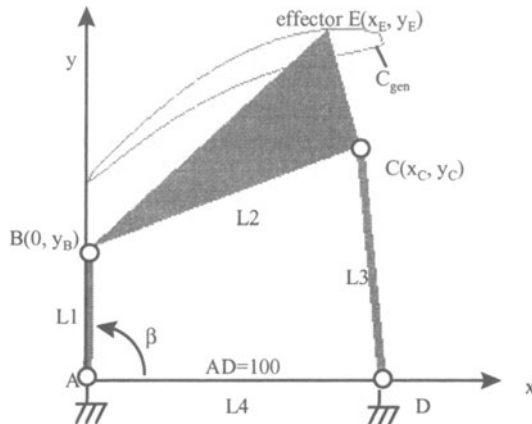


Fig. 1: Parametrisation of the fourbar mechanism (normalised)

3. Decision Maker's Definition

The optimising process is distributed between different actors that are able to modify subvectors of the two design vectors X_{sh} and X_{po} . This allows the integration of the designer, as a particular actor, in the process loop, thanks to virtual reality immersion devices. Actually, the designer has at his disposal the mouse to influence the X_{po} , and the keyboard for the X_{sh} . The proposition is to separate the agents in different groups according to their own abilities (as constraint agents, optimising agents, morphology

agent...). The global objective function is defined by the "distance" between the desired path and the generated path (see 3.2). The amplitude of the iterative actions of the agents is limited. The priority of these actions are managed with a time scaling. All the limitations are consistent from one agent to another. This strategy is described further.

3.1. THE AGENTS

The agents are set as simple as possible. There is no global optimiser, only the collaboration described further generates a global behaviour. They are:

The designer (d): in a first part, its contribution consists in indicating a variation of the X_{po} vector thanks to the mouse direction and different clicks. Only the mouse direction is recorded, whereas the variation X_d is limited to a maximum value. His vision is supposed to be global: the visual feedback of the simulator gives intuitive indications of the X_{po} solution. Another possible type of action of the designer concerns the X_{sh} vector, by acting on the lengths of the bars or the position of effector point E. The agent operating in the distributed process is a simulated designer, who participates with a relatively global proposition. This is to ensure the repeatability and the stability of the processes in order to validate the testability conditions.

The optimiser: as in a conventional optimisation approach, the optimiser proposes to move along the gradient of the distance function (see 3.2) taking into account all the coordinates of X_{sh} and X_{po} . No special penalty exists for an opened curve. It means that the optimiser is not able to "close" the generated path. The predetermined step gradient method has been chosen because of its simple descent direction method. The step is small and constant in order to have a consistency of the actions of the different agents. The pertinence of the agent is strongly local and should be efficiently coupled to the designer's contribution and with constraint agents contributions.

The Grashov actor: is a constraint agent which verifies the Grashov conditions defined with the bar lengths, in order to ensure the complete rotation of bar 1. The objective is to get a closed generated path. Its actions are limited to vector X_{sh} . The Grashov agent allows brief incursions out of the design domain in order to avoid local minima.

The bounding box actor: it intends to give the same perimeters to the bounding boxes of generated and the desired paths. This is not a constraint agent, but its success criterion is different from the distance function one (see 3.2). It should behave as a complementary agent in the cooperation process.

The symmetry agent: the point D is defined on x axis with $x_D > 0$. We intend to cover the whole range of possibilities of morphologies. The symmetry agent is dedicated to check whether or not a symmetrical configuration would lead to a better value of the objective function. Its priority level is lower than the other one considering the strong alteration of the variables. Its participation is not incremental but radical.

The global participation of all actors generates a recovering (see fig. 2) on several design variables on both X_{sh} and X_{po} . The possible conflicts, due to the coupling of the different agents, are controlled with the priority set (see §4).

global variables Agent	X_B	X_C	Y_C	X_E	Y_E	X_A	Y_A	alpha	zoom
Designer	x	x	x	x	x	x	x	x	x
simulated designer						x	x	x	x
Optimiser	x	x	x	x	x	x	x	x	x
"Grashov agent"	x	x	x						
Singularity	x	x	x						
Bounding Boxes						x	x		x
Symmetry		x	x	x	x	x	x	x	

Fig. 2: participation and recovering of the agents on the nine global variables

3.2. THE DISTANCE FUNCTION

To measure the performance of the cooperation of the agents, we give a distance between both paths. This distance is here considered "time independent" (see fig 3): it does not take into account the leading angular variable β for a particular point of the generated path. For each point X_{des} on the desired path, point \hat{X}_{gen} is determined on

the generated path, and: $f_{criterion} = \frac{\sqrt{\sum d^2 (X_{des}, \hat{X}_{gen})}}{\text{step number}}$.

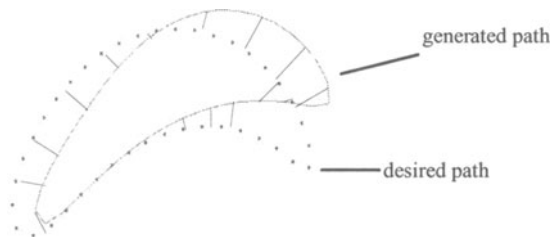


Fig 3: example of construction of a "time independant" criteria function

This is the function used for the gradient method (3.1). A penalty is given for an opened curve to ensure the "crank" state of bar 1 at the end of the cooperation.

4. Cooperation Strategy

The proposition consists in considering the "decision making agents": the designer, the constraints actors (and others ?), working simultaneously, introducing a time sampling for each of their actions (fig. 4) (Chedmail et al, 1996).

In a conventional sequential approach, the designer validates, refuses and modifies the solutions which are proposed by an artificial decision maker. The time samplings t_d and t_a which are attached to the designer, and to the artificial decision maker, are different: $t_a \ll t_d$. Their actions are sequential. In the proposed process of cooperation, the time scaling (fig. 4) is coherent with the priority level permitted to each agent, since their participation is supposed to be geometrically limited.

The question is the conflict management between these agents all along the evolution of the shared variables. The shorter the time base is, the higher the priority is given to an agent. We intend to characterise the best coupling between the different types of agents, in order to achieve the mechanism synthesis with the cooperation of simple agents.

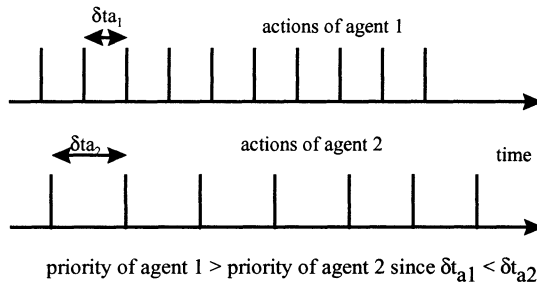


Fig. 4: example of time sampling for shared common variables X

5. Results

The agents have different goals to achieve, with different criteria functions. They work independently, accessing a shared memory. However, the results of their actions are coupled. Moreover, no one of them is able to perform independently the complete optimisation of the whole process. We observe the convergence of their cooperation.

In the following study, the initial conditions for X_{sh} and X_{po} , and the given desired path are shown on fig. 5. The trajectory are discretised with 40 points here.

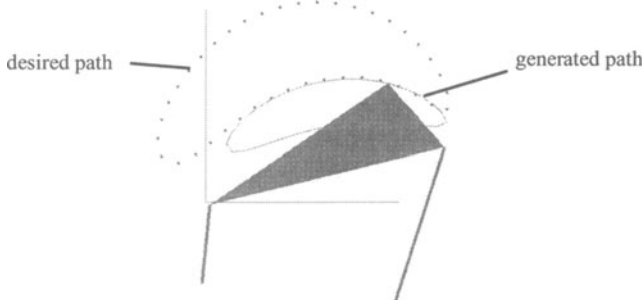


Fig. 5: Initial conditions for the study of the mechanical synthesis

We represent the result of the cooperation of the agents with different surfaces where the performance of the global process is represented as a function of different time scaling rates dt_{aj} .

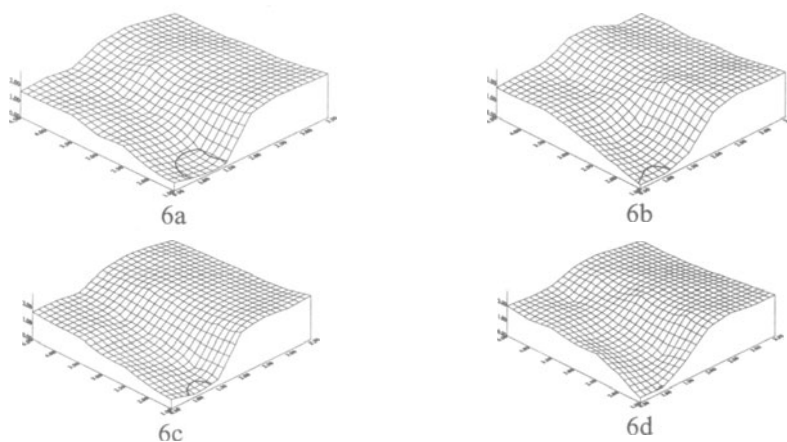


Fig. 6: surfaces representing the global criteria function of the coupling of agents

The performance index of the global process is the distance function between the desired path and the real one at the end of the design process. It is a function of the designer priority, of the optimiser agent priority, of the symmetry agent priority, of the bounding agent priority, with a given time scales for the Grashov agent. The surfaces shown in fig. 6, represent the performance of a coupling where, for each surface, the dt are fixed for the Grashov agent, the Bounding box agent, and the singularity one. The δt of the optimiser and the designer are varying from their minimum (depending on the average CPU time of an iteration), for a given calculation time (800 s). The cases presented are for $\delta t_{\text{BoundingBox}} = 2.0$ s (it is fixed) and:

<u>case a</u> $dt_{\text{Grashov}} = 1.0$ s $dt_{\text{Singularity}} = 1.0$ s	<u>case b</u> $dt_{\text{Grashov}} = 5.0$ s $dt_{\text{Singularity}} = 1.0$ s
<u>case c</u> $dt_{\text{Grashov}} = 1.0$ s $dt_{\text{Singularity}} = 2.0$ s	<u>case d</u> $dt_{\text{Grashov}} = 2.0$ s $dt_{\text{Singularity}} = 2.0$ s

The curve which is represented on the surfaces is the isocriteria at $f=0.3$, which is a rather good performance for the mechanism (it visually satisfies the designer). That is to say that a set of priorities for the δt_{OPT} , and the δt_{DES} is optimal for the problem, and ensures the global convergence of the cooperation. Out of this domain, the organisation fails in local minimum, or the calculation time is not reasonable. This optimal area is (in the case of Fig 5a) included in $\delta t_{\text{OPT}} \in [1.5, 2.1]$, $\delta t_{\text{DES}} \in [0.8, 1.6]$. The consequences are that a lack of priority is unfavourable to the system for the two agents optimiser and

designer ; but a too high priority of the simulated designer is prejudicial to the cooperation as well. One may notice that the set can vary according to the constraint agents priorities.

6. Conclusion

We can conclude with the description and the analysis of such surfaces that the collaboration set in this design process achieves the convergence of the whole process, and that the priority given with time scaling is a factor of success. We proposed an optimized set of priorities for designing a four bars mechanism with given initial conditions and a given desired path.

A more tractable result remains to be established: is it possible to prescribe a priority set independently from initial conditions and desired paths ? Such an answer would bring a new approach for the fourbars mechanism synthesis. This second stage is currently under study. A third stage would be the generalisation to any planar morphology.

7. References

- Bond AH, Gasser L, 1988, "Reading in distributed artificial intelligence", Morgan Kaufmann Publishers Inc, pp. 135.
- Chaudron L, Erceau J and Trousse B (1993): "*Cooperative decisions and actions in multiagent worlds*".
- Chedmail, Damay and Rouchon (1996): "*Integrated design and artificial reality: accessibility and path planning*". Proc ASME Engineering System Design and Analysis, ESDA'96, Vol 8, pp 149156.
- Chedmail, "*Optimization of MultiDOF mechanisms*". In Angeles J. and Woessner H. (Editors): NATO ASI Computational methods in mechanisms, Springer Verlag.
- Ferber J, 1995, "*Les systèmes multiagents : vers une intelligence collective*", InterEdition.
- Freudenstein F., and Maki E.R. (1979): "*The creation of mechanisms according to kinematics structure and function*". Environment and Planning B 6, 375391.
- Garro O, Brissaud D, 1995, "*un modèle distribué de conception*", colloque SMA et IAD.
- Lees B and Jenkins DG, "*Agent oriented support for conceptual, concurrent and collaborative engineering design*", IIA'97, Nîmes, France.
- Ramos C, Oliveira E, "CIARC: *a multiagent community for intelligent assembly robotic systems with real time capabilities*"
- Sichman, Demazeau et Boissier, 1992, "*When can knowledge based systems be called agents ?*", SBIA.
- Vasiliiu A.A (1997): "*Une approche CAO pour la préconception des mécanismes plans générateurs de trajectoire : Realisme*". Doctoral Thesis, Ecole Centrale de Paris, ChâtenayMalabry, February.

STUDY OF COMPLEX TACKLES : LIFTING SYSTEMS WITH PULLEYS AND CABLES

A BILLEREY, P. CLOZEL & D. CONSTANT
*Design Team, Department of Solid Mechanics, Mechanical Engineering,
Civil Engineering
Ecole Centrale de Lyon, BP163, 69131 ECULLY Cedex, FRANCE*

This article presents a study on complex tackles. Classical Cad tools are badly adapted to the study of this type of system. We have tested original tools (DesignView and Mechanical Advantage), to study movements of parcels transported by tackle, the efforts in cables, the amplitude of oscillations of the parcel... Others studies with Mechanical Advantage are also presented. One shows that this style of tools can allow to approach very various problems in phase of preliminary studies.

1. Introduction

This article is based on a study of complex tackles proposed by a Company to students of Ecole Centrale de Lyon (Billerey *et al.*, 1996). A complex tackle results of the utilization of pulleys and cables whose points of fasteners, on the support as well as on the volume to displace (parcel), are determined to obtain some functions :

- reduction of efforts,
- reduction of oscillations,
- mastery of displacement (notably 3D rotation of the parcel),

The number of cables is equal to the number of degrees of freedom that one wants to suppress. For a simple tackle, one cable is used and simply allows to lift the parcel. With six cables, it is possible to insure the small displacement of the parcel following 3 translations and 3 rotations. The amplitude of displacement is limited when the tension in one of the cables is cancelled. When one uses a number less than six of cables, the position of the parcel in the space can be determined by minimizing potential energy of the system, or by studying the static balance of each element of the system. For some tackles, a number greater than six of cables is used for security reasons.

Actually, to design tackles, the construction of physical models is a solution used by many manufacturers and it does not seem to exist others methods. The traditional Cad softwares and their applications dedicated to the study of mechanisms are found maladjusted to process these kinds of problem. Indeed it is necessary to be able :

- to define the length of a cable by adding lengths of the different wires,
- to determine the position of balance of the parcel by minimization of potential energy or by the study of the each wire balance,
- and in a more general way, to determine the position of the fastening points on the parcel and on the support in function of the objectives to reach.

Geometrical and mechanical models of this type of system have been made with the help of variational tools. DesignView (Computervision) and Mechanical Advantage (Cognition) softwares have been tested. These softwares allow to make a model of a problem by 2D sketch and the writing of mathematical equations. It is then possible :

- on a sketch to specify geometrical constraints : parallelism, coincidence from points, fixed length...
- to define the sketch with parameters,
- to write mathematical equations between variables,
- to have the parameters vary, to look for the optimums...
- to plot the evolution of variables.

With these functionality many mechanical engineering problems can be studied. Especially, diagrams can be easily animated and optimized.

A great part of this article is devoted to tackles. The utilization of this type of softwares in an other area of application will be nevertheless presented at the end of this paper, in order to show how interesting are these type of softwares for preliminary studies.

2. Planar tackle

In a first time, the models of different types of tackles have been made in 2D. In this paper, we will talk about a particularly simple 2D tackle, with 2 cables and 3 wires (fig.1).

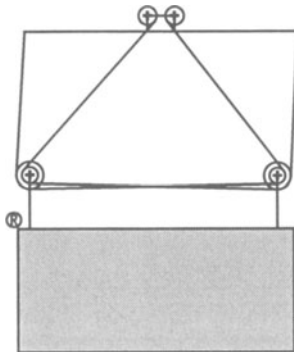


Fig.1 : Tackle composed of 2 cables and 3 wires

In order to simplify the problem, and not to overload calculations of software, pulleys and fasteners will be thereafter modelised with points. These first models allow to obtain a first series of results for planar systems. Two methods have been used :

2.1. DETERMINATION OF THE POSITION OF BALANCE

This tackle is made of two cables. There is a degree of freedom left, for a 2D system. To determine the position of the parcel for fixed cable lengths, it is necessary to study the balance of the system. Two methods have been used:

2.1.1. *Minimization of potential energy*

Mechanical Advantage software has a built in optimization algorithm. It is then possible to determine the angle between the parcel and the horizontal in order to minimize the potential energy of the system. Then, by neglecting the weight of cables, one just has to require a minimum value for the vertical position of the gravity center. This method is very simple to do.

2.1.2. *Study of the balance of elements of the system*

For the writing of the balance of the parcel, one introduces its weight and tensions in cables. Then, by using the principles of the graphical static resolution (fig.2), one graphically defines that the sum of efforts applied on the parcel is null, and that tensions in the wires of one cable are identical. The software then determines automatically the position of balance.

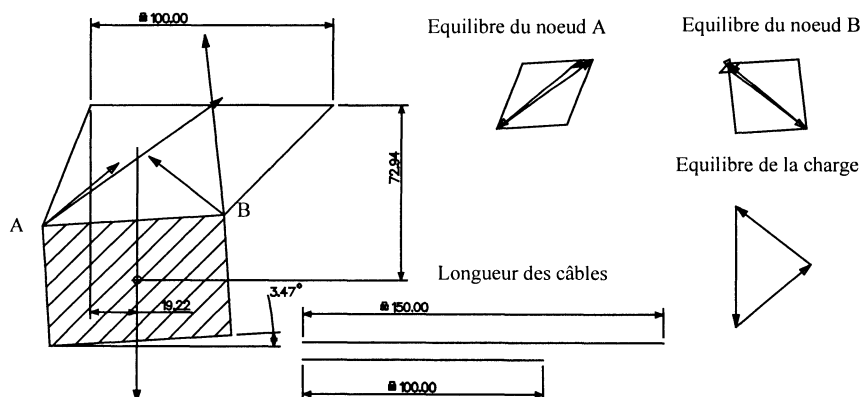


Fig.2 : Position of balance of the parcel for different lengths of the two cables

The second method is a lot better than the first one, because it allows to find rapidly the position of balance of the system after that one has made a variation of a parameter. This avoids, contrarily to the first method, to have to start a new

optimization for each variation of length of a cable. More, this method allows to have the different efforts in cables and therefore to know what are most solicited cables.

2.2. MINIMIZATION OF EFFORTS

The first objective of a tackle is to allow the raising of important parcel by distributing the load on a certain number of cables. More the number of cables and wires will be important, more the maximal load that one will be able to displace will be great, if the loads distribute almost in the same way between the different cables.

After having made the balance of the parcel, one observes that when the lengths of the two cables are identical, they support the same tension. On the other hand, when one makes vary the length of one alone of the two cables, so as to displace the parcel sideways, one observes that the shorter cable supports a more important part of the load. One also notices that for a too important length of the cable 1, the tension gets null, and that limits the lateral displacement of the parcel.

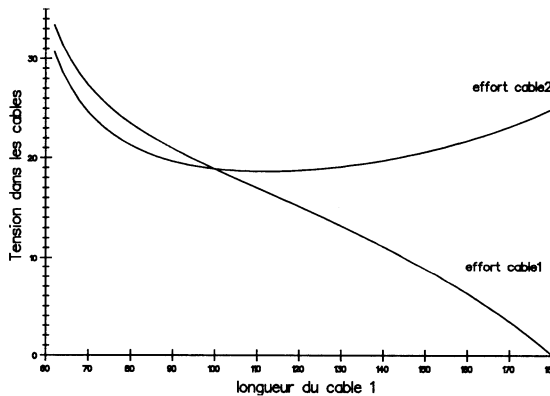


Fig.3 : Tension in cables according to the length of the cable 1

2.3. REDUCTION OF OSCILLATIONS

For safety reasons, a tackle has to minimize oscillations due to a shock on the parcel or to a brutal displacement of the parcel. For this study, we are going to compare the behavior beside oscillations of the proposed 2D tackle to that of a simple tackle. For the 2D tackle, the oscillatory movement is a composition of a translation and a rotation. For the simple tackle, one will only take into account oscillations in translation of the parcel. The method here is to compare potential energy curves of the parcel according to its lateral displacement. The tackle will be more stable if its potential energy curve is more convex (or "closed on itself"). The display of energy potential curves demonstrates that the 2D tackle is better than the simple tackle, as long as oscillations are concerned.

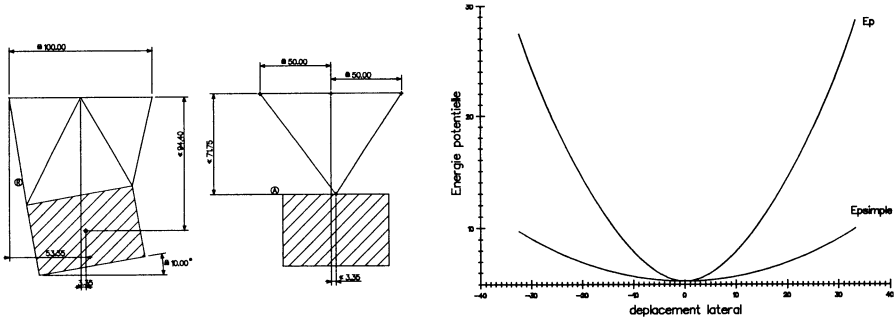


Fig.4 : Comparison of the oscillations between the 2D tackle and a simple tackle

2.4. MASTERY OF DISPLACEMENT

It can be interesting to displace the parcel sideways by acting on one or several cables to have a precise positioning. Thanks to the parametrization of the problem, one can easily modify the position of the fastening points, as to obtain the displacement wished. One observes that for the case of the studied 2D tackle, in order that the parcel could displace sideways without rotation, it is necessary to position points of fasteners of cables as represented (fig. 5). Thus by reducing the length of a cable, the parcel will be able to displace sideways without rotation.

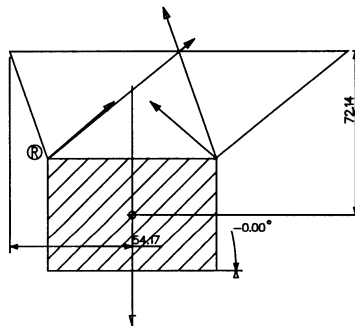


Fig.5 : For a translation in the plan of the parcel

3. 3D tackle

In a second time, the objective was to process totally 3D cases. The problem has been to define a model for a 3D system with a 2D tool, as these softwares just work with 2D problems (Mechanical Advantage also has 3D modeling capabilities, but no real 3D geometrical constraints capabilities). This problem can be bypassed by working with the software as on drawing board (projections in several views...). The method has been to represent the system on at least two views, in order to entirely define 3D position of all elements of the system. It has sometimes been interesting to add views,

and to be redundant, to improve the comprehension of the tackle and the visualization of the movements of the parcel (fig.6).

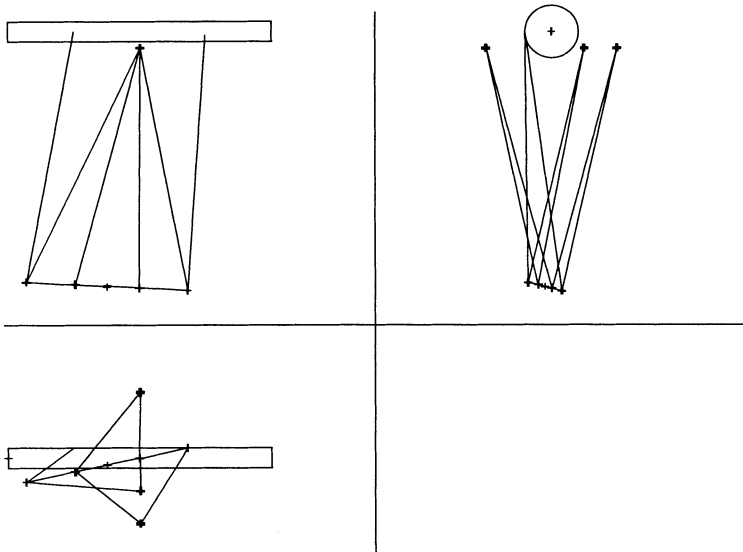


Fig.6 : 3 views model of a 3D tackle made of one cable and 8 wires.

For this model, one has to take into account the constant dimensions of the mobile elements : cables, parcel... It is possible to introduce equations (Pythagore theorem) in order to create new constraints in the drawing, or to treat the problem just graphically (fig.7) where the length of the cable is defined as the sum of the lengths of the wires (each wire length being obtained by the construction of a rectangle triangle with the measures taken on the front and top views of the tackle)

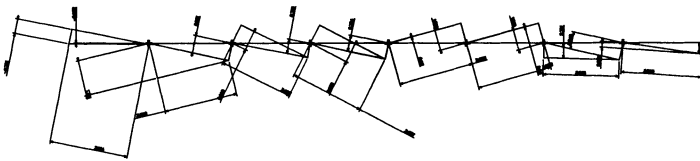


Fig. 7 : Cable unfolded.

But this model is still very complex. In fact, to suppress the remaining degrees of liberties, it would be necessary as for the 2D modelisation, to write the balance of the parcel. For the presented problem, as the parcel still has 5 degrees of freedom, it would be necessary to minimize potential energy according to 5 variables. Mechanical Advantage only supports optimization with 3 variables. On the other hand, it is possible to study the static balance of each element of the system. In 3D that becomes quickly very complicated to define and to manipulate. We have not yet found 3D

variational software, working with geometrical constraints, as 2D Mechanical Advantage or 2D DesignView.

4. Preliminary study of a crane

This example of preliminary study has been built from information from (Cetim, 1996).

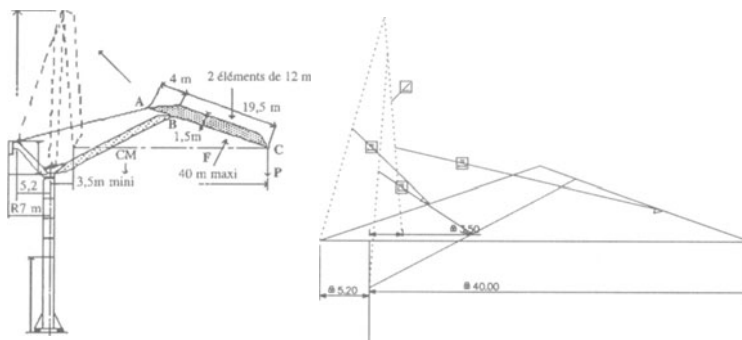


Fig.8 Scissors crane. Model with the software.

It has been possible in a limited time, approximately 12 hours, with persons who never had used previously the software to solve the following problems :

- Determination of the length of each element of the crane in order that the maximal reach is 40 meters, and that for the inferior reaches, the extremity moves almost following a horizontal line. This problem equals to the synthesis of a 4 bars system, which has to better follow a trajectory. The problem can be solved completely graphically (fig.8), in a very simple way without having to use difficult optimization methods as in (Vasiliu *et al.*,1997).
- Determination of the position of the contacts with the ground, of the mass and position of the counterweight in order that the balance of the crane is good for a load between 0 and 3 tons, whatever is the reach between 3,5 and 40 meters.
- Determination of the maximal load, depending on the reach of the crane.
- Mechanical solicitation determination in each element for the maximal admissible load, depending on the reach.

5. Conclusion

Softwares as Mechanical Advantage and DesignView allow to find models for most various mechanical systems, with geometrical 2D constraints, and mathematical equations. Their algorithms for resolution of equations and optimization systems, without being very effective, allow to study many problem types as soon as their is a good model.

For the tackles, without a computer tool, it is difficult to imagine movements of the parcel, to calculate tensions in cables and to understand why, with some tackles, oscillations of the parcel are limited. In a company, designers often use existing solutions, because they know their behavior. With the softwares we have used, it is very fast to study and optimize a 2D tackle. On the other hand, the problem becomes very difficult with 3D tackles. Nevertheless, the use of this type of tools is very interesting, waiting for totally 3D variational software, working with geometrical constraints, or for a specific application to be developed on an existing Cad software.

The crane example also shows that in preliminary study phase, one can define dimensioning parameters for a product according to requirements very quickly. This step is necessary for new Cad systems generations (Constant, 1997) And as we know that savings on the cost of a product depends a lot from the preliminary choices, the use of these tools can be very profitable for a company.

References

- A. Billerey, R. Fillon, D.Bauer, B. Debaud (1996) Modélisations des mouflages complexes à l'aide outils de CAO mécanique, Rapport de projet d'élèves ingénieurs, Ecole Centrale de Lyon (France).
- Centre Technique des Industries Mécaniques (1996) Conception des pièces mécaniques en plastique et composite, CETIM, N°2E16, Senlis (France).
- A. Vasiliu, B. Yannou. (1997) Synthèse dimensionnelle de mécanisme générateurs de trajectoires par reseaux de neurones Actes du 5^{ème} colloque PRIMECA sur la Conception Mécanique Intégrée, La Plagne (France), avril 1997, pp 315-324
- D. Constant. (1997) Elaboration d'un modèle fonctionnel de produits pour une nouvelles générations de systèmes de CMAO, Actes du 5^{ème} colloque PRIMECA sur la Conception Mécanique Intégrée, La Plagne (France), avril 1997, pp 263-269

Computervision 100 Crosby Drive, Bedford, MA 01730 USA
Cognition Corporation 209 Burlington Rd. Bedford MA 01730 USA

APPLICATION OF A FUZZY LOGIC ORDERING METHOD TO PRELIMINARY MECHANISM DESIGN

J.C. FAUROUX, C. SANCHEZ, M. SARTOR, C. MARTINS
*Laboratoire de Génie Mécanique de Toulouse, INSA Toulouse
Complexe scientifique de Rangueil, 31077 TOULOUSE Cedex
Tel : 05.61.55.97.18 Fax : 05.61.55.97.00
E-Mail : [JC.Fauroux | Marc.Sartor]@gmm.insa-tlse.fr*

1. Introduction

Fuzzy logic has experienced a considerable growth in various fields, even if it is still underused in mechanical engineering. However, it seems to be of promising interest in the early stages of design, where qualitative reasoning is mostly performed without taking exact dimensions into account [1]. Our preliminary design system for geared mechanisms already works well using a conventional multi-criterion ordering method. In order to assess the interest and advantages of fuzzy logic in the early design stages, we have integrated it into the above system and improved certain points where the conventional method has proved inadequate.

2. Nature of the problem

Our aim is to improve with fuzzy logic our existing preliminary design system for geared mechanisms [2]. This program provides a list of mechanical solutions which comply with given specifications. It is based on a three-step method (Figure 1) :

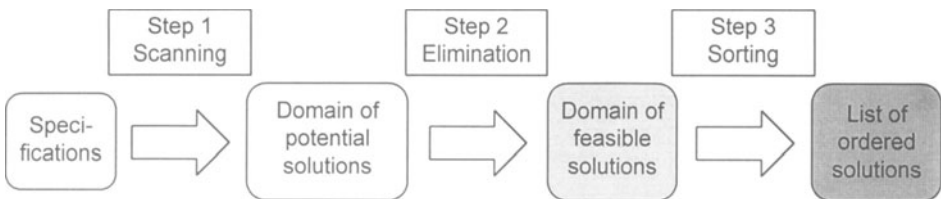


Figure 1. Structure of the preliminary mechanism design program

1. Scanning of the mechanical solution domain ;
2. Elimination of the candidates which do not meet the design rules ;
3. Sorting of the remaining candidates by order of preference.

In this article, we shall concentrate more particularly on step 3. Each of the mechanical solutions is given a mark, which will facilitate subsequent ordering. The following hypotheses are made :

- Each mechanical solution M_i is made up of N_e stages, being elementary mechanisms serially connected and taken from a mechanism database ;
- Each of the elementary mechanisms has previously been given several marks by an expert, according to N_c criteria. The marks are recorded in the database.

The process for calculating the mark for a mechanical solution can be found below (Figure 2) :

- The mark for solution M_i is the mean of the N_e elementary stage marks ;
- Weighing coefficients K_c allow us to adjust the respective influence of criteria.

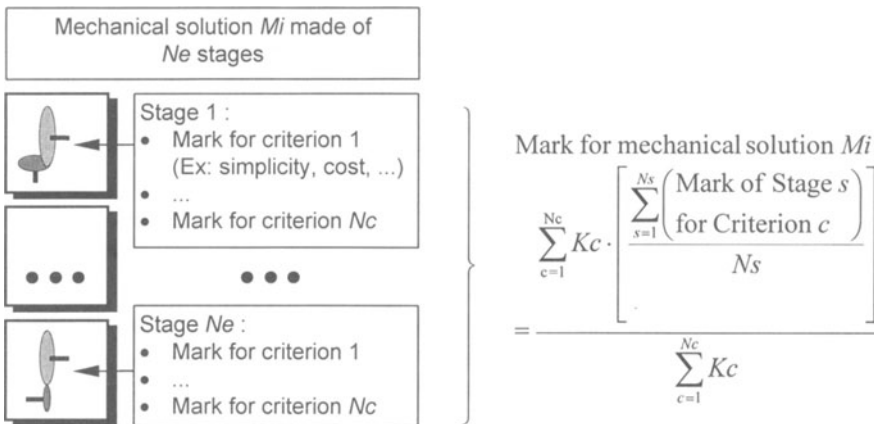


Figure 2. "Conventional" way of obtaining the mark for a mechanical solution M_i

Advantages of this rather conventional multi-criterion process :

- Simplicity (for programmer as well as for user) ;
- Speed of execution ;
- Reliable results confirmed in practice.

Drawbacks :

- Designers generally reason qualitatively with linguistic rather than numerical

variables. They know, for instance, that a cylindrical gear is “less expensive” and “easier to mount” than one which is conical. By using such a method, they give a mark (out of 100 for example) to each elementary mechanism in the database (Table 1).

TABLE 1. Examples of marks given to mechanisms

Nature of criterion	Gear type	
	Cylindrical	Conical
Manufacturing cost (mark out of 100)	50	15
Mounting simplicity (mark out of 100)	50	10

It is difficult to justify every mark “point by point” as the marks are relative rather than absolute. If conical gears are given a mark of 15 instead of 40, it is because several other mechanisms must be inserted between cylindrical and conical gears. Moreover, the spread of these marks must be readjusted each time we add or suppress elementary mechanisms from the database.

- Obviously, the overall mark is a mixture of several quantities which are not of the same nature.

Consequently, these reservations justify our interest in a new type of process based on fuzzy logic [3]. We will try to determine if it is worth using fuzzy logic and what are its strong and weak points in a mechanical context such as ours.

3. Fuzzy algorithm

We now introduce, through a simple example, the fuzzy algorithm which was chosen for comparing two solutions. As soon as the “comparison” notion is defined, it will be easy to implement a “sorting” method for step 3.

3.1. SIMPLE EXAMPLE

Two mechanical solutions, called A and B, each made up of two stages (respectively A1, A2 and B1, B2) and evaluated according to criteria (C1 and C2) must be compared (Table 2).

TABLE 2. Nature of the compound mechanisms to be compared

Criteria	Solution A		Solution B	
	Stage A1	Stage A2	Stage B1	Stage B2
Criterion C1	G	VB	G	M
Criterion C2	VB	B	B	VG

With the following abbreviations :

VB : Very Bad	B : Bad	M : Medium	G : Good	VG : Very Good
---------------	---------	------------	----------	----------------

These initial data are of a qualitative nature and relatively vague. They are expressed in a way similar to the one used by an expert to give his point of view.

In this simple case, five quality classes are used, each one being defined by a triangular shape membership function (Figure 3). Such a distribution between two extremes, with a medium and two intermediate classes will suit small examples like this but might subsequently be refined.

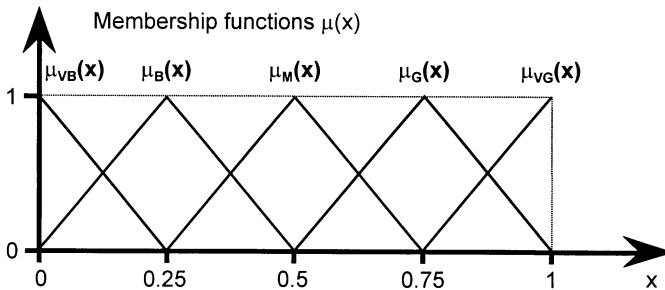


Figure 3. Membership functions of the five quality classes

3.2. COMPARISON PRINCIPLE

Comparison between two solutions A and B is a three-phase process (Figure 4) :

- Firstly, each solution is evaluated according to each criterion ;
- Then solutions are compared criterion by criterion ;
- Finally, all the comparisons are mixed up in a global comparison.

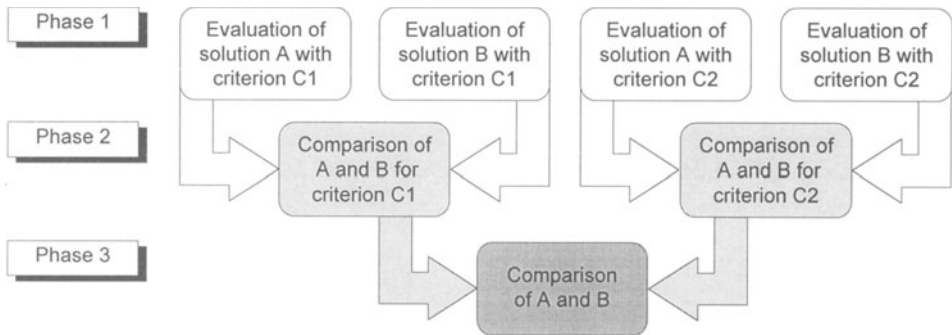


Figure 4. Comparison principle between two solutions A and B

3.3. PHASE 1 : EVALUATING A SOLUTION ACCORDING TO A CRITERION

Let us evaluate, for instance, the quality of the constituent stages of solution A according to criterion C1 (Table 3).

TABLE 3. Evaluation of solution A according to criterion C1

Criteria	Solution A	
	Stage A1	Stage A2
Criterion C1	G	VB

According to the Mamdani method, the barycentre of the areas delimited by the corresponding membership functions has to be calculated (Figure 5).

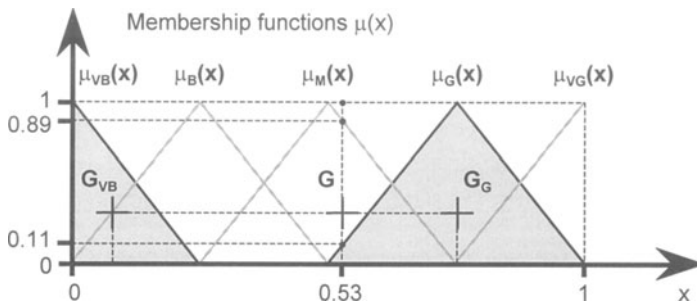


Figure 5. Mamdani barycentre principle

The abscissa of the global barycentre ($x = 0.53$) thus obtained gives the membership degrees of solution A to each of the five quality classes (Table 4).

TABLE 4. Membership degrees of solution A to the 5 quality classes according to C1

VB	B	M	G	VG
0.00	0.00	0.89	0.11	0.00

This calculation is repeated identically for solution B and criterion C2. The corresponding results are shown in Table 5 :

TABLE 5. Membership degrees to the 5 quality classes

Evaluation of :	Value of x	VB	B	M	G	VG
A according to C1	0.53	0.00	0.00	0.89	0.11	0.00
B according to C1	0.63	0.00	0.00	0.50	0.50	0.00
A according to C2	0.19	0.22	0.78	0.00	0.00	0.00
B according to C2	0.47	0.00	0.11	0.89	0.00	0.00

3.4. PHASE 2 : COMPARING SOLUTIONS FOR EACH CRITERION

The problem is now to compare solution B to solution A, knowing their quality degrees according to criterion Ci. The following rules are given :

- **If** (B has the same quality degree as A) **Then** (B is Equivalent to A)
- **If** (B has one more quality degree than A) **Then** (B is Superior to A)
- **If** (B has two or more quality degrees than A) **Then** (B is Very Superior to A)
- ...

These rules are summarized in Table 6, where the five possible degrees of comparison can be seen.

TABLE 6. Comparison of B with A according to criterion Ci

Solution A	Solution B				
	VB	B	M	G	VG
VB	E	S	VS	VS	VS
B	I	E	S	VS	VS
M	VI	I	E	S	VS
G	VI	VI	I	E	S
VG	VI	VI	VI	I	E

With the following abbreviations :

VI : Very Inferior	I : Inferior	E : Equivalent	S : Superior	VS : Very Superior
--------------------	--------------	----------------	--------------	--------------------

A and B may now be compared according to C1. The previous rule :

If (B has the same quality degree as A) **Then** (B is Equivalent to A)

can be reformulated in the following way :

If ((B='VB' **And** A='VB') **Or**
 (B='B' **And** A='B') **Or**
 (B='M' **And** A='M') **Or**
 (B='G' **And** A='G') **Or**
 (B='VG' **And** A='VG')) **Then** (B is Equivalent to A)

The Mamdani definition [4] is then used for the **And** connector :

$$\mu_{P \text{ and } Q}(x, y) = \min (\mu_P(x), \mu_Q(y))$$

This definition is applied and illustrated in Table 7 : the numerical value in each cell is obtained by taking the minimum of the corresponding row and column values.



TABLE 7. Comparison of B with A according to C1 (example)

Solution A (val.)	Solution B (with membership values)				
	VB (0.00)	B (0.00)	M (0.50)	G (0.50)	VG (0.00)
VB (0.00)	E (0.00)	S (0.00)	VS (0.00)	VS (0.00)	VS (0.00)
B (0.00)	I (0.00)	E (0.00)	S (0.00)	VS (0.00)	VS (0.00)
M (0.89)	VI (0.00)	I (0.00)	E (0.50)	S (0.50)	VS (0.00)
G (0.11)	VI (0.00)	VI (0.00)	I (0.11)	E (0.11)	S (0.00)
VG (0.00)	VI (0.00)	VI (0.00)	VI (0.00)	I (0.00)	E (0.00)

Then, the Mamdani definition for the **Or** connector is used :

$$\mu_{P \text{ or } Q}(x, y) = \max(\mu_P(x), \mu_Q(y))$$

Next, Table 8 is constructed in this way : for each comparison degree in Table 7 (grey cell areas), only the maximum value is retained.

TABLE 8. Degrees of comparison of B with A

Criteria :	VI	I	E	S	VS
Criterion C1	0.00	0.11	0.50	0.50	0.00
Criterion C2	0.00	0.00	0.11	0.78	0.22

Thus, for instance, we can see from Table 8 that there is a 50 % probability that B is superior to A according to C1 and 78 % according to C2.

3.5. PHASE 3 : FINAL COMPARISON

Our purpose is now to combine the various comparisons (one per criterion) into a single comparison. We use the following reasoning : “If there is superiority according to C1 and inferiority according to C2 then there is equivalence”. This can be translated into :

If ((C1='S') **And** (C2='I')) **Then** ('E')

Next, we apply the same process as in Step 2 (min operator for Table 9, max operator for Table 10).

TABLE 9. Mixing criteria C1 and C2

Criterion C1 (val.)	Criterion C2 (with membership values)				
	VI (0.00)	I (0.00)	E (0.11)	S (0.78)	VS (0.22)
VI (0.00)	I (0.00)	I (0.00)	I (0.00)	I (0.00)	E (0.00)
I (0.11)	I (0.00)	I (0.00)	I (0.11)	E (0.11)	S (0.11)
E (0.50)	I (0.00)	I (0.00)	E (0.11)	S (0.50)	S (0.22)
S (0.50)	I (0.00)	E (0.00)	S (0.11)	S (0.50)	S (0.22)
VS (0.00)	E (0.00)	S (0.00)	S (0.00)	S (0.00)	S (0.00)

TABLE 10. Final comparison of B with A

I	E	S
0.11	0.11	0.50

Proposition “S” (i.e. $B > A$) seems to be the most plausible because its membership function has the highest value of all. Thus, this result confirms what Table 2 already seemed to suggest.

4. Comparative example

Now, let us compare the conventional ordering method with its fuzzy version. Not wanting to lose the subtleties contained in the expert database, we have chosen to use a seven quality degree representation (instead of five for the example). Of course, this choice leads to a heavier computational load.

For a same set of 1016 mechanical solutions, the ordering time is about three minutes long for the fuzzy algorithm instead of about ten seconds for the conventional method.

As for the quality of the resulting set (that is to say the correct ordering of solutions), it is similar in both cases.

5. Conclusion

Undeniably, fuzzy logic perfectly suits the representation of qualitative information, such as those used in the beginning of a design process. The fuzzy algorithm previously described gives correct results, similar to those obtained with the conventional method. It is more satisfactory for representing expert knowledge and accurately reflects everyday speech or thought. However, these qualities are obtained at the cost of heavier computations.

References

1. THURSTON D.L., CARNAHAN J.V. (1994) Fuzzy ratings and utility analysis in preliminary design evaluation of multiple attributes, *Journal of Mechanical Design* **114**, 648-658.
2. FAUROUX J.C., SARTOR M. (1997) Conception qualitative de mécanismes. Application aux réducteurs à engrenages, *Proceedings of AUM'97*, Poitiers (France), 1^{er}-5 septembre 1997, Vol. 3, pp. 319-322.
3. DUBOIS D., PRADE H. (1994) Ensembles flous et théorie des possibilités : notions de base, *ARAGO 14 - Logique Floue*, Masson (France), ISBN 2-22-584474-7, pp. 29-62.
4. FOULLOY L., TITLI A. (1994) Aspects généraux de la commande floue, *ARAGO 14 - Logique Floue*, Masson (France), ISBN 2-22-584474-7, pp. 64-79.

Chapter 1

RVS: A ROBOT VISUALIZATION SOFTWARE PACKAGE

John Darcovich*, Jorge Angeles**, Pierre Montagnier**, Chu-Jen Wu**

* *CAE Electronics Ltd.*

8585 Cote de Liesse Rd., Saint-Laurent, Quebec, Canada, H4L 4X4

** *Department of Mechanical Engineering & Centre for Intelligent Machines,*

McGill University, Montreal, Quebec, Canada, H3A 2K6

angeles@cim.mcgill.ca

Abstract RVS is a software package that was developed at McGill University's Centre for Intelligent Machines. Its name stands for Robot Visualization System. This package, written in C and platform-independent, combines superb 3-D graphics with a high degree of usability. RVS is a 3-D visual tool whose applications span from virtual prototyping to trajectory-planning in a dynamic environment. The aim of this paper is to introduce the main features of the RVS package. The paper gives an introduction to the windows driven environment on which RVS is built; each of its functionalities is described and illustrated with real-life applications. The paper concludes with a case study of the design of a spherical wrist.

1. INTRODUCTION

Visualization tools have been increasingly used in robotics as they can provide invaluable help to users in design and manufacturing applications. They have been used in many different situations, including designing a robotic manipulator, off-line robot programming, evaluating a workcell layout, or choosing between alternative robot arms for a given manufacturing task.

A number of software packages are commercially available. BYG Systems Ltd. (Nottingham, UK) have developed GRASP, a 3-D graphical simulation tool applicable to general kinematic modelling for design, evaluation, and programming of jointed structures. IGRIP (Interactive

Graphics Robot Instruction Program), developed by Deneb Robotics Inc. (Auburn Hills, USA) is also used for designing, evaluating, and off-line programming robotic workcells. Tecnomatix's (Herzeliya, Israel) ROBCAD is a set of computer-aided production engineering tools for design, simulation, optimization and off-line programming of automated and manual manufacturing systems. CimStation Robotics, a product of SILMA (San Jose, California, USA) can be used to create, simulate and optimize robot programs off-line.

Thanks to its built-in versatility, RVS is equally useful for educational, design and manufacturing purposes. A new robot can be created with minimal input from the user, who is then immediately presented with a 3-D rendering of the manipulator and has access to the full range of RVS features, namely,

- customization of the robot (e.g. joint limits, prestored configurations, end-effectors or payload);
- forward kinematics;
- inverse kinematics;
- trajectory planning and collision avoidance (including moving obstacles).

Each of these features will be described in detail in the sections below.

2. SOFTWARE DESCRIPTION

This section outlines the basics of RVS based on an implementation on *Silicon Graphics Inc.* workstation with OpenGL. RVS can run on other types of platforms, the only required modifications being those related to device-dependent features.

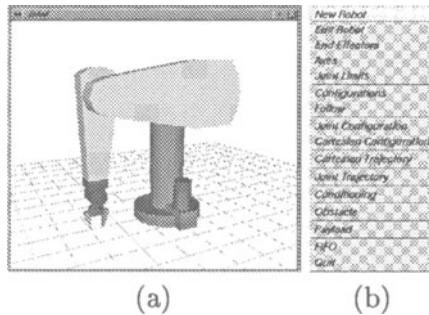


Figure 1: (a) RVS workspace; (b) Pop-up menu.

2.1 STARTING UP RVS

When RVS is executed, a window that contains the workspace with the default robot will appear on the screen (Fig. 1(a)). The workspace is the area of the screen where the robot is displayed and animated. RVS is a window-driven environment. Each of the main commands has its own window (dialog box). Multiple windows can be opened at the same time. The user be able to navigate inside the RVS environment using the mouse.

2.2 DISPLAY FEATURES

The user can rotate and translate the robot as a rigid body as well as zoom in and out by means of the mouse. Pressing on the left mouse button and at the same time dragging the mouse pointer will rotate the object inside the workspace with respect to the viewer. Similarly, pressing the middle mouse button and at the same time dragging the mouse pointer will translate the object. By pressing the left and middle mouse button and at the same time dragging the mouse pointer vertically zooms in and out. All these parameters, in addition to the background features, can equally be set in a pop-up menu.

The base frame as well as the frame attached to each link can also be displayed.

2.3 FUNCTIONS

All RVS commands are grouped in the **Functions** pop-up menu (Fig. 1(b)). To activate the pop-up menu, presses the right mouse button. A menu item is then selected by dragging the mouse pointer over the item and releasing the right mouse button.

2.4 CREATING A NEW ROBOT

Creating a robot simply requires reading its corresponding Denavit-Hartenberg (DH) parameters (Angeles, 1997) from a text file previously created by the user. Immediately and without any further user input, the skeleton of the robot is generated and rendered graphically. In other words, its representation as a chain composed of rigid links and either revolute or prismatic joints, without geometric detail on the physical shape of the links is displayed. If required, the full rendering of the actual robot can also be viewed after programming the detail of the robot-link geometry using graphic primitives from any software library (e.g. OpenGL or Xforms).

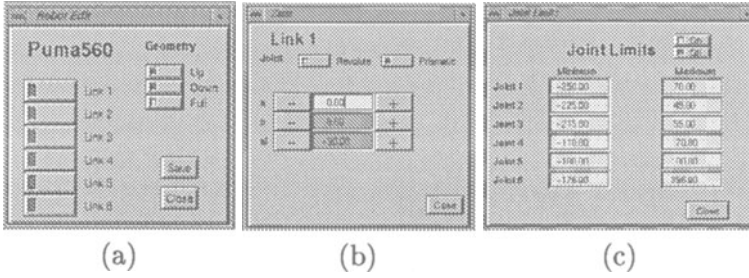


Figure 2: Menus: (a) Edit robot; (b) Edit link; (c) Edit joint limits.

The user can obtain an enhanced model of the robot, for instance, by imposing joint limits or, by selecting a different end-effector (gripper, welding tool, etc.), depending on the intended application. These features can either be directly set in the initial text file, or changed on-line by using the **Edit Robot** command (Fig. 2(a)). Updated architectures can be saved at any time and are integrated to the available robot library.

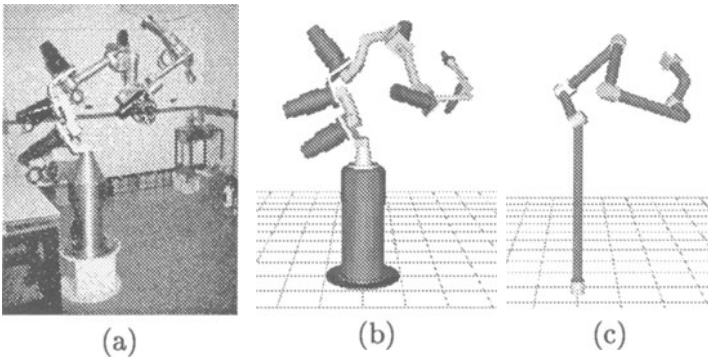


Figure 3: REDIESTRO 1: (a) Real; (b) Full rendering; (c) Skeleton.

One of the main application of RVS is using it as a tool during the early stages of design. A virtual prototype can be constructed without the need to invest in a real prototype, which saves both time and cost. During the mechanical design stage of REDIESTRO 1 and REDIESTRO 2¹, RVS was used to monitor issues such as collisions among links, actuator capabilities, constructibility, and other kinematic design issues (Ran-

¹REDIESTRO 1 and REDIESTRO 2 are full-scale seven-axis isotropic manipulator designed and manufactured at the McGill Centre for Intelligent Machines (CIM) of McGill University.

jbaran, 1997), see Fig. 3. By exploring other general architectures using RVS, it is possible to design a robot for particular or general applications. Figure 4(a) shows REDIESTRO 1 at a configuration known as isotropic (Angeles, 1997).

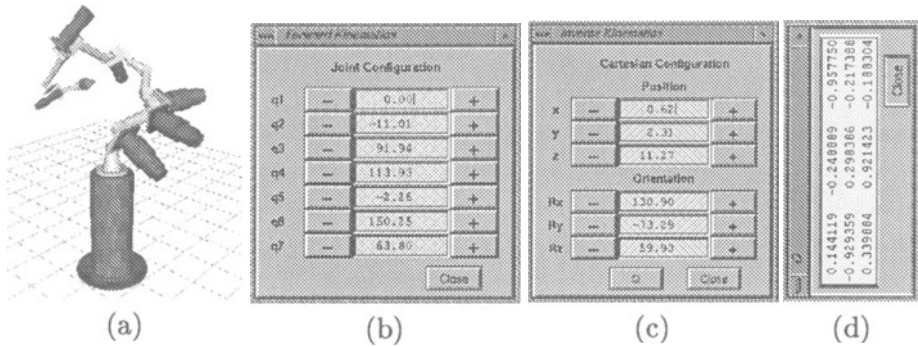


Figure 4: (a) REDIESTRO 1 at the isotropic configuration; (b) Joint configuration; (c) Cartesian configuration; (d) Rotation matrix.

2.5 FORWARD KINEMATICS

The **Joint Configuration** (Fig. 4(b)) command positions the manipulator in a given configuration. The robot can either 'jump' to the prescribed configuration or, alternatively, follow a trajectory based on a spline interpolation.

The user can modify each joint variable independently, while having simultaneous access at the corresponding Cartesian coordinates of the end-effector (Fig. 4(c)), its 3×3 orientation matrix (Fig. 4(d)) with respect to the base frame and the condition number of this matrix at any position.

2.6 INVERSE KINEMATICS

RVS has the capability to move the manipulator in a Cartesian frame, thus solving the inverse kinematics (IK) problem. All the features detailed for the forward kinematics remain available. RVS can also be interfaced with existing IK solving code, such as the contour method (Zanganeh, 1997). At the call of the function, a window displaying all the possible solutions for a given pose pops up. Clicking on any of these will move the robot to the corresponding configuration.

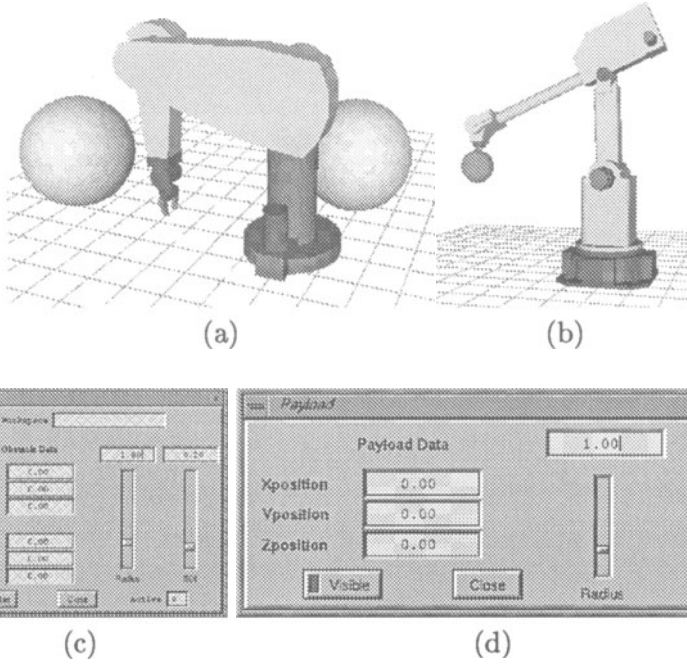


Figure 5: (a) Puma 560 with obstacles; (b) Fanuc S300 with a payload; (c) Obstacle menu; (d) Payload menu.

2.7 TRAJECTORY-PLANNING AND COLLISION-AVOIDANCE

RVS also allows the visualization of a precomputed trajectory. The joint angles obtained via an external IK program need only be written in a text file. The file is read by RVS using the **Joint Trajectory** command. RVS then displays the corresponding trajectory inside the workspace. The manipulator can then follow this trajectory forwards or backwards in a continuous fashion, stop at the prompt of the user or jump to designated points.

Moreover, obstacles can be included inside the workspace to check for collisions with the manipulator in real time. In the current version of RVS obstacles are modelled by spheres whose radii can be set by the user (Figures 5(a) & 5(c)). A distinction can be made between the hard contact zone and a safety zone. The user has the freedom to assign the starting location of the obstacle in the Cartesian space, and can also set a velocity in order to simulate a moving obstacle. Finally, with

the **Payload** command, the user can attach a payload to the tip of the end-effector (Figures 5(b) & 5(d)).

RVS was used to test the trajectories produced using redundancy-resolution schemes (Arenson, 1994). The trajectories were implemented first in RVS, then in the C3 Arm², see Fig. 6.

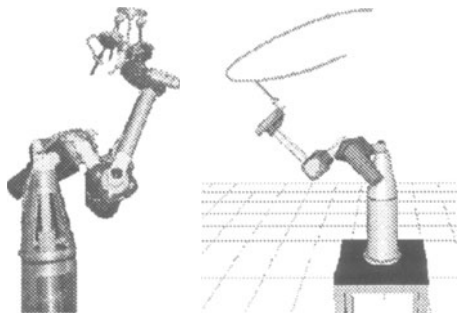


Figure 6: C3 Arm following a prestored trajectory.

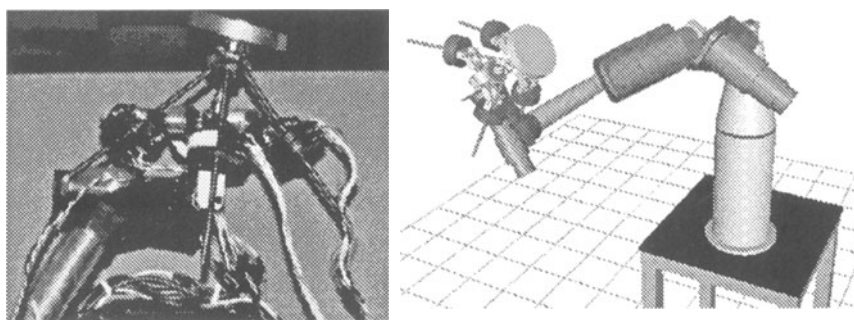


Figure 7: Three-dof spherical wrist.

3. CASE STUDY: DESIGN OF A THREE-DOF SPHERICAL WRIST

The case studied in this section is the design of a 3-dof spherical wrist with parallel architecture and actuation redundancy (Becker et al., 1994), (Fig. 7). The function of the wrist is to provide orientational capabilities to any positional manipulator. The spherical wrist has the

²The McGill-IRIS C3 Arm is an isotropic, four-revolute redundant manipulator designed and manufactured at McGill's Centre for Intelligent Machines.

advantage of higher stiffness and lighter design. However, it has inherent drawbacks, such as lower dexterity, smaller workspace, and kinematic complexity. With the help of RVS, a compact and light robotic wrist was built. Using the trajectory planning feature, RVS was used to monitor collisions between the links, to analyze the workspace, and to study the kinematics of the spherical wrist. The virtual model of the spherical wrist was mounted on the terminal link of the virtual C3 Arm to study the feasibility of the design.

4. CONCLUSIONS

Compared to other existing packages targeting specific fields of applications, RVS offers a development environment which can be adapted to the specific requirements of each user. This makes RVS a flexible and versatile tool. It is by no means restricted to 'conventional' industrial manipulators and has proven an invaluable tool in real life situations as diverse as modelling and simulation of rolling robots, landing gears (Angeles and Darcovich, 1993), kinematic design of a seven-axis redundant manipulator (Ranjbaran, 1997) and of a parallel, redundantly-actuated, three-dof spherical wrist (Becker et al., 1994), or the feasibility study of a manipulator for aircraft maintenance.

References

- Angeles, J. (1997). The Mechanical Design of Redundant Manipulators. In *Proc. 6th International Workshop on Robotics in Alpe-Adria Danube Region (RAAD'97)*, pages 15–26.
- Angeles, J. and Darcovich, J. (1993). The animation of vibration in landing gear systems. Technical report, Dept. of Mechanical Engineering & Centre for Intelligent Machines Technical Report, McGill University.
- Arenson, N. (1994). Real-time redundancy-resolution schemes for robotic manipulators. Master's thesis, Department of Mechanical Engineering, McGill University, Montreal, Canada.
- Becker, M., Hayward, V., Ranjbaran, F., and Angeles, J. (1994). The Kinematics of a Parallel Wrist with Actuation Redundancy. In *Proceedings of the First World Automation Congress*, volume 2, pages 405–410.
- Ranjbaran, F. (1997). *A Methodology for the Kinematic Design and Performance Evaluation of Serial Manipulators*. PhD thesis, Mechanical Engineering, McGill University.
- Zanganeh, K. (1997). The contour method: An interactive approach to the inverse. Technical report, Dept. of Mechanical Engineering & Centre for Intelligent Machines, McGill University.

Chapter 5
ANALYSIS AND OPTIMIZATION
OF MATERIAL FORMING PROCESSES

Clinch joining modeling with the static explicit method and remeshing	275
V. HAMEL, J.M. ROËLANDT, J.N. GACEL and F. SCHMIT	
 Theoretical and practical aspects in modeling of the metal powder compaction process	283
A. GAKWAYA, H. CHTOUROU, and M. GUILLOT	
 Study and evaluation of different formulations of the optimization problem applied to the stamping process.....	291
J. PAVIE, E. DI PASQUALE, S. BEN CHAABANE and V. BRAIBANT	
 Design optimization of metal forming processes	299
O. GHOUATI and J.C. GELIN	
 Modeling and blank optimum design of thin car panels obtained by sheet metal forming.....	307
Y.Q. GUO, H. NACEUR, J.L. BATOZ, C. KNOPF-LENOIR, O. BARLET, F. MERCIER and S. BOUABDALAH	
 Shape and thickness optimization of an aeronautical structure manufactured using age creep forming process	315
J.P. BOURDIN, J.P. BONNAFE, J. DELMOTTE, E. GROSJEAN and J.M. ROËLANDT	
 Two component finite element model for the simulation of shaping of prepreg woven fabric	323
A. CHEROUAT, J.L. BILLOET and S. BELHOUS	
 A sensitivity analysis for the spring back of the arched tubes.....	331
J.C. DJENI, P. PATOU , H. SHAKOURZADEH and V. BRAIBANT	

CLINCH JOINING MODELING WITH THE STATIC EXPLICIT METHOD AND REMESHING

V. HAMEL^{*,**}, J.M. ROELANDT^{*}, J.N. GACEL^{**}, F. SCHMIT^{**}

** Université de Technologie de Compiègne, LG2mS UPRES A 6066,
Pôle de Modélisation Picardie,*

B.P. 20529, 60206 Compiègne cedex, France.

*** C.E.D., Usinor Sollac,*

B.P. 109, 60206 Montataire Cedex, France.

Abstract - This paper presents a fast and efficient FE method for studying clinch forming with respect to process parameters. The basic principle of this mechanical joining technique is to clamp together several metal sheets by stamping and extrusion between a punch and a die.

The resolution of the updated lagrangian formulation is based on a static explicit approach. The contact conditions are insured by a penalty method. In addition, due to large mesh distortions, remeshing techniques are used in order to compute an accurate solution. After designing a new mesh, fields variables are transferred by a diffuse approximation technique.

The results computed with the static explicit method are compared with experimental data and numerical results calculated with a static implicit method (ABAQUS). The influence of process parameters (tools geometry, friction, material behaviour) is in very good agreement with experimental results.

1 . Introduction

Owing to its low cost and flexibility, mechanical press joining is finding extensive applications by complementing or replacing spot welding joints. However, the basic mechanisms of these cold forming processes are not well studied, and more insight knowledge on the process can be obtained by use of the numerical simulation.

In this paper we present an elastic-plastic incremental finite element computer code that has been developed to simulate the clinch joining process. The resolution of the updated lagrangian scheme is based on a static explicit approach. In addition, in order to compute an accurate solution, a sufficient mesh geometrical quality is insured by use of remeshing techniques. A clinch forming simulation is compared with experimental results as well as numerical solutions obtained with a static implicit method (ABAQUS). The good correlation between numerical and experimental results is also demonstrated to study the influence of process parameters.

2. The static explicit approach

This method was developed by [6] and was studied at UTC in the scope of sheet metal assembly [4 - 5]. This method is based on the following principles.

2. 1. MODEL DESCRIPTION

The principle of virtual velocity can be written in the following form, as proposed by [6]:

$$\int_V \left\{ \left(\dot{\sigma}_{ij}^J - 2\sigma_{ik} D_{kj} \right) \delta D_{ij} + \sigma_{jk} L_{ik} \delta L_{ik} \right\} dv = \int_{S_f} \dot{f}_s \delta v_i ds \quad (1)$$

for which

- * $\dot{\sigma}_{ij}^J$ represents the Jauman dérivative of σ_{ij}
- * L is the velocity gradient.
- * D is the symmetric part of L
- * f_s represents the known external forces applied on the system.

2. 2. CONSTITUTIVE EQUATION

The metal is modeled as an elastic - plastic material described by a Prandtl - Reuss constitutive equation. The equivalent stress - equivalent plastic strain relations are represented by a n power law of the form

$$k(p) = K(\varepsilon_0 + p)^n \quad (2)$$

with p representing the equivalent plastic strain and $k(p)$ the yield strength.

The integration of the elasto - plastic behavior law is realized with a Simo & Taylor algorithm.

2. 3. FINITE ELEMENT APPROXIMATION

The spatial discretization of the incremental virtual work equation and substitution of the constitutive equation, following a standard finite element procedure, yields a matrix equation of the form

$$K\Delta U = \Delta F \text{ with}$$

$$K = \sum_{e=1}^{nelt} \int_{V_e} \left[B^T (D_{ep} - F) B + E^T G E \right] dv \quad (3)$$

In these equations, ΔU denotes the nodal displacement increment, ΔF the nodal force increment, K the global tangent stiffness matrix, D_{ep} the elemental elasto-plastic constitutive matrix, B the strain matrix, E the velocity gradient, and F and G the Cauchy stress correction matrices. Their expressions are given in [5].

Equation (1) and (2) are originally derived in rate form and therefore, are valid only for infinitesimal displacement increment. Thus, a step control method is adopted to limit the size of each incremental steps.

2. 4. CONTACT MODELIZATION

The penalty method [2], is implemented to insure the planar and axisymmetric contact inequalities, due to its low computational cost and simplicity. This procedure involves sticking, frictional sliding and separation under large deformation. The friction law derives from the Coulomb model.

2. 5. AUTOMATIC REMESHING AND FIELDS MAPPING

In forming processes, contact conditions and localised strains often lead to a significant distortion of the elements on the domain boundary that is such that accurate calculations are not possible. In order to insure sufficient mesh quality along the calculation, it is necessary to periodically regenerate the whole mesh. An automatic adaptive remeshing based on the h - refinement is adopted.

These procedure follows the next three steps:

* Remeshing decision: In the elasto plastic code, remeshing becomes necessary when the errors due to spatial discretization of the boundaries become too large, or is user controlled.

* Automatic remeshing: first, a new discretization of the geometrical boundaries upon the deformed state of the part is designed. The mesh quality is then increased by locally modifying the element size on the boundary. This adaptive method can be controlled with a local error estimate. In our case, we chose to adapt the node density on the boundaries, depending on local equivalent plastic strain gradient. Finally, new meshes of the domains are created with an automatic mesh generator.

* Fields mapping: the most usual fields mapping method consists of extrapolating the fields to the node of the old mesh then interpolating those values to the integration points of the new mesh [1]. However, this method does not interpolate and does not generally insure that stresses at the integration point of the new mesh verify the plastic admissibility when their neighbours in the old mesh do.

Instead, a weighted least squares approximation method on a local window, is used. This has recently been proposed in the scope of the diffuse element formulation [7].

At a given point x of the new mesh, let σ be the field to estimate. It is searched in the form $\sigma = \langle p(x) \rangle \{ \alpha \}$ with $\langle p(x) \rangle$ a polynomial basis and $\{ \alpha \}$ a coefficient vector depending on x that is determined by minimizing the following function:

$$\sum_{i=1,N} w_x(x_i) \left(\langle p(x_i) \rangle \{ \alpha \} - \sigma_i \right)^2 \quad (4)$$

where x_i and σ_i are the coordinates and the fields values at the integration points of the old mesh. w_x is a weighting function centered on x , whose value is 1 at x , with a bounded support. The approximation is based on the k closest neighbours of x . With $r(x)$ the $(k+1)^{st}$ closer neighbour of x , we choose

$$w_x(x_i) = \exp\left(\frac{\ln(\epsilon) \|x_i - x\|}{r(x)} \right) \quad (5)$$

The minimization of function (4) leads to solve the following linear system:

$$\{\alpha\} = [A]^{-1} \{b\} \quad (6)$$

with $[A] = \sum_{i=1,N} w_x(x_i) \{p(x_i)\} \{p(x_i)\}^T$ and $\{b\} = \sum_{i=1,N} \sigma_i w_x(x_i) \{p(x_i)\}$

This method is not interpolating. However it does not require fields extrapolation to the old mesh nodes, and so is more accurate than the finite interpolation method.

3. Clinch forming simulation using remeshing techniques

3. 1. PROCESS DESCRIPTION

Mechanical joining techniques described by [3] work by forming spots, in one operation, without thermal effects, and allow to assemble parts by mutual shear insertion with cutting or upsetting of material between a punch and a die.

In particular, the TOX process, studied in this article, creates a so called clinch locking by mutual insertion of the metal sheets, without cutting. The punch presses on the surface of the upper work piece and spreads the material by upsetting into the shape of the die. The clinch joint is formed with TOX tools: punch 52100 (5.2 mm diameter, 10 mm height) and die BB8018 (8 mm diameter, 1.8 mm depth) whose geometry is displayed in Fig. 1.

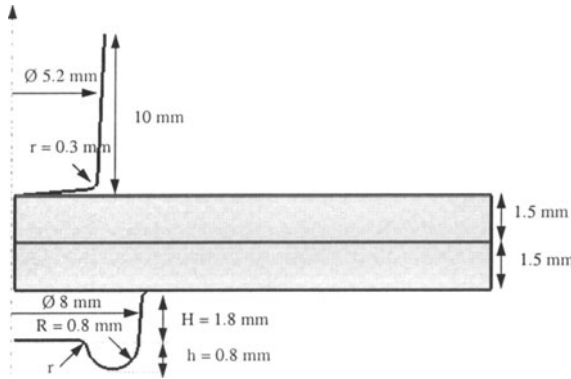


Figure 1. Process geometry

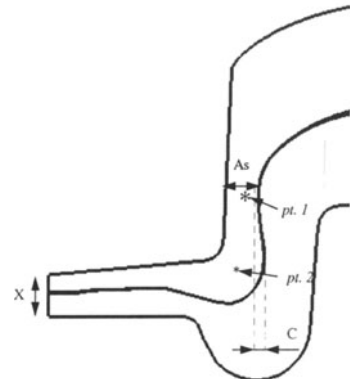


Figure 2. Clinch joint geometry

For a given forming punch displacement, the resulting geometry of a clinch joint is characterized by the following geometrical quantities: the axial thickness X, the minimum upper sheet thickness A_s , and a measure of the clinch lock C (Fig. 2).

The sheets are made of an extra mild isotropic steel. The elastic constants are: $E = 210000$ MPa: Young's modulus, $\nu = 0.3$: Poisson's ratio, $\sigma_y = 175$ MPa: Yield strength.

The isotropic hardening law is described by the following relation:

$$k(p) = 728(p+0.002)^{0.227} \text{ MPa} \quad \text{where } k(p) \text{ is the flow stress.}$$

3. 2. REMESHING VALIDATION

Experimentally, the punch force is set up in order to obtain an axial thickness X of 0.75 mm. The influence of friction is neglected in our calculations ($\mu=0$) and experiments, thanks to insertion of Teflon films (thickness 1/100 mm) between the metal sheets and the tools. For the experiments, a TOX clinch press type CEU15 is used to form the joints. The applied load and punch displacement are measured with piezo-electrique captors. Static explicit calculations without remeshing result in a poor accuracy of the deformed shape when compared with the experimental one. Furthermore, the evolution of the global load applied to the punch numerically is not comparable to the experimental one (fig. 5).

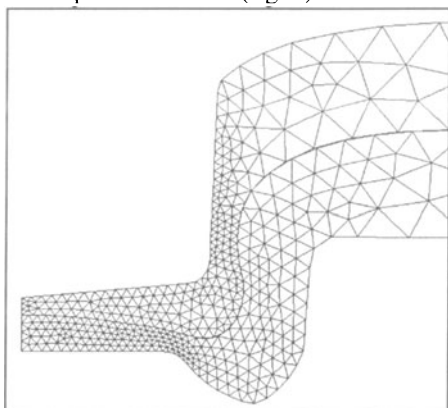


Figure 3. Static explicit calculation

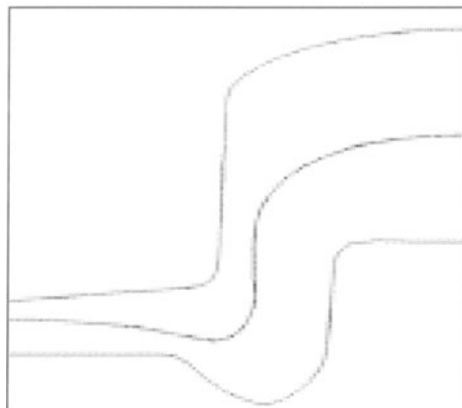


Figure 4. Experiment

Numerically, computations made with static explicit method (Fig. 3) and remeshing, and static implicit method without remeshing (ABAQUS) are similar and close to the experiment. The comparison of the applied punch force demonstrates the good correlation between the experimental and numerical solution obtained with T3 elements and remeshing (Fig. 5). For a 1400 d.o.f. model, CPU time on a Silicon Graphics Solid Impact R10000 workstation are 25'24" for ABAQUS and 15'36" for the static explicit method with remeshing.

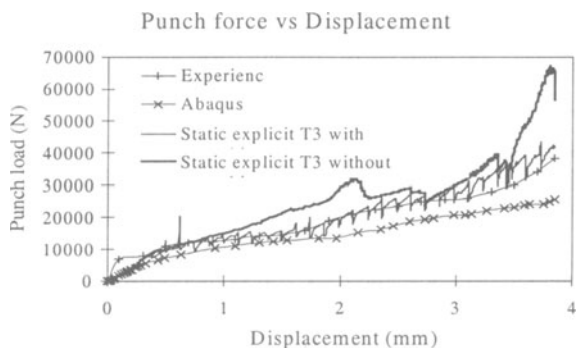


Figure 5. Computed punch force variation

3. 3. PROCESS PARAMETERS INFLUENCE

3. 3.1. Friction

The tests are realized with the prior metal sheets and tools (3. 2.). The influence of the friction parameter upon the final geometry of the clinch joint is evaluated by use of Teflon films. Wherever friction is applied between surfaces, the Coulomb friction coefficient is chosen as $\mu=0.1$. The joints are formed with a constant punch force of 40830 ± 20 N, while friction is applied alternatively on all surfaces. Joint final geometries are then computed by imposing a punch displacement such that the final axial thickness of the joint is similar to the experimental one.

The comparison between experiments and calculations are presented for two out eight different friction configurations (Fig. 7 -8.).

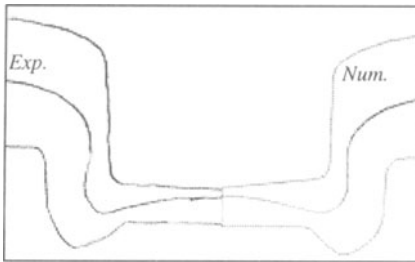


Figure 7. Die friction

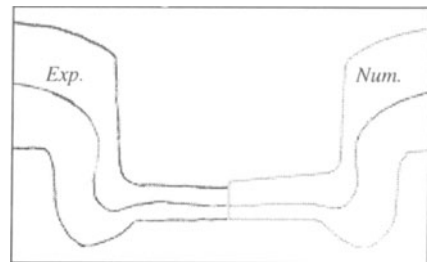


Figure 8. Punch friction

With a similar forming punch force, a minimum thickness of 0.6 mm is obtained when Teflon films are used on all surfaces, and a maximum thickness of 0.95 mm is obtained when no Teflon film is used.

The axial thickness ratio between the metal sheet also varies according to the friction applied between parts. This tendencies are confirmed by the numerical simulation. In addition, at a given punch displacement, the calculated punch force is equivalent to the experimental forming load.

3. 3.2. Materials characteristics

The same procedure as 3.3.1 is used to study the influence of the material characteristics on the clinch forming process. Two materials are used: the prior extra mild steel (XMS) and a high strength steel (HSS) whose mechanical characteristics are the following: $E = 210000$ MPa, $\nu = 0.3$, $\sigma_y = 417$ MPa, $k(p) = 1020(p+0.002)^{0.114}$ MPa.

The influence of the friction is neglected in the calculations, and experiments. Clinch joints are formed with a constant punch force of 40530 ± 15 N. Four clinch joint configurations are studied: XMS over XMS, HSS over XMS, XMS over HSS and HSS over HSS.

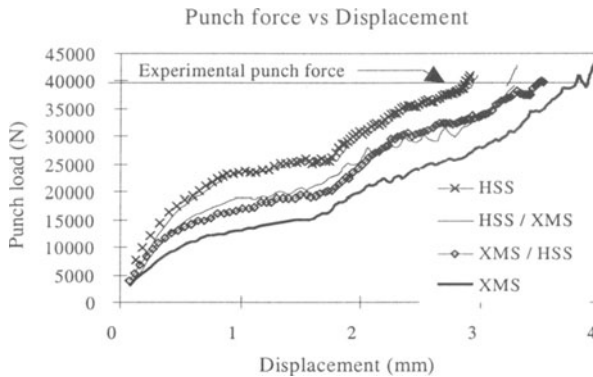


Figure 9. Computed punch force variation with different metal hardening

The influence of the material hardening is shown to be greater than the influence of the friction. With the same applied load, the axial thickness X varies between 0.6 mm for a soft steel to 1.6 mm for a hard hardening metal (Fig. 9).

The computed punch force is in very good agreement with the experimental one.

3.3.3. Tools geometry

In this experiment, the influence of the tool geometries is studied. Clinch joints are formed with extra mild steel sheet of 1 mm thickness. The punch diameter varies between 3.8 mm and 4.6 mm. The die has a constant diameter, and its height varies between 0.8 mm and 1.6 mm. The experiments are made with friction, and a constant Coulomb coefficient $\mu=0.1$ is applied in between every surfaces in contact. The experimental joints as well as numerical one are made such that the final thickness $X=0.75$ mm. The variation of the other two geometrical characteristics of the joint A_s and C (Fig. 2) are compared between the experiments and the calculations, and are reported in the following charts (Fig. 10).

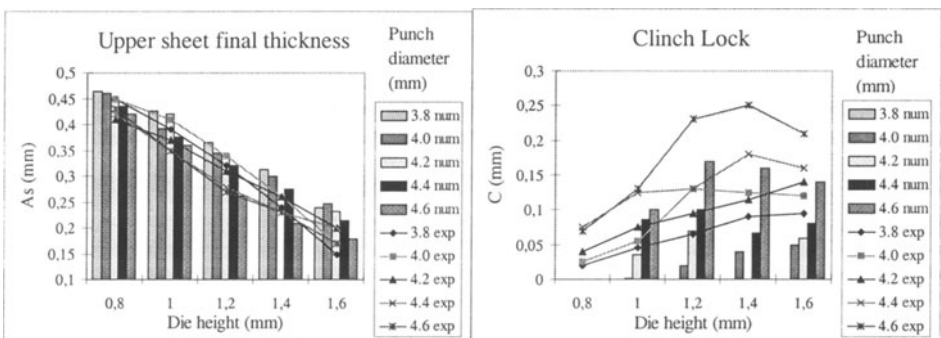


Figure 10. Evolution of the experimental and computed final thickness and clinch lock for metal sheets 1 mm / 1 mm, with different punches and dies

The main variations of clinch joint geometry with a constant outer diameter are the following:

First, for a given die height, an increase in punch diameter leads to a decrease in minimum thickness A_s and an increase in the clinch lock C .

Second, for a given punch diameter, an increase in die height results in a uniform decrease in the minimum thickness A_s . It has been shown in latter experiments using a bottom less die, that this trend is confirmed until the thickness is small enough to induce a rupture by necking. Inversely the clinch lock tends to increase when the die height increases. However this trend has a limit and an optimum value is reached for C .

Finally, experimental measures and computed results correlates well with regards to the tendencies demonstrated.

4. Conclusion

The simulation of clinch joint forming using a static explicit approach appears to be a fast and efficient numerical method to thoroughly study the clinch forming process. We have shown the necessity and suitability of the remeshing and fields mapping tools that have been developed in order to accurately simulate the clinch process while taking into account the main non linearities that are involved in the process.

Comparisons with experimental results show that numerical computations display a similar sensibility to the process parameters. The friction between tools and sheets influences slightly the intensity of the punch force and the distribution of deformation between upper and lower sheet. Metal hardening has an even greater influence. Finally, the tools geometry is the main factor that determines the final joint geometry and thus its mechanical strength.

5. References

1. Cheng J.H., Automatic adaptive remeshing for finite element simulation of forming processes., *Int. J. Num. Meth. Eng.*, vol. 26, pp.1-18, 1988.
2. Endo T., Oden J.T., Becker E.B., Miller T., A numerical analysis of contact and limit-point behavior in a class of problems of finite elastic deformation., *Comput. Struct.*; vol. 18, pp. 899-910, 1984.
3. Gao S., Budde L., Mechanism of mechanical press joining, *Int. J. Mach. Tools Manufact.* Vol. 34, No 5, pp. 641 - 657, 1994.
4. Hamel V., Roelandt J.M., Gacel J.N., Benzegaou A., Etude du comportement des aciers au clinchage par la simulation numérique et l'expérimentation. *StruCoMe*, France, 1996.
5. Hamel V., Roelandt J.M., Schmit F., Gacel J.N., Benzegaou A., FE modeling of clinch forming with automatic remeshing. *Comp&Struct*, to appear.
6. Makinouchi P., Ogawa H., Simulation of sheet bending processes by elastic-plastic finite element method., *Annals of the CIRP*, Vol. 38, n°1, pp. 279-282, 1988.
7. Nayrolles B., Touzot G., Villon P., Diffuse approximation and diffuse elements., *New Advances Comp. Struct. Mech.*, pp. 143-157, 1992.

THEORETICAL AND PRACTICAL ASPECTS OF MODELING OF THE METAL POWDER COMPACTION PROCESS

A. Gakwaya , H. Chtourou* and Michel Guillot****

P/M Laboratory , Précitech Inc. & Université Laval

Department of Mechanical Engineering

Laval University, Québec, CANADA

*research associate, ** professor*

ABSTRACT

Modeling and simulation of the compaction process in Powder Metallurgy is considered. The features of the mechanical behavior of metal powders are reviewed and a multisurface elastoplastic material constitutive law of the cap type is presented. The experimental characterization of the material model is done through resonant frequency measurements, uniaxial compression, hydrostatic and triaxial tests. A sensitivity study gives the relative influence of various parameters. Finite element simulations are performed and simulated results are validated by using experimental Vickers macrohardness measures in the context of industrial applications. The main conclusion of the study is that further experimental work is still needed in order to accurately identify the elasticity and the shear failure mode parameters.

1. INTRODUCTION

Powder Metallurgy (P/M) is now a well established manufacturing process because of its economical and technological benefits [19]. Complex physical mechanisms, induced by effects such as internal friction, elasto-plastic deformation and frictional contact at tools' walls, take place during the forming process and may lead to non-uniform density distribution and damage. The production of uniform and crack free compacts satisfying both dimensional tolerances and mechanical strength requirements is the ultimate goal of P/M industry[8]. Although for the design of routine parts, an extensive "know-how" has been developed in setting up tools and compaction sequences, however, when dealing with more complicated designs, costly trial and error procedures tend to be used. Therefore, an alternative design tool based on the finite element (FE) method has recently been used and allows for the prediction of density and stress level distributions in the compact prior to any tooling design and manufacturing activity. Accurate predictions require, however, a good treatment of the boundary conditions and a material model that can faithfully describe the physical mechanisms taking place during compaction. Therefore, a great care should be taken during the determination of the material parameters and the experimental calibration of the model [4]. The commonly used single surface plasticity model for compaction modeling does not properly cope with all the observed mechanisms[2,14]. Here, we rather consider a more complete model of the cap type [1, 18]. It involves however a large number of parameters and there is not yet a well established calibration procedure. More research work is needed in order to fully understand and reliably

apply this model to a given powder material.

This paper provides informations about the modeling of the compaction process. Section 2 presents features of the mechanical behavior of ductile metal powders compaction and the characteristics of the adopted particular material cap model. Section 3 presents the results of experimental calibration of the model and its application for the case of 316L stainless steel powders. Finally, the results of FE simulation are validated via Vickers macro-hardness method applied to an industrial PM part.

2. METAL POWDERS COMPACTION AND CONSTITUTIVE MODELING

2.1 Experimental observations and basic modeling hypotheses

The compaction of metal powders is commonly performed by using a set of rigid tools consisting of a die, punches and sometimes, core rods. The compaction process yields what is called a green part and involves three main phases [16] : (i) rearrangement phase during which bridges between particles are partially eliminated and the medium is densified by particle movement under the applied pressure; (ii) deformation phase in which the particles undergo elastoplastic deformations resulting in the hardening of the powder medium, and (iii) the fracture phase during which, if the densification continues beyond a critical level, inter-particle as well as intra-particle cracks may occur. Chemical composition, granulometry of the blend, particle shape as well as intensity and compacting mode affect the quality of the green compact. Its density distribution and average void size have the most influence on the final mechanical strength of the P/M part and subsequent sintering process. In order to minimize springbacks and residual stress effects during the ejection stage, assessing a uniform compaction ratio throughout the part by using multiple punches is highly desirable. However, the presence of either interparticles or tool walls friction always induce density gradients. For practical modeling applications, we use a macromechanical approach and considers the powder blend as a continuum medium that undergoes large elasto-plastic deformations. Moreover, we assume that the compacted powder remain globally isotropic, and for relative low tool speed, the process can reasonably be considered as inviscid and isothermal [1, 2, 14].

2.2 Powder material constitutive model

Within our continuum approach, two generic classes of models are generally used: (i) "classical elastoplasticity" based models, and (ii) "soil or geomechanics" based models. Models of the first group, also known as the "Kuhn-Shima-Gurson" type of model [11, 15, 19], were initially developed for sintered compacts and are thus an extension of the classical J_2 -flow theory to the compressible range. Recent works have shown [3] that these models correctly represent the late stages of compression but are not suitable for modeling the early stages where shear behavior and internal friction are important. These models use associative flow rule and isotropic hardening and also assumes that particle rearrangement is negligible and hence that particles only undergo plastic deformation. Among the models of the second group, the Cap model is one of the most popular. It was originally developed for rocks, soils and other geological materials [7, 18]. It is a multi-surface elastoplasticity model that describes all the compaction stages and thus accounts for the observed elastic behavior (springbacks, residual stresses), shear dilatancy (particle frictional slip and volumetric plastic strain increase with shear loading), work hardening and/or softening (under hydrostatic loading), and tensile fracture modes which may occur during the consolidation process. Compared to the first type of model, this one involves a large number of parameters whose full understanding and control

require a significant amount of experimental work. It has been successfully adapted and used to simulate the cold die compaction of hard metal powder [6] and was applied recently to the ductile case [Tra89, 4]. Hence as for soils or geological materials, grain sliding and rotations are the dominating plastic mechanisms in the early stages of compaction of the loose powder. And as higher pressures are applied, densification increases, particles rearrangement becomes negligible and particles undergo more elastic-plastic deformation. Its mathematical representation is still evolving but must include all the basic mechanisms. The multisurface cap plasticity model seems to be the most suitable to represent the above described and observed material behavior. Table 1 gives a summary of the equations of the main modes and figure 1 gives their graphical representation in the stress state space [5,10] where it is seen that the three yield surfaces intersect in a non smooth manner and that the state of stress is expressed in term of the pressure p , related to the first stress invariant J_1 by $p = J_1/3$, and the norm s of the stress deviator S defined by $S = \sigma - \frac{1}{3}J_1 \mathbf{1}$.

Table 1: Multisurface plasticity Cap model for powder compaction:

1. Hyperelastic compressible granular solid: $\psi(\varepsilon_v, \varepsilon_d, \rho) = \frac{1}{2}K(\varepsilon_v \bar{\mathbf{I}} : \bar{\mathbf{I}})^2 + G\varepsilon_d : \varepsilon_d$ $\sigma = \bar{\mathbf{C}}\varepsilon^e = \bar{\mathbf{C}}(\varepsilon - \varepsilon^p)$; $\bar{\mathbf{C}} = \frac{\partial^2 \psi}{\partial \varepsilon^2} = 2G(\rho)\bar{\mathbf{I}} + (K(\rho) - (2/3)G(\rho))\mathbf{1} \otimes \mathbf{1}$
2. Multi-yield surface a) Surface Tension limit : $f_1(\sigma) = T - J_1 = 0$
b) Shear failure surface: $f_2(\sigma) = s - F_e(J_1)$ for $-T \leq J_1 \leq L(k)$; $F_e(J_1) = \alpha - \gamma e^{-\beta J_1} + \theta J_1$ where $L(k)$ is equal to k if $k > 0$ or is equal to 0 if $k \leq 0$
c) Cap hardening surface: $f_3(\sigma, k) = F_c(J_1, s, k) - F_e(k) = 0$ for $L(k) \leq J_1 \leq X(k)$, $F_c(J_1, s, k) = \sqrt{s^2 - \frac{1}{R^2}[J_1 - L(k)]^2}$, variable aspect ratio: $R(\rho) = (X(k) - k) / F_e(k)$
3. Evolution equations: a) flow rule : $\dot{\varepsilon}^p = \sum_{i=1,3} \dot{\lambda}_i \frac{\partial f_i(\sigma, k)}{\partial \sigma}$ b) hardening law: $\bar{\varepsilon}_v^p [X(k)] = W[1 - e^{-DX(k)}]$, if $\dot{\varepsilon}_v^p > 0$ or $k > 0$ and $k > J_1$ then $\bar{\varepsilon}_v^p = \varepsilon_v^p$, otherwise $\bar{\varepsilon}_v^p = 0$ c) updating of density: $\rho = \rho_0 e^{-\varepsilon_v^p}$

3. EXPERIMENTAL CHARACTERIZATION OF THE CAP MATERIAL MODEL

3.1 Methodology:

The methodology used for experimental characterization of the cap model, is described in details in [4]. A blend of Alcan 316 L stainless steel powder with 0.75 wt % premixed Acrawax lubricant was used and it had a loose relative density of 0.33 (2.64g/cm³). The

testings started by pressing hydrostatically the specimens at different pressures ranging from 20 to 90 Ksi (138-610Mpa). This generated parts with quasi-constant densities. Then, specimens were machined into bars having an appropriate shape for the remaining tests. First ,

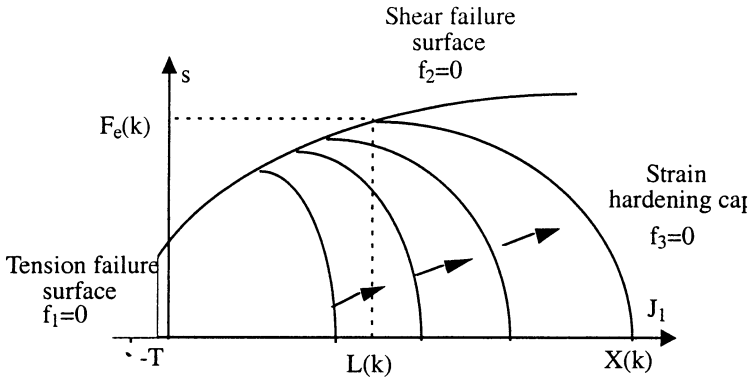


Figure 1 : Cap model yield surfaces

elastic moduli were determined from resonant frequency measurements[20]. The hardening law parameters were then determined from a series of hydrostatic compression tests. Then additional triaxial and uniaxial compression tests were required to determine the parameters of the cap and shear failure surfaces. Finally, considering that tensile loading is irrelevant for rigid die compaction modeling, the tension limit was assumed to be equal to zero (Figure 2). A detailed description of the equipment used in this research and detailed experimental results are presented in [4, 13]. The next step was the calibration of the model, usually performed through numerical trial and error process without following a clear methodology. However, a rigorous mathematical approach can also be utilized by considering the task of parameter identification as an optimization problem, provided reliable experimental data is available. The following observations were drawn from the obtained experimental results:

- resonant frequency method for measuring the elasticity parameters seems to be not very reliable (very small values were obtained). It would have been better to extract them from loading/unloading cycles in an instrumented hydrostatic press. Therefore, only average constant values will be used for the determination of the final density distribution.
- for the hardening law describing the compressibility of the studied powder, hydrostatic compression of a loose powder specimen in an instrumented hydrostatic chamber was used. Then if W is a measure of the maximum achievable volumetric plastic strain, the model retained can take the form: $\epsilon_v^p = W \cdot (1 - e^{-D \cdot J_1})$ with $W=91.64\%$ and $D=1.97 \cdot 10^{-3} \text{ Ksi}^{-1}$.

A series of triaxial compression tests were carried out during which online measurements of the axial and volumetric strains, fluid pressure and axial force were obtained [13]. The data recordings were then analysed and various material data were extracted from them. It was observed that no relevant information could be used to determine the shear failure mode parameters. Data from uniaxial compression were used to draw the initial critical surface and since no data was available in high pressure range, the shear failure surface was approximated by a straight line, thus leaving open its full characterization. But it was possible to extract parameters for the cap aspect ratio given by: $R(\rho)=r_1(\rho-r_2)^{r_3} = 0.778(\rho-.3)^{0.343}$. The preliminary yield surfaces obtained from the partial experimental data are shown in Figure 2. A sensitivity

study [4] of the model showed that the lack of information concerning the shear failure surface, as well as the lack of accuracy of the apparatus, does not represent a major handicap for the global characterization procedure. It was, in fact, found that as long as one deals with powder compaction with no excessive distortion, the parameters, influencing most the final density distribution, are those related to the material hardening law [4,5]. Table 2 summarizes the preliminary model parameter values obtained for the 316L stainless steel powder, as well as their relative influence on the final density distribution in a compact, as determined by the

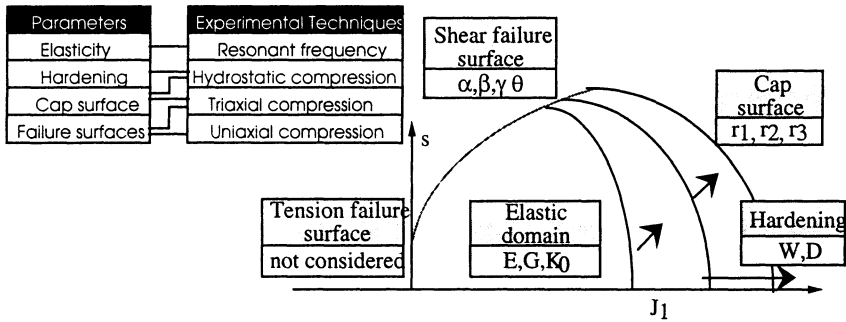


Figure 2 : Cap model parameters and associated experimental measuring techniques

Table 2: Values and relative influence of the 316 L parameters:

parameters	units	values	Relative Influence(%)
E	Ksi	$0.0299e^{12.9p}$	19,32
G	Ksi	$0.0078e^{13.8p}$	11,29
α	Ksi	0	0,83
β	Ksi^{-1}	0	0,06
γ	Ksi	0	0,68
θ	--	0,617	0.32
W	--	0,916	54,47
D	Ksi^{-1}	0,00197	12,21
R	--	$0,778(p-0,3)^{0.343}$	0,64
K_0	Ksi	0,001	0,01

sensitivity analysis. It should be noted that the initial intersection of the cap with the J_1 axis was not determined experimentally but was simply taken as a very small value, implying that the powder had no elastic behavior when in the loose state.

3.2 Validation of the material parameter set

The developed cap material model has been implemented into ABAQUS software [12] and a series of simple FE simulations was performed in order to validate the material parameters by first trying to reproduce the experimental results and tests conditions. The isostatic and triaxial compaction tests were used in this calibration process. The results of the two series of

simulation are graphically shown, in terms of achieved relative density, in Figures 3, 4 and 5.

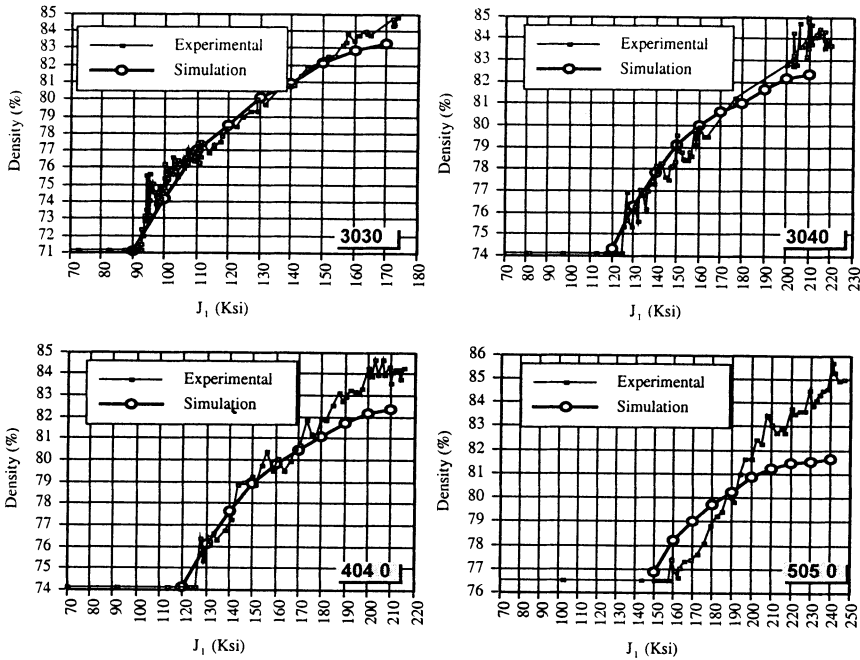


Figure 3. Simulation results of the triaxial compression tests

It is seen that a good agreement between experimental and simulated results was achieved for most cases. Except for the 5050 triaxial compaction test, the discrepancy never exceeded 1.5% (in relative density) and it appears only at the late stages of compression. This may be due to the data processing hypothesis which assumed that during the triaxial test, no permanent

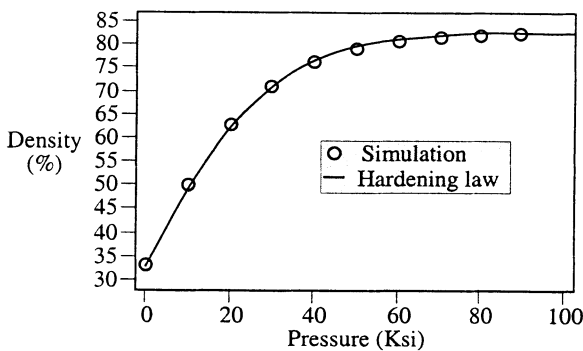


Figure 4. Simulation results of the hydrostatic compression tests

densification occurs before the pre-compaction pressure (first 2 digits in e.g. 5050) is reached, and that all subsequent deformation is totally plastic. However, it appears that, by the end of a test, accumulated elastic strain is not negligible as we assumed, but can reach as much as 3%.

Globally, the results obtained from the model are very acceptable, knowing that the experimental tests involved considerable noise [13]. Accordingly, the obtained values for the material parameters are considered valid and are retained for the rest of simulations.

4. EXPERIMENTAL VALIDATION AND FINAL RESULTS

Results of density distribution measured on industrially produced parts through Vickers macrohardness method[9,14] were compared with those obtained through numerical simulation. Fig. 6 shows the density distribution obtained after adjustment of the tool sequence, following a first calculation showing failure in the lower part.

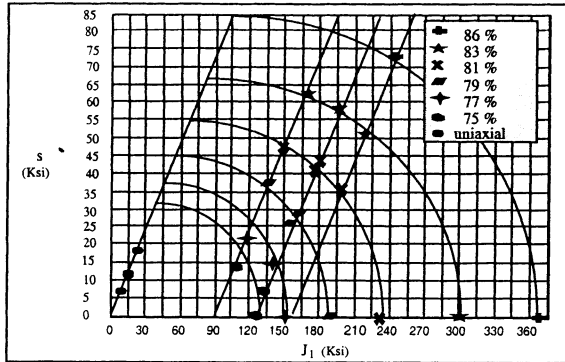


Figure 5: Fitting of the cap surfaces and the shear failure surface

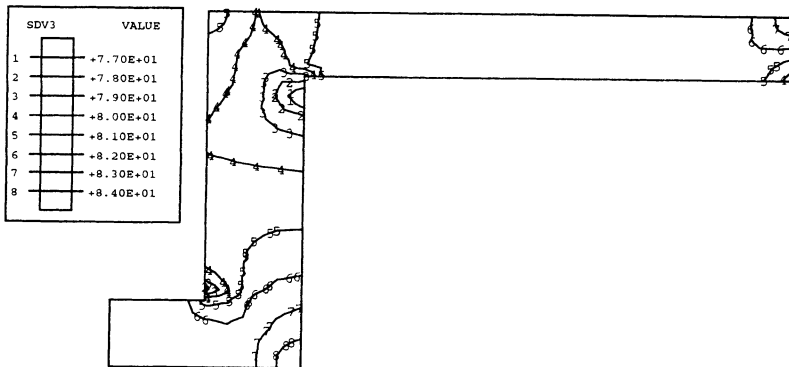


Figure 6.. Simulation results obtained using the modified sequence

5. CONCLUSION

Due to its ability to represent all the compaction stages, the cap material model, originally used for geological materials, has been adapted for ductile powders. Some of its parameters and other characteristics have been presented. An experimental characterization procedure was developed and applied for the case of 316L stainless steel powder to obtain a set of material

parameters which was validated by simulating the characterization tests. The relative influence of each parameter on the global relative density was determined through a sensitivity analysis. Despite the lack of information about the shear failure mode, as long as compaction does not involve excessive distortion, the parameters related to the material hardening law, have most influence on the final density distribution. The validation of the modeling approach was done by comparing the FE predicted density distribution with an experimental map density obtained from Vickers macro-hardness measurements. Although a good agreement was obtained, the incomplete material model characterization calls for further experimental work better parameter identification techniques aimed at providing a better description of the powder elastic behaviour, cap hardening and shear failure mode. This is the subject of on-going research.

ACKNOWLEDGEMENT

We acknowledge the support of the National Sciences and Engineering Research Council of Canada (strategic grant 0167091 and grant no. CRD-186296)

REFERENCES

1. Alm O.(1983), "Mechanical Testing of Powders and Powder Compacts", *Scandinavian Journal of Metallurgy*, Vol. 12, pp 302-311 .
2. Bockstiegel G.(1968), Relations between pore structures and densification mechanisms in the compacting of iron powder, *Perspectives in powder metallurgy*, Vol. 3, pp 54-71.
3. Brown S. and Abou-Chedid G.(1993), Evaluation of Yield Functions Due to Powder Characteristics, *Advances in Powder Metallurgy and Particulate Materials*, vol. 3,, pp. 245-255.
4. Chtourou H.(1996), "Modélisation par Éléments Finis du Procédé de Compression des Poudres Métalliques de l'Acier Inoxydable 316-L", *Ph.D Thesis, Laval University, Quebec*.
5. Chtourou H., Gakwaya A., Guillot M. and Hrairi M.(1995b), Implementing a Cap Material Model for the Simulation of Metal Powder Compaction, *Net Shape Processing of Powder Materials, ASME, AMD-vol 216*, pp. 19-27, San Fransisco.
6. Crawford J. and Lindskog P.(1983), Constitutive Equations and Their Role in the Modeling of the Cold Pressing Process, *Scandinavian Journal of Metallurgy*, vol. 12, pp. 271-281.
7. Dimaggio F. and Sandler I.(1971), Material Model for Granular Soils, *J. Engng Mechanics Division*, pp. 935-950.
8. German R.M.(1984), Powder Metallurgy Science, MPIF, Princeton N.J.
9. Guillot M. and Chtourou H.(1996), "Generalization of the Vickers Hardness Local Density Measurement Technique to Different Powder Materials", *Proceedings of the World Congress on Powder Metallurgy and Particulate Materials* , vol. 1, part 4, pp. 31-40, Washington D.C., 1996.
10. Chtourou H. Guillot M., and Gakwaya A.(1995a), "Modeling the Rigid Die Compaction of 316L Stainless Steel Powder", *Advances in Powder Metallurgy and Particulate Materials*, vol. 1, part 2, pp. 169-183, Seattle.
11. Gurson A.L. and Posteraro R.A.(1992), Yield Functions for Metal Powders for Use in the Numerical Simulation of Powder Compaction, *TMS Conference*, San Diego CA.
12. HKS Inc., "ABAQUS Theory Manual", Version 5.4, 1995, Hibbit, Karlsson and Sorensen, Inc., Rhode Island.
13. Innovare Inc.(1993), "Advanced Metalworking System ", Bath PA., Vol.114, #2.
14. Koopman M.G., Rachakonda V.B.S., Gurson A.L. and McCabe T.(1992), Material Models for the Finite Element Simulation of Compaction of Metal Powder, *TMS Fall Meeting*, Chicago.
15. Kuhn A.H. and Downey C.L.(1971), Deformation Characteristics and Plasticity Theory for Sintered Powder Materials, *Int. Journal of Powder Metallurgy*, vol. 7 (1), pp. 15-25.
16. Lenel F.V.(1980), Powder Metallurgy, Principles and Applications, MPIF, Princeton, N.J.
17. MPIF86. MPIF, Standard 42 (1986): "Determination of Density of Compacted and Sintered Metal Powder Products", Princeton, N.J.
18. Sandler I. S. and Rubin D.(1979), An Algorithm and a Modular subroutine for the Cap Model, *Int. Journal for Numerical and Analytical Methods in Geomechanics*, vol. 3, pp. 173-186.
19. Shima S. and Oyane M.(1976), Plasticity Theory for Porous Material, *International Journal of Mechanical Science*, vol. 18, pp. 285-291.
20. Yu C.J., Henry R. J., Prucher T., Parthasarathi S. et Jo J.(1992), "Resonant Frequency Measurements for the Determination of Elastic Properties of P/M Components", *Proceeding of P/M'92 World Congress*, vol. 6, pp 319-332.

STUDY AND EVALUATION OF DIFFERENT FORMULATIONS OF THE OPTIMIZATION PROBLEM APPLIED TO THE STAMPING PROCESS

S. BEN CHAABANE⁽¹⁾, J. PAVIE⁽²⁾, V. BRAIBANT⁽³⁾,
E. DI PASQUALE⁽⁴⁾

(1) Dept Mécanique des systèmes, Pôle Universitaire Léonard de Vinci, 92916 La Defense cedex, France

(2) CEA-CESTA, BP 2, 33114 Le Barp , France

(3) MECALOG, 2 rue de la renaissance 92184 Antony cedex, France.

(4) SIMTECH, 37 rue des Accacias, 75017 Paris, France

Abstract

The application of optimization algorithms to the numerical simulation of stamping process is due to the low computational cost obtained with software based on an inverse approach. However, the definition of the optimization problem is difficult because several objectives must be satisfied simultaneously. The formulation that we propose in this paper allows to separate the feasibility criteria from the quality criteria, and to simplify the formulation of the multi-criteria problem. We, also compare several methods to solve the optimization problem and show the advantages of the methods based on sensitivity analysis.

1. Introduction

In order to make the task of the designer easier, the industrials are interested in the automation of the design and the development of the stamping process. Because of the fastness of software based on the inverse method, we have decided to link them to optimization algorithms.

If the design variables seem to be easy to define, through the understanding and the control of the stamping process, the formulation of the optimization problem appears to be more difficult. In fact, several objectives must be achieved simultaneously: the workpiece should neither break nor wrinkle. It should not include unstretched areas.

Thus, we propose a multi-criteria formulation, allowing to separate the quality aspects from the feasibility aspects. Then, we focus on the resolution strategy of the problem, showing in particular the advantages of the local approaches compared to the sequential ones.

2. Formulation aspects

2.1. FEASIBILITY CRITERIA IN STAMPING

In sheet metal forming there are many feasibility criteria, related primarily on the types of workpieces and on the experience of the workers. We call n_c the number of used criteria. Usually we consider three types of criteria : wrinkling, rupture, and unstretched areas. These criteria are function of the principal strains in the plane of the sheet : (ϵ_1, ϵ_2 , with $\epsilon_1 \geq \epsilon_2$).

A first evaluation of the risk of rupture can be carried out when we consider the thinning of the part. If ϵ_3 denotes the strain in the direction of the thickness of the part, we have :

$$f_{rup} = \epsilon_1 + \epsilon_2 + \ln(1 - t_{accep}) \tag{1}$$

where f_{rup} is the function representing the rupture criteria, and t_{accep} is the maximum thinning tolerated. Other more complex evaluations of the risk of rupture are possible, with, for example, the use of the distance to the forming limit curve.

In some parts, we note the appearance of blemishes related to low values of plastic strain : unstretched areas. If we denote ϵ_{eq} the equivalent plastic strain measured in the mid-plane of the sheet, the absence of defects will be ensured by a minimal value ϵ_{acc} of ϵ_{eq} . Thus we have :

$$f_{unst} = \epsilon_{acc} - \sqrt{\frac{3}{2}(\epsilon_1^2 + \epsilon_2^2)} \tag{2}$$

The wrinkle results from local buckling associated with compressive stresses. This results in a relation of the type $\epsilon_1 \leq -\epsilon_2$. In order to soften this criterion, we introduce the parameter α , which represents the angle between the axis of maximum principal strain ϵ_1 and the line representative of the wrinkling criterion :

$$f_{wr} = -\epsilon_1 - \cos(\alpha_{acc} - \frac{\pi}{4})\epsilon_2 \tag{3}$$

The space of acceptable strains is represented in figure 1.

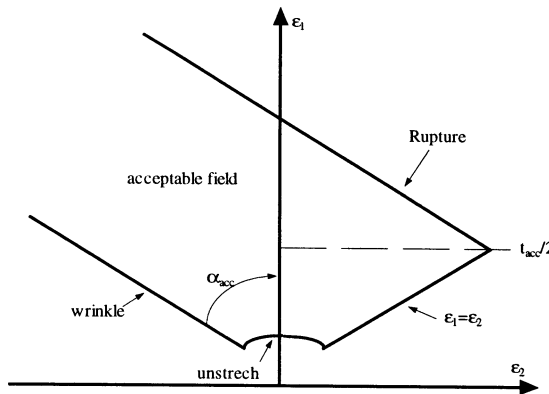


Figure 1. Acceptable field for principal strains

2.2. EXPRESSION OF GLOBAL CRITERIA

To evaluate the global state of the workpiece, we frequently use a global quality function, which is supposed to reflect each of the criteria on the whole of the workpiece. Thus we can take into account the influence of the areas where the criterion is not satisfied while a maximal local value of this criterion is used. A global criterion can be written as :

$$F_i = \left[\sum_{k=1}^{n_{elem}} \mu_k \langle f_i^k \rangle^q \right]^{\frac{1}{q}} \quad (4)$$

where f_i^k is the positive part of f .

For the element number k , μ represents the weight of the element k and q is a factor of normalization.

To avoid the problems caused by the choice of the type of normalization and weighting, we consider local aspects of the criteria. The optimization problem will be formulated using the $n_t = n_c \times n_{ele}$ criteria f_i^k , and not the n_c global criteria F_i .

2.3. MULTI-CRITERIA ASPECTS

In industrial cases, (complex workpieces) several criteria have to be satisfied simultaneously. The resolution of a multi-criteria problem is often difficult, so we generally use a single scalar function with new techniques of normalization ([KOS85], [STA88], [HAF92] and [SAN94]).

So, we can use :

$$\phi = \left[\sum_{j=1}^{n_c} \omega_j \langle \varphi_j \rangle^p \right]^{\frac{1}{p}} \quad (5)$$

where $\langle \varphi_j \rangle$ is the positive part of the criterion φ_j , ω_j is the weight associated to the criterion and p is the normalization factor. A priori, there is no standard method to calculate the weight and the factors to use for a known workpiece. Several resolutions of the problem $P(p, \vec{\omega})$ are needed to reach an acceptable solution for the user. This explains the fact that in the most of the studies carried out, the quality of the workpiece is evaluated using only one criterion. The worker tries to solve the predominating problem, and not to alter the other criteria (mono-criterion formulation with $n_c - 1$ constraints).

2.4. FEASIBILITY CRITERIA : CONSTRAINTS

In order to separate the feasibility problem from the quality problem, we have introduced the feasibility criteria as constraints in the optimization problem. So a relaxation formulation using the n_t local criteria f_i^k is developed. The principle of this

formulation is to try to bring back the f_i^k criteria inside the acceptable field of the principal strains (ϵ_1, ϵ_2) . Let δ_i^k be the distance separating the criterion i from its acceptable field. δ_i^k is calculated for the n_i criteria f_i^k such as δ_i^k is strictly negative if the criterion is satisfied, and δ_i^k is positive, if not. The calculation of δ_i^k in the (ϵ_1, ϵ_2) plan, allows to obtain criteria which are homogeneous to a strain.

2.5. OBJECTIVE FUNCTION : QUALITY CRITERIA

Since the problems of feasibility and quality are uncoupled, we can use any quality function without the unique dependence with respect to ϵ_1 and ϵ_2 . We can for example plan to optimize the depth of the workpiece, the strain gradients, etc ...

The first objective function, that we propose, consists in increasing the security factor with respect to the least satisfied feasibility criterion :

$$\phi = \underset{1 \leq i \leq n_c}{\text{Max}} \left(\delta_i^k \right) \quad (6)$$

$$1 \leq k \leq n_{ele}$$

With this method there is no more difficulty to define explicitly the weights. The concept of weighting persists, but it is taken into account implicitly through the definition of the acceptable field. However the acceptable field is often well defined according to the type of the part to analyze.

The Kresselmeir-Steinhauser function is another type of normalization, which allows to obtain a negative quality function, even if the part is acceptable ::

$$\phi = \frac{1}{\rho} \ln \left[\frac{\sum_{i=1}^{n_c} e^{\rho \delta_i^k}}{n_i} \right] \quad (7)$$

Where ρ is a factor to check the type of formulation to be used (global or local criteria). This expression of ϕ allows to overcome the numerical problems which can occur with the formulation (6), and increases the quality of convergence of the optimization algorithms. So, we suggest the following formulation for the optimization problem :

$$\begin{cases} \text{Min}(\phi) \\ \bar{x} \\ \text{Subjected to} \\ \delta_i^k(\bar{x}) \leq \delta_{\max} & \forall i = 1, \dots, n_c & \text{et} \forall k = 1, \dots, n_{elem} \\ \underline{x}_j \leq x_j \leq \bar{x}_j & \forall j = 1, \dots, n_{vc} \end{cases} \quad (8)$$

where \underline{x}_j and \bar{x}_j are the technological constraints applied to the design variables x_j . The workpiece will be feasible if, and only if, $\delta_{\max} \leq 0$. However, for many optimization algorithms, the definition of an acceptable field is a major difficulty. In this cases we choose to use a relaxation formulation for the constraints. The value of δ_{\max} can be updated at each iteration as following :

$$\delta_{\max} = \alpha \cdot \underset{i=1, \dots, nele}{Max} (\delta_i^k) + \beta \quad (9)$$

α and β are user defined coefficients.

3. Resolution strategies

We focus in this part on the resolution strategy planned to solve the non linear optimization problem under non linear constraints. The functions which are used in stamping problems are, a priori, non convex, so the presence of local optima is frequent, in particular if the number of design variables is large.

The first resolution strategy called “global optimization strategy”, consists in determining a global optimum on the design space. These methods (for example experience plans, Monte-Carlo, genetic algorithms) will not be detailed in this paper. Using these methods we can not obtain a good approximation of the optimum. Furthermore these methods require a significant number of function evaluation. But they often constitute an excellent starting point for the local optimization methods.

The local optimization methods constitute the second strategy considered. They allow the enhancement of the performance of a given initial design. Based on the use of the concept of approximations, the various local approaches are characterized only by the type of the approximation of the response surface, and by the technique used to build this surface.

We also distinguish, a sequential approach, based on the refining of the local approximation during the iterative process, and on the determination of an approximated response surface near the current point, from the calculations of the sensitivities.

3.1 SEQUENTIAL APPROACH

The sequential approach is based on the determination of a (polynomial) approximation of the objective function and of the constraints. The software HYPEROPT developed by Altair Eng., is based on this approach, by building and reactualizing a quadratic approximation of the objective function and the constraints. The complete Hessian matrix of the response surface, and the approximation are updated by weighting the results according to their respective performances.

3.2 LOCAL APPROACH

The convex linearization method is based on a linear or inverse approximation of the objective function and the constraints. This method gives a fast convergence but

becomes unusable when no constraint is active near the optimum. The recursive quadratic method is based on a quadratic approximation of the objective function, and a linear approximation of the constraints.

The local approaches need the knowledge of the derivatives of the objective function and the constraints with respect to the design variables. We generally calculate only the first derivatives, because the cost of calculation of higher orders, becomes quickly prohibitive. In the case of quadratic approximation, the inverse of the Hessian matrix is generally evaluated by a BFGS schema.

The performance of this approach is directly related to the type of sensitivity calculations. The calculation of the sensitivities has the considerable advantage to allow the use of a filtering on the criteria of feasibility. Indeed, in the case of a degenerated element or of an independence of the feasibility criteria or objective functions with respect to the design variables, the optimization process is stopped. In this case, and by the use of filters we can overcome these difficulties, by eliminating, for example, from the formulation of the problem, the constraints checking :

$$\left\| \frac{\partial \delta_i^k}{\partial x} \right\| \leq d_{limit} \quad (10)$$

3.3 APPLICATION

We present in this section the results obtained for a simple test case. The finite element calculations are realized with a software called SIMEX based on the inverse method. In this problem we optimize the two lines of drawed retaining forces. So the design variables are in fact the percentage of these forces compared to the forces obtained for a standard snapping.

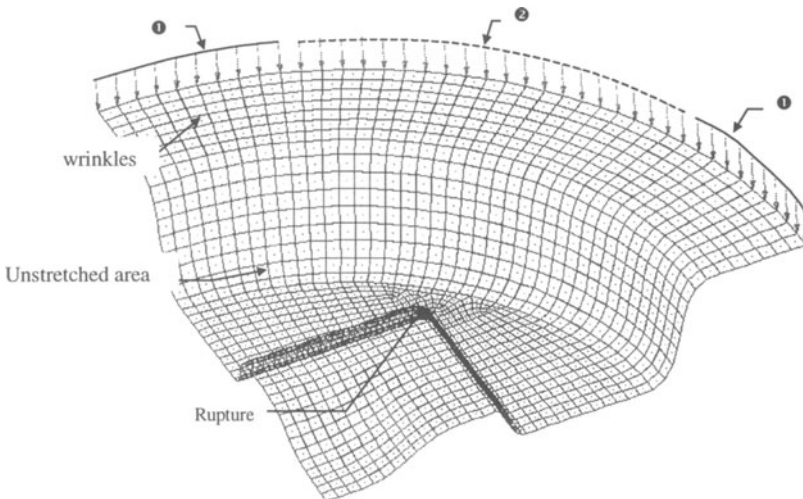


Figure .2. Quarter of the model used

In a first step, we compare the sequential approach (Hyperopt) to the local ones.

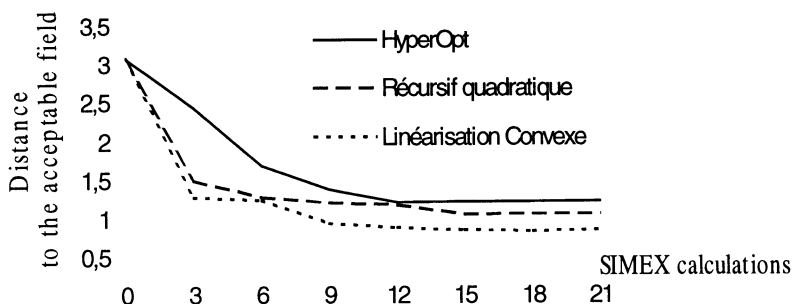


Figure 3. Distance to the acceptable field for the different approaches

The definition of the acceptable field, that we have used, does not allow a feasible part in the design space that we have fixed. However we can make some remarks. Since the first iteration the results are generally more efficient for local approaches. Finally, let us note that the optimal solution is obtained with the algorithm based on a convex linearization independently of the type of the objective function (infinite standard or Kresselmeier function with several values of ρ).

The results shown in figure 3, are obtained with sensitivities calculated with left finite difference method. This method seems to be very expensive when we consider a great number of design variables, or when we need to restart the calculations changing boundary conditions. So it is necessary to develop explicit derivative methods to obtain the sensitivity functions.

Additionally, we have noted that the convergence of the convex linearization algorithm can be improved using the Kresselmeier objective function. This function allows to obtain a more realistic evaluation of the quality of the workpiece.

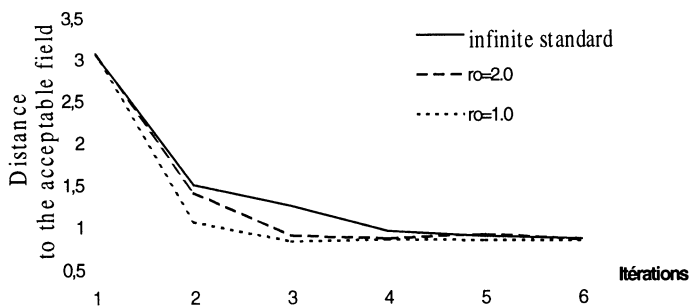


Figure 4. Influence of the objective function

4. Conclusion

By formulating the optimization problem using the local criteria, we avoid the use of an arbitrary smoothing of these criteria on the part. In the same manner, by representing these criteria in the principle strains plan, the formulation of the multi-criteria problem is carried out implicitly through the definition of the acceptable field. The acceptable field can be well defined for a given type of workpiece.

Then we have proved that the most suitable strategy of resolution is the one based on a construction of an approached problem by a sensitivity analysis. This approach allows, to obtain very satisfactory approximations since the first iterations, to include filtering techniques and in addition to reduce the total cost of the optimization by a judicious calculation of the sensitivities. The future efforts will be set on the enhancement of the precision of these derivations in order to build an approximation of good quality around the current design point.

5. References

- [GUO.90] GUO, Y. Q., BATOZ, J. L., DETRAUX, J. M., DUROUX, P. (1990) Finite element procedures for strain estimations of sheet metal forming parts, International journal for numerical methods in Engineering, Vol. 30, pp. 1385-1401.
- [HAF.92] HAFTKA, R., GÜRDAL, Z. (1992) Element of structural optimization, Kluwer Academic Publishers Dordrecht/Boston/London.
- [KOS.85] KOSKI, J. (1985) Defectiveness of weighting method in multi-criterion optimization of structures, Communications of Applied Numerical Methods, 1, 333-6.
- [SAN.94] SANDGREN., E., (1994) Multi-criteria design optimization by goal programming, Advances in design optimization, Adeli.
- [STA.88] STADLER, W. (1988) Multi-criteria Optimization in Engineering and in the Sciences, Plenum Press New York.

DESIGN OPTIMISATION OF METAL FORMING PROCESSES

O. GHOUATI, H. LENOIR and J-C. GELIN

Laboratoire de Mécanique Appliquée R. Chaleat UMR CNRS 6604

Université de Franche-Comté

24 rue de l'Épitaphe, 25030 Besançon Cedex - France

Tel. : +33 (0)3 81 66 60 34 - Fax : +33 (0)3 81 66 67 00

Email : oghouati@univ-fcomte.fr

Abstract:

A process optimisation technique is proposed on the base of the combination of a numerical optimisation procedure and a finite element method. The optimisation algorithm is based on an augmented lagrangian method and is used to minimise an objective function subject to constraint functionals. This allows to adjust process parameters in the finite element model. The finite element method allows an accurate simulation of the process under consideration by taking exactly into account boundary conditions, applied loads and operating conditions. Furthermore, a sensitivity analysis is associated with this method in a consistent manner so as to assess accurately the gradient of the reponse function and the constraint functionals with respect to process parameters. An application to the control of springback during deep drawing of sheet metals is presented.

1. Introduction

Significant demand exists in the industry to have convenient methods for determining optimal process parameters for forming operations. At present this demand is poorly met. This leads to an under-usage of CAD/estimation software which is nevertheless very powerful. On the other hand, the finite element method has experienced a significant progress, turning it into a powerful tool for the simulation of various forming processes in different operating conditions. This allowed to formulate the design of forming processes as a non linear mathematical programming problem, the finite element method providing the overall behaviour of the process for a fixed set of design parameters [1]. The goal of the optimisation is to achieve the minimisation (or maximisation) of a reponse functional S subject to equality and/or inequality constraint functionals g_i ($i=1,nc$) and h_j ($j=1,nic$) [2,3]. Design parameters can be of different kinds. They can represent the material behaviour, the operating conditions such as the

temperature, strain rate, friction conditions etc..., or the geometry of the process including the shape of both the tools and the workpiece.

In this paper, a design optimisation technique for forming processes is presented. This technique is based on the coupling of the finite element method and an optimisation technique allowing to solve the mathematical problem stated above. The finite element allows to evaluate for a fixed set of design parameters, the objective functional S and the constraint functionals g_i and h_j . The constrained optimisation problem is solved using an augmented Lagrangian method. The Lagrangian is minimised with respect to the design parameters \mathbf{p} as an unconstrained functional. The method used to do so is a variable metric method.

The finite element formulation utilises two different approaches: a quasi-static implicit one which is based on an updated Lagrangian formulation with a consistent tangent matrix, and a transient explicit one where a diagonal mass matrix is computed. The finite element method uses two-dimensional or three-dimensional thin shell elements with mixed interpolation of transverse shear strain components in order to avoid shear locking [4]. Material properties of the sheet metal are described using an elasto-plastic behaviour either isotropic or anisotropic. The elasto-plastic behaviour is described by an orthotropic Hill criterion taking into account the hardening and an associated flow rule [5]. Treatment of the contact between the sheet and the tools uses a master-slave scheme where penetration has to be detected first. Then conditions are adjusted after reaching the equilibrium. To provide an effective deep drawing process, after the simulation of the loading stage, the unloading sequence is modelled. For the first step, the control of the blank-holder force is taken into account during the deep drawing process. For the second step, a mechanical modelling of the springback is proposed. All nodal contact forces with tools are taken into account and decreased. In the case of explicit transient analyses, all tools are removed. So the sheet metal is set free from contact nodes [6].

The process optimisation method developed is applied to the design of a deep drawing process. The goal is to find the optimal design parameters leading to the minimal springback. The process parameters considered here are geometry parameters of the tools.

2. Problem formulation

Consider a sheet metal S occupying a domain Ω_0 with boundary Γ_0 in the initial configuration and the domain Ω with boundary Γ in the current configuration. On boundaries Γ_u and Γ_σ ($\Gamma_\sigma \cap \Gamma_u = \emptyset$, $\Gamma_\sigma \cup \Gamma_u = \Gamma$), the displacement $\bar{\mathbf{u}}$ and the traction $\bar{\mathbf{f}}_s$ are prescribed. The sheet metal undergoes a deformation process specified by the displacement field $\mathbf{u}_t(\mathbf{p}, t)$ where t is time or a time like parameter for the quasistatic process and \mathbf{p} is the vector of process parameters. In a finite deformation process the initial configuration C_0 is deformed into C_t with $\mathbf{x}_t = \mathbf{x}_0 + \mathbf{u}_t$.

The following weak form associated with the equilibrium equations for the sheet metal S is used in the finite element method:

$$G(\mathbf{u}_t(\mathbf{p}), \eta) = \int_{\Omega_t} \mathbf{T}(\mathbf{u}_t(\mathbf{p})) : \nabla_{x_t}^s \eta dV - \int_{\Gamma_\sigma} (\bar{\mathbf{f}}_s \cdot \eta) dS = 0 \quad (1)$$

where \mathbf{T} is the Cauchy stress tensor, η is an homogeneous displacement field ($\eta=0$ over Γ_u) and $\nabla_{x_t}^s \eta$ is the symmetrical gradient of η in the current configuration.

Equation (1) is non-linear with respect to $\mathbf{u}_t(\mathbf{p})$. The solution process is performed using a Newton iterative scheme and leads to the following equation:

$$\int_{\Omega_t} \mathbf{C}(\nabla_{x_t}^s \mathbf{u}_t(\mathbf{p})) : \nabla_{x_t}^s \delta \mathbf{u}_t(\mathbf{p}) : \nabla_{x_t}^s \eta dV + G(\mathbf{u}_t(\mathbf{p}), \eta) = 0 \quad (2)$$

where $\delta \mathbf{u}$ represents the displacement increase. The term $\mathbf{C}(\nabla_{x_t}^s \mathbf{u}_t(\mathbf{p}))$ represents the tangent operator consistent with the algorithm of evaluation of stress and internal variables.

In the displacement based finite element method, the discretized form of the equation (2) is used to calculate an estimated incremental displacement $\delta \mathbf{u}_{n+1}$ between t_n and t_{n+1} [7,8], following the implicit iterative equation:

$$[\mathbf{K}_T]_{n+1}^{(i)} \delta \mathbf{u}_{n+1}^{(i)} = [\mathbf{F}_{ext}] - [\mathbf{F}_\sigma(\nabla_{n+1}^s \mathbf{u}_t(\mathbf{p}))]_{n+1}^{(i)} \quad (3)$$

$[\mathbf{F}_{ext}]$ represents the nodal vector of external loads, $[\mathbf{F}_\sigma(\nabla_{n+1}^s \mathbf{u}_t(\mathbf{p}))]$ the nodal vector of internal loads, and $[\mathbf{K}_T]$ represents the tangent stiffness matrix.

In the case of the transient explicit solution procedure, the acceleration is taken into account, the virtual work principle can be written in an Eulerian manner as:

$$\int_{\Omega_t} \mathbf{T}(\mathbf{u}_t(\mathbf{p})) : \nabla_{x_t}^s \eta dV - \int_{\Gamma_\sigma} (\bar{\mathbf{f}}_s \cdot \eta) dS + \int_{\Omega_t} \rho \gamma \eta dV = 0 \quad (4)$$

After discretization, the integral form (4) is transformed as:

$$[\mathbf{M}]_{n+1} \gamma_{n+1} = [\mathbf{F}_{ext}] - [\mathbf{F}_\sigma(\nabla_{n+1}^s \mathbf{u}_t(\mathbf{p}))]_{n+1} \quad (5)$$

where γ_{n+1} is the nodal accelerator vector and \mathbf{M}_{n+1} the mass matrix.

Nodal accelerations vector are obtained by solving equation (5) and velocities, respectively displacements are obtained by a central difference formulae. In the particular case where \mathbf{M} is a diagonal matrix, the solution process is easy and fast.

3. Design problem

3.1. FORMULATION OF THE DESIGN PROBLEM

The solution of the design problem can be formulated in the form of a non linear problem of mathematical programming as [1-3]:

$$\min_{\mathbf{p}} S_0(\mathbf{p}, \mathbf{u}) \quad (6)$$

subject to constraints

$$\begin{cases} h_j(\mathbf{p}, \mathbf{u}) \leq 0 & (1 \leq j \leq n_{ic}) \\ g_i(\mathbf{p}, \mathbf{u}) = 0 & (1 \leq i \leq n_c) \end{cases} \quad (7)$$

where n_{ic} is the number of inequality constraints and n_c is the number of equality constraints.

The cost function S_0 is defined in the case of springback analysis as the amount of displacement after unloading while the constraint functions h_j and g_j usually concern the nodal displacements, element stresses, technological limitations and so on.

To solve this constrained optimization problem an augmented Lagrangian method is used by the definition of the Lagrangian associated with the problem as following:

$$\mathbf{L}_r(\mathbf{p}, \mathbf{u}, \lambda) = S_0(\mathbf{p}, \mathbf{u}) + A_1(\mathbf{p}, \lambda, r) + A_2(\mathbf{p}, \lambda, r) \quad (8)$$

with

$$\left\{ \begin{array}{l} A_1(\mathbf{p}, \lambda, r) = \sum_{i=1}^{n_{ic}} [\lambda_i \psi_i + r \psi_i^2] \\ \psi_i = \max \left[h_i(\mathbf{p}), \frac{-\lambda_i}{2r} \right] \\ A_2(\mathbf{p}, \lambda, r) = \sum_{i=1}^{n_c} [\lambda_i g_i + r g_i^2] \end{array} \right. \quad (9)$$

A gradient-based method is used to minimize $\mathbf{L}_r(\mathbf{p}, \mathbf{u}, \lambda)$ with respect to \mathbf{p} . The iterative solution process is as follows . At the k th iteration, for $r^{(k)}$ and $\lambda^{(k)}$ fixed, an estimation $\mathbf{p}^{(k)}$ for the design parameters is evaluated in a way to minimize $\mathbf{L}_r(\mathbf{p}, \mathbf{u}, \lambda)$. The Lagrange multipliers are updated using the equation :

$$\begin{cases} \lambda_i^{(k+1)} = \lambda_i^{(k)} + 2r g_i(\mathbf{p}^*) & i = 1, n_c \\ \lambda_i^{(k+1)} = \lambda_i^{(k)} + 2r \max[h_i(\mathbf{p}^*), (-\lambda_i^{(k)})/(2r)] & i = 1, n_{ic} \end{cases} \quad (10)$$

The penalty coefficients are evaluated as follows:

$$r^{(k+1)} = r^{(k)}\beta \quad \beta > 1 \quad (11)$$

The solution process needs the evaluation of the gradient of the Lagrangian function and thus of both the cost function S_0 and the constraint functions h_j and g_i . This is performed by the means of a sensitivity analysis.

3.2. SENSITIVITY ANALYSIS

A sensitivity analysis for sheet metal forming problems has been developed on the base of direct differentiation of the solution process for the mechanical problem [9].

Sensitivity of displacements is obtained, in the implicit case, by solving the following equation:

$$\frac{d(\Delta \mathbf{u}_{n+1})}{d\mathbf{p}} = -[\mathbf{K}_T]^{-1} \left[\frac{\partial}{\partial \mathbf{p}} [\mathbf{F}_\sigma] - \frac{\partial \mathbf{K}_T}{\partial \mathbf{p}} \Delta \mathbf{u}_{n+1} \right] \quad (12)$$

The inverse of the stiffness matrix can be obtained from the solution of the direct problem. It remains therefore to evaluate the sensitivity of the stiffness matrix and the sensitivity of the internal load vector.

In the explicit case, first stage is to evaluate sensitivity of the acceleration vector using the following equation:

$$[\mathbf{M}]_n \frac{d\gamma_{n+1}}{d\mathbf{p}} = \left[\frac{d\mathbf{F}_{\text{ext}}}{d\mathbf{p}} \right] - \frac{d\mathbf{F}_\sigma}{d\mathbf{p}} - \frac{d[\mathbf{M}]_n}{d\mathbf{p}} \gamma_{n+1} \quad (13)$$

This equation provides sensitivity of accelerations at time t_{n+1} knowing sensitivity of the mass matrix, sensitivity of the external load vector and the sensitivity of the internal load vector, at time t_n . On the other hand, since the sensitivity analysis is performed once the mechanical problem has been solved, the quantities \mathbf{M}_n and γ_{n+1} are known.

4. application

To illustrate the use of the optimisation algorithm described above, the drawing of a channel is presented. Dimensions of the sheet are $200 \times 40 \times 1.0 \text{ mm}^3$ and the geometry of the tools is presented in figure 1.

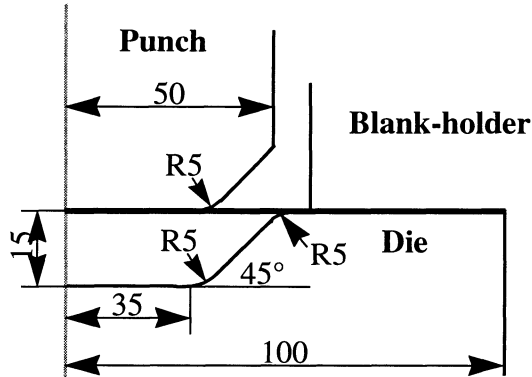


Figure 1. Geometry of the channel test

The sheet material is mild steel with an elastoplastic behaviour and an isotropic hardening law. The flow rule is of Hollomon type with material properties reported in table 1. A blank-holder force of 8 kN is applied to the sheet.

TABLE 1. Material properties for the channel test

Parameter	E (MPa)	ν	σ_0 (MPa)	K (MPa)	n
Value	206 800	0.29	160	563	0.256

The finite element simulation of the process uses plane strain shell elements. Besides, for evident symmetry reasons, only one half of the test is considered.

Process parameters considered here represent the geometrical description of the tools. Each tool is described by a set of elementary lines and arcs following figure 1. Therefore, the punch is made of 3 lines and 1 arc, the die is made of 3 lines and 2 arcs, and the blank-holder of 1 line. Each line is represented by the geometrical positions of its edges (4 parameters) and each arc is represented by its radius (1 parameter), the geometrical positions of its edges being implied by connectivity with other lines. So, for the problem considered here, the number of parameters is 31 parameters (13 for the punch, 14 for the die and 4 for the blank-holder).

Figure 2 represents the gap between the obtained shape after springback and the desired shape before optimisation. It can be noticed that springback effects are very strong for this test, with a maximal shape error of about 7.0 mm.

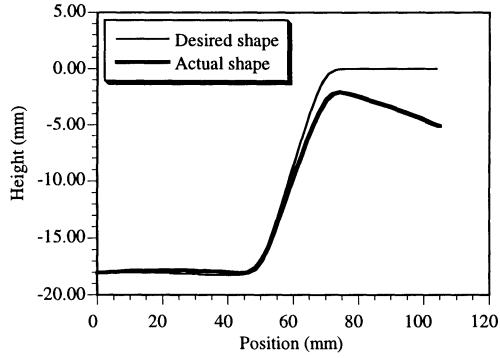


Figure 2. Obtained and desired shapes before optimisation

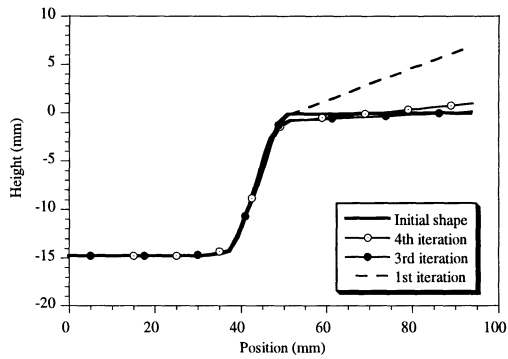


Figure 3. Evolution of the die shape during the optimisation process

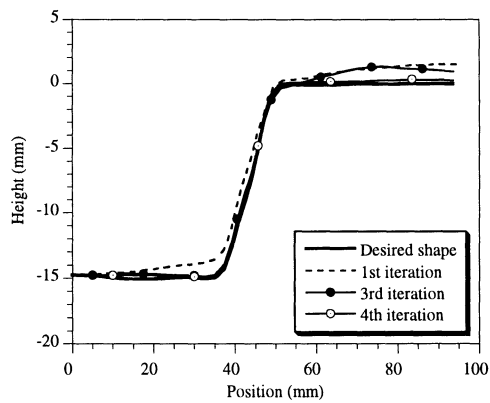


Figure 4. Sheet shape corresponding to the calculated die shape

In the optimisation process, the objective function is defined as the gap between the actual shape and the desired shape. The minimisation of this objective function is subject to constraint functionals to ensure geometrical consistency of the tools. In this optimisation, only the shape of the die was optimised.

Figure 3 represents the evolution of the shape of the die during the optimisation process, whereas figure 4 represents the corresponding shape of the sheet deformed using the calculated die shape.

5. Conclusion

An algorithm for process optimisation is presented. This algorithm is made of an optimisation technique based on a gradient method and a finite element method. The finite element method used allows to simulate the process studied with sufficient accuracy making possible the adjustment of the design parameters. Associated to this algorithm, a sensitivity analysis is developed on the base of a direct differentiation of the finite element formulation. An application is presented to demonstrate the efficiency of the proposed method.

6. References

1. Ghouati, O., and Gelin, J.C.: "Sensitivity analysis and optimization of shape and process parameters in metal forming", Engineering Systems Design and Analysis Conference 1996, Vol.3, pp.221-226.
2. Kegl, M., Butinar B.J., and Oblak, M.M.: "Shape optimal design of elastic planar frames with non linear response", Int. J. Numer. Methods Eng., Vol.38, 3227-3242, 1995.
3. Schramm U., and Pilkey, W.D.: "Optimal shape design for thin walled beam cross-sections", Int. J. Numer. Methods Eng., Vol.37, 4039-4058, 1994.
4. Gelin, J.C., Boulmane, L., and Boisse, P.: "Quasi-static implicit transient analyses of sheet metal forming using a C^0 three node shell element", J. Mater. Processing Technology, vol. 50, n° 1-4, 54-69, 1995.
5. Boubakar, L., Boulmane, L., and Gelin, J.C.: "Finite element modelling of the stamping of anisotropic sheet metals", Engineering Computations, Vol.13, pp 143-171, 1996.
6. Joannic, D., and Gelin, J.C., "Accurate simulation of springback in 3D sheet metal forming processes", 5th Int. Conf. on Numerical Methods in Industrial Forming Processes - Numiform'95, Ed. by S.F. Shen and P.R. Dawson, A.A. Balkema Publ., 729-735, 1995.
7. Bathe, K.J., *Finite Element Procedures in Engineering Analysis*, Ed. Prentice Hall Int., New York, 1982.
8. Zienkiewicz, O.C., and Taylor, R.L., *The Finite Element Method*, Fourth Edition, vol.1, *Basic Formulation and Linear Problems*, Mc Graw Hill Book compagny, 1989.
9. Gelin, J.C., and Ghouati, O.: An Inverse Solution Procedure For Material Parameters Identification In Large Plastic Deformations, *Comm. in Num. Meth. in Eng.* **12** (1996), 161-173.

MODELING AND BLANK OPTIMUM DESIGN OF THIN CAR PANELS OBTAINED BY SHEET METAL FORMING

Y. Q. GUO, H. NACEUR, J.L. BATOZ, C. KNOPF-LENOIR,
O. BARLET, F. MERCIER, S. BOUABDALAH
*Université de Technologie de Compiègne, Lab. LG2mS
Département GSM, B.P. 20529, 60205 Compiègne Cedex, France*

ABSTRACT : We first present our simplified finite element method called the Inverse Approach (I.A.) for the analysis of thin shell structures obtained by deep drawing. We recall the basic assumptions of the I.A. and then present some recent developments such as the consideration of bending effects and the improvements in the resolution algorithms. In the second part, we present our shape optimization procedure coupling the I.A. and SQP (Sequential Quadratic Programming). The sensitivities are computed analytically using the adjoint variable method. The procedure is applied to the blank optimum design of the TWINGO dashpot cup.

1. Introduction

A number of powerful industrial softwares (mainly based on incremental dynamic explicit approaches) are nowadays available for the analysis of sheet metal forming problems [1], [2]. These tools are appropriate for the analysis when an initial set of forming parameters is available. However they cannot be used to generate the forming parameters in an iterative optimization procedure, mainly for prohibitive computer costs. On the other hand, some simplified numerical procedures are also developed for the analysis of sheet forming parts [3]. Their efficiency and precision have been the subject of a number of publications [4]. Several industrial softwares based on these approaches are now available.

The efficiency of our simplified Inverse Approach (I.A.) developed at UTC since 1987 is based on the following assumptions : (1) a priori knowledge of the workpiece shape (useful part), (2) total path independent deformation theory of plasticity, (3) simplified representation of the tool actions. Despite the crude assumptions, very good results have been obtained for benchmark tests (LDH tests [2]) and industrial parts.

The present I.A. appears to be an attractive way to obtain the strain and stress states in the optimization loops of forming parameters. Since 1995 our I.A. has been combined with Mathematical Programming Techniques for the optimum design of axisymetrical or general 3D parts [5,6]. To our knowledge such optimum blank design procedures have not been described so far.

In this paper, we give a brief description of the I.A. and present some recent developments : the bending effects are considered using a simple triangular shell element

without increasing the number of degrees of freedom (dof) ; an initial (starting) solution method and a damping factor are implemented to reduce the iteration number and improve the robustness of the resolution procedure. In the shape optimization part, we present the procedure coupling the I.A. and SQP using an adjoint variable method for the sensitivity computations. The objective functions, design variables and limitations are also discussed. The results of an industrial problem are presented.

2. Brief description of I.A. including bending effects

Our I.A. including bending effects has been presented in detail in [7,8,11]. Only the basic ideas and assumptions are given in this paper. The I.A. is based on the knowledge of the final workpiece shape. Starting with a finite element mesh on the final workpiece, we iterate to find the original node positions on the initial flat blank and then we calculate the strains, stresses and the thickness variations. The first estimation can be made by the simple vertical projection of the nodes, then the Newton -Raphson procedure is used to adjust the node positions in order to satisfy the equilibrium in the final workpiece.

Two basic simplifications are adopted : the deformation theory of plasticity based on the proportional loading assumption is used to avoid the incremental procedure of plastic strain computations; the contact-friction forces due to the tools (punch, die, blank holders) are replaced by nodal forces defined from the knowledge of the vertical reactions.

The bending effects are taken into account using the DKT12 shell element [8] which is composed of the CST membrane element and the DKT6 plate element proposed by Batoz and Dhatt. In the DKT6 element , the two virtual rotation components of the normal are expressed with linear semi- C^0 approximations in terms of the normal and tangential rotations at the three mid-nodes. Then the normal mid-rotations are expressed in terms of the transverse displacements using the Kirchhoff assumption. The DKT12 element has 3 translation displacements at the corner nodes and one tangential rotation at the mid-side nodes.

In the Inverse Approach, only two horizontal displacements per node are unknown (2 dof per node) since the vertical displacements and the rotations can be obtained easily from the knowledge of the final workpiece shape. The above basic ideas, assumptions and element model lead to a total, path-independent approach and to an efficient and robust finite element code. Since 1997 several international benchmark tests and industrial parts have been studied showing the advantages and limitations of the I.A.

3. Improvements in resolution algorithms

The inverse approach leads to highly nonlinear equation systems due to the large strains and elasto-plastic materials. To overcome the convergence difficulties several resolution algorithms have been developed and tested [9] such as the Newton-Raphson static implicit method, static explicit method, Levenberg-Marquardt method, dynamic explicit algorithm, dynamic relaxation method, dynamic viscous relaxation method,

Among these resolution methods, the standard N-R method appears to be very attractive (efficiency, simplicity, verification of equilibrium). However, it requires a good initial solution and a well-conditioned tangent matrix. One of our important improvements is to use a good initial solution. So far the initial guess for the solution was obtained by vertical node projection, but this simple guess leads to very large strains and stresses in the elements belonging to quasi-vertical walls of the workpiece. Therefore very small steps are needed to avoid divergence problems. Recently we develop a geometric mapping method to define a good initial guess : the nodes situated on the known mid-surface of a 3D workpiece are mapped on the horizontal plane along the radial directions from the gravity center of the workpiece. This initial guess considerably reduces the number of steps and the CPU time.

The large strains and weak material hardening often induce an ill-conditioned tangent matrix and convergence troubles. A relaxation factor ω is introduced to keep the solution within the radius of convergence and a positive damping factor λ is used to improve the conditioning of the stiffness matrix :

$$(\{K_T\} + \lambda^i \{I\}) \{\Delta U^i\} = \{R^i\} \quad (1)$$

$$\{U^{i+1}\} = \{U^i\} + \omega^i \{\Delta U^i\} \quad \text{with } (0 < \omega^i \leq 1) \quad (2)$$

The norm of the residual forces $\|\{R\}\|$ is a very complicated function in terms of ω^i . A line search technique is used to find ω^i minimizing $\|\{R\}\|$.

4. Shape optimization procedure

The size and shape of the blank have both a great influence upon the quality of the workpiece. When the blank is too large, the material flow into the die cavity is limited and the risk of the excessive thinning (necking) increases. On the other hand, a too small blank size can cause wrinkling problems. For practical applications the thickness is a good indicator of the formability of the workpiece since a thickening is often correlated with wrinkling and a thinning may lead to rupture (necking). These considerations are relevant for the definition of the objective function F of our optimization problem which can be stated as:

$$\min F(\mathbf{v}) = \left(\sum_e^{\text{net}} (h^e - h_0)^p \right)^{1/p} \quad (3)$$

$$\text{with } \mathbf{c}(\mathbf{v})=0, \mathbf{g}(\mathbf{v}) \leq 0, \mathbf{v}_l \leq \mathbf{v} \leq \mathbf{v}_u, \mathbf{v} \in \mathbb{R}^n \quad (4)$$

where h_0 and h^e are the initial and final thickness of an element, \mathbf{v} is the vector of design variables, \mathbf{c} and \mathbf{g} are equality and inequality constraints, \mathbf{v}_l and \mathbf{v}_u the lower and upper geometrical constraints (bounds). The use of $p=1$ consists in minimizing the sum of the thickness variations on the whole workpiece ; the high order powers ($p=2,4,8,\dots$) allow to reduce the most important thickness changes (peaks). Other objective functions have been considered in [5, 6].

The design variables are the positions of the curve control knots describing the workpiece contour (Fig.1). A parametrization with a B-spline curve is used to reduce the number of design variables. Some limitations on the design variables are introduced in order to satisfy technological requirements. At each optimization iteration, the objective function, constraints and sensitivities are computed using the strains and stresses obtained using I.A. which has the advantage of low computer time with acceptable accuracy. A Sequential Quadratic Programming method is used as optimization algorithm. This algorithm is quite robust and efficient for optimization with a small number of variables and highly non linear constraints. The sensitivity calculation is based on the differentiation of the equilibrium equations of the I.A and the adjoint variable method. The analytical formulas implemented in the optimization procedure give the accurate gradients with a small amount of computer time.

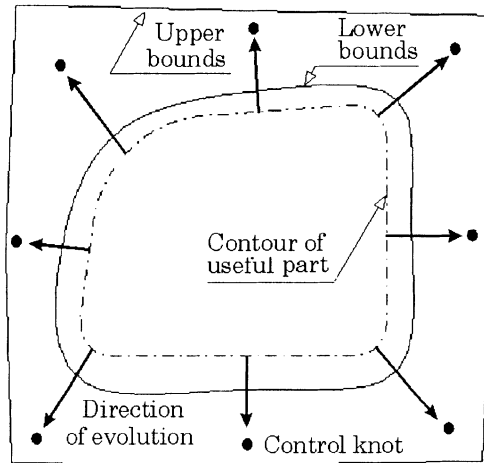


Figure 1. Parametrization of the contour with eight design variables

The optimization process starts with a preliminary workpiece contour. A nonlinear analysis is carried out using the I.A. in order to obtain the thickness, strain and stress distributions. Using these results, the objective function, constraints and gradients are evaluated. Then the optimization algorithm updates the set of the design variables. The iterative process continues, producing a succession of designs, until an optimal workpiece contour is achieved. It is also possible to optimize directly the contour of the initial blank and compute the corresponding contour of the workpiece.

5. Blank shape optimization of the TWINGO DASHPOT CUP

The optimum design of the blank contours of axisymmetrical parts and square cups has been considered in previous papers [5, 6] before considering more difficult industrial problems.

The TWINGO dashpot cup was presented as an industrial test for sheet forming analysis [10] (Fig.2). The workpiece is produced with a rectangular blank (Fig.5) and this case is taken as the reference for the comparison of the results (thickness variations). The blank holder is flat but inclined. The material data are : $E=206.8$ Gpa, $\mu=0$ (friction), $h_0=1.97$ mm, $\bar{r}=0.995$ (anisotropy), $\sigma = 624(0.007 + \epsilon_p)^{0.167}$ Mpa .

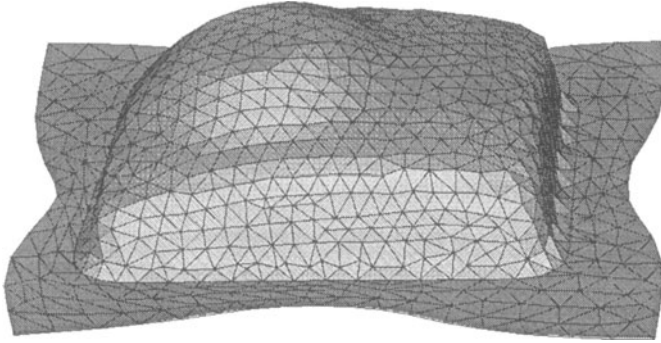


Figure 2. TWINGO dashpot cup obtained by the I.A. with a rectangular blank

Our finite element mesh consists of 1634 elements. An important thinning (-20%) was found in the punch zone by our I.A. (Fig.5). For the optimization calculation, we consider the lower bound as the preliminary solution for the design variables. The contour of the workpiece is defined by a B-spline curve using eight design variables : the positions of the control knots along the normal directions of the contour (Fig.1).The CPU time for an optimization calculation is about 2 hours on a HP J280 (PA8000) workstation. The evolution of the objective functions is shown in Fig. 3. About 10-20 iterations are needed to reach the convergence. The variations of the thickness and sheet volume for $p=1, 2, 4, 8$ are presented in Table 1. A 16% reduction of the volume has been obtained using $p=8$. The optimal contours of the final workpiece corresponding to different values of p are given in Fig. 4. The optimal contours for $p=4$ and $p=8$ are quite close to the lower bounds but they give smaller thickness variations. The figures 5 and 6 show that the optimization allows to obtain a better thickness distribution with a smaller amount of material.

Table 1. Optimization results

	Rect. blank	Low. bound	P=1	P=2	P=4	P=8
$-\Delta h_{\max}$ (%)	-20.27	-13.28	-18.85	-16.55	-13.03	-12.92
$+\Delta h_{\max}$ (%)	+17.44	+17.87	+13.86	+13.09	+13.56	+13.41
Vol.(cm ³)	314	256	311	269	263	261

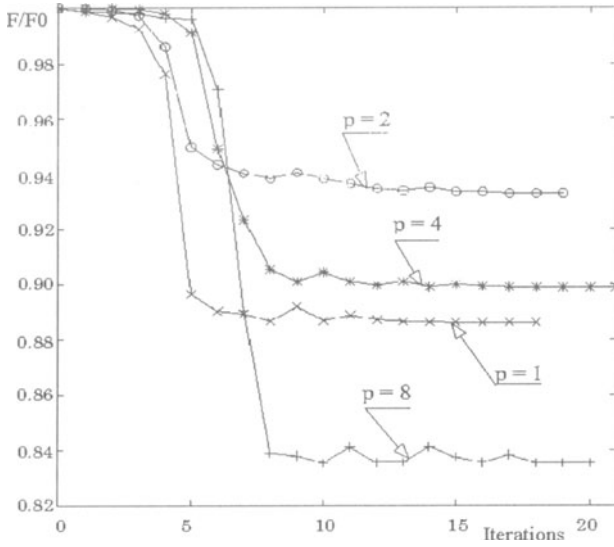


Figure 3. Evolution of the objective function ($p=1,2,4,8$)

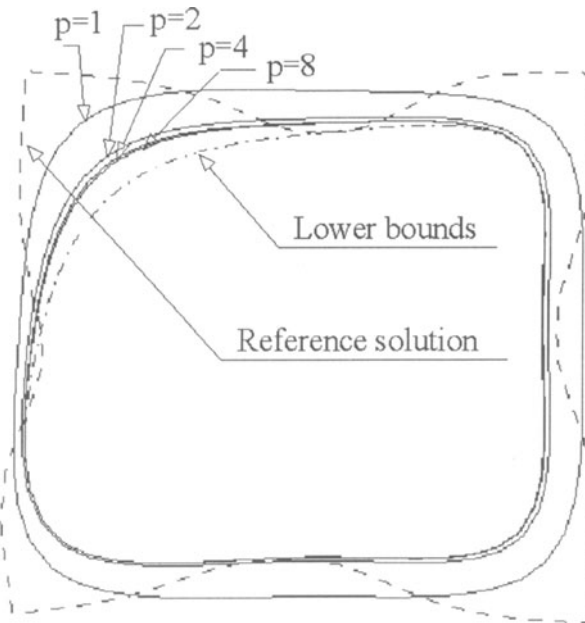


Figure 4. Optimum contours of the workpiece obtained with $p=1, 2, 4, 8$.

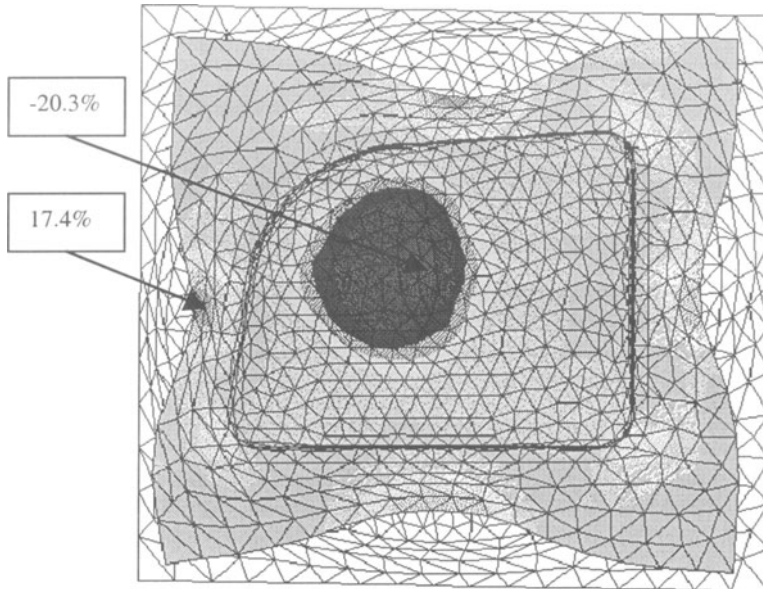


Figure 5. Thickness distribution obtained by I.A. with a rectangular blank (reference)

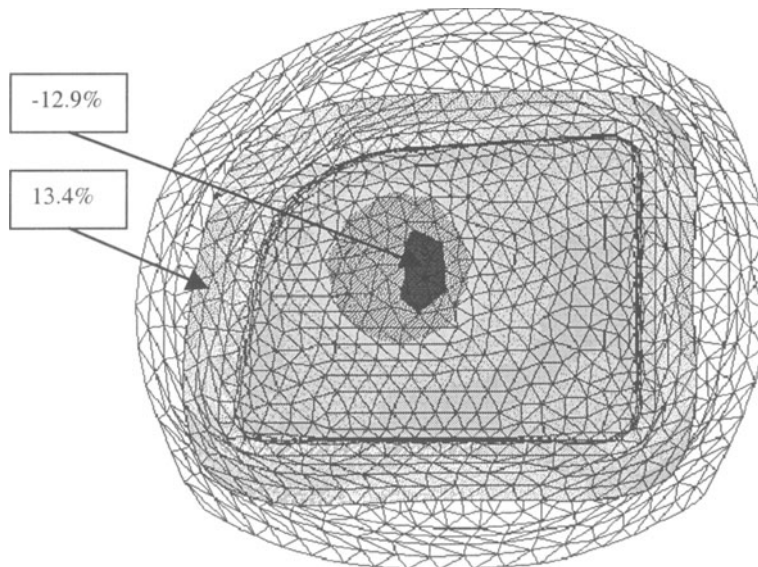


Figure 6. Thickness distribution obtained by blank shape optimization ($p=8$)

6. Concluding remarks

A simplified FE procedure called the Inverse Approach is used to quickly estimate the large elasto-plastic strains involved in the sheet forming process. The DKT12 shell element model is introduced without increasing the number of dof (only 2 dof per node). Some improvements in the N-R resolution procedure make the I.A. more efficient and robust. The results for recent international benchmark tests show that the I.A. is not only very efficient but also quite precise compared to available numerical and experimental results. An automatic procedure to optimize the blank shape is proposed. The analytical (explicit) computation of the sensitivities leads to a considerable reduction of CPU time in the optimization loop compared to a numerical (finite difference) approach. From the above satisfactory results, we believe that the I.A. combined with a mathematical programming algorithm appears to be a valuable tool for the automatic design of 3D industrial metallic blanks in deep drawing process. Other parameters (material properties, drawbead geometry) can also be optimized using similar procedures for the design of thin walled products and the corresponding tools.

7. References

1. S.F. Shen et al. Eds, *Simulation of material processing : theory, methods and applications*, NUMIFORM'95, Balkema, Rotterdam, Brookfield, 1995.
2. J.K. Lee et al. Eds, *Numerical Simulation of 3D Sheet Metal Forming Processes, Verification of Simulations with experiments*, NUMISHEET'96, Ohio State University, Dearborn, Michigan, 1996.
3. Y.Q. Guo, J.L. Batoz, J.M. Detraux, P. Duroux, Finite element procedures for strain estimations of sheet Metal forming parts, *Int.J.Num. Meth. Eng.* Vol.30, p1385-1401, 1990.
4. D.R.J. Owen et al. Eds, *Computational plasticity - Fundamentals and Applications*, COMPLAS V, CIMNE, Barcelona, Spain, 1997.
5. O. Barlet, J.L. Batoz, Y.Q. Guo, F. Mercier, H. Naceur, C. Knopf-Lenoir, The inverse approach and mathematical programming techniques for optimum design of sheet forming parts. *ESDA'96*, 3rd Biennial European Joint Conf. on Eng., Montpellier, 1996.
6. O. Barlet, J.L. Batoz, Y.Q. Guo, F. Mercier, H. Naceur, C. Knopf-Lenoir, Optimum design of blank contours using the inverse approach and mathematical programming techniques. *J.K. Lee et al. Eds, NUMISHEET'96*, 1996.
8. J.L. Batoz, Y.Q. Guo, Analysis and design of sheet forming parts using a simplified inverse approach, *COMPLAS V*, Barcelona, pp.178-195, 1997.
8. J.L. Batoz, Y. Q. Guo, F. Mercier, The inverse approach with simple triangular shell elements for large strain predictions of sheet metal forming parts, *J. Engineering Computations* Vol. 15, n° 6, 7, p. 864-892, 1998.
9. X.B. Hu, Y.Q. Guo, J.L. Batoz, Inverse Approach for sheet metal forming using explicit, implicit static and DR algorithms, *Advanced Technology of Plasticity*, 5 th ICTP, Columbus, USA, p.861-864, 1996.
10. M. EL Moutassim, B. Thomas, J.P. Jameux, E. DI Pasquale, An industrial finite element code for one step simulation of sheet metal forming. *NUMIFORM 95*, Balkema, Rotterdam, Brookfield, p 761-766, 1995.
11. Guo Y.Q., Batoz J.L., Naceur H., Bouabdalah S., Mercier F., Barlet O., "Recent developments on the analysis and optimum design of sheet metal forming parts using the simplified inverse approach", to appear in *Computers and Structures*, 1999.

SHAPE AND THICKNESS OPTIMIZATION OF AN AERONAUTICAL STRUCTURE MANUFACTURED USING AGE CREEP FORMING PROCESS

J.-P. BOURDIN*, J.-P. BONNAFÉ**, J. DELMOTTE***,
E. GROSJEAN***, J.-M. ROELANDT*

* *Université de Technologie de Compiègne, LG2mS, UPRES A 6066
Pôle Interrégional de Modélisation (Haute Normandie - Picardie)
BP 20529, 60205 Compiègne cedex, France*

** *AEROSPATIALE, Espace et Défense, Etablissement des Mureaux,
route de Verneuil, BP 96, 78133 Les Mureaux cedex, France*

*** *AEROSPATIALE, Centre de Recherche Louis Blériot
12, rue Pasteur, 92152 Suresnes cedex, France*

Abstract : We present a numerical method to optimize the age creep process for the manufacturing of spatial structures. In particular, we study the forming of Ariane 5 bulkheads. They are obtained by assembling eight segments which have to be a portion of sphere. Each one is formed by blowing a sheet against a die following a predetermined thermo-mechanical cycle (temperature and pressure). To take into account viscoplastic strains we have identified a non-isothermal Chaboche-Lemaître model.

The process optimization is done through iterative computations using ABAQUS software. It consists in the minimization of the gap between the deformed sheet and the final shape required and the cumulated plastic strain minimization. The optimization parameters define the shape and the thickness distribution of the undeformed sheet and the die geometry. Our numerical model enables to obtain a configuration that respects industrial specifications (geometry and toughness).

1. Introduction

This work concerns the age creep forming process of aluminium sheets for the manufacturing of spatial structures (Bonnafé *et al.*, 1996).

The process consists in applying pressure on a sheet of metal to maintain it in contact with the die. Simultaneously the temperature is increased following a predetermined cycle, that decreases the mechanical material characteristics and generates the development of irreversible viscoplastic deformations. After returning to room

temperature and the pressure being suppressed, the sheet keeps a residual curvature (Bourdin *et al.*, 1997).

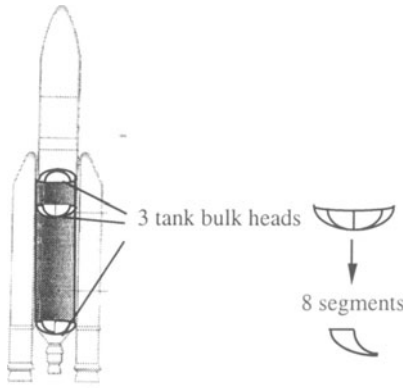


Figure 1. Ariane 5 bulkhead segments

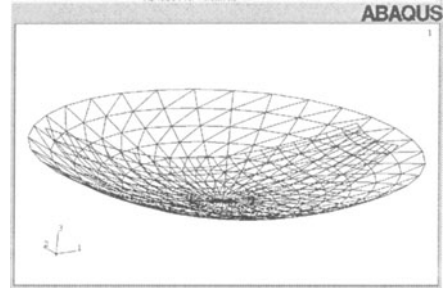


Figure 2. Die and deformed sheet

In particular, we study the forming of Ariane 5 bulkhead segments. They are obtained by assembling eight spherical segments (Fig. 1). The aim of our work is to study and optimize the age creep forming process so that the deformed shape becomes as close as possible to the targeted shape (ideally spherical segment in our case) (Fig. 2).

We first present the experimental and numerical approach that has been used to identify the chosen viscoplastic behavior law. Then we validate our mechanical model on a free blow up test. After that, we show the effect of the springback concerning the residual stress distribution in the formed bulkhead segments.

An iterative process to relocate the nodes has been used to optimize the shape of the die and the outline of the initial sheet.

Finally, we present the numerical method used to optimize the sheet thickness distribution, minimizing the maximum cumulated plastic strain

2. Visco-plastic model

2.1. IDENTIFICATION

The material behavior is described by an isotropical additive strain hardening-viscoplasticity model (Lemaître *et al.*, 1985). described by the following relations:

$$(\dot{\sigma}) = [D] \{ (\dot{\epsilon}) - (\dot{\epsilon}_p) \} \tag{1}$$

$$(\dot{\epsilon}_p) = \frac{3}{2} \dot{p} [P] \frac{(\sigma)}{J} \tag{2}$$



$$\dot{p} = \left\langle \frac{J - R(p) - k}{K} \right\rangle^N \quad (3)$$

$$R(p) = Q_1 p + Q_2 (1 - e^{-bp}) \quad (4)$$

where:

(σ): stress tensor, (ϵ): total strain tensor, (ϵ_p): viscoplastic strain tensor

$$p : \text{cumulated plastic strain defined by : } \dot{p} = \left(\frac{2}{3} \right) \dot{\epsilon}_p \left([P] (\dot{\epsilon}_p) \right)^{\frac{1}{2}}$$

$$J : \text{von Mises equivalent stress : } J = \left(\frac{3}{2} \right) \sigma \left([P] (\sigma) \right)^{\frac{1}{2}}$$

$$[P] = \frac{1}{3} \begin{bmatrix} 2 & -1 & 0 \\ -1 & 2 & 0 \\ 0 & 0 & 6 \end{bmatrix} \quad [D] = \frac{E}{1-\nu^2} \begin{bmatrix} 1 & \nu & 0 \\ \nu & 1 & 0 \\ 0 & 0 & \frac{1-\nu}{2} \end{bmatrix}$$

E: Young's modulus, ν : Poisson's ratio

k, K, N, Q_1, Q_2, b are six parameters depending of the temperature to be identified.

The process has to be achieved respecting a predetermined temperature cycle to obtain required material properties. To identify the model we used the tension-relaxation test. Two series of tensile specimens have been chosen, respecting the direction of the metal fibres or across. The tests have been completed at different temperatures and times of the process cycle (increase of temperature, flat part of the temperature curve, return to room temperature).

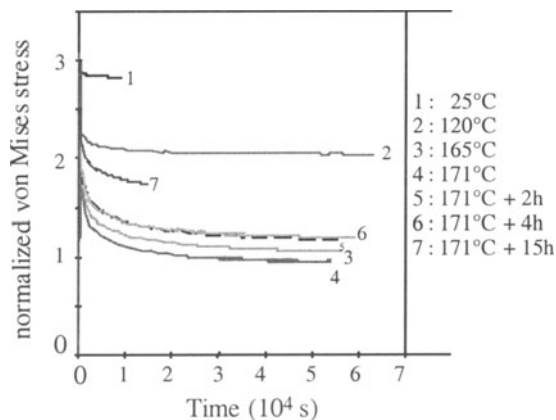


Figure 3. Tension-relaxation test corresponding to different times of the cycle for an imposed strain.

For all these times, different strain values have been tested. SiDoLo software has been used [REV.93] to identify the parameters evolution during the age creep forming temperature and pressure cycle. In Fig.3 above, we represent the strain variation during the different times of the process cycle for an imposed strain (curves deduced from identified parameters).

2.2. MODEL VALIDATION: FREE BLOW UP TEST.

The application of this model to free blow up of a clamped rectangular sheet in a cylindrical hole (Fig.4) is presented here as a validation. Fig.5 shows the inelastic strain contour around the rupture.

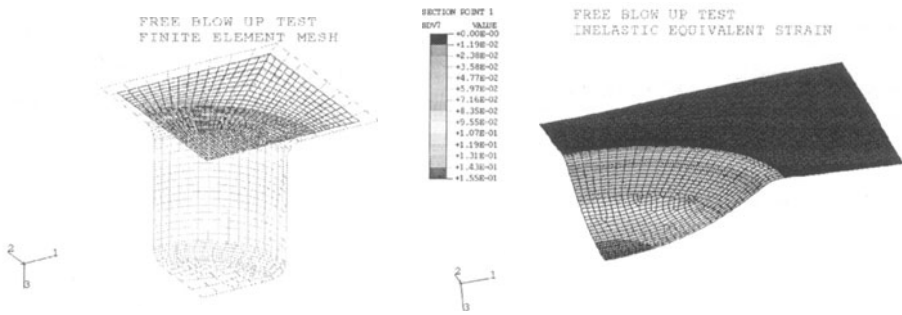


Figure 4. Free blow up test: sheet and tool discretizations Figure 5. Inelastic equivalent strain distribution

The simulation of that process is done in large transformations with evolving conditions of contact. We used ABAQUS/Std software to compute the deformed sheets that have been discretized using triangular and quadrangular shell elements taking into account the evolution of thickness and the transverse shear stiffness. Plastic strains are integrated by a Simo and Taylor scheme (Simo *et al.*, 1985) in a UMAT subroutine.

The simulation results are very close to the reality. Experiments and the corresponding simulations have been achieved and compared.

The values of sheet center deflection and thickness, were checked. In every case the error between modelization and experiment was far less than 5% (see Tab.1 for an illustration of two examples).

TABLE 1. Comparisons between experiments and numerical simulations.

Example	center deflection (mm)	center thickness (mm)
First example modelization	15.7	0.466
First example experiment	16.8	0.455
2d example modelization	13.7	0.492
2d example experiment	13.2	0.94

3. Age creep forming process simulation

We have simulated the age creep forming process of one eighth Ariane 5 bulkhead segment using a spherical die discretized with rigid elements and a half deformed segment (symmetrical) discretized with shell elements taking into account the decrease of thickness from the edge to the center (Fig. 1). This simulation corresponds to a constant thickness distribution in the segment central part. Von Mises equivalent stress in the deformed sheet can then be computed for the half sector and is shown in the following Figures 6 and 7 for two steps corresponding to the maximum pressure applied and the end of the process. Von Mises equivalent stress at the end of the process is less than 141 MPa; and less than 50 MPa in the greater part of the sheet.

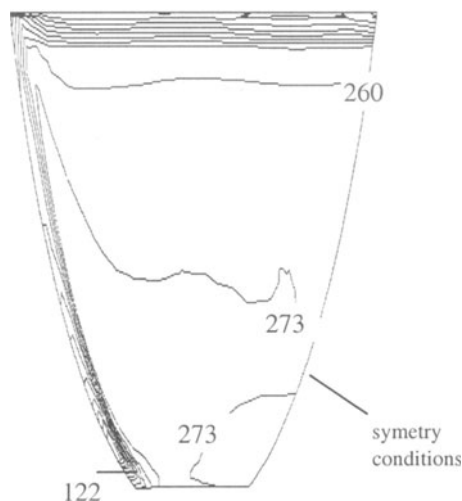


Figure 6. Von Mises equivalent stress corresponding to the maximum of the pressure.

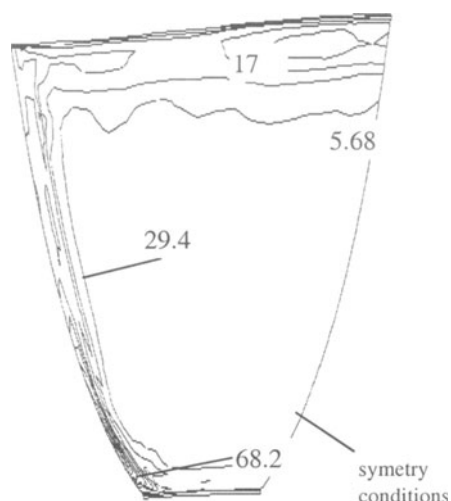


Figure 7. Von Mises equivalent stress at the end of the process.

4. Shape optimization

4.1. OVERVIEW OF THE PROBLEM

The final springback has been taken into account to optimize the initial shape of the sheet and the die. The objective function is representative of the gaps between the theoretical and the numerical shapes, using curvature and edge straightness criteria applied to the deformed sheet. The optimization defines the shape of the die and the outlines and the thickness of the flat initial sheet in order to obtain a spherical formed segment with targeted outline and thickness.

We show the gap between the deformed sheet and the ideal shape before (Fig. 8) and after (Fig. 9) the optimization defined below. An automatic procedure to modify and

optimize the initial shapes and thicknesses of the sheet and the die has been programmed around the ABAQUS software.

4.2. SHAPE OPTIMIZATION OF THE SHEET AND THE DIE

We have used an automatical procedure of nodes relocalization to optimize the shapes of the die and the outline of the initial sheet. We have studied an example in which datas were :

- the initial die is spherical. Its radius is the ideal segment one ($R_{\text{idéal}}$).
- the initial sheet shape is a flat segment.
- the contact die-sheet is modelled by a Coulomb law.

The ideal deformed shape is a troncated spherical segment of 45 degrees with an ideal radius $R_{\text{idéal}}$. After each computation, to reach the ideal shape, we relocate the nodes that define the lower part of the die and the outline of the initial sheet.

From these datas, it redefines :

The position of the nodes of the die located under the sheet. The die geometry is parametrized with a three dimensionnall Bézier surface.

The position of the initial sheet edge nodes so that the deformed shape is coincident with the targeted segment.

4.3. RESULTS

This numerical procedure has reduced the gaps between deformed and targeted sheet more than 80 % on the curvature, and more than 95 % on the final position of the edges. Figures 8 and 9 show the reduction of the gap between deformed and targeted sheet (gaps are given in mm). These results have been obtained after 8 iterations of nodes relocalization for the die and 3 for the outline of the initial sheet.

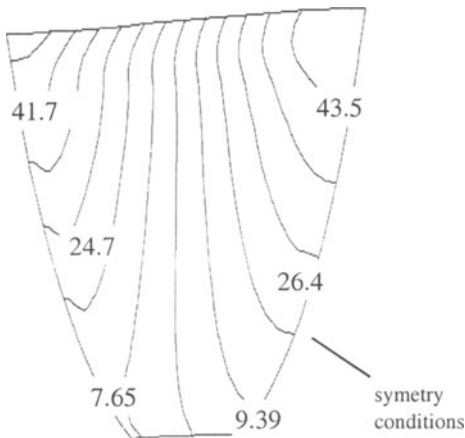


Figure 8. Initial gap (47.6 mm max) between the deformed sheet and the ideal one before optimization.

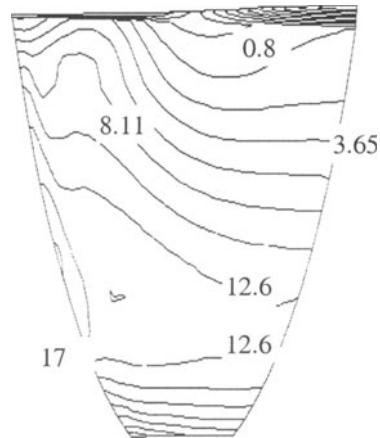


Figure 9. Final gap (0.63 mm max) between the deformed sheet and the ideal one after optimization.

5. Thickness optimization (strain minimization)

5.1. OVERVIEW OF THE PROBLEM

We want to minimize the maximum cumulated plastic strain which has to verify:

$$p \leq p_0 \quad (5)$$

When we use a constant thickness distribution, the cumulated plastic strain is too important and concentrated in a local area near the extra thickness of one of the edges (see Fig.10 above). The decrease of the maximum cumulated plastic strain is obtained by modifying the sheet thickness before forming. It has to remain between $e_{p_{\min}}$ and $e_{p_{\max}}$.

5.2. NUMERICAL SIMULATION

Every integration point P of an element of the initial sheet can be parametrized by its cylindrical coordinates (r, θ , z). For each integration point the thickness will be given by the following R and Θ polynomial:

$$e(R, \Theta) = \sum_{i=0}^m \sum_{j=0}^n a_{ij} R^i \Theta^j \quad (6)$$

with $R = \frac{r}{R_{\text{Idéal}}}$ and $\Theta = -4 * \frac{\theta}{\pi}$ so chosen to remain between 0 and 1

The parameters $(a_{ij})_{i,j \in I}$ have to be determined so that we can obtain the lowest maximal cumulated plastic strain.

The previous problem consists in minimizing the function $f((a_{ij})_{i,j \in I}) = E_{\text{plas max}}$.

where $E_{\text{plas max}}$ is the maximal cumulated plastic strain obtained in the deformed sheet with the parameters $(a_{ij})_{i,j \in I}$.

We add the following limitations :
$$\begin{cases} e_{p_{\min}} - \min(e(R, \Theta)) \leq 0 \\ \max(e(R, \Theta)) - e_{p_{\max}} \leq 0 \end{cases}$$

The minimization of the function is performed using the code FFSQP Version 3.6 for constrained nonlinear optimization problems. FFSQP implements two algorithms based on Sequential Quadratic Programming. Practically the gradients are obtained using the finite differences method.

5.3. RESULTS

We ran the shape and thickness optimization using an automatic procedure as many time as necessary. In our example the optimum was obtained after five optimization iterations. The reduction of the geometrical gaps and the maximum strain

in the deformed sheet are quite important. The decrease of strain is shown on the two following Figures 10 and 11.

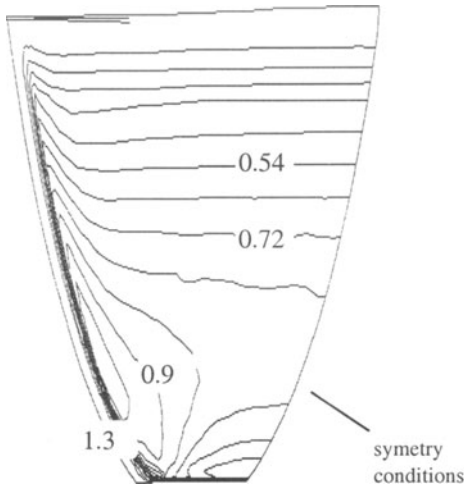


Figure 10. Strain ratio p / p_0 (max 1.3) in the deformed sheet before thickness optimization.

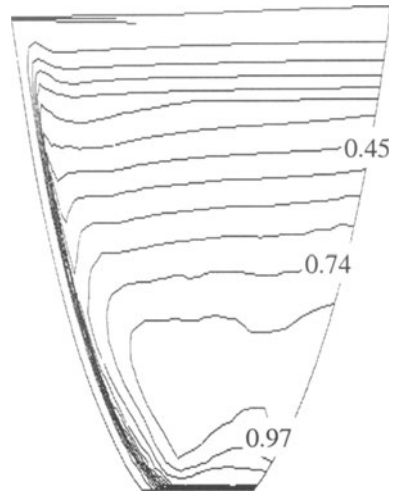


Figure 11. Strain ratio p / p_0 (max 0.97) in the deformed sheet after thickness optimization.

6. Conclusion

The implemented procedure allows to optimize the age creep forming process. This optimization procedure can be adapted to the simulation of other processes used in aeronautical applications. The next improvement of the age creep forming process could be the regulation of the temperature and pressure cycle.

7. References

- Bonnafé, J.P., C. Destandau & J. Fougeras (1996) Age creep forming process modeling and experimentation in aluminium alloys - Validation on Ariane 5 main tank bulkhead segments. *Proceedings of the 4th European Conference on Residual Stresses (ECRS4), Cluny France, june 1996.*
- Bourdin, J.P., J.P. Bonnafé, J. Delmotte, P. Revel & J.M. Roelandt (1997). Simulation numérique du procédé de formage-revenu de tôles en alliage d'aluminium. *3ème colloque national en calcul de structures, Giens, France.*
- Lemaître, J. & J.L. Chaboche (1985) *Mécanique des matériaux solides. Dunod editions.*
- Revel, P., M. Clavel, G. Beranger & P. Pilvin (1993). Mechanical properties and microstructural evolution of a cobalt base alloy coating. *Materials Science and Engineering.* A169: 85-92.
- Simo, J. C. & R. Taylor (1986) A return mapping algorithm for plane stress elasto-plasticity. *International Journal for Numerical Methods in Engineering.* 22: 649-670.

TWO COMPONENT FINITE ELEMENT MODEL FOR THE SIMULATION OF SHAPING OF PREPREG WOVEN FABRIC

A. CHEROUAT***, J.L. BILLOET** & S. BELHOUS**

* LASMIS - GSM University of Technology of Troyes BP 2060 10010 Troyes, France

** LM2S secteur ENSAM of Paris 151 Boulevard de l'Hôpital 75013 Paris, France

1. INTRODUCTION

Continuous fibre reinforced composites are now firmly established engineering materials for the manufacture of components in the automotive and aerospace industries. They offer design engineers enormous opportunities for introducing new design concepts whilst reducing costs. In this respect, prepreg gives flexibility in the composite shaping and is already playing an important role in increasing the use of advanced composites. The ability to define, in advance, the ply shapes and material orientation allows engineers to optimize the composite structural properties of the part for maximum strength, maximum material utilization and maximum lay-up efficiency.

The formulation of the new efficiency numerical models for the simulation of the composite shaping processes should make it possible to reduce the time needed to manufacture of complex pieces and to optimize costs in an integrated design approach. Actually, the prepreg composite corresponds to a structure composed of the combination of the yarn network and resin membrane.

Some models are proposed to homogenize elastic properties of a composite material and to simulate the deformation of these materials by forming process. Geometrical and micro-macro mechanical approaches are proposed in the literature to simulate the transformation of fabrics during the draping process Cherouat (1994), Gelin (1996) and Blanlot (1996). It is difficult to globally characterise, by homogeneous methods, the behaviour of this fabric without losing mechanical characteristics. The new numerical finite element model developed at a mesostructural level permits to take into account the various mechanics of physics of the mechanical transformation of prepreg fabrics during the shaping process, namely large angular variations of yarns, viscoelasticity of resin and evolution of possible damages in yarns. The different advantages of this modelling is first to give the ability to obtain a very good material orientation of yarns and consequently to introduce good data in the pre-processing of the calculation of the

final piece after polymerization, secondly to give the mechanical limits of the fabric during the forming process and to limit the falls of the fabric thanks to a better definition of the flat form. The forming process of prepreg woven fabric usually includes complex mechanisms which can have a significant effect on mechanical properties of the finished product.

The overall behaviour of prepreg composite is based on a finite strain membrane model and must take fabric weaving (geometrical undulation of yarns), fibre properties and resin behaviour into account. The development of a numerical model for prepreg woven fabric behaviour can be defined as :

1. the most appropriate weaving of the reinforcements for the forming process,
2. fibre positions in the composite structure,
3. the holding force of the composite during the forming deformation, and
4. the state of impregnated fabric (wrinkling, folding, fibre damage and resin strains).

The proposed model is described by meso-structural approach for finite strains and geometrical non linearities. The bi-component finite elements for modelling prepreg fabric behaviour are based on an association of 3D membrane finite elements representative of resin behaviour and truss finite elements representative of warp and weft fibres behaviour. The efficiency of the proposed model resides in the simplicity of its numerical formulation and the performance of its mechanical approach.

2. MESO-STRUCTURAL FINITE ELEMENT APPROACH

It is easily shown that a large rotation of the fibres is followed by straightening phenomena which intervene in the kinematic transformation of fabrics during the shaping deformation and determine the aptitude of prepreg woven fabrics to make up complex shapes. The shaping operation is strongly affected by the fabric behaviour, which is different from that of a conventional sheet metal.

The simulation of the shaping process is based on the numerical and mechanical approaches specific to the composite reinforced fabric behaviour. The meso-structural model is a 'biphase model' in which the elastic fibre and viscous resin components are treated separately. The fibres are assumed to be embedded in the resin and move with inter-fibre shear deformation. The proposed finite element makes it possible to model the deformation of composite fabrics by taking into account the various dominating mechanisms in the physics of the mechanical transformation of fabrics such as geometrical non linearity (large displacements and finite rotations of fibres), material non linearity (viscoelastic behaviour of resin in shearing, variation of fibres due to weaving of fabric) and contact with friction between tools and prepreg material.

In the numerical model, the behaviour of the fabric is represented by structural truss finite elements corresponding to the behaviour of warp and weft fibres and the resin is modelled by 2D membrane finite elements (Figure 1). The interaction effects and friction phenomena between fibres are negligible. The proposed bi-component finite elements can take into account geometrical non linearities such as large displacements and finite rotations of fibres, material non linearities such as viscoelastic behaviour of

resin in shearing and undulation of fibres due to the weaving of fabric. A co-rotational formulation associated with rigid body rotation, derived from the polar decomposition, is used to describe the kinematic motion and the deformation mechanism that woven material undergo during shaping process.

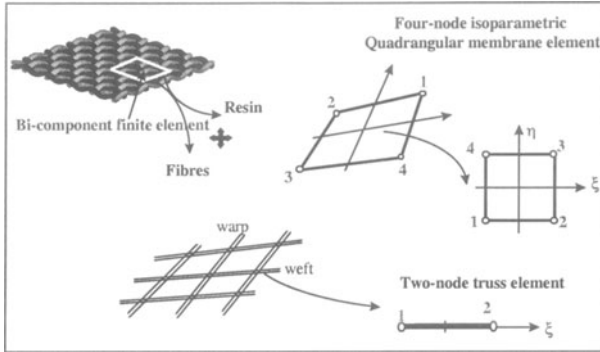


Figure 1. Two-component finite element for the simulation of mechanical behaviour of woven fabric

3. MODELLING OF PREPREG WOVEN FABRIC BEHAVIOUR

Large angular variations of yarns, viscoelasticity of resin and evolution of damage in yarns are the main mechanical mechanisms which control the shaping process of impregnated fabric. The kinematic transformation of impregnated material in large displacements and finite strains is based on the following assumptions :

A1 : Non-sliding inter-fibre during the shaping process can be experimentally observed by the following transformation of aligned straight lines drawn on the fabric. For each point of continuum material the current position is defined in current configuration by

$$\vec{x}^{fibres} = \vec{x}^{resin} = F\vec{X}^{fibres} = F\vec{X}^{resin} \quad (1)$$

F describes the deformation gradient of the composite fabric.

A2 : The current longitudinal orientation of each fibre $\vec{n}_L^f(F, \theta_0)$ is calculated from the geometrical transformation defined by the linear application

$$\vec{n}_L^f(F, \theta_0) = \frac{F\vec{N}_L^f(\theta_0)}{\sqrt{\vec{N}_L^f(\theta_0)^T F^T F \vec{N}_L^f(\theta_0)}} \quad (2)$$

A3 : The shear angle deformation of fibres can be associated with the rotation of the rigid body of the fibre. This assumption can be written using the following kinematic relation

$$\vec{N}_L^f(\theta_0) \cdot \vec{N}_T^f(\theta_0) = \vec{0} \Rightarrow \vec{n}_L^f(F, \theta_0) \cdot \vec{n}_T^f(F, \theta_0) = \vec{0} \quad (3)$$

Considering the previous assumptions in the proposed model, we introduce a new pseudo-gradient of transformation **F'** as a function of the gradient of transformation of composite fabric **F** (Figure 3). The motion of different material points of fibres are defined in the current configuration by

$$\begin{cases} F^f = \lambda_i^f n_i^f \otimes N_i^f & \text{fibres} \\ F^m = F = RU^m & \text{re sin} \end{cases} \quad (4)$$

The non linearity of the shaping problem imposes the use of incremental formulation. The spatial velocity gradient in the current configuration, is expressed in a reference frame by

$$\begin{cases} L^f = \dot{F}^f F^{f-1} = \frac{\dot{\lambda}_i^f}{\lambda_i^f} n_i^f \otimes n_i^f + \dot{n}_i^f \otimes n_i^f & \text{fibres} \\ L = FF = D + W & \text{re sin} \end{cases} \quad (5)$$

and in the rigid body rotation frame as

$$\begin{cases} \bar{L}^{fR} = \frac{\dot{\lambda}_i^f}{\lambda_i^f} N_i^f \otimes N_i^f = \bar{D}^{fR} + \bar{W}^{fR} & \text{fibres} \\ \bar{L}^R = R^T L R + \dot{R}^T R = \dot{U} U^{-1} = \bar{D} + \bar{W} & \text{re sin} \end{cases} \quad (6)$$

The constitutive equations for finite-strains use objective derivatives. In a above equations the rotation rate of the local frame in which a simple derivative would give objective derivative is defined by Green-Naghdi's co-rotational formulation. To characterise the objective behaviour of the fabric, the stretching tensors are written in the rigid body rotation frame as

$$\begin{cases} \bar{D}_L^f = \begin{pmatrix} \dot{\lambda}_L^f \\ \lambda_L^f \end{pmatrix} & \text{fibres} \\ \bar{D}^R = \bar{L}^R & \text{re sin} \end{cases} \quad (7)$$

Using Kirchhoff's and Green-Naghdi's tensor stress, the stress rate in the fibre and the resin can be written at any time by :

$$\begin{cases} (\bar{\sigma}_L^{fR})_{n+1} = (\bar{\sigma}_L^{fR})_n + \int_{t_n}^{t_{n+1}} E_L^f(\lambda_L^f) \frac{\dot{\lambda}_L^f(\tau)}{\lambda_L^f(\tau)} d\tau & \text{fibres} \\ (\bar{\sigma}^{mR})_{n+1} = (\bar{\sigma}^{mR})_n + \int_{t_n}^{t_{n+1}} C^m(\tau) \bar{D}^R d\tau & \text{re sin} \end{cases} \quad (8)$$

The internal vector load is defined by summation of elementary forces which are function of Cauchy's stresses, material surface area S and normal vector to the surface \vec{n}_s

$$\begin{cases} \vec{f}^{fibres} = \sum_{fibres} \int_{S^f} \bar{\sigma}^{fR} \vec{n}_s dS & \text{fibres} \\ \vec{f}^{re sin} = \int_{S^m} \bar{\sigma}^{mR} \vec{n}_s dS & \text{re sin} \end{cases} \quad (9)$$

The behaviour of prepreg woven fabric in a non-polymerized phase is obtained by superimposing the membrane behaviour of the resin and the behaviour of each fibre in the material frame :

$$\vec{f}^{comp} = \sum_{elts S^m} \int \bar{\sigma}^{mR} \vec{n}_s dS + \sum_{warp S^f} \int \bar{\sigma}_{warp}^{fR} \vec{n}_s dS + \sum_{weft S^f} \int \bar{\sigma}_{weft}^{fR} \vec{n}_s dS \quad (10)$$

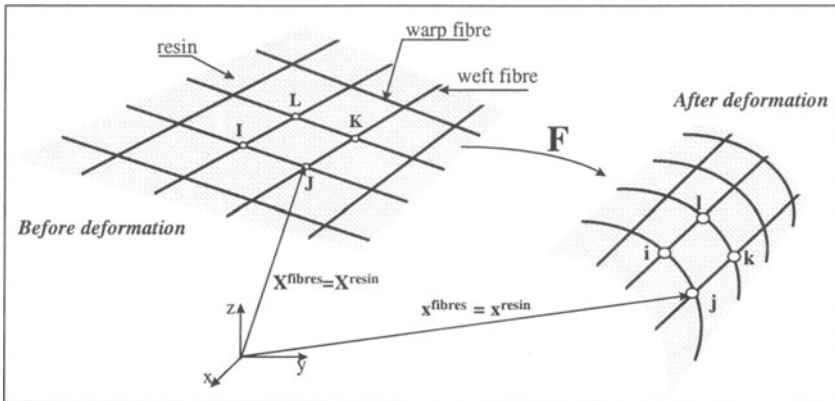


Figure 2. Geometrical transformation of fibre-resin linkage points

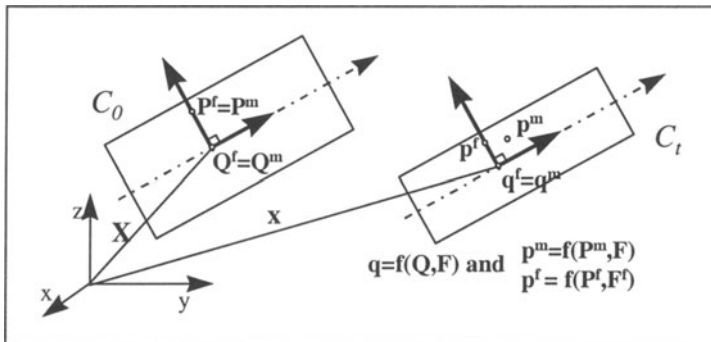


Figure 3. Geometrical transformation of the woven fabric and-resin material point

4. NUMERICAL SIMULATION OF SHAPING PROCESS

To validate the proposed approach for the mechanical behaviour of the prepreg woven fabric and the computational finite element modelling, some numerical simulations were carried out. The laying-up of prepreg fabric on a non developable surface was built inside our laboratory in order to cover hemispherical surface (Figure 4) Blanlot (1996). The numerical simulation is carried out with Abaqus software using an explicit formulation. With the numerical simulation, we can visualize fibre orientations and ply shapes after the forming process and predict manufacturing problems.

4.1. SIMULATION OF LAYING-UP SHAPING PROCESS

An initially square non polymerized woven fabric made of carbon fibre (350 x 350 mm) is draped on a hemispherical surface ($r = 120$ mm). Eight loaded springs are used to maintain the fabric during the shaping transformation. The formability of composite fabric during the laying-up process is tested by using two directions of fibres $\pm 45^\circ$ (Figure 5a) and 0° (Figure 5b). The final experimental shapes for a 300 mm displacement of the mould are shown in Figure 6a for $(-45^\circ, +45^\circ)$ fabric deformation and in Figure 6b for $(0^\circ, 90^\circ)$ fabric deformation. We can notice that these shear angles values are very large ($>40^\circ$) along the diagonal line for the $(0^\circ, 90^\circ)$ fabric on Figure 8 and along the median line for the $(-45^\circ, +45^\circ)$ fabric Figure 7. These numerical results show that the proposed finite element model takes into account the highly anisotropy of fabric behaviour.

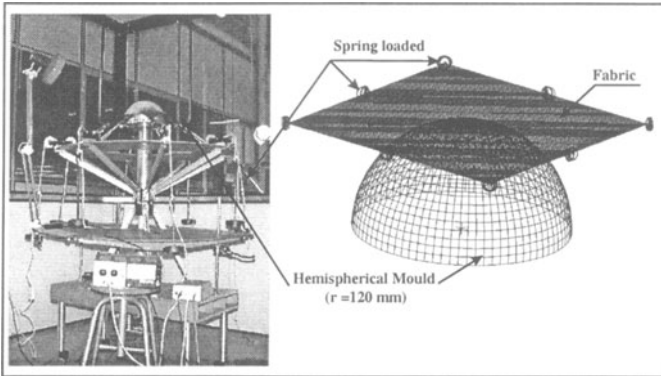


Figure 4. Laying up on the hemisphere



Figure 5. Experimental shape obtained with woven fabric $\pm 45^\circ$ (a) and 0° (b)



Figure 6. Simulation shape obtained with woven fabric $\pm 45^\circ$ (a) and 0° (b)

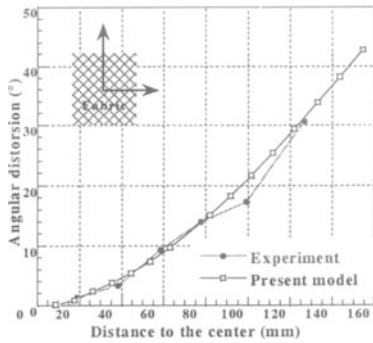


Figure 7. Angles between yarns on the median $\pm 45^\circ$

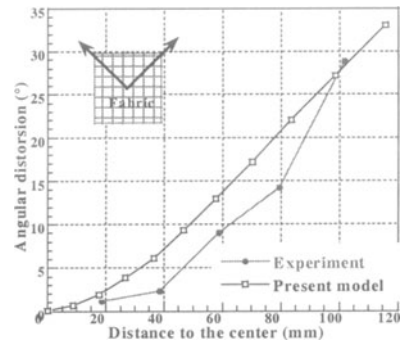


Figure 8. Angles between yarns on the median 0°

4.2. SIMULATION OF DEEP DRAWING PROCESS

An initially square blank (280 x 280 mm) and a circular blank ($r = 140$ mm) made of a glass fibre are shaped into a square box (Figure 9). The forming process of composite fabric usually includes large angular variation of the warp and the weft directions which can have a significant effect on the mechanical properties of the finished product. Results of simulations of the shaping operation are shown in Figure 10. Figures 11 and 12 show the shear angles of the fibres for three sets of radius (5, 10 and 15 mm) for the punch. These radii mainly influence the maximum values of the angular variations of the fibre directions. The square blank leads to shear angles greater than 80° which values cannot be used for the fabric. On the contrary, the circular blank leads to shear angles smaller than 60° and the shaping operation appears to be possible.

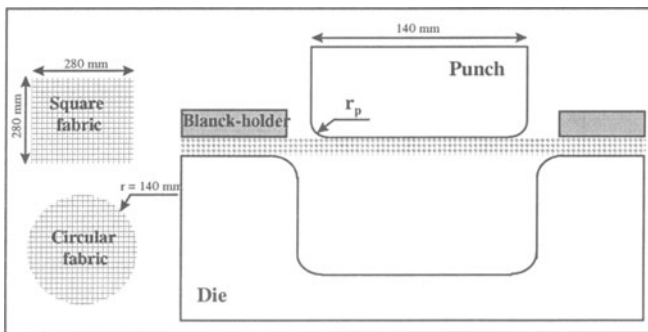


Figure 9. Trial of punch-drawing

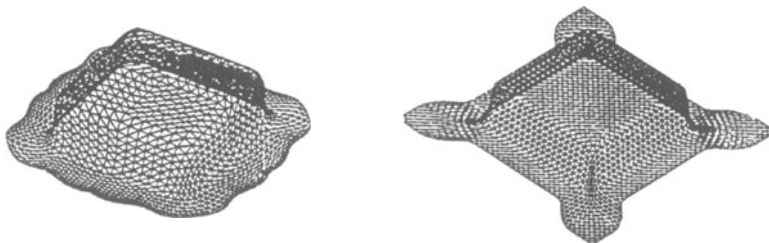


Figure 10. Simulation shape obtained with circular (a) and square woven fabric 0° (b)

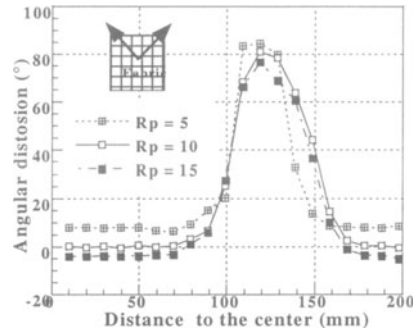
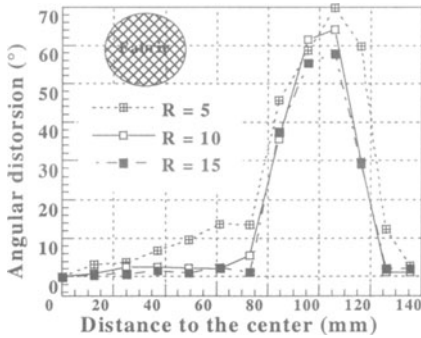


Figure 11. Angles between yarns on the circular diagonal Figure 12. Angles between yarns on the diagonal square

5. CONCLUSION

A numerical mesostructural approach is proposed for modelling the behaviour of the preimpregnated composite fabric. Numerical examples show the concordance of the computed final shapes and relative distortions between fibres with experimental ones. The numerical results of shaping processes (deep drawing and laying-up) prove the validity of the proposed formulation. The numerical tool is an efficient means of evaluating factors related to manufacturing process and an efficient help to design a preforming sequence for manufacturing fabric reinforced composites. It is possible to detect the main defects occurring during the shaping deformation in order to obtain good, quantitative information on the forming process and to pre-determine the mechanical properties of the composite parts and tool shapes.

Extensions of the numerical model have been carried out with a view to take the viscoelasticity of the resin and the undulation of fibres into account.

6. REFERENCES

- Billoët, J.L. (1996), Contribution à la compréhension des problèmes en grandes transformations, rapport interne LM2S ENSAM Paris.
- Blanlot, R. & Billoët, J.L. (1996), ICCE/3 New Orleans USA, 117-118.
- Boisse, P., Borr, M., Buet, K. & Cherouat, A. (1997), Finite Element simulation of textile composite forming including the biaxial fabric behavior, Composite Part B Engineering Journal, N° 28, 453-464.
- Cherouat, A. (1994), Simulation numérique de l'emboutissage des tissus de fibres de verre par la méthode des éléments finis, PhD thesis, University of Franche-Comté Besançon France.
- Cherouat, A., Gelin, J.C., Boisse, P. & Sabhi, H. (1995), Modelling the glass fiber fabrics process by the finite element method; Revue Européenne des Eléments Finis, Vol. 4 N° 2, 195-182.
- Dhat, G. & Batoz, J.L. 990), Modélisation des structures par éléments finis, Tome 2 et 3, Edition Hermès, Paris.
- Gelin, J.C., Cherouat, A., Boisse, P. & Sabhi, H. (1996), Composite Sciences and Technology, 56, 711-718.
- Gilormini, P. (1993), A.C. Académie des Sciences Paris, 316, Série II, 1153-1159.
- Hibbit, Karlsson & Soresen (1995), ABAQUS theory, User's Manual Version 5.5.

A SENSITIVITY ANALYSIS FOR THE SPRING BACK OF THE ARCHED TUBES

J.C. DJENI^{*}, P. PATOU[♦], H. SHAKOURZADEH^{*}, V. BRAIBANT[‡]

* Pôle Universitaire Léonard de Vinci
12, Avenue Léonard de Vinci
Département Mécanique des Systèmes
92916 Paris La Défense CEDEX
France

♦ SOLLAC / FOS
Centre de Recherches
ZA 13776 FOS-SUR-MER CEDEX
France

‡ MECALOG
2 rue de la Renaissance
92184 ANTONY Cedex

Abstract

As well as sheet metal, the tube is an intermediate product which should be formed, covered and assembled. Among all of the known processes of tube forming as bell mouth, burnishing, ovalization, bending, it is this last one which is more often used. However, in industry, the use of this process causes some problems such as the flatness of the elbow, risks of failure on the outer face, the crumpling on the inner face and finally the spring back. Understanding spring back for the arched tubes constitutes a major problem for every tube manufacturer. Even when the allowable fluctuations are limited to tenth of degrees, angular fluctuations of several degrees are usually observed. This indicates the importance of the problem.

The aim of this study is to understand the role of material characteristics in the spring back of bent tubes. The first stage of the this work consists in determining analytical, semi-analytical, numerical or even empirical models in order to formulate the spring back. These models are then validated by experimental tests. In the second step, an analysis of sensitivity is carried out in order to determine the influence of various parameters like the geometry, the process, or material.

1. Introduction

The objective of tube bending is to deform the tube in a permanent way. The various techniques of bending aim at resolving the problems which occur in the course of bending such as necking, wrinkling, ovalization or flatness. Those are solved overall

thanks to the means of tube supports during the operation of forming. However, spring back (a phenomenon which appears at the end of the bending) remains always an insoluble problem depending on a certain number of influential factors. The spring back appears in other manufacturing processes like stamping. It is a quasi linear phenomenon which proceeds from the elastoplastic behavior of steel. It is due to the existence of residual stresses. The principal problem arising from the spring back in the manufacturing process of the curved tubes, is in the control of scattering. The bibliographical studies point out that the influential factors on the spring back and its scattering were especially studied in the case of sheet metal forming. In particular the characteristics related to the base metal, with its geometry and those related to the process of forming (force and speed of punch) can be distinguished. In a concrete way, the more the time of load (the force is supposed to be constant) is important, the more the spring back (as like as its scattering) decreases. To make the process of bending reliable, the expert should be ensured that according to the batch of tubes in its possession, scattering of spring back will not exceed a certain tolerance level. Consequently, a sensitivity analysis of the engaged parameters during the process of bending is necessary. The first stage of the work thus consists in finding analytical, semi-analytical, numerical or even empirical models in order to formulate the spring back. These models are then validated by experimental tests. In second stage, a sensitivity analysis is carried out in order to determine the influence of various parameters like the geometry, the process or the material. This study shows the important role of the bending process and in particular the precision of the machine tool on the spring back. It confirms that the role of material is little compared to other influential parameters.

2. Objectives

The objective of this study is composed of three parts:

i) develop and/or adapt an analytical model of the spring-back estimation having as input variables the tube characteristics, ii) carry out a Monte-Carlo analysis allowing to obtain the spring back scattering from those of the tube, iii) reverse approach aiming at specifying new tolerances on the tube from a known scattering (and allowable) on the spring back. We present only the first two parts in this paper.

3. Bending of tubes

3.1. PROCESSES OF BENDING

Techniques of bending can be classified in two categories: the hot and the cold processes. The choice of one approach or the other depends on the nature of the arch to be realized and its operational limits. The cold processes are used when a large ray of curved tube is needed. Various methods of cold bending are shown by Djeni (1997). Hot bending is necessary and essential when the ray of bending is short or when tubes of large diameter are used. Beyond the expensive costs, the hot processes require care (to realize).

3.2. MECHANICAL ASPECTS OF BENDING

Mechanically, the bending of tubes results from the superposition of traction and bending stresses which lead to a displacement of the neutral fibre towards the interior. The original circular sections of the tube will be flattened and become elliptic. Indeed, the moment of inertia of the cross-section is not constant any more. This reduction of cross-section involves a substantial fall of the normal constraint in fibres far away from the neutral axis. The simulation tools can be used in order to determine the limits of tube formability and to study mechanical instabilities. Geometrical instabilities are related to the constraints imposed on the tube in the course of forming. They generally appear by the necking in the outer-surface, wrinkling in the inner-surface or the ovalization (flatness) of the sections. These instability problems are solved thanks to techniques of internal tube support during the bending operation.

4. Spring back

Under the bending moment imposed by the machine, the tube yields an angle α_0 . When this effort is not maintained any more, the tube is slackened and the aperture passes to a value α_f different to α_0 (fig. 1). It is thus an unbending. The spring back is not a phenomenon inherent in bending only. It appears for example during a simple tension test or a folding operation when the imposed forces are suspended. Generally, it is a quasi linear phenomenon which proceeds the elastoplastic behavior of steel. In a welded tube, the spring back results from the elastoplastic behavior of material, the desovalisation of the cross-sections, and the residual stresses. The spring back can be interpreted using the SACHS coefficient noted S. This coefficient is equal to the ratio of the angles α_f after spring back and α_0 before, so $S = \alpha_f / \alpha_0$. It is also common to use the difference $\Delta\alpha = \alpha_f - \alpha_0$. The values of $\Delta\alpha$ highly depend on the mechanical characteristics of the metal, the geometrical characteristics of the requested element (sheet, tube), the characteristics of process as the speed of forming, dieing forces, lubrication, etc.

4.1. DEVELOPMENT OF A SPRING BACK MODEL

The interactions between the factors engaged during operations of folding, as analyzed previously, justify that we cannot calculate the spring back with precision. An order of magnitude seems more suitable.

Some analytical or semi-analytical models were proposed for the case of the sheet folding. These models use especially the mechanical and geometrical characteristics of sheet and a process parameter (the ray of folding). In the case of Queener and De Angelis (1968) models and also those of Gardiner cited by Marron and Bou elier (1994), an expression of the Sachs coefficient is provided which is easily usable for calculations. The results of the Queener and Gardiner models were compared with experimental tests on rectangular test-bars (100x70 mm) by Djeni (1997). The comparison shows that the results of the models are in agree with the experiments and the Queener's model is more precise. The Queener's model takes into account the work hardening of the material by using the Hollomon work-hardening law. The Sachs coefficient is expressed in the form:

$$S = 1 - \left\{ \frac{3.k.(1 - \nu^2)}{E.(n + 2).(0.75)^{(n + 1)/2}} \right\} \cdot \left\{ \frac{2.R_0}{e} \right\}^{1 - n} \tag{1}$$

where ν is the Poisson’s coefficient, k the load factor, n the work-hardening coefficient, E the Young modulus, R_0 the initial ray of folding and e the thickness of sheet.

On the other hand for tube bending few models exist in the literature. In the case of bending by rolling up, the model of the Sumitomo group presented by Akiyama et al. (1989), makes possible to consider the initial ray to give to the bending tool by introducing the ray of the tube after spring back. Its principle idea includes two stages: (i) the deduction of the behavior law of the tube by traction and compression tests (with the Bauschinger effect), (ii) the modeling of bending and spring back by taking into account the position of neutral fibre only. This approach of the Sumitomo group is original because it does not use any bending test. Moreover, it integrates all of the stiffness changes due to the tubification (effects of the weld bead and the rolling thus the residual stresses). However, it should be noted that we have not enough information neither on the type of used constitutive law, nor on the angles of bending. Indeed the implementation of the method requires the results of traction and compression tests on the tubes which are not available. In the case of our study where we are interested in the analysis of reliability of the spring back, the method of Sumitomo group is not very usable and the development of the analytical models seems necessary.

4.2. AN ANALYTICAL MODEL FOR THE SPRING BACK

Here, we propose an analytical model for the spring back of tubes according to the method suggested by Queener for the sheet folding. In his formulation, the model takes into account the influential factors of the spring back: geometry of the tools (rollers), characteristics of the material, geometrical characteristics of the tube. This method is based on the works of Sorkin and Tonkil (1993). It is admitted that: the bending is calculated without ovalization and crumpling, the deformation is primarily uniaxial and thus controlled by axial stress (as in the model of Sumitomo group), the tube section is divided into the elastic and plastic zones (fig. 2). With y the distance from the neutral axis, the expression of the normal stresses are written as:

$$\sigma_{x\text{élast}} = E \cdot \frac{y}{R_0} \text{ in the elastic zone ; } \sigma_{x\text{plast}} = k \cdot \left| \frac{y}{R_0} \right|^n \text{ in the plastic zone} \tag{2}$$

By integrating the quantity $\sigma_x(y)y$ over the tube section, we obtain successively the following terms:

$$M_1 = \int_0^\lambda dz \cdot \int_{\sqrt{(D/2)^2 - z^2}}^r y \cdot \sigma_x dy \tag{3} \quad M_2 = \int_\lambda^{d/2} dz \cdot \int_{\sqrt{(d/2)^2 - z^2}}^{\sqrt{(D/2)^2 - z^2}} y \cdot \sigma_x dy \tag{4}$$

$$M_3 = \int_{d/2}^{D/2} dz \cdot \int_0^{\sqrt{(D/2)^2 - z^2}} y \cdot \sigma_x dy \tag{5} \quad M_4 = \int_0^\lambda dz \cdot \int_r^{\sqrt{(D/2)^2 - z^2}} y \cdot \sigma_{x\text{plast}} dy \tag{6}$$

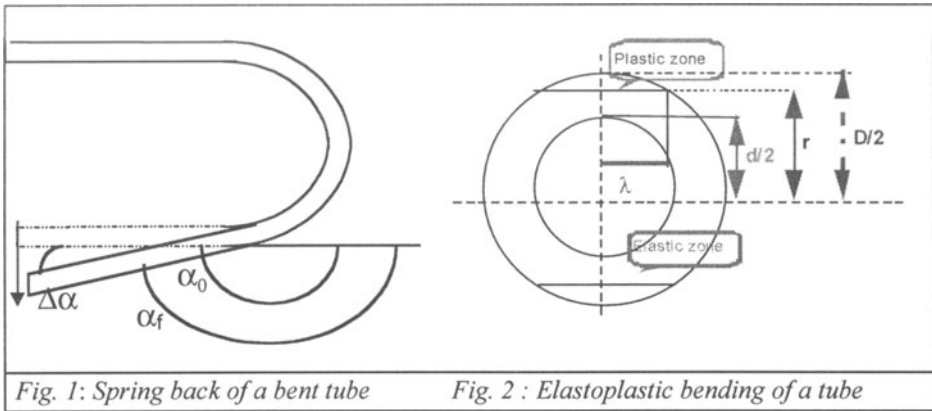
The maximum moment M_{max} is the sum of the calculated moments. Without giving more details, we note that the calculation of these integrals lead to relatively complex

terms. The reader can consult the works of Djani (1997) and Sorkin and Tonkii (1993) for more information. The moment-curvature relation according to Queener's approach is adopted here:

$$\frac{1}{R_0} - \frac{1}{R_f} = \frac{M_{\max}}{[\partial M_e / \partial (1/R)]} \quad (7)$$

where M_{\max} indicates the maximum moment applied to the tube, M_e is the bending moment during the elastic discharge and R_0 and R_f the rays before and after spring back, both taken to the axis of the tube. As Queener and De Angelis (1968) and Stelson (1982) in the case of the sheet folding, we use the following fundamental geometrical relation:

$$\frac{R_0}{R_f} = \frac{\alpha_f}{\alpha_0} \quad (8)$$



The results of the tests carried out by the CRPC (Sollac-Fos), enable us to check this relation in the case of bending of tubes. By analyzing the values taken by the R_0/R_f ratio, the Sachs coefficient and the $\Delta\alpha$ angle, we find that the relation (8) is valid with close measurement uncertainties. By using the relations (7) and (8), we can write:

$$\frac{R_0}{R_f} = 1 - \frac{R_0 \cdot M_{\max}}{[\partial M_e / \partial (1/R)]} = \delta \quad (9)$$

Finally, we have by identification:

$$\Delta\alpha = \alpha_0 - \alpha_f = (1 - \delta) \cdot \alpha_0 \quad (10)$$

In equation (9), if the quantity M_e is known, it is possible to deduce the expression of δ . If ratio R_0/D is very large, we can adopt the classical theory of beams in deflection. Then:

$$M_e = E \cdot I_z / R_0 \quad \text{with} \quad I_z = \frac{\pi}{64} (D^4 - d^4) \quad (11)$$

The equations (9) to (11) are obtained by admitting some simplifying assumptions. We present later some correction factors in order to introduce the effects related to the geometrical deformation of the cross-section (flatness, distortion, ovalization) and to

the displacement of the position of neutral fibre. These corrections allow to take into account: the reduction of rigidity caused by the flatness of the deformed tube (Sorkin and Tonkii, 1993), the displacement of the neutral fibre and the modification of the inertia of the section (Djeni, 1997), the restrictions of the profile of the cross-section (Sorkin and Tonkii, 1993). A detailed formulation of the correction factors is given by Djeni (1997).

4.3. VALIDATION OF THE SPRING BACK MODEL

The model was validated on the basis of the works of the Sumitomo group (Akiyama et al., 1989). The comparison of the results of our model to those of Sumitomo shows that the Sumitomo model is more precise and our model underestimates the spring back (fig. 3). The differences observed between the results come from the simplicity of the model presented here. Indeed, in our model the Bauschinger effect is neglected and several simplifying assumptions make possible to set up an analytical formula to calculate the Sachs coefficient. The analytical form of the model is expressed according to the geometrical characteristics of the tube and the properties of material.

The method of Sumitomo is numerical. It also requires the results of traction and compression tests on the tubes actually unavailable.

In a first approach to order to simplify the problem, we used the model presented in this paper to study the reliability of the spring back.

5. Sensitivity analysis and reverse approach

The development of a model for the sensitivity analysis and the computation of reliability in the processes of tube bending, are the principal objectives of this study. Two different approaches are used:

- (i) the direct approach based on a Monte-Carlo method, allows to calculate the scattering of spring back from the industrial scattering on the design parameters,
- (ii) the reverse approach aiming at specifying the material characteristics in term of allowable scaling for a given level of reliability on the spring back. This last approach will be the subject of a later publication.

6. Direct approach

6.1 MONTE-CARLO METHODS (SAPORTA, 1990 AND JUSTENS 1990)

When the statistical density functions of the various basic variables are known (with their possible correlation), it is possible to simulate a great number of structures whose geometrical and mechanical characteristics are represented by random and/or deterministic variables.

6.2. ESTIMATE OF RELIABILITY

Considering Y as a random characteristic of a device. Y is a function of the parameters X_i (with average μ_i and standard deviations σ) of the same device. So Y follows a normal distribution. The operation of the device is correct when Y lies between the y_1 and y_2 , then reliability (noted θ) will be:

$$\theta = \text{Prob}(y_1 < Y \leq y_2) = \text{Prob}(Y \leq y_2) - \text{Prob}(Y \leq y_1) \quad (12)$$

By using the law $N(0,1)$, we obtain:

$$\theta = \phi\left(\frac{y_2 - \mu_Y}{\sigma_Y}\right) - \phi\left(\frac{y_1 - \mu_Y}{\sigma_Y}\right) \quad (13)$$

For our study, we identify Y with $\Delta\alpha$, Φ with the analytical model of spring back, variables X_i as the six influencing and useful parameters for our sensitivity analysis.

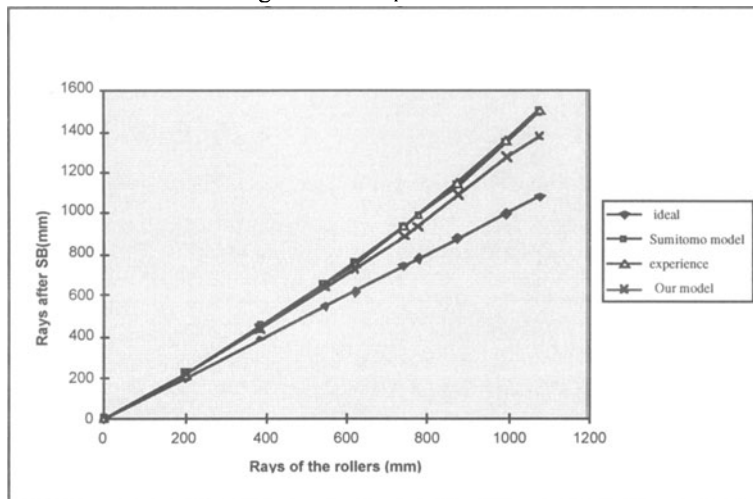


Fig. 3 : Validation of the spring back model presented in this paper

6.3. RESULTS

The Monte-Carlo method was implanted using Excel version 5. The automating of the all procedures by macro-command appeared necessary because a high number of operations should be realized. The macro carries out the whole of the statistical processing directly from the data input (average and variation-types) of the problem.

Few information available in terms of scattering of the spring back, did not allow a validation on several examples. Only nuance XC in diameter 32 and thickness 1.5 was used for which we had some experimental results of scattering. In order to have the most reliable information, it was necessary to treat data resulting for 200 test sheets on tubes with all nuances. We checked the results obtained on nuance XC by carrying out the experimental tension tests on tubes. These tests aimed moreover at determining the coefficients k and ν of the Hollomon law. With nuance XC, three cases were analyzed: a study of the single influence of scattering related to the tube on those of spring back (it is the first case), plus two other studies more or less identical whose objective were to study the share of fluctuations due to the diameter if the thickness is constant (case 2) and conversely (case 3).

An example of the Monte-Carlo simulation is presented in Figure 4, where the influence of diameter on scattering of the spring back is studied. The analysis of the results using the Monte-Carlo method shows that in the case of a decoupling of the tube effects and bending process, the scattering related to the tube alone is very small (about 1°). However, these results should be considered with caution because tubes and process interact together throughout the operations. In addition, the spring back model used for the sensitivity analysis does not take into account all factors whose influence,

certainly relative, cannot in the absolute being neglected. These factors are in particular the welding which introduces not only a variation of the inertia of the cross-section, but also the residual stresses which the share of responsibility cannot currently be estimated (Maeder and Lebrun, 1993).

7. Conclusions

This study showed that in an approach aiming at uncoupling the effects of the tube and the process of bending, the share of responsibility for the first one is small compared to industrial scattering observed. The interaction «process-tube», which was underestimated in this first approach, is to be considered. On the other hand, this work proposes a future orientation of the work in the sense that the tube manufacturers should work on the process of bending to reduce the spring back effects.

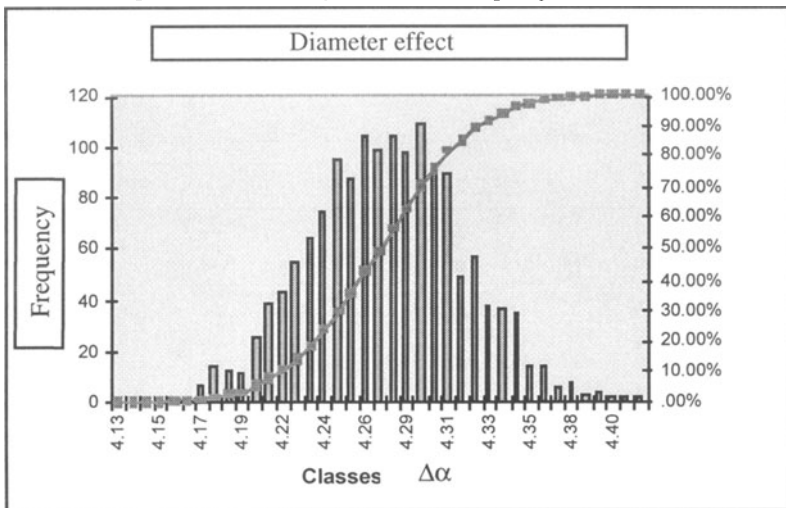


Fig. 4. Diameter effect on dispersal of spring back

References

- Akiyama M., Kobayashi, K., and Nakaï, T., 1989, "Optimum design of roll radius for the tube bending", The SUMITOMO search n° 40, pp 71-80.
- Djeni, J.-C., 1997, "Analyse de fiabilité du retour élastique", Technical note FPG97, University Léonard de Vinci, Département of Mechanical Systems, Paris La Défense.
- Justens, D., 1990, "Statistiques pour les décideurs", Entreprise De Boeck, Editions Universitaires, 2nd edition.
- Maeder, G., and Lebrun, J.L., 1993, "Contraintes résiduelles et mise en forme", Physique et mécanique de la mise en forme des métaux, Ecole d'été d'Oléron, CNRS Publishing, IRSID, pp 627-628.
- Marron, and Bouhéliar, 1994, "Le pliage des aciers HLE : prévision et maîtrise du retour élastique ", Tôles en acier HLE, choix et mise en oeuvre, Publications CETIM-OTUA, pp. 191-203.
- Queener, C.A., and De Angelis, R.J., 1968, " Elastic springback and residual stresses in sheet metal formed by bending ", Transactions of American Society for Metals, vol LXI, pp 756-766.
- Saporta, G., 1990, "Probabilités, analyse de données et statistiques", Edition Technip.
- Sorkin, L.S., and Tonkii, E.A., 1993, "Determination of axial residual stresses in tubes subjected to elastoplastic bending in cold condition", Zavodskaya Laboratoriya, vol 59, n°10, pp 28-30.
- Stelson, K.A, 1982, " An adaptative press-brake control using an elastic-plastic Material Model ", Transactions of American Society for metals, Journal of Engineering for Industry, vol.104, pp 389-393.

Chapter 6
MODELING FOR CONTROL AND MEASUREMENT
TOLERANCING AND ASSEMBLY IN MANUFACTURING

Influence of the Machine-Tool defects on the formation of the residual defects on a surface : application to turning	341
A. GOUSKOV and S. TICHKIEWITCH	
Certification of free-form machining : a comprehensive approach from CAD/CAM to measurement	349
D. FEAUTRIER, F. THIEBAUT, G. TIMON and C. LARTIGUE	
Nominal and actual geometry explicit declaration Application to dimensional inspection	357
C. CUBÉLÈS-VALADE and A. RIVIÈRE	
Adaptative digitization of mechanical parts	365
F. BENNIS and F. DANIEL	
Geometric tolerance transfer for manufacturing by an algebraic method	373
F. BENNIS, L. PINO and C. FORTIN	
Modeling dispersions affecting pre-defined functional requirements of mechanical assemblies using jacobian transforms	381
L. LAPERRIERE and PH. LAFOND	
Toward a computer aided tolerancing system for parts and mechanisms	389
E. BALLOT, F. THIEBAUT and P. BOURDET	
Interactions between tolerancing and structural analysis views in design processes	397
S. SAMPER and M. GIORDANO	
Fixturing effects on workpiece quality in milling	405
A D'ACUNTO, J. LEBRUN, P. MARTIN and M. GUEURY	

INFLUENCE OF THE MACHINE-TOOL DEFECTS ON THE FORMATION OF THE RESIDUAL DEFECTS ON A SURFACE: APPLICATION TO TURNING

A. GOUSKOV^{*} & ^{**}, S. TICHKIEWITCH^{**}

^{*} *Bauman Technical University*

^{2nd}, *Baumanskaya st. 5, 107005 Moscow, Russia*

^{**} *Soils, Solids, Structures Laboratory*

Domaine Universitaire, BP 53, 38041 Grenoble Cedex 9, France

Abstract

In order to obtain a surface by a machining process, a kinematics has to move a tool along a trajectory defined in relation with the geometry of the part. Regarding the second order, the complete dynamics of the technological system 'machine-tool-part' and the state of the initial surface disturb the cutting phenomenon and cause form defects on the tooled surface. This paper presents a modelling of the surface defects, giving a classification between the global defects and some specific defects. As the resulting surface is a true signature of the technological system, an example shows the possibility of the association of some typical defects to a particular characteristic of the machine-tool.

1. Introduction

The technological system in machining process (TS), composed of the machine-tool, the tool and the part, leaves its signature on the surface of a tooled part in form of defects. These defects can be represented with a lot of components of a numerical matrix, that can be identified during the metrology of the part. The integral characteristics of a defect are : *the deviation relatively to the dimensions, the mean quadratic deviation and the amplitude of the surface*. However, these characteristics give a minimum information on the surface, a lot of collected information being lost until we can describe the possible structure of the defects. In this work, we consider a global structure of the defects for a lateral surface of a cylindrical part obtained by turning. This structure is built on a panel of nine defects successively named : *eccentricity, conicalness, barrel-saddle, ellipticity, cylindrical waves, twisted waves, axial waves, form of the axle and parallelism*.

The majority of the works dedicated to the study of the dynamics of the TS (Kelson *et al.*, 1996)(Jen and Magrab, 1996), excludes the modelling of the surface formation. The cutting loads are presented as the result of an harmonic excitation with given amplitude and frequency, taking into account the state variables of the dynamic system but without the variables which describe the state of the surface. Such an approach is oriented for the research of the conditions of the removal of the vibrations of the TS (increase of the static stiffness of the constitutive elements, increase of the absorption, lagging of

the spectrum for the proper vibrations). But it will be technologically impossible to suppress all the imperfections of the TS, as such as it will always exist some deformation of the TS. For this, we will always have some form defects on the tooled surface.

The question we try to answer in this work is to find a modelling of the surface formation during tooling, linking this formation to the dynamics of the TS with its own defects. The simulation of the comportment of the system must allow us to find a correlation between the defects of the machine-tool and the induced defects on the surface. We are here very near of the work done by Coffignal *et al.* (1996). However, we have introduced a complementary hypothesis in the fact we take into account the variation of the superficial layer of the part during tooling. This layer remains thin and so we do not propagate this fact on the stiffness matrix and on the generalised masses. This allows us to treat the surface with a geometrical manner, using bilinear surface-elements on an orthogonal mesh which is considered as the propriety of a perfect cylinder, named the basic cylinder. It allows us also to determinate the cutting effects as a function of the section of the chip. In Gousskov and Tichkiewitch (1996) we have presented the dynamic model of the TS, taking into account the defects of the machine-tool and of the initial geometry of the considered surface : vibration from the ground, excitation at the headstock, at the chuck and at the tool-holder, defect of the initial surface of the part and possible mass eccentricity of the part.

As a continuity of the previous paper, we present here the modelling of the nine defects chosen in order to characterise the cylindrical surface. We also present an example of the influence of the defect in centring the part by the chuck, with an excitation from the ground and some defects of the headstock considered as constant.

2. Mathematical Definition of the Defects on a Cylindrical Surface

The radius of the basic cylinder is the nominal radius of the wished cylinder. The radial coordinates of the surface are measured from the basic cylinder and are normalised relatively to the machined depth H . These coordinates form the matrix:

$$\mathbf{X}(i, j), i = \{1, \dots, n\}, j = \{1, \dots, m\}$$

where $(n - 1)$ is equal to the number of partitions of the length L of the part, $(m - 1)$ is equal to the number of partitions of the circumference with radius $(R - H)$ of the basic cylinder, with R the nominal radius of the initial surface.

With such coordinates, the mean value $\mu[\mathbf{X}]$, first integral characteristic, defines the deviation relatively to the cylindrical surface:

$$\mu[\mathbf{X}] = \frac{1}{m \cdot n} \sum_{i=1}^m \sum_{j=1}^n X_{ij}$$

The form defect of the lateral surface $\Delta\mathbf{X}$ is:

$$\Delta\mathbf{X} = \mathbf{X} - \mu[\mathbf{X}] \cdot \mathbf{E}_{m,n}$$

where $\mathbf{E}_{m,n}$ is a matrix with unitary components, and the mean quadratic deviation, second integral characteristic which gives the accuracy of the surface, is given¹ by:

$$\sigma[\mathbf{X}] = \|\Delta\mathbf{X}\| \cdot (m \cdot n)^{-1/2} \quad \text{with} \quad \|\Delta\mathbf{X}\| = \text{Trace}(\Delta\mathbf{X}^T \cdot \Delta\mathbf{X})$$

¹ We use in this text the MATLAB syntax

The third integral characteristic of the defect of the surface is the amplitude:

$$V[\mathbf{X}] = \max_{i,j}(\mathbf{X}) - \min_{i,j}(\mathbf{X})$$

The normalised ratio:

$$\varepsilon^{(0)} = \frac{V[\mathbf{X}]}{\sigma[\mathbf{X}]}, \quad \sigma[\mathbf{X}] \neq 0$$

gives an idea of the plenitude of the space filled by the surface².

In order to be able to compare the defects, whatever the radial scale of the surface, we found interesting to consider the surface defect in a normalised form relatively to the mean quadratic deviation:

$$\Delta\mathbf{X}^\sigma = \Delta\mathbf{X} \cdot \sigma[\mathbf{X}]^{-1}$$

and in this case, the defect may be presented with the following relation:

$$\mathbf{X} = \mu[\mathbf{X}] \cdot \mathbf{E}_{m,n} + \sigma[\mathbf{X}] \cdot \Delta\mathbf{X}^\sigma$$

The representation of the panel of the nine types of considered defects is realised with nine test surfaces that are compared with the form defect of the lateral surface. Each of the test surface is defined with :

$$\mathbf{X}^{(\text{test } i)} = \mathbf{f}^{(i)}(\mathbf{Y}, \mathbf{Z}, \mathbf{p}^{(i)})$$

$$\text{where } \mathbf{Y} = (0 : m-1)^T / (m-1) \text{ and } \mathbf{Z} = (0 : n-1)^T / (n-1)$$

and is dependent of a parameter vector $\mathbf{p}^{(i)}$ determined with the least square method:

$$\mathbf{p}^{(i)*} \leftarrow \min_{\mathbf{p}} \|\mathbf{f}^{(i)}(\mathbf{Y}, \mathbf{Z}, \mathbf{p}^{(i)}) - \Delta\mathbf{X}\|^2$$

The rate of surface defect is given with the "signal-noise" ratio:

$$\eta^{(i)} = \frac{\|\mathbf{f}^{(i)*}\|}{\|\Delta\mathbf{X} - \mathbf{f}^{(i)*}\|} \quad \eta^{(i)} \in [0; \infty)$$

This ratio is so much important as the noise is weak, i.e. the test surface well approximate the form defect. An other way to characterise the defects is to use the normalised defect:

$$\varepsilon^{(i)} = N(\mathbf{p}^{(i)*})$$

N being specific to each considered defect. This way allows particularly to evaluate the global defect that we can express in meter:

$$e^{(i)} = H \sigma[\mathbf{X}] \varepsilon^{(i)}$$

The characterisation of each of the test surfaces is given after.

² See the R/S method or the HERST's factor in FRACTAL (1991, Feder Edition)

2.1. ECCENTRICITY (N°1 DEFECT)

Two parameters characterise the axle deviation of the test cylindrical surface, parallel to the basic axle, in the two radial directions. We can consider also the amplitude and the phase of the first harmonic on a circumference direction:

$$\mathbf{X}^{(\text{test } -1)} = (p_1^{(1)}(\cos(2\pi \mathbf{Y}) - \Phi_1) + p_2^{(1)}(\sin(2\pi \mathbf{Y}) - \Phi_2)) \cdot \mathbf{E}_n^T$$

with $\mathbf{E}_s \in R^S$ has components equal to 1 and:

$$\begin{aligned} \Phi_1 &= \mathbf{E}_m \cdot (\mathbf{E}_m^T \cdot \cos(2\pi \mathbf{Y})) / m & \Phi_2 &= \mathbf{E}_m \cdot (\mathbf{E}_m^T \cdot \sin(2\pi \mathbf{Y})) / m \\ \varepsilon^{(1)} &= \|\mathbf{p}^{(1)*}\| \end{aligned}$$

2.2. CONICALNESS (N°2 DEFECT)

One parameter characterise the amplitude of the difference between the two extreme radii of the test surface:

$$\begin{aligned} \mathbf{X}^{(\text{test } -2)} &= p_1^{(2)} \cdot \mathbf{E}_m \cdot (\mathbf{Z}^T - 0.5 \cdot \mathbf{E}_n^T) \\ \varepsilon^{(2)} &= p_1^{(2)*} \end{aligned}$$

2.3. BARREL-SADDLE (N°3 DEFECT)

One parameter characterise the amplitude of the rounded or the hollow of the parabolic test surface, the axle of this surface being parallel to the basic axle:

$$\begin{aligned} \mathbf{X}^{(\text{test } -3)} &= p_1^{(3)} \cdot \mathbf{E}_m \cdot (-(n-2)/(n-1) \cdot \mathbf{E}_n^T / 6 + \mathbf{Z}^T - (\mathbf{Z}^T \cdot \mathbf{Z}^T)) \\ \text{where } \mathbf{Z} &= (0 : n-1) / (n-1) \\ \varepsilon^{(3)} &= p_1^{(3)*} \end{aligned}$$

2.4. ELLIPTICITY (N°4 DEFECT)

Two parameters characterise the amplitude and the phase of the second harmonic on a circumference direction:

$$\begin{aligned} \mathbf{X}^{(\text{test } -4)} &= (p_1^{(4)}(\cos(4\pi \mathbf{Y}) - \Phi_1) + p_2^{(4)}(\sin(4\pi \mathbf{Y}) - \Phi_2)) \cdot \mathbf{E}_n^T \\ \text{with} & \\ \Phi_1 &= \mathbf{E}_m \cdot (\mathbf{E}_m^T \cdot \cos(4\pi \mathbf{Y})) / m & \Phi_2 &= \mathbf{E}_m \cdot (\mathbf{E}_m^T \cdot \sin(4\pi \mathbf{Y})) / m \\ \varepsilon^{(4)} &= \|\mathbf{p}^{(4)*}\| \end{aligned}$$

2.5. CYLINDRICAL WAVES (N°5 DEFECT)

Two parameters characterise the amplitude and the phase of the harmonic with k order, upper than 2, on a circumference direction, and which minimises a least square deviation:

$$\mathbf{X}^{(\text{test } -5)} = (p_1^{(5)} (\cos (2 k \pi \mathbf{Y}) - \Phi_1) + p_2^{(5)} (\sin (2 k \pi \mathbf{Y}) - \Phi_2)) \cdot \mathbf{E}_n^T$$

where $k \in [3, k_{\max}]$, $k_{\max} = \text{int}(m/5)$ and

$$\Phi_1 = \mathbf{E}_m \cdot (\mathbf{E}_m^T \cdot \cos (2 k \pi \mathbf{Y})) / m \quad \Phi_2 = \mathbf{E}_m \cdot (\mathbf{E}_m^T \cdot \sin (2 k \pi \mathbf{Y})) / m$$

$$\varepsilon^{(5)} = \|\mathbf{p}^{(5)*} (k^*)\|$$

2.6. TWISTED WAVES (N°6 DEFECT)

Two parameters characterise the amplitude and the phase of the best harmonic with k order, upper than 2, on a circumference direction, taking into account a r twist ratio:

$$\mathbf{X}^{(\text{test } -6)} = (p_1^{(6)} (\cos (\Phi) - \Phi_1) + p_2^{(6)} (\sin (\Phi) - \Phi_2))$$

$$\Phi = 2 \cdot \pi \cdot k \cdot (\mathbf{Y} \cdot \mathbf{E}_n^T - r \cdot \mathbf{E}_m \cdot \mathbf{Z}^T)$$

$$\mathbf{s}_1 = \mathbf{E}_m \cdot (\mathbf{E}_m^T \cdot \cos (2 k \pi \mathbf{Y})) / m \quad \mathbf{s}_2 = \mathbf{E}_m \cdot (\mathbf{E}_m^T \cdot \sin (2 k \pi \mathbf{Y})) / m$$

$$\mathbf{t}_1 = \mathbf{E}_n \cdot (\mathbf{E}_n^T \cdot \cos (2 k r \pi \mathbf{Z})) / n \quad \mathbf{t}_2 = \mathbf{E}_n \cdot (\mathbf{E}_n^T \cdot \sin (2 k r \pi \mathbf{Z})) / n$$

$$\Phi_1 = \mathbf{s}_1 \cdot \mathbf{t}_1 + \mathbf{s}_2 \cdot \mathbf{t}_2 \quad \Phi_2 = \mathbf{s}_2 \cdot \mathbf{t}_1 - \mathbf{s}_1 \cdot \mathbf{t}_2$$

$$k \in [1, k_{\max}], \quad k_{\max} = \text{int}(m/5); \quad r \in [-2; +2], \quad \Delta r = 0.1$$

$$\varepsilon^{(6)} = \|\mathbf{p}^{(6)*} (k^*, r^*)\|$$

2.7. AXIAL WAVES (N°7 DEFECT)

Two parameters characterise the amplitude and the phase of the best harmonic with l order, upper than 2, on an axial direction (l being real), and which minimises a least square deviation:

$$\mathbf{X}^{(\text{test } -7)} = \mathbf{E}_m \cdot (p_1^{(7)} (\cos (2 l \pi \mathbf{Z}) - \Phi_1) + p_2^{(7)} (\sin (2 l \pi \mathbf{Z}) - \Phi_2))^T$$

with $l \in [l_{\min}, l_{\max}]$, $l_{\min} = 0.25$, $l_{\max} = \text{int}(n/5)$, $\Delta l = 0.2$

$$\Phi_1 = \mathbf{E}_n \cdot (\mathbf{E}_n^T \cdot \cos (2 l \pi \mathbf{Z})) / n \quad \Phi_2 = \mathbf{E}_n \cdot (\mathbf{E}_n^T \cdot \sin (2 l \pi \mathbf{Z})) / n.$$

$$\varepsilon^{(7)} = \|\mathbf{p}^{(7)*} (l^*)\|$$

2.8. FORM OF THE AXLE (N°8 DEFECT)

The test surface is composed of a lot of circular sections with mean radius computed relatively to the sections of the surface with form defect, using a least square deviation. Two parameters characterise the amplitude and the phase of the first harmonic evaluated for each of the sections:

$$\mathbf{X}^{(\text{test } -8)} = (\cos (2 \pi \mathbf{Y}) - \Phi_1) \cdot \mathbf{p}_1^{(8)T} + (\sin (2 \pi \mathbf{Y}) - \Phi_2) \cdot \mathbf{p}_2^{(8)T}$$

with

$$\Phi_1 = \mathbf{E}_m \cdot (\mathbf{E}_m^T \cdot \cos (2 \pi \mathbf{Y})) / m \quad \Phi_2 = \mathbf{E}_m \cdot (\mathbf{E}_m^T \cdot \sin (2 \pi \mathbf{Y})) / m$$

$$\Psi_1 = (\cos (2 \pi \mathbf{Y}) - \Phi_1) \quad \Psi_2 = (\sin (2 \pi \mathbf{Y}) - \Phi_2)$$

$$a = \Psi_1^T \cdot \Psi_1, \quad b = \Psi_1^T \cdot \Psi_2, \quad c = \Psi_2^T \cdot \Psi_2, \quad D = a \cdot c - b^2$$

$$\mathbf{p}_1^{(8)} = \Delta \mathbf{X}^{\sigma T} \cdot (c \cdot \Psi_1 - b \cdot \Psi_2) / D \quad \mathbf{p}_2^{(8)} = \Delta \mathbf{X}^{\sigma T} \cdot (-b \cdot \Psi_1 + a \cdot \Psi_2) / D$$

$$\varepsilon^{(7)} = \sqrt{\max_i (\mathbf{p}_1^{(8)*} \cdot \mathbf{p}_1^{(8)*} + \mathbf{p}_2^{(8)*} \cdot \mathbf{p}_2^{(8)*})}$$

2.9. PARALLELISM OF THE REAL AXLE RELATIVELY TO THE THEORETICAL ONE (N°9 DEFECT)

The test surface is a cylindrical surface with a radius equal to the mean radius. This surface is situated relatively to the surface with form defect in order to minimise the least square deviation. Parameters take into account the deviation and the orientation of the axle of the test surface relatively to the basic axle:

$$\mathbf{X}^{(\text{test } -9)} = (\cos(2\pi \mathbf{Y}) - \Phi_1) \cdot \mathbf{p}_1^{(9)T} + (\sin(2\pi \mathbf{Y}) - \Phi_2) \cdot \mathbf{p}_2^{(9)T}$$

with $\varepsilon_{HL} = H/L$ and

$$\theta_1 = \varepsilon_{HL} \cdot \sigma[X] \cdot \frac{6(n-1)}{n(n+1)} (\mathbf{E}_n^T - 2\mathbf{Z}^T) \cdot \mathbf{p}_2^{(9)*} \equiv \varepsilon_{HL} \cdot \sigma[X] \cdot \vartheta_1$$

$$\theta_2 = \varepsilon_{HL} \cdot \sigma[X] \cdot \frac{6(n-1)}{n(n+1)} (\mathbf{E}_n^T - 2\mathbf{Z}^T) \cdot \mathbf{p}_1^{(9)*} \equiv \varepsilon_{HL} \cdot \sigma[X] \cdot \vartheta_2$$

$$a_1 = \frac{2}{n(n+1)} [3 \cdot (n-1) \cdot \mathbf{Z}^T - (n-2) \cdot \mathbf{E}_n^T] \cdot \mathbf{p}_1^{(9)*}$$

$$a_2 = \frac{2}{n(n+1)} [3 \cdot (n-1) \cdot \mathbf{Z}^T - (n-2) \cdot \mathbf{E}_n^T] \cdot \mathbf{p}_2^{(9)*}$$

$$\mathbf{p}_1^{(9)*} = a_1 \cdot \mathbf{E}_n + \vartheta_2 \cdot (\mathbf{E}_n - \mathbf{Z}) \quad \mathbf{p}_2^{(9)*} = a_2 \cdot \mathbf{E}_n + \vartheta_1 \cdot (\mathbf{E}_n - \mathbf{Z})$$

$$\varepsilon^{(9)} = \sqrt{\vartheta_1^2 + \vartheta_2^2}$$

Type of defect	$\varepsilon^{(i)}$	$\eta^{(i)}$
Eccentricity	0.0001	0.0001
Conicalness	-1.631	0.5372
Barrel-Saddle	9.708	1.072
Ellipticity	0.0001	0.0000
Cylindrical waves	0.0000	0.0000
Twisted waves	0.0141	0.01
Axial waves	1.4047	10.45
Form of the axle	0.0034	0.0015
Parallelism	0.0001	0.0001

Tab.1 : Perfect system

Type of defect	$\varepsilon^{(i)}$	$\eta^{(i)}$
Eccentricity	0.0054	0.0038
Conicalness	1.645	0.5434
Barrel-Saddle	3.239	0.2515
Ellipticity	0.0109	0.0077
Cylindrical waves	0.9013	0.8294
Twisted waves	0.9013	0.8294
Axial waves	16.74	0.6347
Form of the axle	0.0255	0.0095
Parallelism	0.0313	0.0075

Tab.2 : Excited system

Using the definition of these nine defects, we can describe each studied surface with the identification of their integral characteristics $\mu[\mathbf{X}]$, $\sigma[\mathbf{X}]$ and $V[\mathbf{X}]$, and also with the tables of the normalised defects $\varepsilon^{(i)}$ and the rates of defects $\eta^{(i)}$. Each line of these tables represents the corresponding values for each of the previously defined defect.

3. The Influence of Centring the Part in the Chuck

As an example of such a definition of the tooled surfaces, we have now a look on the problem of the influence of a bad centring of a part in the chuck. We consider that the turning machine transmits from the ground an excitation. Its amplitude a_{BX} is defined at the chuck level on a vertical direction and its frequency is f_{BX} . The defects of the headstock are characterised by an eccentricity R_1 on a direction α_1 , giving excitation with amplitude a_1 and frequency f_1 . The defects of the chuck are characterised by an eccentricity R_0 on a direction α_0 , giving excitation with amplitude a_0 and frequency f_0 . The problem here is to evaluate the state of the lateral surface for the tooled part for different values of the eccentricity R_0 .

In order to compare our results, a first step considers the perfect technological system with zero defect:

$$\{ \{ a_{BX}, f_{BX} \}, \{ R_1, \alpha_1, a_1, f_1 \}, \{ R_0, \alpha_0, a_0, f_0 \} \} \equiv 0$$

The initial surface is also a perfect cylinder. With some values taken for the definition of the machine, of the tool and of the part, the table 1 gives the resulting defects of the tooled surface. The axial waves is mainly the result of such machining, signature of the initial technological system. The integral characteristics of the tooled surface are:

$$V[X] = 2.751; \quad \sigma[\Delta X] = 7.239 \cdot 10^{-4}; \quad \mu[\Delta X] = 1.263 \cdot 10^{-3}$$

Figure 3 exhibits the defect of the tooled surface in the normalised form. The generatrix of the surface is approximately the influence line of a rod, which is tailed on a side and placed on a free support on the other side, with the loading of a radial punctual force.

For a second step, we add an excitation to the technological system such as :

$$\begin{cases} a_{BX} = 0.05 \cdot H, & f_{BX} = 2.5 \cdot f_P \\ \{ R_1 = 0.005 \cdot H, & \alpha_1 = 2 \cdot \pi \cdot rand, & a_1 = 0.005 \cdot H, & f_1 = 5 \cdot f_P \\ \{ R_0 = 0.01 \cdot H, & \alpha_0 = 2 \cdot \pi \cdot rand, & a_0 = 0.005 \cdot H, & f_0 = 7 \cdot f_P \end{cases}$$

With the same initial perfect surface, we obtain a new tooled surface. The table 2 gives the resulting defects of this new tooled surface which have for integral characteristics:

$$V[X] = 4.755; \quad \sigma[\Delta X] = 3.679 \cdot 10^{-3}; \quad \mu[\Delta X] = 7.634 \cdot 10^{-3}$$

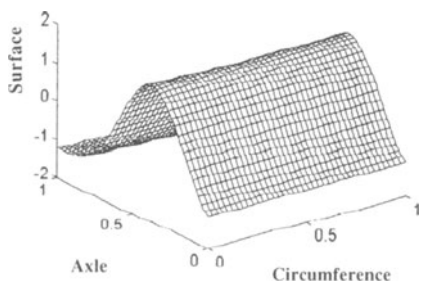


Figure 3 : The defect of the tooled surface for the perfect system

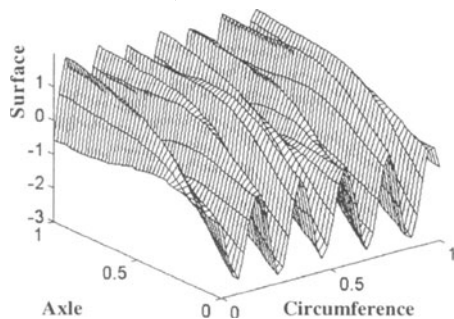


Figure 4 : The defect of the tooled surface for the excited system

The nearest test surface is now the cylindrical waves (the same values for the cylindrical waves and the twisted waves indicates that their is no more twist effect). Figure 4 exhibits the defect of the new tooled surface in the normalised form.

Starting with the same initial surface, we successively change the R_0 parameter in order to analyse its influence on the defect generation. Figures 5 gives the variation of the nine normalised defects $\epsilon^{(i)}$ computed at the chuck level for an eccentricity of the headstock axle converted from $R_0 = 0$ to $R_0 = 0.001 H$ with a step of $0.0002 H$. Computed points are given by * symbol.

A first analysis shows that the defect of the eccentricity at the chuck level is more easily detected by the normalised defect of the surface corresponding to the axial waves. The study of the correlation has to be done now on order to obtain some indicators allowing the easiest identification of the defects on a machine-tool.

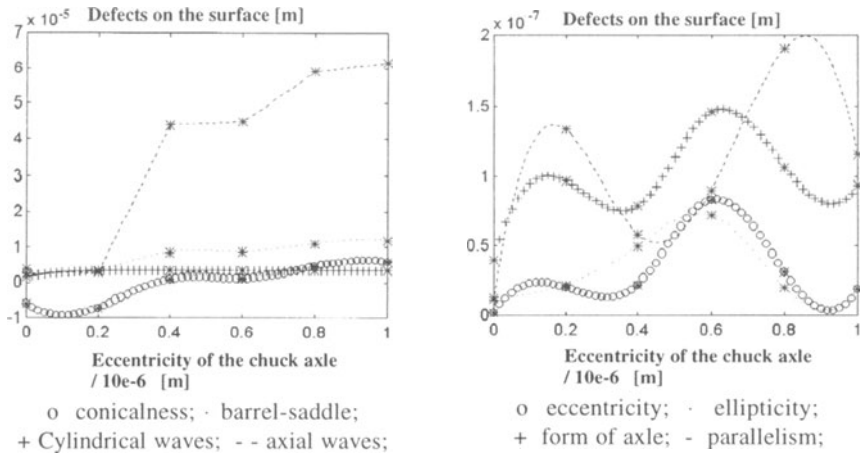


Figure 5 : Normalised defects : interpolation with cubic splines

4. Conclusion

After the modelling of the technological system used in a machining process in Gousskov and Tichkiewitch (1996), we have proposed a new classification of the defects of a surface and a method in order to identify these defects. We show how it is possible to correlate a particular defect of the surface with a specific defect of the machine-tool. We hope with such a correlation to be able to characterise a machine-tool. We have also an other goal in the possibility to specify a machine-tool in order to get a given quality of the wished surface.

5. References

- Gousskov, A., Tichkiewitch, S. (1996) Modélisation de l'opération de tournage : prise en compte des aspects dynamiques dans la formation de la surface usinée, *IDMME'96*, Nantes (France), Vol.1, pp.245-254.
- Yen, K.Z., Hsueh, W. (1996) Suppression of Chatter Vibration in Inner-Diameter Cutting, *ISME, Inter. Journal*, Series C, Vol. 39, No.1, p.25-33.
- Jen, M.U., Magrab, E.B. (1996) The Dynamic Interaction of the Cutting Process, Workpiece, and Lathe's Structure in Facing, *J. of Manuf. Science and Eng.*, August, Vol. 118, p. 349-358.
- Coffignal, G., Beauchesne, E., El Bab, K.D., Hakem, N. Mechanical simulation of machining using cutting tools, *Proceedings of IDMME'96*, Nantes (France), Vol.1, pp.145-154

CERTIFICATION OF FREE-FORM MACHINING:

A comprehensive approach from CAD/CAM to measurement

D. FEAUTRIER, F. THIEBAUT, G. TIMON and C. LARTIGUE

Laboratoire Universitaire de Recherche en Production Automatisée

ENS Cachan

61 Avenue du président Wilson

94235 Cachan Cedex - France

e-mail: lartigue@lurpa.ens-cachan.fr

ABSTRACT

Nowadays, the quality of free-form surfaces is directly linked to the precision of each step of the machining process, from the tool-path calculation using a CAM system to the milling of the part on a machine tool. The assessment of the whole process can be done through a measurement of the final machined surface. The measured geometrical deviations are the sum of the different errors occurring at each step. After an analysis of all the sources in the process, an identification of the different models that allow us to estimate each type of errors is performed. Particularly, the loss in precision due to tool-path calculation and the tool geometry are clearly described. An application on a well-known surface is performed.

1. Introduction

The paper deals with the quality of free-form machining by means of Computer Aided Milling. In general, if the machined surface meets the required geometrical specifications the process is satisfying. The quality of the final part is linked to the accuracy of each step of the process i.e. part design, tool path generation using a CAM system and milling process on a machine tool. As a result, form deviations can be modeled as the sum of errors due to the CAD/CAM system and the machining process itself.

In a previous work [5] we proposed a test part allowing to bring out possible errors linked to both the tool path generation and the milling process. The test part is composed of a set of geometrically defined surfaces the function of which is to give samples of possible failures either in the tool path generation or in the milling process (the surfaces are chosen and spread such that each difficulty can be taken separately). This previous work led to the proposition of an inspection method that only allows us to check the tool path generation.

The inspection of the whole machining process obviously requires the machining of the part on a machine tool. A possible approach to assess the milling process is to carry out the measurement of the part. In fact, the part measurement gives global deviations including tool path generation errors, that are well known since determined in the previous step. Therefore, errors due to the milling process can be calculated by subtraction of the tool-path generation errors to the global errors.

The aim of the present paper is to illustrate this approach through one of the test part surfaces: the *smooth surface*. It consists of a revolution surface obtained by rotation of a five degree Bezier curve. The main interests of this surface relatively to the milling process are to allow us the study of tool deflection effects on the final geometry and the possibility to deduce from the latter the Numerical Controller milling center errors.

In the present work, the measurement is performed with a numerical controlled Coordinate Measuring Machine (CMM) that is obviously imperfect. So, we have to take into account this new source of errors on the deviations.

The first section is dedicated to the analysis of all the sources of errors setting apart those that are quantifiable from the others. Next we present the experimental procedure, from the milling of the part to its measurement on the CMM. In the last section, experimental results are commented and, particularly, the identification of the different types of errors allows us to conclude on the efficiency of the proposed approach to certify the free-form machining process.

2. Analysis of the deviations between the final shape and the nominal model

The analysis concerns the 3-axes milling process of free-form surfaces with a ball-end cutter tool. This section presents the sources of errors at each level of the process (see Figure 1) that cause final form deviations from the nominal model. We can distinguish errors coming from the milling process from those linked to the measurement of the machined part.

2.1. SOURCES OF ERRORS IN THE PROCESS

As the CAD modeling is assumed to be perfect in this study, the main errors occurring during the milling process may come from the tool-path generation (using the CAM system) and the part milling on the NC center. In fact, the error represents the deviation between the final machined surface and the nominal model and obviously results from the sum of both errors (tool-path generation and milling process). From the nominal surface, the CAM system calculates the successive locations of the tool-path points with respect to given criteria. The resulting error is the deviation between the envelope surface of such calculated tool-paths and the original surface [2], [3]. Note that the calculation of the tool-path is performed with a perfect tool geometry. From the generated tool-path, the part is machined on a machine tool. The main sources of errors may come from the machine tool

behavior (tool-path treatment by the numerical controller, rigidity of the machine-tool, ...) and the tool behavior during the cutting process (deflection,) [7].

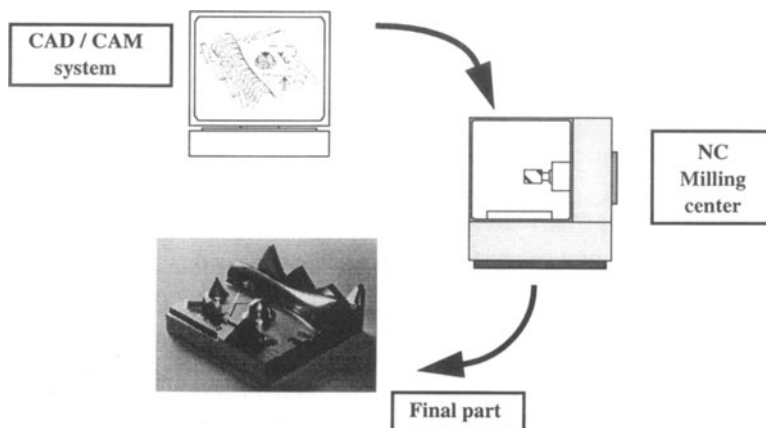


Fig. 1 Manufacturing process

At this stage, the error is the deviation between the machined surface, which is the envelope of the tool motions, and the nominal model. For our purpose, this deviation is defined in terms of a geometrical deviation e , at each point P_o of the original surface : $e = P_o P_m \cdot \vec{n}$, where P_m represents the corresponding point on the machined surface and \vec{n} , the normal to the nominal surface at P_o .

The final geometrical deviation can be evaluated at each point by a measurement of the part on a CMM. Obviously, the measuring process is a new source of error. Besides the measurement uncertainties, we have to consider the errors due to the CMM behavior, including the CMM geometry and the probe repeatability.

2.2. CLASSIFICATION OF THE MAIN DEVIATIONS

In the scope of this study, our working hypothesis concerning the specificity of each error is presented in table 1. Each source gives rise to a specific error which is of the following types: calculated from a given model, derived from measurements, known by experience or unknown a priori.

	CAM	Machining	Measurement
Calculated	geometrical deviation	tool deflection	
Measured		tool geometry	uncertainty
Known by experience			probe certification
Unknown a priori		machine tool behavior	CMM geometry

Table 1 : Classification of the sources of error

In the case of the first two types, the error can be evaluated at each point of the surface either by calculation from a model or by measurements. On the other hand, for the last two types, the error is generally quantified using an upper-bound value for the whole surface.

In a previous work, we proposed a model to assess the tool-path generation using a CAM system [5]. The geometrical deviation at each point is calculated after the determination of the machined point P_m using the Z-buffer method. A covering of the nominal surface by a cartesian grid of vertical lines is performed and the machined point is the lower intersection between a vertical line and the envelope of the tool-path.

With an accurate measurement of the tool geometry, the non-perfect tool geometry effects can be taken into account. In fact the knowledge of the real tool geometry allows us to presuppose the final machined shape and so, to quantify the resulting geometrical deviation.

Concerning the tool deflection it seems difficult to quantify its effect at each point of the surface with greater precision. However numerous models show that in most cases, errors are linked to the orientation of the normal at each point relative to the tool axis.

Although it is known that some models can be used to determine the influence of the CMM geometry on the measured deviation [4], we classify these errors as unknown a priori. This assumption will be clarified in the following sections.

3. Description of the manufacturing process

This section presents a description of the whole milling process and the measurement of the smooth surface. Remember that the process is divided in: tool path generation on a CAM system, milling of the part on a NC milling center, and measurement of the part on a NC CMM.

For the tool path generation, we choose the driving tool direction to be in parallel planes, as it is currently done. The planes are vertical and perpendicular to the revolution axis of the surface. The line is commonly the description format of the tool-path : the tool-path is a set of points linked together by line segments. This set of points results from the approximation of the surface using two parameters that characterize the quality of the final part : the maximal chordal deviation, M_t , and the maximal scallop height, h_c [1]. The maximal chordal deviation defines the discretization step for a single path (distance between two points on a single path) and the maximal scallop height defines the distance between two successive single paths. Note that the driving tool direction defines the direction of a single path.

Although there is no obvious link between the form deviation specification and those parameters, they are chosen so that : $-M_t \leq e \leq M_t + h_c$ [6]. For our experimentation, $M_t = 5 \mu\text{m}$ and $h_c = 5 \mu\text{m}$. This implies the geometrical deviations to be included in $[-5 \mu\text{m}, 10 \mu\text{m}]$. Results are shown in figure 2. It can be seen that machining such a shape does not cause problem to the CAM system for the calculated deviations e_{CAM} remain in the authorized interval $([-4 \mu\text{m}, 4 \mu\text{m}])$. Considering the driving tool direction this is not surprising.

During the next step, the part machining is implemented with conventional feedrate and cutting speed on a 3-axes milling machine. The part material (aluminum alloy 2017) and the overall machining conditions, induce the milling to be achieved mark free : neither slow-down linked to the numerical controller treatment nor cutting problems.

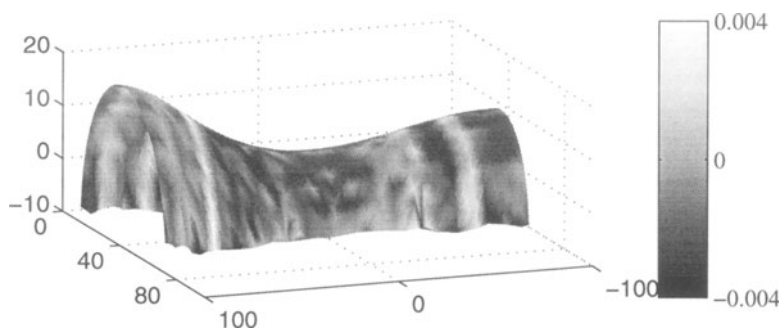


Fig. 2 Geometrical deviations on the tool-path

As said above, the certification of the milling process is done through the measurement of the part. Before setting up the experiment, one has to generate the set of measuring points. This set can be derived from the knowledge of the tool path generated by the CAD/CAM system, i.e. a set of Cutter Location Points (CLP). To get the probe path we project each point of the tool-path on the nominal surface in the direction of the corresponding normal vector. So we take out 767 points that form the probe path. In this case, both the probe path and the tool-path follow circles defined in planes perpendicular to the revolution axis (the single path is a circle, intersection between the nominal surface and the driving tool direction).

Before acquiring the points, we run an alignment procedure by measuring three remarkable surfaces of the test part eventually forming a coordinate system. In addition, to avoid random errors we measure each point 25 times. Finally, during the acquisition we use the probe tip compensation along the approaching direction, i.e. the direction of the normal vector to the surface. We end up with a set of 19175 actual points which take 10 hours to measure. The measurement is performed with a NC CMM that is obviously imperfect. In order to ensure that such errors are negligible with respect to the global deviations, the part is measured in several locations of the CMM working volume.

Nota Bene: for the experiment we checked that both the temperature and humidity were controlled to guarantee the stability of both the CMM and the part.

4. Results

The objective is of course to be able to evaluate the deviations between the actual surface (defined by the measured points) and the nominal model (defined by the CAD system). The way points are measured involves that the geometrical deviation is directly given by the distance between the measured points and the corresponding points on the nominal.

As we supposed before, the influence of the CMM geometry is unknown a priori. In fact, CMM geometry errors essentially depend on the location of the measured point in the working space. So, four measurements of the surface are performed in different locations of the measuring space. If variations of the deviation at each point occur, they only come from the CMM geometry. We compare the deviations on several isoparametrics (circles) for the different locations and we notice that the overall mean variation of the deviations between the

positions is of about $3\mu\text{m}$ ($\text{std}=1.7\mu\text{m}$). We can then assume that the CMM errors are relatively low with respect to the global deviations.

Figure 3 presents measured geometrical deviations, e_m , corresponding to one experiment. The amplitude of the geometrical deviations is 0.095 mm. A few aberrant data can be noticed, and the probe repeatability can be estimated to $1.5\mu\text{m}$. The deviation at each point presented in figure 3 is the average of the deviations calculated from the 25 measurements. So we assume that the measurement uncertainty is eliminated.

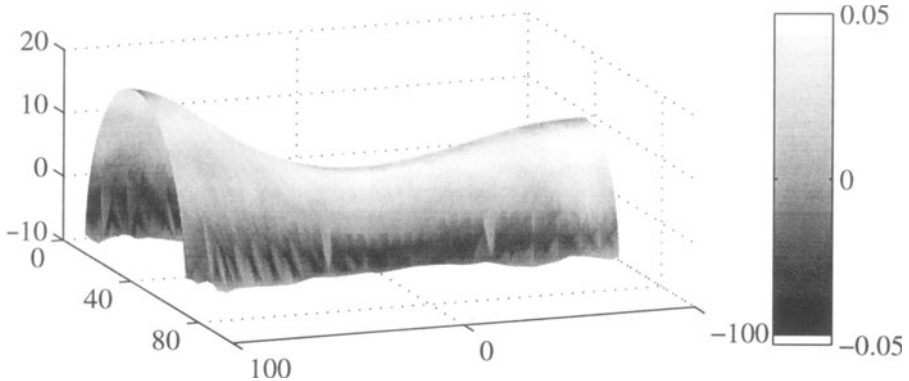


Fig. 3 Deviations from nominal

After this first analysis, the influence of the errors linked to the measurement process are small enough to be negligible in the following analysis.

At this stage of the study the remaining deviations are issued from the milling process. The possible causes considered for the remaining deviations are: the tool geometry, the tool deflection and the machine tool behavior (servo-control, geometry, vibrations...).

Concerning the tool geometry, the measurement of the real tool shape is performed. Each cutting edge is measured using an optical bench. Besides the dimension which is not right, the shape of the tool is not hemispherical. In fact, each edge can be approximated by an arc of circle whose radius value is greater than the theoretical one ($R_0 = 5\text{ mm}$), and whose centre does not belong to the tool axis (see table 2). Even though the tool shape is far from the perfect shape, this can be explained by the grinding method.

edge	Radius (mm)	dx (mm)	dz (mm)	Form deviation (mm)
1	5.214	0.116	0.206	0.020
2	5.176	0.095	0.188	0.018

Table 2 : Geometry of the tool edges

In order to take into account these effects, we adopt the model proposed in figure 4. The parameter dz is determined considering that the virtual ideal tool and the real tool have the same length. The link between the two edges is characterized at N by a tangent discontinuity. The distance between N and the axis tool is measured : 0.16 mm . Moreover, the analysis shows that edge 2 is shifted back

relative to the other one. We thus only consider the effect of the shape of edge 1. In order to evaluate the deviations induced by the non perfect tool geometry, we compute the distance between the point M , that belongs to edge 1 and M_o , that belongs to the theoretical edge. The variation of the deviations e_{tool} , with the angle θ , that defines the normal orientation relative to the tool axis, is presented in figure 4.

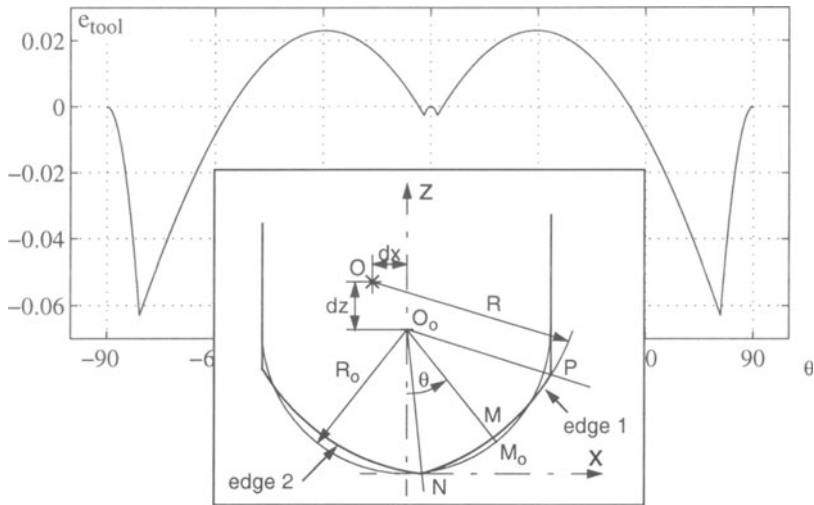


Fig. 4 Deviations due to the tool geometry

Note that the amplitude of these deviations is significant in comparison to the deviations due to the CAM system : 0.09 mm (thereof 0.008 mm only result from the CAM system).

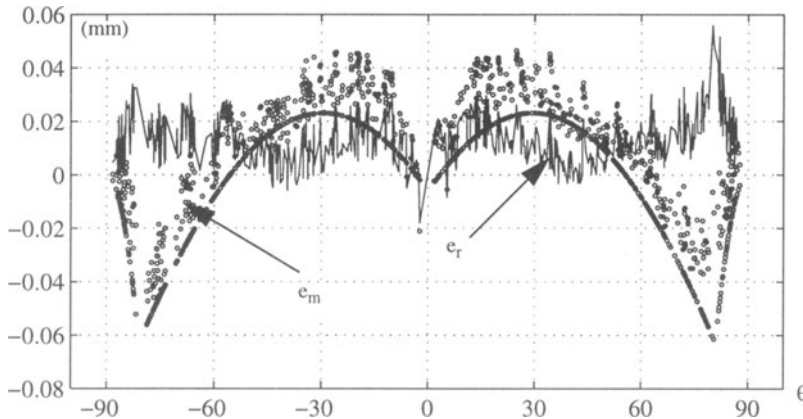


Fig. 5 Residual deviations

The evolution of the measured geometrical deviations with θ is shown in figure 5. We notice that the general form of the mean curve of the deviations is similar to the one in figure 4. The tool geometry is thus the essential source of errors in our experimentation.

Finally, to achieve the assessment of the process, we have to separate the identified errors and the residual deviation e_r is given by : $e_r = e_m - e_{CAM} - e_{tool}$ at each point. Errors issued from the measuring process are bounded by $-2 \mu\text{m}$ and $2\mu\text{m}$. So the residual deviation essentially includes the effects due to the machine tool behavior. The evolution of the residual deviations with θ are shown in figure 5. Figure shows a significant systematic error, close to 0.015 mm , which is surprising and can not only be explained by the effect of the machine tool behavior. Among the most likely explanations, the effect linked to the adjustment of the tool geometry model seems to be the most pertinent. In fact, through the hypothesis that the effect of the tool deflection is negligible on the points whose normal is vertical, such points are used to define the zero deviation of the tool geometry model. An error on the origin obviously implies an offset on the deviations. The separation of the remaining deviations is not yet realized for not identifiable simply.

5. Conclusion

An approach to certify the machining process of free form surfaces is proposed. Besides the evaluation of the process performance performed by the part measurement, an identification of the different sources of error is proposed. Even though it is not possible to clearly estimate the effects of each actor of the process, some of them are quantified at each point using models, or measurements. That is the case for errors linked to the CAM system (i.e. tool path calculation) and these due to the non-perfect tool geometry, that can be thus estimated before the part machining. The remaining geometrical deviations (obtained by subtraction of CAM and tool geometry errors to the measured geometrical deviations) include effects not qualifiable easily (servo-control, machine tool geometry,). The application of the method to a well-known part surface shows the efficiency of the proposed models. However, the final measurement of the part has to be carried out with some caution so that the measuring process does not become a new source of unknown errors.

References

- [1] CHOI B.K., LEE C.S., HWANG J.S. and JUN C.S, Compound surface modelling and machining, *Computer Aided Design*, **20**, no 3 (1988) 127-136
- [2] JERARD R.B., HUSSAINI S.Z., DRYSDALE R.L. and SCHAUDT B., Approximate methods for simulation and verification of numerically controlled machining programs, *The Visual Computer*, n 5 (1989) 329-348
- [3] KIM C.B., PARK S. and YANG M.Y., Verification of NC tool path and ,manual and automatic editing of NC code, *International Journal of Production Research* **33** n 6 (1995) 1683-1697,
- [4] SARTORI S. and ZHANG G., Geometric error measurement and compensation of machines, *Annals of the CIRP* **44**, no 2 (1995) 599-609
- [5] THIEBAUT F., LARTIGUE C., and DUC E., A certification method for the milling process of free-form surfaces using a test part, *International Journal of Production Research* **37** n 2 315-327
- [6] TOURNIER C. Evaluation des modes de generation des trajets outil pour l'usinage de formes gauches. Etude de cas, *DEA de Production Automatisee* - ENS Cachan, 1996
- [7] YEUNG M.K., WALTON D.J., Curve fitting with arc splines for NC toolpath generation, *Computer Aided Design* **26**, n 11 (1994) 845-849

NOMINAL AND ACTUAL GEOMETRY EXPLICIT DECLARATION

Application to Dimensional Inspection

Catherine CUBÉLÈS-VALADE, Alain RIVIERE

*Institut Supérieur des Matériaux et de la Construction Mécanique,
3 Rue Fernand Hainaut,
93407 SAINT-OUEN Cedex, FRANCE, Tél. : 33.1.49.45.29.20
email : ariviere@ismcm-cesti.fr*

1. Geometry and tolerancing

1.1. DECLARATIVE GEOMETRY

1.1.1. TTRS Model version 1.

A TTRS (Technologically and Topologically Related Surface), [CLE 94] and [CLE 97], is composed of either a pair of surfaces or a pair of TTRS's, or a surface and a TTRS. The notion of inheritance is integrated into the model: each TTRS entity X inherits the general structure of the model shown in Fig. 1. The model has 7 classes of surfaces. The first three classes of surfaces - spherical, cylindrical and plane - are said to be **simple** surface classes, compared to the other four surface classes which are helicoidal, generated by rotation, prismatic or any other type and are said to be **complex**. 6 cases of surface relations result from the association of the three classes of simple surfaces and define **13 relative positioning constraints**. TTRS entities are comprised of several types of attributes: those considered as elementary--points, straight-lines or planes—denoted elementary MGRE's (Minimum Reference Geometric Elements) and those considered as elementary constructed MGRE's, for instance running points. The TTRS also has relative positioning, topological and chirality type constraints as attributes.

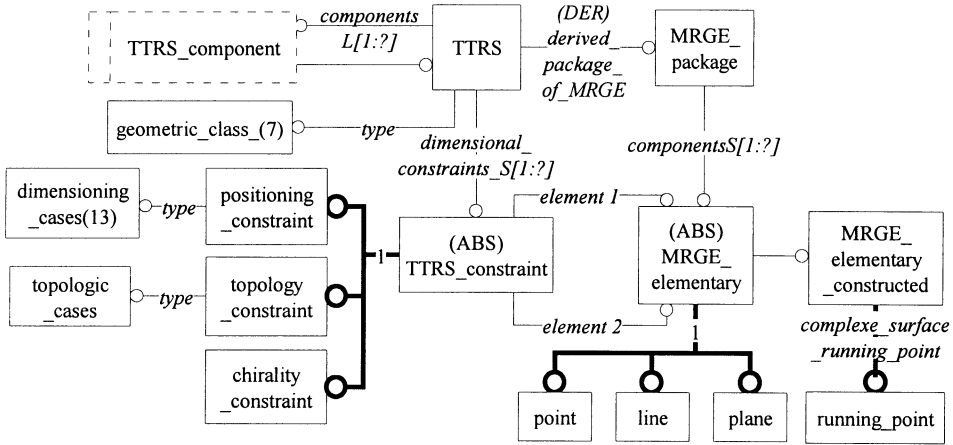


Fig. 1 : TTRS Model

1.1.2. Review of the 13 relative positioning constraints

Each relative positioning constraint, [CLE 98], possesses a mathematical expression which has been prepared using the following hypotheses :

A point M in space is defined by its original vector, as : $\vec{m} = \overrightarrow{OM}$. A straight-line D in space is defined by two perpendicular vectors : \vec{t} , directive unit vector and \vec{p} , as $\forall M_D \in D : \vec{p} = \overrightarrow{OM}_D \wedge \vec{t}$. A plane P in space is defined by a normal unit vector, \vec{n} , and a scalar, d , as $\forall M_P \in P : d = \overrightarrow{OM}_P \cdot \vec{n}$.

These 13 constraints constitute a necessary tool, sufficient for the explicit definition of the positioning of any simple or complex surface in relation to any other simple or complex surface. Utilization of the thirteen relative positioning constraints enables the **explicit constraint-assisted declaration** of the tolerancing and dimensioning of a mechanical part to be made, in a very flexible manner. For instance, the constraint C13 between two lines may be expressed like :

$$Ang(D_1, D_2) = arcsin(\|\vec{t}_1 \wedge \vec{t}_2\|) = arccos(|\vec{t}_1 \cdot \vec{t}_2|)$$

C13 : distance and angle (line, line)

$$d(D_1, D_2) = \frac{|\vec{t}_1 \cdot \vec{p}_2 + \vec{t}_2 \cdot \vec{p}_1|}{\|\vec{t}_1 \wedge \vec{t}_2\|}$$

1.2. EXAMPLE OF A CURVE

1.2.1. De Casteljau's construction declaration

The objective is to **declare** the De Casteljau curves, [CAS 86], defined by their poles and to describe their dimensioning by a list of positioning constraints. To be more precise, these constraints not only enable the **positioning** of the curve to be **declared** with respect to its poles but also allow **dimensioning** the declared curve or surface.

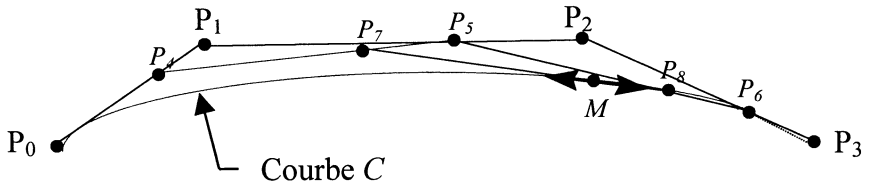


Fig 2 : De Casteljau Curve

Let C be the De Casteljau curve to be declared in a 3D space. Let P_0, P_1, P_2 and P_3 be its four poles, as per De Casteljau definition. Full declaration of the curve C includes that of each of the points constructed from these poles (Fig 2), P_4, P_5, P_6, P_7, P_8 , and from the point P_9 , called the running point, of the geometric locus curve C . The successive declaration of these sub-poles is carried out.

For each declaration of constructed sub-poles, two C2 relative positioning constraints and one topological constraint have to be applied : C2 : distance (first pole, constructed pole) and C2 : distance (constructed pole, second pole) ; the constructed pole belongs to the segment [first pole, second pole], [CLE 98]. The system of constraints (S) for the complete declaration is thus expressed by :

$$\begin{aligned}
 & \forall i \in [0,3], \text{ (2nd degree curve pole construction) } \\
 & d(P_i, P_{i+4}) = \|\vec{m}_{P_{i+4}} - \vec{m}_{P_i}\| \\
 & d(P_{i+4}, P_{i+1}) = \|\vec{m}_{P_{i+1}} - \vec{m}_{P_{i+4}}\| \\
 & \|\vec{m}_{P_{i+4}} - \vec{m}_{P_i}\| / \|\vec{m}_{P_{i+1}} - \vec{m}_{P_{i+4}}\| = k \\
 & d(P_i, P_{i+4}) + d(P_{i+4}, P_{i+1}) - d(P_i, P_{i+1}) = 0 \\
 & \forall i \in [4,6], \text{ (1st degree curve pole construction) } \\
 & d(P_i, P_{i+3}) = \|\vec{m}_{P_{i+3}} - \vec{m}_{P_i}\| \\
 & d(P_{i+3}, P_{i+1}) = \|\vec{m}_{P_{i+1}} - \vec{m}_{P_{i+3}}\| \\
 & \|\vec{m}_{P_{i+3}} - \vec{m}_{P_i}\| / \|\vec{m}_{P_{i+1}} - \vec{m}_{P_{i+3}}\| = k \\
 & d(P_i, P_{i+3}) + d(P_{i+3}, P_{i+1}) - d(P_i, P_{i+1}) = 0 \\
 & \text{Pour } i = 7, \text{ (0 degree curve pole construction) } \\
 & d(P_i, P_{i+2}) = \|\vec{m}_{P_{i+2}} - \vec{m}_{P_i}\| \\
 & d(P_{i+2}, P_{i+1}) = \|\vec{m}_{P_{i+1}} - \vec{m}_{P_{i+2}}\| \\
 & \|\vec{m}_{P_{i+2}} - \vec{m}_{P_i}\| / \|\vec{m}_{P_{i+1}} - \vec{m}_{P_{i+2}}\| = k \\
 & d(P_i, P_{i+2}) + d(P_{i+2}, P_{i+1}) - d(P_i, P_{i+1}) = 0
 \end{aligned}
 \tag{S}$$

A 3rd-degree De Casteljau curve is defined by 4 poles. Consequently, the declared and constructed sub-poles P_4, P_5 and P_6 define a 2nd-degree De Casteljau curve; the same declared and constructed sub-poles, P_7 and P_8 define a 1st-degree De Casteljau curve (that is, a straight-line) and the running point P_9 , defines a 0-degree De Casteljau curve, that is, the point itself. According to the above explanations, the system (S) is composed of three sub-systems. The running point P_9 has several specificities : it is therefore declared in the same manner as the other sub-poles, it belongs to the curve and defines the exact position of the tangent to the curve. This tangent is a 1st-degree curve (a straight-line) which passes through the constructed sub-poles, P_7 and P_8 . Let (P_7, P_8) be

the tangent to the curve at P_9 . It is declared using the two C4 constraints coinciding with

points (P_7 and P_8) and can be expressed by :

$$\begin{cases} \vec{m}_{P_7} \wedge \vec{t}_{(P_7, P_8)} = \vec{P}_{(P_7, P_8)} \\ \vec{m}_{P_8} \wedge \vec{t}_{(P_7, P_8)} = \vec{P}_{(P_7, P_8)} \end{cases}$$

1.3. NORMALIZATION ADVANCEMENT

Since the beginning of the 80's, the technological advancement of CAD-CAM has enabled digitized surfaces to be defined as close as possible to the projected functions (aerodynamics, design, etc.). These surfaces, of a new type, are increasingly complex. What do we understand by complex surface ?

These are quite simply surfaces that we are not accustomed to handling. What responses do the tolerancing and verification standards of such surfaces provide? CAD-CAM systems provide designers with nominal definitions as close as possible to the functions expected from the product. On the other hand, the geometry of the shapes drawn is more and more complex. Maximum admissible deviation for complex products - generally called tolerances by the mechanical engineer - must be expressed in a language that is common to all the actors in a company : this is the standardized language of industrial design. If we look at standards for technical design, such as AFNOR or ISO, these have been built up gradually according to industrial requirements, using examples, and they take little or no account of the tolerancing of complex surfaces. The French E04-562 standard project, [NOR E04], entitled « Geometric Product Specification (GPS), Complex surfaces, Specifications for design », proposes an initial response for the tolerancing of these complex surfaces, together with a possibility for referencing them.

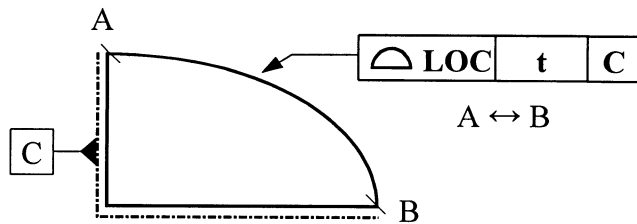


Fig. 3 : Tolerancing of a complex form in relation to a prismatic reference

The example shown in Fig. 3 illustrates the type of symbol proposed by the standard project. The form symbol, standardized for simple surfaces, together with the letters « LOC » is used to indicate that the specification is a localization of a complex surface. The reference system is constituted by the surface C, which is a complex surface. It is indicated on the drawing by a dot-and-dash line. This reference system is a prismatic surface which corresponds to the association of two plane surfaces. The standard project also provides for the resolution of **progressive** and **offseted** tolerance areas; however, this case is not covered in this article. The TTRS model advancements, particularly as regards the surface running point, deal with the geometrical declaration of complex surfaces, as well as their tolerancing and dimensional inspection.

2. Tolerancing declaration/actual geometry integration

2.1. DECLARATION OF THE MODELS

2.1.1. Tolerancing declaration

As per the ISO 10303-47 standard, [ISO 97], commonly called part 47 of the STEP standard, the model (Fig. 4) defines a geometric tolerance by the relative positioning of the tolerated element and the tolerance zone in relation to the datum system. Any TTRS tolerance zone boundary is positioned in relation to a tolerated element using one or several relative positioning constraints. This unit (tolerance area \cup tolerated element) constitutes the tolerancing TTRS which is itself positioned in relation to the TTRS datum, using one or several relative positioning constraints and constitutes the tolerancing TTRS, as shown in Fig. 4.

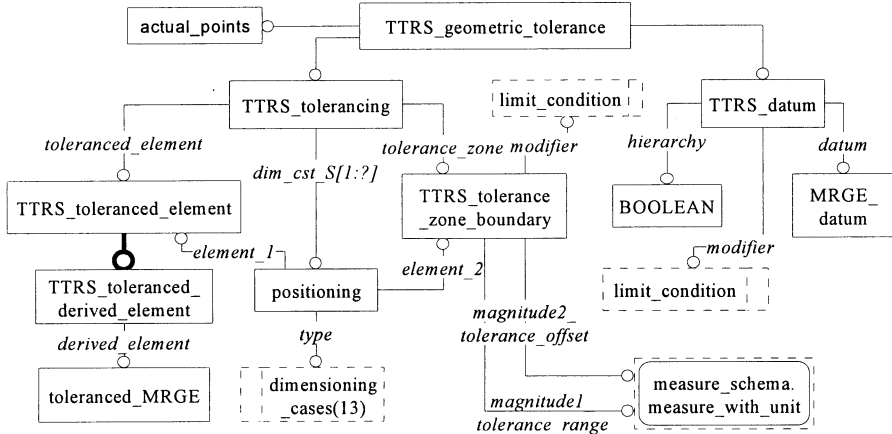


Fig. 4 : Tolerancing model

2.1.2. Actual geometry integration

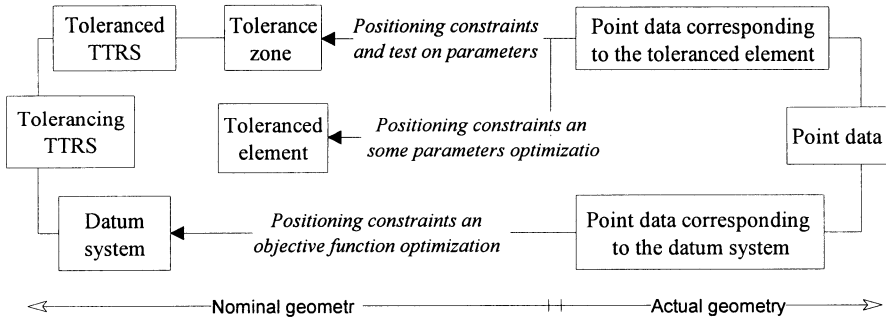


Fig. 5 : Nominal model and actual model

Fig. 5 shows the integration diagram for nominal and actual geometry. The significance of the method presented here is the constraint-assisted **declaration of relative positioning** of the **extracted actual point data** representative of the datum system and the element tolerated, directly and respectively corresponding to the **nominal, declared elements**.

2.2. EXAMPLE OF THE LOCALIZATION OF A BEZIER CURVE

2.2.1 Dimensioning

The example examined in this paragraph relates to the localization of a Bezier curve in relation to a prismatic surface, as shown in Fig. 3.

Dimensioning of the part is composed of two parts. The surface comprised between points A and B is a complex surface whose dimensioning is described in paragraph « 1.2.1. De Casteljaun's construction declaration », and which provides us with knowledge of its running point (used later for tolerancing and metrology). Dimensioning the datum, that is to say the surface or TTRS C, composed of two perpendicular plane surfaces, is declared by a C7 constraint, angle (plane, plane), so the angle equals 90°. Completeness of dimensioning is achieved by positioning the running point of the complex surface in relation to the TTRS C.

2.2.2. Tolerancing

Declaration of the tolerancing is a declaration identical in conformity with dimensioning, to which is added the declaration of the tolerance zone boundary. This declaration is also achieved using the running point principle, as shown in Figure 6. This boundary is limited by surfaces S_1 et S_2 , whose running points are respectively M_1 and M_2 .

The two running points M_1 and M_2 are positioned in relation to the running point P_9 , at a fixed distance of $t/2$ (half of the tolerance) and by a topological constraint indicating that the point P_9 belongs to the segment $[M_1, M_2]$. The corresponding system of equations is :

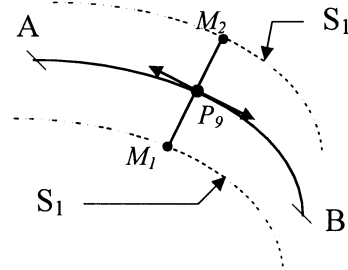


Figure 6 : Tolerance area

$$\begin{cases} C_2 : d(P_9, M_1) = \|\vec{m}_{P_9} - \vec{m}_{M_1}\| = f(k) \\ C_2 : d(P_9, M_2) = \|\vec{m}_{P_9} - \vec{m}_{M_2}\| = f(k) \\ d(M_1, P_9) + d(P_9, M_2) - d(M_1, M_2) = 0 \end{cases}$$

Function $f(k)$ gives the value of the tolerance, in the case of a progressive and displaced tolerance, in relation to the position of the point courant. In this case, the value of the zone is considered to be constant, thus $f(k)$ is constant and equal to $t/2$.

2.2.3. Metrology

Datum system association :

The datum point data is composed of two types of points : C_i , points corresponding to a plane and the point C_j , the other plane. For the declaration of this association, the distance of each of the points $C(i \text{ or } j)$ from the TTRS C_{ass} sought is declared, [BAL 92], in the sense of the least square criterion (criterion chosen), together with the perpendicularity constraint between the two plane surfaces. The form of the system is :

$$\begin{cases} Dist(M_i, plan A_{ass}) = \|\vec{m}_i \cdot \vec{n}_{A_{ass}} - d\| = \varepsilon_i \\ Dist(M_j, plan B_{ass}) = \|\vec{m}_j \cdot \vec{n}_{B_{ass}} - d\| = \varepsilon_j \\ Ang(plan A_{ass}, plan B_{ass}) = \arcsin(\|\vec{n}_{plan A_{ass}} \wedge \vec{n}_{plan B_{ass}}\|) = \Pi / 2 \\ Min[\sum(\varepsilon_i^2 + \varepsilon_j^2)] \end{cases}$$

The datum association here is an « exterior to matter » constraint, [BAL 92], [CUB 98]. Therefore, it is now necessary to declare the determination of an exterior to matter point (one for each datum plane). Let P_A be an approach point determining the exterior in relation to surface C . The objective is to declare the construction of a TTRS C_A (plane A_{approach} , plane B_{approach}), passing through the approach point. Declaration is achieved using the constraints :

C3 : distance (point P_{approach} , plane A_{approach} , parallel), where the distance is 0 and C6 : distance (plane A_{ass} , plane A_{approach}), so that the distance is d_A ; C3 : distance (point P_{approach} , plane B_{approach} , parallel), where the distance is 0 and C6 : distance (plane B_{ass} , plane B_{approach}), so that the distance is d_B . This list of constraints is expressed mathematically by the system :

$$\left\{ \begin{array}{l} d(P_{\text{approach}}, \text{plan } A_{\text{approach}}) = |\vec{m}_{\text{approach}} \cdot \vec{n}_{\text{approach}} - d_{A_{\text{approach}}}| = 0 \\ \vec{n}_{A_{\text{ass}}} \wedge \vec{n}_{\text{approach}} = \vec{0} \\ d(\text{plan } A_{\text{ass}}, \text{plan } A_{\text{approach}}) = |(\vec{n}_{A_{\text{ass}}} \cdot \vec{n}_{\text{approach}}) \times d_{A_{\text{approach}}} - d_{A_{\text{ass}}}| = d_A \\ d(P_{\text{approach}}, \text{plan } B_{\text{approach}}) = |\vec{m}_{\text{approach}} \cdot \vec{n}_{\text{approach}} - d_{B_{\text{approach}}}| = 0 \\ \vec{n}_{B_{\text{ass}}} \wedge \vec{n}_{\text{approach}} = \vec{0} \\ d(\text{plan } B_{\text{ass}}, \text{plan } B_{\text{approach}}) = |(\vec{n}_{B_{\text{ass}}} \cdot \vec{n}_{\text{approach}}) \times d_{B_{\text{approach}}} - d_{B_{\text{ass}}}| = d_B \end{array} \right.$$

The distance of each of the points M_i and M_j is declared in relation to their respective approach plane.

$$\left\{ \begin{array}{l} d(M_i, \text{plan } A_{\text{approach}}) = |\vec{m}_{\text{approach}} \cdot \vec{n}_{\text{approach}} - d_{A_{\text{approach}}}| = d_i \\ \text{Sup}(d_i) \\ d(M_j, \text{plan } B_{\text{approach}}) = |\vec{m}_{\text{approach}} \cdot \vec{n}_{\text{approach}} - d_{B_{\text{approach}}}| = d_j \\ \text{Sup}(d_j) \end{array} \right.$$

$\text{Sup}(M_i)$ and $\text{Sup}(M_j)$ indicate the exterior to matter points. The two exterior to matter planes still have to be declared by the constraints : C3 : distance (point $M_{\text{external matter}}$, plane A_{ass} , parallel), where the distance is 0 and C6 : distance (plane A_{ass} , plane A'), so that the distance is $d_{A_{\text{ext}}}$; C3 : distance (point $M_{\text{external matter}}$, plane B_{ass} , parallel), where the distance is 0 and C6 : distance (plane B_{ass} , plane B'), so that the distance is $d_{B_{\text{ext}}}$. This list of constraints is expressed mathematically by the system :

$$\left\{ \begin{array}{l} d(M_{A_{\text{ext mat}}}, \text{plan } A') = |\vec{m}_{\text{ext mat}} \cdot \vec{n}_{A'} - d_{A'}| = 0 \\ \vec{n}_{A_{\text{ass}}} \wedge \vec{n}_{A'} = \vec{0} \\ d(\text{plan } A_{\text{ass}}, \text{plan } A') = |(\vec{n}_{A_{\text{ass}}} \cdot \vec{n}_{A'}) \times d_{A'} - d_{A_{\text{ass}}}| = d_{A_{\text{ext}}} \\ d(M_{B_{\text{ext mat}}}, \text{plan } B') = |\vec{m}_{\text{ext mat}} \cdot \vec{n}_{B'} - d_{B'}| = 0 \\ \vec{n}_{B_{\text{ass}}} \wedge \vec{n}_{B'} = \vec{0} \\ d(\text{plan } B_{\text{ass}}, \text{plan } B') = |(\vec{n}_{B_{\text{ass}}} \cdot \vec{n}_{B'}) \times d_{B'} - d_{B_{\text{ass}}}| = d_{B_{\text{ext}}} \end{array} \right.$$

Each point Pt_i of the point data is positioned in relation to the tolerance zone MGRE, that is to say the running point of the complex surface (AB). For each of the positions of the running point, the position of the tangent to the surface and, therefore, the normal is known (Fig. 7). Then, for each of the points Pt_i , the distance ε_i is declared in relation to the respective position of the running point P_9 , by including the topological constraint that point Pt_i belongs to the segment $[M_1, M_2]$.

For complex surface measure for design engineering, the $\text{Sup}(\varepsilon_i)$ is declared. The corresponding system of equations is :

$$\begin{cases} C_2 : d(Pt_i, P_9) = \|\vec{m}_{P_9} - \vec{m}_{Pt_i}\| = \varepsilon_i \\ d(M_1, Pt_i) + d(Pt_i, M_2) - d(M_1, M_2) = 0 \\ \text{Sup}(\varepsilon_i) \end{cases}$$

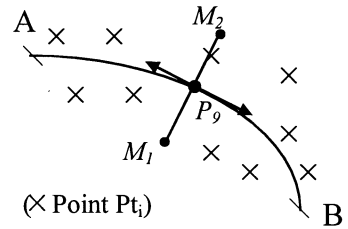


Fig. 7 : Complex surface point data

3. Conclusion

In this paper, we have presented a full declarative diagram, integrating dimensioning, tolerancing (from the CATIA Fd&T module) and the relationship between the nominal geometry and actual geometry of the mechanical parts. This declaration is expressed by a system of equations, inequations and target functions that will constitute input data for the solver. This new approach to dimensional inspection seems to us to possess particularly interesting exhaustivity and integration qualities. We are currently testing the exhaustivity of our declarative language, as well as the capacity of some solvers to resolve all our declarations.

4. References

- [CLE 94] CLEMENT A. et al, Cotation tridimensionnelle des systèmes mécaniques, PYC Edition, (1994).
- [CLE 97] CLEMENT A., VALADE C. et RIVIERE A., « The TTRSs : 13 Oriented Constraints for Dimensioning, Tolerancing & Inspection », Advanced Mathematical Tools in Metrology III, published by P. Ciarlina, M.G. Cox, F. Pavese & D. Richter, Ed. World Scientific Publishing Company, 1997, pp. 24-42.
- [BAL 92] BALLU A., « Identification de modèles géométriques composés pour la spécification et la mesure par coordonnées », Ph.D, 1992.
- [CLE 98] CLEMENT A., SERRE P. et RIVIERE A., « Géométrie et topologie déclarative : un nouveau paradigme pour la CFAO », 2ème Conférence Internationale sur la Conception et la fabrication intégrées en Mécanique, IDMME'98, UTC Compiègne France, 27-29 Mai 98.
- [CUB 98] CUBELES-VALADE C., RIVIERE A., SERRE P., CLEMENT A., « Intégration de la géométrie nominale et réelle », MICAD conference, Paris, 17-20 May 1998.
- [ISO 97] ISO/FDIS 10303-47, « Industrial automation systems - Product data representation and exchange : Shape variation tolerances », generic resources, ISO, 1997.
- [CAS 86] CASTELJAU P. (de), « Mathématiques et CAO 2, Formes à pôles », Hermes Ed., 1986.
- [NOR E04] Draft of French standard E04-562, proposed to ISO, « Spécification géométrique de pièces (GPS), Surfaces complexes, Spécifications sur le dessin ».

ADAPTIVE DIGITIZATION OF MECHANICAL PARTS

F. BENNIS and M. DANIEL*

Institut de Recherche en Cybernétique de Nantes (IRCyN) UMR 6597

**Institut de Recherche en Informatique de Nantes (IRIN)*

1, rue de la Noë, B.P. 92101, 44321 Nantes cedex 03

email :Fouad.Bennis@lan.ec-nantes.fr, Marc.Daniel@ec-nantes.fr

Abstract

This paper proposes an automatic and adaptive method for the digitization of numerical parts using Coordinate Measuring Machines (CMM). We present a methodology for scanning inspired by optimization algorithms and contour determination in Computer Aided Design. Relevance of the proposed method and its advantages compared to existing methods are illustrated by an example of industrial application consisting in measuring the profile curves and sections of parts of revolution. We finally set up the bases of an algorithm devoted to the surface digitization of any mechanical part.

1. Introduction

Digitization has different objectives. The first one is to create the CAD model of an existing part. A second application is to check part conformity to designer specifications.

There exist many techniques for mechanical part digitization. Some are adapted to products to measure (spotlight of profile, camera for plane parts,...) [2], [4]. Due to its speed of measurement, digitization using laser and camera seems a good technique. It has nevertheless some drawbacks and measurement through probes by contact is often required. Among these drawbacks, we can mention, the measurement accuracy, the low depth, the important equipment dimensions. This technique is not suitable for transparent or refractive parts, like plastic bottles. Moreover, organizing the point cloud is a difficult problem.

All the existing CMM machines propose programs based on digitization methods whose parameters are not all well mastered. Moreover, these methods are not adaptive since they uniformly digitize points on the surface. They are unable to adapt the number of points according to the geometrical complexity of the explored region. This yields the measurement of useless points and thus a waste of time.

2. General digitization algorithm with CM Machines

We present in this section the outlines of a general algorithm for the digitization with a Coordinate Measuring Machine. A scanning technique is proposed in order to precisely follow a predetermined trajectory on the part to digitize.

Let us introduce the following notations:

x_i : i-th digitized point known by its coordinates,

$X_i = \{x_i\}$: ordered "structured" list of the first i digitized points,

y_i : i-th valid or accepted point characterizing the line to digitize.

$Y_i = \{y_i\}$: ordered "structured" list of the first i y_i .

All the digitized points belong to X_i list. Y_i is sufficient to provide a good definition of the curve to be digitized (with respect to the accuracy required by the user). Y_i is obtained during the scanning process by suppressing points x_i which do not add a worthwhile complement of information.

Algorithm:

```

begin
step 1: obtention of the data limiting the region to digitize
repeat /* in the current situation, we have  $X_n = \{x_n\}$  and  $Y_p = \{y_p\}$  .
    step 2: estimation of the following point  $x_{n+1}$ :  $\tilde{x} = \Psi(x_1, \dots, x_n)$ 
    step 3: measurement of point  $x_{n+1}$  by sighting: estimated point :
         $X_{n+1} = X_n \cup \{x_{n+1}\}$ ,
    step 4: computation of the difference between estimated point  $x$  and
        measure point  $x_{n+1}$ .
        If point  $x_{n+1}$  satisfies the criteria do :
             $Y_{p+1} = Y_p \cup \{x_{n+1}\}$  and  $(y_{n+1} = x_{n+1})$ 
until digitization is complete
step 5: computation of the offset region.
end
  
```

The first step of our algorithm consists in defining the limit of the region to digitize and the initial situation. The second stage estimates the point to digitize through an evaluation function Ψ . Then, the point is picked by sighting the predicted point. Evaluation and measurement are repeated until the region to digitize has been entirely covered. Finally, the radius of the probe must be taken into account to shift the digitized region for obtaining the true image of the part. Steps 2 and 3 of previous algorithm are closed to optimization techniques. Both require the definition of an efficient evaluation function Ψ . With a CMM, the prediction step is of fundamental importance because the prediction point is quickly computed while the measurement process involves the motion of the machine axis in order to posit the probe. Digitizing a point requires that the probe must move to the predicted point \tilde{x} , and must grope in its neighbourhood. In general, the probe moves straight from a starting point P_d (see figure 1). For safety

reasons, the probe moves at a nominal speed until point \mathbf{x}_s (defined by safety parameter d_s) and with a speed for measuring (very low in general) between \mathbf{x}_s and potentially up to \mathbf{x}_f (defined by search parameter d_r). The digitized point (limit of the material) must necessarily belong to interval $[\mathbf{x}_s, \mathbf{x}_f]$. Estimator ψ must therefore take into account these technical aspects to avoid wasting too many time in the groping process. *The predicted point must be as close as possible to the measured point, but without lost of safety.*

Digitizing a part whose CAD model exists is a very interesting particular case. Assuming an appropriate wedging between the part and the model, the latter can be used to compute the prediction of digitized points, which really speeds the process up.

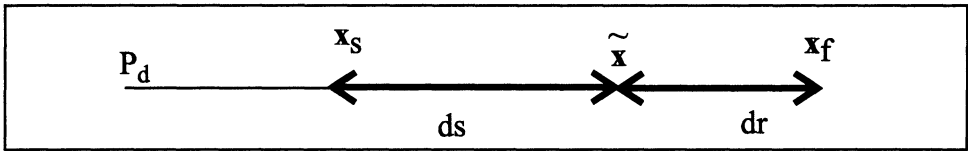


Figure 1. Parameters defining the probe working space

The proposed algorithm must allow us to define correctly the entity being digitized (a line for example). The difficulty is equivalent for marching methods in Surface-Surface Intersection (S.S.I.) problem. One must avoid to digitize or compute too many useless points. For an intersection curve, it is always possible to have an a posteriori control checking the good definition of the curve. This can entail the computation of some intermediate points [1]. For our digitization algorithm, this technique must be proscribed. We should avoid a loop including steps 2, 3 and 4 and devoted to the obtention of a 'good' point y_{p+1} . The progression step must automatically be adapted to directly obtain the good number of points. This automatic step adaptation depends on several tolerances which are difficult to master and on objects themselves. Results are proposed in [3] for S.S.I. search. We present our approach in section 3.2.

With a spherical head probe, each measurement provides the coordinates of the probe centre. We obtain a digitized point shift of the sphere radius from the "true" curve. An exact procedure must shift back every point along the normal direction to the surface at the given point. As far as we know, all scanning software propose a shift in the measurement plane and consider the normal direction on the digitized curve but not to on the surface. Applications proposed in the following allow us to estimate the surface normal vector and thus to propose a correct shift.

Offset curves and surfaces often contain singular points. Since the radius of the probe head is small, and the studied surfaces have to be digitized with this probe (rather "fair" surfaces) we do not consider singularities. Even by reducing the probe radius, some information on the part can not be reachable (singularities on the digitized curve).

3. Digitization of a surface of revolution

Our proposed method has the advantage of being an automatic, fast, generic and accurate method. It can be applied to all parts of revolution and does not require any specific installation. The digitization of the part takes place in two steps:

- determination of the revolution axis: for this purpose the user selects four points on the part. The system deduces the normal vectors to these given points and then the location of the axis through an automatic measurement of 8 additional points.
- Measurement by scanning of a profile curve or section or both depending on the user's choice.

3.1. DETERMINATION OF THE REVOLUTION PART AXIS

Searching the revolution axis is an essential step to avoid a manual alignment. Since the revolution axis is known, the final shift of the curve can be done in the plane defined by the current point and the axis. Another important point concerns visibility: every point to measure must be visible for the probe.

Let us introduce our notations, illustrated on Figure 2 and used in the following:

- * p_i a point on the surface of revolution,
- * n_i the normal to the surface of revolution at point p_i ,
- * D_i the line defined by vector n_i and point p_i , written $D = (p_i, n_i)$,
- * v the vector defining the revolution axis,
- * Δ the revolution axis, also written $\Delta = (m, v)$
- * p_{i0} the intersection point between lines D_i and Δ ,

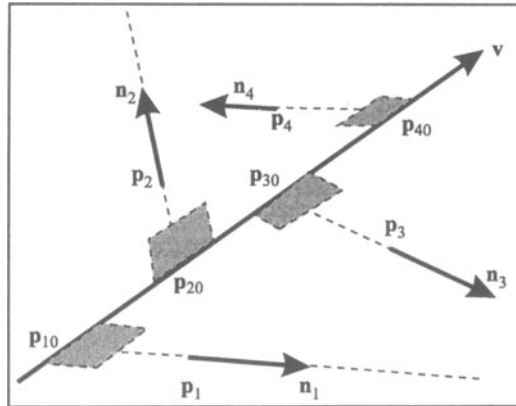


Figure 2. Location of the four points, the normal vectors and the axis

Normal vectors n_i can be measured with the M.M.C. The user chooses the position of points p_i and the machine automatically digitizes additional points in their neighbourhood (by picking two close points of p_i , we can determine two vectors whose cross-product approximates normal vector n_i).

We assume that coordinates of \mathbf{p}_i and \mathbf{n}_i are known and that coordinates of \mathbf{p}_{i0} , \mathbf{m} and \mathbf{v} are unknown. As \mathbf{m} is a free point on Δ , we will merge \mathbf{p}_{10} (first point \mathbf{p}_{i0}) and \mathbf{m} . Moreover vector \mathbf{v} can be deduced from any couple of points on Δ . Finally, let us consider: $\mathbf{m} = \mathbf{p}_{10}$ and $\mathbf{v} = \mathbf{p}_{10}\mathbf{p}_{20}$.

Our problem reduces to determine the 6 unknown coordinates of points \mathbf{p}_{10} and \mathbf{p}_{20} . Since point \mathbf{p}_{i0} belongs to line D_i ($\mathbf{p}_i, \mathbf{n}_i$), there exists a scalar value λ_i such that:

$$\mathbf{p}_{i0}\mathbf{p}_i = \lambda_i \mathbf{n}_i \quad (\lambda_i > 0 \text{ and } i = 1, \dots, 4) \quad (1)$$

Each equation of type (1) introduces an additional parameter λ_i . The balance between equations and unknowns requires four points \mathbf{p}_i .

As points \mathbf{p}_{i0} are aligned, we can introduce the following convention:

$$\mathbf{p}_{10}\mathbf{p}_{20} = \mathbf{v} \quad , \quad \mathbf{p}_{10}\mathbf{p}_{30} = k_1 \mathbf{v} \quad \text{and} \quad \mathbf{p}_{10}\mathbf{p}_{40} = k_2 \mathbf{v} \quad (2)$$

Applying the relations ($\mathbf{p}_{i0}\mathbf{p}_{i0} = \mathbf{p}_{10}\mathbf{p}_1 + \mathbf{p}_1\mathbf{p}_i + \mathbf{p}_i\mathbf{p}_{i0}$ ($i=1, \dots, 4$)) and combining (1) and (2), we obtain the system of 9 unknowns and 9 equations:

$$\begin{cases} \mathbf{v} = \lambda_1 \mathbf{n}_1 + \mathbf{p}_1\mathbf{p}_2 - \lambda_2 \mathbf{n}_2 \\ k_1 \mathbf{v} = \lambda_1 \mathbf{n}_1 + \mathbf{p}_1\mathbf{p}_3 - \lambda_3 \mathbf{n}_3 \\ k_2 \mathbf{v} = \lambda_1 \mathbf{n}_1 + \mathbf{p}_1\mathbf{p}_4 - \lambda_4 \mathbf{n}_4 \end{cases} \quad (3)$$

the unknowns being : λ_i ($i=1, \dots, 4$), k_1 , k_2 and the three coordinates of vector $\mathbf{v} = \mathbf{p}_{10}\mathbf{p}_{20}$.

To solve this system, we decompose the problem on basis ($\mathbf{n}_1, \mathbf{n}_2, \mathbf{p}_1\mathbf{p}_2$). Selecting a point so that the vectors define a basis can be easily achieved by the operator. We write the following linear decomposition:

$$\begin{aligned} \mathbf{n}_3 &= \alpha_3 \mathbf{n}_1 + \beta_3 \mathbf{n}_2 + \gamma_3 \mathbf{p}_1\mathbf{p}_2 \\ \mathbf{n}_4 &= \alpha_4 \mathbf{n}_1 + \beta_4 \mathbf{n}_2 + \gamma_4 \mathbf{p}_1\mathbf{p}_2 \\ \mathbf{p}_1\mathbf{p}_3 &= \alpha_{13} \mathbf{n}_1 + \beta_{13} \mathbf{n}_2 + \gamma_{13} \mathbf{p}_1\mathbf{p}_2 \quad (4) \\ \mathbf{p}_1\mathbf{p}_4 &= \alpha_{14} \mathbf{n}_1 + \beta_{14} \mathbf{n}_2 + \gamma_{14} \mathbf{p}_1\mathbf{p}_2 \end{aligned}$$

If vectors \mathbf{n}_3 and \mathbf{n}_4 are chosen so that their component on $\mathbf{p}_1\mathbf{p}_2$ does not vanish, we can assume that $\gamma_3 = 1$ and $\gamma_4 = 1$. Equations (4) leads to:

$$\begin{cases} \lambda_1 (k_1 - 1) = -\lambda_3 \alpha_3 + \alpha_{13} \\ \lambda_1 (k_2 - 1) = -\lambda_4 \alpha_4 + \alpha_{14} \\ \lambda_2 k_1 = -\lambda_3 \beta_3 + \beta_{13} \\ \lambda_2 k_2 = -\lambda_4 \beta_4 + \beta_{14} \\ k_1 = -\lambda_3 + \gamma_{13} \\ k_2 = -\lambda_4 + \gamma_{14} \end{cases} \quad (5)$$

From the two last lines in (5), we eliminate λ_3 and λ_4 . After substitution in the other equations and elimination of λ_1 and λ_2 , we have the following equations:

$$\begin{cases} k_1 k_2 (\alpha_3 - \alpha_4) + k_1 (\gamma_{14} \alpha_4 - \alpha_{14} - \alpha_3) + k_2 (\alpha_{13} - \gamma_{13} \alpha_3 + \alpha_4) + (\gamma_{13} \alpha_3 - \alpha_{13} - \gamma_{14} \alpha_4 + \alpha_{14}) = 0 \\ k_1 k_2 (\beta_3 - \beta_4) + k_1 (\gamma_{14} \beta_4 - \beta_{14}) + k_2 (\beta_{13} - \gamma_{13} \beta_3) = 0 \end{cases} \quad (6)$$

Introducing intermediate parameters e_i and f_i , equations (6) can be written:

$$\begin{cases} k_1 k_2 e_1 + k_1 e_2 + k_2 e_3 + e_4 = 0 \\ k_1 k_2 f_1 + k_1 f_2 + k_2 f_3 = 0 \end{cases} \quad (7)$$

from which we obtain:

$$\begin{cases} k_2 = A k_1 + B \\ k_1 k_2 f_1 + k_1 f_2 + k_2 f_3 = 0 \end{cases} \quad \text{with : } A = \frac{f_1 e_2 - e_1 f_1}{e_1 f_3 - f_1 e_3} \quad \text{and } B = \frac{f_1 e_4}{e_1 f_3 - f_1 e_3} \quad (8)$$

Finally, eliminating k_2 yields a second degree equation in k_1 :

$$A f_1 k_1^2 + (B f_1 + f_2 + A f_3) k_1 + B f_3 = 0 \quad (9)$$

We considered the general case where all parameters do not vanish (the particular cases entail simpler relations). Equation (9) provides two roots for k_1 . It is then possible to compute the two solutions for unknowns k_2 , λ_3 , λ_4 , λ_1 and λ_2 . Finally, two solutions for vector \mathbf{v} are obtained. One of them can be eliminated with relatively simple conventions. In our case, we have chosen $\lambda_i > 0$ writing $\mathbf{p}_{i0} \mathbf{p}_i = \lambda_i \mathbf{n}_i$.

We should note that our tests proved that the direction of the axis is not very sensitive to the choice of the 4 points on the part, provided that a reasonable distance between points is respected and to avoid that normal vectors lie in the same plane.

3.2. DIGITIZATION OF A PROFILE CURVE

The goal is to obtain, in optimal time, the best sampling of a profile curve. Geometric details must not be forgotten and a concentration of digitized points must exist where the profile have important shape variations. Digitization is achieved in a plane $(\mathbf{o}_1, \mathbf{v}, \mathbf{y})$. We define an orthogonal frame with unit vectors $R(\mathbf{o}_1, \mathbf{v}, \mathbf{z})$ with the knowledge of a point \mathbf{p}_0 on the profile, and axis $\Delta = (\mathbf{m}, \mathbf{v})$:

$$\mathbf{y} = \frac{\mathbf{o}_1 \mathbf{p}_0}{\|\mathbf{o}_1 \mathbf{p}_0\|} \quad \text{and} \quad \mathbf{z} = \mathbf{v} \wedge \mathbf{y} \quad (10)$$

\mathbf{o}_1 , being the intersection between the plane containing \mathbf{p}_0 and perpendicular to Δ

We just have to apply our general digitization algorithm to the profile of the revolution part. The definition of the measurement plane corresponds to step 1 in the algorithm. We should note, that by definition of revolution parts, normal vectors to digitized points are necessary in plane $(\mathbf{o}_1, \mathbf{v}, \mathbf{y})$. The shift process can then be realized without particular care.

As discussed in the general algorithm, the most crucial issues concern the estimator definition and criteria for point acceptance. The prediction of the following point can be decomposed into estimations of a direction and of a step.

Prediction of $\tilde{\mathbf{P}}_{i+2}$ is located on the tangency in \mathbf{P}_{i+1} at the parabola defined by \mathbf{P}_{i-1} , \mathbf{P}_i , \mathbf{P}_{i+1} as illustrated in figure 3 (\mathbf{t}_{i+1} being the unit vector on this tangency).

Points \mathbf{P}_{i-1} , \mathbf{P}_i and \mathbf{P}_{i+1} allow us to compute an approximation of the radius of curvature \mathbf{P}_i . A step estimating function of the radius (see figure 4) fixes the location of \mathbf{P}_{i+2} . The smaller the radius of curvature, the smaller the step. But when the radius is important, the step quickly increases up to a maximum value Stepmax. Steps must be smaller than the smallest information to detect.

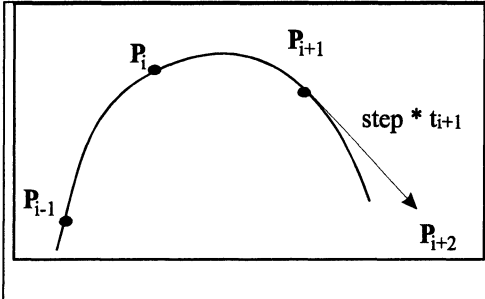


Fig. 3 : parabolic estimation of P_{i+2}

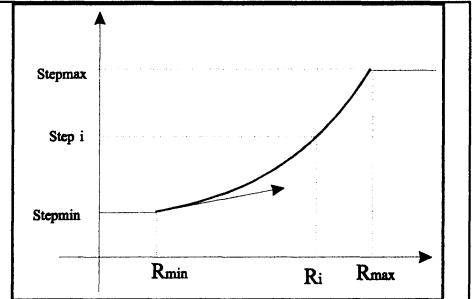


Fig. 4 : Step estimating function

However, for a part with long cylindrical or conical sections, it is convenient to apply a rather large step. The risk is then to skip a fundamental detail (a groove for example). An efficient way to avoid this problem is to allow the operator to pick some characteristic points by hand.

Remarks : To measure more than one profile of the part we consider the points of the first profile as estimators, which is greatly time saving (while avoiding all groping around points to digitize). This method is equivalent to the one applied to digitize parts with known CAD models. The difference is that the part is already aligned. Without loss of generality, the criteria for point acceptance is based on the minimum angle between two successive line segments.

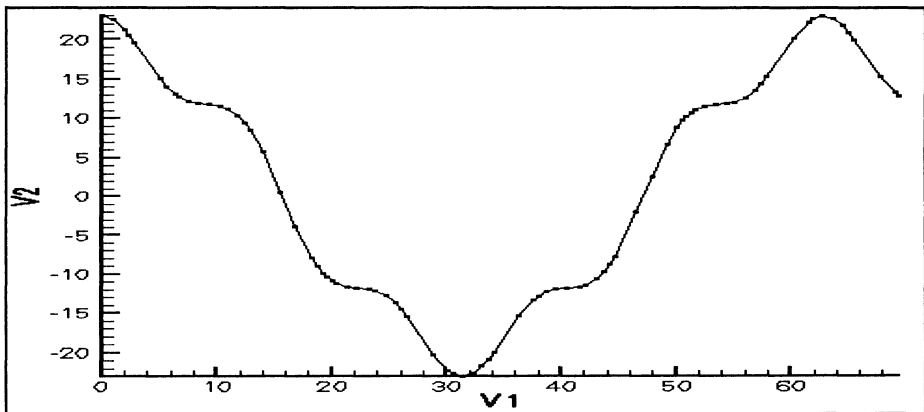


Fig. 5 : simulation example using a parabolic estimation

In figure 5, we propose a simulation of the algorithm based on the above criteria. We should note that the different parameters (Stepmax, Stepmin, Rmax et Rmin) depend on the part complexity and on the probe radius. They should be chosen by the operator in regard of her (his) quality requirement. In figure 6, we propose an example with a groove in which the characteristic points have been initially picked by the operator.

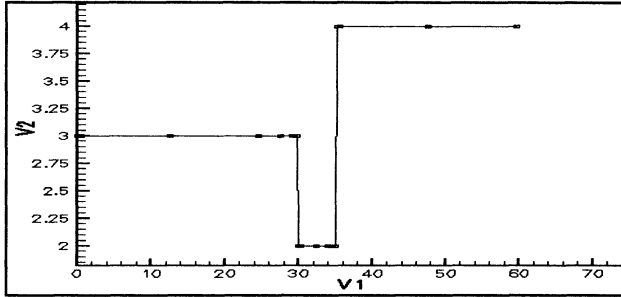


Fig. 5 :digitizing a part with a groove

4. Conclusion

An original method for digitizing parts has been proposed. The achieved tests prove its generality and its efficiency. The latter can always be improved by introducing more and more accurate estimators. Our first goal is to adapt the method to different types of parts defined by a geometric characteristic (such as ruled surfaces for example).

A second goal is to propose a digitization method available for any mechanical part. The methods often proposed are based on the use of parallel planes. In each plane, a curve is digitized and offset in the same plane. However, this technique does not consider the true normal vector to the surface and produces a "wrong" final curve. We propose to construct a progressive Delaunay mesh (see also [5]). Each digitized point is introduced into the mesh and allows us to adjust at best the prediction of next point. This process is repeated until a break criterion is satisfied (minimal size of a triangle, angle between two triangles,...). In that case, the estimator ψ considers all measured points to predict next point. On the other hand, at every point of this mesh, normal vector is easily approximated.

References

- [1] R. BARHNILL, G. FARIN, M. JORDAN, B. PIPER, "Surface/surface intersection", Computer Aided Geometric Design 4 (1987), pp. 3-16.
- [2] Z. CHEN, T-L CHAI and S-Y HO. "Measuring 3-D Location and Shape parameters of cylinders by a spatial technique", IEEE Transaction on Robotics and Automation, Vol. 10, n. 5, October 1994, pp. 632-647.
- [3] E. MALGRAS, "Contribution à la détermination de l'intersection de surfaces paramétriques par des techniques de suivi de contours", PHD, Nantes University, january 1998.
- [4] A. NOBLE, R HARTLEY, J. MUNDY and J. FARLEY. "X-Ray Metrology for Quality Assurance". IEEE International Conference on RA, pp. 1113-1119.
- [5] H. PARK and K. KIM. "An adaptive method for smooth surface approximation to scattered 3D points". Computer-Aided Design, Vol. 27 (12), december 1995, pp. 929-939.
- [6] A. SPYRIDIS and A. REQUICHA, "Accessibility Analysis for Automatic Inspection of Mechanical Parts by C.M.M.". IEEE International Conference on Robotics and Automation, Cincinnati Ohio, May 1990, pp. 1284-1289

GEOMETRIC TOLERANCE TRANSFER FOR MANUFACTURING BY AN ALGEBRAIC METHOD

F. BENNIS, L. PINO, C. FORTIN*

Institut de Recherche en Cybernétique de Nantes (IRCyN)

1, Rue de la Noë - BP 92101 - 44321 Nantes Cedex 3 - France

Laurent.Pino@lan.ec-nantes.fr

** Ecole Polytechnique de Montréal*

Departement of Mechanical Engineering - Montréal H3C 3A7 - Canada

Abstract

The increasing need of high quality products, leads industry to improve the tolerancing of their products. It is thus necessary to calculate, as precisely as possible, every tolerance to achieve functional requirements and to take into account the influence of manufacturing processes and the results of the final assembly. An algebraic method is proposed which can help tolerance analysis and synthesis, and in particular tolerance transfer. It is a continuation of previous work developed particularly by Louis Rivest, Clément Fortin and others. The method allows the algebraic determination whether a tolerance can be transferred, and what will be its shape after transfer. This result is obtained from a second degree equation. The study of this equation determines whether the transfer is possible. The calculation time is reduced since no simulation is required. Finally, two examples are used to show that the method can solve some complex cases.

1 Introduction

To design a part, the designer defines the shape of surfaces of this part as perfect forms. Although production tools are more and more precise, they can only realise parts that only approach the perfect form. Tolerancing allows the designer to define variation limits of real surfaces with respect to perfect surfaces. Tolerancing of a part is a very important task, since the final quality of the product depends on it. It is only with a rigorous tolerancing method that interchangeable parts can be assembled.

One of the first authors who tried to develop a formal model of tolerancing for CAD was Requicha. In 1983 he proposed a mathematical theory of geometric tolerancing [1]. This theory is based on the offset surface model. Srinivasan and Jayaraman, extended the Requicha's theory and proposed the theory of Virtual Boundary Requirements [2][3]. André Clément and Alain Rivière proposed the concept of Technologically and Topologically Related Surfaces (TTRS) [4] which structures the tolerance definition into a limited sub-set and proposes a general typology of tolerances. Louis Rivest proposed a kinematics model of tolerancing [5][6]. In particular, this model was developed to answer the fundamental question of tolerance analysis: the tolerance transfer, which can

be defined as follows: « *given an uncertainty zone defined in a reference frame A, how do we compute the value of this uncertainty zone in a new reference frame B, knowing the uncertainty zone associated to the surfaces composing the reference frame?* »

The current paper extends the concepts presented in [5]. The goal is to obtain an explicit solution of the transfer tolerance equation. It is recognised that an explicit solution is indispensable for tolerance synthesis. In the following, the kinematics model introduced by Rivest is presented. Finally, the analytic transfer method of a tolerance zone is developed.

2 The kinematics model

This model was developed by Louis Rivest [6]. It is based on the kinematics character of tolerance analysis. It uses the analogy between the tolerance zone and the workspace of a robot manipulator. The aim of the kinematics model is to define the region of space in which a toleranced feature must be found. In order to model a tolerance zone, Rivest et al propose a kinematics structure, similar to those used in robotics [5][6]. The limits of a tolerance zone correspond to the envelope of the workspace of the manipulator. As in robotics where the model of an end effector can be added to the model of a robotics mechanism, the kinematics models can be assembled to one another. In this way, a tolerance chain is formulated like a kinematics chain. The toleranced feature is free to move anywhere in the tolerance zone, as the terminal link of a robot can be located at any orientation or position within its workspace. This model can model all types of tolerances and it takes into account the role of the modifiers and the effect of datum precedence [5]. With the kinematics model, the resolution of the problem of tolerance transfer, is carried out in five stages. After defining the tolerance chain between the different features as well as the kinematics structure of this chain, it is necessary to make a discreet sweep of certain tolerance parameters to determine the extreme deviation of the controlled feature. The admissible state of the primary DRF is thus characterised in the target DRF. As soon as the state of the primary DRF is known with respect to the target reference frame, the extreme states of the tolerance zone in the target DRF can be calculated. Once we have these states, the intersection of the associated zone must be calculated to obtain the neutral zone in the target DRF. As the shape of this neutral zone cannot be directly used in manufacturing, the radius of a circular zone inscribed within the neutral zone must be calculated. This resolution raises several problems. Indeed, determining the neutral zone from sweeps can be obtained in two ways: either from a Boolean operation of solid models of each tolerance zone state, or from an analysis of the meaningful steps of the sweep. The first approach requires a solid modelling system that can easily operate several intersections of solid images of tolerance zones. Since the tolerance zones are very small, this approach usually exceeds the resolution of the solid modeller which is thus incapable of solving the Boolean operations. The second approach requires setting up an analysis for every sweep. This approach can make the generalisation of the problem more difficult.

We are now presenting a model that avoids these constraints, and calculates the image of the neutral zone in the target DRF. The method we describing uses a second degree

equation. The study of this equation permits to determine the possibilities of the tolerance transfer.

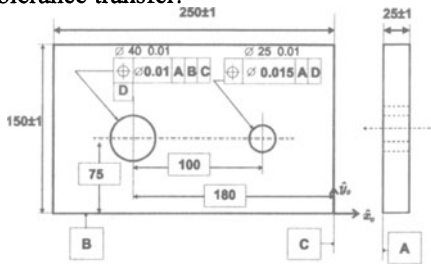


Figure 1. Definition drawing [5]

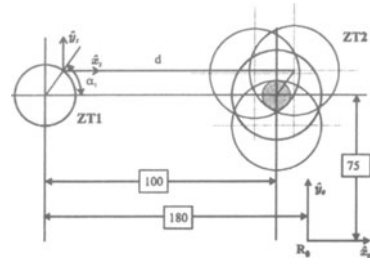


Figure 2. Tolerance zone definition

3 Analytic tolerance transfer: General case

A geometric tolerance applied to a feature defines a tolerance zone within which the real feature must be included. Let Z_i be the tolerance zone representing the space domain in which the real feature must be found. Every manufactured feature in this tolerance zone Z_i will be called an actual feature of Z_i . Apart from the tolerances of form which are intrinsic to the feature, all other tolerances are defined with respect to a functional DRF noted R_{fonct_i} . It is chosen for a given feature from a functional standpoint which is often related to the assembly characteristics of the mechanism.

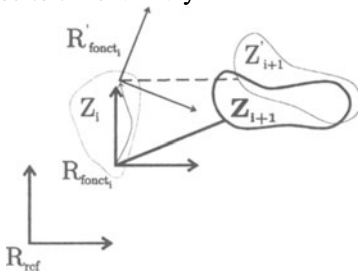


Figure 3. Datum frame definition

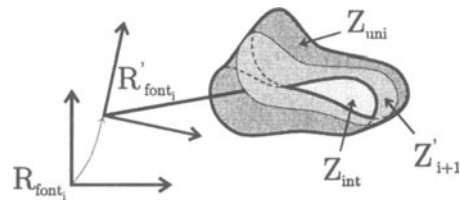


Figure 4. Tolerance zone definition

Let R_{ref} be the DRF in which we want to calculate the new tolerance zone (R_{ref} is the target DRF defined by Rivest et al). There is a tolerance chain between the R_{fonct_i} DRF and the R_{ref} DRF (Fig. 3). On this figure, every actual feature of Z_i participates to the definition of the Z_{i+1} functional DRF called R_{fonct_i} . If R_{fonct_i} is defined from tolerated features, it can be in an infinity of locations and orientations with respect to the R_{ref} DRF. R'_{fonct_i} is a possible situation of R_{fonct_i} , the zone Z'_{i+1} is obtained from zone Z_{i+1} with the same transformation which transforms R_{fonct_i} into R'_{fonct_i} . It is equivalent to move simultaneously with a rigid-body transformation the Z_{i+1} zone and the DRF R_{fonct_i} as shown in Figure 4. The complete set of locations of the Z_{i+1} tolerance zone for all locations of the R_{fonct_i} DRF defines the Z_{uni} zone (Fig. 4). Z_{uni} is therefore the union of all Z_{i+1} zones. A necessary condition of conformity of a feature is met when it belongs to the

Z_{uni} zone. Since it depends on the location of the R_{fonct_i} DRF, this condition is not sufficient. The Z_{int} zone represents the zone where all actual features must be located. It is constituted by an infinite number of intersections of the Z_{i+1} zone. It is called the neutral zone because it does not depend on the location of the R_{fonct_i} DRF. A sufficient condition of feature conformity is thus met when it belongs to the Z_{int} zone.

Then, the case of two successive tolerance zones Z_1 and Z_2 will only considered, as in the Figure 3 with $i=1$.

Let us designate a space point by the symbol χ . χ is within the tolerance if and only if its expression in the R_{fonct_i} DRF (noted $^{fonct_i}\chi$) is within the Z_{i+1} tolerance zone. If the transformation noted $^{fonct_i}T_{ref}$ is known, (Fig. 5) permitting a transformation from the R_{fonct_i} DRF to the R_{ref} DRF, the fundamental relation of the tolerance transfer for a point can be written in the following form:

$$^{fonct_i}X = ^{fonct_i}T_{ref}^{ref} X \tag{1}$$

$$^{fonct_i}X = \begin{bmatrix} ^{fonct_i}A_{ref} & ^{fonct_i}P_{ref} \\ \mathbf{0} & 1 \end{bmatrix}^{ref} X$$

Where $X = [\chi \ 1]^T$. Matrix $^{fonct_i}A_{ref}$ is the orientation matrix of the R_{ref} DRF expressed in the R_{fonct_i} DRF. Matrix $^{fonct_i}P_{ref}$ is the location matrix of the R_{ref} DRF expressed in the R_{fonct_i} DRF.

It is often more convenient to use the nominal element of the tolerance zone. So two new DRF leaning on the nominal conditions can be introduced. Let R_1 (respectively R_0) be a DRF obtained from the R_{fonct_i} DRF (respectively R_{ref}) with a constant transformation as shown in Fig. 5.

The R_1 DRF corresponds to the nominal situation of the Z_2 zone with respect to the R_{fonct_i} DRF. For every location and orientation of the R_{fonct_i} DRF corresponds a R_1 DRF. There is a rigid-link between the R_{fonct_i} DRF and the R_1 DRF. The R_0 DRF corresponds to the nominal situation of the Z_2 zone with respect to the R_{ref} DRF.

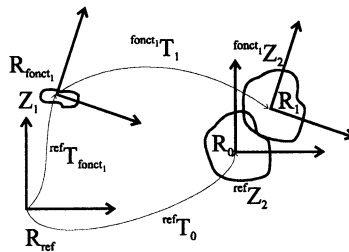


Figure 5. Transformations definition

Let $^{ref}T_0$ be the transformation which makes the R_0 DRF move to the R_{ref} DRF (this matrix is given by manufacturing values). Let $^{ref}T_{fonct_i}$ the transformation which moves

the R_{fonct_1} DRF to the R_{ref} DRF (it depends on parameters q_i which defines the location and the orientation of the two DRF one with respect to the other). And let ${}^{fonct_1}T_1$ be the transformation which moves the R_1 DRF to the R_{fonct_1} DRF (this matrix is obtained by the nominal product definition values).

Let ${}^0\chi$ be the χ point coordinates in R_0 , and let ${}^1\chi$ the χ point coordinates in R_1 . The general equation (1) can now be written:

$$\begin{aligned} {}^{fonct_1}X &= {}^{fonct_1}T_1 {}^1T_0 {}^0T_{ref} X \\ {}^1T_{fonct} {}^{fonct_1}X &= {}^1T_{fonct} {}^{fonct_1}T_1 {}^1T_0 {}^0T_{ref} X \\ {}^1X &= {}^1T_0 {}^0X \end{aligned} \quad (2)$$

Where ${}^1X = [{}^1\chi \ 1]^T$ and ${}^0X = [{}^0\chi \ 1]^T$

The development of this relation is thus:

$${}^1\chi = {}^1A_0 {}^0\chi + {}^1P_0 \quad (3)$$

Then, a necessary and sufficient condition to meet a tolerance specification can be written as:

$${}^1\chi \text{ meets the tolerance if and only if } {}^1\chi \in {}^{fonct_1}Z_2$$

It means that if the point after being transformed is not anymore in the tolerance zone ${}^{fonct_1}Z_2$, then the tolerance does not meet this transformation. The set of points ${}^1\chi$ that remains in the ${}^{fonct_1}Z_2$ tolerance zone for any location of this zone, defined the neutral zone Z_{int} .

4 Analytic transfer: Particular case

In order to clarify the demonstration, circular positional tolerances in a plane are presented. Point ${}^1\chi$ can be manufactured if this point remains in the ${}^{fonct_1}Z_2$ circle, otherwise it means that this point is located outside of the tolerance zone after the transformation 1T_0 . Thus, the tolerance is not met anymore. Since ${}^1\chi$ must be in the ${}^{fonct_1}Z_2$ circle, it is necessary that the distance between the centre of this circle ${}^{fonct_1}Z_2$ and the ${}^1\chi$ point must be lower than r_1 , the radius of the ${}^{fonct_1}Z_2$ circle. The R_1 DRF being originally the centre of the ${}^{fonct_1}Z_2$ circle, the equation

$$\|{}^1\chi\|^2 \leq r_1^2 \quad (4)$$

with :

$$\begin{aligned} \|{}^1\chi\|^2 &= ({}^1A_0 {}^0\chi + {}^1P_0)^T ({}^1A_0 {}^0\chi + {}^1P_0) \\ &= \|{}^0\chi\|^2 - 2 {}^0\chi^T {}^0P_1 + {}^1P_0^2 \end{aligned}$$

Equation (4) gives :

$$\|{}^0\mathcal{X}\|^2 - 2 {}^0\mathcal{X}^T {}^0\mathbf{P}_I + {}^1\mathbf{P}_0^2 - r_I^2 \leq 0 \quad (5)$$

${}^0\mathbf{P}_I$ and ${}^0\mathcal{X}$ are written in polar form:

$${}^0\mathbf{P}_I = [\rho \cos\theta \quad \rho \sin\theta \quad 0]^T \text{ with } \rho \geq 0 \text{ and } {}^0\mathcal{X} = [r \cos\alpha \quad r \sin\alpha \quad 0]$$

Then :

$$r^2 - 2 r \rho \cos(\theta - \alpha) + \rho^2 - r_I^2 \leq 0 \quad (6)$$

The left hand side of equation (6) is a second degree equation, with two real roots r' and r'' if and only if its discriminant Δ is positive. Since the coefficient of r^2 is positive, the solutions of this equation are negative between these two roots r' and r'' . So, the inequality (6) can be verified between the two r' and r'' . Calculating the two r' and r'' roots. Letting $\phi = \alpha - \theta$, the discriminant of the equation is:

$$\Delta = r_I^2 - \rho^2 \sin^2 \phi \quad (7)$$

Δ is positive if :

$$r_I^2 \geq \rho^2 \sin^2 \phi \quad (8)$$

Since Δ must be positive for any value of ϕ , it is necessary that:

$$r_I^2 \geq \min_{qi} \rho^2(q_i) \quad (9)$$

If this condition is not fulfilled, it means that there is no Z_{int} neutral zone. It is a necessary condition for the existence of Z_{int} and therefore for the realisation of Z_{int} too.

If $\Delta > 0$, then we have two real roots r' and r'' . Since the $r'r''$ product is always negative or nil the two roots have opposite signs. So The r' root is positive and the r'' root is negative. As r' must always be positive, therefore: $0 \leq r \leq r'$

For every value of Δ , the radius of the Z_{int} neutral zone can be calculated:

$$r_n(\alpha) = \min_{qi} (\sqrt{\Delta} + \rho(q_i) \cos\phi) \quad (10)$$

This equation is the neutral zone polar equation. For each value of α , the radius of the neutral zone can be calculated. If α is varied between 0 and 2π , the form of the neutral zone is thus obtained. The r_n neutral zone radius of the circle inscribed within Z_{int} and centered on the nominal location is given by the smallest value of $r_n(\alpha)$. This value must be independent of α and ϕ . The minimum of $r_n(\alpha)$ is therefore:

$$r_n = \min_{qi} (r_I - \rho(q_i)) \quad (11)$$

An equation allowing the direct determination whether the transfer is possible or not has therefore been developed. Another equation which helps to determine the shape of the neutral zone after the transfer is also available. These are now applied to two examples.

1. Examples

4.1 PROBLEM OF ONE VARIABLE POSITIONING

In this example, a simple 2D case which includes positional tolerances is considered as shown in Figure 1. The Z_1 zone has a radius in the worse case equal to r_1 .

The different transformations matrices between the different DRF can be defined systematically. Then:

$$\|{}^1\chi\|^2 = r^2 - r_1^2 - 2 r r_1 \cos(\alpha - \alpha_1) \quad \text{and} \quad \|{}^1\chi\|^2 \leq r_2^2$$

$$\text{So } r^2 - r_1^2 - 2 r r_1 \cos(\alpha - \alpha_1) \leq r_2^2 \quad \text{and} \quad \Delta = r_2^2 - r_1^2 \sin^2(\alpha - \alpha_1)$$

Δ is positive for any value of α or α_1 if $r_1 \leq r_2$. This condition is a necessary condition for the existence of a neutral zone. It is in this case an obvious condition since the radius of the Z_2 zone must be superior to the radius of the Z_1 zone.

$$\text{If } r_1 \leq r_2, \text{ then } r' = r_1 \cos(\alpha - \alpha_1) + \sqrt{\Delta}$$

The radius of the neutral zone is given by $r_n(\alpha) = r_2 - r_1$

It is very interesting to note that this result is generic and does not require very little computational effort. Indeed, it can be applied directly to any circular positional tolerance case equivalent to the case shown above. In the next example, a more complex DRF is defined which can lead to more complex calculations and less foreseeable results.

4.2 MULTI-VARIABLE PROBLEM

The example that follows has been presented by Louis Rivest in [5]. It covers the transfer of tolerances for the manufacturing of a hole positioned in relation with two other holes. These last two are defined in the manufacturing set-up reference frame as shown in Figure 6. The various DRF are first defined as shown in Figure 7. Then the transformation matrices are defined and $\|{}^i\chi\|^2$, Δ , $r_n(\alpha)$ are calculated. The following a_i and b_i values are then set at:

Parameters	a_1	b_1	a_2	b_2	a_3	b_3
Values in inches	1.1748	1.6450	1.3239	2.8025	-0.8430	-0.4860

Table 1 : Parameters value

The following results are then obtained:

	radius in inches		L.Rivest	Current results
case 1	$r_1 = r_2 = 0.0025$	r_n	-	-
	$r_3 = 0.0025$	min Δ	-	$-2.90 \cdot 10^{-5}$
case 2	$r_1 = r_2 = 0.0005$	r_n	0.0013	0.00126
	$r_3 = 0.0025$	min Δ	-	$4.83 \cdot 10^{-6}$

Table 2 : Calculation results

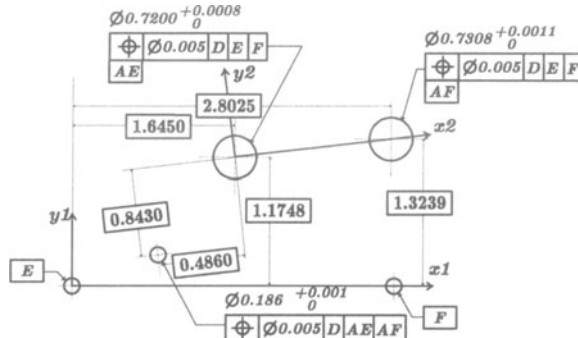


Figure 6. Example 2 from [5]

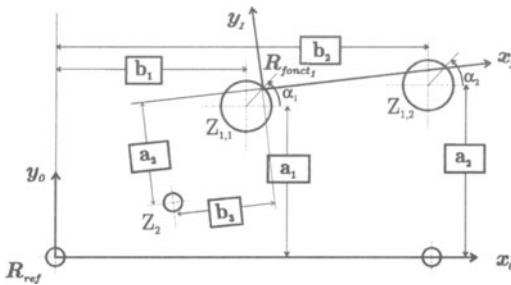


Figure 7. DRF definitions

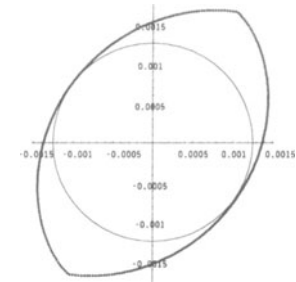


Figure 8. Z_2 in R_0 for case 2

5 Conclusion

An analytical method to determine a tolerance zone transfer for manufacturing applications has been developed. This method based on the kinematics aspect of the tolerance zone transfer process determines analytically the shape of a transferred tolerance zone. It can also be used to solve the tolerance synthesis problem. Since it permits the algebraic determination of a transferred tolerance zone, it can be used for the optimisation of the tolerance zone size in a tolerance synthesis program. The next step is to validate the method for the various types of ISO standard geometric tolerances for two and three dimensional cases.

References

- [1] Requicha A. A. G. : Toward a theory of Geometric Tolerancing. *The International Journal of Robotic Research*. 2(4) : 45-60, 1983.
- [2] Jayaraman R. and Srinivasan V. : Geometric Tolerancing : I. Virtual Boundary Requirements, *IBM J. Res. Develop.* 33(2) : 90-104, 3 1989.
- [3] Srinivasan V., Jayaraman. R. : Geometric Tolerancing : II. Conditional tolerances. *IBM J. Res. Develop.* 33
- [4] Clément A., Rivière A. and Temmerman. M. : *Cotation tridimensionnelle des systèmes mécaniques*, PYC Edition, 1994
- [5] Rivest L. : *Modélisation et analyse tridimensionnelles des tolérances dimensionnelles et géométriques*. PhD thesis, - Ecole Polytechnique de Montréal ,1993.
- [6] Rivest L., Fortin C., and Morel C. : Tolerancing a solid model with a kinematic formulation, *Computer-Aided Design*. 26(6) : 465-476, 6 1994.

MODELING DISPERSIONS AFFECTING PRE-DEFINED FUNCTIONAL REQUIREMENTS OF MECHANICAL ASSEMBLIES USING JACOBIAN TRANSFORMS

LUC LAPERRIÈRE and PHILIPPE LAFOND
Université du Québec à Trois-Rivières
Dept of Mechanical Engineering
3351, Des Forges Blvd
Trois-Rivières, Québec
Canada, G9A 5H7
luc_laperriere@uqtr.quebec.ca

Abstract

Assuming that a method exists for exhaustively generating 3-D tolerance chains around a desired functional requirement, this paper describes a method to mathematically quantify the relationship between the effects that the functional elements dispersions implied in a chain have on the dispersions of the desired functional requirement. This is achieved by using the concept of six virtual joints associated to each functional element implied in a chain. These virtual joints then become the basis for modeling virtual kinematic chains around the desired functional requirement. By associating each virtual joint with a coordinate frame, the impact of various small displacements of the individual functional elements on the overall functional requirement can be computed using a Jacobian matrix.

1. Introduction

Functional analysis consists of using expertise to determine Functional Requirements (FRs), generally in terms of gaps, clearances and fits, between pairs of Functional Elements (FEs) in an assembly. Once the FRs have been determined by the designer, an important task is to identify every possible FE of the whole assembly which can have an effect on the upper and lower limits of these FRs, with the general definition that a FE can be a point, curve or surface or a part, either real or fictive. In this paper we assume that an appropriate representation of an assembly in terms of the FEs that have some influence on the FR in a chain is already available, for example the graph model in figure 1. Indeed, this graph model explicitly *identifies* which FEs of an assembly have an influence on the FR by including them in closed kinematic (tolerance) chain.

Clearly, a tolerance chain around a FR passes through pairs of FEs, two types of which can be distinguished: internal pairs, which are pairs on the same part, and

kinematic pairs, which are pairs on different parts in contact. The tolerance chain will generally go through internal pairs and kinematic pairs alternatively. In this paper, the goal is to mathematically *quantify* the functional relationship between the FEs dispersion values to the FR dispersion value: $FR \text{ dispersion} = f(\text{FEs dispersions})$.

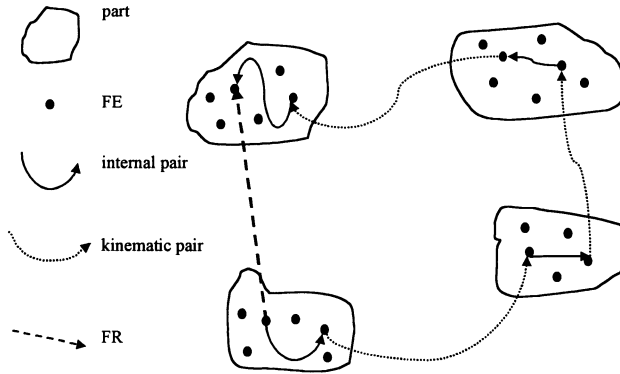


Figure 1. Graph model representation of a tolerance chain around the FR of a 4-parts assembly.

2. Relevant Literature

A tolerance chain around a FR can be seen as a kinematic chain. For this reason, robotics concepts have been recently applied for modeling tolerancing data. Rivest et al. (1993) and Whitney et al. (1994) were among the first to describe a kinematics approach to model tolerance information and buildups. The approach finds its roots in robotics, where models for representing movements of consecutive kinematic joints, expressed in a global coordinate frame, have been thoroughly studied and used (Spong and Vidyasagar, 1989). Indeed, the authors suggest using a similar scheme, i.e. associating coordinate frames to the kinematic pairs of an assembly to model their possible movements. The former paper focuses on modeling small movements resulting from dispersions inside pre-defined tolerances zones, the latter on statistical distributions of accumulated tolerance buildups. Ongoing research results have also been published on both projects (Gaudet et al., 1999), (Matripragada and Whitney, 1998).

Desrochers and Rivière (1997) describe a tolerance model based on the TTRS concept (Desrochers, 1991). The effects of tolerance buildups in a chain are modeled using kinematic torsors to which small displacements theory is applied.

The approach presented in this paper uses homogeneous matrix transforms and their partial derivatives in terms of a Jacobian matrix to relate FE's dispersions to FR's dispersions in a tolerance chain. The next section of the paper focuses on modeling nominal spatial relationships between FEs in both internal and kinematic pairs. Section

4 describes the modeling of infinitesimal spatial relationships (tolerances) using a Jacobian transform. Section five concludes the paper.

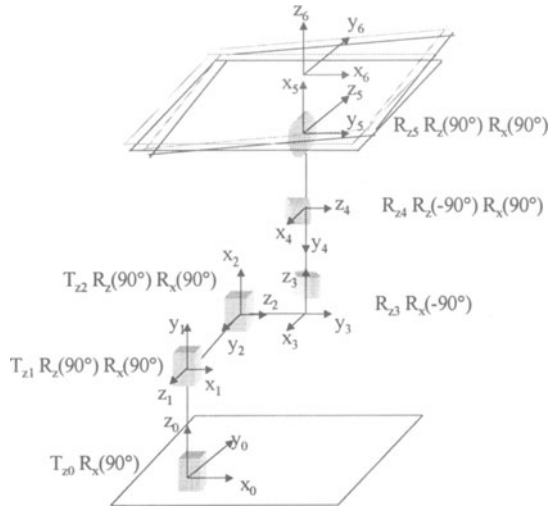


Figure 2. Adding virtual joints and coordinate frames to FE to model spatial relationships.

3. Modeling Nominal Spatial Relationships

Consider figure 2. It shows a pair of FEs to which a set of six virtual joints have been associated. In turn, each virtual joint is mathematically modeled using a homogeneous 4x4 transform matrix. Without loss of generality, this pair can be considered to be either internal or kinematic. We will now demonstrate how the spatial relationship between both FEs in this pair can be modeled using coordinate transforms.

3.1. INTERNAL PAIRS

In figure 2, the “z” axis of the first three frames O_0 to O_2 are assumed to be the translation axis of three corresponding translational virtual joints, while the “z” axis of the next three frames O_3 to O_5 are assumed to be the rotation axis of three corresponding rotational virtual joints. Assuming that the three translational “z” axis are mutually perpendicular and that the three rotational “z” axis are also mutually perpendicular (as was done in the frame setup in figure 2), then we can explicitly formulate the general nominal spatial relationship between two consecutive FEs in the chain, using simple 4x4 homogeneous transform matrices. For the first three translation transformations we have:

$$T_0^1 = T_{z_0} \cdot R_x(90) \quad (1)$$

$$T_1^2 = T_{z_1} \cdot R_z(90) \cdot R_x(90) \quad (2)$$

$$T_2^3 = T_{z_2} \cdot R_z(90) \cdot R_x(90) \quad (3)$$

$$T_0^3 = T_0^1 \cdot T_1^2 \cdot T_2^3 = \begin{bmatrix} 0 & 1 & 0 & D_2^3 \\ -1 & 0 & 0 & -D_1^2 \\ 0 & 0 & 1 & D_0^1 \\ 0 & 0 & 0 & 1 \end{bmatrix} \quad (4)$$

and for the next three rotational transformations we have:

$$T_3^4 = R_{z_3} \cdot R_x(-90) \quad (5)$$

$$T_4^5 = R_{z_4-90} \cdot R_x(90) \quad (6)$$

$$T_5^6 = R_{z_5+90} \cdot R_x(90) \quad (7)$$

$$T_3^6 = T_3^4 \cdot T_4^5 \cdot T_5^6 = \begin{bmatrix} C(\Omega_3^4)C(\Omega_4^5)C(\Omega_5^6) - S(\Omega_3^4)S(\Omega_5^6) & C(\Omega_3^4)S(\Omega_4^5) \\ S(\Omega_3^4)C(\Omega_4^5)C(\Omega_5^6) + C(\Omega_3^4)S(\Omega_5^6) & S(\Omega_3^4)S(\Omega_4^5) \\ -S(\Omega_4^5)C(\Omega_5^6) & C(\Omega_4^5) \\ 0 & 0 \\ C(\Omega_3^4)C(\Omega_4^5)S(\Omega_5^6) + S(\Omega_3^4)C(\Omega_5^6) & 0 \\ S(\Omega_3^4)C(\Omega_4^5)S(\Omega_5^6) - C(\Omega_3^4)C(\Omega_5^6) & 0 \\ -S(\Omega_4^5)S(\Omega_5^6) & 0 \\ 0 & 1 \end{bmatrix} \quad (8)$$

We conclude that the relative position and orientation of the upper plane in figure 2 with respect to the lower plane, expressed in the base frame O_0 , is given by:

$$T_0^6 = T_0^3 \cdot T_3^6 = \begin{bmatrix} S(\Omega_3^4)C(\Omega_4^5)C(\Omega_5^6) + C(\Omega_3^4)S(\Omega_5^6) & S(\Omega_3^4)S(\Omega_4^5) \\ S(\Omega_3^4)S(\Omega_5^6) - C(\Omega_3^4)C(\Omega_4^5)C(\Omega_5^6) & -C(\Omega_3^4)S(\Omega_4^5) \\ -S(\Omega_4^5)C(\Omega_5^6) & C(\Omega_4^5) \\ 0 & 0 \\ S(\Omega_3^4)C(\Omega_4^5)S(\Omega_5^6) - C(\Omega_3^4)C(\Omega_5^6) & D_2^3 \\ -C(\Omega_3^4)C(\Omega_4^5)S(\Omega_5^6) - S(\Omega_3^4)C(\Omega_5^6) & -D_1^2 \\ -S(\Omega_4^5)S(\Omega_5^6) & D_0^1 \\ 0 & 1 \end{bmatrix} \quad (9)$$

where :

D_i^j : variable quantifying the translation from frame_i to frame_j (part's linear dimension);

Ω_i^j : variable quantifying the rotation from frame_i to frame_j (part's angular dimension);

3.2. KINEMATIC PAIRS

The same model as above can be used to express the relationships between FEs at different point in the tolerance chain resulting from various configurations of the assembly as permitted by the Degrees Of Freedom (DOF) of its kinematic pairs. To this end, we can now regard figure 2 as being a plane-plane contact, and we can simply reformulate eq. (9) as follows:

$$T_0^6 = \begin{bmatrix} S(\omega_3^4)C(\omega_4^5)C(\omega_5^6) + C(\omega_3^4)S(\omega_5^6) & S(\omega_3^4)S(\omega_4^5) \\ S(\omega_3^4)S(\omega_5^6) - C(\omega_3^4)C(\omega_4^5)C(\omega_5^6) & -C(\omega_3^4)S(\omega_4^5) \\ -S(\omega_4^5)C(\omega_5^6) & C(\omega_4^5) \\ 0 & 0 \\ S(\omega_3^4)C(\omega_4^5)S(\omega_5^6) - C(\omega_3^4)C(\omega_5^6) & d_2^3 \\ -C(\omega_3^4)C(\omega_4^5)S(\omega_5^6) - S(\omega_3^4)C(\omega_5^6) & -d_1^2 \\ -S(\omega_4^5)S(\omega_5^6) & d_0^1 \\ 0 & 1 \end{bmatrix} \quad (10)$$

where :

d_i^j : variable quantifying a permitted translation DOF from frame_i to frame_j;

ω_i^j : variable quantifying a permitted rotation DOF from frame_i to frame_j ;

It follows that the relative position and orientation of *any* FE in the chain with respect to the base FE at O_0 , as a result of *both* nominal dimensions and DOF of the FEs implied in the tolerance chain, is given by:

$$T_0^n = T_0^6 \cdot T_6^{12} \cdot T_{12}^{18} \dots T_{6n-6}^{6n} \quad (11)$$

with the understanding that the matrices of eq. (9) and eq. (10) are alternatively multiplied and that “n” represents the total number of FE pairs (both internal and kinematic) involved in a tolerance chain.

4. Modeling Dispersions

Consider figure 3, which shows schematically a tolerance chain around a FR for a three parts assembly. This chain involves three internal pairs and two kinematic pairs. Each pair is assigned a set of six virtual joints with coordinate frames attached to them as in figure 2, which gives a total of 30 such virtual joints and frames. The frame numbers are labeled in the figure for each FE pair, for example O_0 to O_5 for the first internal pair, O_6 to O_{11} for the first kinematic pair, and so on. We will focus on the second internal pair at the top of figure 3 where frames O_{12} to O_{17} have been explicitly displayed with emphasis on their bolded “z” axis.

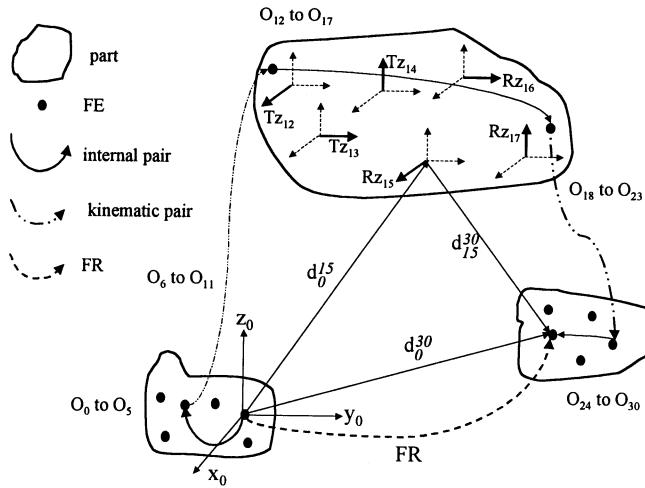


Figure 3. Schematic representation of a tolerance chain for a 3-parts assembly.

Once the perfect spatial relationships have been modeled using the method described in section 3, we are interested in determining what happens if we let the relationships deviate from their true values. Conceptually, this is equivalent to performing small translations and small rotations around each local “z” axis of all frames in the chain. In order to quantify the relationship between such individual local dispersions and the dispersions of the FR at the end of the tolerance chain, we simply apply the theory of small displacements on kinematic chains using standard Jacobian matrices.

Let’s focus on small translations first. Assuming there is a small translation along some axis of some virtual joint (z_{12} to z_{14} in figure 3), and assuming that all parts are rigid and are not moving except for the one to which this small translation is applied, then clearly this small translation will contribute entirely both in direction and magnitude to only a translation (no rotation) of the last part in the chain, in particular at O_{30} of the FR. This result is true for every small translation at any translational frame of any part in the chain. This observation dictates how those columns of the Jacobian that are associated to small translation virtual joints should be computed, see eq. (14).

Looking now at the contribution of small rotations (z_{15} to z_{17} in figure 3), we first realize that a rotational joint contributes to both linear and angular displacements of the last FE in the chain at FR. For linear contributions, the small rotation must be multiplied by its lever arm to the point where the linear contribution is to be computed, which implies the use of the cross product operator. For rotational contributions, small rotations at individual virtual joints contribute to small rotations of the last FE in the chain and this contribution is both in direction and magnitude corresponding to a rotation of the last FE at FR. These observations dictate how those columns of the Jacobian that are associated to small rotation virtual joints should be computed, see eq. (13).

We can now summarize the previous results in a general model as follows (the details can be found in Laperrière and Lafond, 1999):

$$\begin{bmatrix} \delta \vec{s} \\ \delta \vec{\alpha} \end{bmatrix} = \begin{bmatrix} [J_1 J_2 J_3 J_4 J_5 J_6]_{FE_1} \cdots [J_{6n-5} J_{6n-4} J_{6n-3} J_{6n-2} J_{6n-1} J_{6n}]_{FE_n} \end{bmatrix} \cdot \begin{bmatrix} \vec{\delta}_{FE_1} \\ \vdots \\ \vec{\delta}_{FE_n} \end{bmatrix} \quad (12)$$

where :

$\delta \vec{s}$: 3-vector of point of interest's small translations, expressed in the base frame;

$\delta \vec{\alpha}$: 3-vector of point of interest's small rotations, expressed in the base frame;

$[J_{6i-5} \dots J_{6i}]_{FE_i}$: i^{th} 6x6 Jacobian matrix associated with the tolerated FE of the i^{th} FE pair (internal or kinematic), $i = 1$ to n ;

$\vec{\delta}_{FE_i}$: i^{th} 6-vector of small dispersions associated with the tolerated FE of the i^{th} FE pair (internal or kinematic), expressed in the local frames, $i = 1$ to n .

For small rotational virtual joints, the i^{th} column of the Jacobian matrix J_i is computed as:

$$J_i = \begin{bmatrix} \vec{z}_0^{i-1} \times (\vec{d}_0^n - \vec{d}_0^{i-1}) \\ \vec{z}_0^{i-1} \end{bmatrix} \quad (13)$$

where "x" denotes the vector cross product operator and:

\vec{z}_0^{i-1} : 3rd column of T_0^{i-1}

\vec{d}_0^{i-1} : last column of T_0^{i-1}

For small translational virtual joints, there is no contribution to small rotational displacements of the point of interest and the i^{th} column of the Jacobian matrix J_i is simply computed as:

$$J_i = \begin{bmatrix} \vec{z}_0^{i-1} \\ \vec{0} \end{bmatrix} \quad (14)$$

5. Conclusion

This paper has presented a novel approach to model the influence of individual functional element dispersions on a point of interest of a mechanical assembly. The model is based on a theory of small displacements using standard Jacobian matrices computations. The model uses sets of six coordinate frames associated to consecutive pairs of functional elements around a functional requirement. Assuming that such functional elements are accessible in a CAD database, then this association should be

straightforward to implement, either automatically (the user identifies both ends of a functional requirement and the CAD system computes the chains), or interactively (the user manually selects the functional element pairs in the chains). Most CAD modelers have inherent frame definition capabilities which could be exploited after the chains have been identified, and all CAD modelers have inherent homogeneous transformation matrices computation capabilities which can be exploited to obtain the resulting equations.

6. References

- Desrochers A. (1991) "Modèle Conceptuel du Dimensionnement et du Tolérancement des Mécanismes: Représentation dans les Systèmes CFAO", *Ph.D. thesis*, École Centrale de Paris
- Desrochers A. and Rivière A. (1997) "A Matrix Approach to the Representation of Tolerance Zones and Clearances", *International Journal of Advanced Manufacturing Technology*, v13, pp. 630-636
- Gaudet P., Cloutier G., and Fortin C. (1999) "The validation of a process plan by propagated dispersion zones", *Proceedings of the 6th CIRP seminar on computer-aided tolerancing*, Enschede, The Netherlands, pp. 73-82
- Laperrière L. and Lafond P.: (1999) "Modeling tolerances and dispersions of mechanical assemblies using virtual joints", *Proceedings of ASME DETC '99*, Las Vegas, USA
- Matripragada R. and Whitney D.E. (1998) "Modeling and controlling variation propagation in mechanical assemblies using state transition models", *Proceedings of IEEE international conference on robotics and automation*, pp. 219-226
- Rivest L., Desrochers A. and Fortin C. (1993) "Tolerance Modeling for 3-D Analysis: Presenting a Kinematic Formulation", *Proceedings of the 3rd CIRP Seminar on Computer-Aided Tolerancing*, Cachan, France
- Spong W.S. and Vidyasagar M. (1989) "Robot Dynamics and Control", *John Wiley and Sons*, USA, 1989
- Whitney D.E., Gilbert O.L. and Jastrzebski M. (1994) "Representation of geometric variations using matrix transforms for statistical tolerance analysis in assembly", *Research in engineering design*, v6, pp. 191-210

TOWARD A COMPUTER AIDED TOLERANCING SYSTEM FOR PARTS AND MECHANISMS

Eric BALLOT*, François THIEBAUT and Pierre BOURDET****

** Centre de gestion Scientifique de l'Ecole des Mines de Paris*

*** Laboratoire Universitaire de Recherche en Production Automatisée de l'Ecole Normale Supérieure de Cachan*

Email : eric.Ballot@cgs.ensmp.fr

Abstract

The works carried out in the fields of tolerancing or mechanism specifications are performed using two complementary approaches: the mathematization of tolerances and the definition of efficient tools for Computer Aided Tolerancing. After explaining our model of geometric deviations, we present the different possibilities to aid the designer. A tolerancing strategy is then presented and exemplified with a gear.

This study permits to bring out the contribution of the behavior laws of a mechanism to the part specification. Indeed, the sensible choice is made with the help of the mathematical description of the functional requirements. This mathematical description gives all the necessary deviations to be constrained for each part.

Introduction

Current works on tolerancing or geometric specifications of mechanism are performed using two complementary approaches. One is a mathematical description of the part variability, completed for a standardization objective (mathematization of tolerances). The other one consists in modeling the geometric variations of the mechanism features in order to provide assisting tools for the determination of specifications (Computer Aided Tolerancing).

In this paper, we consider that using functional requirements as the starting point to assist designers on the tolerance synthesis is interesting. We thus present a calculation model based on the parameterization of geometric deviations. Then we develop the ways designers may be assisted. We present topics that are already widely studied and note that research opportunities are left on less developed approaches. An example of a tolerancing strategy linked to a CAD system is then presented corresponding to one of these latest approaches.

1. Current approaches of mechanism specification

Every tool of geometric specification relies on a deviation model of parts. Most of them can be classified into two model families : the envelope models and the variational models. The envelope models gather models for which real geometry is included between two offset surfaces of the nominal one [6]. This family of models corresponds to most of the mathematical representations of tolerances. Nevertheless, their use in calculation methods is still difficult and is barely initiated.

The variational models gather models for which the real geometry of the part is modeled through the variations of the nominal geometry [5], [4]. A substitute surface is created, whose form corresponds to the nominal one but whose size, position and orientation may vary . The variations correspond to the translatory components and to the rotation components necessary to express the deviation from the initial surface to the substitute surface. The set of deviation components constitute a mathematical space called deviation space. The variational models permit the mathematical definition of the standard specifications, if we make the analogy between substitute surfaces used in our model and identified surfaces used in metrology. They also provide strong basis for the development of the specification tools, since geometric specifications of parts may be seen as a domain in the space of deviation. The method we propose to use to express the geometric deviations is the Small Displacement Torsor (SDT).

2. Expression of geometric deviations

The proposed method links the initial geometry of the mechanism to the substitute geometry. The position and orientation of the features of the substitute model are deduced from the initial model ones. We use three kinds of torsors to express these deviations:

- the surface torsor expresses the deviations between the initial location of the surface and the location of the substitute surface,
- the gap torsor expresses the deviations between two substitute surfaces of two different parts,
- the part torsor expresses the deviation between the initial location of a part and the location of the substitute part.

Compared to the TTRS model [3] or the one presented by J. Turner [8], our model brings out a difference between the deviation components for which the variation domain is searched and those that leave the nominal surfaces unchanged. The acceptable variation domain of the deviation components is called tolerance zone on the surface.

In particular, this parameter difference permits the determination of the form of the gap torsors which describes the gaps in the mechanism links. It also permits the combinatory calculation of possible contacts between two sets of surfaces [2].

When we want to establish the link between the geometric deviations of part features and a particular geometric specification defined by datums and a tolerance zone, one set of surfaces defines the substitute part and the other characterises the geometric specifications (see figure 1). We define a nominal frame according to standard datums and we locate the tolerance zone relatively to the datums. The substitute surface, corresponding to the toleranced

feature, has to be included into the tolerance zone. The deviation components of the substitute part are bounded by the tolerance zone, the geometric specification is then mathematically defined.

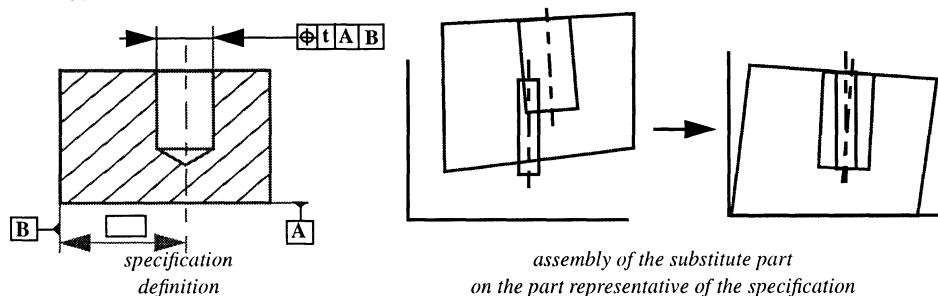


Fig. 1 Assembly of a substitute part on a part representative of a specification

If both sets of surfaces belong to different parts, the set of assembly configurations of the mechanism is then determined (see figure 2). The necessary operators for the calculation are given in [1]; so are the links which permit the computation of the behavior laws. These behavior laws directly link each functional requirement to the deviation components of the concerned parts. Moreover, these laws moreover give a specific expression for each assembly configuration of the mechanism. This means that tolerancing has to take into account the nature of the contact for a complete assembly and the configuration combinatory for assembly with mobilities.

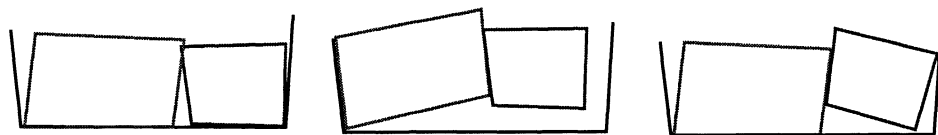


Fig. 2 Different assembly configurations on a mechanism

3. The ways designers may be helped

3.1. DESIGNERS' NEEDS FOR GEOMETRIC TOLERANCING

To define an assisting tool for specification, we first make the hypothesis that it is possible to know the set of functional requirements according to a mechanism, and its working configurations. These conditions, which are not necessarily exhaustive, may be completed with constraints coming from components or machining processes.

Starting with these data, the designer has to answer the following questions: what kind of specifications is required on each part of the mechanism? and what is the authorized range of deviation for these specifications? The knowledge of the functional requirements or tolerancing as a starting point implies two different approaches of tolerancing: the tolerance analysis

and the tolerance synthesis. It is also necessary to check the consistency of a specification or of a set of specifications. We propose typical assisting methods relative to these needs.

3.2. FIVE TYPICAL ASSISTING METHODS

From a research point of view, we find interesting to quote the five following assistance methods in order to define associated calculation methods. We obviously keep in mind the necessity of their integration in a unique and complete tolerancing system of the mechanism and the necessity to take into account the management of the valid working configurations of the mechanism.

3.2.1. The designer imposes the geometric specifications and their values.

The aim consists in validating the tolerances on a part after their mathematical modeling. The system then validates the geometric specifications by analysing the respect of the functional requirements. This is carried out either using assembly simulation (using Monte Carlo method) or by the search of extreme positions of the mechanism, in order to check if the functional requirements are respected even in these extreme configurations (using an optimization method). Such a method, called tolerance analysis, is at present widely developed but only permits the validation of the tolerancing proposed by the designer.

3.2.2. The designer imposes specifications without values.

From a calculation standpoint, the treatment of this problem is still more complicated since the tolerance values and mean values must be determined. The assistance also requires a repartition function of tolerances between parts and surfaces. This function is often based on an economic criterion or a machining simulation. Such a method, called tolerance synthesis, is hardly developed on three dimensional tools of tolerancing. As in the previous method, only the validation of the nature of specifications is performed.

3.2.3. The assisting tool gives the optimum specifications on parts of the mechanism and the designer gives the tolerance zone values.

Such a tool, which answers the question "what kind of specification?" does not yet exist [7]. In the following section, we present an original method which gives a first approach to answer this problem. It is important to underline that such a method allows us to know whether the tolerancing of the parts is necessary and sufficient.

3.2.4. The assisting tool gives the nature of the specification and the associated value of the tolerance zone for each mechanism part.

This tool corresponds to the best assistance tool but requires the most complex calculations. As this assistance tool may be seen as a combination of tolerance analysis and synthesis, it seems possible to integrate their both principles. However, this kind of problem induces combinatory calculations, and its validation on industrial cases is quite difficult.

3.2.5. The designer imposes both the specification and the tolerance zone values on one part.

In this case, we have the complete tolerancing of one of the mechanism part. Analysis and synthesis methods do not give information on each specification relevance and on the compatibility between the different specifications. A way to reach this goal is to

define the links between the geometry constrained by the specifications and the values of the deviation components in the deviation space. The knowledge of these links permits to ensure the real necessity of each specification and its geometric coherence.

4. Application to a assisting tool of tolerancing in a CAD environment

The assisting tool we propose to the designer is based on the knowledge of both the mechanism behavior laws and the geometric functional requirements. These data are given for a set of working configurations of the mechanism.

The aims of this assistance are:

- to inform the designer, for each part of the mechanism, on the deviation components of the surfaces which need to be constrained so that the functional requirements are respected,
- to allow the designer to define specifications between some part surfaces, identifying which deviation components remain still not constrained and which ones are non usefully constrained,
- to check that the deviation domain defined by the specifications is included into the deviation domain associated to the functional requirements.

The method used to perform this study is the following: consider a mechanism defined by its nominal geometry and each pair of surfaces initially in contact. It is possible to compute the behavior laws of the mechanism that provide the links between the components of the surface deviations and the gap components.

The mechanism illustrating the proposed method (figure 3) consists of three parts: a frame and two pinions. Each pinion is modeled by two coaxial cylinders, one representing the shaft connected to the frame and the other the effective pinion whose diameter is equal to the pitch diameter

The required features to compute the behavior laws are extracted from the CAD model: the pairs of surfaces representing the contacts and their geometric description.

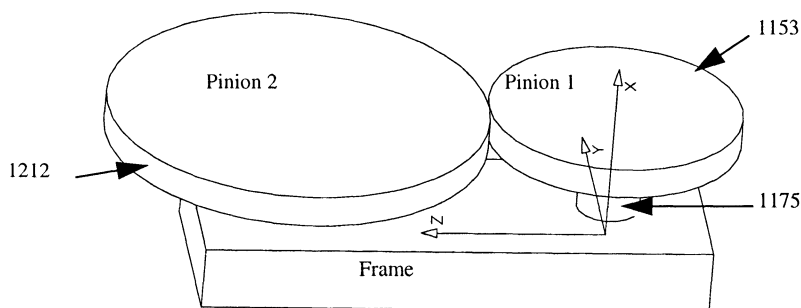


Fig. 3 CAD model

```
Pinion1=  {{175,      {-10,0,0},   {1,0,0},   10,  0,   CylExt},
           {1153,    {-10,0,0},   {1,0,0},   40,  0,   CylExt}}...
Contacts = {{1042, 1239}, {1062, 1175}, {1153, 1212}}
```

The geometric description of each surface includes the surface identifier (number), a representative point of the surface, a director vector representing either the axis of the feature or the normal vector, then the surface radii (if defined) and the surface nature. This set of data is sufficient to compute the behavior laws of the mechanism. These behavior laws give the part's positions relative to the frame and the links between the deviation components and the gap components. These equations are similar to the dimension chains and mathematically express the technologic concept of hyperstatism.

For example, we obtain the value of the translatory deviation in the direction z for a point of the pinion axis relative to the frame, as a function of the gap components and the deviation components of the part surfaces

$$v[\mathbf{C},\mathbf{R}] = 10 c[1062,A] - 10 c[1175,C] - \text{Cos}[t[1175,1062]] dr[1062,A] - \text{Cos}[t[1175,1062]] dr[1175,C] + 10 J[rz,1175,1062] + J[ty,1175,1062] + v[1062,A] - v[1175,C] + v[A,R]$$

So we know the formal description of the links between the deviation components of the surfaces relatively to the nominal ones, the position of the different parts relatively to their CAD position and the gap components between parts. The following step of the method is the determination of the geometric specification.

From the behavior laws and the functional requirements, we propose to deduce the geometric features which have to be constrained in order to respect a given condition. The first condition to be respected, is the non interference condition between the parts of the mechanism. The expression of this condition is made by specifying that for each contact point, the gap component has to be positive or null (a sampled geometry is used to write the functional requirements). This only condition constrains nearly all the deviation components, but the designer needs to limit the gap amplitude, in order to restrain the part displacements or to limit local gaps... To assist the designer in his work, the behavior laws permit to identify the set of influent components on a given functional requirement, that has to be necessary constrained in order to impose the respect of the given condition.

In the particular case of our mechanism, we wish to ensure a gearing with an acceptable deviation equal to 0.3 mm between the pitch diameters and a parallelism condition with an acceptable value of 0.1 mm between the pitch cylinders. These functional requirements are expressed using the following approach: for each nominal contact point between the two pinions, the gap projection between the cylinders along the Z axis is less than 0.3 mm and the gap variation between two points of the contact line is less than 0.1 mm. These equations are verified along the contact line if they are verified at the ending points due to the hypothesis of linear model.

For example, the equation that formalises the parallelism condition between the two cylinder axes is:

$$10(b[1042,A]-b[1062,A]+b[1153,C]+b[1175,C]-b[1212,B]-b[1239,B]-J[ry,1175,1062]+J[ry,1239,1042]) < 0.1 \quad (1)$$

All the equations have to be checked independently, and to ensure the interchangeability of the part, the components relative to each part have to be separated. Weight coefficients (c1,c2...) are used to quantify the components values relative to each part according to the repartition function. We directly obtain the components to be constrained on each part from equation (1).

On the frame: $10 (b[1042,A]-b[1062,A]) < c1 0.1$

On the pinion 1: $-b[1212,B]-b[1239,B] < c3 0.1$

and also the sum of the admissible gaps: $J[ry,1175,1062]+J[ry,1239,1042] < c4 0.1$

The signification of the relations between the surfaces of each part is immediate. It corresponds to the angular expression of a parallelism between the axes. The gap values $J[ry,1175,1062]$ and $J[ry,1239,1042]$ correspond to the dimension range induced by the radius difference in the kinematic links.

These equations define the domain attributable to the deviations and give the necessary information to achieve the tolerancing of the different parts. On the frame: the radius has to be specified, the axes have to be parallel and the distance between axes has to be specified. The extreme values of the different gaps are obtained by searching the local maximum with regards to the dimensional parameters. The proposed specification is given figure 4.

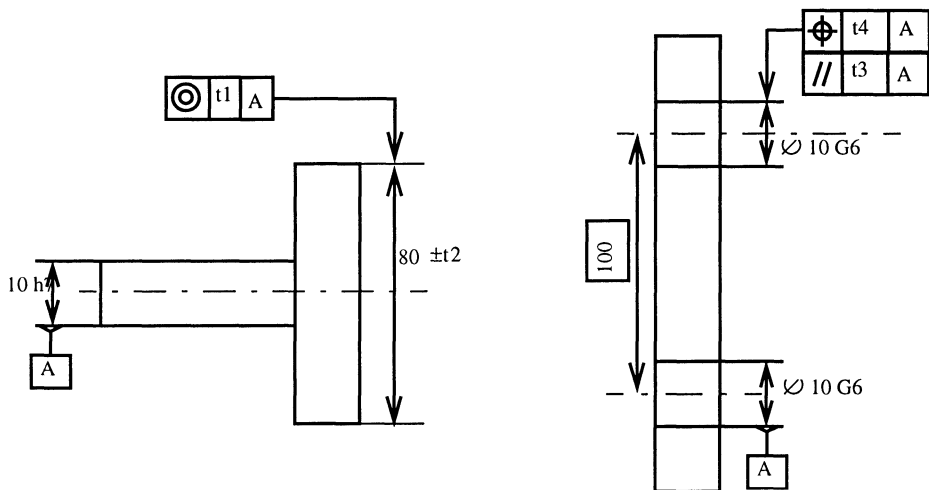


Fig. 4 proposed specification

The description of the specification is then realized. It is now possible to know the set of components which have to be constrained and the ones which are over constrained. Note that we do not know if the chosen specification is optimal but only if it constrains the defined components. The attribution of the parameter values to the specifications permits to check the inclusion of the deviation domain into the functional domain.

In this section, the knowledge of the behavior laws permits to know which components contribute to the respect of the functional requirements. The separation of the components on each part of the mechanism permits to set the nature of the specification between the surfaces of each part. The choice of the specifications is free for the designer, then this choice is validated first by checking that all the deviation components which need to be constrained are effectively constrained and then that the authorized geometry by the specifications implies the respect of the functional requirements.

Conclusion & perspectives

The study proposed in the current paper permits to point out the interest of the behavior laws on specification choice. The knowledge of the components that have to be constrained on each part allows the designer to decrease time in the choice of the nature of the specification to apply on different parts. The part tolerancing is then validated on the whole mechanism by checking that the functional requirements are respected. This method is only a step toward a more precise assistance to the designer in the choice of the nature of the specification and in the value setting of the tolerance intervals. Nevertheless it permits to rationalize quickly the choice of the nature of the geometric specification.

The following step of the study consists in automatically proposing the possible specifications relative to the functional requirements. These specifications should be completed by minimizing the difference between the functional deviation domain and the domain resulting from the geometric specifications. The expected matching between the domains is hardly achievable with standardized specifications, because they constrain too much the geometry as regards the functional requirements.

References

- [1] Ballot E., Bourdet P., A computation method for the consequences of geometric errors in mechanisms, *5th CIRP Int. Sem. on Computer Aided Tolerancing*, Toronto - Canada, 27-29 april, 1997.
- [2] Bourdet P., Ballot E., Geometrical behavior laws for computer aided tolerancing *Computer Aided Tolerancing* edited by Fumihiko Kimura and published by Chapman & Hill, (1996), 119-131.
- [3] Charles B., Clement A., Desrochers A., Pelissou P., Rivière A., Toward a computer aided functional tolerancing model, *The international conference on CAD/CAM and AMT*, Jerusalem, Vol. II, 1989.
- [4] Clozel P., MECA master: outil de conception mécanique et de cotation 3D pour les bureaux d'études, *Actes de la conférence Int. du MICAD 1*, Paris, (1991), 196-209.
- [5] Gupta S., Turner J. U., Variational solid modeling for tolerance analysis, *IEEE Computer Graphics & Applications* **17**, No. 5, (1993) 64-74.
- [6] Requicha A.A.G., Mathematical meaning and computational representation of tolerance specification, *Proc. of the 1993 Intl Forum on Dimensional Tolerancing and Metrology* **27**, Dearborn, Michigan (1993) 61-68.
- [7] Turner J. U., Current tolerancing packages, *Proc. of the 1993 Intl Forum on Dimensional Tolerancing and Metrology* **27**, Dearborn, Michigan (1993) 241-248.
- [8] Turner J. U., A feasibility space approach for automated tolerancing, *Journal of Engineering for Industry*, **115**, (1993) 341-346.

INTERACTIONS BETWEEN TOLERANCING AND STRUCTURAL ANALYSIS VIEWS IN DESIGN PROCESSES

Serge SAMPER*, Max GIORDANO*

** Laboratoire de Mécanique Appliquée/CESALP*

Ecole Supérieure d'Ingénieurs d'Annecy

41 Avenue de la plaine BP806 74016 Annecy Cedex FRANCE

samper@esia.univ-savoie.fr - giordano@esia.univ-savoie.fr

ABSTRACT

In a classical sequential design process, the designer first makes mechanical and structural analyses then global drawings of a mechanism, then tolerancing before manufacturing. So tolerancing is made without the knowledge of the deformations of the mechanism. And the structural analysis is made with the assumption that the mechanism is perfect with regard to its geometry. In most cases, we can see that deformations of mechanisms are of the same order as tolerances. So a methodology is built in order to mix tolerancing analysis with the elastic analysis. This method implies either to input distortions of parts in elastic analysis or to input deformations of parts in tolerancing.

This methodology has the three following parts: tolerancing view, elastic view and synthesis of those views. Those views are explained through a simple gear box.

1. The tolerancing model

1.1. TOLERANCING ANALYSIS AND SYNTHESIS

Most studies about geometric tolerances are based on models of rigid bodies. Among these models, the geometric deviations of functional surfaces or features of a mechanical part are defined by vectors or torsors. We can call vectorial tolerancing models these types of models. For A. Wirtz, ([7]) vectorial tolerancing means that the functional surface locations and orientations are described by vectors and the tolerances limit the values of the components of these vectors. L. Mathieu proposes a more general method to describe the different deviations which is more compatible with standard tolerance representations. A. Clément ([2], [1]) uses the concept of « Technologically and Topologically Related Surfaces » and introduces the torsor tolerancing concept. The model is interesting for the determination of surfaces or features that must be toleranced in relation to another one, but for the determination of values for tolerance zones it is necessary to use the traditional chains of dimensions. In other approaches like Turner's

« feasibility space approach », the tolerances are expressed as constraints that define a region of a cartesian space of model variations ([6]). The aim of these different models is to provide computational approaches to the tolerance analysis but none of these models give a systematic method for the determination of the tolerance values. On the other hand, in all these models it is assumed that the bodies are perfectly rigid. In this paper, a method is developed through an example, for the determination of tolerances that take the deformations into account.

1.2. MECHANISM OF RIGID BODIES, A MODEL FOR TOLERANCE DETERMINATION

The first model for tolerancing is defined by the following hypothesis :

- The bodies are absolutely rigid.
- There are no form errors. For example, a cylindrical nominal surface is assumed to be a perfect cylinder.
- The geometric deviations and clearances are small enough so that the corresponding displacements may be represented by small displacement torsors.
- The two functional requirements are considered : possibility of assembly without any constraints and accuracy of relative positions or relative motions between two parts.

Two sorts of geometric deviations are considered, and each one is limited by tolerances:

- size deviations limited by size tolerances,
- location and orientation deviations between two surfaces, limited by geometrical tolerances.

For example, when considering a cylinder (cylindrical surface of revolution), the diameter is defined by a nominal dimension and the tolerances by two real numbers : the lower and upper deviations. A geometrical tolerance is defined by a reference frame and by a tolerance zone. The reference frame may be complete or not and it is designed by a letter.

1.3. THE PROPOSED METHOD FOR TOLERANCE DETERMINATION

In this following method, the choice of the shape of tolerance zones is given from the assembling requirements. The maximum material condition lead to inequalities that must be respected. Indeed, the maximum material condition is the most unfavourable case for assembling.

The types and the shapes of joint surfaces allow the determination of "clearance spaces". We call "clearance space" of an actual joint, the set of the possible values of small displacement torsors, between the two links of the joint ([3]).

For each independent close loop of the mechanism, it is possible to write an equation between small displacement torsors. The equations are similar to those obtained for kinematic loop equations. But, on the one hand, the relations concern small displacements instead of velocities and on the other hand, the clearances between two parts of each joint, and the deviations between two joint surfaces of each body are taken into account. The resolution of these equations leads to tolerancing equations.

Tolerancing equations are the relations between the components of clearance torsors and deviation torsors only. But the values that can be taken by these torsors are limited. For given actual parts, the deviation torsor components and the dimensions are defined. The clearance torsor values depend on the forces applied on the mechanism, but whatever these forces, the tolerancing equations have to be respected, and in the assumption of rigid bodies, the components of clearance torsors are limited. The general method is here applied with a simple example .

1.4. EXAMPLE FOR A SHAFT SUPPORTED BY TWO BEARINGS.

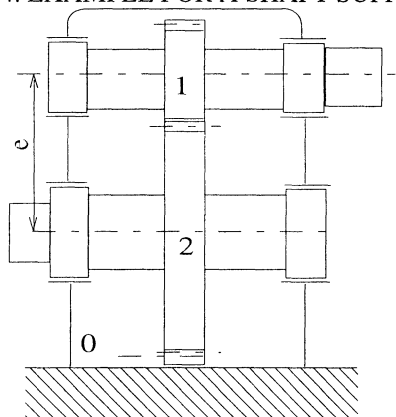


Figure 1. Gear box

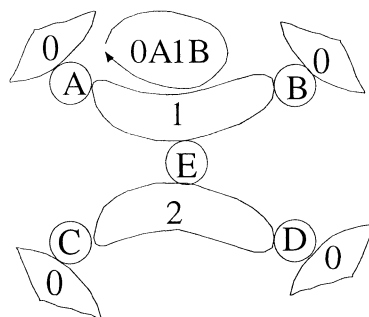


Figure 2. Graph of the mechanism

1.4.1. Shafts and bearings tolerancing

Let us consider two cylindrical joints between two bodies : shaft and support (the base 0). In nominal position the coaxiality between the two joint axes is assumed. With the hypothesis of small displacements, we get the following close loop (0A1B) equation:

$$C_{0A1} + J_{0A1} + E_{A1B} + C_{1B0} + J_{1B0} + E_{B0A} = 0 \quad (1)$$

Where : $C_{0A1} = (C\alpha_{0A1} \mathbf{x} , Cu_{0A1} \mathbf{x})_0$ is a joint torsor. $C\alpha_{0A1}$ and Cu_{0A1} are respectively the small rotation and small displacement of the point O, allowed by the cylindrical joint. The letters A and B refer to the joints and the numbers 0 and 1 refer to the links.

$J = (J\beta \mathbf{y} + J\gamma \mathbf{z} , Ju \mathbf{y} + Jv \mathbf{z})_0$ is the clearance torsor, representing a small displacement allowed thanks to the gap between the two surfaces of the joint (the indices are omitted here).

$E = (E\beta \mathbf{y} + E\gamma \mathbf{z} , Eu \mathbf{y} + Ev \mathbf{z})_0$ is the deviation torsor, representing a small displacement possible between the two cylindrical surfaces of the same part.

In the nominal configuration, the torsors J and E are equal to 0. The closed loop equation gives 6 scalar equations. The terms of the joint torsor C are considered as unknowns. There are four unknowns for this example. The rank of the linear system is equal to two. So that four compatibility equations (6 - 2) have to be checked. These equations are composed of the terms of torsors J and E only. We call tolerancing equations these scalar equations.

In this example, only the components of small rotations around axes Oy and Oz and the components of small displacements of point O along the axes Oy and Oz, appear in these tolerancing equations. They are the following :

$$\begin{aligned}
 J\beta_{0A1} + E\beta_{A1B} + J\beta_{1B0} + E\beta_{B0A} &= 0 & Jv_{0A1} + Ev_{A1B} + Jv_{1B0} + Ev_{B0A} &= 0 \\
 J\gamma_{0A1} + E\gamma_{A1B} + J\gamma_{1B0} + E\gamma_{B0A} &= 0 & Jw_{0A1} + Ew_{A1B} + Jw_{1B0} + Ew_{B0A} &= 0
 \end{aligned}
 \tag{2}$$

For given dimensions of the two surfaces, the limitations of clearance torsor components are defined by the clearance space, built in the small displacement space.

For a given geometrical tolerancing, the deviation torsor components are limited by a tolerance space, which is in fact a representation of the tolerance zone represented not in the conventional three-dimension space but in the small displacement space that has six dimensions in the general case. However, the tolerancing equations show that, for the example, only four components have to be taken into account.

The equations between the different components may be written under as follows: $E = -J$ where J and E are four-component vectors.

The different possible values of J result from the composition of the different values of clearance torsors that appear in the tolerancing equations and are limited by the clearance space and are noted {J}.

The assembling condition gives the minimum possible resulting deviation space. It is the resulting clearance space (with the minus sign : -{J}). This condition may be written in a mathematical form :

$$\forall E \in \{E\}, \exists J \in \{J\} \Rightarrow E + J = 0 \tag{3}$$

This condition may be translated in the following form : The deviation space {E} must be included in the clearance space -{J} [SA.96].

In consequence, the minimum deviation space which may be chosen, coincides with the clearance space.

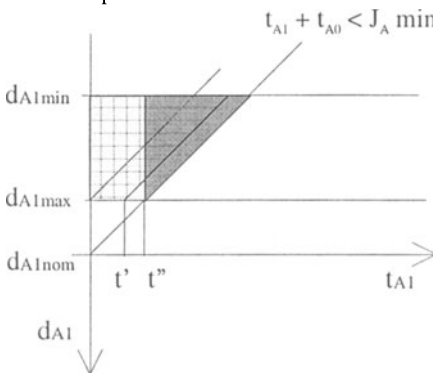


Figure 3. Representation of inequalities

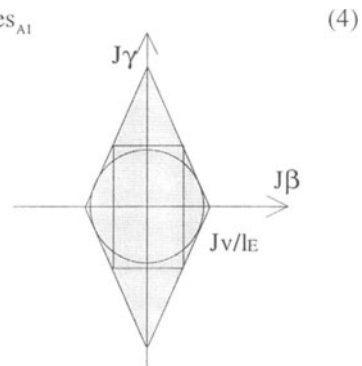


Figure 4. Clearance space projection

So that the two conditions $t_{A1} < -es_{A1}$ and $t_{A0} < ei_{A0}$ are sufficient to ensure that any shaft fits any base (interchangeability condition).

If the maximal material condition is used, the corresponding inequality is :

$$t_{A0} < ei_{A0} + (d_{A0} - d_{A0min}) \tag{5}$$

Fig. 3 gives a graphic representation of these conditions.

If the bearings are ball bearings, the clearance space is slightly different but the result is close to the previous one.

1.4.2. Gear tolerancing

Assuming that all the tolerances are defined for the shafts and bearings, it is possible to determine the clearance between each shaft and the base that result of the assembling of the two bearings. A single joint is then considered between each shaft and the ground. The closed loop for gear tolerances is then :

$$C_{0AB1} + J_{0AB1} + E_{AB1E} + C_{1E2} + J_{1E2} + E_{E2CD} + J_{2CD0} + C_{2CD0} + E_{CD0AB} = 0 \quad (6)$$

The linear system is composed of 6 equations and 4 unknowns (the two rotations shaft and the 2 d.o.f. for the gear linear contact). The rank of this system is equal to 3 so that 3 tolerancing equations are obtained : two equations for rotation components and one equation for the small displacement.

Then the method previously exposed may be applied: the clearance space for the three joints is built, and the deviation space is chosen so that this space is minimum (fig.4).

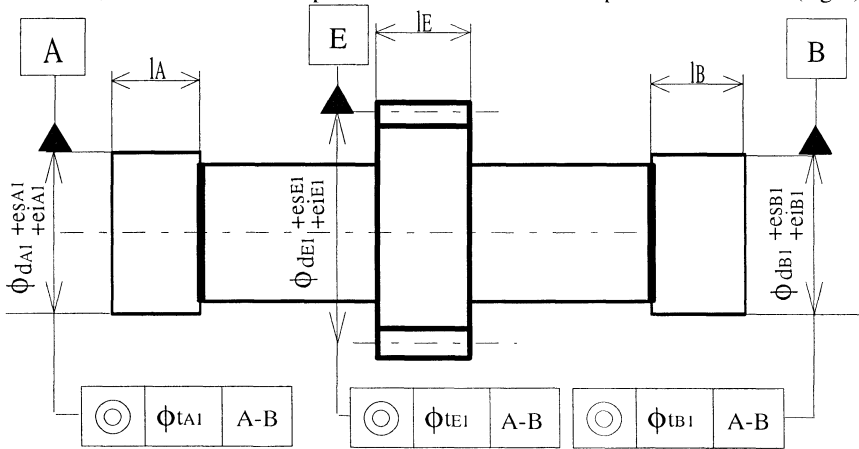


Figure 3. Shaft tolerancing

2. Elastic analysis view

Some results from the rigid tolerancing view are needed to make this analysis. So it must be done after the former. In fact, we must know the configuration of all parts and joints with the load and displacement constraints to deduce the elastic displacements in joints and parts [4]. Those displacements (and reaction forces) are the results of this view.

2.1. METHODOLOGY

Every elastic study may be done in an analytical way (beam model, ...) a numeric way (F.E.M., experiment, ...) or a mixed way. The analysis of the mechanism is made

with an finite element method. The finite element model is an assembly of "part elements" (structural stiffness of parts between two joints) and "joint elements" (« contact » stiffness) between parts. Then with the global model, we can determinate little elastic displacements in joints (elastic clearance) and little elastic displacements in parts (elastic clearance) which can be mixed in the synthesis view with those of the previously analysed tolerancing view.

2.2. MODELIZATION

In the case of our example, we use an analytical method (the beam model and the Hertz theory) to build the stiffness matrix of the assembly. This matrix is built with elementary ones and allows us to make a static analysis of the mechanism.

2.2.1. Stiffness study

To start with, a stiffness matrix of every element of the finite elements model has to be built. In this aim, all degrees of freedom (in the structural analysis way) are identified. This can be done by using the kinematic graph of the previous view.

With this graph, we can find all the joint and part frames of the mechanism (forbidden movements are structural d.o.f.'s). So we get the elastic degrees of freedom in every joint. They are the same as clearance d.o.f.'s. For example, **A** is a revolute joint with the (A, \vec{x}) axis between parts 0 and 1. In **A** we have the d.o.f. vector $\delta_A = \langle \delta_{Ax} \ \delta_{Ay} \ \delta_{Az} \ \theta_{Ay} \ \theta_{Az} \rangle$. Joint by joint, we build all the d.o.f.'s vectors.

If a part is linked to other ones with joints **A B C**, its d.o.f. vector will be an « addition » of δ_A , δ_B and δ_C . It is then possible to build the stiffness matrix of this part. For a joint matrix, we need the joint d.o.f. vector.

Finally when every component (part or joint) matrix is known, we can make the assembly in the global stiffness matrix of the mechanism (in which parts and joints are elements and nodes are frames).

Remarks

-1- The concept of component leads us to study a piece of mechanism like a single element (thus a single element matrix). For example, a ball bearing (which is a mechanism) is a component (such as a spherical or ring joint) regardless what is happening inside.

-2- The structural analysis model of the mechanism is not the same as the tolerancing analysis. In this reducer, we introduce in part 1 the sub-components pinion 1.1 and pinion 1.2 (in elastic analysis view) to input the elastic behaviour of the link shaft-pinion (part 2 becomes shaft 2.1 + pinion 2.2).

-3- There are several gear tooth links between 1.2 and 2.2. Those links are linear contact joints (4 kinematic d.o.f.'s so 2 elastic d.o.f.'s). We build a single gear joint (1.2-2.2) as a compilation of all these line links.

When all d.o.f.'s are known we can analyse the stiffness relations of parts and joints which are concerned by them. For shaft elements, we can use a beam model (two beam elements linked with a pinion element). In a first approach, we suppose the base to be

rigid (it is possible to study a flexible one by using stiffnesses at bearings A, B, C, and D). In every cylindrical bearing we can study the stiffness by using either the Hertz-Radziowski theory ([5]) or experiments or manufacturer's data. The main problem of contact analysis is that stiffness depends on contact configuration. At this step the latter is necessarily known. But this problem only appears for the joints with clearances. In the case of joints with preloads, there is no problem unless external loads are lower than internal ones.

We can divide pinion analysis into two models:

-1- **A part model** to take into account deformations in the pinion independently of the relative position of pinions. This model can be a single disk with a load at a peripheral point (tooth loads).

-2- **A local joint model** to know the behaviour of the tooth/tooth contact with two sub models. The first one is a tooth beam model to take the tooth flexibility into account. The second one is a local Hertz contact model (cylinder/cylinder) in which the stiffness depends on contact configuration. The angular position between 1.2 and 2.2 gives the number of teeth in contact and contact directions. If there is preload of the gear, there will be contact on both sides of the teeth.

For the gear joint model, stiffness matrices have been assembled to build a single gear joint matrix at point E. This matrix will depend on configuration. There are several configuration parameters. In this example, the angle α between pinions can be used as one of them and the pivot pitch clearance e as the other one if negative. The matrix is studied in particular configurations of α (i.e. with one or two tooth contacts). In those cases, the pivot pitch only is a parameter (the assembly pivot pitch has been chosen).

2.2.2. Resolution

Once all component matrices have been built, their assembly is made as a classical finite element analysis. The static resolution then gives unknown displacements and forces in every node (frame) of the model. With the object of making the synthesis, the displacement results must be "distributed" in elastic clearances and elastic distortions.

The elastic clearance in a joint is the little displacement torsor between the two frames which link the joint with parts (most of the time they match at the beginning of the elastic analysis). The elastic distortion in a part is the little displacement torsor between two frames which links the part with joints (a single part linked by more than two joints has got several elastic distortions).

When the elastic clearances and distortions are known, it is possible to check closing loop equations of the perfect flexible mechanism.

3. Synthesis of the two models

Small displacements are due as much to the elastic displacements as to geometric deviations, but are also due to clearance. This fundamental hypothesis leads to linear equations from the geometric closed loop. The different torsors describe all these small displacements.

A first application of the stiffness matrix consists in the assumption that the assembly conditions without pre-stresses is not required. On the contrary, we assume that the system can support pre-stresses within reasonable limits. This method allows to reduce the clearance between gearwheels and consequently to reduce noises and vibrations and also to improve the accuracy of the mechanism.

Another application consists in determination of the maximum angle between the shaft axis and the bearing axis by taking geometric deviations and elastic distortions simultaneously into account. This determination is important for the elastic-hydrodynamic behaviour of the bearings.

The tolerancing method leads to qualitative choices and relations between tolerancing parameters. Structural analysis gives other relations between forces and displacements. Design optimisation must take these different relations into account.

4. Conclusion

Starting with the hypothesis of small displacements, coming from the manufacturing deviations as well as elastic displacements, it is possible to use a model for tolerances then elastic analysis and their interactions.

Basically, this model is simple, unfortunately, there are many real variables for the definition of dimensional and geometric tolerances and the difficulty is to have enough conditions for a unique solution. The design of clearance deviation is also a difficulty because it is necessary to make projections of a space with more than three dimensions. A software seems necessary to aid for the determination of tolerance zones.

Elastic analysis gives stiffness matrices and tolerancing analysis gives the qualitative determination of tolerances. The definitive values that totally determine these tolerances must take into account these different requirements. This paper is a contribution to reach this aim.

5. References

1. GAUNET D. (1994) Modèle formel de tolérancement de position. Contribution à l'aide au tolérancement des mécanismes et CFAO Ph. D. Thesis ISMCM ENS Cachan France.
2. CLEMENT A., DESROCHERS A., RIVIERE A. (1991) : "Theory and practice of 3-D tolerancing for assembly" *CIRP International Working Seminar on Tolerancing* pp 25-55
3. GIORDANO M., DURET D. "Clearance Space and Deviation Space. Application to three-dimensional chain of dimensions and positions", *Proceedings of 3rd CIRP.Seminars on Computer Aided Tolerancing. , France, April 27-28 1993, EYROLLES Ed. pp.179--196.*
4. SAMPER S., GIORDANO M. (1996) Taking into account elastic displacements in 3D tolerancing. Models and application, *Proceedings of the 5th International Conference on Achievements in Mechanical & Materials Engineering, Wisla, POLAND, Elsevier Ed. Dec. 1996.*
5. RADZIMOVSKY E.I. (1953) Stress distribution and strength conditions of two rolling cylinders pressed together *Eng. Exp. Sta. Univ. Ill. Bull.* 408, 1953
6. TURNER J.U. (1993) A feasibility space approach for automated tolerancing, *Journal of engineering for industry* vol. 115 n°3 Aug. 1993 pp 341-346
7. WIRTZ A. (1993) Vectorial tolerancing, a basic element for quality control *3rd CIRP seminar on Computer Aided Tolerancing ENS Cachan France* April 1993

FIXTURING EFFECTS ON WORKPIECE QUALITY IN MILLING

A. D'ACUNTO*, J. LEBRUN**, P. MARTIN*, M. GUEURY**

* ENSAM, Metz, 4 rue A. Fresnel, 57070 Metz, France.

** ERIN, ESSTIN, Université Henri Poincaré, Nancy 1, 2 rue J. Lamour, 54500 Vandoeuvre, France

1 INTRODUCTION

Nowadays, industrial companies have to manufacture a large variety of complex products in short time. Reduced lot size and increased product quality requirements result from the pressure of market. Product quality requirements lead to the necessity for the manufacturers to "produce good quality from the start". This obliges us to provide assistance tools allowing for the prediction of surfaces. In fact, it is imperative to better understand the workpiece behaviour on the machine tools. The modelling of cutting processes is needed for the development of simulation and prediction of machining. Models of the milling process can be used in adaptive control on NC machine tools or for the choice made during the selection of machining operations in process planning. In this paper we present the definition of resources, which enable us to describe the default sources. Thus, we propose an approach for the prediction of milled surfaces. This approach is useful for workpieces with a high added value (accurate tolerances) or for workpieces deformed by residual stresses. We made experimentation with the Design of Experiments method. We treated the influence of the fixturing acting on the surface flatness in the "Workpiece/Machine/Tool" (WMT) framework. The finite element methods (FEM) is used for simulation and prediction.

2 CONTEXTE

Our research work focuses on the workpiece. The defaults of surfaces are the important characteristics to identify the causes and sources in order to undertake corrective tasks. We submit the various relationship between the workpiece and the milling process, resources, process planning (no reported in this section) . The framework of ours study is the behaviour of the "Workpiece/Machine/Tool" (WMT).

2.1 MILLING PROCESS

Usually, the cutting process is the means of machining. However, we distinguish two modelling levels. The first level is the interaction between material and cutting edge (orthogonal and oblique cutting). The second one is the interaction between the tools and the workpiece.

The first of these approaches concerns the modelling part of cutting with a microscopic regard on mechanical, thermal, dynamic behaviours. Those works are developed on a tool-chip interface by (Merchant,1945) or with experimental and analytical methods (Oxley,1989) and with numerical method (Shih,1995).

The second approach is based on the macroscopic part of cutting because the chip's geometry is used for modelling. We can quote the first articles on milling processes by (Martellotti,1941).(Martellotti,1944) which define the path of the cutter cutting edge and the chip thickness for up and down milling. (Koenigberger,1961) and (Saberwall,1962) defined the relationship between chip thickness and the cutting force compounds. A mechanistic model are proposed by (Tlusty,1975), and Fu (Fu,1984).

The comprehensive forces system takes account of some defaults of the "Machine-Tool-Workpiece" (Spiewak,1994), the run-out (Kline,1983), the cutter deflection (Sutherland,1986), the tilted spindle.

Both approaches can lead to a better understanding of cutting process and milling process phenomena. Nevertheless, those approaches are not linked. The second approach needs to define different parameters (K_S , K_T) in milling process especially for each material family. It demands a lot of experimentation on machine tools providing for reliable information. It is necessary to link the two approaches in order to reduce experimentation and cost.

2.2 RESOURCES

The introduction of the concept of resources enables us to define the means of manufacturing. We will consider the resources in terms of functional tasks and a physical system. From the functional point of view, the resources aim at removing material, moving and inspecting the workpiece. Following this description, the resources can be machine tools, robots or co-ordinate measuring machines. From the physical point of view, the resources consist of:

- Mechanical structure (slide ways, spindle, base, bed, and so on) ;
- Automation structure (CNC, dialogue, monitoring, and so on) ;
- Actuators and sensors structure (Drives motors, measuring system, and so on) ;
- Technical structure (tools, tool-holders, jigs and fixtures, clamping, and so on).

The resources can breakdown resulting in various problems. The origins of these defaults are caused by the mechanical and technical structure stemming from geometry, kinematics, dynamics, thermal, and vibration. We can say the same thing for technical structure. Actuators and sensors structure can lead to defaults of stability and motions errors. These errors are less important than those within the mechanical and technical structures, except for the control of high speed machining. To reduce the errors, feed drives must be directly linked with the mechanical structure. Sensors must be correctly located to give the best information concerning the position and motion of the workpiece. The defaults caused by the automation structure are often problem of models implementation.

Our research work deals with the fixturing influence on the workpiece during the end milling operation. This phenomenon belongs to the technical structure, thus we will study mechanical gripping acting on surface quality

3 EXPERIMENTATION

The centre of interest is the gripping effects influence on workpiece in end milling. The equipment is a horizontal milling center. The end milling cutter of 63 mm diameter was equipped with carbide inserts. The workpiece holder is a standard vice. The jaws were shoulder shaped. The clamping torque was controlled by a dynamometer spanner. We used the co-ordinate-measuring machine measuring the surface before, during and after the milling and gripping action.

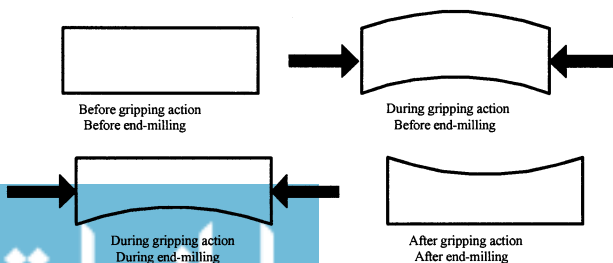


Figure 1. Gripping problem

The workpiece material is an aluminium alloy (Fortal: Ref.7075). The dimensions of workpiece were : $l = 200\text{mm}$, $w = 60\text{mm}$ and $h = 20$ or 15 mm

3.1 DESIGN OF EXPERIMENT

The flatness, lengthways and transversal deformations were the responses of Design of Experiment. The workpiece was submitted to strains. The other parts (mechanical structure and vice, tool-holder, milling cutter of technical structure) were regarded as rigid bodies. Thermal, dynamics and vibration effects of the resource were considered negligible. In this experimentation the cutting time was very short and the cutter wear was of insignificant influence on the surface quality. The cutting conditions were optimised with a semi roughing criterion. We considered that the regarded parameters are mutually independent.

3.2 METHOD

The applied method was based on the Taguchi method. The plan has two levels (min – max) realised with two repeated tests (figure 2). We realised the tests to verify if the behaviour between two levels is linear. The parameters were the cutting speed, rate feed, depth of cut, the gripping torque, and rolling direction.

Parameters	Level 1	Level 2
Cutting speed	360 m/min	200 m/min
Plate feed,	0,2 mm	0,5 mm
Depth of cut	3 mm	5 mm
Workpiece thickness	20 mN	20 mm
Gripping torque	15 mm	30mN
Rolling direction	transverse/length	lengthways/length

Figure 2. Parameters for experimentation

We measured flatness by CMMs. Lengthways and transverse deformation were calculated with the results of measurement. The experimental values example is described in figure 3.

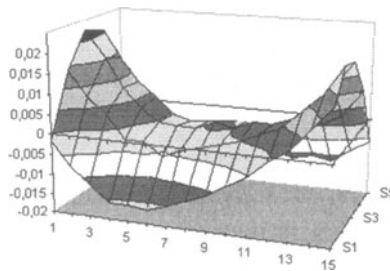


Figure 3. Example of measuring on CMMs - For the vertical axis, the unit is in mm and the others are the position of measured points.

3.3 RESULTS AND INTERPRETATIONS

Regarding the results, we can give the following series of information.

- Confirmation of the partial independence of parameters.
- Confirmation that lengthways deformations are superior to transverse deformations
- Confirmation that the gripping forces increased the transverse deformation values.
- Confirmation that the effect of gripping is inversely proportional to lengthways deformations.
- Invalidation that the thickness of the workpiece has a significant influence on the flatness.

From these observations we can state :

- Confirmation of the significant role of residual stresses derived from rolling process. The material behaviour is anisotropic. The default is more important where the direction of feed rate is perpendicular to rolling direction.

4 MODELING AND SIMULATION BY FINITE ELEMENTS METHOD

4.1 MODELING METHODOLOGY BY FEM

After experimentation, we will present a prediction method for the workpiece flatness by the finite element method (Zienkiewicz,1991). We only treated the influence of gripping forces. We used calculation codes like "DiagueBiDim" and "DiagueTriDim" (Gueury,1998). The software is implemented on PC. Firstly, we made a bi-dimensional model with "DiagueBiDim". Subsequently, we made a tri-dimensional model with "DiagueTriDim".

The direct formulation of finite element characteristics applied in manufacturing was outlined in two steps. The first step treats the rolling residual stresses. The second step describes simulation with a virtual eraser tool of material. A machined part is manufactured out of block in which residual stresses are present. Frequently the evaluation of this compound force is omitted. The residual stresses in the workpiece must be considered as imbalanced internal forces.

The constitute law was linear elastic behaviour. The relationship (1) between stresses and strains (Zienkiewicz,1991) is linear and we can state :

$$\boldsymbol{\sigma} = \mathbf{D}(\boldsymbol{\varepsilon}_0 - \boldsymbol{\varepsilon}) + \boldsymbol{\sigma}_0 \quad (1)$$

$\boldsymbol{\sigma}$: Euler-Cauchy Stress tensor, \mathbf{D} : Element stress matrix - $\boldsymbol{\varepsilon}_0$: Initial deformation tensor, (thermal origin for example) - $\boldsymbol{\varepsilon}$: Deformation tensor, $\boldsymbol{\sigma}_0$ Initial stresses tensor (residual stresses for example).

The relationship (2) between stresses and displacements is defined as :

$$\boldsymbol{\varepsilon} = \mathbf{B} \mathbf{a} \quad (2)$$

\mathbf{a} : global displacement - \mathbf{B} : Strain shape function.

With the formula of constitute law and stresses and displacements relationship, the principle of virtual (internal and external) work we can write :

$$\mathbf{K} \mathbf{a} + \mathbf{f} = \mathbf{r} \quad (3)$$

\mathbf{K} : Stiffness matrix, \mathbf{f} : Global forces of nodes - \mathbf{r} : External forces,

In our application case, each removal material breaks the internal equilibrium of the whole workpiece. It is necessary to reconstitute the internal equilibrium of the workpiece. The numerical simulation of the end milling operation must be defined by a statical study and brought into balance again for each material removal. We calculated the equilibrium of the whole workpiece at time t_i and at time t_{i+1} , thus :

$$\int_V \mathbf{B}^T \boldsymbol{\sigma}_i dV = \mathbf{r}_i \quad \text{and} \quad \int_V \mathbf{B}^T \boldsymbol{\sigma}_{i+1} dV = \mathbf{r}_{i+1} \quad (4)$$

The equilibrium of the whole body cured of residual forces :

$$\Delta \mathbf{r} = \mathbf{r}_{i+1} - \mathbf{r}_i \quad (5)$$

We used the displacement approach and the minimisation of total potential energy and the weighted residual approach.

$$\mathbf{K} \Delta \mathbf{a} = \Delta \mathbf{r} \Rightarrow \mathbf{a}_{i+1} = \mathbf{a}_i + \Delta \mathbf{a} \Rightarrow \boldsymbol{\sigma}_i = \boldsymbol{\sigma}_0 + \Delta \boldsymbol{\sigma} \quad (6)$$

With this approach we can update the mesh after each calculation of equilibrium of the workpiece. This is possible because the material removal is only considered as a small perturbation. We neglect the initial strains of the thermal effect because they are insignificant on workpiece during end milling. The residual stresses cannot be considered because before milling the workpiece is in the state of self-equilibrium and

the initial stresses are unknown. The latter were considered null the initial stresses at the beginning of simulation :

Numerical simulation of the gripping and machining action were carried out in three steps:

- Loading of mobile jaw was simulated by an imposed displacement (0.1 mm) in transversal direction. This is a realistic behaviour because the jaws of the vice are infinitely rigid.
- Milling process was considered as a material eraser. Usually, we took into account the effects of material removal. The numerical treatment was the same in both simulation studies.
- The loosening of the moving jaw is considered as unloading of gripping action with elastic recovery.

4.1.1 Bi-dimensional simulation (Modeling: Plan Strain State)

The following method refers to the three steps that we defined in methodology paragraph. We considered the calculation in a plan strain state. The workpiece was represented by a beam in transversal direction. The section is discretized by 60 isoparametric finite elements. The Serendipity element is described by eight nodes of quadrilateral elements in a Cartesian Co-ordinate System (thus 213 nodes and 416 degrees of freedom). The layers of meshes were chosen to take into account the depth of cut (2 mm) and the height of jaws (4 mm). The height of layers isn't constant; the dimensions are 2 mm, 1.25 mm and 1 mm. The mesh of the workpiece is represented in figure 4.

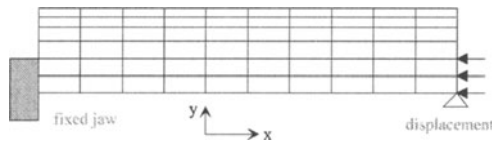


Figure 4. Modelling by FE in 2D

- Steps 1: gripping effect of jaws

The figure n° 5 presents the amplified deformation of the middle section. We can observe that the jaws gripping bring about the curved shape of the section.

- Step 2: material removal with eraser material.

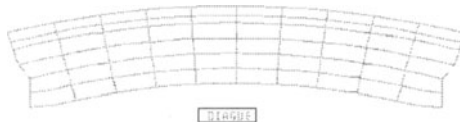


Figure 5. Amplified deformation ; convex form

Material removal of 10 finite elements corresponding to the first depth of cut caused imbalance of the nodal forces. It was necessary to correct the nodal forces. The section of the mesh was updated respecting the initial stress defined in step 1. The second depth of cut corresponds to the removal of 10 finite elements. This section of the mesh was updated again in concordance with the stress defined by the first depth of cut. In figure 6, the plan plot of relative Von Mises stress is presented.

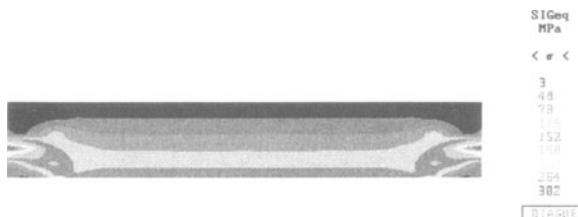


Figure 6. Von Mises stress in the beam section

We distinguished high density of stress where the jaws of vice and the workpiece are joined. The stress level is low on the milled surface. The level of Von Mises stress value (minor of elastic stress) enable to define that the behaviour of workpiece material is linear.

- Step 3: beam unloading

This task consisted in applying the equal and opposite loading of the initial nodal forces defined in step 1. The simulated workpiece surface is a concave curvature. The results are in accordance with the transverse deformation observed in experimentation.

- Concluding remarks for 2D simulation

The results of the first simulation are very instructive. The influence of the gripping actions is high on the flatness. The residual stresses are non-existent at the beginning of the simulation, afterwards they were taken into account. However, the measured transverse deformation gaps can enable us to evaluate residual stresses. Concerning the transversal deformations, the mean values of the experimentation are equivalent to the values of the beam deflection after milling and unloading actions resulting from the simulation.

4.1.2 3D simulation (Modelling in three dimensions)

We simulated the workpiece behaviour in three dimensions with “DiagueTriDim” finite elements code. The workpiece was considered as an elastic body. Due to the symmetric shape (workpiece and jaws) and the loading geometry we can reduce the problem to a quarter of the workpiece. Figure 7 represents system and surface references.

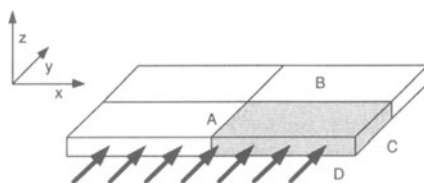


Figure 7. System and surface references of a quarter of the workpiece.

The quarter of the workpiece was discretized by 200 iso-parametric finite elements. The Lagrangian elements were eight nodes of element in a cartesian co-ordinate system (thus 330 nodes and 990 degrees of freedom). Modelling of the quarter of the workpiece (figure 7) needed new boundary conditions. We must take into account supports and (geometric and loading) symmetry. The jaws of vice and the vice were considered as rigid bodies.

- On face A, all nodes were blocked following the Ox axis.
- On face B, all nodes were blocked following the Oy axis.
- On face D, nodes were blocked following the Oz axis for all z=0.
- The loading of the mobile jaw was simulated by an imposed displacement (0.1 mm) following the Oy axis.

Like in bi-dimensional simulation, the meshes were chosen to take into account the depth of cut and the height of the jaws. The height of layers isn't constant; the dimensions are 4 mm, 1.25 mm and 1 mm (dimension of depth of cut)

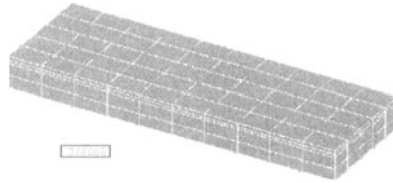


Figure 8. 3D mesh of a quarter of the workpiece

The 3D mesh was realised by the extrusion of the bi-dimensional mesh of face A (figure 8). The boundary conditions due to the gripping jaws were applied to the bottom layer. The imposed displacement has the same value as in the 2D simulation.

- Gripping effect

Figure 9 depicts the deformation of the chosen workpiece section. We can note that the gripping action provokes:

- Convex curvature of the workpiece section in the transversal direction where it is applied
- Raising of the workpiece edges in the lengthways direction.

Both phenomena on the whole workpiece give a look of "horse saddle". This shape corresponds to the experimental results.

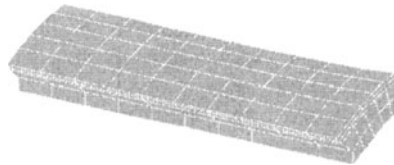


Figure 9. Amplified deformation of the workpiece section

Figure 10 confirms the low level of stresses on the milling surface. The stress distribution is not uniform in lengthways direction. In the area of contact of the gripping action the stress level is high.

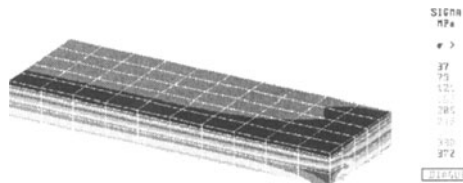


Figure 10 : Von Mises Stress on the surface of the workpiece.

- Concluding remarks for 3D simulation

Material removal with eraser material and unloading of the workpiece were treated like in the 2D simulation. The resulting shape - a horse saddle - was the same as observed in experimentation. The simulation by finite element method provides for correct results, because the mean values of flatness, lengthways and transversal deflection correspond to the evaluations of defaults resulting from the tests.

5 CONCLUSION

Our work consisted in developing a model that enables to predict the quality of a workpiece surface. The criterion is the flatness of the milled surface. Concerning the conditions of machining we treated the effects of the fixturing actions of a standard

vice and the end milling operation. By using the design of experiments method we realised a series of tests. We presented the influence of fixturing effects on the flatness of the workpiece. We took into account the residual stresses that increased the defaults of clamping.

The finite elements method permitted to simulate the behaviour of the workpiece subject to the gripping jaws and the end milling operation.

The approach presented here is dedicated to validate the use of the finite element method, which can be applied for the prediction of surface quality in milling. We verified that it is possible to apply the finite element method to foresee the workpiece behaviour submitted to gripping action and milling forces.

The finite elements method is not enough for the efficient simulation. It is necessary to understand the global behaviour of the mechanical and technical structures acting on the workpiece.

The approach can be reduced to experimental tests because they are very expensive in terms of time and money. Also, this approach can provide a method of prediction in milling operations for added value and deformable workpieces.

Lastly, it is possible to use this approach in process planning, where the difficulties of its application are great because :

- firstly, the automation of the approach needs the integration of CAD and CAM,
- secondly, the process planning staff usually is not familiar with the finite elements method. In prospect, we will make simulation of slotted and bored workpieces with the same rigid vice. We will take into account vice deformations and treat the vibration behaviour and the influence on the roughness.

6 REFERENCES

- Fu H.J., DeVor R.E., Kapoor S.G. (1984) A mechanistic model for the prediction of the force system in face milling operations, *Journal of Engineering for Industry*, Vol **106**, 81-88.
- Gueury M. (1997) "Diaguebidim, and DiagueTridim", Finite element software, Version 4.12, Equipe de Recherche en Interface Numérique (ERIN) in Ecole Supérieure des Sciences de l'Ingénieur de Nancy, France.
- Kiritzis D. (1995) A review of knowledge-based expert systems for process planning. Methods and problems, *International Journal of Advanced Manufacturing Technology*, N° **10**, 240-266.
- Kline W. A., DeVor R.E. (1983) "The effect of runout on cutting geometry and forces in milling", *International Journal of Machine Tool Design and Research*, Vol **23**, N° **2/3**, 123-140.
- Koenigberger F., Sabberwal A.J.P. (1961) An investigation into the cutting force pulsations during milling operations, *International journal of Machine Tool Design and Research*, Vol **1**, 15-33.
- Martellotti (1941) An analysis of milling Process, *Transaction of ASME*, Vol **63**, pp 667-700.
- Martellotti (1944) An analysis of the milling process, Part II – Down milling, *Transaction of ASME*, Vol **67**, 233-251.
- Merchant M.E. (1945) Mechanics of the metal cutting process, orthogonal cutting and type two chips, *Journal applied Physic*, p 267-312
- Oxley P.L.B. (1989) A strain Hardening solution for shear angle in orthogonal metal, *International Journal Mechanical of Sciences*, Vol **3**, pp 68-79.
- Saberwall A.J.P. (1962) Chip section and cutting force during milling operation, *Annals of C.I.R.P.*, Vol **10**, 197-203
- Shih A.J. (1995) Finite element simulation of orthogonal metal cutting, *Journal of Engineering for Industry*, Vol **117**, 84-93.
- Spiewak S.A. (1994) Analytical modelling of cutting point trajectories in milling, *Journal of Engineering for Industry*, Vol **116**, 440-448.
- Sutherland J.W., DeVor R.E. (1986) An improved method for cutting force and surface error prediction in flexible end milling systems, *Journal of Engineering for Industry*, N° **104**, 272-278.
- Thusty J., MacNeil (1975) Dynamic of cutting forces in end milling, *Annals of C.I.R.P.*, Vol **24**, 21-25.
- Zienkiewicz O.C. (1977) "The finite element method", Mac Graw Hill Edition, New York.

Chapter 7
OFF LINE PROGRAMMING AND OPTIMAL PARAMETERS
FOR MACHINING, WELDING AND ROBOTICS

Subassemblies detection with genetic algorithms	415
P. DE LIT, E. FALKENAUER and A. DELCHAMBRE	
Tool path correction on a numerically controlled machine-tool by characterisation of scattering in relation to type of machining	423
G. DESSEIN, J.M. REDONNET, P. LAGARRIGUE and W. RUBIO	
A ring-shaped mechanical assembly line optimized by a genetic algorithm.....	431
F. FONTANILI, A. VINCENT, T. SORIANO and R. PONSONNET	
Side milling of ruled surfaces-optimum tool radius determination and milling cutter positioning.....	439
J.M. REDONNET, G. DESSEIN, W. RUBIO AND P. LAGARRIGUE	
Optimization of end-mill roughing operation sequence.....	447
F. VILLENEUVE	
A model for the optimization of the relation between product means and product	455
S. TASSEL, F. VILLENEUVE and O. LEGOFF	
Optimal mill positioning in five axis machining on free form surfaces Application at roughing path of moulds.....	463
W. RUBIO, J.M. REDONNET, G. DESSEIN and P. LAGARRIGUE	
Avoiding the need for deburring by analyzing burr formation during product design.....	471
L. BLONDAZ, D. BRISSAUD and D. DORNFELD	

SUBASSEMBLIES DETECTION WITH GENETIC ALGORITHMS

P. DE LIT, E. FALKENAUER and A. DELCHAMBRE
Université Libre de Bruxelles
Department of Applied Mechanics
50, Av. F. Roosevelt CP. 165/41
B-1050 Brussels, Belgium

Abstract. The determination of an “optimal” assembly sequence for a product is known to be a hard task, due to the combinatorial explosion proper to permutation problems. A possible way to reduce the number of sequences to be studied is to subdivide the product into subassemblies. We here propose an original approach, based on a grouping genetic algorithm (GGA) to tackle the problem. We first describe a mathematical model reporting the topological characteristics of a product. We then explain the constraints the GGA developed deals with, and the cost function (which is expressed according to a connectivity criterion, and the stability of the proposed subassemblies). Finally, the algorithm is applied to an industrial case study and the corresponding results are presented and commented.

Key words: subassemblies, grouping genetic algorithms.

1. Introduction

The determination of the assembly sequences of a product suffers on combinatorial explosion. It is therefore mandatory to apply qualitative and quantitative criteria to reduce their number, like the number of re-orientations or the components stability during assembly. Another way to limit the number of possible assembly sequences is to subdivide the final product into subassemblies, for each of which an assembly sequence is generated. We thus transform the original problem into several less important instances of it. Moreover, the decomposition allows the simultaneous assembly of each subassembly increasing parallelism and allows tests on the subassemblies before final assembly of the whole product.

There has been considerable growth of interest in recent years in developing algorithms to detect subassemblies in a product. (Dini and Santochi, 1992) proposed an enumerative method to detect stable subsets of the one associated to the whole product, a subassembly being considered as a subset composed of strongly connected components, stable in the different insertion directions, and allowing the final assembly of the product from its subassemblies. They used a matrix

formalism to model the topological constraints between the components. (Citotolin, 1997) proposed an algorithm using the matrix formalism of (Fleury, 1993). To avoid the shelf of the enumerative feature of Dini's method, he proposed an heuristic, detecting the stable subsets of the whole product once the most external fixation links have been broken. (Lee, 1994) described a heuristic of recursive decomposition of a product from a liaison graph representation of the assembly. The selection of a so-called preferred subassembly is based on performance indexes.

We propose here an original method for subassemblies, using a Grouping Genetic Algorithm. This paper is organized as follows. Section 2 is devoted to the description of the subassemblies detection algorithm. It explains the product model, the constraints the GGA will deal with and the cost function we chose to evaluate the individuals. Results of an industrial case study will be given and commented at section 3. We draw conclusions at section 4.

2. Subassemblies Detection

2.1. PRODUCT MODEL

The formalism used in this paper is inspired from (Dini and Santochi, 1992) and (Fleury, 1993). It is supposed that (Wolter, 1988) the assembly sequence is sequential, that the insertion directions are parallel to the axes of a cartesian orthogonal system, that the insertion trajectories are linear translations, the sequence is monotone. We associate a positive and a negative sense to each axis and note \overline{d}_t the opposite direction of d_t .

2.1.1. Contact Constraints Model

We call *contact constraint* the contact link a component c_i possesses with the component c_j , the link preventing the translation—for amplitudes greater than the one under which components are considered to be in contact—of c_i in direction d_t . These contact constraints create a set of relations between the different components. We expressed them with a binary square matrix so that $S_{d_t(ij)} = 1$ if there exists a contact between c_i and c_j in direction d_t .

By definition a component never constrains itself. Note that if there exists (or if there does not) a contact between c_i and c_j in direction d_t , the same goes for c_j and c_i in direction \overline{d}_t . So

$$S_{\overline{d}_t} = {}^t S_{d_t}. \quad (1)$$

2.1.2. Interference Constraints Model

An *interference constraint* arises between two components c_i and c_j in direction d_t when c_j is on c_i disinsertion trajectory in direction d_t , no contact constraint existing between them in that direction. We represented these constraints with a

binary square matrix so that $G_{d_t(ij)} = 1$ if there exists an interference between c_i and c_j in direction d_t . As for contact matrices

$$G_{\bar{d}_t} = {}^t G_{d_t}. \quad (2)$$

For example, the contact and interference matrices in direction z^+ for the fictitious product illustrated in Figure 1 are

$$S_{z^+} = \begin{matrix} & \begin{matrix} 0 & 1 & 2 & 3 \end{matrix} \\ \begin{matrix} 0 \\ 1 \\ 2 \\ 3 \end{matrix} & \begin{pmatrix} 0 & 1 & 1 & 0 \\ 0 & 0 & 0 & 0 \\ 0 & 0 & 0 & 1 \\ 0 & 0 & 0 & 0 \end{pmatrix} \end{matrix} \quad G_{z^+} = \begin{matrix} & \begin{matrix} 0 & 1 & 2 & 3 \end{matrix} \\ \begin{matrix} 0 \\ 2 \\ 3 \end{matrix} & \begin{pmatrix} 0 & 0 & 0 & 1 \\ 0 & 0 & 0 & 0 \\ 0 & 1 & 0 & 0 \\ 0 & 1 & 0 & 0 \end{pmatrix} \end{matrix}$$

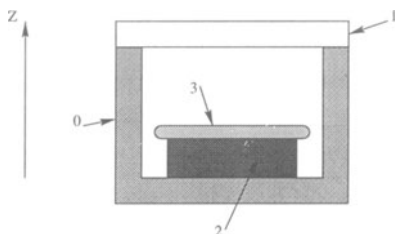


Figure 1. Fictitious product.

Note that properties (1) and (2) allow us to work only with matrices associated to positive axes directions.

2.1.3. Attachment Links Model

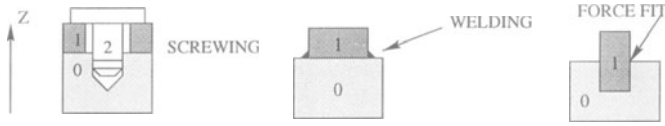
Attachment constraints can be represented with a symmetric matrix, F , valid for all directions. Although the diversity of existing attachment types, this kind of link stays easy to model. Figure 2 shows the attachment matrices for three simple examples.

We distinguish components specifically used to establish an attachment link from the others. Constraints matrices are modified too. A fixation component does not introduce contact links with the one it is fixed to in directions orthogonal to the insertion axis. The contact constraint actually becomes an interference constraint in these directions.

2.2. DECOMPOSITION OF THE PRODUCT INTO SUBASSEMBLIES

2.2.1. Definitions

Bourjault (Bourjault and Henrioud, 1987) introduces the concept of a “subset” as a set of m components among the n the product is composed of, so that the functional links subgraph generated by the corresponding m vertices is connected.



$$F = \begin{matrix} 0 \\ 1 \\ 2 \end{matrix} \begin{pmatrix} 0 & 1 & 2 \\ 0 & 0 & 1 \\ 0 & 0 & 0 \\ 1 & 0 & 0 \end{pmatrix} \quad F = \begin{matrix} 0 \\ 1 \end{matrix} \begin{pmatrix} 0 & 1 \\ 0 & 1 \\ 1 & 0 \end{pmatrix} \quad F = \begin{matrix} 0 \\ 1 \end{matrix} \begin{pmatrix} 0 & 1 \\ 0 & 1 \\ 1 & 0 \end{pmatrix}$$

Figure 2. Attachments matrices for different kinds of fixtures.

This definition stays applicable to our model, the functional links graph (Bourjault, 1984) being replaced by the one associated to *all* contact and attachment constraints. We associated a weighted graph to the above definition, to give more weight to an attachment than to a contact, yielding matrix S (the weights α and β will be discussed later):

$$S_{ij} = \alpha \sum_{d_t} S_{d_t(ij)} + \beta F_{ij}. \tag{3}$$

We define a *subassembly* as a subset of strongly connected components, preferably stable in some directions. This definition is more constraining than Bourjault’s one of a subset, without requiring the total stability of the subassembly.

2.2.2. *Stability Heuristic for Subassemblies*

We consider a subassembly stable along a direction if a translation of the referential associated to any of its components provokes the translation of the referential associated to each component in the subassembly. The different constraints matrices previously introduced only express the *direct constraints* existing between components in a direction d_t . It is clear that if c_i is constrained by c_j , c_j being constrained by c_k , c_i will be constrained by c_k . The identification of these *indirect constraints* between components asks for the transitive closure of the associated oriented graph; we used Warshall’s algorithm to detect it (Sedgewick, 1984). The direct constraints matrix P_{d_t} we used is:

$$P_{d_t} = S_{d_t} \bigvee F. \tag{4}$$

The fact that the translation of the whole subassembly must occur for any of its components being translated is crucial in our definition, because it restrains the stability directions to an axis, the transitive closure NC_{d_t} of P_{d_t} having to be a clique.

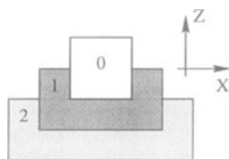


Figure 3. Fictitious product to illustrate the stability heuristic.

As an example, let us consider the pyramid presented in Figure 3. No fixtures are used, so $F = 0$. We have :

$$P_{x^+} = \begin{pmatrix} 0 & 1 & 0 \\ 1 & 0 & 1 \\ 0 & 1 & 0 \end{pmatrix} \quad P_{z^+} = \begin{pmatrix} 0 & 0 & 0 \\ 1 & 0 & 0 \\ 0 & 1 & 0 \end{pmatrix} \quad NC_{x^+} = \begin{pmatrix} 0 & 1 & 1 \\ 1 & 0 & 1 \\ 1 & 1 & 0 \end{pmatrix} \quad NC_{z^+} = \begin{pmatrix} 0 & 0 & 0 \\ 1 & 0 & 0 \\ 1 & 1 & 0 \end{pmatrix}$$

which indicates that the subassembly is stable along x axis, but not along z .

2.3. FEATURES OF THE PROPOSED GROUPING GENETIC ALGORITHM

2.3.1. Adaptation of the GGA Operators

The grouping genetic algorithm (GGA) (Falkenauer, 1998) differs from the classic GA (Holland, 1975; Goldberg, 1989) in the following aspects: a specific encoding scheme is used so that the relevant structures of grouping problems become genes in chromosomes and special genetic operators are used to suit the new encoding scheme. We here detail two genetic operators which properties have slightly been modified to suit the hard constraints of our problem.

The crossover operator is the same as the one exposed in (Falkenauer, 1998), except that the groups from which items should be eliminated are emptied, and re-injected randomly. This insures that the groups remain connected subgraphs. The applied mutation only consists to empty a random group, and to randomly re-assign the extracted items.

2.3.2. Invalid Decompositions Detection

Once assembled, a subassembly must not prevent the final assembly of the product. Determination of invalid decomposition uses a binary generalized interference constraints matrix I_{d_i} , defined as follows:

$$I_{d_i} = S_{d_i} \bigvee G_{d_i}. \quad (5)$$

The detection of invalid decompositions occurs in two steps: contraction of I_{d_i} yielding $I_{d_i}^c$, related to the proposed subassemblies, and verification of the existence of *any* valid assembly sequence for the proposed decomposition. The

contraction of I_{d_i} matrix traduces the passage from constraints between components to those existing between subassemblies, a subassembly $s_i = \{c_k\}$ having a constraint with $s_j = \{c_l\}$ if one of its components $c_k \in s_i$ interferes with a component $c_l \in s_j$. This matrix $I_{d_i}^c$ also allows the detection of a possible assembly sequence applied to a proposed decomposition into subassemblies. Disinsertion of a subassembly will be possible in direction d_i if it is submitted to no constraint in that direction. Thus, we just have to detect null lines or columns in $I_{d_i}^c$ (these columns correspond to null lines in $I_{d_i}^c$). We used the following algorithm:

1. Is it possible to disassemble a still non extracted component or subassembly i in any direction d_i ? If it is, go to 2, else decomposition is invalid.
2. Disassemble i and update all $I_{d_i}^c$ matrices, nullifying the corresponding lines and columns. Go to 1.

The update of $I_{d_i}^c$ traduces the fact that a disassembled subassembly introduces no more constraints on the remaining subassemblies.

2.3.3. Cost Function

The definition of a subassembly given at section 2.2.1 takes two features into account: intra- and inter-group connections and stability. The problem is to find a partition P of the weighted graph $G = (S, L)$ into K subgraphs $G_k = (S_k, L_k)$, $S_{(k)}$ being the set of vertices representing the components, $L_{(k)}$ the set of edges characterizing connections between components, the value of each edge illustrating the strong- or weakness of the links. We used the following cost function to evaluate the partitions proposed by the GGA:

$$\sum_{i,j \in S_k} \frac{l_{ij}}{2\gamma \text{card}(S_k)} - \sum_{\substack{u \in \omega(S_k) \\ \text{card}(S_k) > 1}} \frac{l(u)}{\gamma \text{card}(S_k)} + \sum_{k=1}^K \text{Stab}(k), \quad (6)$$

where γ and $\text{Stab}(k)$ are parameters and

$$l_{ij} = S_{ij} = \alpha \sum_{d_i} S_{d_i(ij)} + \beta F_{ij} \quad \text{from (3)}.$$

$\omega(S_k)$ is the cocycle of S_k . Simulations led to the following values: $\alpha = 1$, $\beta = 4$, $\gamma = 2$, and $\text{Stab}(k) = 1$ if S_k is stable along 2 axes or totally stable ($\text{card}(S_k)$ must be greater than 1), 0 otherwise.

3. Industrial Case Study

The industrial case study we propose to study is an electric signalling relay studied previously by (Delchambre, 1992). It is composed of 34 pieces, described in Figure 4.

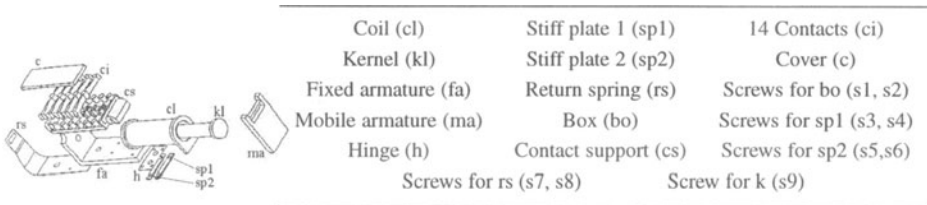


Figure 4. Components of the signalling relay.

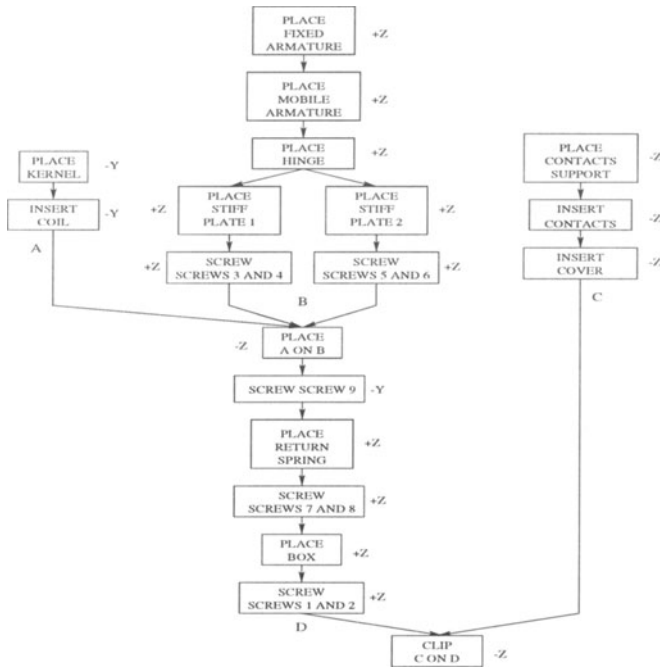


Figure 5. Precedence graph resulting from the proposed decomposition.

The GGA detects the following subassemblies: $\{cl, kl\}$, $\{cs, c1-c14, c\}$, and $\{fa, ma, sp1, sp2, s3-s6\}$. This decomposition leads to the assembly sequence illustrated in Figure 5.

4. Conclusions

Subassemblies detection appears to be a precious tool in establishing an assembly sequence of industrial products, drastically reducing the number of possible sequences. We developed a Grouping Genetic Algorithm to detect subassemblies, essentially based of connections between pieces that compose them, and only requiring topological characteristics of the product, expressed with seven matrices: three contacts matrices, three interferences matrices, and one attachments matrix.

The algorithm presented applicable to important instances of the problem. The results we showed in the previous section were obtained in about 30 seconds on a modest 166 MHz Pentium.

The precedence graph resulting from the proposed decomposition showed in Figure 5 is not the “best one”. A better precedence graph exists, presented in (Delchambre, 1992), requiring one more less turning to assemble the whole product. In the future, we will couple the subassemblies detection algorithm to an assembly planner, to have a feedback from this planner on the proposed decompositions.

Aknowledgements

This paper is based on results of the project “Outil d’aide à la conception interactive des produits et de leurs systèmes d’assemblage”. We particularly thank the “Région Wallonne” which has funded this project.

References

- Bourjault, A. (1984). Contribution à une approche méthodologique de l’assemblage automatisé : élaboration automatique des séquences opératoires. Thèse d’État, Université de Franche-Comté.
- Bourjault, A. and Henrioud, J.-M. (1987). Détermination des sous-assemblages d’un produit à partir des séquences temporelles d’assemblage. *Automatique-Productique Informatique Industrielle*, 21(2):117–127.
- Cittolin, A. (1997). Étude de filtres universels en vue d’une détermination et d’une sélection automatique de gammes d’assemblage de produits industriels. Mémoire de Thèse, Lausanne, EPFL.
- Delchambre, A. (1992). *Computer-aided Assembly Planning*. Chapman & Hall, First edition.
- Dini, G. and Santochi, M. (1992). Automated sequencing and subassembly detection in assembly planning. *Annals of CIRP*, 41(1).
- Falkenauer, E. (1998). *Genetic Algorithms and Grouping Problems*. John Wiley & Sons Inc., First edition.
- Fleury, J.-P. (1993). Détection des sous-ensembles durant la détermination des gammes d’assemblage. Technical report, DMT-IMT Institut de microtechnique, EPFL - École Polytechnique Fédérale, Lausanne (Suisse).
- Goldberg, D. E. (1989). *Genetic Algorithms in Search, Optimization and Machine Learning*. Addison-Wesley Publishing Company Inc.
- Holland, J. H. (1975). *Adaptation in Natural and Artificial Systems*. University of Michigan Press, Ann Arbor.
- Lee, S. (1994). Subassembly identification and evaluation for assembly planning. *IEEE Transactions on systems, man, and cybernetics*, 24(3):493–503.
- Sedgewick, R. (1984). *Algorithms*. Addison-Wesley.
- Wolter, J. D. (1988). *On the automatic generation of plans for mechanical assembly*. PhD thesis, The University of Michigan, USA.

TOOL PATH CORRECTION ON A NUMERICALLY CONTROLLED MACHINE-TOOL BY CHARACTERISATION OF SCATTERING IN RELATION TO TYPE OF MACHINING

G. DESSEIN^(*), J.M. REDONNET^(**), P. LAGARRIGUE^(**), W. RUBIO^(**)

() Laboratoire de Conception de Produits et de Systèmes industriels*

Ecole Nationale d'Ingénieurs de Tarbes

47, avenue d'Azereix - BP 1629 - 65016 TARBES Cedex

*(**) Laboratoire de Génie Mécanique de Toulouse*

Université Paul Sabatier

Bât. 3PN - 118, route de Narbonne 31062 TOULOUSE Cedex

Abstract

When manufacturing a part, distortions of the machine, tool, workpiece and machining assembly lead to defects. These will vary according to the type of machining and the machine used. Given the large number of influential parameters, it therefore appears a delicate matter to develop generally representative modelling.

The aim of the present study is to develop and validate a procedure to identify defects and provide systematic correction of the NC-Code program.

Having neutralised the inherent machine parameters, we chose a method to identify scattering in relation to the product being machined, based on certain interpolations and cutting conditions. The correction method used modifies the initial NC-Code program by inserting intervals and by calculating new movement co-ordinates before actual machining takes place.

1. Introduction

In a previous study, we saw how to highlight those machine characteristics likely to lead to lack of precision [1] and how to derive a simplified experimental model [2]. Obtaining reliable results meant we had to use a method that neutralised the grouping of tool, workpiece and machining assembly parameters. However, these factors cannot be neglected, especially where components subject to deformation are concerned (tool flexion, assembly rigidity, etc.)

We now need to quantify scattering according to the type of interpolation and the machining context. We therefore propose to draw up a breakdown of a complex machining process into sufficiently basic machining tasks for us to be able to quantify defects and assign them to a precise working configuration. All the data gathered will

then enable us to construct an overall correction strategy for the type of machining concerned.

2. Choice of basic machining processes

Choosing the machining process and classification into analogous groups is directly related to the goal to be attained ([3],[4]). Drawing on knowledge of the various existing methods, we can make a complete list of all the possible machining processes on a 4-axis machining centre.

Family	Product	Precision
Surface grinding	Spur, simple surface, recesses	Z
Surface grinding and form milling	Shoulders, recesses	X or Y and Z
2-sided surface grinding and form milling	Grooves, recesses	X or Y and Z
Surface grinding and contour milling	Complex shoulders, recesses	X or Y and Z
2-sided surface grinding and contour milling	Complex grooves, recesses	X or Y and Z
Form milling	Side milled surface	X or Y
2-sided form milling	Open grooves	X or Y
Contour milling	Complex side milled surfaces	X or Y
2-sided contour milling	Shallow complex grooves	X or Y
Point to point	Drilling, tapping, etc.	X or Y

TABLE 1. Machining families

Linear 1-axis (X, Y, Z or B) $\Leftrightarrow 2 \times 4$ possibilities
Linear 2-axis simultaneous $\Leftrightarrow 4 \times 6$ possibilities
Linear 3-axis simultaneous $\Leftrightarrow 8 \times 4$ possibilities
Linear 4-axis simultaneous $\Leftrightarrow 16 \times 1$ possibilities
Circular XY $\Leftrightarrow 4$ possibilities
Circular XZ $\Leftrightarrow 4$ possibilities
Circular YZ $\Leftrightarrow 4$ possibilities

Cut depth
Feed
Cutting speed
Machined width
Material resistance
Up or down milling
Cutting force direction

TABLE 2. Various cases of interpolation and the machining context

Assuming we use a 2-cut side and face shell end mill, this list can be broken down into 7 machining families each corresponding to an elementary case and to the axis constrained by the level of precision. (TABLE 1).

For each case of machining, we shall have several possibilities for interpolation together with a clearly defined machining context (TABLE 2).

3. Studying a machining family

Our aim is to show the method's feasibility on a significant case and the approach to be applied generally. Combined 2-sided surface grinding and contour milling seems to be

the case that contributes most information and is likely to be most fruitful for future application to the various families. In particular, we can machine a groove to obtain results on the X, Y and Z axes.

However, our study will mainly concern the X and Y axes. For significant tool flexion (low radius, large machining depth), scattering over these axes will be predominant.

3.1. EXPERIMENTAL IMPLEMENTATION

The first test workpiece (FIGURE 1) comprised different linear interpolations translating all cases of linear grooves. Machining a reference surface on X, Y and Z with a ϕ 63 milling cutter assumed to be free from the effect of distortion meant we did not have to worry about tool gauge measurement and part datum shift errors. The measurements were performed on 3DMM and with a comparator assembled on the spindle.

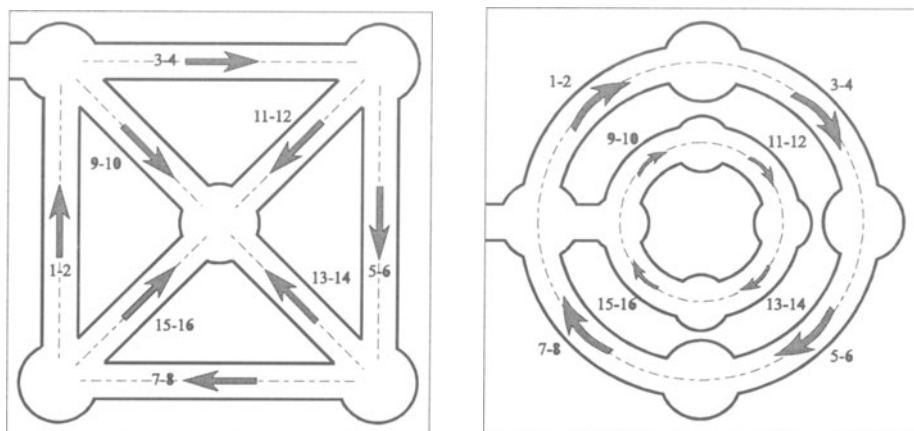


FIGURE 1. Workpieces for linear and circular interpolations

Two similar workpieces (same working conditions) can be used to study circular (anti-trigonometric: FIGURE 1 and trigonometric) interpolations.

To determine the influence of the machining direction and the interpolation radius, we worked in the four quadrants machining two different radius (40 and 20 mm).

We were then able to quantify the influence of cutting conditions :

- either by repeating previous work in different machining contexts
- or by analysing the effect of these conditions on elementary cases then extrapolating the results

Although the second option increased the risk of erroneous interpretation, it was perfectly suited to well defined zones where the behaviour of the grooves remained constant during interpolation.

3.2. RESULTS OF THE GROOVE CASE

A measurement strategy is essential for reliable interpretation. We first sensed the reference surfaces to construct the workpiece reference framework and then sensed the points on one side of the groove. We kept the measurement depth constant so that tool flexion did not lead to additional errors.

We then applied the least squares method to compare the position of the test surfaces with the reference surfaces so as to deduce the scattering corresponding to the machined workpieces.

We also used the comparator on the spindle to check these calculations.

TABLE 3 shows the condensed experimental results with coefficients ΔA , ΔB , ΔI , ΔJ and ΔR for equations :

$$Y = (A + \Delta A).X + (B + \Delta B) \text{ and } (X - (I + \Delta I))^2 + (Y - (J + \Delta J))^2 = (R_{\text{initial}} + \Delta R)^2$$

N° Surface	Linear		Circular Anti-trigonometric			Circular Trigonometric		
	ΔA (degree)	ΔB (mm)	ΔI (mm)	ΔJ (mm)	ΔR (mm)	ΔI (mm)	ΔJ (mm)	ΔR (mm)
1-2	-0.004	-0.085	0.017	-0.033	0.110	-0.028	0.063	-0.124
3-4	-0.005	0.072	0.044	0.070	0.023	-0.006	0.011	-0.113
5-6	0.001	0.094	-0.033	0.037	0.110	0.037	-0.068	-0.148
7-8	-0.003	-0.096	-0.028	-0.042	0.051	0.038	0.045	-0.056
9-10	-45.013	0.182	0.012	-0.036	0.107	-0.018	0.044	-0.102
11-12	45.006	-0.128	0.034	0.063	0.040	-0.026	-0.030	-0.066
13-14	-45.003	-0.143	-0.043	0.059	0.127	-0.016	-0.016	-0.081
15-16	44.999	0.077	-0.069	-0.102	-0.020	0.025	0.042	-0.070

TABLE 3. Groove case results for each kind of interpolation

It is difficult to find a correlation between the different linear and circular cases. Behaviour patterns are extremely varied and the least squares method applied to the circle will render responses on centre or radius offsets irregular. Use of a modelling approach thus remains of limited relevance. Analysis of TABLE 3 and FIGURE 2 show that :

- ΔA orientation defects on linear interpolations are extremely and can be considered to be negligible. We can observe scattering that is noticeably constant around 0.1 mm (ΔB), this being appropriate to tool flexion in these work conditions.
- Cutting conditions FIGURE 2 have a number of specific influences : increase in feed causes an amplification of scattering only in the case of a machined width equal to the tool diameter. This scattering is also dependent on the cut depth d and the machined width w , but to a less significant extent.
- Up milling leads to defects opposed to those previously mentioned. This appears to be normal as the cutting loads change direction.

- However, we shall obtain stable results regardless of the other factors, with scattering close to -0.02 mm.

All experiments on the groove family were performed with a cut depth of 4 mm, working fully within the material and with feed of $F = 0.05$ mm/tooth, providing elementary scattering of 0.05 mm for our model.

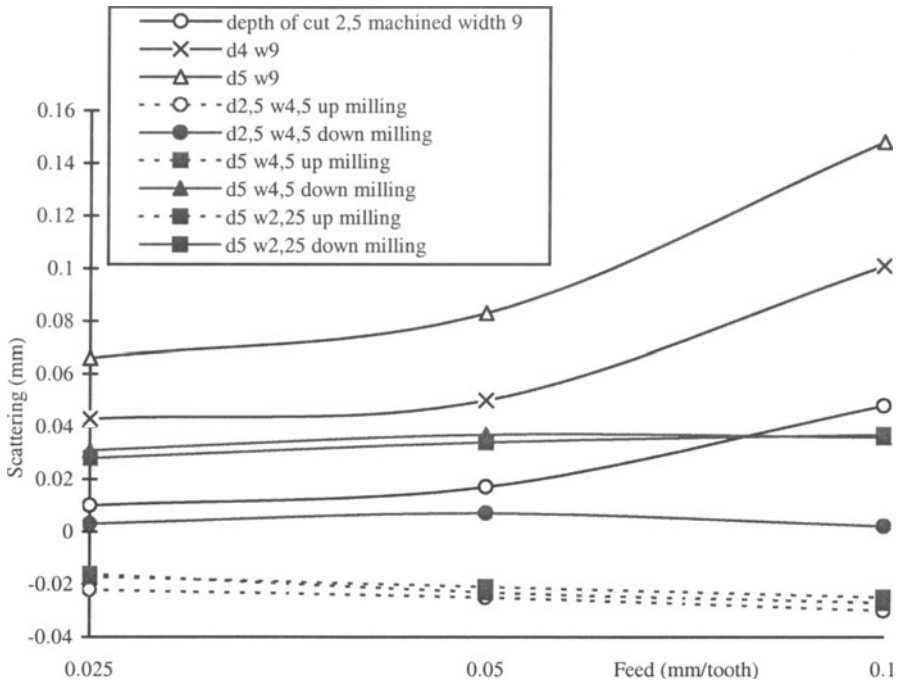


FIGURE 2. Influence of cutting conditions on a groove

Using these results will only remain valid within experimental limits.

3.3. CORRECTIONS TO BE CONSIDERED

Using this data bank on scattering for the case of grooves to draw up a behavioural law proves to be difficult. We can, nevertheless, try to find a correction method that integrates experimental values to the greatest extent possible.

We can assume that an extremely small movement will not modify our results [5]. Indeed, the defects measured (≈ 0.1 mm) are negligible compared with the tool diameter. Resetting the tool positioning cannot therefore change the behaviour of machining. We can then apply a mirror type correction (offset by a value opposed to the defect).

The examples in TABLE 4 show the results of a correction limited to coefficients B, I and J. For a circular interpolation, defect ΔR is carried over onto ΔI and ΔJ . Maximum defects are now of the order of 0.02 to 0.03 mm. Gain thus exceeds 50 % and residual values are due to random scattering of the machine, tool, workpiece and machining assembly. When performing a complete intervention on coefficients I, J and R, accuracy of the correction appears to be equivalent to the previous results.

N° of machined surface	Linear	Circular Anti-trigonometric			ΔI only	ΔJ only
	ΔB (mm)	ΔI (mm)	ΔJ (mm)	ΔR (mm)		
1-2	0.024	0.123	-0.142	0.110	0.013	-0.031
3-4	0.000	0.011	-0.010	0.003	0.014	-0.007
5-6	0.016	-0.088	0.118	0.110	0.022	0.008
7-8	-0.016	0.056	0.023	0.037	0.019	-0.014
9-10	-0.013	0.137	-0.136	0.115	0.022	-0.021
11-12	-0.029	-0.014	-0.041	0.035	0.021	-0.006
13-14	0.007	-0.084	0.114	0.102	0.018	0.013
15-16	-0.024	-0.002	-0.039	-0.022	0.020	-0.017

TABLE 4. Rectified results for grooves– limited intervention

4. Correction

Overall and systematic experimentation on different machining families would be cumbersome. The creation of standard workpieces integrating several families in a number of work conditions is needed to reduce experimentation time [6].

The problem posed by the influence of cutting conditions is complex, as the relation between cutting loads and the scattering measured appears to be difficult to model. This suggests to us the following reasoning: overall correction can either use all experimental results or be limited to a certain number of results only. Correction and the desired level of precision will then depend on the machining considered..

Correction on the NC machine-tool is conducted in two stages :

- Reading and interpreting the NC-Code program
- Correction by intervening on programming codes

The experimental results appear in the form of offsets on X, Y and Z according to the different parameters. For cutting conditions, we can construct a relation between the levels and their effects, thus allowing either for modelling of the parameter values ([7],[8]) or extrapolation.

Three main types of corrections can thus be envisaged :

- Insertion of a constant offset before a programming block.

- Modification of interpolation values.
- Modification of cutting conditions [9].

The experimental design method applied to NC machine tool inherent parameters identifies scattering in relation to the machining configuration. The constant offset G59 is entirely appropriate in this case.

However, experimental results on machining families relate to each machine movement. We therefore need to bring interpolation co-ordinates into consideration, thus the need to modify the programmed lines.

Finally, the tool work conditions only require an offset along certain directions. The real difficulty lies merely in real time control over their effects and cyclical re-positioning.

The correction retained for linear and circular interpolations is the mirror method. For linear interpolation, the modifications made to the co-ordinates for the points of departure and arrival are identical and the offset is thus constant. For the groove family, we experimented linear interpolations along all combinations of the X and Y axes at 0°, 45° and 90° [10]. By cutting the XY plane into eight parts, we can extrapolate our experimental results.

Where circular interpolation does not remain solely in a quadrant, we shall need to proceed with a breakdown of the interpolation. There will thus be a discontinuity between the different corrected circular interpolations. We can deal with this discontinuity using linear interpolation which is adequate considering the maximum correction errors (0.03 mm). This will minimise the distance of the join and allow for simple programming (FIGURE 3).

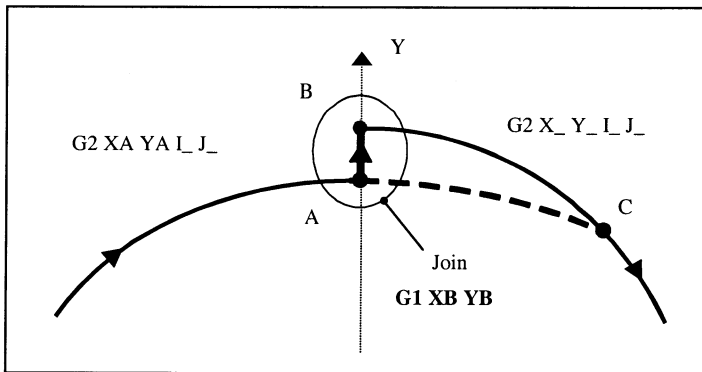


FIGURE 3. Circular interpolation join

5. Conclusion

ISO standardisation of the NC-Code program allows for the insertion of programmed offsets, additional lines and modification of movement co-ordinates subsequent to

reading and ensuring overall analysis of the syntax used.

This suggests that we can use our experimental results to ensure adequate machine characterisation to predict machining behaviour in contexts different from those tested. This means that we can model the machine within a field of validity using a data bank enriched with a minimum number of machining tasks only.

The large number of interventions in the program can readily be automated, meaning we can easily computerise the process. Obviously, the modelling methods adopted will reduce the need for material iteration of machined surfaces. But this has the advantage of simplifying the approach, whereas more accurate and complex correction is likely to hinder optimisation of scattering.

The reasoning put forward fits in with a defect reduction approach. However, corrections will depend on the machines concerned in addition to our results. Application of the strategy on a different machine will use the same procedure but the conclusions may be at variance. Taking dispersions due to changes in heat conditions of the machine into account is under way. In this, we shall apply the same experimental philosophy.

6. Bibliographical References

- [1] Dessein, G., Lagarrigue, P. and Rubio, W. (1996) Analyse des dispersions d'usinage liées aux configurations de centres d'usinage à commande numérique par une approche expérimentale, *IDMME'96*, Nantes, pp. 747.
- [2] Soulier, B. (1994) *Sur la modélisation expérimentale en mécanique : précision, optimisation et applications industrielles*, PhD Thesis, Ecole normale supérieure, Cachan, pp. 109.
- [3] De l'etang, C., Goutte, D., Vendeville, Y. (1975) Applications des groupements analogiques aux fabrications mécaniques, *CETIM 11/2*.
- [4] Groupe GAMA (1990) *La gamme automatique en usinage*, Hermes, Paris.
- [5] Seo, T., Hascoet, J.Y., Depince, P.H. and Furet, B. (1997) Compensation de trajectoires déformées d'usinage, *Colloque Primeca*, April, pp. 117.
- [6] Mery, B. (1997) *Machines à commande numérique*, Hermes, Paris, pp. 344.
- [7] Bouzakis, K.D., Efstathiou, K. and Paraskevopoulou, R. (1992) NC-Code preparation with optimum cutting conditions in 3 axis milling, *Annals of the CIRP 41/1*, pp. 513.
- [8] Takata, S., Tsai, M.D., Inui, M. and Sata, T. (1989) A cutting simulation system for machinability evaluation using a workpiece model, *Annals of the CIRP 38/1*, pp. 417-427.
- [9] Schulz, H. and Bimschas, K. (1993) Optimization of precision machining by simulation of the cutting process, *Annals of the CIRP 42/1*, pp. 55.
- [10] Dessein, G. (1997) *Qualification and optimising of the accuracy of numerically controlled machine-tool*, PhD Thesis, Université Paul Sabatier, Toulouse, pp. 109-133.

A RING-SHAPED MECHANICAL ASSEMBLY LINE OPTIMIZED BY A GENETIC ALGORITHM

Franck FONTANILI*, Arnault VINCENT*, Thierry SORIANO**
Raymond PONSONNET***

*GRPI IUT Cergy Dept OGP, 95 rue Valère Collas 95100 Argenteuil
fontanil@u-cergy.fr

**LIISI ISMCM-CESTI Toulon Maison des technologies 83000 Toulon
thierry.soriano@toulon.ismcm-cesti.fr

***GRPI IUT Place du 8 Mai 1945 St Denis 93000
ponsonet@iut-sd.univ-paris13.fr

Abstract

We seek to optimize a ring-shaped mechanical assembly line. Within a Just In Time context we wish to reduce the manufacturing lead time for a batch of pallets by specifying the best inter release time between two consecutive pallets. We have conducted experimental calculations combining a simulation model and a genetic algorithm. A simple case was chosen so the results thus obtained could be compared with those obtained from a closed form mathematical solution.

Résumé

Nous nous intéressons à l'optimisation d'une ligne flexible d'assemblage mécanique en anneau. Dans un contexte de production en juste à temps, nous cherchons à réduire le temps de production d'un lot de palettes en contrôlant en particulier le temps inter lancement de deux palettes consécutives. Nous avons expérimenté l'application de la combinaison d'un modèle de simulation et d'un algorithme génétique. Nous avons comparé les résultats avec la solution analytique pour un cas simple où elle peut être évaluée.

1. System under study and problems encountered

1.1. PRESENTATION OF THE CELL

Ring-shaped mechanical assembly lines provide both great flexibility and easy maintenance which today's machines and plans require. These lines have been studied by different authors with different points of view : either with respect to the decisional system level or their physical organization especially as regards the problems surrounding machine to machine transfer [FER.94] [MAN.97].

Our study is supported by an experimental plat-form constituted by six by-pass workstations situated along a ring-shaped pallet transfer line. A secondary line connected to the previous one is used for production preparation by loading batches of pallets off-line and unloading processed pallets (see figure 1) .

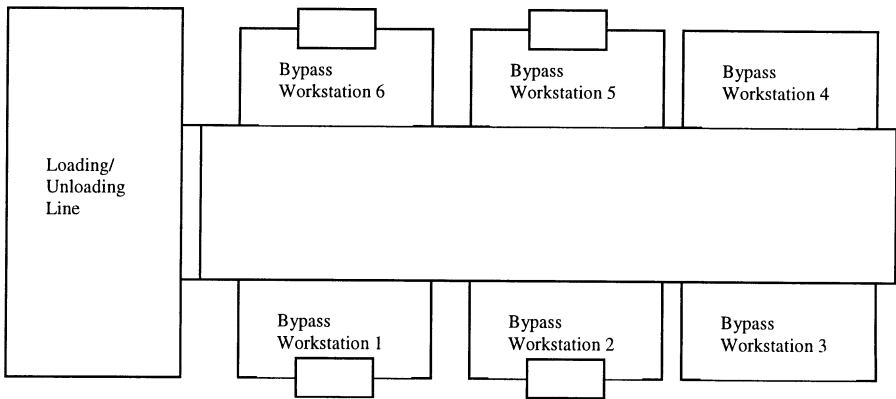


Figure 1: Scheme of the ring assembly line
 Schema de la ligne d'assemblage en anneau

1.2. HYPOTHESIS

We are operating within a Just In Time context for pallet batch production [PAR.96]. We seek to optimize a very short term line load. An important element needed to decide when production for a given batch must begin is knowledge of the time interval between the introduction of the first pallet and the exit of the final pallet from the line. We will call this time the Manufacturing Lead Time MLT and it will be an important variable for the system. The ring structure of the system does not allow an easy calculation of the number of revolutions a given pallet could execute. An approach is developed in [BRU.97] in which each pallet is an object, in the Object Oriented Approach sense. This object has communication and decision capacities so that it is able to set its own timetable with the workstations on the line and to calculate its exit date. For the moment, we adopt a simpler and more pragmatic approach where the decision level is at the line and the workstation, and not at the pallet which supports only attributes . Another hypothesis is that a batch is constituted of identical pallets.

I.3. OPTIMIZATION PARAMETERS

In accord with the foregoing treatment, the first criterion that we sought to optimize was the Manufacturing Lead Time MLT for a batch of pallets with a known size and assembly operating range.

The operating range is a constraint imposed by the product ; while the batch size is a function of the manufacturing order, having as an upper limit the maximum number of pallets that can be stocked in the waiting zone. These two given data provided constraints for our initial optimization.

The parameters whose variation does not entail any transformation in the assembly cell's physical layout can be used to decide short or medium term production schedules.

Such parameters are:

- The Inter Release Time IRT: launch interval between pallet departures for a batch of identically built products.
- The production-model limit for the stock upstream from a bypass workstation.
- The production-model limit for the stock downstream from a bypass workstation.
- The priority rules for entry onto the main line when leaving a workstation (six switches)

I.4. LIMITS ON EXHAUSTIVE CASE BY CASE ANALYSIS

If one were to consider a typical batch of 20 pallets with fixed operating times, fixed upstream stocks, fixed downstream stocks, and fixed priority rules, that is, if the Inter Release Time IRT was taken as the only parameter for optimization varying over a range of twenty values $\{1, \dots, 20\}$ for example, the resulting number of cases would be 20^{19} . Consequently, we must seek two types of tools :

- a means of reducing the length of on-line testing
- a means of reducing the number test cases

The first goal was achieved by performing massive simulations to assess the effects of changes in Manufacturing Lead Time MLT without any on-line testing.

The second goal was achieved through the use of methods borrowed from artificial intelligence such as genetic algorithms which both reduce the number of combinations to consider and display within a reasonable time limit solutions converging to some optimum value.

Other techniques, closely allied to artificial intelligence such as constraint programming are feasible as well; a kindred method was applied by Huguet [HUG.94] to a scheduling problem; however his method required that the system be described by a set of equalities and inequalities, which is not currently the case for our system. The genetic algorithm does not require models based on equalities or inequalities but merely

the updating of a numerical criterion which fits well with our simulation model.

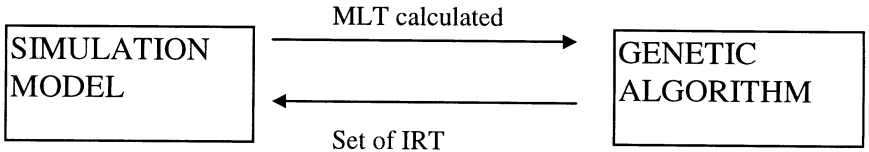


Figure 2: Our approach: a couple simulation - genetic algorithm
 Notre approche: un couple simulation - algorithme génétique

2. Using simulation and genetic algorithm

2.1. SIMULATION MODEL FOR THE CELL

Our model was written in the simulation language Witness. It provides a truly formalized graphic language which combines major ergonomic features and a powerful programming language. The cell model, once developed, was both perfected and confirmed by a variety of comparisons between those Manufacturing Lead Time MLT measured on the experimental production cell and those obtained by simulation.

At present, the relative error has been brought to below five percent. The simulation model could be undergo further improvement by introducing a random variable in the operating time parameters.

2.2. THE GENETIC ALGORITHM

Based on the work of Renders [REN.95], this algorithm is quite complex but a simplified presentation of the structure is that follows:

1. Random creation of a population of individuals: each individual has a gene
2. Calculation of the objective function for each individual
3. Selection of the two individuals having the best objective function
4. Reproduction: Using a subset of the gene of each parent
5. Evaluation of the new population; back to step 2

It offers the possibility of separating the gene into two subsets :

- One subset is linked to the idea of the individual classically found in this type of algorithm
- Another linked to the algorithm itself and independent from the individuals

A gene contains either numerical or Boolean numbers; reproduction between two individuals results by taking a subset from each parent's gene.

The program embodying the algorithm has a declarative structure which can evolve as well as a kernel with recursive behavior.

The declarative features adds greater versatility; once a new function is specified and coded; the user can give it a new gene which increases the genealogical possibilities. For example, the probability of a cross between two individuals who have been selected according to a survival constraint, or even the mutation rate of a given individual, are coded in the form of the gene which can be easily modified.

From the user's point of view, there exists a crucial feature that allows the extraction of a specific population whose members will either reproduce or mutate ; we can specify a criterion, in the present case the Manufacturing Lead Time MLT, which steadily decreases from generation to generation.

A partial confirmation of the algorithm was performed in simple cases for which the absolute optimum could be analytically calculated. One of them will be presented later in this text. The results thereby obtained correspond to the calculated results; however a major study concerns the convergence speed with respect to the initial random values as well as the algorithms ability to escape form local optimums.

3. Experimentation

3.1. THE CASE CHOSEN

Suppose that we want to produce a batch of $N = 25$ pallets, having the same assembly range which is:

$[P_1^9 , P_2^{12} , P_5^8 , P_6^6]$ where P_i^j is the operation on workstation i during the operation time $OT = j$ seconds. We have included in OT everything that is performed between the entrance shunt and the output shunt of the workstation

We denote by Inter Release Time IRT the time interval from the release of one pallet to the release of the next.

3.2. ANALYTICAL SOLUTION FOR A THEORETICAL MINIMUM MLT

The smallest value for the Manufacturing Lead Time MLT is obtained when no pallet spends time in a waiting cycle on the ring and enters each workstation when required conforming to the assembly range. However such a situation is purely ideal.

We can see that the first pallet will not spend time in a waiting cycle because every workstation is initially free. We will call T_d (Time of delivery) the time necessary for merely one pallet. It corresponds to MLT for a batch consisting of one pallet.

For a multi-pallet batch we suppose that there will be cycles for some pallets.

We will focus on bottleneck on the ring line as developed in the OPT approach [FOX.82].

Consider the workstation having the longest operation time OT . Let's call OT_g the operation time for this workstation.

According to the fact that every pallet must pass through this workstation, we can say that the MLT for the (N-1) pallets following the first one is greater than the value of (N-1) x Tg. This value is encountered when the bottleneck is always running. It is obtained when each pallet is released after the previous one with a Inter Release Time IRT equal to the greatest operation time Tg.

Therefore, we obtain for this particular ideal case the numerical relationship:

$$MLT = T_d + (N-1) \times T_g$$

The numerical application for the above case is as follows:

T_d depends on operation times and transfer times on the ring line, which we have measured ; T_d = 187 s

$$N = 25$$

T_g is the Operation Time OT of the second workstation : T_g = 12 s . According to the condition required , the Inter Release Time IRT equals T_g . It is a constant.

With these numerical values we obtain MLT = 475 sec

3.3. RESULTS WITH THE COUPLE SIMULATION – GENETIC ALGORITHM

We choose a gene constituted of the 24 IRT for the batch of 25 pallets. All the initially numerical values were identical but could become different from one generation to the next .

We used a population of 8 individuals; this value was not derived from the application but rather from calculating time considerations. The reasons for such a choice must be more fully examined in the future research.

The objective function was the Manufacturing Lead Time MLT. Each new generation of individuals had to reduce the value of this function to be able to be parents.

The following graph (figure 3) displays the evolution of the MLT when the number of generations is limited to 50. The application took 15 minutes to perform the calculation. The results showed that the MLT, initially evaluated at 555 seconds dropped to 479 seconds after 50 generations.

The final result was obtained with the gene:

12-11-9-6-1-12-4-6-4-4-18-3-9-11-5-1-6-15-3-8-3-10-2-15

This result is very close to the minimal value calculated analytically (about 1%) .

We can see that this gene has a form vastly different from the gene which gives the minimal value by analytical calculation (12 – 12-12)



Figure 3: Manufacturing Lead Time MLT function of number of generations
Temps de production d'un lot en fonction du nombre de générations

3.4. EXPERIMENTAL FEATURES

Current experiments use the simulation application Witness communicating through OLE links on Windows with the genetic application written in DELPHI on a PC with a 166 MHz pentium processor. The latter's performance may provide an inadequate number of necessary iterations over a very short time span. Therefore a distributed version is under study. The presence of efficient interapplication communication norms greatly facilitated our experimental study.

4. Conclusions

We have described an optimization method for a ring assembly line which has provided promising results. The method is based on the combined use of a genetic algorithm and a simulation which has proved both rapid and precise.

The use of genetic algorithms in optimization problems offers attractive possibilities but raises several fundamental questions. The lack of a formal language or a graph-language in the genetic algorithm renders the results more conceptually difficult to explain.

This application uses one genetic algorithm but there are multiple variations on this with more elaborate evolution rules , using emergent phenomena observed in insects, which provide a swifter convergence towards good solutions. The flexibility of genetic algorithms makes also possible to add to our system some particular constraints; for example inequalities between variables, special functions and so on without limiting calculating speed.

The satisfying results of the approach in the case presented constitute validation elements. We will try it now for cases with no analytical solutions.

Our future research on application of genetic algorithms to production systems will have to take into account unexpected events such as machine failures or conveyor delays. In this case the solution delivered should not only be a good solution but also a robust solution and thus easily implemented in industrial systems.

5. References

- [BRU.97] D. BRUN-PICARD « *The product as an active element of distributed production control* » proceedings of IFAC-IFIP CIS 97 Belfort (France) 1997
- [FER.94] M.FERRARINI « *Contribution à l'étude et à la mise en oeuvre de la décentralisation de la décision pour la commande de systèmes flexibles de fabrication* » Thèse de doctorat Université d'Aix-Marseille III (France) 1994
- [FOX.82] R.E. FOX « *OPT: An answer for America* » Part II Inventories and production magazine 2(6) (USA) 1982
- [HUG.94] M. HUGUET « *Approche par contraintes pour la l'aide à la décision et à la coopération en gestion de production* » Thèse de doctorat INSA Toulouse (France) 1994
- [MAN.97] H. MANIER, P. BAPTISTE « *How to improve the productivity of a reactive method of control for a flexible manufacturing ring* » proceedings of IFAC-IFIP CIS 97 Belfort (France) 1997
- [PAR.96] J.L. PARIS, H. PIERREVAL , L. TAUTOU « *Une méthode d'optimisation-simulation par algorithme évolutionniste en gestion de production juste à temps* » Jesa vol 30, N°7 Hermès Paris (France) 1996
- [REN.95] M. RENDERS « *Algorithmes génétiques* » Hermès Paris (France) 1995

SIDE MILLING OF RULED SURFACES - OPTIMUM TOOL RADIUS DETERMINATION AND MILLING CUTTER POSITIONING

J.-M REDONNET, G. DESSEIN, W. RUBIO, P. LAGARRIGUE
Laboratoire de Génie Mécanique de Toulouse
Université Paul Sabatier - Filière Génie Mécanique - Bât. 3PN
118, rte de Narbonne 31062 Toulouse Cedex – France
e-mail : jmax.redonnet@gmm.insa-tlse.fr

Abstract

Side milling is a process that enables machining time, and thus costs, to be reduced. This type of machining is particularly well suited to ruled surfaces and all surfaces one of whose main curvatures is very small before the tool's radius, and subject to only minor change over the surface. These surfaces must be treated with great care, as they often concern parts with high value added such as helicoid parts as used in fluid dynamics. We then need to calculate and minimise interference that may arise if the ruled surface cannot be developed. Whereas machining is mostly carried out by setting the tool according to the rule, we suggest a new setting of the tool allowing interference to be reduced considerably. The computation algorithms for tool setting and determination of the optimal tool radius were developed so as to be used in real time by CAD/CAM software.

1. Introduction

Side milling has been less frequently addressed by researchers than tip milling (see [2], [5]). But it may be very useful, especially for ruled surfaces.

We shall first briefly recapitulate the principle for ruled surfaces and settings that are currently adopted in existing CAD/CAM software before going on to introduce a new setting for the tool, allowing interference to be reduced considerably. The third section of this paper is devoted to the presentation of two algorithms. The first allows the optimal tool radius for machining of a given ruled surface to be determined and the second allows all the tool positions for this surface to be determined.

1.1. « STANDARD » POSITIONING

A ruled surface (Fig.2) is generated by a set of straight lines based on two driving curves : the directrices $C_0(u)$ and $C_1(u)$.

The equation corresponding to this ruled surface is

$$S(u,v) = (1-v)C_0(u) + v C_1(u) \quad (u,v) \in [0,1]^2$$

With "standard" positioning the tool's axis is colinear with the rule under consideration. The tool can then be placed at a tangent to one of the two directrices (Fig. 1a) or so as to distribute the error between its two extremities (solution proposed in [10] – Fig. 1b).

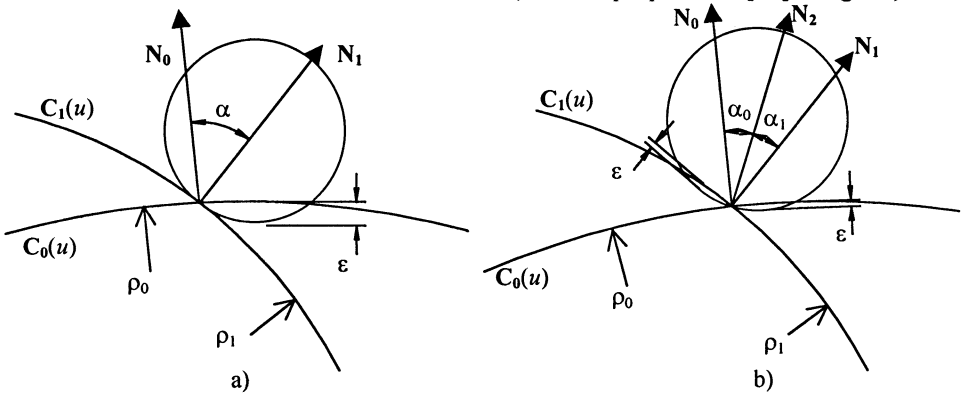


Figure 1 : Standard tool positioning

According to Rubio [10], we then obtain in case of a) :

$$\epsilon = \rho_1 + R - \sqrt{R^2 + \rho_1^2 + 2R\rho_1 \cos(\alpha)}$$

in case of b) :

$$\epsilon = \rho_0 + R - \sqrt{R^2 + \rho_0^2 + 2R\rho_0 \cos(\alpha_0)} = \rho_1 + R - \sqrt{R^2 + \rho_1^2 + 2R\rho_1 \cos(\alpha_1)}$$

These equations can be used to determine the radius R needed to respect a given tolerance. In the case of infinite curvature radii (straight directrices), error calculation for standard setting will give (see [6]):

in case of a) : $\epsilon = R(1 - \cos(\alpha))$

in case of b) : $\epsilon = R(1 - \cos(\alpha_0))$

2. Optimum Positioning

2.1. PRESENTATION

The setting we suggest is the fruit of a trade-off between two contradictory objectives : reducing interference by a more complex tool setting that is therefore longer to calculate than standard setting and the need to be able to calculate this setting rapidly enough to enable real time utilisation in CAD/CAM type software. This optimum setting as described in Fig. 2 is based on 3 tangential points :

- tangency of the tool lower generating line to the rule (P_0P_1) : point M_2
- tangency to the two directrices $C_0(u)$ and $C_1(u)$ on both sides of the extreme points of the rule : points M_0 et M_1 .

Taking into consideration a rotation of γ allowing passage from standard setting to optimum setting, the tool position could be completely defined by the angle γ between

the tool's axis and the rule and the axis of this rotation going through point M_2 of the rule P_0P_1 . Marciniak first proposed that the tool be shifted along the rule (see [7]).

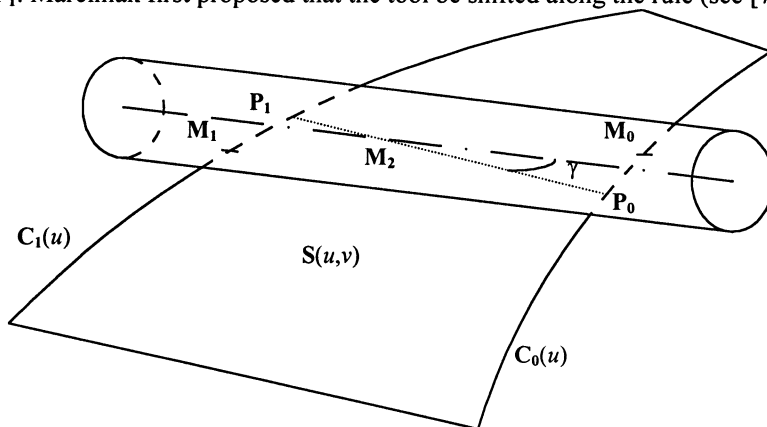


Figure 2 : Optimum positioning

Liu, in [6], presents a method based on two offset points (the Double Point Offset method) also introducing an angle between the rule and the tool's axis.

2.2. DETERMINING SETTING PARAMETERS

One could refer to [9] for detailed description of setting parameters determination. Let y_2 be the rotation axis allowing the passage from standard setting to optimum setting, y_2 being defined as the vector N_2 of Fig. 1b) with $\alpha_0 = \alpha_1$ (see Fig. 3).

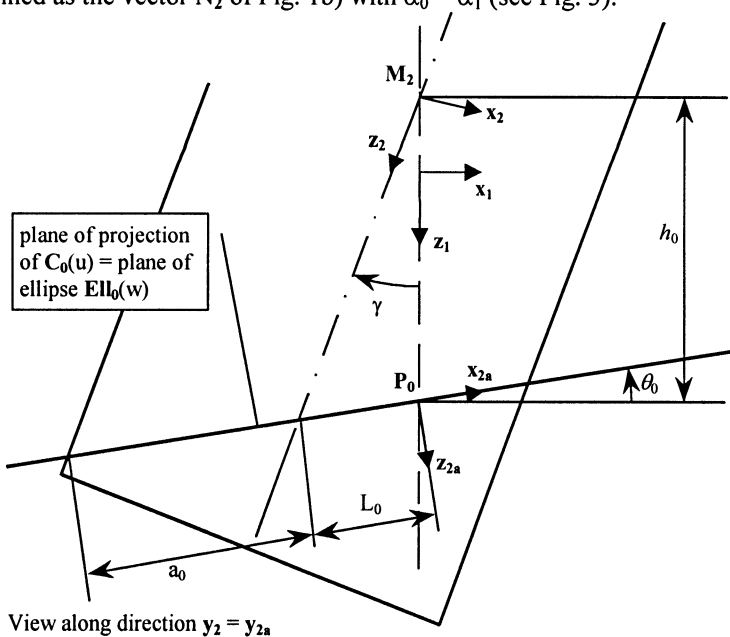


Figure 3 : Definition of references

We take into consideration the ellipse $Ell_0(w)$ defined as the intersection of the tool and the plane (P_0, x_{2a}, y_{2a}) ; itself defined by y_2 and the tangent line to $C_0(u)$ going through P_0 (see Fig. 4). At the tangent point M_0 (see Fig. 2), the intersection of $C_0(u)$ and $Ell_0(w)$ is translated by $C_0(u_0) = Ell_0(w_0)$, whence we deduce two significant equations by projection onto the reference R_{2a} . The tangency condition between the tool and directrix $C_0(u)$ is translated by the unicity of this intersection. By defining $\tan Ell_0(w)$ as the vector tangent to ellipse $Ell_0(w)$, we can express this tangency condition by the fact that $\tan Ell_0(w_0)$ and $C_0(u_0)$ have the same slope in the reference R_{2a} (see Fig. 4). Thus at both sides of the rule, we can determine two equations translating intersection between the ellipse and the rule and one equation translating the tangency condition at this point. Further, if we posit h_p the length of the rule, by postulating $h_1 = d(P_1, M_2)$ and $h_0 = d(P_0, M_2)$, we shall obtain $h_0 + h_1 = h_p$.

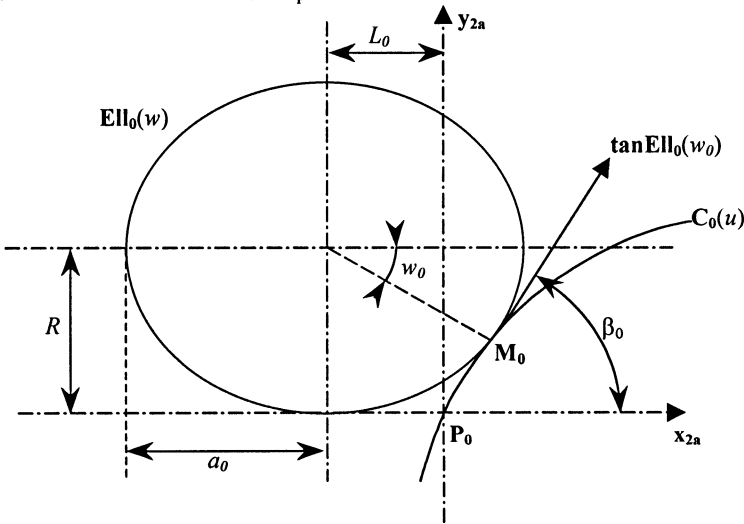


Figure 4 : Ellipse Ell_0

Whence a system of 7 equations with 7 unknown values ($u_0, u_1, w_0, w_1, h_0, h_1$ et γ) that can be resolved numerically in a sufficiently short time.

2.3. RESULTS AND ANALYSIS

One could refer to [9] for more detailed analysis of results provided by optimum setting. As the setting parameters calculation could not be carried out analytically, the calculation of error machined for a given positioning should be performed numerically. A dichotomial algorithm with variation in the two parametric directions will be adopted as the resolution algorithm. For example, we present in this section a comparative study of errors for any ruled surface defined by :

$$S(u, v) = \begin{cases} 30u^2 + 10u + 30 + 20vu^2 - 10vu - 10v \\ 100\sqrt{u} - 50 - 100v\sqrt{u} + 90v - 60v\sin\left(\frac{1}{2}\pi u\right) \\ 70 - 30u^2 - 130v + 50vu^2 \end{cases} \quad (u, v) \in [0, 1]^2$$

This surface is shown on Fig. 5.

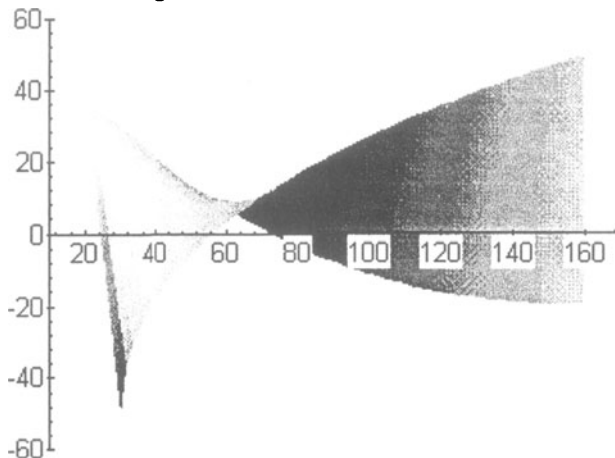


Figure 5: Ruled surface

For this surface, comparison of machined errors using each positioning is presented in Fig. 6. It would appear that the positioning we suggest allows for considerable reduction in interference error. Quantitatively this improvement could be evaluated by a ratio of at least 1 to 10. Further, for the lowest performance ratio obtained, the gain is greater from a quantitative point of view. We can observe qualitatively similar curve shapes.

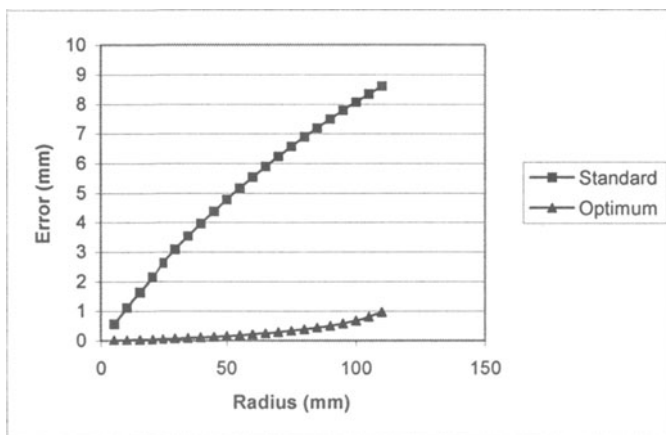
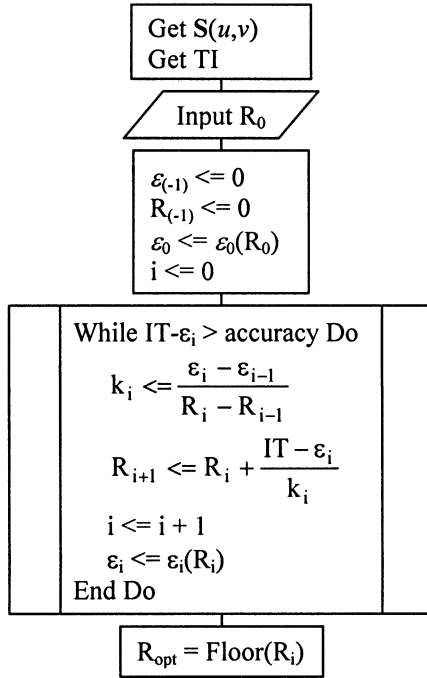


Figure 6 : Error curves for a ruled surfaces

3. Machining Algorithms

3.1. OPTIMUM TOOL RADIUS

From the optimum positioning described in section 2, we shall determine the optimum tool radius for machining a given surface respecting a given tolerance.



Algorithm 1 : Determination of optimum tool radius

The tool radius sought for should be as great as possible to reduce machining time but should remain small enough to respect tolerance which is expressed as $S(u, v)_0^{+IT}$.

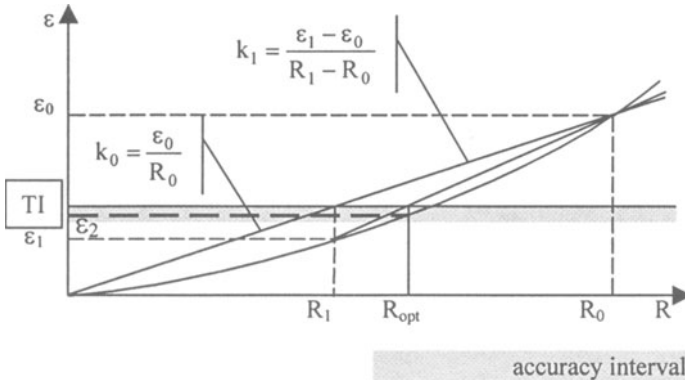
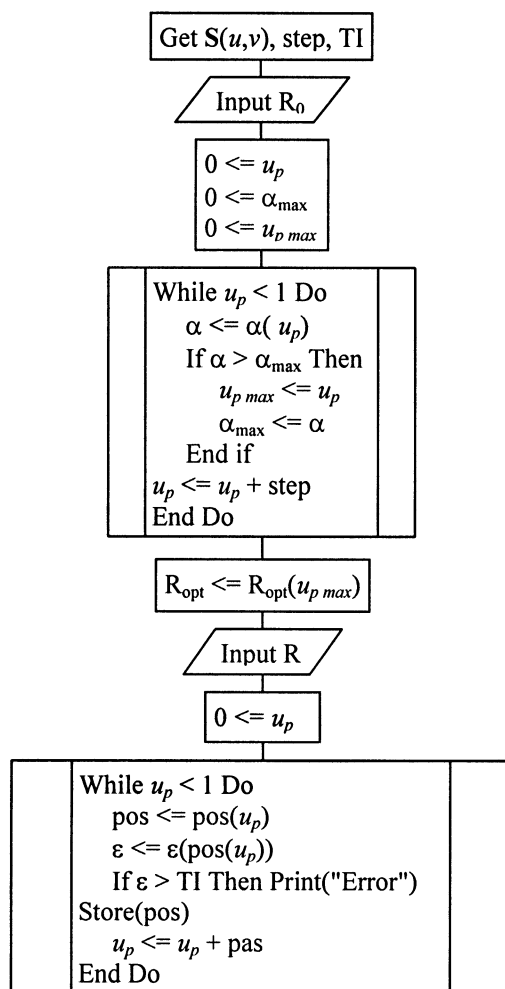


Figure 7 : Determination of R_{opt}

From the input of the initial radius R_0 , this algorithm allows optimum tool radius to be determined with a minimum number of iterations (see Fig.7). Taking into consideration the shape of the error curve in relation to radius (see Fig. 6), the optimum tool radius obtained will always be lower than the theoretical tool radius.

3.2. MILLING THE ENTIRE SURFACE

Algorithm 1 allows the optimum tool radius to be determined for a given configuration, i.e. for a given value of parameter u which shall be called u_p . To be able to determine the optimum tool radius for the entire surface, this algorithm should be applied to each value of u , then the lowest value for results should be chosen : $R_{opt}^S = \min(R_{opt}^{u_p})$.



Algorithm 2 : Tool positioning calculation for the entire surface

However, this systematic method increases calculation time dramatically. We therefore chose to develop an indicator allowing us to make an initial estimate of the position u_p for which error will be at maximum. Main parameters having an influence on error are : the tool radius R , the angle α (see Fig. 1a) and h_p , but experience shows that α has the greatest influence. This parameter will therefore provide our indicator to determine the value for u for which calculation should be carried out. Although it does not give us

exactly the location at which error will be maximum, this indicator will be accurate enough considering the various reductions applied subsequently to the value obtained. Indeed, algorithm 1 provides a value for the optimum tool radius that is lower than the permitted theoretical value. Further, in practice, the machining process will be carried out using a tool whose radius will be the first available. In the algorithm 2, the set of positioning values for the tool in relation to the surface for a given value $u = u_p$ is called $\text{pos}(u_p)$ and the error for this position is called $\varepsilon(\text{pos}(u_p))$. Further a tolerance verification loop has been included. This algorithm thus enables us to calculate all the positioning parameters for all the values of u .

4. Conclusion

For side milling of ruled surfaces, this study allows calculation of successive positionings of the milling cutter and interferences with the surface. Calculation is carried out rapidly enough to enable real time utilisation in CAD/CAM type software. This positioning considerably reduces machined error and furthermore preserves directrices of the ruled surface. That is very useful for piecewise ruled surface approximation of any free-form surface (see [3]) in order to preserve joins and make finishing operations (polishing sequence) easier. Study variations in error in relation to tool radius shows that such error increases concomitantly. This fact enables us to adopt an algorithm that converges systematically and rapidly towards the optimum tool radius. Considerable savings in calculation time are thus made through establishing an indicator to estimate the position of the the tool where error will be at its maximum.

References

1. CARMO, D. : *Differential Geometry of Curves and Surfaces*, Prentice-Hall, 1976.
2. CHOI, B.K., PARK, J.W., and JUN, C.S. : Cutter-location data optimization in 5-axis surface machining, *Computer Aided Design*, **25** (1993), pp. 377-386.
3. ELBER, G., and RUSS, F. : 5 Axis free-form surface milling using piecewise ruled surface approximation, *ASME Journal of Manufacturing Science and Engineering*, **119** (1997), pp. 383-387.
4. FAUX, I.D., and PRATT, M.J. : *Computational Geometry for Design and Manufacture*, Ellis Horwood Ltd, 1985.
5. LEE, Y.S. : Admissible tool orientation control of gouging avoidance for 5-axis complex surface machining, **29** (1997), pp. 507-521.
6. LIU, X.-W. : Five-axis NC cylindrical milling of sculptured surfaces, *Computer-Aided Design*, **27** (1995), pp. 887-894.
7. MARCINIAK, K. : *Geometric Modelling for Numerically Controlled Machining*, Oxford University Press, 1991, pp. 233,234.
8. QIULIN, D., and DAVIES, B.J. : *Surface Engineering Geometry for Computer Aided Design and Manufacture*, Ellis Horwood Ltd, 1987.
9. REDONNET, J.M., RUBIO, W., and DESSEIN, G. : Side milling of ruled surfaces - Optimum positioning of the milling cutter and calculation of interference, *The International Journal of Advanced Manufacturing Technology*, **14** (1998), 459-465.
10. RUBIO, W., LAGARRIGUE, P., DESSEIN, G., and PASTOR, F. : Calculation of Tool Paths for a Torus Mill on Free-Form Surfaces Five-Axis Machines with Detection and Elimination of Interference, *The International Journal of Advanced Manufacturing Technology*, **14** (1998), 13-20.
11. RUBIO, W. : "Génération de trajectoires du centre de l'outil pour l'usinage de surfaces complexes sur machines à trois et cinq axes" (*Generation of cutter location paths for machining of complex surfaces for three- and five-axis machines*), PhD thesis presented at *University of Toulouse III, France*, 1993.

OPTIMISATION OF END-MILL ROUGHING OPERATION SEQUENCE

F. VILLENEUVE

*LURPA -University Laboratory in Automated Production Research
ENS Cachan, 61 avenue du Président Wilson, 94235 Cachan Cedex
Tel : 33 (0)1 47 40 22 21 Fax : 33 (0)1 47 40 22 20
email : villeneuve@lurpa.ens-cachan.fr*

Abstract. The aim of this work is the optimisation of end-mill roughing operation sequences on "open-slot" machining features. Some experiments have been carried out to highlight the limits of the process. Cutting data and limits of usage are modelled on the basis of the experiments and the industrial data. An optimised choice under end-milling constraints and their cutting data is then proposed. A computer model using the optimisation algorithm is presented.

Key words. CAPP, Process Ascending Generation (PAG), Optimisation under constraints, milling, Open-slot machining feature.

1. Introduction

This article aims at analysing and then generating an optimised choice for end-milling processes for the roughing of open-slot machining features. It is part of the works which for two years have been carried out, whose first target was roughing operations under circular interpolation conditions for hole machining features (Villeneuve, 1996 and Muller, 1997). We are here using the concept of Process Ascending Generation (PAG) (Villeneuve, 1990). The finished state of the machining feature is thus known. An end-mill whose diameter and length will be compatible with this feature is then searched for, as well as a radial cutting depth to generate the former state of the feature described. An optimisation function allows to better target the choice. Thanks to the quality of the feature, roughing end-milling can be used

Most works carried out on the notion of choice of tools focus either on geometrical analyses as in pocketing (Lee *et al.*, 1994), giving little importance to the actual technological criteria of the use of the tools and essentially to the cutting data, or on optimisation algorithms of the cutting data (wear modelling) sometimes associated with the choice of the tools mostly in the field of turning (Anselmetti, 1994). We wish to combine both these preoccupations into a more global approach that will use "realistic" data.

The issue is as follows: to machine a volume of a workpiece known, what are the milling tool(s) (Do), the axial and radial cutting depths, the cutting data (V_c , f_z) that fit the work while respecting maximum flow criteria (i.e. minimum machining time). A series of experiments will first be described. It aims at validating the hypotheses and confirm the data given by the world of industry. A modelling of the cutting data is then

proposed as well as an analysis of the limits of use. This modelling includes varied constraints that will act on the tool. An optimised choice under constraints of end-milling and their cutting data is then proposed. A computer model using an optimisation algorithm under constraints is used to validate it.

2. Experiments

2.1. OBJECTIVE

The experiments herein proposed aim at observing the general behaviour of the machining on open slot features.

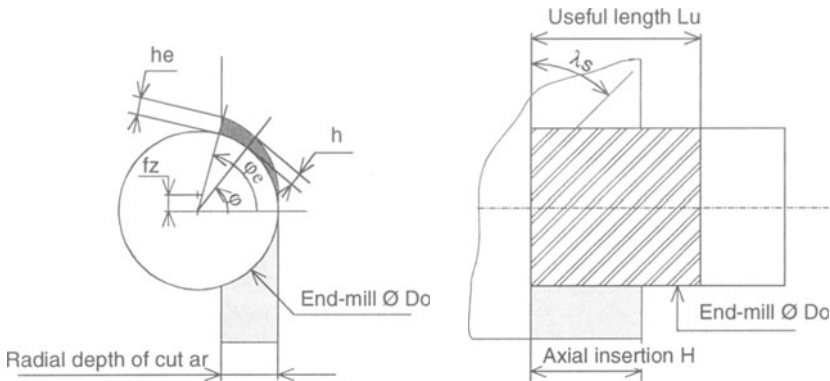


Figure 1. Linear end-milling parameters

We have characterised this general behaviour by the observation of the chips obtained and of the vibrations during machining as well as by the state of the end-mills after machining. This study was completed by the analysis of the features realised according to the following criteria : surface geometry, dimensions, surface finish. This stage of experimentation also allows to validate the cutting data proposed at the Citroen factory in Meudon (cf following chapter on modelling) at least for a certain number of cases. The parameters that were taken into consideration for the operation are defined in figure 1. The dimensional characteristics of the features tested were chosen so as to reach critical cutting depth, reaching the limit of the usage conditions of the tools.

2.2. THE OPEN SLOT FEATURE STUDIED AND THE EXPERIMENTS

The feature studied is a combined open-slot machining feature composed of two open-slot machining features. The trials were carried out over four test samples with three different geometrical cases (figure 2). The material used is a XC38 steel.

With the cutting data provided by Citroen, it can be shown (Villeneuve, 1996) that the limits of the usage conditions of the tools are: maximum chip thickness, minimum chip thickness, minimum number of working teeth and dimensional limits due to the tool's dimensions (a_r and H). The machining strategies presented tend to reach these limits (Figure 3, Table 1).

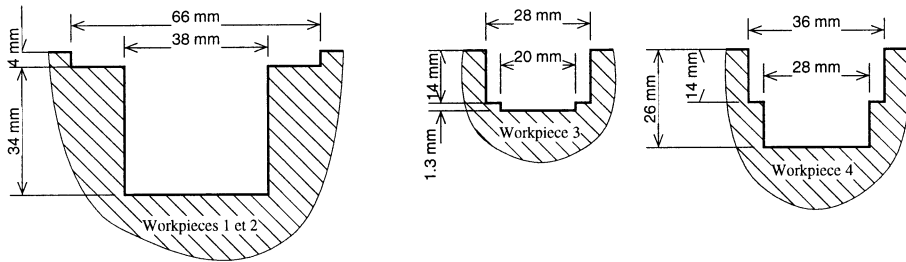


Figure 2. 'open step' machining features geometry

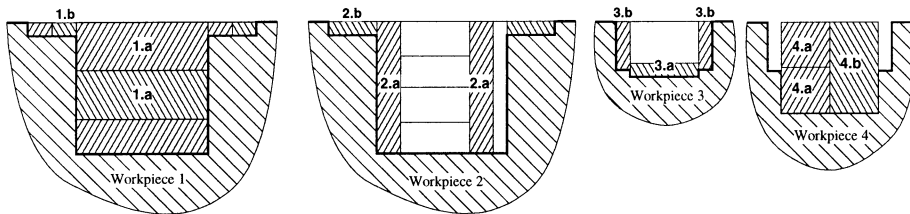


Figure 3. Machining strategies

TABLE 1. Machining strategies and process limits

Workpiece 1	1a : ar = 20	H = 14	End-mill Ø20, 4 teeth	ar maxi. and mini. chip
	1b : ar = 7	H = 4	End-mill Ø10, 4 teeth	Maximum chip
Workpiece 2	2a : ar = 7	H = 38	End-mill Ø20, 4 teeth	H maxi. and optimum ar
	2b : ar = 14	H = 4	End-mill Ø20, 4 teeth	Maximum chip
Workpiece 3	3a : ar = 20	H = 4	End-mill Ø20, 4 teeth	ar maxi. and maxi. chip
	3b : ar = 4	H = 14	End-mill Ø20, 4 teeth	Less than 1 tooth working
Workpiece 4	4a : ar = 14	H = 13	End-mill Ø14, 4 teeth	ar maxi. and mini. chip
	4b : ar = 14	H = 26	End-mill Ø20, 4 teeth	Minimum chip

2.3. ANALYSIS OF THE RESULTS

The full material paths (1a, 3a and 4a) have led to the highest vibrations and consequently to the worst surface finish. These defects are even more exaggerated when the diameter of the tool is larger. The defects of the positioning of the slots realised also take values that cannot really be neglected any more.

The realisation of the so-called critical paths did not really pose any problem. In particular, the H limit = useful length (Lu) was not particularly problematic. The limit of the number of working teeth could also be easily overcome. The most sensitive limitation is that of the minimum chip, which is highly important for full material paths.

The fact that the tools did not break confirms the accuracy of the cutting data proposed by the Citroen factory at Meudon.

The degree of geometrical defects of the surfaces realised shows constraints that will not be taken into consideration in our study (vibrations and distortions).

3. Modelling cutting data

We are proposing to model realistic cutting data and to identify their limits. The industrial cutting data devised by the Production Unit at Citroen Meudon give the feed-rate V_f and the rotation speed N that are to be considered on the part material, the tool diameter D_o , on H and a_r for roughing end-milling in linear interpolation (IL) with HSS tools (Figure 1).

3.1. MODELING DATA

It can be noted that, in the Citroen cutting data, the feed-rate V_f varies with D_o , a_r , H and the material machined. The engagement angle ϕ_e is more generic than the radial cutting depth a_r as it can be used in circular interpolation (Villeneuve, 1996). The objective is then to express $V_f = \text{function of } (D_o, H, \phi_e, \text{mat.})$.

When analysing the feed-rate V_f in relation with H or ϕ_e for an end-mill diameter (D_o) and a given material, it can be noted that there is an almost linear decreasing evolution on a logarithm scale (Figure 4). Do these feed-rate values correspond to the respect of a maximum mechanical solicitation criterion of the tool ?

A numeric simulation of the cutting forces induced by these cutting data was carried out. The model of forces chosen for this simulation is that developed by Bouzakis *et al.* (1985). A tooth element with a dz height is submitted to the tangent (dF_t), radial (dF_r) and axial (dF_z) components of the elementary cutting force (dF).

$$\begin{cases} dF_T = K_t \times h^{(1-m_t)} \times dz \\ dF_R = K_r \times h^{(1-m_r)} \times dz \\ dF_Z = K_z \times h^{(1-m_z)} \times dz \end{cases} \quad (1)$$

There exist at least two possible modes of tool breakage : a local mode that leads to the breaking of one of the tool's teeth, and a global mode that leads to the complete breaking of the end-mill. The local mode is characterised by a maximum dF_t , the global mode by a maximum flexion moment (M_{flex}). dF_t et M_{flex} have been numerically computed for all the Citroen's cutting data. It can be noted that the feed-rate data proposed do not all lead to a maximum dF_t and M_{flex} value (Figure 5). For each end-mill, we have thus chosen the maximum computed value of dF_t and M_{flex} as constraints on the feed-rate.

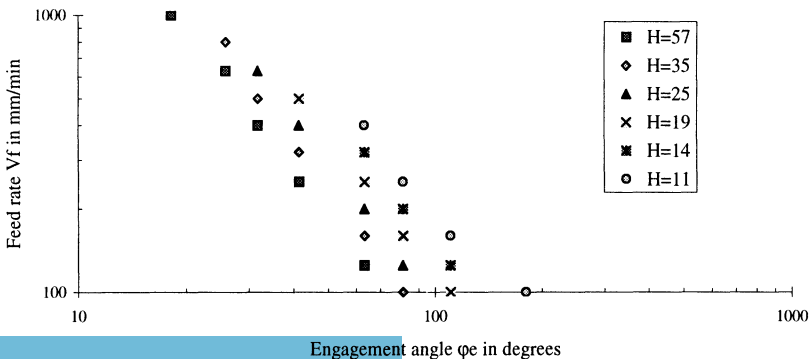


Figure 4. Citroën data : Vf function of ϕ (End-mill $\varnothing 40$, material XC 38)

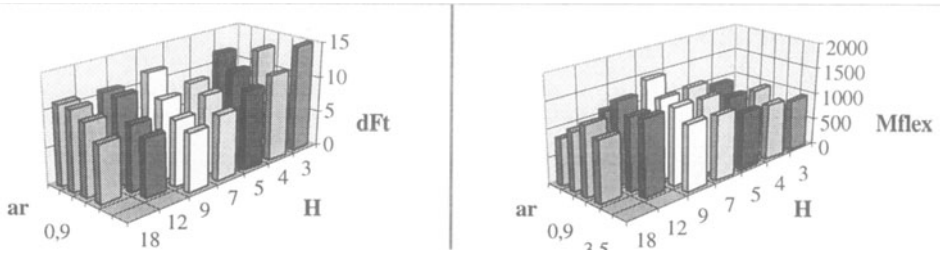


Figure 5. Citroën data ; dFt and Mflex function of H and ar

The cutting speed V_c of the Citroën data varies with the material machined but also with the engagement angle ϕ and the tool diameter D_o . The lower the engagement, the more V_c can be increased as the tool gets cooled better. Hence the following modelling and an idea of the correlation with the data (Figure 6) :

$$V_c = KI(mat.) \left(\left(\frac{D_o}{5} + 30 \right) + \left(\frac{3 \cdot D_o}{40} + 11 \right) \cdot \left(\frac{1620}{\phi^2} - \frac{\phi^2}{180^2} \right) \right) \quad (2)$$

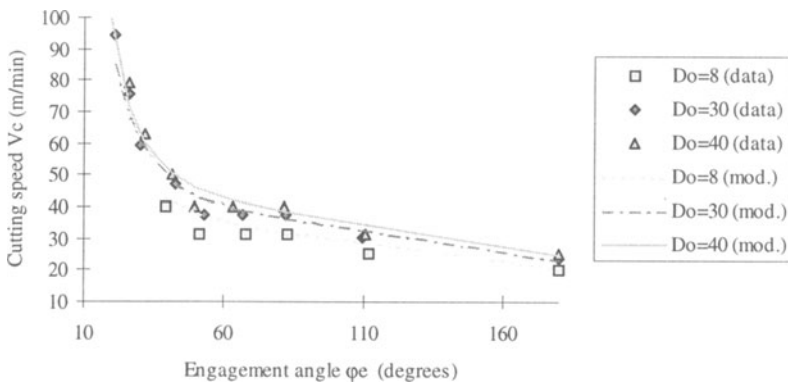


Figure 6. Cutting speed V_c , data/modelling correlation

3.2. DETERMINING THE LIMITS

In the Citroën Charts of data, there are limits for H and ar beyond (and under) which the feed-rate is not given. We are interpreting these limits in relation with different criteria (Figure 7). Considering he, the maximum chip thickness of the milling operation (Figure 1). For given material and tool diameter, he is limited by a maximum and a minimum.

$$he_{min}(Do, mat.) \leq he \leq he_{Max}(Do, mat.) \quad (3)$$

he_{min} corresponds to a minimum chip under whose value the cutting is done in bad conditions as the chip cannot be formed any more. he_{min} can be modelled as follows:

$$he_{min} = \frac{K2(mat.)}{K1(mat.)} \cdot 13 \cdot 10^{-4} \cdot Do \tag{4}$$

he_{Max} corresponds to a limit beyond which there is a risk of breaking the mill's teeth:

$$he_{Max} = \frac{K2(mat.)}{K1(mat.)} \cdot 5 \cdot 10^{-3} \cdot Do \tag{5}$$

There can be a total absence of feed-rate in the Citroën's data at a stage when the maximum limit of the thickness he has not yet been reached. It then means there is a physical limit that requires to have at least one tooth working during roughing. This constraint depends on Do, H, λs (Figure 1) and z (number of teeth) and can be translated with the following geometric relation :

$$\varphi e \geq \left(\frac{1}{z} - \frac{H \cdot tg(\lambda s)}{\pi \cdot Do} \right) \cdot 360 \tag{6}$$

HSS end-mill, diameter 8 mm, short length		Number of teeth z = 3							Hemin = 0.01
		Feed-rate Vf (mm/min), function of H and φe							HeMax = 0.04
ar mm	φe degrees	H = 18	H = 12	H = 9	H = 7	H = 5	H = 4	H = 3	N tr/min
		0.9	39	160					
1.5	51	100	125						1250
2.5	68	80	100	125					1250
3.5	83	50	63	80	100	125			1250
5.5	112		40	50	63	80	100		1000
8	180			32	40	50	63	80	800

Less than one tooth working area (the ratio H/ φe is too small)

Minimum chip area (If Vf is smaller then he < hemin)

Maximum chip area (If Vf is greater then he > hemax)

Figure 7. Constraints on feed-rate Vf, end-milling (Citroën data)

4. Optimised choice of end-mills under constraints

The aim of the study is to find a tool and cutting conditions that will minimise production time at the roughing stage of a given feature. The study presented here is limited to the case of open slots (Figure 8).

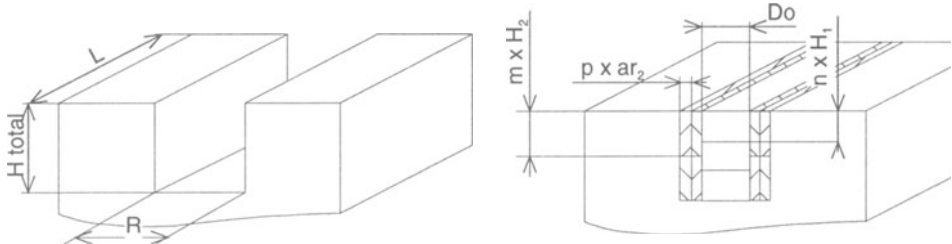


Figure 8. 'open slot' machining features and path parameters

The machining time of such features can be considered under the angle of the time the tools take to move at working feed-rate, supposing that the time at high feed-rate is negligible. This means that the distances to cover between two paths can be considered short and that the high feed-rate is really higher than the working feed-rate. If one makes use of these hypotheses, the machining time (t_u) is then equal to the total of the machining times for the full material paths plus the total of the times of the lateral paths.

$$t_u = \sum_1^n t_{u_i}(\text{full material}) + \sum_1^{m-p} t_{u_i}(\text{lateral paths}) \quad (7)$$

4.1. TARGET : MINIMUM TIME

During the roughing operations, the distance is equal to the length L of the part + a margin G that depends on the path. One then gets :

$$t_{u_i} = \frac{(L+G_i)}{Vf_i} \quad \text{so} \quad t_u = \sum \frac{(L+G_i)}{Vf_i} \quad (8)$$

So as to simplify the problem, we have decided upon the following constraints (fig. 8)

- The full material paths are all identical ($Do \times H_1$), flow Q_1 .
- The lateral paths are all identical ($ar_2 \times H_2$), flow Q_2
- The full material and lateral paths are machined with the same tool.
- The margin G is the same for all the paths.

$$\begin{cases} Q_1 = Do \cdot H_1 \cdot Vf_1 \\ Q_2 = ar_2 \cdot H_2 \cdot Vf_2 \end{cases} \quad \text{and} \quad \begin{cases} n = \frac{H_{total}}{H_1} \\ m = \frac{H_{total}}{H_2} \\ p = \frac{R - Do}{ar_2} \end{cases} \quad (9)$$

$$\text{Hence, to minimise } t_u \text{ means to minimise: } \frac{Do}{Q_1} + \frac{R - Do}{Q_2} \quad (10)$$

4.2. IDENTIFYING CONSTRAINTS

On top of the limits put to the cutting data presented in 3.2, we wish to recap the constraints that act on the optimisation variables:

$$\text{Useful length of the end-mill} \quad Lu(Do) \geq H_{total} \quad (11)$$

$$\text{Maximal radial cutting depth equal to the tool's diameter } Do \geq ar_2 \quad (12)$$

$$\text{Axial insertion inferior to the depth of the feature} \quad H_{total} \geq H_i \quad (13)$$

$$\text{Radial cutting depth inferior to the width of the feature} \quad R \geq ar_2 \quad (14)$$

$$\text{Respect of the maximum flexion moment} \quad M_{flexMax} \geq M_{flex} \quad (15)$$

$$\text{Respect of the admissible force criterion} \quad dF_{TMax} \geq dF_T \quad (16)$$

4.3. IMPLEMENTATION

A computer model of the optimisation under constraints of the milling operation sequence of an open slot feature has been made. An optimisation algorithm under Matlab was used. This computer model was used for a series of optimisation trials in varied conditions. The conditions studied were:

- Influence of the tool's diameter D_o and the axial insertion H on the full material machining flow.
- Influence of the engagement angle ϕ_e during lateral milling.

It can be shown that:

- The $D_o/Q1$ ratio decreases with D_o and that it is therefore interesting to look for a large diameter end-mill.
- $(R - D_o)$ is thus decreased, which means that one only has to look for conditions that lead to a maximum $Q2$ machining flow.

5. Conclusion

The aim of this work was the optimisation of end-mill roughing operation sequences on "open-slot" machining features. The experiments carried out have validated the hypotheses proposed. A modelling of realistic cutting data was then proposed as well as an analysis of the limits of use of the tool. An optimised choice under constraints of end-mill and their cutting data was then proposed and a computer model using the optimisation algorithm was used to validate it.

The correlation of the proposed models with the data is satisfactory and the optimisation results allow for the choice of both a tool and its cutting data for the roughing of an open slot feature in a minimum of time.

This work will potentially open onto the generalisation of the conclusions drawn to all of the features to be machined with an end mill.

References

- Anselmetti, B. (1994) Génération automatique de gammes de tournage et contribution à la gestion d'une cellule de production, Habilitation à diriger les recherches, Université de Nancy I, January.
- Bouzakis, D. and Methenitis, G. (1985) Determination of the values of the technological parameters which are used to describe the time course of cutting force components in milling, *Annals of the CIRP*, Vol.34/1/1985, pp. 141-144.
- Lee, K., Kim, T. J. and Hong, S. E. (1994) Generation of toolpath with selection of proper tools for rough cutting process, *Computer Aided Design*, vol. 26, n°11, pp. 823-831.
- Muller B. (1997) Contribution à l'optimisation des processus d'ébauche en fraisage 2 tailles, mémoire de recherche de DEA, DEA de Production Automatisée, LURPA, ENS de Cachan.
- Villeneuve F. (1990) Génération ascendante d'un processus d'usinage. Proposition d'une formalisation de l'expertise. Application aux entités alésage, thèse de Doctorat, Ecole Centrale de Paris, LURPA, ENS de Cachan.
- Villeneuve F. (1996) Choix optimisé de fraises 2 tailles en interpolation circulaire ébauche, colloque PRIMECA, Nantes.

A MODEL FOR THE OPTIMIZATION OF THE RELATION BETWEEN PRODUCT MEANS AND PRODUCT.

S. TASSEL, F. VILLENEUVE and O. LEGOFF.

LURPA, ENS CACHAN.

61, Avenue du Président Wilson 94235 Cachan Cedex, France

Tel : 33(0)1 47 40 27 57 Fax : 33(0)1 47 40 22 20

e-mail : tassel@lurpa.ens-cachan.fr

Abstract. In this article we propose an optimal response to the problem of integrating manufacturing constraints at the stage of the definition of the manufacturing process, taking a class of means selected and the definition of the part into account. This solution is expressed in terms of means in adequacy with the definition of the part. The first part of the work consisted in defining a model of the data associated with a means of machining. The information thus modeled renders an account of the set of relevant characteristics associated with a machine-tool. The model suggested uses the EXPRESS-G formalism. Once the model defined, we endeavor to define the processing which makes it possible to obtain an answer about the workability of the part. The works completed mainly consider the kinematics of a given class of machines and aims at checking then optimizing the workability of the part, which is then represented by an extension of machining feature, the extreme situations.

Key words. DFM, kinematic, data model, extrem situation, machining feature.

1. Introduction

The Design For Manufacturing (DFM) concept represents a set of tools and methods that allow for the qualitative or quantitative measuring and/or the validation (Mony, 1994) of the solution of design.

This article deals with the DFM issue or how to validate, alter or even direct the design stage according to the constraints linked with production. We will be more specifically interested in the machining processes. Among the constraints that machining techniques generate, one is the analysis of the existence of a machine-tool that answers the requirements of the surfaces to machine. T. Chang (Feng and Kusiak, 1995) proposes a classification of the constraints of the machine-tool. We thus propose a modeling of the machine-tools using the formalism EXPRESS-G (ISO 10303-11) (ISO, 1991) in order to put a machine in adequacy with a part.

Delbressine (Delbressine and Van Der Wolf, 1990), (Delbressine and Hijink, 1991), splits the problem of manufacturability into three sub-problems : interferences materialized by the "delta volume", precision of the "manufacturable object" and its setup. It is on this last point that we propose a strategy to validate the manufacturing properties of a set of machining features of a part in term of tool accessibility. A machine-tool model is presented. The geometrical model uses a parameter setting that results from robotics, Denavit-Hartenberg's model. A definition of the product to be

realized is introduced under the form of machining features and "extreme situations". The model can be used from two different points of view. One describes a method of validation of the accessibility of a workpiece for a given configuration. The other illustrates the research for a setup of the workpiece that will be compatible with the described constraints.

We place ourselves within the field of the search for an optimal solution for the problems of accessibility posed during the development of the manufacturing process of the product. This solution is expressed in terms of means to put in adequacy with the definition of the part. The first part of the work consisted in defining a model of the data associated with a mean of machining. The modeled informations render an account of the set of relevant characteristics associated with a machine-tool (kinematics, power, tool-attachment...).

2. Machine-tool model

The model suggested uses the EXPRESS-G formalism (ISO, 1991), increasingly widespread in the CAD / CAM field, which makes it possible to define models that one can describe as "conceptual data models". Its development enabled us to specify many informations and to define the associated data which will then be taken into account into a more important model relating to the step of concurrent engineering. We will not develop all of the points dealt with in this model ; it can however be noted that the research carried out in order to establish the model is related to the following fields :

- Machine power : study of the various curves of power engines and of the associated characteristics.
- Cutting parameters : study of the feed rates and cutting speed, definition of the relevant characteristics according to the technology used for transmission power.
- Geometrical model : study and choice of a model in order to define the kinematics of the machine, this point will be detailed further on.

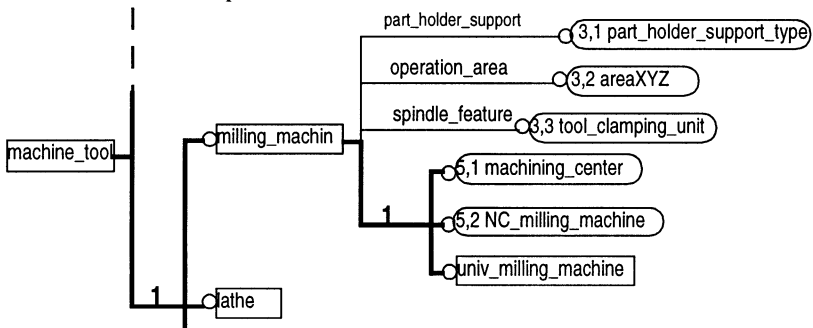


Figure 1 : Partial model of a machine-tool

- Accessible volume : approximate definition of the machining maximum lengths on each axis.
- Connection part/machine : study of the part holder supports and part holders, of the various systems of part holders positioning, and of the standard systems of positioning the parts on the machine-tool.
- Connection tool/machine : study of the types of tool-holders.

The major difficulties related to this aspect is due to the fact that it is a question of formalizing the manufacturers' know-how; and introducing numbers of concepts and methods of calculation that result from the research tasks. Figure 1 partly represents the model carried out in order to account for the set of characteristics relating to the machine-tool associated with a setting operation (Krajewski, 1997).

2.1. GEOMETRICAL MODEL

After studying various approaches used for modeling of the machine-tools, we chose to use a model resulting from research in the field of robotics : Denavit and Hartenberg's Modified (DHM) model (Dombre and Khalil, 1988) (Guerin, 1994), (Mery, 1997). This model regards a robot as a set of solids (body) connected by a rotoide or prismatic joint. The used parameters allow to describe the structure of the considered robot.

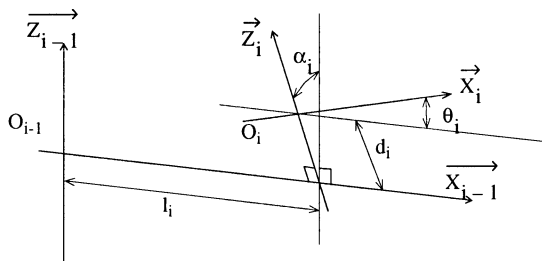


Figure 2 : Changing of reference mark

Thus, a machine-tool is regarded as a particular robot and the table of the machine as the base of the robot. The main point of this model is its genericity: it makes it possible to describe any machine architecture, in terms of a number of axes and types of joints; moreover the algorithms used in robotics are directly exploitable (collision detection, calculation of trajectories...).

We define the reference mark R_i with axes X_i and Z_i . Z_i is the direction of the joint, and X_i is the common perpendicular to Z_i and Z_{i+1} . If Z_i and Z_{i+1} are parallel then X_i is selected thanks to considerations of symmetry and simplicity. We call q_i the articular variable associated with a joint, $q_i = \theta_i$ for a rotoide (one sets $\sigma_i = 0$, like determining variable the type of joint), or $q_i = d_i$ for a prismatic joint ($\sigma_i = 1$). We can write that $q_i = (1 - \sigma_i)\theta_i + \sigma_i d_i$.

The four geometrical parameters are the following ones : a translation along Z_i length d_i , a rotation of axis Z_i angle θ_i , a translation along X_{i-1} length l_i , and a rotation of axis X_{i-1} angle α_i . We thus obtains the matrix of change of the reference mark:

$$T_{i-1,i} = (R_{i-1}, R_i) = \begin{bmatrix} \cos \theta_i & -\sin \theta_i & 0 & l_i \\ \cos \alpha_i \sin \theta_i & \cos \alpha_i \cos \theta_i & -\sin \alpha_i & -d_i \sin \alpha_i \\ \sin \alpha_i \sin \theta_i & \sin \alpha_i \cos \theta_i & \cos \alpha_i & d_i \cos \alpha_i \\ 0 & 0 & 0 & 1 \end{bmatrix}$$

We can thus define the matrix of change of reference mark between each body: $T_{0,1}$, $T_{1,2}$, ..., $T_{n-1,n}$, with R_0 related to the machine. So, the resulting matrix is $T_{0,n} = T_{0,1} T_{1,2} \dots T_{n-1,n}$. The representation of DHM model in the data model is presented Figure 3. Thanks to the model, it's possible to know if each joint is prismatic or rotoide as well as the values of the higher and lower limits of the routes corresponding to this axis. In addition, we know the values of the articular characteristics (alpha, l, teta,

d, and sigma). Having the characteristics of each axis, it is easy to install the matrix of the change of reference mark that corresponds to the machine.

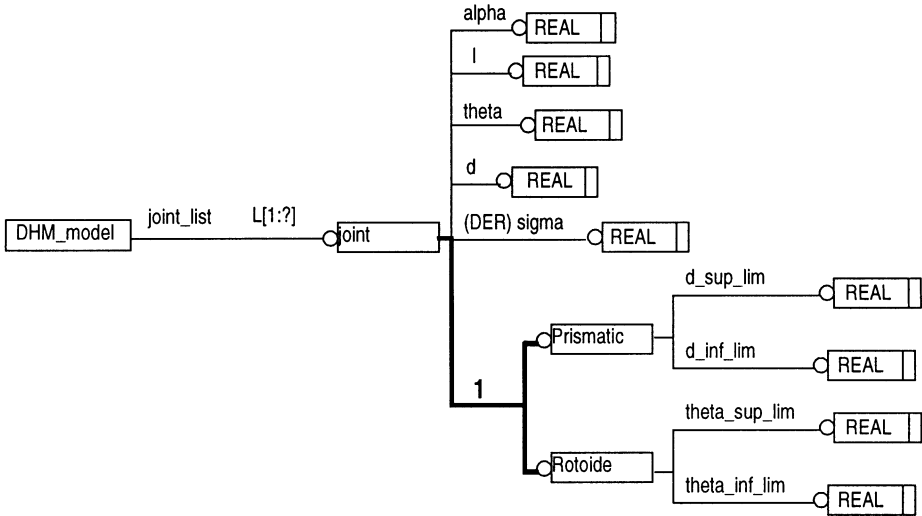


Figure 3 : Modeling of DHM model

2.2. EXAMPLE OF APPLICATION

Taking presented model into account, we are proposing an example of the use of this model in the case of a 4 axis-machining center. The structure of the machine considered is represented on figure 4.

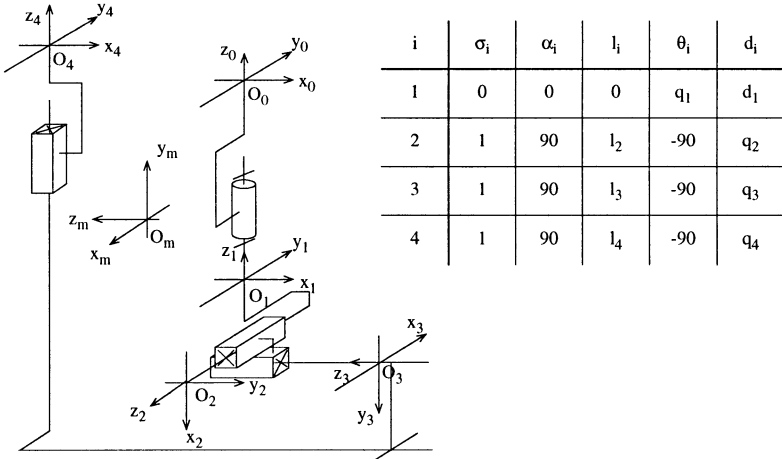


Figure 4 : Modeling of a 4 axis machining center

Hereunder the matrix $T_{0,4}$ which represents the transformation associated with the articular parameters q_i for a four axis machining center.



$$T_{0,4} = \begin{bmatrix} \cos q_1 & -\sin q_1 & 0 & -l_4 \sin q_1 - q_3 \cos q_1 + l_2 \cos q_1 + q_2 \sin q_1 \\ \sin q_1 & \cos q_1 & 0 & l_4 \cos q_1 - q_3 \sin q_1 + l_2 \sin q_1 - q_2 \cos q_1 \\ 0 & 0 & 1 & q_4 - l_3 + d_1 \\ 0 & 0 & 0 & 1 \end{bmatrix}$$

Once the machine-tool model defined, we endeavour to define the process which makes possible to obtain an answer on the workability of the part.

3. The extreme situations

We are presenting a representation method of the machining features (Anselmetti et al., 1996) that allows to do without the knowledge of the full process planning : the extreme situations.

The knowledge of the extreme situations of a feature allows looking for a machine-tool that can machine the feature from a kinematic point of view. It also allows defining a space permitting to setup the workpiece on the machine-tool.

Here are the working hypotheses we have chosen:

- The machining features are of the two-and-a-half axis type, i.e. they can be machined on a two-and-a-half axis machine-tool. Let us for instance mention the feature flat bottom pocket, a hole, a thru hole, a slot or a step.
- The use of a machine-tool whose number of axes is greater than three allows the machining of several features that require varied spindle-axis directions. We nevertheless consider that the rotation axes complementary to the basic translations X, Y, Z are only used to direct the workpiece and that they are not activated when machining a feature.

We can pinpoint two points of view on the extreme situations of machining features. The first point of view, intrinsic to the feature and to its geometric definition, is that of the minimum technological trajectories. The second point of view appears when the feature is positioned on the machine-tool, i.e. the extreme kinematic situations.

3.1. MINIMUM TECHNOLOGICAL TRAJECTORIES

For each type of feature corresponds one or several directions of the spindle. Let us admit that, once a direction is chosen for a feature, the whole set of machining operations of the feature will use the same direction of spindle. For a given direction of the spindle, we define a minimum technological trajectory required in a plane perpendicular to this direction.

We have defined these directions of spindle and these technological trajectories for a certain number of machining features (pocket, slot, step, hole).

For the machining features of the pocket, slot or step type, we define a minimum tool radius using distortion and tool vibration criteria. The tool radius depends on the depth of the feature.

We then define the minimum technological trajectory (fig. 5) as the contour of the trajectory that allows to reach the finish of the machining feature while including technological data. This contour is made of segments which are materialized by the associated bipoints and of arcs of circles represented by their centers and radius.

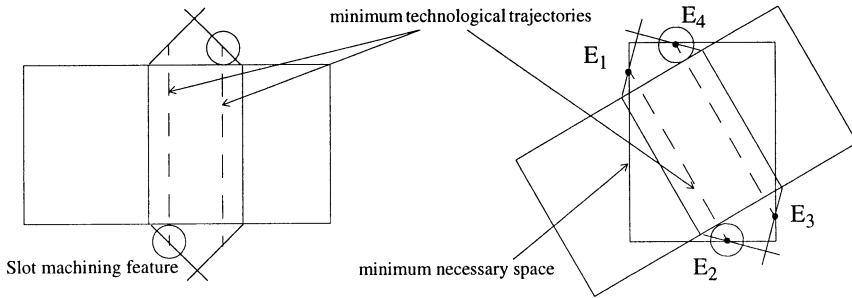


Figure 5 : Minimum technological trajectories and extreme kinematic situation

3.2. THE EXTREME KINEMATIC SITUATIONS

If one takes the hypotheses chosen hereabove, the minimum technological trajectories can be translated in terms of extreme kinematic situations when the setup of the workpiece on the machine-tool is known. The extreme situations E_j are taken into consideration when relating machine-tool and workpiece. Let us suppose that the orientation of a feature k in relation with the machine-tool is known. This orientation is translated by the orientation component of the transformation matrix $T_{O,C}$, a characteristic matrix of the position of the workpiece in the machine-tool space (figure 5). When the spindle axis is lined up with the axis of the feature k , one can define the minimum space that has to be reachable for the machine-tool to follow the minimum technological trajectory of the feature k .

Let us, for instance, consider the case of a slot feature whose minimum technological trajectory is defined in figure 5. When the direction of this feature is known in the machine-tool space, one can determine the minimum space of figure 5. This space holds the set minimum technological trajectory. One then only has to select the four points E_1 , E_2 , E_3 and E_4 as characteristic points of the feature.

4. Method for relating machine-tool and workpiece

The method we are about to describe aims at making the machine-tool and the workpiece fit. We have distinguished two cases:

- validation of a setup already known on a machine-tool,
- research for a setup of a workpiece on a machine-tool to reach a finite number of extreme situations.

It's on the second point that we present a method to optimize the research of a setup.

4.1. GENERAL ISSUE

Let us consider the transformation matrices of the references represented :

- $T_{0,4}$ represents the kinematics of the machine-tool considered, e.g a four-axes machining center (2.2)(fig. 4)
- $T_{4,P}$ the transformation matrix from R_4 to the reference P characteristic of the tool, extreme point placed on the axis and the end of the tool.

- $T_{0,C}$ represents the setup of the workpiece defined by the reference R_C in the working space of the machine-tool (R_0).
- $T_{C,E}$ is the transformation matrix from the reference R_C to a reference R_E associated with an extreme situation.

An extreme situation is reached if and only if the reference R_P linked to the tool can be blended into the reference R_E , linked with the extreme situation, save on one rotation around the tool, i.e if and only if $T_{E,P} = Id(\varphi)$:

$$T_{E,P} = \begin{bmatrix} \cos\varphi & -\sin\varphi & 0 & 0 \\ -\sin\varphi & \cos\varphi & 0 & 0 \\ 0 & 0 & 1 & 0 \\ 0 & 0 & 0 & 1 \end{bmatrix}$$

φ is the degree of freedom corresponding to the tools rotation around its axe.

4.2. RESEARCH FOR A SETUP

Here, if one excludes the bilimited conditions on the articular variables of a model, i.e. considering infinite routes, it is first a matter of defining sub-sets of extreme situations that can be machined with the same setup. Then one tries to seek a setup of the workpiece that will make the extreme situations reachable, under the constraints of the characteristics of the machine-tool used.

The data of the problem then appear as follows:

- The kinematics of a workpiece represented by the matrix $T_{0,4}$ and the constraints on the q_i .
- The set of the extreme situations j represented by the set of all the T_{C,E_j}
- The lengths of the different tools used for the finish of the k machining features, the T_{4,P_k} .

First stage.

Consider the set of the extreme situations materialized by the matrices T_{C,E_j} . One extracts the directions \vec{z}_{E_j} corresponding to the spindle directions. From this set $\{\vec{z}_{E_j}\}$,

all the vectors \vec{b}_{mn} are computed such that: $\vec{b}_{mn} = \vec{z}_{E_m} \wedge \vec{z}_{E_n}$

If one tries to maximize the number of features realized in the same setup, one has to seek for a \vec{b}_{mn} that will have as many perpendicular directions \vec{z}_{E_j} as possible.

So a subset of extreme situations that can be machined in the same setup is defined.

Secondary stage.

From this subset, we use a optimizing algorithm to find a setup represented by $T_{0,C}$ such that the q_{ij} that permit to reach all the selected extreme situations E_j according to the respective limits of the q_i . It is therefore a problem of optimization under constraints. The

variable to be determined is the translation component of $T_{0,C}$. The constraints concern the articular variables

$$\begin{cases} q_{ij} \leq q_{iMax} \\ q_{ij} \geq q_{iMin} \end{cases}$$

for any q_{ij} such that : $T_{E_q, P_k} = Id(\varphi) = T_{C, E_q}^{-1} \cdot T_{0,C}^{-1} \cdot T_{0,4} \cdot T_{4, P_k}$

5. Conclusion

A machine-tool model has been presented. The geometrical model has been detailed. It uses a set of parameters resulting from the field of robotics. The genericity of the model proposed allows to define any type of machine-tool. The set of the data relating to the machine is taken into account; in particular the limit kinematic limits necessary to the validation of accessibility. The suggested method is based on the concept of extreme kinematic situations which are an extension of the machining features. This representation, which depends on intrinsic data (minimum technological trajectories) and on the orientation of the entity, makes it possible to check or optimize the setting in position of the part in the workspace of the machine-tool modeled beforehand. The method of setting the part in adequacy with its means of production was presented.

The issue of optimization under constraints that permits to validate or seek an optimal setup starting from the extreme kinematic situations has been applied in a computer model using the solver of the Matlab software.

In the view of coming works, the integration of the notion of extreme kinematic situation will have to be carried out as early as the design stage of the surfaces of the product, after a manual or automatic recognition of the machining features.

References

- Anselmetti, B., Chep, A., Mawussi, K., and Villeneuve, F. (1996) Approche entité-état pour la conception de processus d'usinage. *IDMME 96 april 15-17*, tome 2, 593-602.
- Delbressine, F. L. M., and Van Der Wolf, A. C. H. (1990) Integrating Design and Manufacturing. *In annals of the CIRP* vol. 39, CIRP 15 Jan. , 149-152.
- Delbressine, F. L. M., and Hijink, J. A. W. (1991) Discrete part Design by Taking Manufacturing Restrictions into Account, *in annals of the CIRP* vol. 40, CIRP 15 Jan. , 171-174.
- Dombre, E., and Khalil, W. (1988) *Modélisation et commande des robots*, Traité des nouvelles technologies série robotique, ed. Hermès, 1988.
- Feng, C. X., et Kusiak, A., (1995) Constraint-based design of part, *Computer aided design*, vol. 27, May , 343-352.
- Guerin, F. (1994) Usinage de surfaces complexes, génération de trajectoires hors collision. *Thèse de doctorat de l'Université de Nantes*.
- Norme ISO 10303 Part 11 (1991), EXPRESS language reference manual, external representation of product definition data (release draft).
- Krajewski, S. (1997) Modélisation en vue de l'optimisation du choix d'une machine-outil, *DEA de production automatisée LURPA - ENS de Cachan*.
- Mery, B. (1997) *Machines à commande numérique*, Hermes.
- Mony, C. (1994) DFM : enjeux, tendances et état de l'art, *in Revue d'automatique et de productique appliquées* vol. 7, 1 Jan , 11-14.

OPTIMAL MILL POSITIONING IN FIVE AXIS MACHINING ON FREE FORM SURFACES : APPLICATION AT ROUGHING PATH OF MOULDS

RUBIO W., REDONNET J.M., DESSEIN G., LAGARRIGUE P.
*Laboratoire de Génie Mécanique de Toulouse,
Filière Génie Mécanique, Bât. 3PN
118, rte de Narbonne
31062 Toulouse Cedex, France*

1. Statement of the problem

Machining on five-axis NC machine tools enables us to position a tool at a point while directing its axis at will. When machining a free-form surface using a flat-end cylindrical milling cutter, standard positioning involves setting the tool axis on the plane $(\mathbf{Q}_0, \mathbf{t}, \mathbf{n})$, with \mathbf{Q}_0 being the point of contact between the tool and the workpiece, \mathbf{t} a vector belonging to the plane tangent to \mathbf{Q}_0 defined by the machining strategy (machining along parallel planes, along isoparametric curves, along a principal direction, etc.) and \mathbf{n} the normal vector on \mathbf{Q}_0 (Vickers (1989), Li (1994), Kruth (1994), Mullins (1993), Jensen (1993), Rubio (1997)). We shall assume from the start that the tool axis is parallel to the normal on \mathbf{Q}_0 (Cf. figure 1). When we calculate the intersection between the cylinder corresponding to the tool envelope and the surface $S(u, v)$, we shall obtain points \mathbf{M}_i with co-ordinates (x_i, y_i, z_i) on the reference $(\mathbf{Q}_0, \mathbf{t}, \mathbf{b}, \mathbf{n})$ with $\mathbf{b} = \mathbf{n} \wedge \mathbf{t}$.

Points \mathbf{M}_i on the figure 1 interfere with the workpiece. Our study relates to the angular corrections we have to perform so as to eliminate collisions between the tool and the workpiece while minimising the material left by the tool. This study concerns roughing moulds for parts. Indeed, to reduce machining times, it is advantageous to use a large tool, which leads to the risk of collision between the tool and the workpiece. In this scenario, we cannot assume that the surface geometry at the point of contact between the tool and the workpiece will be constant and it therefore becomes impossible to reason from the surface differential geometry.

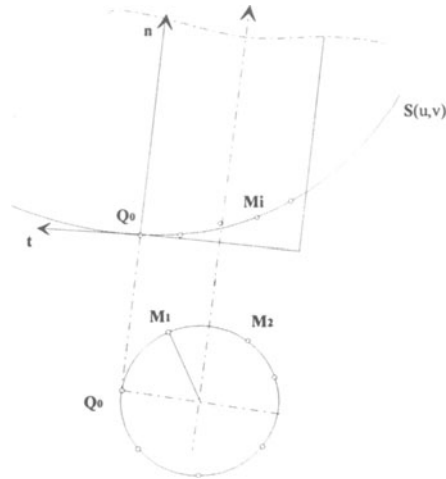


Figure1. Interference between the tool and the surface

The advantage accrued from the distribution of the material left relates to the mould finishing phase. In this case, the tool will work in improved cutting conditions as the pass cutting depth will be more constant, thus limiting cutting changes in cutting loads. This study can, of course, be extended to apply to the finishing pass. In figure 2, we define angles α and β . Other rotations may also be considered (Cho (1993a), Cho (1993b), Lee (1996), Lee (1997).

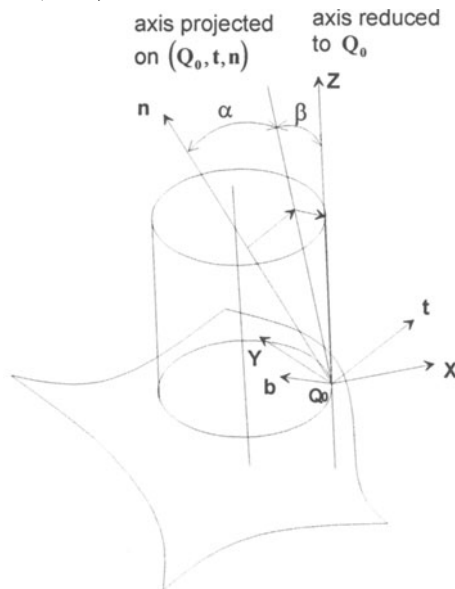


Figure2. Defining the reference change

α corresponds to the tool rotation angle on Q_0 about axis b . From this position, β corresponds to tool rotation on Q_0 about axis X .

We define a tool reference by (Q_0, X, Y, Z) .

Let M_i represent the intersection points between the tool envelope and the surface as defined by co-ordinates (x_i, y_i, z_i) in the local reference of the surface. We bring these points into the tool reference defined by the two angle rotations α and β . The co-ordinates for points M_i will be (X_i, Y_i, Z_i) in the reference (Q_0, X, Y, Z) . The passage of point co-ordinates between the two references is given by the following relation:

$$\begin{cases} X_i = x_i \cos \alpha - z_i \sin \alpha \\ Y_i = -x_i \sin \alpha \sin \beta + y_i \cos \beta - z_i \cos \alpha \sin \beta \\ Z_i = x_i \sin \alpha \cos \beta + y_i \sin \beta + z_i \cos \alpha \cos \beta \end{cases}$$

In the tool reference chosen to characterise the position of the tool in relation to the surface of the workpiece, we need to have all $Z_i \leq 0$ available in order to ensure there is no interference between the tool and the workpiece. In most cases, there are an infinite number of couples (α, β) verifying relations $Z_i \leq 0$. We intend to perform optimisation on the field of solutions so as to minimise the material left by the tool at the point considered. The problem in terms of optimisation can be posed as follows:

Minimise $\text{Max}_{\alpha, \beta} (Z_i) \quad i \in [1, n]$ subject to constraints $Z_i \leq 0 \quad i \in [1, n]$.

2. Study of Z_i functions

It should be noted that the angles are limited by cutting problems or machine end stops. The intervals authorised for the different parameters will be as follows: $\alpha \in [0, 45^\circ]$, $\beta \in [-45^\circ, 45^\circ]$, $x_i \in [-2R, 0]$ and $y_i \in [-R, R]$

It can readily be demonstrated that:

- The Z_i functions are strictly diminishing with α ,
- Z_i values are strictly diminishing with β if $y_i < 0$,
- Z_i values are strictly increasing with β if $y_i > 0$,
- If $y_i < 0$, the domain of validity is located above the curve,
- If $y_i > 0$, the domain of validity is located below the curve.

2.1. SEARCHING FOR THE OPTIMUM SOLUTION

We shall note curves Z_i with $y_i > 0$ as Z_{pos} and curves Z_i with $y_i < 0$ as Z_{neg} .

The limits of the domain are given for equations $Z_i = 0$.

This equation is equivalent to $\tan \beta = -\frac{x_i \sin \alpha + z_i \cos \alpha}{y_i}$ with $y_i \neq 0$.

On figure 3, we have an example of the domain of solutions. We can easily demonstrate that the optimum solution should be found on a limit curve.

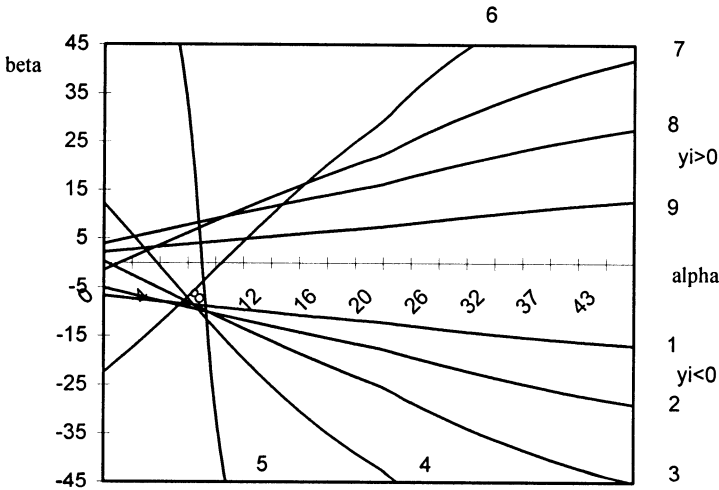


Figure 3. Domain of solutions

Searching for the optimum solution will involve working from the couple $(\alpha_{ab}, \beta_{ab})$ obtained by the intersection of curves $Z_a = 0$ and $Z_b = 0$. This couple belongs to the domain of solutions and has minimum α value.

As the curves are strictly monotonic, this point will be defined from the intersection between a rising curve $Z_{pos} = 0$ and a descending curve $Z_{neg} = 0$. All we need to do is calculate the intersection between these curves inside the domains specified for α and β and take the solution with a maximum value for α . This corresponds to the solution the furthest to the left of the domain.

Let us take two points with indices a and b . The two limit curves of the domain are given by the following equations:

$$\tan \beta = -\frac{x_a \sin \alpha + z_a \cos \alpha}{y_a} \tag{1}$$

$$\tan \beta = -\frac{x_b \sin \alpha + z_b \cos \alpha}{y_b} \tag{2}$$

The intersection between these two curves is given by:

$$\tan(\alpha_{ab}) = \frac{z_b y_a - z_a y_b}{x_a y_b - x_b y_a}$$

Take α_{ab} the solution. We then carry this result over to equation (1) or (2) and obtain the value β_{ab} .

We shall now seek the movement direction inside the domain to find the optimum solution.

Let $(\alpha_{ab}, \beta_{ab})$ be the point of departure for the search. The index a corresponds to the rising curve ($y_a > 0$) and index b to the falling curve ($y_b < 0$).

We shall now calculate all values for $Z_i(\alpha_{ab}, \beta_{ab})$ for $\begin{cases} i \in [1, n] \\ i \neq a \\ i \neq b \end{cases}$. Indeed, if

$i = a$ and $i = b$ functions $Z_i(\alpha_{ab}, \beta_{ab})$ will be null.

We shall now follow the limit curve that will be on the same side as the curve with the maximum value for $|Z_i(\alpha_{ab}, \beta_{ab})|$. Let us take an example:

If $|Z_i(\alpha_{ab}, \beta_{ab})|$ is maximum for a rising curve ($y_i > 0$), we shall follow the curve $Z_a = 0$. Conversely, if $|Z_i(\alpha_{ab}, \beta_{ab})|$ is maximum for $y_i < 0$, we shall follow the curve $Z_b = 0$.

Calculation of movement on the curve $Z_a = 0$

To determine the couple $(\alpha_{sol}, \beta_{sol})$ corresponding to the optimum solution, we shall need two equations. We obtain the first using $Z_a = 0$.

Among the different values for $|Z_i(\alpha_{ab}, \beta_{ab})|$, we shall take the two biggest values on curves with opposite slopes. Let us take the two curves indices m and n with $|Z_m| > |Z_n|$ (We can assume, for example, $y_m > 0$). The second equation will be given by $Z_m = Z_n$ which is equivalent to distributing the material equitably on both sides of the tool. The solution will be obtained by resolution of the following system:

$$\tan \beta = -\frac{x_a \sin \alpha + z_a \cos \alpha}{y_a} \quad (3)$$

(we follow the curve $Z_a = 0$ as $y_m > 0$ and $|Z_m| > |Z_n|$)

$$x_m \sin \alpha \cos \beta + y_m \sin \beta + z_m \cos \alpha \cos \beta = x_n \sin \alpha \cos \beta + y_n \sin \beta + z_n \cos \alpha \cos \beta$$

We shall obtain:

$$\alpha_{sol} = \text{Arc tan} \left(-\frac{y_i(z_m - z_n) + z_i(y_n - y_m)}{y_i(x_m - x_n) + x_i(y_n - y_m)} \right)$$

By carrying over into equation 3 we shall obtain β_{sol} . We shall then need to check that the solution is optimum.

3. Example and conclusion

For the example dealt with, we have a diameter 40 milling cutter on a workpiece defined from a B-spline surface of degree 3x3. Calculation of the intersection between the tool and the surface will give points M_i as shown in the following table in the reference (Q_0, t, b, n) :

x_i	-3.49	-12.75	-26.6	-36.6	-39.96	-35.44	-24.8	-12.25	-2.88
y_i	-11.3	-18.6	-18.9	-11.15	-1.17	12.7	19.4	18.44	10.34
z_i	-1.33	-1.67	0.1	2.42	4.93	5.26	0.5	-1.25	-0.39

Table 4. Points M_i in the reference (Q_0, t, b, n)

The co-ordinates (x_i, y_i) for points M_i are to within an acceptable level of tolerance on a circle. The z_i co-ordinates give us the information on the points that are in interference.

The intersection curve between the tool and the surface on projection over the plane (Q_0, t, n) is shown in figure 5.

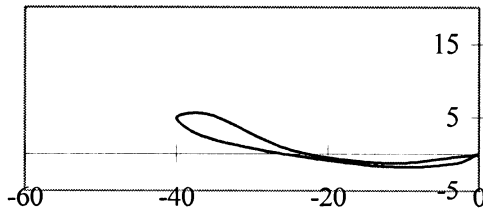


Figure 5. Intersection between the tool and the surface on projection over (Q_0, t, n)

Figure 3 shows curves $Z_i = 0$. The optimum solution is found in the area limited by curves $Z_1 = 0, Z_5 = 0, Z_6 = 0$ and $Z_9 = 0$.

The point of departure to find the optimum position is on the intersection between curves $Z_5 = 0$ and $Z_6 = 0$. The couple $(\alpha_{5-6}, \beta_{5-6})$ is equal to $(7^\circ 14', -3^\circ 67')$.

From this solution we can calculate the values for $Z_i(\alpha_{5-6}, \beta_{5-6})$. We shall obtain the following results:

Z1	Z2	Z3	Z4	Z5	Z6	Z7	Z8	Z9
-1.03	-2.05	-1.99	-1.43	0.00	0.00	-3.82	-3.94	-1.40

Table 6. Calculations of values for $Z_i(\alpha_{5-6}, \beta_{5-6})$

The two biggest values normed on curves for opposite slopes are (2.05, 3.94). The biggest normed value is 3.94 for curve Z_8 which has the same slope as



Z_6 . We can seek the optimum value from the following system:

$$\begin{cases} Z_6 = 0 \\ Z_2 = Z_8 \end{cases}$$

We shall obtain the following result: $(\alpha, \beta) = (8^\circ 17, -0^\circ 75)$. Let us check values for $Z_i(\alpha, \beta)$.

Z1	Z2	Z3	Z4	Z5	Z6	Z7	Z8	Z9
-1.66	-3.22	-3.43	-2.66	-0.79	0.00	-3.29	-3.22	-0.93

Table 7. First approach to the optimum solution

The previous system is verified but we are not faced with an optimum solution as $|Z_3(\alpha, \beta)| > |Z_2(\alpha, \beta)|$ and $|Z_7(\alpha, \beta)| > |Z_8(\alpha, \beta)|$. We then resolve the following system:

$$\begin{cases} Z_6 = 0 \\ Z_3 = Z_7 \end{cases}$$

We obtain $(\alpha, \beta) = (8^\circ 09, -0^\circ 97)$ and again calculate $Z_i(\alpha, \beta)$ as given by the following table:

Z1	Z2	Z3	Z4	Z5	Z6	Z7	Z8	Z9
-1.62	-3.13	-3.33	-2.57	-0.73	0.00	-3.33	-3.28	-0.97

Table 8. Results of $Z_i(\alpha, \beta)$ for the optimum solution

The solution obtained indeed corresponds to the optimum we were seeking. The curve of intersection between the tool and the surface is shown on figure 9.

The entire study of calculations for the points M_i and all searches for optimum positioning was programmed in C language on HP9000 workstation. The results obtained are excellent in terms of reliability and speed. As an example, the full time needed to calculate approximately one thousand tool-workpiece points of contact took just one minute. This work is currently generalised for the torus milling tool and the scallop height criterion will be taken into account in the optimisation process.

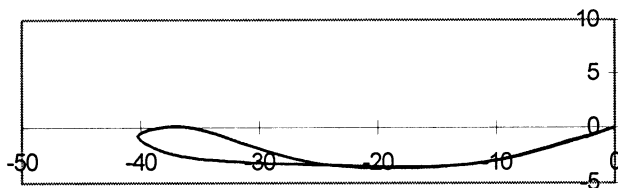


Figure 9. Corrected position for the tool on the surface

4. References

- CHO, H.D., JUN, Y.T., YANG M.Y. "Five-axis CNC milling for effective machining of sculptured surfaces", *International Journal of Production Research*, Vol. 31, N° 11, 1993, pp. 2559-2573.
- CHOI, B.K., PARK, J.W., JUN, C.S. "Cutter location data optimization in 5-axis surface machining", *Computer Aided Design*, Vol. 25, N°6, 1993, pp. 377-386.
- JENSEN, C.G., ANDERSON, D.C. "Accurate tool placement and orientation for finish surface machining", *Journal of Design and Manufacturing*, Vol. 3, 1993, pp. 251-261.
- KRUTH, J.P., KLEWAIS, P. : "*Optimization and dynamic adaptation of the cutter inclination during 5-axis milling of sculptured surfaces*", *Annals of CIRP*, Vol. 43/1, 1994, pp. 443-448.
- LEE, Y.S. "Admissible tool orientation control of gouging avoidance for 5-axis complex surface machining", *Computer Aided Design*, Vol. 29, N° 7, 1997, pp. 507-521.
- LEE, Y.S., JI, H. "Machined surface error analysis for 5-axis machining", *International Journal of Production Research*, Vol. 34, N° 1, 1996, pp. 111-135.
- LI, S.X., JERARD, R.B. "5-axis machining of sculptured surfaces with a flat-end cutter", *Computer Aided Design*, Vol. 26, N° 3, 1994, pp. 165-178.
- MULLINS, S.H., JENSEN, C.G., ANDERSON, D.C.: "*Scallop elimination based on precise 5-axis tool placement, orientation, and step-over calculations*", *Advances in Design Automation*, DE-Vol. 65-2, 1993, pp. 535-544.
- RUBIO, W., LAGARRIGUE, P., DESSEIN, G., PASTOR, F. : "*Calculation of tool path for a torus mill on free-form surfaces of five-axis machines with detection and elimination of interference*", à paraître dans *International Journal of Advanced Manufacturing Technology*.
- VICKERS, G.W., QUAN, K.W. : "*Ball-mills versus end-mills for curved surface machining*", *ASME Journal of Engineering for Industry*, Vol. 111, 1989, pp. 22-26.

AVOIDING THE NEED FOR DEBURRING BY ANALYZING BURR FORMATION DURING PRODUCT DESIGN

L. BLONDAZ* - D. BRISSAUD* - D. DORNFELD**

* *Laboratoire 3S, UJF INPG CNRS UMR 5521, Domaine Universitaire, B.P. 53 - 38041 GRENOBLE CEDEX 9*

** *Laboratory of Manufacturing Automation, University of California at Berkeley - USA*

Abstract

The cost of deburring a part may contribute as much as 30% to the total manufacturing cost. In many cases, it is possible to avoid the problems caused by burrs by integrating preventive actions when designing the mechanical product. Several prevention guidelines for avoiding or simplifying deburring operations during the design to fabrication cycle can be found in the literature. However, a lack of methodology is apparent. This paper presents a methodology whose aim is to compose a strategy for avoiding problems caused by machining burrs through analyses of burr formation at the design stage.

Introduction

A burr is an undesirable piece of material which remains joined to a workpiece, after a manufacturing operation. In particular, a machining burr is a residue of material formed as the result of plastic flow, rather than shearing, from a cutting operation. Burrs cause various types of problems: problems in assembly, corrosion when the burr comes off the workpiece, risks of injuries when handling parts, impediments to the automation of the production, etc.

The cost of deburring a part may contribute as much as 30% to the total manufacturing cost [1]. Burr formation occurs on most of the machined parts. A manual operation of deburring requires a long time. The automation of deburring needs important investments and is often not entirely successful.

A way to significantly decrease deburring costs is to take into account burr formation during the design stage. In many cases, it is possible to avoid the problems caused by burrs, by integrating preventive actions when designing the mechanical product. These preventive actions focus on different levels of the design to fabrication cycle [2]. For instance, burr problems may be avoided by investigations on the design of workpiece forms, on the process planning, on the establishing of tool paths, on the choosing of tool geometry, etc. For each level of investigation, several preventive actions exist. In this panel of preventive actions, a lack of methodology is apparent. How should the best preventive actions be chosen? How should the various actors of the design to fabrication cycle be coordinated? When should decisions be made?

This paper proposes a methodology for taking into account potential burr problems during the design of the product. The objective of this methodology is to avoid deburring operations, or, if it is not possible, to simplify the deburring operation. This methodology provides a cooperation between the different actors of the design to fabrication cycle of the product. From this cooperation, a strategy emerges. This strategy structures the use of preventive actions in order to reach the desired objective. In this paper, the methodology is restricted to machining burrs only.

The first section of this paper situates the research context. The second section quickly presents a classification for machining burrs. This classification is used by the methodology. The third section presents a set of observations for avoiding burr formation, or for reducing problems caused by burrs. The methodology is presented and illustrated in the fourth section.

1. Originalities of the Proposed methodology

1.1 A DFM APPROACH FOR BURR PREVENTION

The goal of Design For Manufacturing is to fit the design of a product to manufacturing objectives. The study focuses on a design for preventing problems caused by burrs and for reducing deburring costs.

1.2 INTEGRATION OF MANUFACTURING DURING STRUCTURAL AND EMBODIMENT DESIGN

Generally, in the literature, the DFM methods concern the detail design of parts. Their goals are to evaluate feasibility, and to give metric measures of manufacturing aspects. The goal of the methodology is to integrate considerations on burrs during global product design (product as a set of parts), and to bring new structural solutions. Decisions taken during the global product design have an important incidence on the manufacturing of each part, and particularly, on the risks of burr formation. Indeed, the various sets of parts and the functional surfaces of each part are first defined at this level of design. In many manufacturing contexts, functional surfaces are generated by machining operations. Thus, strong constraints on burr formation and deburring operations appear during the design of the product structure.

However, the global view of the product does not allow the designer to picture how parts are manufactured. Analyses on manufacturing are made on isolated parts. The methodology considers alternately the view of the product and the different views of the parts. The part view supports embodiment design and enables manufacturing analyses (in particular, an analysis from a burr formation viewpoint can be performed); the product view supports the structural design and receives constraints brought by investigations on manufacturing, particularly on burr prevention, from parts analyses.

1.3 A CONTEXT OF COOPERATION

Making manufacturing easier during design obviously requires investigations from designers and specialists of manufacturing. Especially for accurate aspects of

manufacturing such as deburring, specialists are required because only they have the capacity to raise manufacturing difficulties and to find improvements. The proposed methodology is a support for a cooperation between designers and specialists of manufacturing in order to raise design solutions fitted to the manufacture.

2. Classification of machining burrs

The methodology uses a burr classification derived from Nakayama and Arai [3]. Burrs are classified based on direction and motion between the machining tool and the part edge, during burr formation. An entrance burr (Fig.1a) is formed when the tool encounters an edge of the part. It is a small size burr, and generally, it does not cause much problem. In this paper, the fact that an entry brings no burr formation is considered. An exit burr (Fig.1b) is formed when the tool exits the part. A side burr (Fig.1c) is formed when the tool goes alongside a new part edge. Exit and side burrs are large; they cause problems discussed in the introduction of this paper.

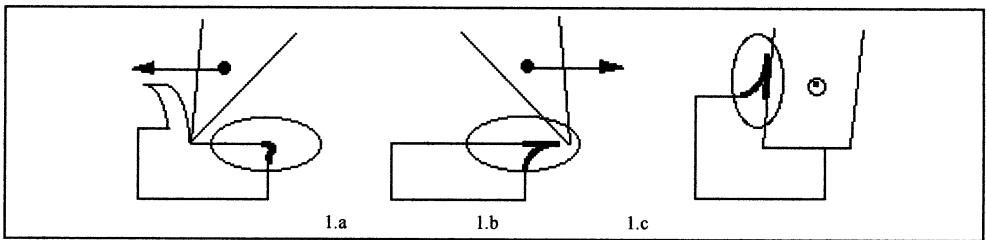


Fig.1: entrance, exit and side burrs. Arrows represent cutting directions.

3. Guidelines for reducing deburring costs in the design to fabrication cycle

Several studies have formalized observations for reducing deburring costs in the design to fabrication cycle [4], [5], [6]. Tab.1 presents some of them. These observations provide a decrease in deburring costs, either by avoiding burr formation or by simplifying deburring operations. During the design, these observations are bound to become guidelines for burr prevention. They enable investigations on the various levels of the design to fabrication cycle.

Tab.1: observations concerning burr formation (type A) and deburring (type B), integrated on various levels of the design to fabrication cycle.

Observations / guidelines for machining tool paths	
A-1	In end milling, up milling generates an exit burr, down milling does not [6], (Fig.2).
A-2	In end milling, a normal entry of the milling tool forms an exit burr, a circular entry can avoid exit burr formation [6], (Fig.3).
A-3	Consequence of observations A1 and A2: in end milling, burr formation can be avoided for machining features such as "plan", "step" or "slot", by an adapted tool path.

Tab 1 is continuing on next page.

Observations / guidelines for process plan sequencing	
A-4	If two machined surfaces abut (share an edge), and if the machining operation of one of these two surfaces forms an entry burr on the shared surface, thus, this machining operation must be processed after the other one, in order to finally obtain an entry burr (no trouble).
A-5	If two machined surfaces abut (share an edge), and if no machining operation of one of these two surfaces forms an entry burr on the shared surface, it can even be possible to put the burr at a place where no problems occur.

Observations on the forms of parts	
A-6	Forms of a part can often be designed in order to put the burr at a place where no problems occur.
A-7	An "edge angle" is the convex angle on a part between two edges which abut (share edge). More the edge angle is large, more the burr size is low. For an edge angle approximately larger than 135°, the burr size is insignificant (Fig.4).
A-8	Part forms can be designed in order to obtain a large edge angle. This result can be reached, for instance, by designing a chamfer.
B-1	Inversely, long and fragile burrs appear on a small edge angle. Thus, deburring is easier on small edge angles (Fig.5).

Example of observation on burr accessibility	
B-2	It can be possible to put the burr at an easy to access place (From [4]).

Example of observations on machining tool choice	
A-9	A form cut operation avoids burr formation. (From [4])

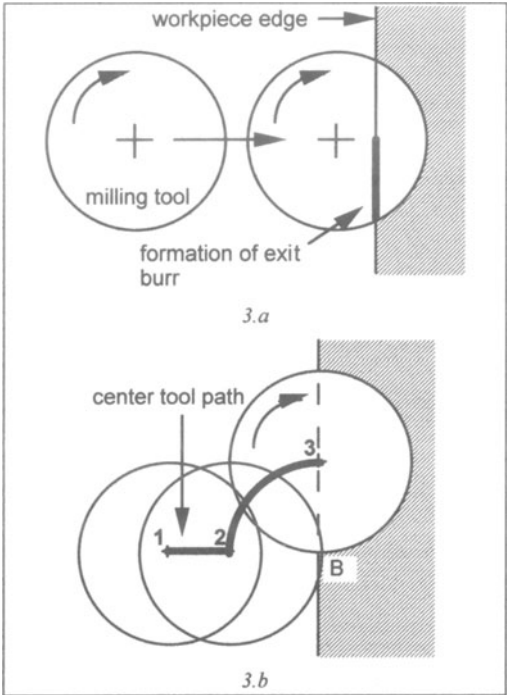


Fig.3: (From [6]) tool entry with orthogonal path (3.a): burr formation; tool entry with a circular path (3.b): no burr formation.

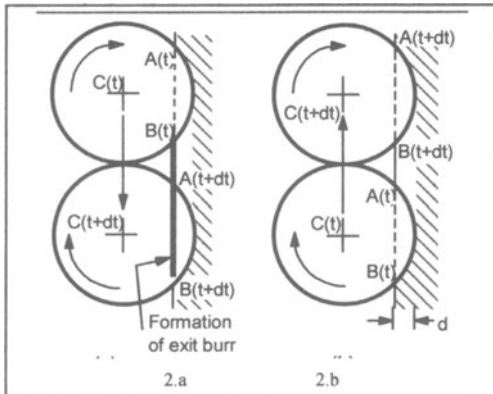


Fig.2: (From [6]) In end milling, up milling generates exit burr (2.a), down milling does not (2.b).

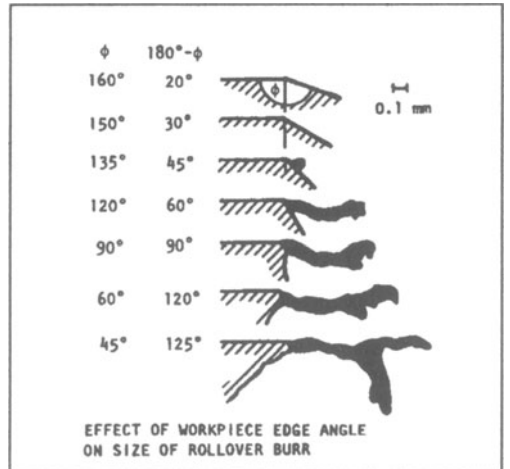


Fig.4: (From [4]) influence of the edge angle on burr size.

4. A methodology to avoid machining burrs in structural and embodiment design

The proposed methodology is presented in this section. The general scheme is shown in figure 6. This presentation is illustrated by an example of design: the design of a pneumatic gripper.

This methodology is integrated during the structural and detail designs. Figure 5 presents an analyzed structure of a product. Some design alternatives are tested at this level: the analyzed structure is characterized by a spring return single acting cylinder and a toggle link. At this level, it is difficult to get

an evaluation on manufacturing (manufacturing costs, feasibility...), and especially on deburring. The aim of the methodology is to enable manufacturing investigation (and particularly investigation on deburring) at that early level of design.

The philosophy of the methodology is not restricted to only burr issues; in a larger view, it comes in the framework of a larger integration of manufacturing. The methodology involves considering burr issues simultaneously with process planning, tool machine selection, tool path generation. However, in this paper, only the burr analysis is described.

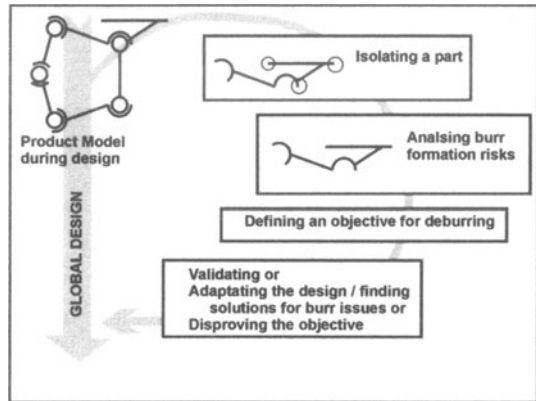


Fig. 6: scheme of the methodology.

FIRST TASK: ISOLATING PART FROM PRODUCT VIEW

Parts must be analyzed one by one, from the manufacturing viewpoint. As proposed in figure 7, the first task consists of isolating a part from the product view and taking stock of the functional constraints, which have already been expressed (Fig.7).

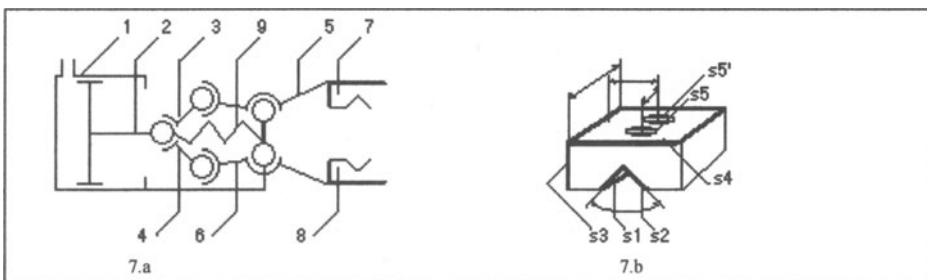


Fig.7: structure of the analyzed pneumatic gripper, and the isolated part (jaw 7). Functional constraints appears on fig.7b as functional surfaces (bold) and functional dimensions .

In the present paper, only the analysis of the jaw part (part 7) is presented. In particular, functional constraints of this part are the various functional surfaces (the V-block imposed form for component handling, planes for positioning, holes and threads for clamping).

SECOND TASK: ANALYZING BURR FORMATION RISKS

The second task consists of analyzing burr formation risks. The part must be analyzed at once from the manufacturing and functional points of view. The manufacturing analysis gives an inventory of the edges on which a burr may be formed (Fig.8). The edges are the border of machined surfaces. The functional analysis focuses on each selected edge. For each one the question is: what is the trouble caused by burr: dysfunction, problems in assembly, risks of injuries?

Concerning the example of the "jaw" part, all the burrs present problems. Burrs on edges e3 and e4 cause problems on the use of "jaw"; e1, e5, e6 hinder assembly operations; the others bring risks of injuries for workers.

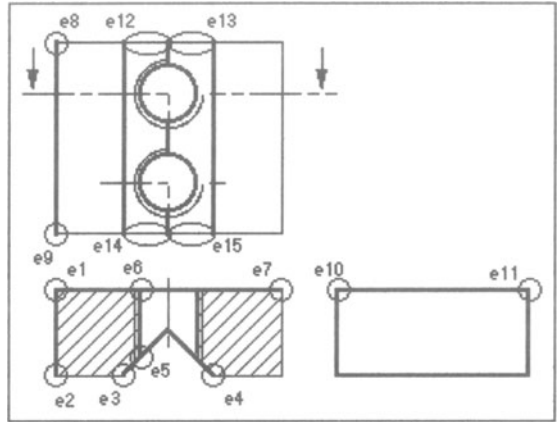


Fig.8: inventory of the edges where burrs can appear.

THIRD TASK: DEFINING AN OBJECTIVE FOR DEBURRING

The third task consists of defining an objective for the deburring of the part. This objective can be either "to avoid totally the deburring", or "to facilitate deburring operations". In the first case, the design of the part will follow type A guidelines (table 1); in the other case, type B guidelines will be used. Fixing an objective is needed at this moment because investigations for avoiding deburring or simplifying deburring are different and require different guidelines. In some cases, they have an opposite effect. For instance, guideline A-8 (table 1) advises enlarging edge angle; in contrast, guideline B-1 advises reducing edge angle.

Concerning the "jaw" part, the fixed objective is to totally avoid deburring operations.

FOURTH TASK: VALIDATING OR ADAPTING THE DESIGN / FINDING SOLUTIONS FOR BURR ISSUES OR DISPROVING THE OBJECTIVE

This task consists of finding solutions for the fixed objective, and validating it, (or, invalidating it if it is not possible). In the case of invalidating, another less ambitious objective will be fixed.

For each edge, a solution must be found in order to reach the objective. It is a design task, thus, the creativity of designers and manufacturers must be involved. However, guidelines presented in table 1 bring suggestions for deburring prevention. Table 2 summaries the solution finding process, in the case of the part taken as example.

Let us see how solutions for deburring prevention can be found in the case of the "jaw" part. Edges e3 and e4 (Fig.8) have a large edge angle (135°). According to the guideline A-7, no burr will be formed on these edges.

Concerning the other edges, investigations on deburring require some piece of information on the machining process of the part (machine-tool selections, process planning, etc). At this state of product development, these pieces of information present obviously some uncertainty. Hypotheses must be made. The way to bring these hypotheses is discussed in the conclusion of this paper.

The jaw part has a plan form, with functional surfaces on each side. Thus, two milling set-ups are required. They are described in figure 9: set-up 10 generates surface s4; set-up 20 generates s1, s2. Surface s4 is end milled, thus edges e1, e7, e10 and e11 (according to guideline A-3) can be avoided. Surfaces s1 and s2 form a step feature, thus edges e12, e13, e14, e15 can be avoided (according to guideline A-3). Surface s3 is generated by horizontal milling, in set-up 10 or 20.

Two problems occur: during the operation where s3 is generated, the fixturing of the part is difficult on the direction orthogonal to s3; generating s3 can form burrs because no guidelines are known for avoiding side burrs.

The solution which has been found is to slightly modify the structure of the product, in order to replace the plane surface s3 by a step feature s3, s3' (Fig. 10); the part 7 just needs a small modification, but the functionality remains identical. According to guideline A3, burr formation can be avoided on the new edge e2. Moreover, the part can be easily positioned and clamped by a parallel vise. Burrs on edge e1 can be avoided if surface s4 is generated after s3 (according to guidelines A-4 and A-3).

Concerning the edges e5 and e6, the proposed solution is: first, generate holes s5 and s5' in set-up 10; generate a chamfer on these holes; turn the part up and generate the step s1-s2 on set-up 20; - realize threads t5 and t5'.

A 4 axis milling machine is needed for set-up 20 because step s1-s2 and threads t5 and t5' have two different machining directions. According to guideline A-8, burr formation is avoided on edge e5 (entry burr only), and on e6 (135° edge angle). A supplementary surface must be machined in set-up 10 for

Cutting op. on surfaces:	edges	preventive action types:
Set-up 10		
s3, s6 and s7	e2, e8, e9	A-3 (step)
s4	e7, e10, e11, e1	A-3 (plane) A-4 (s4 after s3)
hole s5, s5'	-	-
chamfer c5, c5'	-	-
Set-up 20		
s1, s2	e3, e4, e12, e13, e14, e15	A-3 (step) A-7 (>135°)
thread t5, t5'	e5, e6	entry burr, A-8 (chamfer)

Tab.2: Strategy for burr avoidance of the jaw part.

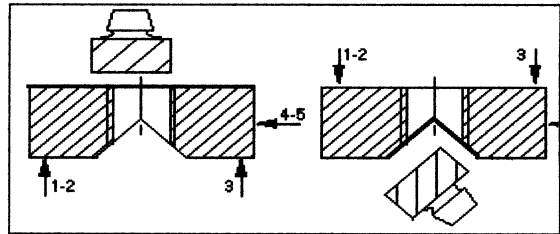


Fig.9: description of machining set-up 10 and 20.

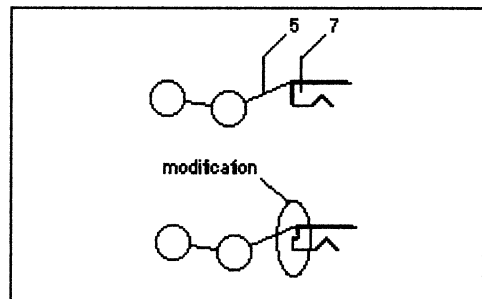


Fig.10: modification of the product.

positioning the part, in order to center the threads with enough precision (abutment on surface s7).

Conclusion

The final part is presented in figure 11. Deburring is totally avoided for machining this part: the fixed objective is successfully reached. Part forms and product structure have been influenced by the burr prevention methodology. Constraints for avoiding deburring are given on different aspects of the design to fabrication cycle: design, process planning, set-up definitions and tool path. An important interest of the presented methodology is to bring all the decisions concerning burr prevention together, at an early stage of design. In this way, it is possible to select the more adapted guidelines for burr prevention.

This presented methodology can bring important savings. A lot of time to deburr parts is eliminated or greatly reduced. Even if the use of type A-3 preventive actions increases the machining time (adapted tool path), this increase is many times smaller than the time which would be necessary to manually deburr the part. Moreover, suppressing deburring operations brings savings on manufacturing management (shorter times, less stock, less workpiece moves...) and on implementation (one less operation to study, no more investments for deburring process...). This methodology can be extended to simplify other aspects of manufacturing. For instance, limiting the number of machining set-ups, validating and simplifying part fixtures, etc. Necessary information on machining, for burr prevention (as seen in section 4-Fourth task) can be obtained in this way.

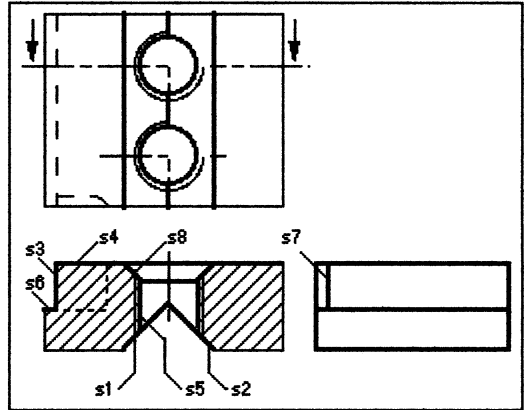


Fig.11: the "jaw" part after applying strategy for deburring prevention.

References

1. GILLESPIE L. K.: *Deburring technology for improved manufacturing*, edited by the Society of Manufacturing Engineers (USA), 1981.
2. STEIN J., DORNFELD D., *Integrated Design and Manufacturing for precision Mechanical Components*, Proc. of 1st IDMME Conference, PRIMECA / CIRP, Nantes (France), 1996.
3. NAKAYAMA K., ARAI M., *Burr formation in metal cutting*, annals of the CIRP, vol. 36, no 1, 1987, pp. 74-80.
4. GILLESPIE L. K., *Basic approaches to minimizing deburring costs*, in *Advances in deburring*, edited by the Society of Manufacturing Engineers (USA), 1978.
5. NARAYANASWAMI R., *A burr advisor for collaborative CAD system*, Ph.D. Thesis, University of California at Berkeley (USA), 1995.
6. BLONDAZ L., DORNFELD D., 1996, *Avoiding exit burr in CNC end milling by determining an adapted tool path*, U. C. Berkeley, Engineering Systems Research Center Technical Paper (USA), May 1996.

Chapter 8
INTEGRATED DESIGN METHODOLOGY
AND APPLICATIONS. DESIGN AND COMMUNICATIONS

Engineering design : management of information and uncertainty.....	481
C.A. MCMAHON	
Towards a need satisfaction oriented computer aided design	489
F. LIMAYEM and B. YANNOU	
Aided design of brass musical instruments	497
J.F. PETIOT and J. GILBERT	
Environmentally-conscious design and materials selection	505
ULRIKE G.K. WEGST and M. F. ASHBY	
Design knowledge representation for constrained-based design in CAD systems..	513
C. LENGUIN and P.A. YVARS	
CONCAD Bridging : Managing the integration of technical solutions in a modularized product concept	521
M.W. LANGE	
Mechanical models management in engineering design	529
N. TROUSSIER, F. POURROY, M. TOLLENAERE and B. TRÉBUCQ	

Proposal to control the systems design process Application to manufactured products	537
PH. GIRARD, B. EYNARD AND G. DOUMEINGTS	
Integrated design of mechanical systems by a concurrent engineering approach ...	545
P. RAY, M. NIGROWSKY, G. GOGU, C. DEMARQUILLY and A. MALLON	
Contribution to a multi-views, multi-representations design framework applied to a preliminary design phase	553
MG-IT collective noun (Coordinator : J.C. LÉON)	
Proposal of a functional model of logistics for spare parts preservation.....	561
N. BAUD, M. MEKHILEF and J.C. BOCQUET	
A generic model for know-how capitalization	569
J. LE CARDINAL	
Web-based product information visualization through VRML code generation	577
YOONHO SEO	
Collaborative design in education : the TAXIA project.....	585
B. RAMOND	

ENGINEERING DESIGN: MANAGEMENT OF INFORMATION AND UNCERTAINTY

C. A. McMAHON

University of Bristol

Department of Mechanical Engineering

University Walk

Bristol, BS8 1TR

England

Computers are extensively used in design, but provide limited support in managing the diverse information used by design teams, and in handling design uncertainty. This paper describes research aimed at understanding how engineers use information in design, and how they deal with uncertainty, and then uses this understanding to suggest guidelines for the development of design support tools. The nature of design is first discussed, and then results are presented of studies by questionnaire and case-study of designers' information requirements, and of risk management in design. The importance of experience, personal contacts and informal information is emphasised, as is the need for tools to manage risk information to indicate project risk.

1. Introduction

The engineering design process is today dominated by the use of the computer. Computer-aided design (CAD) systems have replaced the drawing board as the means whereby engineering designs are represented and communicated; reports, letters and other project documentation are generated using computers; for many companies finite element analysis is a standard tool for engineering stress and dynamic analysis. But despite the ubiquitous use of computers, many aspects of the designer's work are not well supported by computer tools. In particular, the process whereby engineering concepts are identified and developed is often much as it was 20 or 30 years ago. In the early design stages, the design process is very dependent on the skills, experience and knowledge of the design team, and in these areas computer support has been limited.

During the design process the design team has to make decisions concerning the concepts to incorporate in the product, the materials and manufacturing processes to employ, the design parameters and so on. The team has to make these decisions with severe constraints on time and on available human and other resources. In the early stages of the design process there is often much information missing on which to base

such decisions, and uncertainties persist throughout the process. The design process can be characterised as “decision making under uncertainty with limited resources”.

In recent years there has been world-wide realisation of the importance of the sharing of information and knowledge to successful product design. This realisation has come from studies of the design process, of designers at work, and of computer tools for design support. From these studies a number of observations can be drawn.

The first group of observations concern the nature of the design process. They identify that design is predominantly a collaboration between specialists, proceeding by their consent at decision points in the design process. Specialists use their own representations and techniques, and share information using a common vocabulary (Bond and Ricci, 1992). During the design process, the understanding of the design problem itself, and of its solution, are developed in parallel (Roozenberg and Cross, 1991). This development involves *refinement* of the design model. Refinement may involve replacing abstract information with that which is more concrete, the addition of detail (addition of information), choosing between alternatives, or replacing approximate information with that which is more exact.

The second group of observations concern information support. During the design process, designers make continual requests for information to support their decisions, and also make extensive use of their personal knowledge and experience for decision making (Kuffner and Ullman 1991, Stauffer and Ullman, 1991). Engineers spend as much as 40% of their time in information search and retrieval (Cave and Noble, 1986), but search is often unsuccessful. They often fail to find useful information, even when it is available, because they do not *know* it is available, or because the cost of obtaining it in a useful form is too high (Salzberg and Watkins, 1991).

The importance of knowledge and information is so great that it is seen as a foundation for design research. Konda *et al* (1992) view “shared memory” as a mechanism for embodying context and shared meaning in design and as a central issue in design research and practice. This arises from the view that “design demands the linkage of disciplines without being a discipline in itself”, but that “it is impossible *a priori* even to identify completely which disciplines are required to be involved for a specific design problem except through past records of similar cases - shared memory”.

From these observations can be seen the need to go beyond the relatively limited support for product modelling and representation provided by the present-day CAD/CAM systems and to embrace new approaches to information management. Mechanisms must be identified for storing and sharing design intent, rationale, function and constraints, as well as to model and represent the design problem. Tools must be provided to assist the designer in organising personal information, and in finding and using information stored by others.

2. Empirical study of engineering design practice

There are two main strands to our design research programmes: the development of computer-based techniques for design support, and the industrially-based study of design practice. This study underpins the work on tool development, and guides its

direction, and involves questionnaires, interviews and case studies involving engineers from various contexts. Two studies in particular are reported here.

2.1 THE INFORMATION NEEDS OF ENGINEERING DESIGNERS

The first of the studies of design practice was concerned with the information needs of engineering designers, and involved a survey of design engineers working at various levels in industry, followed by case studies in a number of design situations.

2.1.1 *Survey of engineering designers*

The questionnaire survey involved 208 respondents from small, medium and large engineering companies. These were design staff at various professional levels, and with various professional qualifications, from Chief Designer to Draughtsman. The questionnaire was concerned with the operating procedures employed in the design functions of the respondents' companies, with the methods for recording design decisions, and with the frequency of use and perceived value of various sources of design information. The key findings from the work were (Court *et al*, 1993):

- Designers spent less than 50% of their time in the process of designing. Searching for information accounted for 18% of time, paperwork 23% and meetings 16%.
- The hand-written design logbook was the predominant means of recording personal design activities, and was used by about half the respondents. Project files were next most popular, used by about one quarter. Very few respondents used a formal quality assurance system to record personal design progress.
- The design handbook was also widely used to record project design decisions (19% of respondents). Other popular mechanisms were project diaries (7%), internal memoranda (19%) and project reports (30%).
- Journals and magazines were considered an important source of information, with over half of respondents considering them “important” or “very important”. However, professional and trade journals were far more widely read than academic journals, which were almost unknown among the respondents. Within journals and magazines, product data and adverts were considered the most useful data sources, although features and articles were also rated highly. Magazines were stored by 46% of respondents, but only indexed by 15%, in spite of their perceived value.
- Company libraries were maintained in a variety of ways, but only about 15% of respondents used a formal organisation. There was some use of external libraries - mainly for information about standards, and on specific techniques and processes.
- Suppliers are a very important source of information. The most important information entities obtained from these were data and specification details, technical performance data, drawings and operating and applications information.
- Catalogues were regarded as important sources of product knowledge and ideas, specifications and details, product data and supplier/competitor information.
- Drawings were stored as hardcopy, as microfilm or microfiche or as CAD files, with no dominant mechanism. Indexing was by drawing or project number, with little formal attempt to index by other attributes.
- Perhaps the most important information sources are the designer's personal

experience and that of his or her colleagues, rated by the majority of respondents as highly important, and, from within the companies, product design specifications, previous design schemes, design reports, data handbooks, parts catalogues, design guides and manufacturing data were also perceived as very important. Many of these are not incorporated in formal Product Data Management systems.

- Data storage mechanisms were highly traditional. Personal information systems mainly consisted of desk and drawer, or filing cabinet and shelf.
- Subsequent work has shown that the operation of group information storage systems - e.g. shared filing systems or technical libraries - can be very variable even within one company. The success of such systems is very dependent on the trust that the group members have in the person responsible for maintaining the system.

2.1.2 Case studies

The questionnaire survey highlighted the importance of personal and local information sources, the strong role of suppliers, and the role of informal information entities such as catalogues, reports, sketches or handbooks. This was reinforced by case studies which examined twenty design cases drawn from seven companies of various sizes and engineering domains. These are reported by Court *et al* (1996), and show a strong preference among engineers for following well-established, proven information access paths, and for using familiar information sources. Also shown strongly was the widespread use by engineers of information from memory. On average about 30% of information used in the case studies (e.g., choice of a material, a dimension or a tolerance) was from memory. The studies supported the observation that “the essence of mechanical design seems to rely very little on problem solving techniques but rather on a richness of knowledge” (Stauffer and Ullman, 1991). What was surprising was that the observations varied much less with company type or design task than expected.

2.2 A SURVEY OF RISK MANAGEMENT PRACTICE IN INDUSTRY

In 1997 a second survey was carried out, this time to investigate risk management practice in design. Again, the survey comprised a questionnaire followed by a number of case studies. In this work we wished to explore a number of aspects of risk management, including the perceived need, the techniques applied, the software tools used, where risk was perceived to be most difficult to identify, and what differences there were in practice between different sectors. The work was carried out against a background of rapidly increasing interest in risk management in industry, and the publication of important books on the topic (Chapman and Ward, 1997)(Carter, 1994).

The questionnaire was completed by 63 respondents from industries including aerospace, automotive, power generation, coastal engineering, petrochemicals and manufacturing, as well as consultants. The questionnaire was in two parts, and distinguished between technical risk and project risk. Technical risk is the risk that a programme will not meet technical objectives - e.g. that the performance of the artefact will be lower than required, or that weight or manufacturing costs will be too high. Project risk concerns risks that the project will over-run its time or cost budgets.

In the early part of the study, a general risk management model was identified. This

models risk management as a cyclic sequence of risk identification, prioritisation and modelling, the stages of which are broadly as follows:

- *Goal definition.* This involves identification of measurable control parameters and determination of a base plan (the planned structure of project elements if no risk events occur) and risk management plan. The identified and recorded risks represent deviations from this plan.
- *Identification.* This stage involves identification of both risks and opportunities, and of the members of the project team who are most closely concerned with those risks (the “owners”). Techniques such as brain storming and checklists are used. Risks are often recorded in a risk register.
- *Risk impact and probability evaluation.* The impact and probability of risks is identified and recorded where possible. Numerical evaluations are given wherever possible, and recorded in the register.
- *Risk prioritisation.* The evaluated impact and probability for each identified risk are used to determine which risks should be included in the risk model.
- *Modelling relationships.* Relationships are modelled in terms of time, cost, performance or other measures. Some methodologies reduce everything to cost.
- *Mitigation and contingency.* The base plan is changed to reduce probability or impact. Contingency plans are triggered and trade-offs identified.
- *Budgets.* Budgets are allocated and monitored for measurable/controllable parameters.
- *Risk monitoring.* Monitoring of the identified risks takes place. Probabilities and impacts are updated. New risks arise. Existing risks are eliminated. Trigger events are monitored.

The respondents to the questionnaire survey identified a significant need for risk management. The pressure to incorporate it into the product introduction process comes from demands by clients (especially government clients e.g. for military hardware), from the needs of decision makers, and from the reduction in cost-plus type contracts. Nevertheless, despite the need, there is some reluctance on the part of companies to implement serious risk assessment procedures.

The risk management techniques that were applied by the respondents’ companies were mainly qualitative, with widespread use of “risk registers” to record risks, owners and actions. Quantitative methods were not widely used, but if used were always probabilistic and not fuzzy. The software packages that were used were generally quite simple. A number of programs were developed in-house, and also a number of respondents used spreadsheets with Monte Carlo simulation capabilities added.

Some of the most interesting results of the survey came from the question concerning the sources of technical risk. Respondents were asked to identify potential sources of technical error as “not difficult”, “quite difficult”, “difficult”, or “extremely difficult” to deal with. The aspects considered “difficult” or “extremely difficult” to deal with by the most respondents were aggregate budget overruns (55%) (where budgets include cost, weight etc.), design errors (53%), sub-system interactions (47%) and product usage (43%) (understanding the loads and usage that a product will be subjected to during its life). Respondents were also asked how often technical risk

arises in each area, and here usage, sub-system interactions, materials and aggregate overruns were the most important areas. Design error was considered to occur only “occasionally” or “never” by 62% of the respondents.

The survey covered a number of other topics, and is reported in full by Crossland *et al* (1998). The most important conclusion from the work from the point of view of future design methodologies is that while many companies collect data about risk, the incorporation of quantitative models into risk management is rare. Improved techniques are needed to link data collection with predictive and modelling methods.

3. Requirements for support tools

Throughout the information survey work the themes that arose repeatedly concerned the importance to the designer of personal contacts, of informal information sources such as magazines and catalogues, and above all the issue of *experience*. Far Eastern companies are able to organise and exploit this experience because their engineers move jobs relatively infrequently and accept long training and learning periods. In the West, especially in Anglo-Saxon countries, engineers move jobs frequently and often want to progress rapidly to supervisory and managerial positions. It is contended that, if the West is to compete in knowledge-intensive industries, it should move towards a system where the accumulated experience of an enterprise is stored within its information systems, and engineers will then be able to develop generally applicable information handling and problem solving skills which will be used to manipulate these resources.

To some extent, knowledge-based systems have addressed the question of knowledge representation and retention, but they have perhaps gone too far in removing the processing of information from the user. Knowledge-based engineering is very appropriate for well-defined parametric engineering problems, but for less well-defined problems they should support but not replace the engineer’s decision-making processes.

The risk management survey also showed that experience is very important. “Personal experience of similar projects” was the most widely used technique for identifying risks. Industrial experiences may make engineers more or less sensitive to risk. In this area we therefore need mechanisms that allow understanding about risk to be shared, recorded and re-used. This implies the development and use of risk databases, with the use of numerical data where possible, and implies also a better understanding and recording of the design process.

The remainder of this section will explore what might be the nature of the tools that can support the management of information and uncertainty in design.

3.1 INFORMATION SUPPORT

Through the development of CAD/CAM and Product Data Management systems, tools have been provided for the management of product data within an enterprise. Where present-day computer systems have failed to provide support is in tools for personal

information management, for information management among small groups, and for management of informal design data such as catalogues, guidelines, magazine articles and so on. If design logbooks and paper files are used, much of the information they contain is inaccessible to the enterprise except through the memory of those who have produced the documents. The survey results imply that new support needs to be provided at three levels:

- At the lowest level, a designer should be provided with tools to record and index all manner of computer files together with notes, sketches, telephone conversations and even video, in effect to provide a computerised design notebook.
- At the next level, design teams should be provided with mechanisms for indexing and then organising their collected information. These team information sets should build on the designers' information resources, to allow the designer's experience to be shared.
- At the top level, supply organisations, publishers and other large groups should be provided with the mechanisms for making their information available to others. This information might include catalogues, articles, even advertisements.

In each case, the support tools should be compatible with those at the other levels. The design team tools should be able to build on the designers' information sets, and should be able to cross-refer to or incorporate the information from supply organisations, publishers and so on. A key factor in the ultimate success of such systems will however be the capability of including information entered as brief sketches and notes, and also the facilities for the rapid entry of historic paper-based data.

Importance of personal contacts in design also suggests that, as design activities become more widely spread geographically, video conferencing and shared workspace systems will become more important. It also suggests that techniques are needed to assist individuals in maintaining their networks of connections to information sources, and that a computer tool capable of storing, managing and displaying these networks, for example using the technology of the World Wide Web, would be most useful.

3.2 RISK MANAGEMENT

The risk management survey suggests that in this area there is also a pressing need to provide tools to assist design teams in accumulating and sharing knowledge and information, but there is also a need to provide tools to process and manipulate this information. Some risk information comes into the category of informal design information, but much must be recorded within formal product models, which should be extended to allow for uncertain attributes, and also to allow other aspects of uncertainty to be modelled such as missing information or unresolved choices.

The primary requirement for assistance in the processing and manipulating of risk information concerns the need to be able to use collected or historic risk information to give an indication of the risk status of a new project. In particular, a project manager needs to be able to estimate the effect of the accumulated risk elements within a project on the overall risk in the programme. This implies the need to be able to accumulate uncertainties in the attributes of parts and sub-assemblies in a design to given an

overall design risk. Decision making should be on the basis of accumulation of measured data.

Finally, in risk management there is a need for simple mechanisms to assist in risk identification. These might include automated risk checklists, prompts or aids to brainstorming and methods of storing historical records of types of risk.

4. Conclusions

In recent years the development of design support tools has concentrated on assisting the representation of models of the product, and on attempting to formalise design processes and tools. The surveys of designers reported in this paper have shown the importance of less tangible factors such as the designer's experience, local sources of knowledge and information, contacts with colleagues and suppliers and the like. They have also indicated the aspects of design in which uncertainty is found to be important, and have highlighted the need for risk management methodologies.

5. Acknowledgements

The author is grateful to Andy Court, Rose Crossland, Steve Culley and Jon Sims Williams, whose work is reported here. Support for the work by grants from the UK Engineering and Physical Science Research Council is also acknowledged with thanks.

References

- Bond, A.H. and Ricci, R.J. (1992) Co-operation in aircraft design, *Research in Engineering Design* **4**, 115-130
- Carter, B. (1994) *Introducing RISKMAN Technology: The European Project Risk Management Methodology*, NCC Blackwell Ltd., Oxford.
- Cave, P.R. and Noble, C.E.I. (1986) Engineering design data management, *Proc. 1st Int. Conf. Engineering Management*, Swansea, UK
- Chapman, C.B. and Ward, S. (1997) *Project Risk Management: Processes, Techniques and Insights*, John Wiley and Sons, Chichester, UK
- Court, A.W., Culley, S.J. and McMahon, C.A. (1993) A survey of information access and storage amongst engineering designers, The University of Bath, Bath, UK
- Court, A.W., Culley, S.J. and McMahon, C.A. (1996) Information access diagrams: a technique for analysing the usage of design information, *Journal of Engineering Design* **7**, 55-75
- Crossland, R., Sims Williams, J.H. and McMahon, C.A. (1998) Survey of current practice in managing design risk, EPSRC Grant No. GR/L38745, Final Report, University of Bristol.
- Konda, S., Monarch, I., Sargent, P. and Subrahmanian, E. (1992) Shared memory in design: a unifying theme for research and practice, *Research in Engineering Design* **4**, 23-42
- Kuffner, T.A. and Ullman, D.G. (1991) The information requests of engineering designers, *Design Studies* **12**, 42-50
- Rozenberg, N. and Cross, N. (1991) Models of the design process- integrating across the disciplines, *Proc. Int. Conf. Engineering Design (ICED '91)*, Zurich
- Salzberg, S. and Watkins, M. (1991) Managing information for concurrent engineering: challenges and barriers, *Research in Engineering Design* **2**, 35-52.
- Stauffer, L.A. and Ullman, D.G. (1991) Fundamental processes of mechanical designers based on empirical data, *Journal of Engineering Design* **2**, 113-125

TOWARDS A NEED-SATISFACTION ORIENTED COMPUTER AIDED DESIGN

F. Limayem, B. Yannou

Laboratoire Productique Logistique

Ecole Centrale Paris

92295 Châtenay-Malabry, France

limayem / yannou@pl.ecp.fr

ABSTRACT

In this paper, different approaches are presented in order to automatically estimate the relevance of design performances in terms of a global satisfaction. The first part describes a functional needs expression approach: a bottom-up satisfaction model from lower-level functions to the global satisfaction, taking into account data imprecision and uncertainty at each level. The second part introduces a virtual prototyping design platform, which consists in a primary simulation of some solution performances in order to propagate them through the functional model. Redesign, optimization and risk management capabilities can be imagined, since it is possible to measure the influence of the structural parameter choices over the measure of the global satisfaction and its uncertainty.

1. Introduction

In the beginning, CAD systems were dedicated to geometric product modeling. In the last decade, the emergency of *feature based design* led to a new abstraction level: the technological product model, which consists in a know-how oriented design in addition to pure geometric considerations. A new generation of CAD systems including structural, behavioral and functional views, is presently emerging. The structural model represents the product architecture on multiple granularity levels which can concern abstract concepts as well as component parameters. The functional model consists in a mapping from the general needs to the functions expected from the design. Eventually, the behavioral model represents the way the structure achieve the functions.

Today, CAD evolution requires integrated functional models that automatically and soundly estimate, during the design process, the overall satisfaction relative to a current design alternative. After a brief literature overview, presented in section 2, the functional model, detailed in section 3, introduces different ways of expressing needs

and measuring satisfaction. Before concluding, a CAD application issue that consists in a virtual prototyping design platform is presented in section 4.

2. Related works

The research contributions in functional representation are numerous and they mainly belongs to artificial intelligence and mechanical research fields. Many approaches such as causal processes [CHA.94], axiomatic design [SUH95], bond graphs [CHI.95] and many others focused on the expression of how a device contributes to the achievement of a function set. Feature modeling [TOL.95] or behavior representation [EVE.95] are widely used to link both functional and structural models. The mapping from functions to structure is usually related to design while the mapping from structure to functions characterizes diagnosis. Actually, a design process can be described as an alternation of both tasks.

While structural and behavioral modeling are traditionally established in research, functional representation is comparatively a new issue. Many works focus on how to estimate the achievement of a function that belongs to a functional hierarchy. For example, Wood and Antonsson [WOO.89a] focused on how to map from design parameters to satisfaction estimation, comparing the relevance of both fuzzy logic and probabilistic approaches. Another work [SHI.95] presented an integrated approach, based on the *Functional-Behavior-State* model, including a probabilistic description of how a physical parameter influences a function satisfaction.

Among the existing models, the *functional analysis* methodology (FA) approach is one of the most used in practice. It consists in a decomposition of the general needs in a set of expected functions organized in a hierarchical tree. A set of functional criteria is associated to each leaf function in order to measure its contribution to the overall satisfaction for given solution performances. Those aspects are detailed in the French standards NF X 50-150 et 151. In practice other methods, such as Quality Function Deployment (QFD), use a graph representation with non linear propagation. In general it is difficult to state that satisfaction propagates in linear or non-linear manner. This paper aims to present a generic functional model with different alternatives to express the relevance of a design solution in terms of an overall satisfaction measure.

3. A satisfaction model

1.1. THE MODEL STRUCTURE

We assume that the need expression stage leads to a set of functions. The identified functions are organized through an oriented functional graph (Fig. 1). The satisfaction model, based on this graph, aims to evaluate the overall satisfaction of a design alternative. Other approaches, such as multiple criteria decision, lead to an ordered set of solutions with no quantification of their overall satisfaction.

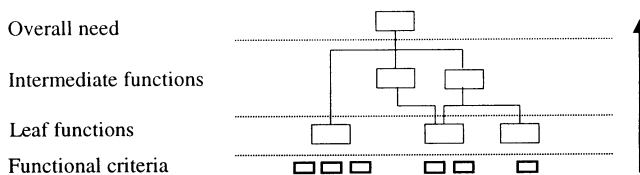


Figure. 1: Functional graph

While building the graph and for automatic estimation sake, each decomposition of an intermediate function F_i into n children functions F_{ij} have to be argued by an explicit satisfaction law of the form¹:

$$S(F_i) = f(S_{i1}(F_{i1}), \dots, S_{in}(F_{in})) \quad (1)$$

In the same way, the satisfaction of a leaf function F_i depends on the performance parameters V_{ij} ² of a given solution as follows:

$$S(F_i) = f(V_{i1}, \dots, V_{in}) \quad (2)$$

Unlike formula (1), the satisfaction of a leaf function depends directly on the performances of a solution and not on some intermediate satisfactions. (see [LIM.96] for further details). In the particular case where functional criteria are not coupled, the notion of criterion satisfaction makes sense and the following simplified formula can be used:

$$S(F_i) = f(S_{i1}(V_{i1}), \dots, S_{in}(V_{in})) \quad (3)$$

1.2. SATISFACTION LAW FORMULATION

In order to express satisfaction laws of the model, a fuzzy logic based approach seems to be the more appropriate. According to Fig. 2, different ways are suggested in order to express satisfaction laws.

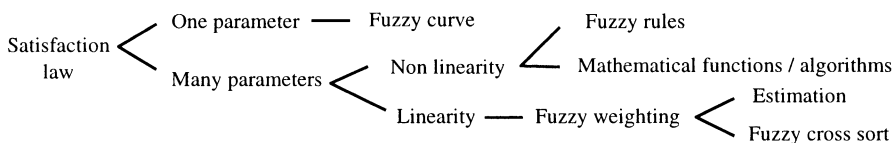


Figure. 2: Satisfaction law formulation alternatives

1.2.1. The satisfaction law depends on one parameter

This happens when, for example, a leaf function is associated to only one functional criterion: $S(F_i) = f(V_i)$ in formula (2). In Functional Analysis, French standards suggests to define for each criterion a target level and acceptance boundaries for which a solution

¹ In this formula, f represents the satisfaction law.

² The performance parameters of a solution correspond to functional criteria that characterize leaf functions.

performance is considered satisfactory. Such a specification, that gives no information about the decrease in satisfaction when the target is not achieved, can be represented by a rung (Fig. 3). In formula (1), each $S_{ij}(F_{ij})$ (respectively $S_{ij}(V_{ij})$ in formula (3)) represents a one-parameter depending satisfaction law.

A fuzzy membership function, which express the imprecision of the statement « this value is satisfactory » (Fig. 3), seems more appropriate for satisfaction representation.

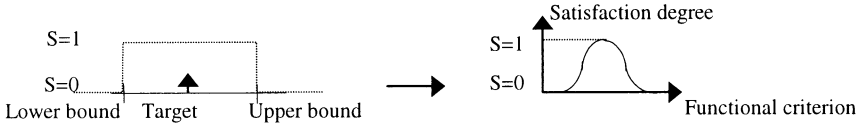


Figure 3: Representation of a one parameter depending satisfaction law

1.2.2. The satisfaction law depends on multiple parameters

When satisfaction depends on multiple parameters, two cases can be considered:

1. The satisfaction law is a linear function of the parameters it depends on. Thus, each parameter can be associated to a weight.
2. The satisfaction law is a non-linear function of the parameters it depends on. Thus, the designer can either approximate it as linear in narrow neighborhoods of a given alternative (redesign) or express this non-linearity.

The non-linear approach that is less common even if more realistic is developed in the following sections. Two ways of expressing a multiple variables non-linear satisfaction can be considered:

1. An explicit formulation using mathematical functions.
2. An implicit formulation using fuzzy rules.

Mathematical functions. The mathematical formalism can be used to represent a linear or a non linear aggregation of a set of parameters. Satisfaction laws aggregation can be of multiple types including either union, intersection or weighted averages. They can be also organized into algorithmic structures that require initial values (performances) to compute the resulting satisfaction.

The way aggregated performances (in an overall solution) are appreciated is often subjective and hard to represent. Thus, aggregation operators must be able to represent different decision approaches. In the field of design optimization, Diaz [DIA.88] used a fuzzy operator that consists in a weighted average between union and intersection to aggregate a set of fuzzy objectives. A sensitivity measure allows the user to adjust the aggregation operator as well as specific objective satisfaction functions. Another application led by L. Thurston [THU.91], consisted in estimating a design alternative relevance using a non-linear aggregation of multiple attributes (performances) utility functions. The aggregation formula includes scaling factors which allow different decision approaches to be represented.

Fuzzy rules. Each fuzzy rule is composed of a premise and a conclusion in the following form:

If price is low **and/or** surface area is medium **Then** satisfaction is medium

An assertion of the type: « *price is low* » is modeled by the *membership function* of « *low* » linguistic value (or adjective) applied to « *price* » linguistic variable. This membership function associates for each price interval value a likelihood degree value between 0 and 1. Starting from a fuzzy rules base giving in conclusion a leaf function satisfaction and referencing solution performances (corresponding to functional criteria) in premises, a fuzzy inference engine will be able to determine the satisfaction level of this function. This satisfaction evaluation benefits from fuzzy logic qualities of robustness and output continuity.

Let us take the example of a rule base expressing the satisfaction for the function « buying a house ». For simplicity, only the three following functional criteria will be considered: *distance* from the workplace, *surface* area and *price*. Each functional criterion plays the role of a linguistic variable. In a first stage, the universe of discourse of each linguistic variable must be defined ; in our case it is similar for all variables and equal to {*low, medium, high*}. Next, all membership functions must be defined for each linguistic variable/value couple (see Fig. 4).

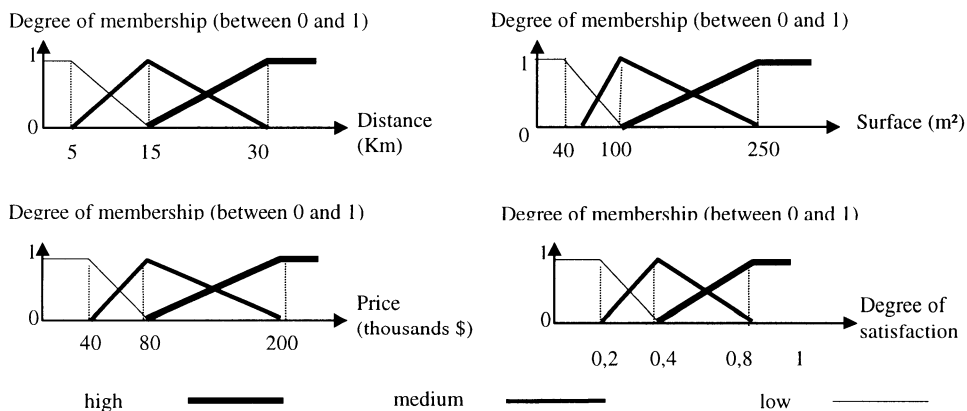


Figure 4: Membership functions definition

The membership function shape is not necessarily triangular nor trapezoidal even if they are the most convenient ways to have a continuous evolving of a property.

The fuzzy rules for the function « buying a house » may be:

1. **If** price is medium **and** surface is medium **or** high **and** distance is low **Then** satisfaction is high
2. **If** price is medium **and** surface is medium **or** high **and** distance is medium **Then** satisfaction is medium
3. **If** price is medium **and** surface is low **and** distance is medium **or** high **Then** satisfaction is low
4. **If** price is low **and** surface is medium **or** high **and** distance is medium **or** low **Then** satisfaction is high

5. **If price is low and surface is low and distance is medium or low Then satisfaction is medium**

Now, let us consider a potential house solution of 60,000\$ (between *low* and *medium* price), of 120 m² *surface* area (between *medium* and *high* surface) and distant of 15 km (*medium*) from the workplace. In this situation, only rules 2 and 4 are applicable.

Considering Zadeh’s aggregation operators [ZAD.75], the inference engine consists in choosing the maximal value of two linguistic values linked by **or** and the minimal value of two linguistic values linked by **and** (see Fig. 5).

In order to conclude on the satisfaction degree of the function « buying a house », one just have to combine with the **or** operator all the rule conclusions weighted by the membership degree. The center of gravity defuzzification method leads to a 70% satisfaction for the example considered above.

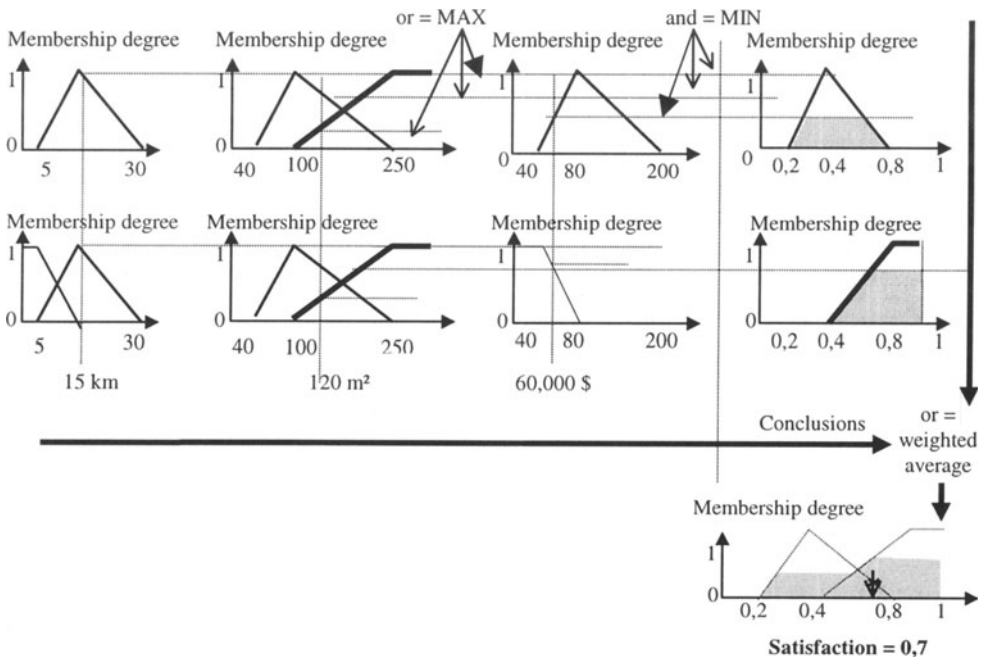


Figure. 5: Example of an inference over a fuzzy rule base

4. Virtual prototyping design platform

During the design process, the designer has some uncertainties over the expected efficiency of his design choices. If he is able to evaluate the probable performances of the current design solution in terms of a fuzzy function, our satisfaction model allows to estimate a global satisfaction by a bottom-up satisfaction propagation (by the way of the α -cuts method [DON.87]). This estimation, also given in terms of a fuzzy function,

gives an idea of the most probable global satisfaction of the current solution, and the degree of uncertainty on the fact to effectively succeed in. When the global satisfaction level is judged satisfactory, one may want to reduce this uncertainty, especially in the final stages of the design process. This risk reduction requires to reduce the current solution performance uncertainties. A focus on the sensitivity of the global satisfaction uncertainty to solution performances (see [WOO.89b]) could help the designer in more precisely determining performance levels. In addition, estimating the costs of these uncertainty reductions could lead to an optimized set of risk reduction actions.

Another issue is to properly estimate the current solution performances from a structural model partially defined. Two cases can occur:

1. The designer realizes an estimation based on his own experience,
2. It is possible to explicit the link between the current solution structural parameters and functional specifications. This link comes from a knowledge capitalization (e.g., a cost parametric model) or it comes from a computer simulation (e.g., a dynamic multi-body simulation to precisely calculate dynamic performances).

As our satisfaction model is able to take into account uncertain performances, it is thinkable, in the case of an explicit structure/specifications link, to evaluate a parameters structural model for which parameters are not already fixed (e.g., defined by an interval or a fuzzy function). Indeed, the α -cuts method would allow to evaluate the sensitivity of the global satisfaction to the variation of the solution structural parameters. This ability allows to develop optimization capabilities for new products and optimal redesign capabilities for existing products. This new framework is called « *virtual prototyping design platform* » in reference to the *virtual prototyping* concept which aims to use, as far as possible, simulation techniques in order to determine the solution performances.

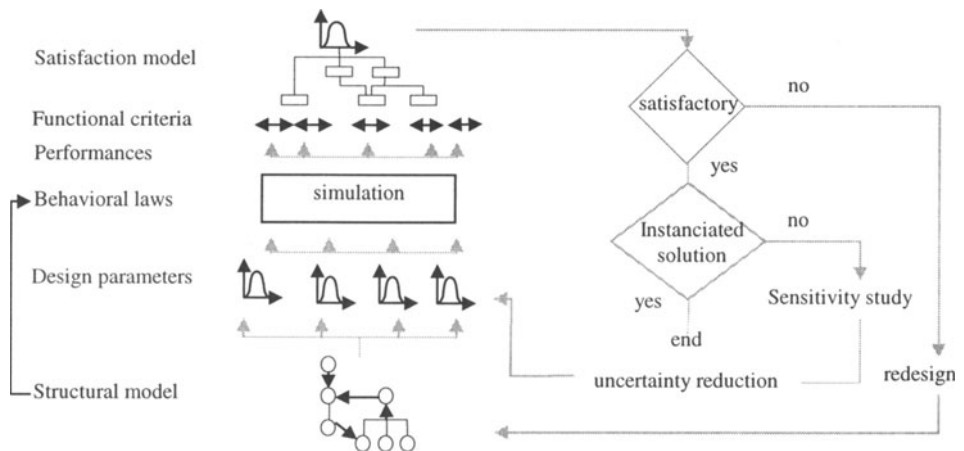


Figure. 6: Virtual prototyping design platform

5. Conclusion

The satisfaction model introduced in section 4 allows to automatically confront uncertain performances to more or less imprecise functional specifications. This evaluation can take place at any moment of the design process to validate a less or more completed structural model. Different approaches were imagined for estimating, through a bottom-up satisfaction propagation, a global satisfaction level relative to the current solution performances. Fuzzy logic provides an ideal framework to represent imprecision and uncertainty of solution performances and, through fuzzy inferences (propagation), to have an idea of the design project feasibility. Such a satisfaction model was the key issue to overcome in CAD systems, especially in redesign, product optimization and design project risk management. A *virtual prototyping design platform* has been proposed for CAD applications. This concept is presently under study.

REFERENCES

- [CHA.94] B. CHANDRASEKARAN. "*Functional Representation*", Advances in computers, vol. 38, 1994, pp. 73 - 138.
- [CHI.95] L. CHITTARO. "*Functional diagnosis and prescription of measurements using effort and flow variables*", IEEE.-Control Theory Applications, vol. 142, 1995, pp. 420-432.
- [DIA.88] A. R. DIAZ. "*Fuzzy Set Based Models in Design Optimization*", presented at Advances in Design Automation, New York (USA), 1988.
- [DON.87] W. M. DONG and F. S. WONG. "*Fuzzy weighted averages and implementation of the extension principle*", Fuzzy Sets and Systems, vol 21, 1987, pp. 183-199.
- [EVE.95] J. O. EVERET. "*A theory of mapping from structure to function applied to engineering thermodynamics*", presented at 9th international workshop on qualitative reasoning, Amsterdam (Netherland), 1995.
- [LIM.96] F. LIMAYEM, 1996, "*Prise en compte de données incertaines et imprécises dans l'établissement du CdCF*", DEA Report, PL - ECP (Paris), 1996.
- [SHI.95] Y. SHIMOMURA et al. "*Representation of design object based on the functional evolution process model*", Design Engineering Technical Conferences, vol. 2, 1995, pp. 351 - 360.
- [SUH95] N. P. SUH. "*Axiomatic Design of Mechanical Systems*", Transactions of the ASME, vol. 117, 1995, pp. 2-10.
- [THU.91] D. L. THURSTON. "*A Formal Method for Subjective Design Evaluation with Multiple Attributes*", Research in Engineering Design, 1991, pp. 105-122.
- [TOL.95] M. TOLLENAERE and D. Constant. "*Un modèle produit générique et réactif pour une conception fonctionnelle*", presented at PRIMECA - 4^{ème} colloque sur la conception intégrée, La Plagne (France), 1995.
- [WOO.89a] K. L. WOOD et al. "*Comparing fuzzy and probability calculus for representing imprecision in preliminary engineering design*", presented at Design Theory and Methodology, Montreal (Canada), 1989, pp. 99-105.
- [WOO.89b] K. L. WOOD et al. "*Computations with imprecise parameters in engineering design: background and theory*", ASME Journal of Mechanisms, Transmissions and Automation in Design, accepted for publication in March 1989.
- [ZAD.75] L. A. ZADEH. "*The concept of a Linguistic Variable and its Application to Approximate Reasoning*", Information Sciences, 1975, pp. 199-249.

AIDED DESIGN OF BRASS MUSICAL INSTRUMENTS

Jean-François PETIOT

*Equipe CMAO et Productique. IRCyN. UMR C.N.R.S. 6597
Ecole Centrale de Nantes. 1, rue de la Noë
BP 92101, 44321 Nantes Cedex 3, France.*

Joël GILBERT

*Institut d'Acoustique et de Mécanique de l'Université du Maine
Laboratoire d'Acoustique UMR CNRS 6613
Avenue Olivier Messiaen
72085 Le Mans Cedex 9, France*

1. Abstract

The manufacture of musical instruments is a domain where the know-how is primordial and rules of the profession are hard to explain and to formalise. In this article we present a new experimental approach with the aim of assisting the manufacture of musical instruments. In this perspective, we have developed an "artificial mouth" that permits to make objective tests on instruments (trumpet or trombone), overlooking the natural adaptation faculty of the musician.

Moreover, the artificial mouth is a useful set-up to understand the basic behaviour of brass instruments, and to improve physical modelling.

2. Introduction

The manufacture of musical instruments is a multi-disciplinary activity. Indeed, to conceive and to manufacture a musical instrument, it is necessary to take into account several requirements [1] [2] :

- ergonomic requirements. The instrument must be adapted to the musician on the physical level and on the perceptive level (domain of psychoacoustics),
- economic and manufacturing requirements,
- musical requirements. It is the most important criteria. Musicians assign to sounds three main qualities : the intensity, the pitch and the timbre. A good instrument must allow the musician to control easily, separately or simultaneously these four parameters.

In centuries, to take these constraints into account, instrument builders have accumulated know-how and experience, constituting the memory of the past. In the past, industry was a craft, but nowadays instrument manufacturing requires modern production devices, adapted to small and average quantities and to the control of product quality. The design and adjustment phases of an instrument are made by the realisation of prototypes, with a test-mistake reasoning.

Recently, a better understanding of the physical phenomenon used in the sound emission has offered an assistance to the design. Furthermore, progress in numerical simulations allows the instrument maker to control the quality of an instrument and to predict some of its performances before the manufacturing. The work presented in this article stands in this context.

This paper is limited to brass instruments (trumpet, trombone, frenchhorn...). Their behaviour is described in section 3. In order to study this type of instruments, we have developed an artificial mouth, presented in section 4. In this section, we expose its contribution to the aided design of musical instruments and their objective characterisation. In the perspectives, we explain how the use of the artificial mouth for the validation of physical model can for the future lead to a Computer Aided Design.

3. Brass Musical Instruments

3.1 FUNCTIONING

Wind instruments (with the exception of those with a flute-like embouchure) are acoustic sources using a valve effect : the acoustic oscillation is a result of the destabilisation of a mechanical element whose movement changes the entrance cross-section of the instrument. This destabilisation is the result of a complex aeroelastic coupling between the mechanical element (the reed of a clarinet or the lips of a trombonist), the air flow entering the instrument as a result of the static overpressure in the mouth of the musician, and the instrument itself (the acoustic resonator) [3] [4].

The vibrations of the lips of the trombonist are controlled both by the musician and the instrument itself [5]. Several parameters condition the natural frequency of lips (tension, geometry, visco-elastic properties, ...). The control and the management in "real time" of these parameters allow to obtain a great variety of musical sounds, this after several years of daily practice for the musician [6].

The resonator is described by its input impedance, giving the amplitude of its acoustic response to an excitation (response in forced oscillations). This characterisation of the instrument alone is not sufficient to define the quality of an instrument. For example, this approach does not enable us to take into account the possibilities for the musician to change the pitch of the playing note, and to play notes of various sounds colours and intensities.

Modern brass instruments have reached a high level of acoustic quality, and it is now very difficult for the manufacturer to improve them. How can one be sure that a slight difference of tone or pitch of note is the consequence of a modification of the bore and not the consequence of an unconscious modification of the "embouchure" (the

way the mouthpiece and lips interact) of the musician ? Is the instrument wrong or does the musician play it incorrectly ?

This sentence sums up the difficulty of objectively characterising the quality of an instrument.

3.2 PERFORMANCE EVALUATION OF AN INSTRUMENT

It is difficult to define the quality of an instrument. Many factors come into play, for example the history of the instrument, its appearance or its price [7].

From an acoustical and musical point of view (for example, aesthetic considerations are not taken into account), one can quote criteria of evaluation of wind instruments in a non-exhaustive way :

- accuracy, and freedom field of pitch,
- ease of playing,
- quality of timbre,
- freedom field of timbre,
- homogeneity of the timbre over the complete range¹,
- freedom field of intensity.

To evaluate an instrument, a musician tester must give an account of the performances of the instrument, according to previous criteria. Essential for the manufacturer, the opinion of the tester is global and can be inaccurate for several reasons :

- a lot of coupled parameters must be evaluated,
- the tester adapts to the instrument, and corrects more or less unconsciously for any possible drawbacks,
- the opinion is subjective,
- comparisons between several instruments are difficult to do,
- it is difficult to do acoustical measurements under playing conditions and it is difficult for the tester to guarantee reproducible playing conditions during such measurements.

In order to complement the opinion of the tester, we have developed an experimental device, the artificial mouth [8]. With this experimental system, it is possible to generate steady and reproducible playing parameters. Previous systems for reed instruments (clarinet, saxophone) have already been used [9]. The main objective is to allow the characterisation of an instrument by objective measurements, in order to answer (at least partially) whether the instrument or the musician plays incorrectly.

4. The Artificial Mouth

4.1 PERFORMANCE SPECIFICATION

The device must satisfy the following functions :

- to guarantee emission of sound in steady conditions (permanent regime),

¹ scale of sounds of an instrument, from lower to higher notes

- to generate several notes over the range of the instrument, by adjusting playing parameters,
- to guarantee a very good reproducibility of adjustments, so that several instruments may be compared with the same embouchure,
- to recreate for each note freedom fields of timbre and intensity characteristic of the musical instrument,
- to fit to several instruments (trumpet, trombone),
- to allow the measurement of pressure and velocity inside the mouth cavity, as well as the visualisation of the lip motion.

After a physiological analysis of a musician playing a brass instrument [10], three control parameters have been kept to change the timbre and the pitch of notes :

- air supply pressure,
- mechanical tension of lips,
- support force of the mouth on lips.

4.2 DESCRIPTION

The artificial mouth (Fig.1) is a hermetically sealed box fed by a high pressure (5 bar maximum) air supply, in which the artificial lips are fixed. The mouth pressure in the box is controlled with a pressure regulator. In order to approach the visco-elastic properties of real lips, the artificial lips are latex tubes filled with water. A jaw presses the lips against the mouth with an adjustable support force.

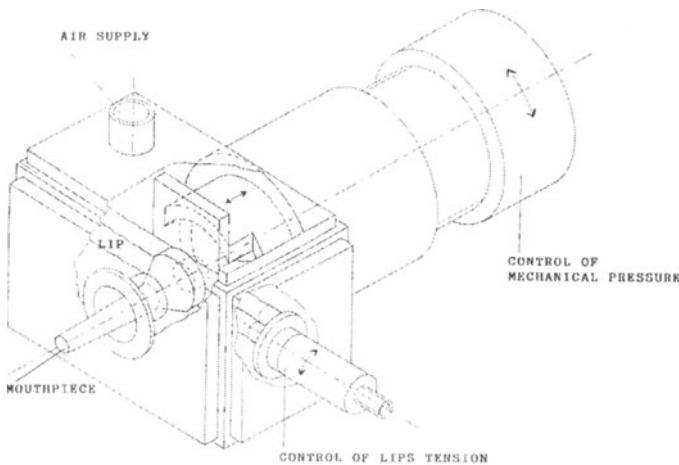


Figure1. The artificial mouth

The adjustment of the support force and the lip tension allows the stiffness of lips, and therefore their natural frequency to be altered. The mouthpiece is clamped and remains fixed with the artificial mouth. Therefore, it is possible to replace one brass

instrument with another without perturbation of the "embouchure" adjustment (the instrument is clamped on the mouthpiece using an adaptation cone). It guarantees a perfect stability of the embouchure when the instrument is replaced by another one.

The timbre obtained with the artificial mouth is quite realistic, the sound can be compared to those obtained with a musician (an opinion confirmed by several professional musicians).

4.3 UTILISATION

The artificial mouth eliminates the musician's natural faculty of adaptation, as the artificial mouth does not adapt its playing parameters according to the produced sound. It is then possible to compare two instruments, being sure that the differences that we observe are not the consequences of a modification of the "embouchure" of the musician. The artificial mouth is integrated into a functional chain, the structure of which is given Fig.2. This SADT representation encapsulates the parameters and data when relevant to our problem.

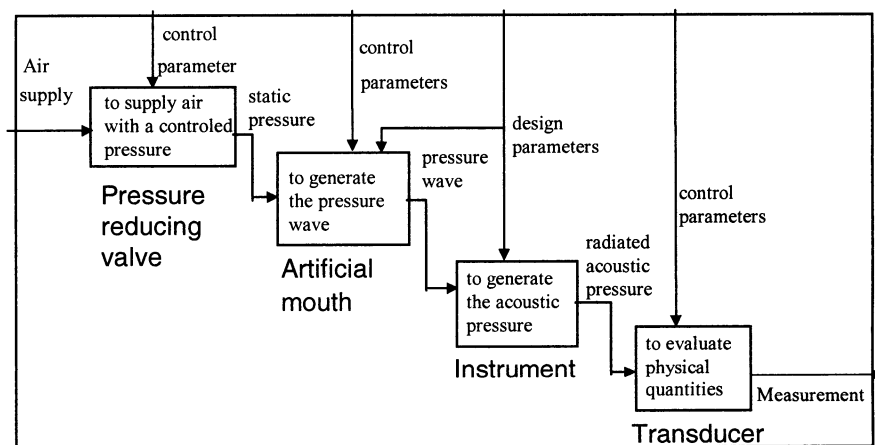


Figure 2. SADT model of the functional chain

The objective is to evaluate the performances of an instrument (according to the previous criteria) by physical measurements.

In fact, to establish such a correspondence is quite ambitious because it involves comparing two quantities of different kinds, i.e. physical quantities (objective) and perceptive quantities. Studies in psychoacoustics show that things are obvious, and that mechanisms of perception are subtle². The major difficulty is in finding sensible physical parameters and the experimental conditions leading to pertinent measurements of the studied criteria. For that, we have chosen :

² For example, the sensation of pitch, relating to the accuracy, is not always dependent only on the playing frequency. It depends in particular on the intensity, the length and the timbre.

- to separate the variables. We take an interest in only one criteria at a time, all others being constant,
- to work by comparison between instruments,
- to have reproducible experimental conditions, for the playing parameters of the artificial mouth, but also for parameters conditioning the measurements (temperature, acoustics of the room,...)

4.4 MEASUREMENTS

We do not claim to define complex criteria, which give an exact account of notions as subtle as "accuracy" or "ease of playing". But we propose to analyse physical quantities, taken directly from measurements which are easily made on our experimental device (static pressure in the mouth, acoustic pressure in the mouth and radiated acoustic pressure). These physics quantities are linked to the criteria of evaluation :

- 1) the study of the accuracy is brought back to the study of the fundamental frequency (also called playing frequency). This frequency is compared to the frequency of the even tempered scale, having for reference the A4 = 440Hz.
- 2) the study of the timbre, the freedom field of timbre, the homogeneity of the timbre over the entire range amounts to an analysis of the spectrum radiated by the instrument for signals in permanent regime. The control parameters are : the air supply pressure, mechanical tension of the lips and the support force of the mouth on the lips.
- 3) we propose to characterise the ease of playing by the measurement of the minimum static pressure necessary to generate a sound. The lower the value of static pressure is, the easier the note production on the instrument is.
- 4) the freedom field of intensity is evaluated by a measurement of the radiated acoustic pressure, according to the supply pressure in the mouth.

Criteria of evaluation and associated measurements are summed up in table 1.

TABLE 1. Criteria of evaluation and associated measurements

Evaluated criteria	Measures
accuracy	fundamental frequency
ease of playing	static pressure supply
timbre freedom field of timbre homogeneity of timbre	internal and radiated spectrum in permanent regime
freedom field of intensity	acoustic pressure/ static pressure

Today, the artificial mouth is not suited to the study of the behaviour of brass instruments in transient regime. The response of the instrument in transient regime is nevertheless essential for the musician. The study of these regimes remains the domain of the tester. The artificial mouth provides a complementary opinion on an instrument, but can never replace the musician. He will always remain the only one who can judge.

4.5 APPLICATIONS

According to the different tests that we have completed, artificial mouth playing tests on instruments can cover two aspects : aided design of instrument or control of production.

4.5.1. *Aided design of instrument*

In case of a new design of an instrument, the major interest is to be able to evaluate the influence of a modification of the instrument (geometry, materials, assembly...) on the criteria of performance, this one without any a priori on the result (the musician is sometimes subject to a "placebo" effect, his opinion changing whereas the instrument is identical). By performing artificial mouth tests, it is possible to quantify the influence of design parameters on the criteria of performance.

These measurements allow the designer to control with accuracy the expected performance of the new instrument.

4.5.2. *Control of Production*

The manufacture of instruments for the general public is of order of small to average quantities. The concern of manufacturers is to control the quality of products, in order to have an homogeneous production. For that, it is necessary to bring under control the variance of the manufacturing processes (assembling, forming, milling, welding,...), because the acoustic result is very sensitive to slight variations of the design parameters (dimensions, surface quality, state of stresses of the material,...).

Artificial mouth measurements, compared to those of a reference instrument, judged high-performance by the tester, will enable the following controls to be made :

- end of production line quality control on the finished product, to provide an initial assessment of the product before seeking the definitive opinion of the tester,
- control on different stages of the manufacturing, in order to control the quality of the manufacturing process.

5. Conclusions - Perspectives

The objective characterisation of musical instruments is an important contribution for the instrument builder. It allows production instruments to be compared one with the other and with reference instruments selected by the musician. The features of the artificial mouth (stability and reproducibility) permit this characterisation using physical measurements taking perceptive notions into account.

The acoustic criteria used in this article are basic. Further work must be done to refine the definition/relation between the perceptive domain and physical measurements (psychoacoustics) [11][12]. This work will be useful for an optimal use of the artificial mouth, with a view qualifying musical instruments.

Artificial mouth measurements complement the opinion of the tester and the musician. They do not permit complete qualification of the instrument because all

playing modes cannot be taken into account. In particular, the study of the transient regime is not yet possible, measurements being limited to the permanent regime. It is not possible to do without the opinion of the musician.

On the other hand, the artificial mouth is an experimental device which is essential for the development of a global physical model of the "instrument and musician" combination [8][13]. In the context of virtual acoustics, it is now possible to listen to very realistic synthesis of brass instrument sounds [14][15]. But important work has to be carried out in order to adapt these tools to a computer aided design approach in the context of virtual acoustics.

6. References

- [1] D.M. CAMPBELL, C.GREATER "The musician's guide to acoustics" Oxford University Press, New-York, 1998.
- [2] D. KOPPE : "La trompette dans la seconde moitié du XXe siècle : Facture, technique et interprétation". Thèse de doctorat. Université de Paris IV, U.F.R. de Musique et de Musicologie. 1996.
- [3] A.HIRSBERG , J.KERGOMARD , G.WEINRACH "Mechanics of musical Instruments" CISM courses and lectures n° 355. Springer Verlag, Wien, New-York, 1995.
- [4] N. H.FLETCHER, T. D.ROSSING. "The physics of musical Instruments" Springer Verlag, New-York, 1991.
- [5] J.GILBERT, J-F. PETIOT "Brass instruments : some theoretical and experimental results". Proc. Institute of Acoustics, Vol 19 Part 5, 1997, pp 391-400.
- [6] J-J.GREFFIN R.PERINNELLI "Méthodologie pour trompette et instruments à embouchure" Editions BIM, Suisse, 1984.
- [7] J-P.DALMONT, J.GILBERT, J.KERGOMARD "Des instruments à vent harmoniques" Pour la Science, n°238, Août 1997, pp. 78-85.
- [8] J. GILBERT, S. PONTIUS, J.F. PETIOT "Artificial buzzing lips and brass instruments : experimental results ". Journal of the Acoustics Society of America,, Vol. 104(3) , pp 1627-1632, 1998.
- [9] J-P.DALMONT,, B.GAZENGEL, J.GILBERT, J.KERGOMARD "Some aspects of tuning an clean intonation in reed instruments". Applied Acoustics N° 46, 1995, pp.19-60.
- [10] L.PIAU "Conception et réalisation d'une bouche artificielle pour instrument à vent de type cuivre". Rapport de recherche de troisième année, Ecole Centrale de Nantes, 1997.
- [11] R.CAUSSE, N.MISDARIIS, S.THORETON "Caractérisation objective de la qualité d'un instrument de musique". Quatrième congrès français d'Acoustique, Marseille, 1997.
- [12] J.KRIMPHOFF "Analyse acoustique et perception du timbre". DEA d'Acoustique appliquée de l'Université du Maine, 1993.
- [13] J.S.CULLEN, J.GILBERT, D.M CAMPBELL, « Brass instruments : linear stability analysis and experiments with an artificial mouth » submitted to ACUSTICA.
- [14] R.MSALLAM, S.DEQUIDT, S.TASSART, R.CAUSSE "Physical model of the trombone including non linear propagation effects" Proc. Institute of Acoustics. Vol 19 Part 5, 1997, pp.419-424.
- [15] C.VERGEZ, X.RODET "Model of the trumpet functioning : real time simulation and experiments with an artificial mouth". Proc. Institute of Acoustics. Vol 19 Part 5, 1997, pp.425-432.

ENVIRONMENTALLY-CONSCIOUS DESIGN AND MATERIALS SELECTION

U.G.K. WEGST and M.F. ASHBY
*University of Cambridge, Department of Engineering,
Trumpington Street, Cambridge CB2 1PZ, United Kingdom
Tel: +44-(0)1223-332791, Fax: +44-(0)1223-332791
ugkw1@eng.cam.ac.uk, mfa2@eng.cam.ac.uk*

Abstract

A materials selection methodology and its software implementation, developed to aid the designer in making environmentally-conscious decisions early in the design process, is described.

1. Introduction

The creation and use of any engineering product carries with it an environmental burden. There is a growing recognition that the minimisation of this burden must become a primary design objective. Materials contribute to it in their production, in the use of products made from them and in the disposal of these products. The minimisation of the environmental burden requires the selection of materials which are less toxic, can give products which — without compromising product quality — are more easily recycled, which are lighter and less energy intensive, and which, where possible, use renewable or non-critical resources. This paper describes the development and use of a software-based design tool, the Cambridge Eco-Selector, which aids the environmentally-conscious selection of materials.

2. The Design Process and Environmental Impact Evaluation

The essential steps in the design process are described in the flow chart of Figure 1. A market need is identified. Concepts to fill it are developed and critically reviewed. Promising concepts pass to the embodiment or 'layout' stage, where the most suitable is selected for detailed design, analysis, production, planning and costing. Finally, the product is manufactured, distributed, used and — when it reaches the end of its lifetime — the materials it contains may be reused, recycled, incinerated or committed to landfill.

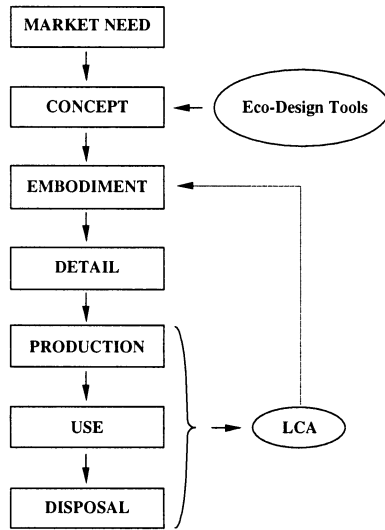


Figure 1. The design process, life-cycle assessment (LCA) and eco-design tools.

The environmental impact of a product is frequently explored using the techniques of Life-Cycle Assessment (LCA). An LCA, as the name implies, examines the whole life-cycle of the product (manufacture, use and disposal — represented as the bottom three boxes in Figure 1) and the total eco-impact it creates. LCA requires information of the life-history of the product at a level of precision which is only available after the product has been produced; it is a tool for the evaluation and comparison of existing products, rather than one which guides the design of those which are new. But decisions taken in the early stages of design lead to commitments which cannot easily be changed later, and for this decision-making, LCA comes too late. Instead, a design tool is required which guides environmental awareness and exploits the information available early in the design process — the 'concept' and 'embodiment' stages of Fig. 1. The Eco-Selector described here seeks to achieve this.

3. The Selection Strategy

Efficient selection (Ashby, 1999; Cebon and Ashby, 1997) involves two main steps which we here call *screening* and *supporting information*. The data requirements and selection and searching strategies in the two steps differ fundamentally.

3.1. THE SCREENING STAGE

Unbiased selection is best achieved by considering *all* materials to be viable candidates until shown to be otherwise. The first step in identifying viable candidates is that of screening. The screening step is effectively performed using a computerised database containing material attributes: values for physical, mechanical, thermal and electrical

properties; and — in a database for eco-selection — attributes relating to the environmental impact of the production of the material itself: its energy content, the greenhouse and acidification gases created by its production, its toxicity and so forth.

Screening is performed by linking the technical and economic requirements of the design with the attribute profiles stored in the screening database using *attribute limits* and *material indices*. Attribute limits are simple limits placed on the values of certain attributes stored in the database. The design requirement that “the service temperature of a candidate material must be greater than 250°C” imposes the limit that the maximum service temperature of any viable candidate must be greater than this; the design requirement of “electrical insulation” imposes a limit on electrical resistivity, and so forth. Attribute limits do not, however, provide any level of performance optimisation.

Optimisation is achieved by the use of *material indices*. These are groups of material properties which characterise performance. They allow ranking of potential candidates: the materials with the largest values of an index maximise some aspect of performance. The specific stiffness, E/ρ , is one such index (E is Young’s modulus and ρ the density); the specific strength σ_y/ρ is another (σ_y is the yield strength). There are many material indices, each measuring some aspect of efficiency for a given function; a catalogue, with derivations, can be found in Ashby (Ashby, 1999).

Indices are used with *material property charts*. These are plots of one material property or a combination of material properties against another. Material indices can be plotted on a material property chart to compare the performance of different materials for a given application. The procedure allows a ranking of materials according to their function per unit weight, or function per unit cost or, as described here, *function per unit environmental impact*.

To summarise: attribute limits isolate candidates which are capable of doing the job; optimising indices identify those among them which can do the job well. The top performers, which satisfy all of the screening criteria, are then short-listed.

3.2. THE SUPPORTING INFORMATION STAGE

The result of the screening step is a shortlist of candidates which satisfy the quantifiable requirements of the design. To proceed further we seek a detailed profile of each: its supporting information.

The data requirements for supporting information differ greatly from those for the screening step. It is not necessary to explore *all* materials in the kingdom, only to find necessary additional information about the few candidates that have already been identified by the screening step. Typically, it is non-quantifiable information which is sought: photographs of microstructures, or case studies of corrosion protection in a particular environment, or details of availability and pricing, and — in an eco-selector — information about environmental impact, toxicity, recyclability and so forth.

Because the data is in ‘free’ format, the search strategies differ completely from the numerical optimisation procedures that are best for screening. Without screening, the candidate-pool is enormous; there is an ocean of supporting information, and dipping into this gives no help with selection. But once viable candidates have been identified by screening, it is only necessary for the supporting information system to provide a mechanism for accessing information about these few materials.

It is, of course, unrealistic to think of minimising the environmental impact of material production and usage as the only objective, there are always other considerations: cost, reliability, performance. The *value-function* method for materials selection, already built into the methodology, can allow an optimum compromise to be reached (Ashby, 1997). A description of the value function method is, however, beyond the scope of this paper.

These ideas are best illustrated by a case study.

4. Case Study: The Monitor Chassis

Monitor chassis are currently made of fire-resistant polystyrene (PS). It has been suggested that the substitution of a magnesium alloy (Mg) or an aluminium alloy (Al) could increase recyclability and lengthen chassis-life, allowing the possibility of reuse. This case study compares the three materials from a mechanical, thermal and environmental perspective.

The approach is based on developing sets of *material indices* for performance-limiting aspects of the chassis design (Ashby, 1999; Ashby and Cebon, 1996; CES 1999). The first index relates to the mass of the chassis: its outer faces, mechanically speaking, act as flat panels loaded in bending, and they must be stiff and strong enough to do this task adequately. The second relates to heat-transfer, important because the electronics contained in the chassis must not get too hot. The third — and the one of principal interest here — concerns its ecological impact ('eco-burden'). The overall aim is to establish whether the use of magnesium (Mg) or aluminium (Al) for the chassis can give a product which equals or surpasses the performance of the current PS chassis in mass and heat-transfer, and whether it can do so with a lesser eco-burden.

4.1. DESIGN REQUIREMENTS

The monitor chassis encases and supports the cathode ray tube (CRT) and associated electronics. These, and the loads imposed externally during normal use, cause the flat panels which form the chassis-walls to be loaded in bending. The structure must be stiff and strong enough to support these bending loads and have heat-transfer properties which are adequate to prevent overheating. It is also known that the natural vibration frequencies of the chassis must be high to avoid annoying resonances. The current PS chassis achieves these goals, but cannot readily be recycled, and is made of a material which creates, in its manufacture, an above-average eco-burden. A substitute must equal or surpass PS in its mechanical and thermal performance and exceed it in recyclability with a lower eco-burden. The requirements are summarised in Table 1.

Table 1. The design requirements for a monitor chassis.

FUNCTION	Plate loaded in bending
OBJECTIVE	Minimise environmental impact
CONSTRAINTS	Match or exceed the properties of fire-retardant polystyrenes(PS): a) Bending stiffness per unit mass b) Bending strength per unit mass c) Heat transfer

4.2. THE METHOD

The Mass. The index for selecting materials for low-mass panels of specified stiffness, S , is found as follows (Ashby, 1999; Ashby and Cebon, 1996). The mass of a panel of dimensions $a * b * t$ ($a < b$, with a , b and t as the width, the depth and the thickness respectively) is

$$m = a.b.t.\rho \quad (1)$$

where ρ is the density of the material of the panel. Its stiffness is

$$S = C_1 \frac{E.I}{b^2} = C_2 \frac{E.a.t^3}{b^2} \quad (2)$$

where E is Young's modulus, I is the second moment of area, and C_1 and C_2 are constants. The minimum thickness of the panel which meets the stiffness constraint is thus

$$t = \left(\frac{S.b^2}{C_2.E.a} \right)^{1/3} \quad (3)$$

Substituting this into equation (1) gives

$$m = a^{2/3}.b^{5/3}.\left(\frac{S}{C_2.E}\right)^{1/3}.\rho \quad (4)$$

Thus the best materials for a flat panel loaded in bending and of minimum weight, with a constraint on stiffness, are those with the highest value of the material index

$$M_1 = \frac{E^{1/3}}{\rho} \quad (5)$$

By a similar argument, the best materials which will perform the same function, but with a constraint on strength, are those with the highest value of the material index

$$M_2 = \frac{\sigma_y^{1/2}}{\rho} \quad (6)$$

where σ_y is the yield strength. The constraints (a) and (b) in Table 1 require that the substitute for PS has values of M_1 and M_2 which at least equal those of PS itself. If they fail to do this, they will be heavier than the existing panels.

Heat Transfer. The heat-transfer rate through a panel (assuming that conduction is controlling) is measured by the heat flux

$$J = A\lambda \frac{\Delta T}{\Delta x} \quad (7)$$

where A is the area of the panel, λ is the thermal conductivity and $\Delta T/\Delta x$ is the temperature gradient.

If the stiffness constraint is assumed to be limiting, then the heat-diffusion distance, Δx , is equal to the thickness of the panel, given by equation (3). Inserting this into equation (7) gives an expression for the temperature difference, ΔT , caused by a heat-flux, J ,

$$\Delta T = \frac{J}{a.b.\lambda} \left(\frac{S.b^2}{C_2 E.a} \right)^{1/3} \quad (8)$$

and the relevant index is

$$M_3 = \lambda E^{1/3} \quad (9)$$

If, instead, the strength constraint is limiting, then the relevant index is

$$M_4 = \lambda \sigma^{1/2} \quad (10)$$

The constraint (c) in Table 1 requires that the substitute for PS has values of M_3 and M_4 which at least equal those of PS itself.

Eco-burden. The performance of the chassis depends on the criteria discussed so far — if these are not met, the substitute is not acceptable. If they are, the question becomes one of the relative environmental impact of the two materials. This is evaluated using two further material indices, derived in ways which parallel those for the mass. High stiffness with low environmental impact is achieved by seeking materials with high values of the index

$$M_5 = \frac{E^{1/3}}{E_I \rho} \quad (11)$$

Here E_I is the *eco-indicator*, a measure of the total eco-burden associated with the production of a unit mass (1 kg) of material. The derivation of these indicators is difficult and requires a great deal of detailed information about energy, greenhouse gasses and wastes of all sorts. At this early point in our study we have drawn on the limited but well-documented data of the IDEMAT software (IDEMAT, 1996) for values for E_I . Incorporating this into the reasoning for material indices gives, when high stiffness per unit mass is the constraint, the index given above; when strength is the constraint, the index becomes

$$M_6 = \frac{\sigma^{1/2}}{E_I \rho} \quad (12)$$

4.3. THE EVALUATION

Figures 2 and 3 show two of the overall six selection stages of this case study. The material indices M_5 and M_6 are plotted as bar-charts for the two classes of materials relevant to this study: polymers (including PS) and metals (among them, Al and Mg). The figures are constructed using the Cambridge Eco-Selector which contains physical, mechanical, thermal and eco-data for 245 materials of five classes (ceramics, composites, metals, natural materials and polymers).

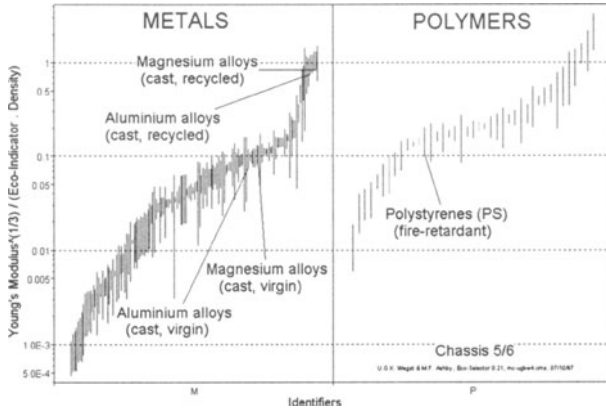


Figure 2. A chart of M_5 against polymer and metal identifiers.

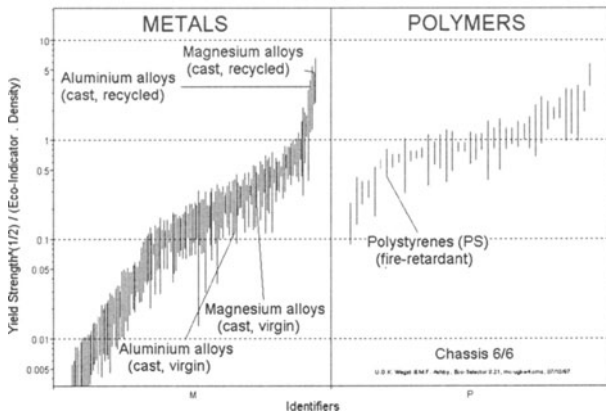


Figure 3. A chart of M_6 against polymer and metal identifiers.

The first two pairs of figures (not shown here, see (Wegst and Ashby, 1998) for reference) allow a comparison of PS, Al and Mg on a mass basis (M_1 and M_2) and on the basis of heat-transfer (M_3 and M_4): The Mg chassis is lighter than one of Al or PS, and both Al and Mg panel exceed PS in thermal performance, with Al being superior to Mg. By these criteria, both Al and Mg would be viable alternatives to PS.

The last pair, Figures 2 and 3, show the eco-indices M_5 and M_6 . The five materials identified are fire-retardant PS (the material of which the chassis is currently made); the second and third are both Al and the fourth and fifth are both Mg. For both Al and Mg a value of eco-indicator for recycled material is used in addition to a value for virgin material. It is clear that while the virgin Mg is comparable in its eco-burden with PS, the recycled Mg is substantially better and recycled Al is almost as good as Mg.

The evaluation of the three alternative materials suggests that Mg alloys provide both from a mechanical and environmental point of view an alternative to fire-retardant PS as long as recycled Mg is used. It is at this point that Supporting Information is

needed. Is magnesium a critical resource? Is the world production enough to support a new market such as this? Who produces and supplies it? A quick search through just one electronic data source — B&H Books (Butterworth Heinemann, 1998) — answers these and other questions quickly and efficiently. The resource base is enormous — about 3×10^{12} tonnes — exceeded, among structural metals, only by iron and aluminium. The world production is about 10^7 tonnes per year, more than enough to cope with the demand expected here. It is produced by Magnesium Elektron Inc, the Magnesium Corporation of America, and others (contact information given). A good Supporting Information source for eco-design would give much more than this; one is in preparation as part of this program.

5. Conclusion

The methodology for environmentally-conscious materials selection described in this paper is still under development. It will be developed further, tested and refined by analysis of case studies in collaboration with industrial and academic partners. It builds on a well-tried methodology and software system. It has potential as a tool for suggesting ecologically-sound materials selection at an early design stage when the details required for conventional life-cycle assessment are still unresolved.

6. Acknowledgements

We wish to thank Narito Shabaik and the Panasonic company for their support for this project and to acknowledge the support of the UK EPSRC through the Engineering Design Centre at Cambridge, and of Granta Design, Cambridge, who developed the software used in this case study.

7. References

- Ashby, M.F. (1999) *Materials Selection in Mechanical Design*, 2nd edition, Butterworth Heinemann, Oxford.
- Ashby, M.F. and Cebon, D. (1996) *Case Studies in Materials Selection*, Granta Design, Cambridge.
- Ashby, M.F. (1997) "Materials Selection: Multiple Constraints and Compound Objectives", ASTM STP 1311 on Computerisation/Networking of Material Databases, ASTM.
- Butterworth Heinemann (1998) *B&H Books: Smithells, the Corrosion Handbook and the Tribology Handbook on CD*, Butterworth Heinemann, Oxford.
- Cebon, D. and Ashby, M.F. (1997) "The Optimal Selection of Engineering Entities", Cambridge University Engineering Department Report CUED/C-EDC/TR59 - November 1997.
- CES Software (1999). Granta Design Limited, Trumpington Mews, 40B High Street, Trumpington, Cambridge CB2 2LS, United Kingdom.
- IDEMAT Software (1996) Faculty of Industrial Design Engineering, Delft University of Technology, Jaffalaan 9, 2628 BX Delft, The Netherlands.
- Wegst, U.G.K. and Ashby, M.F. (1998) Eco-criteria for Materials Selection, *Engineering Designer*, March/April 1998, pp. 8-12.

DESIGN KNOWLEDGE REPRESENTATION FOR CONSTRAINT-BASED DESIGN IN CAD SYSTEMS

Christophe LENGUIN, Pierre-Alain YVARIS
ISMCM-CESTI, GRIEM
3 rue Fernand Hainaut, 93407 SaintOuen Cedex, France

Abstract :

Using constraint programming for routine aided design allows us to model the product to be designed as a set of parameters and a set of constraints. The designer's job consists in valuing all the parameters regarding to this set of constraints. The difficulty relies in the order in which the parameters are valued and in the values which are given. The model proposed aims at representing the design process knowledge in a declarative way.

There are two kinds of design process knowledges : strategic knowledge guiding the design, and failure control knowledge in order to know what to do when a failure occurs during the design.

1. Introduction

For the past fifteen years or so, the CAD environments available on the market have been of considerable assistance to research departments, particularly as regards to geometric modelling.

Traditional modellers have been used to model solid, surface and wire-frame pieces; parameterised geometry allows the various geometrical parameters of a model's entities to be declared and a design history to be described. As for the variational systems, these modellers generalise the parameterised geometry ideas by proposing tools for solving systems of geometrical equations [CHU.89].

However, these tools are really effective only when used for geometrical modelling tasks and do not offer all the functions required to provide assistance of any kind when redesigning industrial products.

Certain types of approaches allow non-geometrical information to be taken into account:

- Object-oriented languages coupled with traditional modellers: These provide an abstract view on a traditional modeller. A developer will directly use a geometrical object layer which includes a predefined hierarchy of geometric classes with a set of manipulation methods and associated calculation. He will thus be able to derive his own classes associated with a given application and initiate calculation methods on the geometry in the course of argumentation. However, the possibility of the implementation of a design process is low. Systems such as ICAD [WAG.90] operate under this mode.

- Inference engines linked to traditional modellers: In these systems, a developer is able to express his expertise in the form of a set of production rules. Due to a rather flimsy coupling with the modellers, it is possible to express geometry operations and calculations within the expertise [TRO.89].

- Constraint managers coupled with traditional modellers: In these systems, the problem is expressed in the form of a set of geometric or other constraints to be met (bi-directional relations between variables). It is also possible in this situation to call up modeller functions on-line.

This last solution appears to be a highly promising one. However, it would seem to require integration of the following into a generic model: the design knowledge set linked to the product to be designed (geometry, structure and functions) and the various design constraints (geometrical and technological) to be met, including the way of obtaining an artefact (design process to be implemented).

Some results obtained recently have culminated in the general constraint-based representation environments now available (the INRIA SHERPA project [GEN.95]). Furthermore, prototypes for research into constraint-based design aid environments are starting to make an appearance (European DEKLARE project [SAU.95]). Finally, constraint-based programming libraries are now available on the market (Ilog Solver, Chip, Prolog III, ...).

II. Problematics

Our objective is to ultimately have at our disposal a real design-aid environment for professional applications. The aim of this environment is to develop knowledge-based redesign or routine design type applications.

To do this, we want to implement object-oriented constraint programming techniques in order to manipulate entities of any type, geometrical or technological [SAU.97].

However, the ability to represent a set of product component elements or a class of products to be designed subject to a set of relations known as constraints strikes us as being a necessary but insufficient step.

Indeed, the majority of constraint-based programming techniques use domain reduction algorithms. Thus, for a set of variables to be instanced, with each variable having a value in a given domain (Boolean, whole or running) and a set of constraints on the 'variable' values, the purpose of the constraint propagation mechanisms is to reduce as far as possible the domains of likely values for each variable in such a way that the declared constraints remain verified. In the most of industrial problems, a supplementary solution level is needed to be able to instance the variables.

Therefore, we would also like to have a formal means of representing the solution process (or design process) and the associated verification. This will enable the representation of the design stages and hypotheses which are connected by various types of links (synchronisation, precedence, back-tracking, resolution methods ...) This formalism could also be advantageous if used with the notion of constraints when defined.

In short, the notion of constraints would enable the following to be defined within a unified declarative model:

- the relations to be met in the design of the product,
- the relations defining the design process to be followed to achieve the desired product.

3. Routine design and constraint-based programming

In routine design, a product can be considered as a set of parameters or variables whose values must meet a certain number of constraints. These constraints can stem from any stage in the product life-cycle. The most immediate are design constraints which can be material resistance constraints, fluid mechanics, kinematics, ... A designer should also keep in mind the numerous manufacturing (machinability, assembly constraints ...) and maintenance constraints. From a concerted engineering viewpoint, a designer must take into account all the constraints to be met by product parameters throughout the design process.

Designers have a reasoning which is quite close to the ideal reasoning described above. However, they can only use intuition to anticipate the impact of their decisions on the constraints to be met by the final product. By dint of their experience, they know the approach to be adopted to avoid back-tracking as a result of failures during the design process.

As for constraint-based programming, this enables constraints to be propagated immediately when set [ILO.97].

Initially, we have a set of variables, each of which has a domain of possible values. Each time a constraint is set between these different variables, the impacted variable domains are recalculated in order to meet the constraints.

If the principle of constraint-based programming is applied to the design approach, we can consider that the product parameters are the constrained variables with certain initial domains. All the constraints to be met by the final product are then set. The domains of the different variables are reduced. If there are one or several empty domains, the design is a failure. If, on the other hand, the domains are all singletons, the constraints only allow a single solution to the design problem. If no domain is empty and domains which are not singletons subsist, the designer must give a value to all the variables still without values. This involves dynamically setting and removing constraints until single value domains are obtained for all the variables. This approach is developed and applied by the implementation of a declarative product metal-model in mechanical engineering, in [SEL.98].

4. Designer approach

The designer approach therefore consists of choosing one variable from those still to be given values, then choosing one value in its domain of possible values and so on until all the variables are allocated values. It is easy to see that, without the designer's knowledge regarding the order of variables to be chosen, the value to be given to them and the choices to be queried in the event of failure, the time taken to solve a design problem can be exponentially increased. In constraint-based design aid, it is vital to take the designer's knowledge into account by means of modelling.

The work described in [VAR.95], constitutes the initial modelling of the design process. Our aim is to enhance this model by adding solution strategy and failure processing capabilities using a declarative approach.

5. Proposal for a design process representation model

During the design process, a designer tends to group the parameters to be allocated values into sub-sets. He breaks his design task down into simpler sub-tasks to be solved until elementary tasks are obtained. A task can be seen as a set of variables to be allocated values. The designer possesses the knowledge required to break the design task down and determine the order in which these various sub-tasks are to be solved. Therefore, he possesses knowledge of the solution strategy for a design problem.

The product to be designed can be considered as a constrained knowledge base. Searching for a solution within a knowledge-based system is an Artificial Intelligence research domain. Modelling of solution knowledge emerges from this domain, structured around task and method concepts ([PIE.96], [ERM.96]).

The model we are proposing uses these task and method concepts.

- A task is an objective to be achieved, a problem to be solved, a set of parameters to be allocated values.

- A method is a possible way of solving a task. A method may be a chain of sub-tasks, thus enabling the designer's strategy knowledge to be modelled. It can also call on a procedure which will generate a value for all the variables to be allocated values by the parent task.

Thus a "beam design" task will comprise a more elementary "determination of the beam section" task which will be solved either by a first "material resistance calculation" method, or by a second "calculation by finished elements" method, or, ultimately "by experience".

The attributes of tasks and methods are their status, the resources they use, their opportunity, pre and post-conditions, strategy and failure processing. In addition, each method has a list of tasks to be executed and each task a list of methods that enable it to be solved.

- The status of a task or method depends on the course of execution. They can be impossible, executable, in process of execution, successfully executed or with execution ending in failure.

- The resource attribute enables the resources allocated to the performance of a task to be stipulated: the user, a given numerical algorithm ...

- The opportunity attribute enables the tasks of the same method to be classified dynamically (or the methods of the same task) so that the most appropriate is always chosen.

- Pre- and post-conditions are constraints to be met prior and subsequent to the task.

- The strategy function allows several heuristics to be defined for the order of the choice of a task's methods and the order of execution of a method's tasks.

Verification of design process execution can be split in two parts: firstly, knowledge of strategy concerning the order of execution of tasks and methods, secondly, knowledge for solving failures.

5.1. KNOWLEDGE OF STRATEGY

In order to use a declarative approach to the modelling of knowledge of strategy, we propose a certain number of relations called connectors which can be set between the tasks and methods. These relations are of two types. Firstly, there are the logic relations which affect the status of the tasks (one task can exclude another, one method can involve another, ...). Then there are temporal relations which model the order in

which tasks and methods are executed.

- Temporal connectors can be as follows: precedence, parallelism, synchronisation, appointment, and initialisation.
Precedence: One task (or method) precedes another task (or method).
Parallelism: Two tasks (or two methods) are executed in parallel.
Synchronisation: Two tasks (or two methods) start at the same time.
Appointment: One task (or method) only starts when the execution of n tasks (or methods) has finished.
Initialisation: Establishes the task or tasks to be executed first, or the method to be used initially.
- Logic connectors are the usual logic relations: AND, OR, exclusive-OR, inclusion,...

All these relations can be n-ary.

In addition, each task or method can have a set of constraints by means of which we know if it is opportune, or can be achieved, given the state of advancement of the design process. These constraints (pre-conditions) allow entry into a method or task to be dynamically verified beforehand.

With the assistance of these primitives, we are capable of modelling design processes for which we have no knowledge of strategy. This then consists simply of modelling the task/method/sub-task breakdown. This breakdown will be an AND/OR tree. One task will be successfully executed if one of its methods is successfully executed. One method will be successfully executed if all its component tasks are successfully executed. One task is successfully executed if all the variables which it is to evaluate are allocated values which meet all the constraints. [LEN.96].

Entirely known design processes can also be modelled with the assistance of these primitives. The process will then be modelled by adding the relations representing this process to the task/methods/sub-tasks tree.

The process model can then be assimilated to a graph whose nodes are task or method-type objects and arcs the connectors listed above. In addition, these relations are constraints in the sense of constraint-based programming.

It is therefore possible to model design processes ranging from completely unknown processes to entirely known processes, including intermediary processes of which we have partial knowledge

5.2. FAILURE VERIFICATION KNOWLEDGE

The second aspect of design process verification is the attitude adopted by the designer in the event of a failure occurring while a solution is being determined.

The designer's knowledge at the level of tasks and methods can then be encapsulated. This processing of failures can be an indication of the task or method to be executed as a priority subsequent to this failure, or may be a modification of certain parameters of the problem before trying out the failed task or method again...

6. Conclusion and prospects

Modelling of the design process could considerably reduce the time taken to solve a constraint-based design problem which would then allow benefit to be derived from the declarativity of constraints. This first model is only the starting point for work currently in progress on constraint-based design process modelling.

It would be ideal if the declarativity of our design process representation model could be reinforced (knowledge of strategy and failure management, in particular) in order to obtain a declarative product and design process model.

Initial implementation of the model is in process using C++ based on the IogSolver constraint library, the IlogViews interface generator and the ACIS modeller.

7. References

- [CHU.89] J.V.H. Chung, M.D. Schussel, "*Comparison of variationnal and parametric design*", Revue Internationale de CFAO et Infographie Vol 4, N°4, Hermès, France, 1989.
- [ERM.96] J.L. Ermine, "*Les Systèmes de connaissances*", Editions HERMES, 1996.
- [GEN.95] J. Gensel, "*Contraintes et Représentation de connaissance par objets - Application au modèle Tropes*", Thèse de Doctorat de l'Université Joseph Fourier Grenoble, France, 1995.
- [ILO.97] "*Ilog Solver 4.0: Référence manual*", Ilog, 1997.
- [LEN.96] C. Lenguin, "*Spécifications pour un langage de représentation du processus de conception en génie mécanique*", Mémoire de recherche, DEA de Production Automatisée, ENS Cachan, Nancy1, CESTI, juillet 1996.
- [PIE.96] C. Pierret-Golbreich, "*TASK, un environnement pour le développement de systèmes à base de connaissances flexibles*", Habilitation à diriger des recherches, LRI, Orsay, 1996.
- [SAU.95] A. Saucier, C. Vargas, P.A. Yvars, "*An environment for mechanical design aid applications development*", Revue Internationale de CFAO et d'Infographie, Vol10, n°1-2, Hermès, France, 1995.
- [SAU.97] A. Saucier, "*Un modèle produit multi points de vue pour le développement et l'utilisation de systèmes d'aide à la conception en ingénierie mécanique*", Thèse de Doctorat, ENS Cachan, 1997.
- [SEL.98] F. Sellini, P.A. Yvars, "*Méta modèle déclaratif pour la représentation d'une classe de produits en conception mécanique*", Actes de IDMME'98, Compiègne, mai 1998.
- [TRO.89] B. Trousse, "*Coopération entre systèmes à base de connaissances et outils de CAO: l'environnement multi-agent ANAXAGORE*", Thèse de Doctorat de l'Université de Nice, Décembre 1989.
- [VAR.95] C. Vargas, "*Modélisation du processus de conception en ingénierie des systèmes mécaniques*", Thèse de Doctorat, ENS Cachan, 1995.
- [WAG.90] M.R. Wagner, "*Understanding The ICAD System*", ICAD Inc, 1990.

CONCAD Bridging: Managing the Integration of Technical Solutions in a Modularize Product Concept

Mark W. LANGE

The Royal Institute of Technology

Computer Systems for Design and Manufacturing

SE – 100 44, Stockholm, Sweden

mark.lange@modular-management.se mla@cadcam.kth.se

Abstract

CONCAD Bridging [ENDREA, 97b], a research project for ENDREA [ENDREA, 97a], is focused on developing a methodology for the earlier integration of product information and data from concept development (CON-) related activities, with detail design (-CAD) related activities. This paper describes a portion of this research focus; managing the integration of technical solutions into modules in a modularized product concept. The identification of technical solutions is provided by a method called modular function deployment. A method is described for supporting the grouping of the technical solutions in the module indication matrix, using a design structure matrix to help clarify the interface interaction relationships. This method is clarified using a case study from a drill motor modularization project. The results of the case study are discussed and conclusions presented to highlight the advantages of applying the method to manage the development of a desired product.

1. Introduction

During the conceptual development phase of a structured product development model [Pahl & Bietz, 94], the needs of the customer are identified. These needs, or customer requirements, are then transformed by the different activities during this phase and result in a specification describing a product concept. This specification is then used as input to the following phases, embodiment and detail design.

The different activities occurring in the concept development phase address the different concerns that a corporation has regarding how a product fulfills the customer needs, such as marketing, design, production and economics [Andreasen & Hein, 87][Olsen, 76]. A method called, Modular Function Deployment (MFD) [Erixon, 98], is a structured means of executing the concept development phase that takes into account these corporate concerns. Using this method to develop a modularized product platform

concept has proved to be successful in a number of Swedish industrial product development applications [Erixon *et al.*, 96][Erixon *et al.*, 94].

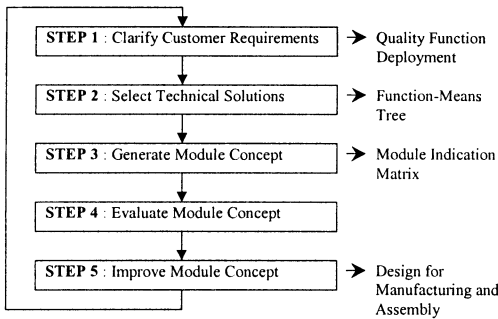


Figure 1. Steps in Modular Function Deployment, adapted from [Erixon, 98]

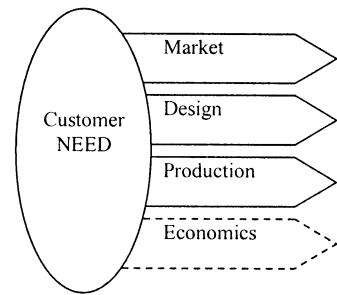


Figure 2. Integrated Product Development adapted from [Andreasen & Hein, 87][Olsen, 76]

At the heart of the MFD method is the Module Indication Matrix (MIM). When using this tool, it is first filled with the technical solutions that have been identified from the function-means tree in step 2. Each technical solution is then weighted to determine its suitability as a module foundation, according to the company specific module driver's. Then the interface interactions and relations, such as geometry, energy, material and information [Pahl & Beitz, 95], with the other technical solutions are defined.

The weights of the module drivers are then summed and those technical solutions that have the highest scores are selected as module foundations, the number of which is determined approximately by the square root of the total number of components in the product [Erixon, 98]. All the remaining technical solutions are then grouped together with the module foundations according to the matching of module driver patterns. It is the grouping of these technical solutions into modules that this article shall address.

2. Problem

2.1. INTERFACE INTERACTIONS

Using the interface matrix in the MIM, interface interactions between technical solutions are represented as weighted "binary" properties. In other words, the results of the interface matrix describe only that there are relationships between technical solutions and their importance. But, interactions are "directional" attributes. This means that the presence of an interface interaction indicates that attributes such as energy, material, and information are transmitted from a technical solution to one or more technical solutions. In order to optimally manage the generation of a modular concept it is important to clearly identify both "binary" and "directional" attributes of interface interactions.

2.2. INTERFACE INTERACTION EFFECTS

Interface interactions have desired and undesired effects. Not only that, there is an "effect transmitter" and an "effect receiver". For example, the transmission of thermal energy between technical solutions, using the principle of conduction, may be the desired effect. In other words, a "transmitting" technical solution provides a "receiving" technical solution with a desired effect. But, the transmission of thermal energy, by the principle of radiation, to the surrounding technical solutions, may be an undesired effect. In this case "receiving" technical solutions are being provided undesired effects by the "transmitting" technical solution. Thus, the management of the integration of technical solutions, in a module concept, must take into account the desired and undesired effects.

2.3. COLLECTION OF TECHNICAL SOLUTIONS

In order to differentiate between the procedure described in the MFD method and the procedure described in this article the following definitions regarding the formation of modules using technical solutions must be made. 1) **Strategic Grouping** – This is the collection of technical solutions into modules based on a module driver profile. This reflects the fact that a number of technical solutions have a similar module drivers that clarify how a corporate organization will manage the resulting module concept. 2) **Technical Integration** – This is the collection of technical solutions into modules based on the interface interactions. This reflects the fact that there are interactions within a module, as well as between modules, that must be managed during the embodiment and detail design phases.

Utilizing just the strategic grouping, or just the technical integration, for the collection of technical solutions in a module concept can have wide spread detrimental effects in a company organization and the desired functionality of a product. To avoid these effects, it is important that both techniques be used in an iterative process and that this process is supported by suitable tools.

3. Solution

3.1. THE SUPPORT TOOL

In order to solve these problems, the interface matrix must be capable of clarifying and

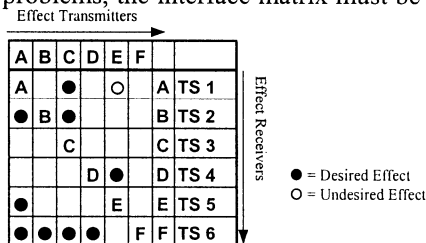


Figure 3. Design Structure Matrix, adapted from [Pimpler & Eppinger, 94]

representing both “binary” and “directional” relationships and the desired and undesired effects of interface interactions. A review of available literature has shown that a design structure matrix (DSM) [Steward, 81], can be used to model this type of information. It has been shown that a DSM can be useful in modeling system architecture based on component relationships [Pimmler & Eppinger, 94]. Additionally, when modeling a project, task and organization structure sequencing can be performed in a DSM, based on information flow relationships [McCord & Eppinger, 93].

3.2. THE METHOD

3.2.1. Interface Interaction Taxonomy

The method described in this article utilizes a component based DSM to clarify the interface interaction relationships between technical solutions. Here, the use of taxonomy is helpful in differentiating between the different types of relationships, as shown in Table 1. This table may be extended with specific interaction forms, depending on the level of product decomposition and technical solutions represented. Thus the taxonomy can take into account solution specific interactions such as electrical energy, thermal energy, mechanical energy, etc.

Table 1. Interface Interaction Relationship Taxonomy, adapted from [Pimmler & Eppinger, 94]

Relationship	Interaction	Interface (description)
Binary	Spatial / geometric	A physical association and/or alignment is necessary.
Directional	Energy	The transmission/exchange of energy is necessary.
Directional	Material	The transmission/exchange of material is necessary.
Directional	Information	The transmission/exchange of information is necessary.

Table 2. Spatial / Geometric Interface Qualifications

Qualification	Symbol	Clarification
Desired	●	Physical alignment is necessary for functionality.
Indifferent	(no symbol)	Physical alignment has no effect on functionality.
Undesired	○	Physical alignment prevents functionality.

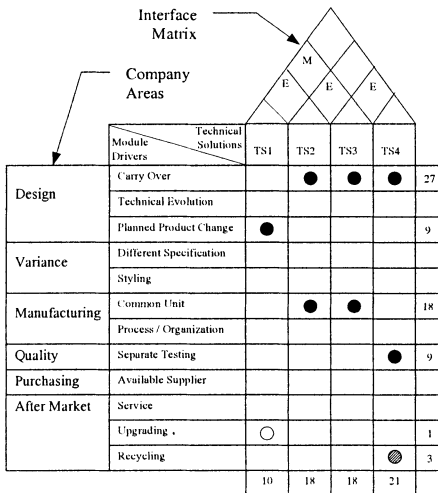


Figure 4. Module Indication Matrix, adapted from [Erixon, 98]

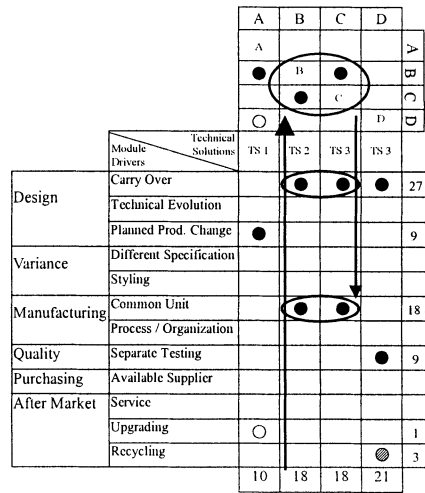


Figure 5. Following the method steps through the DSM augmented MIM matrices

Using the taxonomy selected for the product under investigation, the nature of the relationships between the technical solutions must be qualified. For this method the clarifications are *desired*, *indifferent* or *undesired*, as shown in Table 2. The qualifying symbols are then placed in the matrix according to a directional relationship (i.e. transmitter/receiver) or a binary relationship (i.e. transmitter/receiver “=” receiver/transmitter).

For each type of interaction in a product, a separate DSM layer is generated, producing a three dimensional information structure. This layering enables the focus to be placed on a particular type of interaction that should be addressed while integrating technical solutions into modules. An example of this is an electrical type of product that has spatial relations and energy interactions in the form of wiring connections, or a software type of product that has information interactions.

Grouping is initiated in the MIM by identifying the technical solutions with the highest module driver scores. These high scoring technical solutions are used to initiate the selected DSM. In the DSM, the symbols are then clustered together by sorting the technical solutions so that the symbols come as close to the diagonal as possible. This results in the formation of technical solution “clusters”. These clusters, representing the integration of the technical solutions, are an indication of a module. When a cluster is obtained, it should be referenced back to the MIM to determine if there are any module drivers that are in conflict for the technical solutions in the cluster.

4. Case study

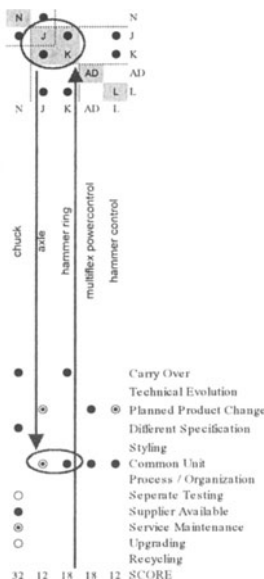


Figure 6. Energy Interaction matrix, Axle Module



Figure 7. Spatial Interaction matrix, AC/DC Transmission Modules

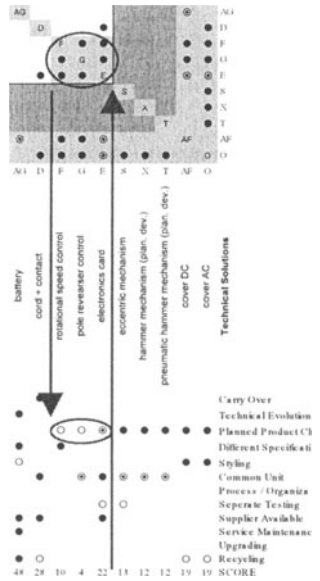


Figure 8. Spatial interaction matrix, Electronics Module



Figure's 6 through 11 are a portion of the project results obtained in a modular product

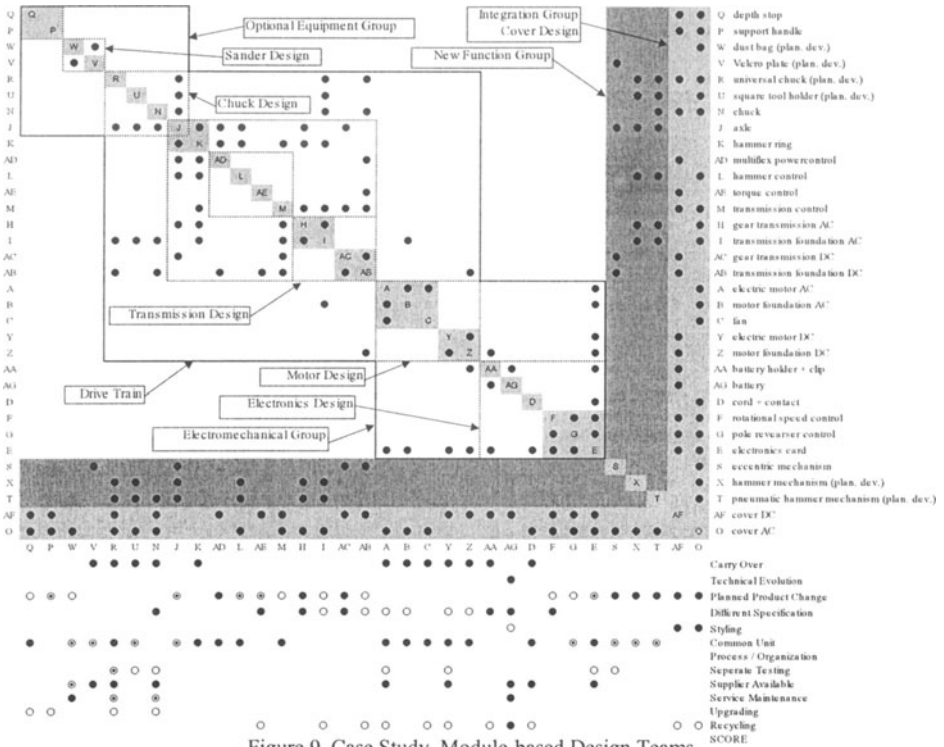


Figure 9. Case Study, Module-based Design Teams

concept for a drill motor. This concept describes a product platform divided into an AC product line and a DC product line. One of the modularization project objectives was to increase the use of common units between the two platforms. Another objective was to identify how these modules could be managed by a company organization using functional design teams.

The interface interactions selected for technical integration to assist in the strategic grouping were “spatial/geometric” (Fig. 7 and 8) and “energy” (Fig. 6). Grouping was initiated in the MIM. Using five of the high scoring technical solutions as module foundations, integration was started using the “energy” DSM to clarify the transmitted mechanical and electrical energies. Effected technical solutions were clustered around these first module foundations to identify potential modules. These results were then used to continue the identification of modules in the “spatial/geometric” DSM. These results were then reflected back to the MIM for verification.

In these results, some of the technical solutions had a great number of interactions with other technical solutions. These were predominately modules identified as having “planned product change” or “styling” module drivers. They were not forced into modules, but moved to the side of the matrix and treated as technical “integration” [Pimmler & Eppinger, 94] modules. Moving these modules to the side of the DSM

assisted in obtaining the necessary clarity so that the remaining technical solutions

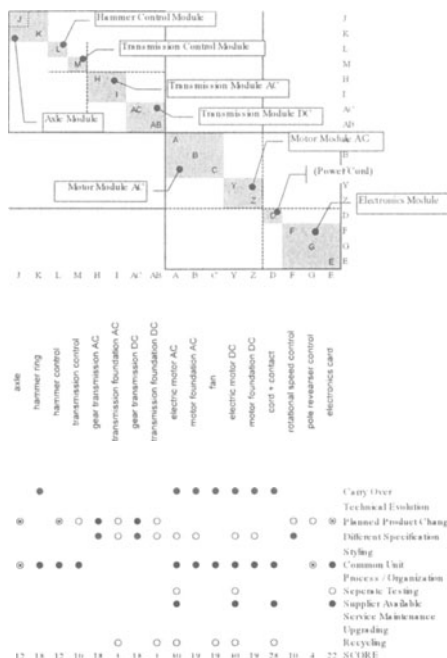


Figure 10. Final Modular Platform Concept

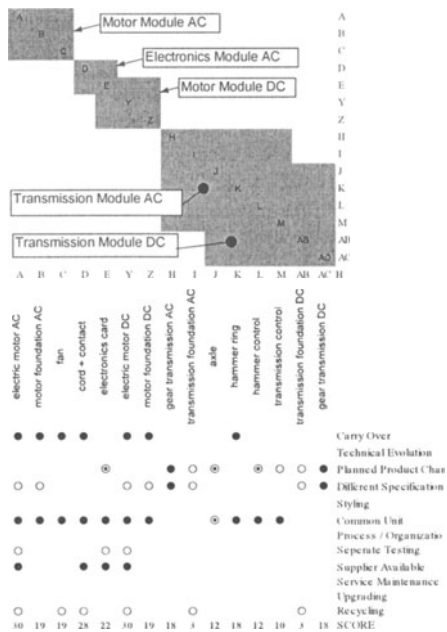


Figure 11. Initial Modular Platform Concept

could be integrated and their groupings verified.

5. Discussion

Moving technical solutions that had a great number of interactions with other technical solutions, to the side of the DSM, helped to clear the matrix of a great deal of information so that integration and grouping could continue. It was observed that the clustering of the symbols reflected a higher level of functional decomposition. In other words, the DSM presented a grouping of “electromechanical”, “transmission” and “optional equipment” functional clusters. These clusters were used to support the identification and recommendation of product design teams, as shown in the figures.

6. Conclusions

This paper has presented a method for managing the integration of technical solutions in a modular product concept. The strength of this method is the ability of the design structure matrix (DSM) to clarify both binary and directional interface interaction relationships that must be taken into account when grouping technical solutions in a module indication matrix (MIM), when they are known to exist. Additionally, this method provides a means of identifying functional project teams that can be implemented by a company organization in a product development effort.

References

- Andreasen, M.M. and L. Hein, Integrated Product Development, IFS Publications Ltd / Springer-Verlag, UK, 1987.
- ENDREA, The Swedish Engineering Research Education Agenda, <http://www.endrea.sunet.se>, 1997
- ENDREA, Collected Project Descriptions, 1997.
- Erixon, G., Modular Function Deployment; A Method for Product Modularization, Doctoral Thesis, The Royal Institute of Technology, Stockholm, Sweden, 1998.
- Erixon, G., Fredriksson, J., Romson, L., and von Yxkull, A., Modulindelning I Praktiken, Sveriges Verkstadsindustrier, ISBN 91-7548-460-9. (in Swedish only), 1996.
- Erixon, G., Erlandson, A., von Yxkull, A. and Östgren, B.M., Modulindela produkten - halvera ledtider och offensiv marknadsorientering. Industrilitterature, ISBN 91-7548-321-1. (in Swedish only), 1994.
- Eppinger, S.D., "A Model-Based Method for Organizing Tasks in Product Development", *Research in Engineering Design*, vol. 6,no 1, pp. 1-13, 1994.
- McCord, K.R. and Eppinger S.D., *Managing the Integration Problem in Concurrent Engineering*. K. R. McCord and S. D. Eppinger, M.I.T., Sloan School of Management, Working Paper, 1993.
- Nordlund, M., *An Information Framework for Engineering Design based on Axiomatic Design*, Doctoral Thesis, KTH, Stockholm, Sweden 1996.
- Olsen, F., *Systematic Design* (in Swedish), Ph. D. Dissertation, Lunds Tekniska Högskola, Sweden, 1976.
- Pahl, G. and Beitz, W., *Engineering Design; A systematic Approach*, Springer-Verlag 1995, ISBN3-540-19917-9.
- Pimmler, T.U. and Eppinger, S.D., "Integration Analysis of Product Decompositions", *Design Theory and Methodology - DTM '94*, DE-Vol. 68, ASME 1994.
- Steward, D.V., "The Design Structure System: A Method for Managing the Design of Complex Systems", *IEEE Transactions on Engineering Management*, vol. EM-28, no 3, pp. 71-74, August 1981.
- Suh, N.P., *Principles of Design*, Oxford University Press, 1990.

MECHANICAL MODELS MANAGEMENT IN ENGINEERING DESIGN

N. TROUSSIER*, F. POURROY*, M. TOLLENAERE** and
B. TRÉBUCQ***

** Laboratoire 3S UJF INPG CNRS UMR 5521, Domaine Universitaire
BP 53 38041 Grenoble Cedex 9 France*

*** Laboratoire GILCO INPG, 46 avenue Felix Viallet 38031 Grenoble
Cedex 1 France*

**** Groupe Schneider, Centre de Recherches A2 F-38050 Grenoble
Cedex 9 France*

Abstract

This paper presents a methodological approach to mechanical models management in engineering design. Numerous models are generated by mechanical designers during product development, and in case of modification and reuse, handling the models remains a costly task. Thus, a methodology for using and reusing mechanical analysis, in relation with the functional specifications of the product, is necessary. To support a methodological approach of calculation, a data structuring on the mechanical analysis in engineering design has been carried out in order to enable both the models management when engineering change occurs and the reuse of previous analysis. Entities and linkage between these entities are described. This paper highlights specific entities, namely “instructional cases”, which are of the utmost importance for the engineering knowledge they carry. It is to be noticed that the methodology supported by the data structuring is useful both for educational and industrial purposes.

1. Introduction

In today's competitive environment, companies are under enormous pressure to reduce time and cost of their design process, and to improve the quality of their products. It is commonly admitted that early good decision making is a key to improve both quality and time to market. Therefore, the use of mechanical analysis, according to specifications, appears earlier and earlier in engineering design. As a multitude of models (experimental or numerical) is generated during a project, the various models management becomes a great challenge to improve engineering efficiency.

Reference [13] provides the main results of the research projects on engineering change over the past twenty years. Two points should be pointed out : firstly, the tracks of the design process are required when engineering change occurs to provide what are the effects on the product. Furthermore, [13] highlights that, in case of engineering change, product functions must remain fulfilled.

In order to help the designer in decision making, it could be interesting to provide him with a way to evaluate the influence of the design parameters on the specifications. Therefore, the design model handled has to be linked to the analysis models. The design / analysis linkage has been considered for a long time only as a link between a geometric CAD model and a single analysis model (figure 1). Then, the problem encountered deals with idealisation and linkage between two geometric representations [11], [3], [9]. More recently, the evolution of models along design has been taken into account through a data model for mechanical analysis [8]. However, the data model doesn't match the management and the use of mechanical models generated to validate product specifications. The latter point is of major importance as the number and kind of models have dramatically increased along the development cycle of the product.

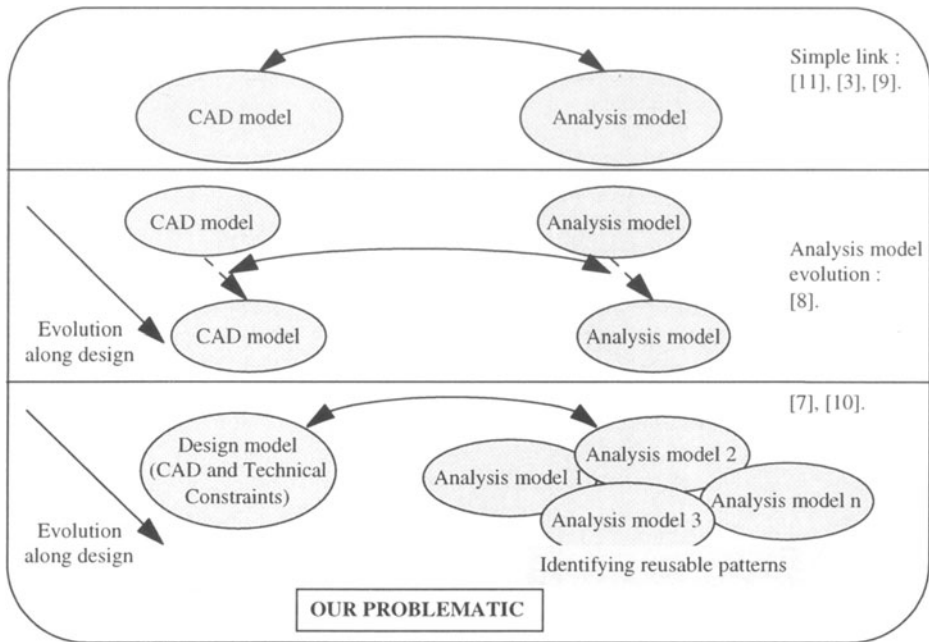


Figure 1. Evolution of research works on Design / Mechanical analysis integration.

Several mechanical models are usually associated with a product development such as kinematic, static, dynamic models in the mechanical field. A kinematic model is often used before a structural analysis. Simplified models could be achieved (beam theory for instance) such as more sophisticated ones (FEM or specific methods for instance for spring calculation [6]). Concerning with the numerical simulation, [10] highlights the difficulties due to the multiplicity of the available mechanical models with respect to the decision making amongst them. [12] provides the qualitative errors implied by choices along a numerical simulation and points out that the reliability of the calculation is in relation with the adequate choice of model, but also with an appropriate formulation of the calculation goal. This last remark emphasises the need for a designer to have a methodological approach for calculation and justifies the need of designer tools to aid him in the management and handling of the different models.

To store and reuse analytical knowledge [5] provided by calculation, data structuring is achieved. However, two reasons have to be mentioned for the present lack of reuse in engineering design :

- In a reuse context, an important feature is to make model modifications very easy. Such modifications are actually somewhat difficult.
- Previously stored models may have to be updated, even when they have not to be reused yet. This is actually made by the designer only if he has an interest to do that.

These two reasons must be taken into account for the methodological tool to be developed.

Reference [4] presents a method to capture the reusable data, that is to say the knowledge created by calculation and the context of its creation in order to reuse it in further design projects. These authors describe a data model, where data are clustered, classified in a confidence matrix and evaluated in an importance matrix.

Nevertheless, this data structuring model isn't presented for reusability and, even if it allows helping for data modelisation, management of numerous entities and links isn't supported.

To enable the management and reuse of different models in relation with product specifications, [7] suggests the development of a specific software environment, especially adapted to engineering design and flexible enough to fit the different industrial needs. Yet, a specific environment is arduous to support in terms of development and maintainability.

The present paper proposes a formal model that enables the designer's management of the analysis models all along the engineering process. To fulfil such a purpose, an identification of entities handled by designers and the linkage between these entities are proposed in the specific field of mechanical analysis.

2. Entities Handled by Designers for Mechanical Analysis

2.1. SUPPORTING EXAMPLE

All along the paper, an example is used to illustrate the purpose : a U-sectional beam that must fulfil the function « robust appearance ». This function is split in many specifications including the following : « when somebody holds one end of the beam and applies a defined transverse load to the other end, the displacement should be less than 2 mm ». The designer is assumed to use numerical simulation (FEM) in order to provide a U-sectional beam that verifies this specification. The different tasks of the design process are :

- evaluate the displacement under transverse load with a beam model,
- see that the beam model provides unexpected results in terms of behaviour, compared with the designer experiment,
- try a shell model,
- have a good behaviour, but the maximal displacement value is over 2 mm,
- decide to add ribs in U-sectional,
- achieve a simulation to evaluate the best rib position,
- evaluate the maximal displacement with the ribs in the U-sectional,
- conclude that the displacements under transverse load are under 2 mm,
- accept the design.

2.2. MAIN CONCEPTS

The product design features are gathered into an entity called “**Design Model**” that contains both the description of the product and the whole set of constrained design parameters. It must be highlighted that the design model evolves rapidly all along the engineering process.

Most of the time, design actions are justified in relation to the product requirement list. The requirement list contains functions that must be verified such as “the product has to be integrated in a casing”. Nevertheless, functions must be translated in design parameters in order to draw evaluation criteria for design options choice. Criteria for engineering choices derived from product function are then called constrained design parameters (for instance, “the total length of the system must be less than a certain value”). Constrained design parameters are fluently used in tolerancing.

However, a function from the requirement list may sometime be concerned with the mechanical behaviour of the product (for example, “no residual default under the user’s weight”). The related constrained design parameter (which could be “the maximum Von Mises stress must be less than half of the yield stress under 100 kg”) has generally to be translated in more accurate mechanical analysis terms for the analyst in order to recognise all data required to complete the analysis. The reformulating of the constrained design parameters leads to a specific entity namely “**Simulation Goal**” that contains both reformulated constrained design parameters and project parameters. The reformulated constrained design parameters are composed of :

- the mechanical features of interest and its particular location (local or global effects of strain, stress, displacement, eigenmodes ...),
- the part(s) of the structure of interest,
- the location of the mechanical features to be observed,
- the situation of the part in its environment from which loads and boundaries conditions will be deduced.

In other words, the reformulated constrained design parameters emphasise the question to be answer by the analyst.

The project parameters are deduced from the purpose of analysis (validation, help for decision making, understanding). They are :

- the evaluated duration for analysis (in relation to the cost of analysis),
- the expected level of accuracy,
- the ability of reuse for the analysis (conclusion, result, models or process) in the same project or, moreover, for other design projects.

The reuse assumes that certain kinds of calculation or results are frequently used. As in software engineering, object based programming has become very popular according to its reuse ability, in mechanical engineering, specific usual analysis could be stored in a database of typical cases.

These project parameters are provided by the analyst and can be modified along the analysis process. They are highly dependent on the context of the analysis (interest of the analyst in the problem, proximity of a project meeting for example). The Simulation Goal express the wish of the analyst in terms of what is the conclusion to be obtained. For example, it could be “verify the global displacement (<2 mm) when the part 10 is in use; a short duration is envisaged, with great accuracy and relatively high reusability”. In the following Figures that illustrate the data structuring, the project parameters are not explicitly given, but are assumed to be taken into account.

The “**Conclusion**” entity is a discussion of the results in relation with Simulation Goal, drawn under consideration of the whole set of hypothesis. The Conclusion may be rather qualitative than quantitative. The analyst observations have to be explicitly associated with Simulation goal in order to provide a meaningful conclusion for the designer.

The analyst observations are based on a “**Result**” entity provided by computation. For example, the Result entity may contain several stress or strain maps, tables of displacement values, curve of sensitivity analysis. It contains the rough output devoid of interpretation and characterised by tolerance provided by computation error indicators (such as error on strain energy convergence in a FEM analysis).

To provide results, a tool (method of calculation and a software or device to be used) has to be chosen. This choice is achieved in relation with the Simulation Goal, according to project parameters and mechanical features of interest. The tool always needs a specific product representation adapted to the simulation method used. This representation, associated with the Simulation Goal, is called “**Simulation Model**”. A FEM model and the associated computation parameters form an example of Simulation Model.

However, both the choice of a tool and the product material and geometric representation depend on the mechanical behaviour of the structure to represent. In other words, the Simulation Model is based on a “**Mechanical Model**” which is a representation of the product from a mechanical behaviour point of view. Mechanical data such as loads, boundary conditions, and material behaviour are deduced from the Simulation Goal to describe the relation between the structure under consideration and its environment. The Mechanical Model geometric representation is deduced from the Design Model by an idealisation step. Its representation is usually a sketch drawn by the designer at the first stage of the analysis. This sketch contains mechanical hypothesis, as the type of structure behaviour assumed under loads, the material behaviour, or some hypothesis on the problem linearity.

The Design model is thus the reference of the product evolution during engineering design in terms of definition (geometric and technical definition) and function (relation with the environment translated by the constrained design parameters).

2.3. HANDLING THE MODELS

The different entities presented above constitute the “Project” entity, reduced to its mechanical analysis viewpoint, on a company wild scale.

Figure 2 shows the described entities joined with two types of links. The graph on the left of the figure provides the general entities and their linkages. The right part of the figure illustrates the structuring with the example.

On one hand, the black straight lines represent informational linkage that associates two entities together. In other words, the informational linkage describes the dependence that exists between two objects. For instance, the Mechanical Model is defined with the help of both the Simulation Goal (loads, boundary conditions...) and the Design Model (geometric representation, material,). Moreover, the Mechanical Model is an informational support to build the Simulation Model.

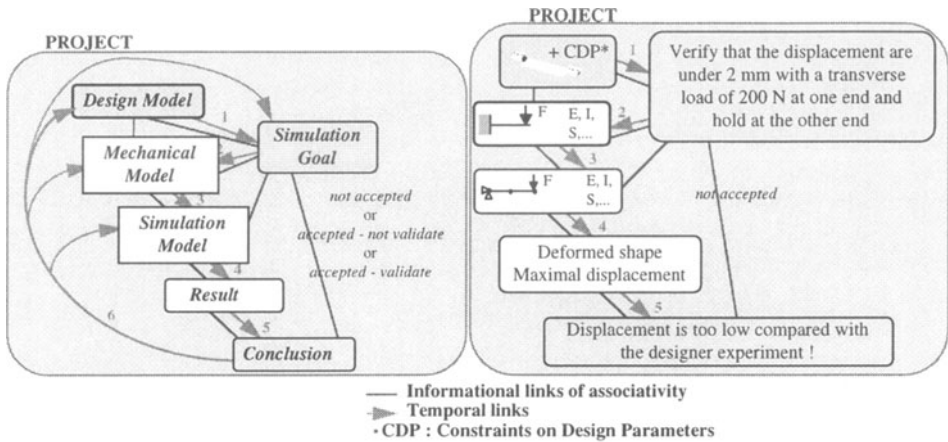


Figure 2. Description of the Project mechanical analysis view point.

On the other hand, the grey numbered arrows support the methodology proposed, and provide the analysis process. This process is given by following the arrows according to the growing numbers.

Thus, two kinds of knowledge are described : the knowledge linked to each entity and the knowledge on the process followed to drive the analysis.

2.4. IDENTIFYING INSTRUCTIONAL CASES

At the higher level that corresponds to the corporation scale, a project often uses data issued from previous projects. The information exchange is achieved with the help of specific entities external to any project, and handled at the same corporation scale as the project entity. These entities are called “**Instructional Case**” and two different cases are distinguished in function of the type of problem they answer. The “**Elementary Case**” brings a solution to a modelisation problem, whereas the “**Simplified Case**” answers to a design options choice. At each Instructional Case type corresponds a specific structuring at the lower level of entities.

The different entities used by the designer, the project entities, and two instructional cases are shown in figure 3. Following the grey arrows enables understanding the analysis process. Afterwards, the informational links are divided in two types :

- the informational links between two different types of entities (like those in Figure 2),
- the informational links between the same type of entities that refer to an “external” analysis (external of the project context).

Let us describe this last type of informational links. They explain the reasons for the entity evolution. For example, at the end of the first analysis, the designer concludes that the maximal displacement is too low compared with his experiment. Then, he assumes that the mechanical model used doesn't match. In order to find a well-adapted model, he decides to complete an analysis on a simplified geometry by comparing the results provided by a beam model and a plate model. This analysis is achieved “out of the project context” and can be reused in another project to make a modelisation choice.

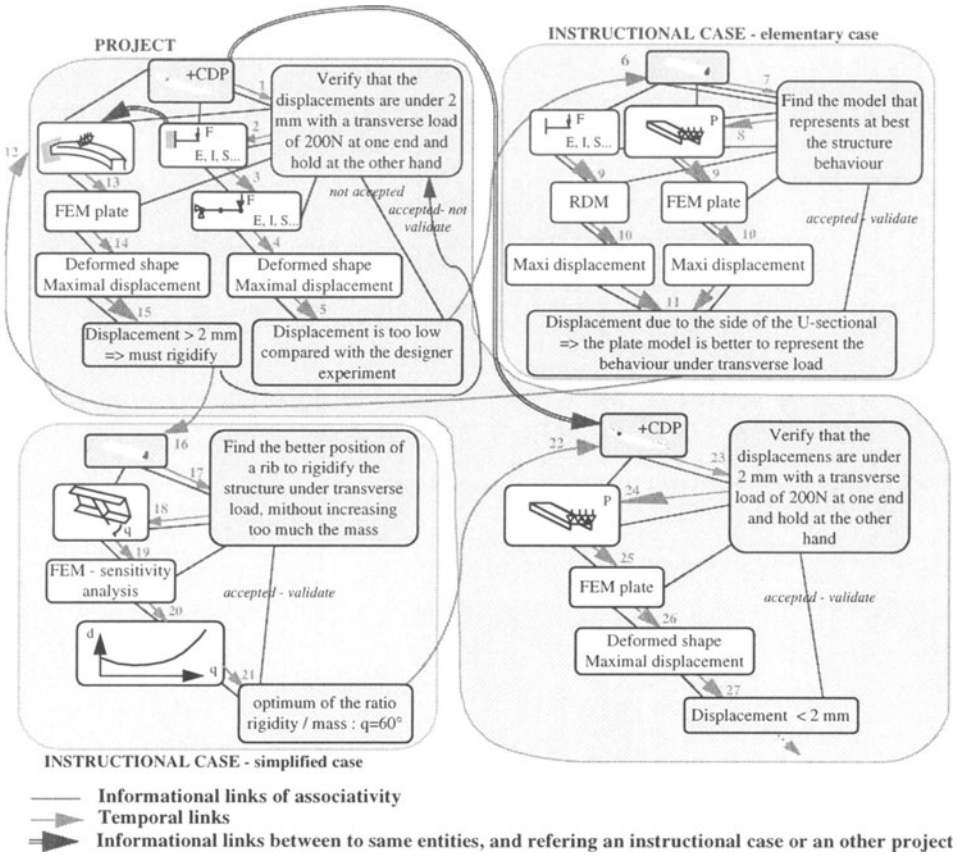


Figure 3. Two types of Instructional Cases.

Then, the data structuring enables us to disconnect the instructional case achieved (which is, in this case, an elementary case that brings an answer in terms of mechanical modelisation) and to reuse it independently of the present project. In a similar way, when the need of more rigidity for the structure appears, an answer to the design problem “how should I place the rib ?” is built with the support of a simplified geometry. The knowledge provided by the instructional case, called here simplified case because it answers a design problem, could be used in another project, independently of the present one. In such a case, it is called simplified case because it answers a design problem. Conversely, the elementary case has been used to answer mechanical modelling questions.

Both the Instructional Cases are of great interest in terms of knowledge improvement and spreading at a company wide scale.

3. Conclusion

The information structuring proposed in this paper for mechanical model management in engineering design constitutes a helpful contribution in an engineering design

methodological approach of mechanical analysis, both for education and industrial purpose. This model improves the design constraints representation and integration by the way of the constrained design parameters of the Design Model entity and their links with other entities. Moreover, this work aims at tracking the engineering choices made by means of mechanical analysis and linked with the product requirements. The track of the linkage between the different entities all along the project improves the management of engineering changes and allows the reuse of previous mechanical analysis.

A design tool is under progress to support the management of the data structuring in order to handle the analysis done, retrieve previous analysis case, navigate through its different entities and load previous entities to handle it in a current process. This tool is achieved with the DBMS ACCESS and Pro/Engineer.

References

1. Amara, B.E., Deneux D., Soënen R., Dogui A.: CAD/Analysis Integration, *First International Conference IDMME'96*, Nantes, France (1996).
2. Armstrong C., Douaghi R., Bridgett S.: Derivation of an Appropriate Idealisations in Finite Element Modeling, *Advances in Finite Element Technology* (1996).
3. Arabshahi S., Barton D.C., Shaw N.K.: Steps towards CAD-FEA Integration, *Engineering with computers* **9** (1993), 17-26.
4. Hamilton J.H., Clarkson J., Burgess S.: The Modelling of Design Knowledge for Computer Supported Aerospace Design, *International Conference on Engineering Design, ICED97*, Tampere (1997).
5. Hashemian M., Gu P.: Modeling the Creative Knowledge of Conceptual Design, *International Conference on Engineering Design, ICED97*, Tampere (1997).
6. Kletz U., Schorcht H.J.: CAD/FEM System for Integrated Shape Design and Calculation of Springs and Spring Systems, *International Conference on Engineering Design, ICED97*, Tampere (1997).
7. Kuhnappel B.: Simulation-Based Evaluation in Conceptual Design, *International Conference on Engineering Design, ICED 97*, Tampere (1997).
8. Remondini L., Leon J.C., Trompette P.: Generic Data Structures Dedicated to the Integrated Structural Design, *Finite Elements in Analysis and Design* **22** (1996), 281-303.
9. Rezayat M.: Midsurface abstraction from 3D solid models : general theory and applications, *Computer-Aided Design* **8** (1996) 905-915.
10. Schweiger W., Löffel C.: Computational Methods in Design-An Ordering Scheme, *International Conference on Engineering Design, ICED97*, Tampere (1997).
11. Shepard M.S., Korngold E.V., Wentorf R.: Design Systems Supporting engineering Idealizations, *Geometric Modeling for Product Engineering*, IFIP (1990).
12. Szabo B.A.: The Problem of Model Selection in Numerical Simulation, *Advances in Computational Methods for Simulation*, Civil-comp (1996), 9-16.
13. Wright I.C. A Review of Research into Engineering Change Management : Implications for Product design, *Design Studies* **18** (1997) 33-42, 1997.

PROPOSAL TO CONTROL THE SYSTEMS DESIGN PROCESS : APPLICATION TO MANUFACTURED PRODUCTS

Philippe GIRARD, Benoît EYNARD and Guy DOUMEINGTS

Laboratoire d'Automatique et de Productique - Groupe GRAI

Université Bordeaux I

351, cours de la Libération - 33405 TALENCE CEDEX - FRANCE

Tél : +33 (0)5 56 84 24 00 - Fax : +33 (0)5 56 84 66 44

e-mail : girard@lap.u-bordeaux.fr

Abstract

This paper presents an extension of the GRAI approach in the scope of the control of design systems of manufactured products and its validation with an industrial application. The product design is defined as the evolution of a flow of informations representing the product knowledge. It is enlightened that both the design process and the product knowledge should be simultaneously and concurrently managed. We propose a model to control the design system, based on the study of the decision sub-system. This control is determined by objectives linked on the one hand, to the product (quality, cost, delay) and, on the other hand, to the system (resources, multi-projects management, cost of activities). The industrial experimentation allows us to conclude on the pertinence of the elements of control which are proposed.

1. Introduction

The performance of the enterprise requires to control cost, quality, flexibility and delay of the manufacturing process. The choice of the relieve date of a product can have important consequences depending on whether the enterprise is a leader or a follower in the market. Tarondeau (1994) specifies that advantages obtained by the leader depend on the delay of followers. If the delay is important, the leader takes advantage from its dominant location to refine the characteristics of its product, to improve its position, and to extend its range. The followers will restrict the leader's advantages by reducing the development duration. A short cycle of development limits risks and costs : the needs to satisfy are better known

when we are near to the launching date, each decision taken during the design reduces the domain of solutions and limits the adaptability of the product to the evolutionary needs of the market. In conclusion, a better control of product development process respecting strategic objectives allows to enlarge the performances of the enterprise. We plan to study the design system with the aim of reviewing the problem of the design in an industrial performance environment. We show that there exists two overlapping unknown strongly : the product and the design process. We insist on the necessity to manage simultaneously and concurrently the evolution of the product knowledge and the planning of design processes activities to achieve the objectives of the industrial strategy. This incites us to identify the decision process both on the design and the planning point of view. We present elements of the control of the design system as part of manufactured products.

2. The design system

In a first approach, the design can be defined as an activity of transformation. The transformed data represent the requirements in input and the definitive layout of product in output. The design, characterised by a flow of informations, uses means and has to satisfy some constraints and objectives . This transformation is influenced by external elements such as the market, the strategy enterprise and the production. But it is not sufficient to study the design only as a set of activities of transformation. It is necessary to consider its evolution with respect with its environment and to be interested in its finality. We propose to study the object design system as an open complex system that we represent as a three subsystems model (Doumeingts, 1984). First the operating system which corresponds to the processes and actors that transform the flow. Output flow, which result from the transformations of input flow in the system, are the products in accordance with the mission of the system. Then the decision system that controls the operating system in order to satisfy its finality. And finally, the information system that stores, memorises, and delivers the set of informations which participate in the process of flows transformation.

Therefore the design is a process of transformation of flow of informations which represent the evolution of the product knowledge. Some elements influence the process without belonging to it : the strategy of the enterprise, the constraints of the market, the resources of the design and the production for example. We talk about a field, considered as an influence capacity which can not be dissociated from the notion of flow. As Ermine *et al.* (1996) present in the SCFC model (Source-Target-Flow-Field), another duality named source/target exists in the processes modelling.

In design (Figure 1) we know the source since it corresponds to the ratified expression of the user's requirements in the form of a functional design contract. The source action is the necessity to solve identified problems to satisfy one or several requirements. The target is a

priori unknown since it is the product knowledge which is obtained by selecting one of the possible solutions defined by the design process.

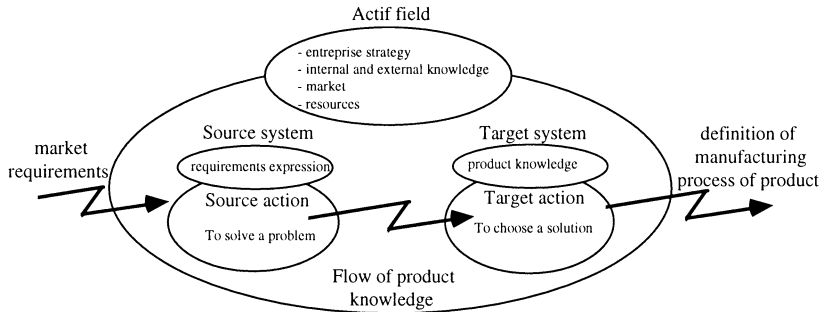


Figure 1 : S.C.F.C model of design process

Another complexity is owed to the fact that we do not know the process which drives the choice of the best solution. This process is built as and when the reduction of incompleteness of the product knowledge and according to the influence of elements of the active field. Therefore two related unknown parameters exist : the design process and the product knowledge.

3. The product and the design process : two unknowns

3.1. MODELLING OF THE PRODUCT KNOWLEDGE

Many researches are involved in the modelling of the product knowledge (Krause *et al.*, 1993). In general, proposed models are sufficiently generic and provide a multi-view representation of the product knowledge as in Tichkiewitch (1996). They have a set of evolutionary rules allowing the achievement of an increasingly detailed modelling. We have shown in Eynard *et al.* (1997) that it was insufficient to propose only as product knowledge the results of the design activity because we have no information on the origin of these results. The product cannot be consider as a simple object for which an analytical modelling (descriptive) could be sufficient. The product model presented in Doumeingts *et al.* (1996), allows the description of the design projects in term of objectives to achieve (Functions). The satisfaction of these functions particularises the representation of the product knowledge thus built. This knowledge is represented with the technological entities (Girard *et al.*, 1994) validated by their relationships with the functions. The building of the product knowledge is made by successive triggering of activities which compose the design process.

3.2. THE DESIGN PROCESS

Lorino (1995) defines the process as a "set of activities connected between them by a flow of informations, ... significant and whose combination allows to obtain an important output". Perrin *et al.* (1997) consider the process as a concept to which we can link up to four dimensions : "the temporal dimension, a process connects several activities according to a predetermined order or not, a process achieves a transformation of product and resources, a process supports a cooperation between actors". For us, the design process consists in transform the requirements expressed by the client into product knowledge according to the resources. This is not a simple succession of activities. It is necessary to know what triggered each activity. These choices are dictated by the state of the product knowledge, the strategic objectives of the enterprise and the market, the resources (technological knowledge, human and material resources,...) that we can associate with this project according to the other projects in development. Bocquet (1996) shows the necessity to adapt the enterprise to each new product and the interest capitalisation of the abilities, this implies the management of the decision process. The fact of saving the memory of decisions allows to question the design (we know their consequences and their sources the choices taken). Saving the memory of decisions may also help us as basic knowledge for future designs. The PROSUS system (Blessing, 1996) based on the study of the process allows to save data of design and proposes a representation as a structured set of questions and activities. But there is not control subsystem of design process of products.

4. The control process of product design

4.1. STATE OF THE ART

The aim of control is the integration of the dimensions design process, product knowledge and time, in evolutionary environment of technological knowledge, enterprise strategy and market. Vargas *et al.* (1996) propose the integration of design process and product. Choices of design are compared with a set of constraints which only concern the product. The SAGEP approach (Ouazzani *et al.*, 1997) proposes the modelling process as elementary activities of design and management, controlled by objectives. Decisional aspects, especially planning, are only partially approached. Dureigne *et al.* (1997) present the basis of the control of design workshop. In the scope of the CIMDEV ESPRIT project (1992-1995) renewed in Integration in Manufacturing and Beyond ESPRIT project (IiMB 1996-1999), it has been shown that to optimise the design, activities did not have to be achieved in a competitive manner but they should rather be structured to obtain an optimal performance. Then Duffy (1995) talks about Design Co-ordination whose eleven main frameworks are presented in Andreasen *et al.* (1996). We are members of this project and

our aim focuses on the following elements activities, decisions, resources and product model which correspond to our point of view of control. To manage well, it is necessary to be able, in a given situation and among the set of possibilities, to take the best decision in order to obtain the optimum behaviour for cost, quality, flexibility and delay. This brings us to study the decision system in the scope of the products design.

4.2. THE DECISION SUB-SYSTEM OF THE DESIGN SYSTEM

Starting from the canonical model of the decision proposed by H.A. Simon and presented in Le Moigne (1990), we propose a control model based on the study of the decision process. It allows the integration of the knowledge of the evolution of the system to be designed with the routing of activities of the design process ; it is what we refer to the control of design system. The model of decision process (based on the concept of decision centre (Marcotte, 1995)) is composed of four phases. The phase of identification of the problems of control whose objective is to identify the difference between unallocated resources and those necessary for each possible action plan. An action plan is a series of activities that allows to reduce the incompleteness of product knowledge. The phase of modelling of problems to be solved whose objective is the formulation of problems to satisfy, to synchronise the use of available allowances with the beginning of action plans. The phase of solutions proposal whose objective is to evaluate action plans allowing to solve problems while respecting external and internal constraints linked to the system to be designed. The phase of solution selection whose objective is the multi-criteria choice of the action plan.

A decision can only be made when compared to a finality. In order to do that, it is necessary to compare the record of the system to be designed with objectives to be achieved. In the case of products design these objectives, known as design objectives, have to take into account two points of view: the product one whose design objectives are to satisfy clients requirements (quality) in time and to a cost satisfying the market ; the design system one, whose objectives are, for the set of products, the optimisation of the use of resources of the design system to a satisfying cost for the enterprise.

5. Experimental study

The studied enterprise is specialised in the design and the manufacturing of storing, distribution and management of fuels equipment. It has a catalogue of products whose production is made at the order (delivery delay of 4 weeks for stocking tanks, 1 to 6 months for tanker trucks, 3 weeks for mechanical equipment whose manufacturing volume varies from 10 to 10 000 pieces by month). The enterprise also studies specific products whose delivery delay varies from 8-10 to 6 months (enclosed 3 months of design). The design department is composed of 25 people (8 engineers) and develops the mechanical, electronic

and software parts of every product. This study, financed in the scope of the European project TBPIIT, consists in enhancing the link between design and production departments. We have used the GRAI approach in the scope of the product design, presented in Doumeingts *et al.* (1996). To study the coordination between each department, we have modelled the decision subsystem of the enterprise with the help of three GRAI grids: a grid of the design department, a grid of the production department and a global coordination grid for the enterprise.

Functions Level	External Info.	To manage project informations	To manage products	To PLAN	To manage human resources	To manage technical resources	Internal Info.
	H = 2 Years P = Event	Decision/ strate. project Tech. info. Market	Strategic projects	Research of components Purchase strategy	To plan strategic projects	Recruiting	Research of technologies Technical investment
H = 1 Year P = Event	Orders	Modifications Project definition	To define purchase (proto, tool)	To plan activities To organise projects	To affect	To affect and to adapt low invest.	
H = 1 month P = 1 week	Demandes modifs. S.A.V.	To analyse modifications	Products modifications	To plan fault treatment	To adapt assignment		

IMAGIM V2.0	Study	Grid Name	Phase	Version	Date	Analyst
		DD	Decisional System of Design Department	Analysis	2	19/02/98

Figure 2 : The decisional model of design department

Each sub-group of synthesis "design department" and "production department" has achieved the corresponding physical and decision models. We present (Figure 2) the grid of the design department ratified by the synthesis group of the enterprise. The results of the analysis phase of the design department shows two strengths : a good assessment of technical tasks of the projects and the existence of a control activity of global times spent by project. However, some weakness concerning the decision system and management of the temporary data are identified (any change between the design department and the production department appears as an abnormality).

In this respect some improvement tracks are proposed. First, it is necessary to implement a control support allowing the planning and the coordination of projects. This implies to identify for each project, the useful project informations to synchronise decision centres of the grid of the design department. Second, it is also necessary to take into account the imperatives of delay, costs, feasibility, ... of each activity as soon as possible (purchases, design, industrialisation ...). It lead us to propose the control of the customer's requirements deployment, market and enterprise according to the evolution of the product knowledge. Currently we are validating the GRAI structure (Figure 3) which allows, with the object

plan, to manage the development of each project according to requirements and, with the action plan, to control the design activities of the set of projects according to the enterprise resources.

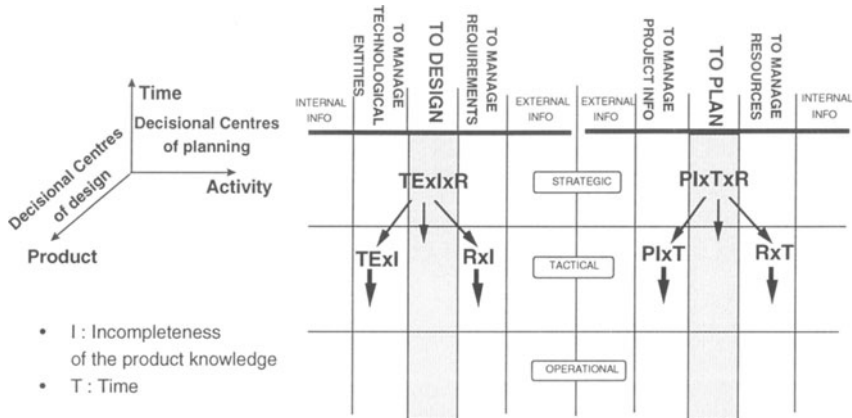


Figure 3 : The GRAI structure

Thus we identify two types of decision centres : design and planning. We propose a model for the coordination and the synchronisation of these decision centres. The coordination corresponds to a classification by temporal level and the synchronisation is made between the functions of the control model for each type of decision (design or planning). The functions of object plan are : to manage the product knowledge (which means the technological entities), to design and to manage requirements. The functions of the action plan are : to manage projects information, to plan and manage resources. The modelling of each decision centre comprises design objectives (product and enterprise), variables of decision (knowledge, capacities, ...), constraints and criteria.

6. Conclusion

Our contribution shows the necessity to strongly integrate the control of the design process with the control of the product knowledge. The control of development evolution implies to model the decision aspects of the design and the planning, considering the strategic, tactic and operating levels. The extension of the proposed GRAI approach, in the scope of system control of product design, includes a dynamic of performance taking into account the evolution of technological knowledge, the enterprise strategy and the market. The first step of the experimentation has allowed us to conclude on the pertinence of the elements of control proposed. The second step would validate the use of the GRAI structure as one key of the efficient implementation of the concurrent engineering philosophy in the enterprise.

7. References

- Andreasen M. , Duffy A., Bowen J. and Storm T. (1996) The design Co-ordination Framework: key elements for effective product development, in A.H.B. Duffy (Ed.), *The Design Productivity Debate*, Springer-Verlag, Berlin.
- Blessing L.T.M. (1996) Design process capture and support, 2nd WDK Workshop on Product Structuring, Delft, The Netherlands, June 3-4.
- Bocquet J.C. (1996) Product/Manufacture a systemic approach for simultaneous engineering, 1st International Conference on Integrated Design and Manufacturing in Mechanical Engineering : IDMME'96, Nantes, France, April 14-17.
- Doumeings G. (1984) Méthode GRAI : méthode de conception des systèmes productiques, Thèse d'état, Université Bordeaux I, France.
- Doumeings G., Girard Ph. and Eynard B. (1996) GIM/GRAI Integrated Methodology for product development, in G.Q. Huang (Ed.), *Design for X - Concurrent Engineering imperatives*, Chapman & Hall, London, pp 153-172.
- Duffy A. (1995) Ensuring Competitive Advantage with Design Co-ordination, 2nd International Conference on Design to Manufacture in Modern Industry, Bled, Slovenia, May 29-30.
- Dureigne M., Geneste L., Grabot B. and Huguet P. (1997) Vers un système de pilotage des ateliers de conception, 2ème Congrès International Franco-Québécois de Génie Industriel, Albi, France, September 3-5.
- Ermine J.L., Chaillot M., Bigeon P., Charreton B. and Malavielle D. (1996) MKSM, a method for knowledge management, in J.F. Schreinmakers (Ed.), *Advances in Knowledge Management*, Ergon Verlag, Vol. 1, pp 288-302.
- Eynard B., Girard Ph. and Chen D. (1997) Un modèle produit support à la conduite du processus de conception, 2ème Congrès International Franco-Québécois de Génie Industriel, Albi, France, September 3-5.
- Girard Ph. and Doumeings G. (1994) Design management of mechanical products, International Conference IFIP TC5-WG 5.3, Valenciennes, France, May.
- Krause F.L., Kimura F., Kjellberg T. and Lu S.C. Y. (1993) Product modelling, *Annals of the CIRP*, Vol.42/2.
- Le Moigne J. L. (1990) *La modélisation des systèmes complexes*, AFCET Systèmes, Dunod, Paris.
- Lorino Ph. (1995) *Comptes et récits de la performance : essai sur le pilotage de l'entreprise*, Les Editions d'Organisation, Paris.
- Marcotte F. (1995) Contribution à la modélisation des systèmes de production : extension du modèle GRAI, Thèse de doctorat, Université Bordeaux I.
- Ouazzani A. I, Bernard A. and Bocquet J.C. (1997) Design Process Management System : SAGEP, International Conference on Engineering Design : ICED 97, Tampere, Finland, August 19-21.
- Perrin J., Forest J. and Micaelli J.P. (1997) Innovation et conception : pourquoi une approche par processus ?, 2ème Congrès International Franco-Québécois de Génie Industriel, Albi, France, September 3-5.
- Tarondeau J.C. (1994) *Recherche et Développement*, Edition Vuibert, Paris.
- Tichkiewitch S. (1996) Specifications on integrated design methodology using multi-view product model, Engineering System Design and Analysis Conference - ASME'96, Montpellier, France, July 1-4.
- Vargas C. and Yvars P. A. (1996) Un langage pour la modélisation de processus de conception en ingénierie des systèmes mécaniques, 1st International Conference on Integrated Design and Manufacturing in Mechanical Engineering : IDMME'96, Nantes, France, April 14-17.

INTEGRATED DESIGN OF MECHANICAL SYSTEMS BY A CONCURRENT ENGINEERING APPROACH

P. RAY*, M. NIGROWSKY*, G. GOGU*,
C. DEMARQUILLY**, A. MALLON**

**Laboratoire de Recherches et Applications en Mécanique Avancée
Institut Français de Mécanique Avancée et Université Blaise Pascal
Campus des Cézeaux - BP 265 - 63175 AUBIERE Cedex
ray@ifma.ifma.fr*

***Manufacture Française des Pneumatiques Michelin
Place des Carmes - 63040 CLERMONT-FERRAND Cedex 1*

Abstract

The limitations of some computer-aided design tools are becoming more and more evident. We refer to their « black box » behaviour, their flexibility and their capacity to integrate the new network technologies and the concurrent engineering concepts. Many approaches have been developed such as Intranet, STEP exchange standards, parametric objects and libraries of reusable object classes. The latter, which have been introduced in the Cas.Cade/SF system proposed by Matra Datavision, is here used by the authors to develop an application on a pneumatic structure modelling. This work has enabled us to implement a tool that seems to have a promising future.

Résumé

Les outils informatiques d'aide à la conception font apparaître des limites liées à leur capacité d'ouverture sur l'extérieur, ainsi ils n'apportent pas la flexibilité nécessaire pour pouvoir s'adapter aux technologies de réseaux et évoluer vers des concepts d'ingénierie simultanée. Des nombreuses approches sont développées comme l'intranet, le standard d'échange STEP, la notion d'objets paramétrés et les bibliothèques de classes d'objets réutilisables. Ces dernières ont débouché sur l'atelier logiciel Cas.Cade/SF de Matra Datavision à l'aide duquel un exemple d'application est développé sur la modélisation d'une structure pneumatique. Ce travail a permis de mettre en place un outil qui semble avoir un avenir prometteur.

1. Introduction

Computer-aided design tools are becoming increasingly important in the process of product manufacturing. Nowadays, these tools are commonly used in the big industrial groups as well as in smaller manufacturing firms. However, after two decades of software development, the CAD systems have begun to reach their limits concerning opening capacity and external communication. Their architecture does not possess the necessary flexibility in order to be able to adjust to new network techniques and to advance towards concurrent engineering.

To overcome these limitations, many approaches have been developed for Computer-Aided Design using the concurrent engineering approach in the broad sense of the term. CAD-dedicated applications represent an interesting solution allowing the users to benefit from computer-aided design tools suited to their job. In addition, they incorporate the designer's know-how and they become more transparent for the user. They represent a good solution by allowing for tool flexibility. However, the development of job-dedicated applications is still reserved for computer scientists. The ideal situation would be to bring the user as close as possible to the development of such applications and to allow him to incorporate his know-how in the final tool in an optimal manner.

The approach of the 1980's has led to the development of complex modelling tools. The software packages proposed a broad range of interconnected applications answering industrial requirements. The modules common to all these products are: geometric modelling, 2D display, machining modules, computation and simulation modules, 3D visualisation, etc. We note that each product is highly efficient in a specific field but that some weaknesses appear elsewhere. Moreover, problems of data compatibility between software have appeared during communication between different users. During the 1990's, the software developers have focused on database management techniques but each supplier offers his own solution, which does not allow us to work simultaneously on the same model.

Nowadays, it is more appropriate to speak about the design process or rather about CAE (Computer-Aided Engineering). This includes the numerical model (DMU - Digital Mock Up), the tools of co-operative distance working, product databases, as well as scientific computing for modelling, simulating and machining. Therefore, we wish to pass from a sequential process to a "concurrent" process which leads to a multiplication of the projects and the removal or reduction of the physical prototype by allowing a 100% numerical definition. This also allows us a real time adjustment of the model's incoherence, an overall reduction in design time as well as the creation of design methodology and a quality approach. Thus, the essential elements of an integrated design chain are: communication between those involved in the process, coherent data management, the setting up of concurrent developments and taking into account the specific requirements of the company.

The various views on CAD are strongly articulated around concurrent engineering and integrated design. This orients the design tools towards a more global approach aimed at integrating the various tools in the production line. [ABO.95]. All these

concepts are tackled in various aspects of the field of CAD research. This is especially the case of Intranet, the STEP standard, the feature concept as well as job specific applications. After developing these different points, we will show how we can work towards integrated design by using software based on reusable object classes.

2. Intranet

This is the greatest innovation of the last few years. We call it “the new communicative CAD” [HAR.97]. The approach is attractive. It involves using the web network as a medium for sharing information within a team or company. All suppliers may access this through a «browser» navigator inside the software that facilitates data exchange and especially allows interactivity on the visualised model. This concept was developed in two projects, one is “SHARE” of Stanford University [KUM.94] which offers a complete communication tool in HTML format, the other is “CYBERCUT” of Berkeley University [SMI.97] using Java language to develop a CAD/CAM tool which shares its resources through the web.

This technique seems promising but industry still remains sceptical because the web does not guarantee an adequate level of information security. Moreover, the network flow remains insufficient to ensure easy use [ANT.97].

3. Data compatibility

Interest in Intranet raises the question of data exchange. The object-oriented approach is nowadays recognised as being that of the future and all current solid modelling is object-oriented. In this perspective, STEP (Standard for Exchange of Product Data) proposes to define a universal data model. The neutral term is used to indicate that context and CAX software are treated separately. STEP data models ensure data exchange throughout the entire product life cycle. For this reason these data models contain the geometry but also the tolerances, the material properties as well as all the attributes used for complete product definition.

The benefits of a common standard for data exchange involve all industrialists. In fact, even if the Intranet is an innovation, concern for data compatibility is a much more immediate problem to solve [MAR.95], [BEL.95].

4. Feature

The work methods using the notion of feature appeared at the end of the 70's [LIG.82], [PRA.84]. However, they have been applied only in the last few years due to improvements in feature modelling coupled with an object-oriented database management system allowing us to manage such information. Nowadays, there are many projects applying this approach in design or manufacturing [QUI.96], [SAB.95],

[VIE.95]. This approach is totally in line with the STEP standard. In fact, we could consider the standard as a generalised feature of all pieces.

5. Adapting tools to jobs

The goal of integrated design is to facilitate the intervention of experts in various jobs at the earliest possible stage in the design process [BEL.95]. This means setting up a platform within the design information system on which all those involved in design and manufacturing could intervene on the product at any given moment.

Some work has been accomplished in this field [BEL.95] and the results are quite encouraging. In any case, one conclusion stands out: setting up work systems capable of reaching this requirement in terms of job specificity requires the customisation of the software so as to reply to specific requirements of each company.

One approach, which allows us to answer to this request of integrating specific job knowledge to software, is via CAD-dedicated applications. However, to be in line with STEP, by using features and concurrent engineering, we cannot develop an application without integrating all the tools used in the design process. For this reason, it is necessary to have a modular approach to each job in order to obtain a homogeneous tool answering to the requirements of all people involved.

The libraries of reusable object classes allow us to satisfy these criteria. Therefore, we are interested in this kind of development tool and will afterwards apply it to an industrial example.

6. Standard libraries

With regard to the points developed previously, we can draw up a non-exhaustive list of requirements to be satisfied, in order to be in accordance with future trends [ABO.95]. It has to be independent from the platform used, to have a broad application architecture, which ensures an open structure, to have centralised and coherent data management, to be based on a future technology and to allow compatibility between different versions.

With a view to evolving towards flexible applications, oriented towards integrated design, libraries of reusable classes represent an interesting approach and several study projects have already led to more or less complete tools. The Cas.Cade/SF software workshop of Matra Datavision is one of them. It seems to be a pertinent and fully mature solution, which might be used at an industrial level in design as well as in manufacture and simulation. This development platform brings together many criteria allowing us to consider, through software, integrated design within the company. This toolbox brings concrete solutions to the points previously mentioned but especially, it proposes a strong basis for further development.

The technology chosen for the development of Cas.Cade/SF is object oriented. There are many advantages concerning the large data modularity and the reutilization of objects. Its philosophy is therefore to develop the necessary specific applications by

using base elements and by creating its own object classes. In fact, the knowledge concerning the job is directly inserted in applications.

Therefore, in connection with Michelin we have decided to tackle a project to highlight the full potential of this tool.

7. Application on an industrial example

7.1. STATE OF THE ART

At present, the company uses a home made software for tyre modelling, developed some years ago. This tool, although highly efficient, has reached its functional limits. The work done in the CAD service aims, in the medium term, to improve the system and, in the long term, to define its replacement. So, we tried to see if the product Cas.Cade/SF could answer the company's requirements.

7.2. THE CURRENT SET-UP

A tyre has a relative complex shape made up of a great variety of products. In this article we will deal with the tread. This is the part of the tyre that is in contact with the road. It has a special profile called sculpture, which confers the adherence to different surfaces. This is a very complex geometry, obtained by the juxtaposition of simple elements called paving structures. Between them we can distinguish the tracks allowing water evacuation when driven on wet surfaces.

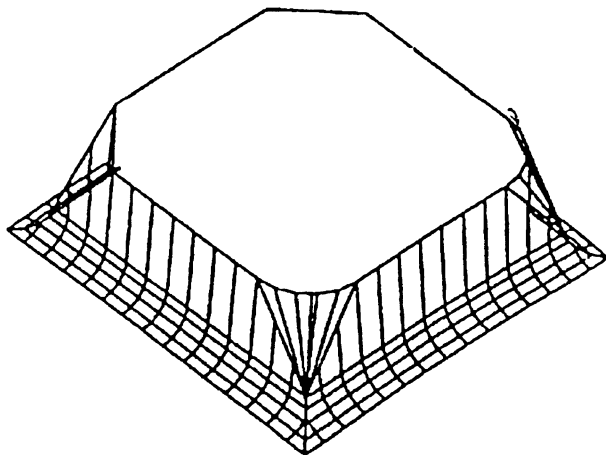


Figure 1. 3D representation of a structural paving.

The idea is to design a paving structure from minimal tyre data allowing the user to achieve the adherence calculation (Fig.1). The top of the paving structure is made by rolling the defining 2D profile on a cylinder whose diameter is a design parameter. The rolled profile is then projected onto the surface representing the tread. The chamfers and the connecting radius are added after setting up the topological surfaces.

7.3. DEVELOPMENT WITH Cas.Cade/SF

7.3.1. *Product Architecture*

The architecture of Cas.Cade/SF software workshop is built up around 4 modules. Firstly, we have C++ object libraries including all the basic algorithms for the creation and the manipulation of classical geometric entities. Afterwards, we have an interactive module (front-end) representing the final user application and containing the structure of the course of operations. The third is a data base management module and the final one is the application development environment allowing us to manage the teams working simultaneously on different projects.

7.3.2. *Application development*

The modules presented share the same development stages. It is achieved in a working space and it is organised on four levels which are: the “factories”, the “workshops”, the “workbenches” and the “development units” (DU). Generally speaking, there is one workbench per project and the object classes are grouped together in various development units called packages. We distinguish other types of DUs such as “engine” or “interface”. This structure of the working space is highly compatible with teamwork.

7.3.3. *Industrial case application*

The construction of a 3D structural paving requires many types of data defined initially in 2D. The type of data that often reappears is a composite curve made up of several curve segments. They are used to define planar objects necessary for the 3D construction. So, to define this structural paving, we use: a planar closed profile, an upper and lower profile, which allow us to generate the upper and the lower surfaces of the tread by revolution, a value for the cylinder radius for the operation of projected rolling and data concerning the topological surfaces for the surface join.

Cutting the process up in this way allowed us to identify the classes for 2D and 3D. This analysis is very important for future development. So, in the final application we find 3 object classes. The class of 3D structural paving (Fig.2) allows us to define the final object. Input is defined as the entities necessary to define the structural paving: the upper and the lower profile, the radius of the cylinder projection, the 2D structural paving and the topological characteristics. The 2D structural paving class allows us to define the composites. We have developed an extra algorithm class to answer to our requirement of projected rolling. This was very interesting because it proves the

product's modularity. These classes can be quickly tested with the tool "Draw" which visualises the geometry created and manipulated (Fig.3). Then a graphic interface is achieved by using predefined functions.

Through this application we have noted that the concept of software workshop and more precisely that of standard classes of reusable objects proves to be highly efficient in developing a dedicated application. In fact, the algorithm classes, which complete the construction stages of the complex geometry of structural paving, have been developed from the components available in the libraries of Cas.Cade/SF.

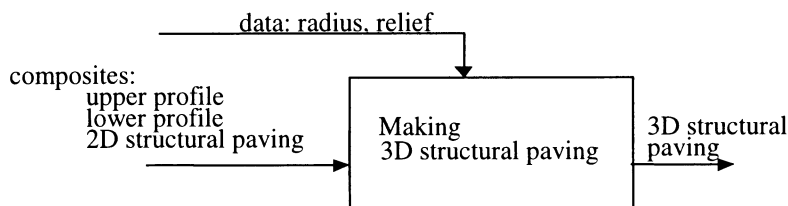


Figure 2. Functional analysis of the 3D structural paving

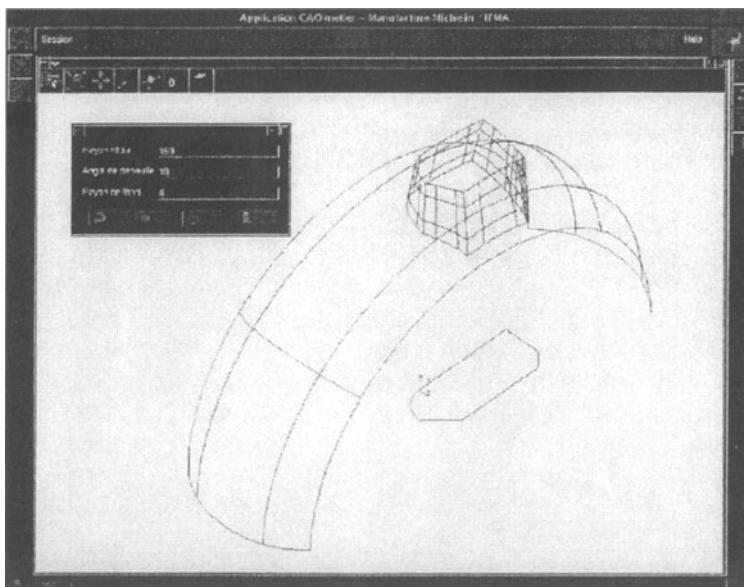


Figure 3. Draw of different entities created.

8. Conclusion

This work emphasised the interest of using the libraries of reusable object classes to develop job-oriented applications. In a concrete example, in an initially unknown application field, which is the job of tyre designer, the use of the Cas.Cade/SF software allowed the completion of the digital model of a complete application. The final application is completely transparent to the user who merely inputs information on the constructive parameters. The classes that are implemented made some specific operations that would require arduous development with a traditional CAD tool.

Object classes are a very well adapted solution to implementing integrated design in a concurrent engineering approach. In fact, they are open to future evolution including, for instance, the STEP standard and new network technologies.

9. References

- Abou-Haidar, S. (1995) A foundation for an integrated design chain within an enterprise, *4^{ème} Colloque PRIMECA*, La Plagne.
- Antoine, J. (1997) CAO: Visez l'excellence, *Industries et Techniques* **780**, 58-86
- Belloy, Ph., Tollenaere, M., Tichkiewitch, S., Chapa, E. (1995) Intégration de connaissances métiers dans les systèmes CAO: exemple de l'usinage et de l'estampage, *4^{ème} Colloque PRIMECA*, La Plagne.
- Harvest (1997) La nouvelle CAO communicante, *Harvest, le journal des bureaux d'études* **39**, 22-28.
- Kumar, V., Glicksman, J., Kramer, G.A. (1994) A shared web to support design teams, *Third IEEE workshop on enabling technologies: infrastructure for collaborative enterprise*.
- Light, R.A., Gossard, D.C. (1982) Modification of geometric models through variational geometry, *Computer Aided Design* **14(4)**, 209-214.
- Marks, P. (1995) Best practices in CAQ/CAM, a survey of nine leading companies, *EDS-Unigraphics*.
- Pratt (1984) Solid modelling and the interface between design and manufacture, *IEEE computer graphics application* **4(7)**, 52-59.
- Quichon, J. (1996) Génération automatique de gammes d'usinage en fraisage pour des machines outils autocontrôlées, *Journées de l'école doctorale: machines performantes et intelligentes*, SPI Clermont-Ferrand.
- Sabourin, L. (1995) L'expertise en conception de gammes d'usinage: approche par entités et propagation de contraintes, *Thèse de doctorat*, LURPA, ENS Cachan.
- Smith, C.S., Wright, P.K. (1997) Cybercut: a world wide web based design to fabrication tool, University of California, Berkeley, <http://kingkong.me.berkeley.edu/>.
- Viel, L., Vernay, P., Lucas, T. 10 applications exemplaires de CAO dans les P.M.I., *L'usine nouvelle* **2514**, 78-93.

CONTRIBUTION TO A MULTI-VIEWS, MULTI-REPRESENTATIONS DESIGN FRAMEWORK APPLIED TO A PRELIMINARY DESIGN PHASE

MG-IT¹

Work group of the Pôle Productique Rhône-Alpes "Geometric Modelling and Technologic Integration"

Laboratoire 3S (Sols, Solides, Structures)- Integrated Design Group, (Grenoble), Laboratoire d'Electrotechnique de Grenoble (LEG), (Grenoble), Laboratoire d'Informatique Graphique Images et Modélisation (LIGIM), (Lyon), Laboratoire LISSE (Laboratoire d'Images de Synthèse de Saint Etienne), (Saint-Etienne), Laboratoire de MECAnique (LMECA), (Annecy),

coordonnator : J-C. Léon : E-mail : Jean-Claude.Leon@hmg.inpg.fr

Abstract. During the design process, several phases involving the use of mechanical, electromagnetic, tolerancing, ... models can take part to this process depending on the product designed. Following the definition of the concepts attached to the notions of "view", of "representation", an analysis is conducted to highlight the nature of the entities used in each "view". Through this analysis, some constraints related to the product models associated with each "view" are stated and illustrated in order to express needs in terms of treatments, data structure organisation, flow of the design process in order to set up an architecture of a design environment meeting these constraints and to express new constraints addressing the organisation of the design process.

1. Introduction

The number of engineers, technicians, taking part to the design process and the various areas and levels of knowledge they offer have an influence on the structure and the content of the computer aided design tools.

The current softwares are capable of fast manipulation of an ever increasing amount of information but the maintenance and the evolution of these software tools increase their cost and their duration of development. In addition, the concept of geometric model forming the basis of most of these softwares effectively acts as a kernel representation, unique and common to various areas of technical knowledge which take part to the design process. However, the engineers and technicians

¹ MG-IT is the collective name of the *work group*. This group is made up from members of the laboratories mentioned above. The participants to the work group are : J-C. Léon (coordinator), A. Bouras, J-M. Brun, E. Chapa Kazuski, S. Foufou, M. Giordano, P. Godhous, S. Guillet, Y. Maréchal, S. Maza, D. Michelucci, F. Noël, E. Pairel, L. Rémondini, S. Samper, M. Seyf, A. Tehari, N. Troussier, P. Véron.
Pôle Productique Rhône Alpes, 74 rue des Acières, BP 755, 42951 Saint Etienne Cedex 9, France.

participating to the design process require more and more access to datasets specific to their technical areas, based on their concepts and relying on geometric models fitting with these concepts as well as with the information specific to their technical fields. The architecture of the current softwares are not enabling the achievement of such an objective.

2. Towards a product model

The representation of objects within a mechanical design environment uses extensively geometric aspects. However, during the design process, various representations of the same object are generated and used, i.e. geometric, technological, mechanical representations, representation for manufacture, ... This analysis has led to the development of “feature-based” approaches [15] or “form features” to provide models dedicated to specific applications and attached to local areas of the object. Nevertheless, these approaches are mainly centred on the geometric treatments of such representations and aim at defining the principles of transfer of the feature attributes when such treatments are performed.

The work introduced here aims at analysing more accurately the relationship between the geometric representation and the data specific to the different “views” to provide a better characterisation of either the adequacy or the deficiency of some intrinsic concepts of the feature approaches.

Works have been also carried out around the concept of product model and focus on the identification and the definition of the structure of the information which are attached to it. However, most these works consider the object representation solely from one point of “view”, thus reducing the context of its geometric representation to only one category of geometric models. Some authors [13] recognise the existence and the prominence of multiple “view” attached to a product but they don’t put forward proposals about that topic.

In fact, the design process requires the use of several models, i.e. kinematics model, model(s) of flexible structures, electromagnetic model, analysis model of geometric tolerances, ..., relying on different geometric representations or even on different geometric models. The Figure 1 illustrates through an example such a configuration. The understanding of some of these models, by the user of a design environment, leads to define the concepts of “representation” and of “view” whose main aspects are recalled hereafter [10].

Representation : here this notion indicates that a given concept can be translated, in a equivalent manner, through different “models”. Each of the “models” used matches a specific criterion. As an example, the geometric representation of an object can be obtained through different “models”, i.e. B-Rep modelling, CSG modelling, if objective performed is to get an identical object geometry as it is seen by the user. The same object can be also represented with a different geometry by different “models” (strength of material model, finite element model) to get a equivalent “representation” in the sense of mechanical strength for example.

To extend this designation, a “representation” could also coincide with an instantiation of a “model” participating to the definition of a product with regard to specific dataset and criterion.

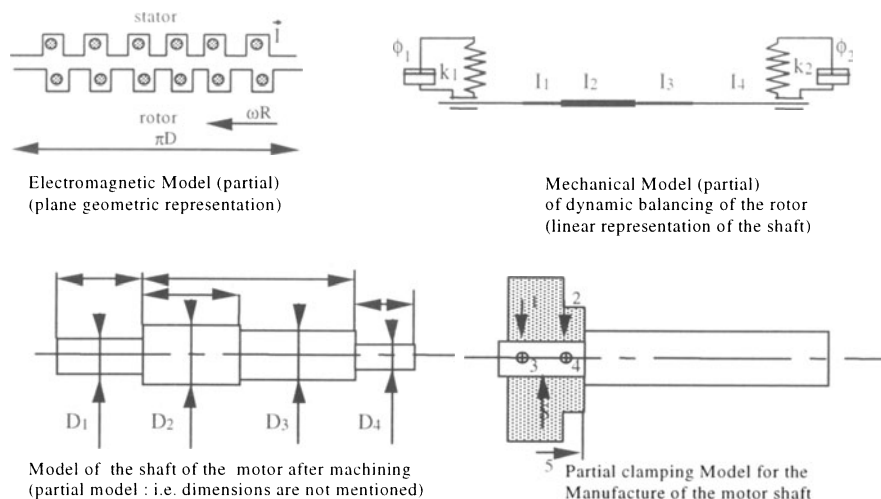


Figure 1 : Various models used during the design of an electric motor. Only some models are taken into account : dynamic analysis model, electromagnetic model, machined shaft model, clamping shaft model, in order to illustrate the diversity of the models set up during the design phase of a product.

View : this concept gets its significance with respect to a user wishing to access a subset of a design environment. The user taken as reference in this definition is a “virtual user” in the sense that he does not represent a physical human being accessing a design environment but he symbolises a human being owning all the required knowledge to manipulate the concepts attached to a given “view”. As a consequence, the elements related to the level and to the scope of the knowledge required to handle the concepts of a “view” are not taken into account.

Within this framework, a “view” stands for the aggregation of data as they exist in “representations” (see the above definition) produced by “models” and focusing on a specific context. As an example, the study of the electromagnetic behaviour of a mechanism, the mechanical analysis of structures, ..., are examples of “views”. As illustrated by the previous list, a “view” does not contain all the information a user could manipulate but is restricted to a specific domain.

A “view” is one of the elements of the dialogue model employed to give a user access to a design environment. In fact, it is necessary to add to the “view” the specific aspects of the man-machine interface needed to adapt the dialog, between the user and the design environment, to the level of knowledge of the user, to his (or her) area of action.

From the above definitions, figure 1 illustrates :

- the data involved in an electromagnetic model, i.e. an “electromagnetic representation” of the motor participating to its electromagnetic “view”,
- the data taking part to the mechanical model of dynamic balancing of the rotor, i.e. a “balancing representation” of the motor shaft incorporated in its mechanical analysis “view”,
- the data partially defining the manufacturing model of the shaft and a clamping model of the same shaft, i.e. a “machining representation” and a “clamping

representation” of the motor shaft. These two “representations” form a part of the machining “view” of this motor shaft.

Starting from these concepts, the current work analyses the constraints and the needs with respect to the information transfer, to the data conversion, to the geometry modifications between different “views” employing different “representations” of a same product.

3. Analysis of different “Views” of a design process

The selected “views” as analysis themes were chosen in accordance to the know-how available through the participants of the work group. Hence, three contexts cover a part of the preliminary design phase of a product : the analysis of the mechanical behaviour of its structural parts, of the electromagnetic behaviour of its subsystems and the analysis of its geometric tolerances [10].

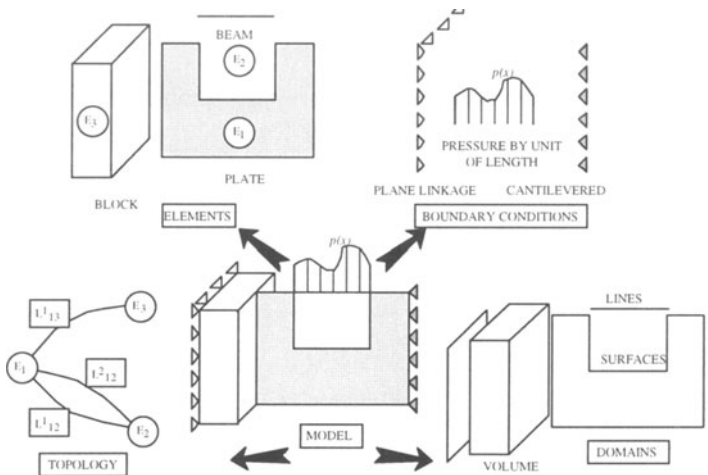


Figure 2 : Example of analysis model of a structure.

3.1. MECHANICAL ANALYSIS “VIEW”

This “view” addresses a subset of the formulation of mechanical analysis problems through analytical methods (strength of materials) or numerical ones (finite element method). Some basic entities take part into it to generate a model. These entities were identified from previous works conducted in the field of the static behaviour of structures [1, 11, 12]. The entities set up allow the description of flexible areas of a part, of boundary conditions, of geometric domains which can be associated with the two previous concepts. Some entities (TOPOLOGY) describe also the way the flexible areas are mechanically as well as geometrically connected and located in 3D space.

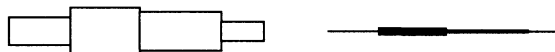
Figure 2 provides an example of a mechanical structure defined as an analysis model. The texts, either boxed or not, define the entities incorporated in its mechanical analysis model.

The geometry of a structure, as required for a specific analysis, may need to be subjected to adaptations or simplifications, i.e. holes, blends, rounds, ... removal, to

generate efficient input data for its analysis in order to reduce the preparation time without changing significantly the results of the analysis. Similarly, choosing a particular model of behaviour either for the entire structure or for one of its subsets may lead to an “idealisation” of the object’s geometry. Whatever the situation, geometric transformations must take place within the mechanical analysis “view”. Figure 3 provides examples of configurations related to geometric transformations of type “idealisation”.

These transformations enforce the prominence of a multi-representations environment.

Transformation of a volume into a line to generate the geometric representation of a “beam”



Transformation of a surface into another surface after removal of several chamfers, rounds or holes



Figure 3 : Examples of geometric transformations for the creation of an analysis model.

3.2. ELECTROMAGNETIC ANALYSIS “VIEW”

This “view” is related to the formulation of electromagnetic analysis problems including, however, specific aspects connected to a problem-solving method of finite element type [9, 14]. Like the mechanical analysis “view”, the entities set up reflect the main characteristics of this sector of the design environment. The set of data involved in this “view” is attached to a geometric representation of the object or of the mechanism studied which has been obtained after simplification or idealisation treatments. Figure 4 shows an example of some entities forming the electromagnetic model of an object.

The analysis conducted has revealed that the geometry of the object used in this “view” as well as the geometry adaptation and idealisation processes for this “view” were distinct from those employed in the mechanical analysis “view”, thus highlighting that these processes must really combine geometric treatments as well as native treatments of the “view” (more precisely treatments using dedicated data of the “view” of interest) to be correctly achieved.

In any case, these treatments produce a transformation of the entities input to generate a description of the object using native entities of the “view” where the adaptation or idealisation process is carried out.

3.3. TOLERANCING “VIEW”

It is a subset of an important “view” of the relationship design-manufacturing and it focuses on the tolerancing problem at its highest level. It handles, for the manufacture, the functional constraints of the “mechanism view”. Only a subset of the main entities of the tolerancing “view” has been identified. However, the structure identified appears to be sufficient to draw significant conclusions related to the structure of a design environment.

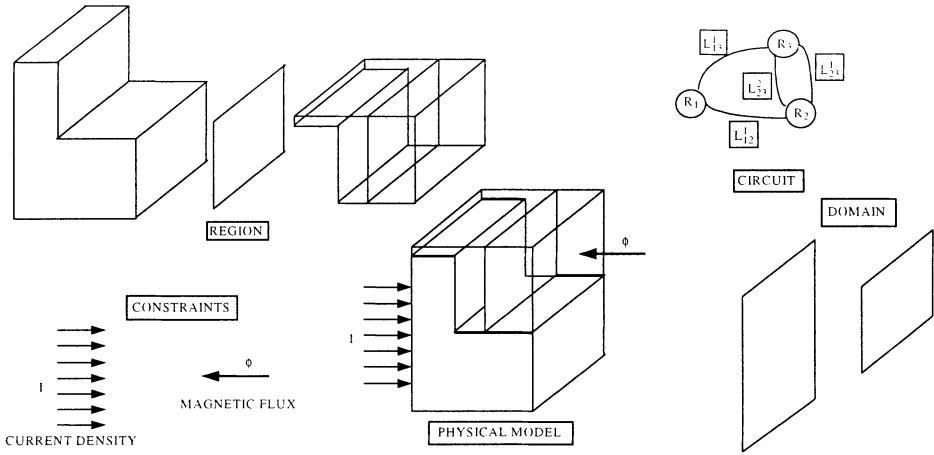


Figure 4 : Example of entities of an electromagnetic model resulting from an adaptation or an idealisation process.

Within this “view”, entities specific to the design phase, i.e. entities attached to the nominal dimension of the parts, as well as others expressing the designer’s perception over the manufacture, i.e. uncertainty about the dimensions really machined. Nevertheless, an analysis of the data specifically attached to this stage uncover new entities and locate them with respect to those belonging to the previous “views”. The entities identified cover only partially the tolerancing phase but, at the current stage of development, they bring a contribution to the proposals centred on the computer structure of a design environment while adding to it a tolerancing model [3, 6].

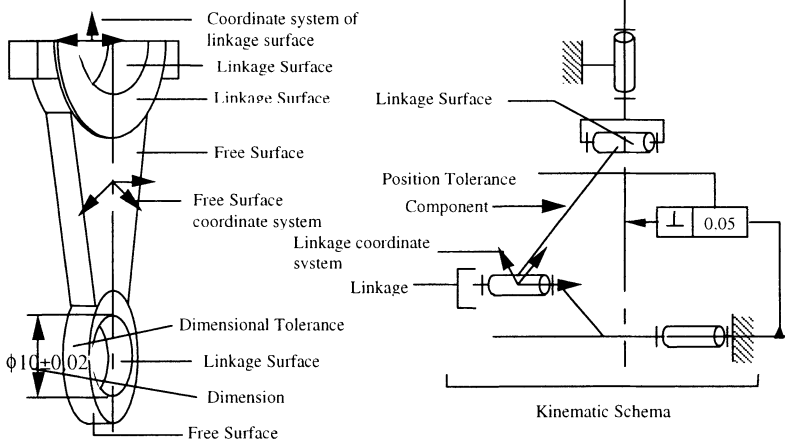


Figure 5 : Example of geometric models and entities taking part to the tolerancing “view” (At left : partial tolerancing of a component, at right : partial tolerancing of a mechanism)

The geometric representation connected to the entities surveyed in the tolerancing “view” is widely diversified due to the various stages where a tolerancing task can take place, i.e. at the preliminary design stage for a functional study, at intermediate design stages where dimension or form specifications may be inserted ; at the stage of the

detailed design where a thorough dimensioning is required. Hence the geometry of the objects representing a subset of the data of this “view” may be either fairly detailed, i.e. the object may be geometrically defined with volume model, when the object is very close to its final shape or schematically represented with a non-manifold representation according to the degree of abstraction of the model and to the development status of mechanism designed. Figure 5 provides an example involving some entities of the tolerancing “view”.

This figure depicts dimensioning stages where the geometric representation of either a component or a mechanism may incorporate geometric models owning significantly different properties. It should be noted that the diversity of the geometric properties and representations just mentioned also applies to the electromagnetic and mechanical analysis “views”.

4. Synthesis of different “views” analysed

The data organisation of each “view” has been described with STEP-based data structures through the graphics representation of EXPRESS-G [5] in order to create an homogeneous environment in adequately fitted with the existing description of basic models (geometric models, finite elements models).

The analysis of each “view” [10] shows that each of them incorporate its specific representation of the product. This leads to address the problem of passing from a given geometric representation to another one as well as mapping geometric models between various “views”. The incorporation of modification processes of the models used during the design process as well as the propagation of their modifications across the modified models are new problems that must be taken into account. This point focuses at least on the geometric data and generate specific constraints when variational or parametric geometry concepts are employed [8, 7]. To this end, coherence checking procedures must be adapted while taking into account geometric (notion of volume, of closed contour, ...) and non geometric (no overlapping of areas of imposed displacements and imposed forces, ...) properties which are attached to these objects. Such a requirement is needed for the preservation of the coherence of the native data of each “view” as well as the coherence of the data exchanged between different “views” of a single design environment. The synthesis of the tolerancing “view” exhibits the relationship between the notions of shape and functionality. In this “view” the enrichment of the geometric representation of the object is subjected to large changes during the design process when technological data are incrementally added.

From the design process point of view, the “views” analysis has shown that strong dependencies exist among some parameters involved into different models acting within different “views”. As an example, there is a strong dependency between the electromagnetic analysis “view” and the mechanical analysis “view”. When the design of an electro-mechanic product relies on the study of its electromagnetic and mechanical behaviours, it is not possible to trigger first a Finite Element (FE) model of its mechanical behaviour and subsequently an electromagnetic FE model. Such a constraint is due to the impossibility of converting forces into current intensity, electric field, ... Conversely, magnetic flux, current density, ... form a set of parameters from which forces may be evaluated to define boundary conditions of a mechanical model.

Obviously, such a situation sets constraints for the integrated design and concurrent engineering concepts.

5. Conclusion

The analysis carried out demonstrates the prominence of a tight connection between geometry and other product data to be able to :

- describe adequately the representations of each “view”,
- maintain the coherence among all the representations and “views” involved in a design process,
- cope with geometric and technical data transformations required to adapt the various data to different design stages.

The structure of the datasets attached to the different “views” is also part of the current work [10]. This aspect is needed to identify basic mechanisms required to propagate data within a design environment and to maintain their coherence. Future work will focus on the detailed definition of data structures and data transformations techniques.

6. References

1. Arabshahi, S., Barton, D.C., Shaw, N.K., “Towards integrated design and analysis”, *Finite Elements in Anal. and Design*, **9**, 1991, 271-293.
2. Brun, J.M., Bouras, A., “Modélisation de Produit: Tendances Actuelles des Conceptions utilisant les Formes Caractéristiques”, Proc. of MICAD'95, Paris, march, 1995.
3. Clément, A., Rivière, A., Temmerman, M., “Cotation fonctionnelle des systèmes mécaniques”, PYC Edition, Paris, 1994.
4. Dabke, P., Prabhakar, V., Sheppard, S., “Using features to support finite element idealizations”, *Comp. in Eng. Conf.*, ASME, Minneapolis, **1**, 1994, 183-193.
5. Norme AFNOR, ISO 10303-11 *The EXPRESS Language Reference Manual*.
6. Giordano, M., Duret, D., “Clearance space and deviation space : Application to the three-dimensional chains of dimensions and positions”, Proc. 3rd CIRP Sem. on Comp. Aided Tolerancing, Eyrolles, Paris, 1993.
7. Lamure, H., Michelucci, D., “Solving constraints by homotopy”, Proc. Solid Modelling Foundations and CAD/CAM Applications '95 Conf., Salt Lake City (USA), 1995, 263-269.
8. Light, R., Gossard, D., “Modification of geometric models through variational geometry”, *CAD*, **14**, n°4, 1982, 209-214.
9. Meunier, G., Sabonnadière, J-C., Coulomb, J-L., “The finite element post processor of Flux3D”, *IEEE Trans. on Magnetics*, **27**, n°5, September, 1991.
10. MG-IT, “Propositions pour une structure d'environnement de conception multi-vues, multi-représentations”, Research Report. Pôle Productique Rhône-Alpes, May, 1997.
11. Rémondini, L., “Un Module d'Analyse de Structures Mécaniques pour la Conception Intégrée”, Ph. D. thesis, INP. Grenoble, December, 1995.
12. Rémondini, L., Léon, J-C., Trompette, P., “Generic data structures dedicated to the integrated structural design”, *Finite Elements in Anal. and Design*, **22**, 1996, 281-303.
13. Rosenmann, M.A., Gero, J.S., “Modelling multiple views of design objects in a collaborative CAD environment”, *CAD*, **28**, n°3, 1996, 193-205.
14. Santana, O., “Analyse et structuration des données dans les logiciels de CAO en électromagnétisme”, Ph. D. thesis INP. Grenoble, September, 1988.
15. Shah, J.J., “Assessment of Features Technology”, *CAD*, **23**, n°5, June, 1991.

PROPOSAL OF A FUNCTIONAL MODEL OF LOGISTICS FOR SPARE PARTS PRESERVATION

Nicolas BAUD, Mounib MEKHILEF and Jean-Claude BOCQUET

*Laboratoire Productique Logistique, Ecole Centrale Paris
Grande Voie des Vignes, 92290 Châtenay-Malabry (FRANCE)
E-mail: mekhilef@pl.ecp.fr*

Abstract

This paper deals with the determination of the optimal logistic chain for the spare parts preservation for the nuclear civil plants. Since a nuclear power plant is designed for a use during at least 30 years, the question relative to the availability of the parts, to be used a long time after the plant design, is crucial and strategic. In other words the question is: "how to preserve the spare parts and where? "

The former points out the fact that we have to choose the preservation technologies in accordance with the parts particularities; the latter rises a localization problem. We examine in this paper the nuclear parts lifeline, by the means of the description of the main aspects. Using a systemic approach for the problem modeling, we build a set of representation models. The global preservation modeling proposed in this paper is a result of the interactions between the company (the logistic chain), the spare parts, the technological solutions for the preservation, the nuclear power plants and the warehouses. Each of the listed components of the system is presented by using the concept of "calling cards". In addition to these formalizations, we suggest a driving model for the objectives and the constraints. The objectives are then transformed to a combinatorial optimization problem solved using simulated annealing and tabou search algorithms.

These functional models have been implemented in a computer platform (MICRO-COST). The validation of the systemic approach and the numerical results has been done by the study of a real case (industrial) stemming from the civil nuclear area.

1. Introduction

Nowadays, the enterprise evolves in an increasingly complex environment, changing and uncertain [PYB96][Ram97]. In order to remain competitive, it has to optimize the use of its internal resources [SCF95]. Electricité de France (EDF) company, that is a partner in this research, does not escape this rule. In order to redefine the whole preservation process for spare parts, we first examine what ideally this process could

be. In other terms, instead of giving an *a priori* solution for the problem, we formalize the need, and the corresponding “perfect” solution. This may help to qualify the potential solution whatever is the way used to obtain it.

2. Context

From a macroscopic point of view, the concerned area is the civilian nuclear. Made up of twenty sites of electricity production (nuclear power stations) allocated on French territory, EDF company uses its existing logistic chain to maintain operational all the plants. The corresponding spare parts (SP in the text) represent a few thousand different¹ equipment² references. Also, EDF regularly practices preventive maintenance schedule and exceptionally curative maintenance (repair). The SP are stored in three distinct places (the national warehouses), and preserved against damaging for an indeterminate duration (from one week to several decades).

From a microscopic point of view, all the parts form a population³ extremely eclectic. There are some heavy and voluminous (ex: turbines, diesel engines...), some others light and tiny (resistors, screws...). Certain spare parts come in a number of varieties (nuts, valves...) or are unique (crank, vortex...). It would also be necessary to talk about the technologies (mechanics, electronics, and hydraulics...), and to consider materials such as metals and polymers; as well as the prices, the supply and demand, the quantities etc. This, in order to truly describe the make up of these parts in store.

The genesis of the problem is an ambitious program of productivity gain, including the logistic process⁴. To this end, our project⁵ is to define what the global system⁶, for preservation (GSP) of spare parts, ideally could be. This subject includes phases of transportation (dynamic phases) as well as those (static) of equipment storage. In other words, the mission is to give some answers (scientifically validated) to the following decision-maker strategic questions:

- ◆ How many warehouses is it necessary to build?
- ◆ Where to place geographically the stores?
- ◆ What technologies of preservation⁷ must be used and for what sorts of SP?
- ◆ How much money to invest in GSP and for what means exactly (site, installation, equipment, etc.)?
- ◆ What gains (financial, temporal, qualitative, etc.) to expect and when?

¹ All in all, several hundred thousand items.

² We will call those sometimes *spare parts*, sometimes *SP* or simply (new) *parts*.

³ In the statistical sense.

⁴ The logistic process (or chain) is made up of all various stages in the life cycle of SP from their manufacturing until their use in the nuclear power stations. There are two stages for the transport and one for the storage.

⁵ According to Le Cardinal [LCa89], a *project* is a regrouping of one or several objectives to realize with some internal or external specified constraints intended to optimize the parameter that represents the quality of results. Likewise, the EDF project intent's seeks to optimize the global cost of preservation with a better quality.

⁶ J. W. Forrester [For84] defined a *system* as a group of elements able to have several states or a group of variables able to take various values.

⁷ For us, a *technology of preservation* is each process that contributes to neutralize at the very least one of aging factors of a spare part.

- ◆ What parts of the existing structure to recycle?
- ◆ What satisfaction for the future GSP may the company obtains?
- ◆ What are risks regarding no availability of nuclear power stations?

Remark:

We consider here that a *class* is a combination of *preservation technologies* (for example: cardboard + plastic film + humidity absorber).

3. Global Approach

The strategic furtherance methodology that we have elaborated is based on a systemic approach of the problem and on the use of a functional analysis tools [Lim96]. This approach allows a global vision – a transversal view – of the project with an important abstraction degree and an unambiguous frontier demarcation of the GSP. Also, it displays the existence of strong interactions between the enterprise (GSP) and products (SP) at all stages. According to *J. Woodward* [Woo71], the technology and the structure are connected, the second depending probably on the first. Likewise, it displays the necessity to capitalize knowledge – all sorts of relevant information on the GSP and on the SP – simultaneously on the two sides before their processing. As *H. A. Simon* [Sim91] has demonstrated, a systemic approach permits the structuring of the system complexity. In our case, the black box has for inputs all the operational spare parts and for outputs these same operational parts. The value-added for the GSP is therefore duration of availability during its transportation and storage activities.

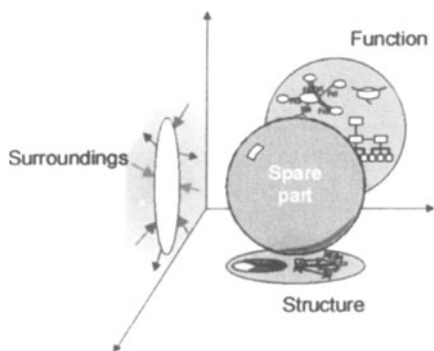


Figure 1: The product model.

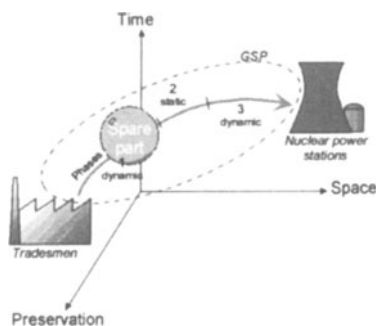


Figure 2: The process model.

To give a clear indication of the *complexity* of the global system of preservation, we use three recent definitions of this term. For *M. Karsky & al.* [KDC+96], a system is complex because its temporal behaviors are often difficult to anticipate, even to short-dated, and they are almost always difficult to analyze. For *J. Mèlèse* [Mél95], the complexity has to be understood as a wealth of the information and the interconnections, a variety of states and possible evolutions, all different things of the complication (in the sense of the overlapping of stable linear connections), often fixed with inflexibility by the system environment. *E. Morin* [Mor94], defines the complexity as a quantitative phenomenon (extreme quantity of interactions and

interference between a great number of units) comprising uncertainties, vagueness, random phenomena.

4. Modeling the Problem

According to *D. Thiel* [Thi93], the modeling of real systems consists in trying to describe, to symbolize, to conceptualize (with a modular and progressive manner) the knowledge of the reality. To formalize our problem, we had to elaborate a functional model of preservation logistics. We built it as a « set of conceptual tools allowing the just necessary description - that is to say, in the senses of the value analysis, aiming the best rate cost/quality of the description more than the minimal cost [Ada87] - of the global system of spare parts preservation ». Its aim is therefore to contribute to the understanding of the structure of the future logistic chain - which purpose is to insure the spare parts integrity- and to improve clearly the actual structure (constituted of several national warehouses).






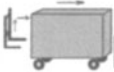








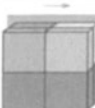
		Time		
		Phase 1 : dynamic	Phase 2 : static	Phase 3 : dynamic
Space	GSP	 <ul style="list-style-type: none"> - Distance - Flow - Access 	 <ul style="list-style-type: none"> - Geographical site - Access 	 <ul style="list-style-type: none"> - Distance - Flow (rate of rotation) - Access
		Average supply duration (or km)	Nb of warehouses, places	Average delivery duration (or km)
	Store (Si)	 <ul style="list-style-type: none"> - Handling - Volume and surface (container) 	 <ul style="list-style-type: none"> - Capacities (volume, surface) 	 <ul style="list-style-type: none"> - Handling - Volume and surface (container)
		Live volume (and max)	Volume, surface of building	Live volume (and max)
	Level (Lj)	 <ul style="list-style-type: none"> - Load (floor) 	 <ul style="list-style-type: none"> - Load (floor) 	 <ul style="list-style-type: none"> - Load (floor)
		Live load (and max)	Live load (and max)	Live load (and max)
Position (Pk)	 <ul style="list-style-type: none"> - Number of compartments 	 <ul style="list-style-type: none"> - Number of compartments - Access to parts 	 <ul style="list-style-type: none"> - Number of compartments 	
	Localization of parts	Localization, duration of reply	Localization of parts	
Preservation	Class (Ci)	 <ul style="list-style-type: none"> - Transportable technologies - Factors of aging 	 <ul style="list-style-type: none"> - Static Techno. (individual or, collective) - Factors of aging 	 <ul style="list-style-type: none"> - Transportable technologies - Factors of aging
		Combination (nber, type)	Combination (nber, type)	Combination (nber, type)

Figure 3: The three axis of the process model.

The validation of the model, recorded in [Baud97], is the result of a classical external functional analysis.

4.1. PRODUCT MODEL

Globally, the functional model of preservation is made up of three parts. The first one (Cf. Fig.1) permits the spare parts description. The underlying desire is the listing of all characteristics (quantitative and qualitative) of SP that are pertinent from the preservation point of view. Thus, the product model - according to *O.Cantzler* [Can97], “a product model is a suite of data in a computing system that characterizes the potential solutions to a particular need, at every moment of the design process” - concatenates three axis (more or less dependent): the functional, structural and surrounding axis.

The first dimension is devoted to the description of the functionalities to be maintained available. For instance, we have the generic functions (kinematics, hydraulics, electronics, and electricity...) and the elementary functions (motor, generator, resistor, filter, and tightness connections: building in, pivot, etc).

The second dimension deals with the description of the parts constitution: material, physics (forms, assemblies) and geometrical (margins) parameters.

The last dimension may be considered as the interaction space between the parts (or product) and the environment potentially harmful for both others dimensions.

In this research field, we defined fifteen aging factors (among them: water, oxygen, ozone, light, temperature...). Each factor may damage a part, but the interaction between two or more factors may also constitute a potential harmful effect on the parts.

4.2. PROCESS MODEL

The second model (Cf. Fig.2) aims at the description of the logistic chain. The process model proposed constitutes a quasi-natural cutting of the problem. Three axes are defined in this space. (Fig.3) gives a vivid representation. At first, the time-axis shows the different positions of use of the preservation process as well as the evolution of the system. We consider for example the notions of part flow, access time, supply, delivery, handling, etc. Then the space-axis expresses the allocation of resources. Accordingly, we determinate among others how many stores are necessary, where to place them and what capacities (volume, load, conveniences...) are required. Finally, the preservation-axis allows the connection with the product model (the third dimension). The main idea is that the determination of the classes is done according to the aging factors, on the one hand, and potentially neutralized by the technologies of preservation, on the second hand.

4.3. DRIVING MODEL

The third model of the triptych is devoted to the objectives and constraints driving. The determination of the parameters has to be undertaken methodically in agreement with the policy of the company. Consequently, the model of objectives and constraints piloting offers the possibility to control priorities of decision-maker by a management of the functions to be optimized. Among all the possibilities, we may point out for

instance, the minimization of the cost of no availability (of the power plants), the annual working cost, the number of warehouses and the access time to sp. Thus, nine objective functions and six constraint functions have been defined.

As previously shown the aim of the functional model is the comparison (on three levels) of the different GSP propositions. First, the comparison of the global cost of technological solutions, second the comparison of the satisfaction between the potential GSP and the ideal system, and third the comparison of risks related to each solution.

5. Implementation

The implementation of this model has trained us to design a software which entry interface (i.e. the man-machine interface) is presented here (Cf. Fig.4). The purpose of MICRO-COST, in French “Logiciel de Conservation Optimisée en Stockage et en Transfert” (Software of Optimized Preservation during Transportation and Storage), is the assistance to strategic. From this perspective, it contributes to the acquisition of knowledge about the problem by the means of five formats of “calling cards” (personalized, validated by EDF experts and enriched by some industrial investigations of technological benchmarking [Kas97]). These cards are designed with the database-processing software Microsoft Access 97 that is actually the best one of the category [Cal97] [ZRD97]. We defined five cards: spare parts, technologies, warehouses, tradesmen and nuclear power station. These cards are trained from the functional model.

The platform MICRO-COST is also made up of a database of rules for preservation (it contains over 300 rules) allowing the quantification of the aging factors (i.e. the third dimension of product model according to the functional and structural description of the parts). The software is used for the constitution and the structuring of the problem database for the purpose of simulation and/or optimization processing with the kernel software LOOPS⁸ [KSM97].

6. Conclusion

One of the main aspect of this work lies on the fact that the literature does not mention examples of global system of preservation. In this work the application of a systemic approach and the design of a functional model of preservation permit a good understanding of the problem and its complexity. The interest of the computer platform MICRO-COST surpasses also the only structuring of the just necessary data in a database for numerical processing. Shortly, this contribution could be used as a “standard” for data exchange between suppliers and users of spare parts. It could also constitute the framework of a future standardization of industrial preservation. Finally, an extension (and generalization) of these conclusions is foreseeable in areas as various as the army, the civil aeronautics, the food, the archaeology and the hospital environment.

⁸ LOOPS is a combinatorial optimization library developed in the “Productique Logistique” Laboratory.

Identité		Carte de visite N° 68	
Libellé :	<input type="text"/>	Matériels et Pièces de Rechange	
Fournisseur :	<input type="text"/>		
N° d'article :	<input type="text"/>		
Description générale			
Prix :	<input type="text" value="0,00 F"/>	Dimensions :	<input type="text" value="0"/> <input type="text" value="0"/> <input type="text" value="0"/>
		Masse :	<input type="text" value="0"/>
		Qté en stock :	<input type="text" value="0"/>
Liste MPR lourds :	<input type="checkbox"/>	MPR mines :	<input type="checkbox"/>
		MPR stratégiques :	<input type="checkbox"/>
		Liste source scellée :	<input type="checkbox"/>
		Taux rotation :	<input type="text" value="0"/>
Coût de non conservation de la pièce :	<input type="text" value="0,00 F"/>	Conservation :	Paliers : CP0 <input type="checkbox"/> CP1 <input type="checkbox"/>
Coût induit pour la centrale si pièce indisponible :	<input type="text" value="0,00 F"/>	individuelle :	CP2 <input type="checkbox"/> P4 <input type="checkbox"/>
Coût de maintenance de la pièce :	<input type="text" value="0,00 F"/>	collective :	P4 <input type="checkbox"/> N4 <input type="checkbox"/>
Remarques :	<input type="text"/>		
Description fonctionnelle			
Fonctions élémentaires :			
1) Mécanique :	<input type="checkbox"/>	2) Electrique :	<input type="checkbox"/>
		3) Electronique :	<input type="checkbox"/>
		4) Hydraulique :	<input type="checkbox"/>
<input type="checkbox"/> Lubrification	<input type="checkbox"/> Actionneurs	<input type="checkbox"/> Composants passifs	<input type="checkbox"/> Robinetterie
<input type="checkbox"/> Protection/étanchéité	<input type="checkbox"/> Moteur	<input type="checkbox"/> Résistance	<input type="checkbox"/> Robinet
<input type="checkbox"/> Mise en position	<input type="checkbox"/> Electro-aimant	<input type="checkbox"/> Inductance	<input type="checkbox"/> Clapet
<input type="checkbox"/> Guidage	<input type="checkbox"/> Vérin électro-magn.	<input type="checkbox"/> Capacité	<input type="checkbox"/> Purgeur
Description structurelle			
Matériaux :			
1) Métaux ferreux :	<input type="checkbox"/>	2) Métaux non-ferreux :	<input type="checkbox"/>
		3) Polymères :	<input type="checkbox"/>
		4) Divers :	<input type="checkbox"/>
<input type="checkbox"/> Fonte	<input type="checkbox"/> Alliage de cuivre	<input type="checkbox"/> Thermoplastique	<input type="checkbox"/> Acide
<input type="checkbox"/> Acier non allié	<input type="checkbox"/> Alliage d'aluminium	<input type="checkbox"/> Thermodurcissable	<input type="checkbox"/> Amiante
<input type="checkbox"/> Acier faiblement allié		<input type="checkbox"/> "Elastomère"	<input type="checkbox"/> Argent
<input type="checkbox"/> Acier fortement allié		<input type="checkbox"/> Groupe R	<input type="checkbox"/> Graphite
<input type="checkbox"/> Elément d'addition	<input type="checkbox"/> Revêtement	<input type="checkbox"/> Groupe M	<input type="checkbox"/> Huile, graisse
<input type="checkbox"/> Cadmium	<input type="checkbox"/> Magnésium	<input type="checkbox"/> Groupe O	<input type="checkbox"/> Mat. radioactive
<input type="checkbox"/> Chrome	<input type="checkbox"/> Manganèse	<input type="checkbox"/> Groupe Q	<input type="checkbox"/> Papier
<input type="checkbox"/> Etain	<input type="checkbox"/> Molybdène	<input type="checkbox"/> Groupe U	<input type="checkbox"/> Verre, céramique
<input type="checkbox"/> Nickel	<input type="checkbox"/> Silicium		
<input type="checkbox"/> Zinc			
Formes et assemblages :			
1) Formes élémentaires :	<input type="checkbox"/>	2) Assemblages courants :	<input type="checkbox"/>
<input type="checkbox"/> Trou borgne	<input type="checkbox"/> Rainure	<input type="checkbox"/> Agrafage	<input type="checkbox"/> Fretage
<input type="checkbox"/> Trou débouchant	<input type="checkbox"/> Forme saillante	<input type="checkbox"/> Boulonnage	<input type="checkbox"/> Liaison par obstacle
<input type="checkbox"/> Chanfrein		<input type="checkbox"/> Collage	<input type="checkbox"/> Soudage
Description environnementale			
Facteurs de vieillissement à neutraliser :			
<input type="checkbox"/> Eau	<input type="text" value="0"/> <input type="text" value="0"/>	<input type="checkbox"/> Pression	<input type="text" value="0"/> <input type="text" value="0"/>
<input type="checkbox"/> Oxygène	<input type="text" value="0"/> <input type="text" value="0"/>	<input type="checkbox"/> Réactifs	<input type="text" value="0"/> <input type="text" value="0"/>
<input type="checkbox"/> Ozone	<input type="text" value="0"/> <input type="text" value="0"/>	<input type="checkbox"/> Rayons	<input type="text" value="0"/>
<input type="checkbox"/> Température	<input type="text" value="0"/> <input type="text" value="0"/>	<input type="checkbox"/> Chocs	<input type="text" value="0"/>
<input type="checkbox"/> Lumière	<input type="text" value="0"/>	<input type="checkbox"/> Vibrations	<input type="text" value="0"/>
		<input type="checkbox"/> Poussières	<input type="text" value="0"/>
		<input type="checkbox"/> Elect. Stat.	<input type="text" value="0"/>
		<input type="checkbox"/> Mat. poisons	<input type="text" value="0"/>
		<input type="checkbox"/> Halogènes	<input type="text" value="0"/>
		<input type="checkbox"/> Micro-organismes	<input type="text" value="0"/>

Figure 4. Example of micro-cost input interface: card "spare parts" (spatial view)

Acknowledgments

The authors would thank *Aleman, Renoux, Briard, Contart* and *Fichter* from EDF, for their important support in this project.

References

- [Ada87] B. ADAM. (1987) *L'analyse de la valeur - Stimulant des ressources humaines*. ESF Editions, Paris, France.
- [Bau97] N. BAUD. (1997) *Un système global de conservation de matériels et pièces de rechange - Application au domaine du nucléaire*. Cahier d'Etudes et de Recherche (confidentiel), Labo. PL, Ecole Centrale Paris (France), N°97-05.
- [Cal97] C. CALLAUD. (1997) Base de données : enfin des logiciels simples. *L'Ordinateur Individuel*, N°84, mai 1997, pp. 148-161.
- [Can97] O. CANTZLER. (1997) *Une architecture conceptuelle pour la pérennisation d'historiques globaux de conception de produits industriels complexes*. Thèse de doctorat, Labo. PL, Ecole Centrale Paris, France.
- [Kas97] M. O. KASSAAGI. (1997) *Benchmarking technologique sur les procédés de conservation*. Mémoire de D.E.A. Labo PL, Ecole Centrale Paris, France.
- [KDC+96] M. KARSKY, G. DONNADIEU, S. COPIN, S. PITARCH and J. FOURCADE. Un modèle de simulation des comportements dynamiques des processus de motivation. *Revue Internationale de la Systémique*, Vol.10, 1996, pp. 447-484.
- [KSM97] S. KEDAD-SIDHOUM and M. MEKHILEF. (1997) LOOPS : outil d'aide à l'affectation d'activités à des ressources parallèles sous contraintes. *PRIMECA'97*, La Plagne, France. Avril 1997, pp. 99-107.
- [Lim96] F. LIMAYEM. (1996) *Représentation fonctionnelle de systèmes physiques*. Rapport bibliographique de DEA, Labo. PL, Ecole Centrale Paris (France), 1996.
- [Mél95] J. MELESE. (1995) *Approches systémiques des organisations*. Les Editions d'Organisation, Paris (France), 3^{ème} édition.
- [Mor94] E. MORIN. (1994) *Introduction à la pensée complexe*. Collection Communication et Complexité, ESF Edition, Paris, France.
- [PYB96] N. PAILLES, B. YANNOU and J.-C. BOCQUET. (1996) Manufacturing Flexibility: A New Evolution. *Proceedings". IDMME'96*, Vol.2, Nantes, France. Avril 1996, pp. 907-916.
- [Ram97] I. RAMONET. (1997) *Géopolitique du chaos*. Galilée. Paris, France.
- [SCF95] F. SUAREZ, M. CUSUMANO and C. FINE. (1995) *An Empirical Study of Flexibility in Manufacturing*. Sloan Management Review. MIT, Fall, USA.
- [Sim91] H.A. SIMON. (1991) *Sciences des systèmes - Sciences de l'artificiel*. Dunod, collection AFCET systèmes, Paris, France. 2^{ème} édition.
- [Thi93] D. THIEL. (1993) *Management industriel - Une approche par la simulation*. Economica, Paris, France.
- [Woo71] J. WOODWARD. (1971) *The Structure of Organisations*. Management & Technology, HMSO, Pugh, USA. pp. 4-21.
- [ZRD97] P. ZEMOUR, Y. ROUX et F. DUPIN. (1997) *Les trois géants en compétition*. Science & Vie Micro, N°147, Paris, France, mars 1997, pp.70-89.

A GENERIC MODEL FOR KNOW-HOW CAPITALIZATION

Modèle générique de capitalisation du savoir-faire

JULIE STAL-LE CARDINAL

*Ecole Centrale Paris, Laboratoire Productique-Logistique
Grande voie des vignes, 92295 Châtenay-Malabry Cedex
email : stalj@pl.ecp.fr*

ABSTRACT

As far as product design is concerned, an important question is what makes an actor in a project capitalize what he knows and does? Capitalizing must become natural and even obvious. Our goal is to reach a very simple and pragmatic level so as to enable any user in a project to capitalize a process. We expect therefore to design a model as generic and convivial as possible so as to fulfill any user's need. The base of our research work is to define what the critical aspects that represent a process without any redundancy are. After a study of the works related to the design process histories and the different tools, we explain how we defined, on the one hand, the objectives for a model and, on the other hand, the just necessary criteria for a given user. In order to validate real needs in capitalization and to perform the response to these needs, we propose here a computerized model of design process history.

RÉSUMÉ

Une réelle préoccupation entoure le domaine de la capitalisation des processus de conception. Tout processus peut être capitalisé, le tout est de savoir comment le « découper » pour en faire une entité réutilisable. La base de notre travail est de réfléchir sur ce qui représente un processus à l'essentiel, en évitant toutes les redondances et notre objectif est de nous situer à un niveau très souple et pragmatique pour permettre à tout acteur d'un projet de capitaliser un processus. Après un état de l'art sur la capitalisation des processus et des différents outils de capitalisation des connaissances, nous expliquons la démarche qui nous permet d'aboutir aux objectifs à atteindre par le modèle et aux critères juste nécessaires pour un utilisateur donné. Nous parvenons ainsi à une structure générale illustrée par une application informatique.

1. Introduction

Studying the project management of an innovative product conception can lead to the discovery of some dysfunctions but it is often difficult to understand why they appear during the realization of the project. Design process history is actually a real preoccupation today as far as conception and management are concerned. Any process in our life can be capitalized, the difficulty lies in capitalizing the parts that form a reusable entity. Our reflection is based on the decomposition of any process into actions. **Our main purpose is to make a generic model that can be adapted to any particular action or process.** In general terms, the idea is that we capitalized, on the one hand, so as to enlarge our stocks of information and to keep it growing bigger and, on the other hand, so as to share all the data. The enrichment and the sharing of information are the two basic ideas of capitalization.

2. Field of Inquiry

A design process is often full of complexities, that makes its decomposition into different parts rather tricky. The strategic, tactical and operational levels have been admitted and recognized for a long time now. But the complexity at the operational level is still so important that it highlights the interest in a process modeling based on capitalization and genericity. Capitalizing allows any company to evaluate, to anticipate dysfunctions, to optimize the innovating design, to understand the reasons of dysfunctions, to take part in the enrichment of its patrimony. People capitalize so as to reuse: reusing « implies » recognizing a situation and recognizing a situation « implies » being able to represent it. Since the beginning of our works, we have been submitted to multiple interrogations, the most important ones are presented here: **How to capitalize the history of the decisions making? How to verify coherence in a system? How to represent a process in its crucial aspects? Is there any single representation of a process that leads to its description and analysis? What are the just necessary functions for capitalization?**

3. State of the Art

With the advent of computer science [GOR.95], design tools and methodologies come out with universal vocation [BLE.94], essentially based on the Hierarchic, Sequential, Informational Model. But the lack of genericity and the disregard of human beings cast some doubt upon the adequacy of the model [PER.94]. An approach to the design activity in terms of organization also appears [MIN.95]. It appeals to different notions such as cooperation, knowledge, retro-actions, communication and apprenticeship. The tool approach gives up competing with the organizational approach with the strategic, tactical and operational stakes. A design process is still very difficult to rationalize [AND.85], [HUB.85], because it depends on multiple factors such as the field of activity (electronics, computer science, building trade), or such as the kind of problem to solve (innovating project, routine project).

As far as the socio-technical approach is concerned, design process cannot be seen only as what passes through the designers' heads [BOU.97]. On the one hand, because designers share their activity with their tools and, on the other hand, because this activity produces traces, called the « intermediate objects » [VIN.94], [TIC.94]. In today's industrial organizations, design histories are rarely archived in an integrated, accessible form [SHA.96]; information about design projects lies scattered about in various formats. The only access to such information may be through conversations with project engineers who work on a given project. So, even if each design process is singular, there is a real need to create generic tools that could help the capitalization, the apprenticeship and the organization of data and knowledge, which are always changing in this concurrent engineering environment.

Regarding the design process representation as a general modeling of the design activity, three different purposes can be identified for the elaboration of a process model: the descriptive and concrete approach [TAK.90], [TOM.87], [ULL.91], the prescriptive and abstract approach [PUG.91] and the mixed approach [CRO.89]. Considering the decision-making processes, flexibility and reliability must be introduced: in any modeling, there is always arbitrariness, simplification and omissions [TSO.91], that lead to multiple problems (differences of interpretation, responsibility of the decision maker in the choice of the decision, unreliabilities, ambiguities). Among all the existing analysis tools, we can present the classical models [KUM.90], the information models [MOL.94], [MAR.94], the capitalization by the goals model [OUA.97] and the consensus model [CRO.92]. We will pay special attention to a conceptual architecture for the design process histories of industrial complex products [CAN.97]. This is a slanted project approach, information that could be used by numerous different people is capitalized, by opposition to the slanted trade approach where the expert's know-how is formalized.

We now use a lot of technics for process/product modeling or optimization and for output management, but we rarely work on the process history. Regarding the design processes history as a special case, works here are even less numerous. The base of our research works is to know what kind of crucial aspects can represent a process without any redundancy and our goal is to be at a very simple and pragmatic level so as to enable any user in a project to capitalize a process.

4. Modeling

As far as the industrial context is concerned, the primary objective of the capitalization is to optimize the conception time which is based on the sharing of information. The industrial need can also be defined as followed: limiting the waste of time spent to accomplish a daily work by capitalizing (structuring and stocking information) and reusing (evaluating, identifying and analyzing) information thanks to a minimal architecture which curbs the user as little as possible and which always allows the extension of the database.

4.1. SOME CONCEPTS DEFINITIONS

4.1.1. *Know-How*

We define **know-how** as data composed of information and semantics and as data progressing by following the different phases of a life line. These stages are structuring, capitalization, reuse, analysis and maintenance. Semantics enables, on the one hand, to structure information which depends on users and tools and, on the other hand, to have intelligent information which is **know-how**.

Our purpose is to structure **know-how** in such a generic way that it will help answering questions such as: when, how long, who, why, what is the aiming at?

4.1.2. *Functions and Criteria*

A functional analysis study has been conducted [STA.97] to **find the functions that must be satisfied by the model** in each of its different situations of use (structuring, capitalization, reuse of data, analysis, maintenance). This list of functions is not exhaustive, it just helps us to define the real need our model has to satisfy. This is the description outline of our model in its different situations of life.

The liberty is given to the user to add other functions or to modify some. Functions from the functional analysis are for instance:

- The object must allow the user to identify a situation, the context of a process.
- The object must allow the user to capitalize his experience on a given design process.
- The object must allow the user to easily and quickly compare two decisions.
- The object must allow optimization of time spent to take a decision.

In order to adapt the model to each user’s need, functions from the functional analysis have been translated into **criteria**: in a given project, a user is able to capitalize a process by choosing criteria which represent his concern in the project.

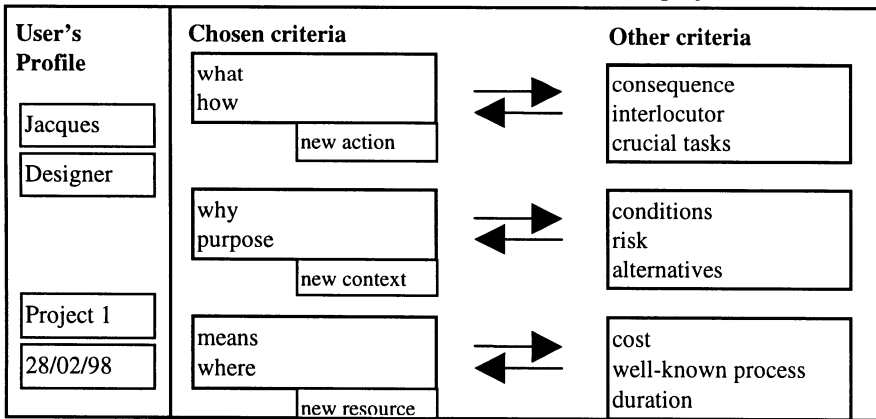


Figure 1. The user chooses here criteria. Selected criteria define his user’s profile.

4.1.3. *Just Necessary Concept*

Criteria depend on the knowledge of the user in a project; one cannot answer to any question regarding a project, it depends on either his function or his action in the project. So, in order to capitalize the just necessary information in a project, each participant can choose his personal criteria.

Translating functions into criteria allows at first the adaptation of the model to a user’s specific need, secondly the definition of a specific profile for each user and finally the satisfaction of a maximum number of functions with the least information possible.

4.1.4. Project of Action

In order to get a generic model, structuring the criteria in a **Project of Action** is necessary. We also propose to decompose any **Project of Action** into Action, Context and Resources which gather numerous criteria chosen by the user and which give access to tools. This represents the minimal architecture for the process (Figure 1).

4.1.5. User's Profile and Bijective Application

By selecting criteria, a user defines a **User's Profile** as shown in Figure 2. This profile gives access to the following potential actions: capitalizing a process, reusing a capitalized process, analyzing a project (group of processes). The **User's Profile** notion answers questions with regards to hierarchy and to diversity as far as specialties are concerned (a user can have numerous functions and also numerous profiles); this is the **direct application between the position of an actor within a project and what he really does**.

	IDEF	PERT	GRAI	VA	Taguchi
crucial criteria	what	what, duration	what, purpose	what, cost	what, purpose, consequence
necessary conditions	action	action, resource	action, context	action, resource	action, context
what, purpose, consequence	IDEF		GRAI		Taguchi
what, purpose	IDEF		GRAI		

Figure 2. This tabular is an extract of the possible relationship between tools and criteria.

Two connections can be highlighted here: the user-tools connection and the user-profile connection. Chosen criteria define the user's profile which gives access to tools. This application is **bijective** because access to a singular tool can be done only by choosing the corresponding criteria. A profile can also be defined by the tools the user wants to use.

4.2. SPECIFICATIONS

Specifications become the followings:

- coherent and generic,
- adaptable model with a free access to data,
- user friendly interface,
- integration of computerized tools (SADT, PERT, GANTT, AMDEC), fitted to all steps of a project and to all granularity levels and which allows a very quick inventory of the database contents.

The other advantages of our model are:

- all keywords used in the application are defined, the language is, on the one hand, informal and natural and, on the other hand, formal,
- the user interface is logic, simple and has a rich vocabulary,
- the possibility for the user to adapt the model to particular needs is done in a very simple way,

- the user can either precise the number of alternatives or add new functions that should be satisfied by the model. He can also use former existing models.

So as to simplify the model, only the just necessary information for the reuse is capitalized, and new tools can be added to analyze a project by a given view.

An application RADO has been implemented on HyperCard so as to illustrate and validate the main functions of the model in its different ways of use.

5. Application: Choice of an Optimization Method

The purpose, here, is to show how a choice of an optimization method can be capitalized so as to be reused to solve an other industrial problem. We just show here the beginning of the capitalization that could help a user to determine the optimum solution.

PA.1 (Project of Action 1):

Action:

What: choose an optimization method

Consequence: find the optimum solution to an industrial problem

How: by finding the appropriated mathematical modeling

Context:

Why: because the way to solve such a problem depends on its own structure (size and complexity)

Purpose: solve an industrial problem

Conditions: have the good definition of the industrial real need (**PA.2**)

Resources:

Means: experts in logistic

Where: in a logistic laboratory

Well-known Process: linear programming, optimization methods

PA.2:

Action:

What: have the good definition of the industrial real need

Consequence: identify the real problem to be formalized

How: by getting the real industrial data from the industrial person

Context:

Why: because sometimes industrial people do not exactly know where the problem really is

Purpose: solve the real problem (**PA.3**)

Conditions: availability of the industrial person

Resources:

Means: experts in logistic

Where: in a logistic laboratory

Well-known Process: linear programming, optimization methods

PA.3:

Action:

What: solve the real problem

Consequence: give the best solution to the industrial person

How: by identifying the size and the complexity of the problem:

1. for a well-known and easy problem: by choosing the appropriated algorithm
2. for a well-known and difficult problem:
 - small size problem: by spending some time to find the solution
 - bigger size problem: by finding only a feasible solution (one may not have the possibility or the time to find the optimum solution)
3. for a unknown problem: by obtaining a feasible solution by heuristic.

5. Conclusion

Our most important question is « what makes an actor in a project capitalize what he knows and does? ». Our main purpose is indeed to make people capitalizing in a real obvious way. We base therefore our research on different notions such as Value Analysis, transparency, information sharing, collaboration. A single representation for any process does not exist yet: processes depend on the considered field, on the kind of project, on the user and on what the user knows about the project. Generic tools are also necessary so as to adapt to anybody's need. Moreover, the minimal architecture proposed here affords us to use the least information possible, the user gives only the information he knows about the project and some subjectivity lies in information just like in any model involving human beings.

Our research work can lead to some future prospects. First of all, in a just necessary view, we could think we just have to capitalize the points involving dilemma in a process. However a process history without any problem is useful to reuse because there is no waste of time and reusing it would let us spend more time resolving other troubles, developing an innovating or strategic aspect. Moreover, we try to structure the language so as to transmit the know-how from the user who capitalizes to the user who reuses the information. But, we still have to solve the problem of the semantics which lies behind words. The language is the real support of the know-how but that must not stand in the way of information transmission. So an other prospect of our work could be the creation of a common language for capitalization and reuse of information. Finally, an other question which still remains is the modeling independence of any product/process modeling. We try here to be as generic as possible by not being linked to any product/process modeling, but this research field is still opened.

6. References

- [AND.85] M.M. ANDREASEN. *"The use of systematic design in practice"*, Design Studies, 1985, pp. 138-144.
- [BLE.94] L. BLESSING. *"A process-based approach to computer-supported engineering design"*, Ph.D. thesis, Université de Twente, Enschede, Pays-Bas, 1994.
- [BOU.97] J.F. BOUJUT. *"Approche sociotechnique des processus de conception"*, Primeca, 1997.

- [CAN.97] O. CANTZLER. *"Une architecture conceptuelle pour la pérennisation d'historiques globaux de conception de produits industriels complexes"*, thèse de doctorat, Ecole Centrale Paris, 1997.
- [CRO.89] N.CROSS. *"Engineering design methods"*, Chichester, Wiley, 1989.
- [CRO.92] N.CROSS, N. ROOZENBURG. *"Modeling the design process in engineering and in architecture"*, Journal of Engineering Design, N°3, 1992, pp. 325-336.
- [GOR.95] I. GORGES. *"The impact of society on CAD research in the USA, France and Germany 1955 through 1985"*, 1995.
- [HUB.85] V. HUBKA. *"Attempts and possibilities for rationalization of engineering design"*, Design Studies, 1985, pp. 133-138.
- [KUM.90] S. KUMARA, I. HAM. *"Use of associative memory and self-organization in conceptual design"*, Annals of the CIRP, n°39, 1990, pp. 117-120.
- [MAR.94] J.C. MARTIN. *"Le traitement de l'information dans l'entreprise, le secret de l'efficacité japonaise transposé en Europe"*, FransOrient, 1994.
- [MIN.95] MINISTERE DE L'ENSEIGNEMENT SUPERIEUR ET DE LA RECHERCHE. *"Concevoir l'activité de conception"*, Rapport annuel, 1995.
- [MOL.94] A. MOLINA, T.I.A. ELLIS, R.I.M. YOUNG, R. BELL. *"Modelling manufacturing resources, processes and strategies to support concurrent engineering"*, Concurrent Engineering Research and Application, 1994.
- [OUA.97] A. OUAZZANI, A. BERNARD, J.C. BOCQUET. *"Proposition d'une méthode d'aide à la gestion des processus et d'intentions de conception : la méthode sagep"*, Primeca, 1997.
- [PER.94] J. PERRIN. *"Définition de l'approche artefact et application de l'approche artefact aux structures organisationnelles"*, Presses Universitaires de Lyon, 1994.
- [PUG.91] S. PUGH. *"Total design: Integrated methods for successful product engineering"*, Wokingham, Addition-Wesley, 1991.
- [STA.97] J. STAL-LE CARDINAL, M. MEKHILEF. *"Démarche pour l'élaboration d'un modèle de capitalisation du savoir-faire"*, CER97-07, Ecole Centrale Paris, 1997.
- [SHA.96] J.J. SHAH, D.K. JEON, S.D. URBAN, P. BLIZNAKOV, M. ROGERS. *"Database infrastructure for supporting engineering design histories"*, Computer-Aided Design, 1996, pp. 347-360.
- [TAK.90] H. TAKEDA, P. VEERKAMP, T. TOMIYAMA, H. YOSHIKAWA. *"Modeling design processes"*, AI Magazine, 1990, pp. 37-48.
- [TIC.94] S. TICHKIEWITCH, D. BRISSAUD, J.F. BOUJUT. *"Prise en compte de la fabrication dans la conception"*, Club Bureau d'études du futur : méthodes de conception, 1994.
- [TOM.87] T. TOMIYAMA, H. YOSHIKAWA. *"Extended general design theory"*, Design Theory for CAD Proceedings of the IFIP Working Group 5.2 Working Conference, 1987, pp. 95-124.
- [TSO.91] A. TSOUKIAS. *"Preference modeling as a reasoning process: a new way to face uncertainty in multiple criteria decision support systems"*, European Journal of Operational Research, N°55, 1991, pp. 309-318.
- [ULL.91] D.G. ULLMAN. *"Design histories: Achieving the evolution of products"*, DARPA Workshop on Manufacturing, 1991.
- [VIN.94] D. VINCK, A. JEANTET. *"Mediating and commissioning objects in the sociotechnical process of product design: a conceptual approach"*, COST A3 Workshop - Management and new technology: design, networks and strategies, 1994, pp. 111-129.

Web-based Product Information Visualization through VRML Code Generation

YOONHO SEO

Product & Process Design Laboratory

Dept. of Industrial Engineering, University of Ulsan

Moogur-dong san#29, Nam-ku, Ulsan, Korea (680-749)

Tel: +82-52-259-2287, Fax: +82-52-259-2180

e-mail: yhs@uou.ulsan.ac.kr

Abstract

VRML (Virtual Reality Modeling Language) is a graphic modeling tool that is used for 3D representation of objects and animation of their behavior through WWW (World Wide Web). Especially, VRML2.0 has such new functions as enhanced static worlds, interaction, animation, scripting, prototyping, etc. By full usage of these capability of VRML2.0, the goal of this research is to develop a software system to automatically generate the VRML2.0 code for demonstrating product shape, product configuration and assembly process with DXF files as input. The VRML code generated can be used to provide a product information through any standard browser, Netscape, Explorer, etc., on WWW. Specifically three algorithms are presented: one for converting CAD to VRML, another for converting BOM to VRML, and the third for generating animation VRML code.

1. Introduction

As the manufacturing systems become automated as well as information-oriented more and more, a methodology is required to integratedly or individually optimize the business processes of the manufacturing enterprise, such as design, fabrication,

procurement, distribution, disposal, etc. Among various techniques for inter-process optimization, concurrent engineering is widely recognized as a feasible approach to obtain the global optimization. By simultaneously considering and providing feasible solutions in the design phase on the problems which may cause at any point of time in the product life-cycle, concurrent engineering design is intended to provide the opportunity for larger improvements in product development cost reduction, the time to market, and quality. For successful implementation of concurrent engineering concepts, it is essential to model and manage the product-related information, and share them between CE team members. Product-related information in manufacturing companies exists in various formats and various departments. For example, product shapes and structural information are in engineering drawings or BOM (Bill of Material) in the form of CAD files or hard-copy documents. Also, process information (including machining and assembly process) exists in process plans in the forms of hard-copy documents, electronic documents, digital files, or database records. Thus, these pieces of product-related information, which may be geographically distributed, inconsistent and incomplete, cannot fully provide what is required to fulfill the cross-functional global optimization among the business processes.

This paper discusses the methodology to represent integratedly and dynamically the product information including product shape and assembly process animation through WWW [2, 4]. The research aims at developing a software tool which encompasses the distributed product-related information in various formats and converts those information into the integrated and dynamically visualized form of information - so called Virtual Reality Modeling Language (VRML) code. This system helps the CE team members share the product information in common by providing the integrated and dynamic realization of product assembly process through WWW or a corporate intranet [1, 3, 5].

2. Proposed System Architecture

In this paper, the development of a software system is proposed, so called Product Assembly VRML Code Generator, which is intended to automatically generate the VRML2.0 code which expresses the product shape and assembly animation process by using and accessing the distributed product-related information in manufacturing companies. The system is composed of three parts, the input/output module, the shape

VRML code generation module including the product shape and structural information and the animation VRML code generation module to visualize the assembly process. The conceptual diagram for the system is presented in *Figure 1*. Detail description for each module is followed.

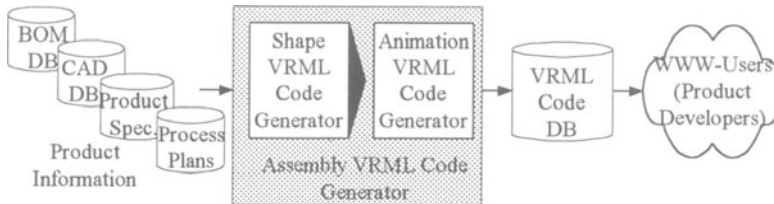


Figure 1. Proposed System Architecture

2.1. INPUT/OUTPUT DATA FORMAT

The Assembly VRML Code Generator takes input data by accessing four data base tables, which include the information on BOM, CAD, product specifications and process plans. The VRML code generated is stored in VRML DB and provided to users according to their requests through the internet. The CAD DB includes the 3D-shapes of component parts. The 3D-shape information is invoked and converted into the VRML codes for part shapes. In this paper, the shape information in the DXF (Drawing Interchange File) format is used. The DXF format is a neutral text file format, which is used to share the 3D-shape information from various CAD systems. Product specification DB includes the product dimensions and tolerances, while assembly relations and sequence are included in the assembly process plan. To produce the assembly VRML code, a two step conversion of raw product information is required, *i.e.*, into the shape VRML code, then the animation VRML code.

2.2. PRODUCT SHAPE VRML CODE GENERATION

Product shape can be illustrated with the component shapes and their combination, *i.e.*, assembly structure and their relations. Traditionally the product structure is expressed in BOM (Bill of Material), which represents the component configuration and material requirements for a product in a tree-like data structure. As shown in *Figure 2(a)*, a product structure is well described in a BOM tree. In the BOM tree, the leaf nodes

represent individual parts, the root node for the final assembly, and the intermediate nodes for the subassemblies. Also the corresponding VRML structure shown in *Figure 2(b)* can explicitly express the inclusion and assembly relationships between component parts.

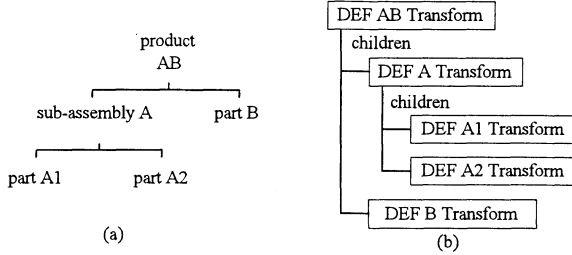


Figure 2. (a) BOM Tree and (b) structure VRML Tree

To produce the VRML code for representing product shape, the product structure in a BOM tree is first interpreted into the VRML code for the tree structure and then the part shape information in the DXF format is converted into the VRML code at each terminal node in the VRML tree. Two algorithms to generate the structure VRML and shape VRML codes are presented in the following two subsections.

2.2.1. Algorithm to Convert BOM into Structure VRML

Variables:

part: data structure including part name and its parent name

List: instance of a linear list class including *part* information

position: current position in *List*

Methods:

List.AddTail(): method function in class *List* to add element into a *List*

List.GetAt(): method function in class *List* to obtain information at any location

List.GetFirst(): method in class *List* to return the first location in *List*

List.GetCount(): method in class *List* to return the number of elements in *List*

List.DeleteFirst(): method in class *List* to delete the first element in *List*.

Make_Node(): assign a node

Insert_ChildNode(): assign a child node

Query_BOM_Database():

Find_Parent_Position(): location that coincides with the parameter.

Main body:

part = product name;

position = 0;

```

List.AddTail(part);
while (position < List.GetCount()) {
    part = List.GetAt (position);
    List.AddTail (Query_BOM_Database (part));
    position ++;
}
while (List.GetCount () != 0) {
    part = List.GetFirst ();
    if (part.parent ==none) Make_Node (part);
    else Insert_Child_Node (Find_Parent_Position (part),part);
    List.DeleteFirst ();
}

```

2.2.2. Algorithm to Convert DXF to VRML

Variables:

dxfl: a DXF text file

dxfl_index: instance of a linear list including XYZ coordinates and string SEQEND.

index_table: instance of a linear list including XYZ coordinates

point: a string for *point* field of coordinate node in VRML

coord_index: a string for CoordIndex field of IndexedFaceSet in VRML

Methods:

DXF_Filter (): to obtain X-, Y-, Z values and SEQEND from a *dxfl* string

DXF_Coord_Filter (): to delete the duplicated coordinates and SEQUEND from a *DXF* string

IndexTable_To_VRML_PointSet(): to convert into VRML *point* field from *index_table*

DXF_SEQEND_To_VRML_Index(): convert into VRML *coord_index* field from set of XYZ coordinates of DXF

Make_Shape(): complete VRML shape node through parameters

Main Body:

dxfl_index = DXF_Filter (*dxfl*);

index_table = DXF_Coord_Filter (*dxfl_index*);

point = IndexTable_To_VRML_PointSet (*index_table*);

coord_index = DXF_SEQEND_To_VRML_Index (*index_table*, *dxfl_index*);

Make_Shape (*point*, *coord_index*);

2.3. VRML CODE GENERATION FOR ASSEMBLY ANIMATION

To generate a VRML code for assembly animation of parts, the parts configuration, assembly sequence and relations for the final assembly should be explicitly represented.

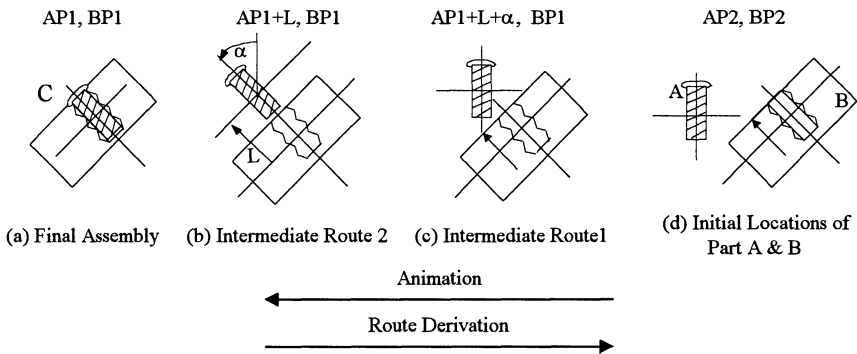
This module uses the VRML codes for product shape and structure generated from the shape VRML code generator in Figure 1, and obtains the final assembly configuration, contact relations and assembly sequences from the assembly process, and the initial location of each component from users.

2.3.1. VRML Code Structure for Animation

The routes of assembled parts are also represented for animation of assembly process. A function Interpolator in VRML is used. The kinds of information are required to use the Interpolator: start and animation time management, shape, location and orientation of each component, and routing part including time elapse and event information.

2.3.2. VRML Code Generation for Animation

In this subsection, the method to generate the intermediate routes of assembled parts is presented. For example, consider a simple assembly C, in which parts A and B are screw-fitted. In Figure 3, the assembly process of two parts can be depicted in three steps: to move a part from the initial position to the position where the center of a moving part is coincide with the assembly direction of the base part, to align the moving part to the assembled direction, and to assemble the part into the base part. For each assembly process, the parameters to conduct the assembly animation can be derived from product specification and the initial position of each component. For example in Figure 3, given the initial positions of part A and B, the rotating degree α and moving distance L can be obtained from the product specification. Therefore, VRML code for assembly animation can be derived from the information described above and by using



*Legends: A, B, C are part name, P means Position, R means Orientation

Figure 3. Animation VRML Code Derivation



the Interpolator NODE in VRML. The complete algorithm is described in the following subsection.

2.3.3. Animation VRML Code Generation Algorithm

Variables:

pos_ori : struct array with position and orientation

t: assembly start time

time: assembly duration

Methods:

Read_VRML_Final(): read the final locations of assembled parts

Read_Relation(): read the assembly relations for animation

Read_Regulation(): read the product specifications

Cal_Contact(): move from the current position to the contact position.

Cal_Fit(): move to the position to be fully fitted

Cal_Screw(): obtain the position and rotating degree in terms of orientation and product dimensionation.

Cal_Orientation(): coincide the orientation of the assembled part with the base

Read_Root_Orientation(): read the orientation of the part in root node

Read_VRML_Init(): read the initial positions for the assembled parts

Add_P&O(): add the time, position and orientation in Interpolator node

Main Body:

index = 0;

pos_ori[*index*++] = Read_VRML_Final()

if(Read_Relation() == Contact) *pos_ori*[*index*++] = Cal_Contact(*pos_ori* [*index*-1], Read_Regulation());

if(Read_Relation() == Fit) *pos_ori* [*index*++] = Cal_Fit(*pos_ori* [*index*-1], Read_Regulation());

if(Read_Relation() == Screw_fit) *pos_ori* [*index*++] = Cal_Screw(*pos_ori* [*index*-1], Read_Regulation());

pos_ori[*index*++] = Calculate_Ori(*pos_ori*[*index*-1]);

pos_ori[*index*] = Read_VRML_Init();

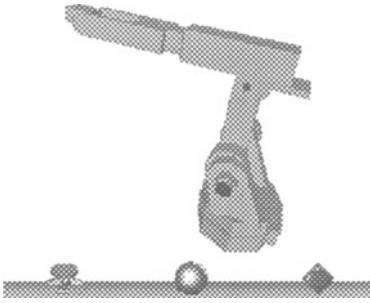
While(*index*>=0) {

 Add_P&O(*pos_ori*[*index*--],*Time*, *t*);

}

3. Implementation

The product assembly VRML code generator proposed is implemented with Visual C++5.0, Netscape Internet Control, Cosmo Player1.0 Plugin, and MicroSoft SQL Server6.5 in Window NT4.0 environment. The final assembly of an industrial robot and its components in the tree structure are depicted in *Figure 4(a)* and *(b)*.



(a) Final Assembly of a Robot



(b) VRML Tree

Figure 4. System Implementation

4. Conclusions and future research direction

Since the proposed system takes DXF format of shape information, BOM and assembly process as inputs regardless their types and general dimensions of the product, the proposed system can be used as a tool for concurrent engineering. Also the software tool can be used for parallel product development since it helps the team members obtain easily and quickly the shape and structural information of products in design phase and assembly animation of the product. The development of interface modules with STEP and JAVA will enhance the system applicability.

5. References

1. Casher, O., Leach, Christopher, Page, Christopher S. and Rzepa, Henry S. (1995) Advanced VRML-Based Chemistry Applications: 3D Molecular Hyperglossary, 2nd ECC Conf.
2. Osawa, N., Morita, H., and Yuba, T. (1997) Animation for Performance Debugging of Parallel Computing Systems, Proc. of VRML97, ACM SIGGRAPH, ACM Press, New York.
3. Ressler, S. *et al.* (1997) Using VRML to Access Manufacturing Data, Proc. of VRML97, ACM SIGGRAPH, ACM Press, New York.
4. Rohrer, Randall M. and Swing, Edward (1997) Web-Based Information Visualization, IEEE Computer Graphics and Application Information Visualization, pp52-59.
5. Silicon Graphics, (1997) The Virtual Reality Modeling Language Specification, <http://vrml.sgi.com/moving-world/spec/>.

Collaborative design in Education : the TAXIA PROJECT

Bruno RAMOND

**Université de Technologie de Compiègne
BP 649 - 60206 COMPIEGNE Cedex, France
Email : bruno.ramond@utc.fr**

RESUME

Douze écoles d'ingénieurs ont décidé d'unir leurs efforts pour concevoir et réaliser un nouveau véhicule automobile. Ce projet, appelé projet TAXIA, a pour but de répondre aux besoins exprimés par les chauffeurs de taxis et leurs clients. L'objectif final est de concevoir et de réaliser un prototype industrialisable du véhicule. Ce projet étudiant est très original dans sa taille, plus de 100 étudiants travaillent sur le même projet simultanément dans différentes écoles, et dans les méthodes utilisées pour les tâches de conception. Ce papier décrit le projet TAXIA et présente certaines observations que nous avons pu faire dès aujourd'hui autour du projet. Une des principales conclusions est que ce type de projet est une expérience pédagogique passionnante à la fois pour les étudiants et les enseignants et que cet exemple pourrait ouvrir la voie à d'autres projets similaires dans l'enseignement supérieur.

ABSTRACT

Twelve French schools have decided to join their efforts to design a new concept of vehicle. The product is designed to respond to the needs of the taxi drivers and their customers. This school project is very original in its size, more than 100 students working together on the same project at different locations in the country, as well as in the methods used to achieve the design, in particular the necessity to use high speed network. This paper describes some observations made concerning the project and reports on some difficulties encountered. One of the main conclusions is that TAXIA is a valuable pedagogic experience for both the students and the teachers, and that it could be an example for future projects in higher education.

I. INTRODUCTION

Since 1995, twelve high schools of Mechanical Engineering in France have been working together on a huge project, the design and the making of a new prototype of vehicle specially intended for taxi drivers: this is the TAXIA project. A prototype will be presented at the "Mondial de l'Automobile", a car-exhibition held in Paris in october 1998. This paper presents the project and a progress report, six months before the deadline.

II. HISTORY

At the beginning, in 1995, two students, passionately interested in cars, contacted other schools and universities to promote this idea :

" We, future engineers, want to show to the world that we are able to develop complex mechanical systems. Even if there are differences in our cultures and our knowledge, we are able to establish communication between ourselves to achieve such a project.

In London, taxis drivers use special cars. In New-York, cabs are yellow. In France, taxis have no distinctive features. Therefore, the taxi drivers using private cars might be a problem when a disabled person wants to hire a taxi.

The French market is too narrow and car makers are not interested in developing special cars for this job.

We are going to design and make a prototype of a taxi. Our objective will be to present a model at the car exhibition - the " Mondial de l'Automobile" - held in Paris in october 98".

So began the TAXIA project...

III. OBJECTIVES

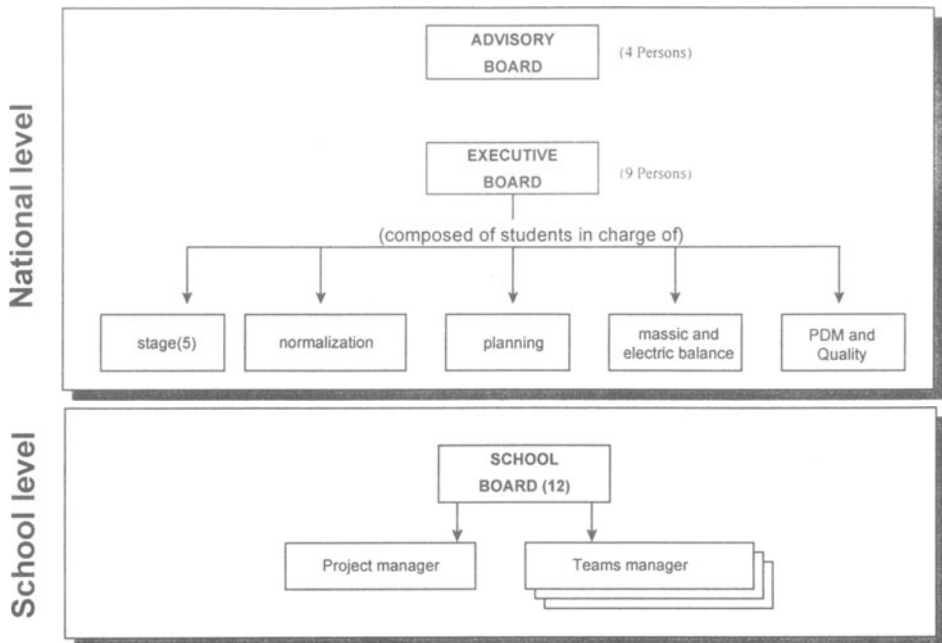
The project has two main objectives :

Firstly, the design and making of a new vehicle. This is certainly the biggest one. This goal is very ambitious as the duration of the project is three years and car makers, specialized in this job, generally spend three years to develop a new car. Furthermore, many innovations will be introduced in the Taxia prototype.

Secondly, communication problems must be solved. With schools distributed all over the country, the organization and the management of this project are complex. One of the challenges of the project is to use (and develop if needed) new concurrent methods and tools to facilitate an efficient work process in a network.

IV. ORGANIZATION

The work is done under the care of the French Society of Car Engineers, the " SIA - Société des ingénieurs de l'automobile".



*Organization of the project
Organisation du projet*

Ecole Nationale Supérieure Electronique Electrotechnique Informatique Hydraulique de Toulouse (ENSEEIH)
Ecole Supérieure de l'Energie et des Matériaux d'Orléans (ESEM)
Ecole Supérieure des Ingénieurs en Electronique et Electrotechnique de Paris (ESIEE)
Ecole Supérieure des Techniques Aéronautiques et de Construction Automobiles (ESTACA)
Institut Supérieur de l'Automobile et des Transports (ISAT)
Institut Supérieur de Design de Valenciennes (ISD)
Institut Supérieur de l'Electronique du Nord (ISEN)
Université de Technologie de Compiègne (UTC)
Institut National des Sciences Appliquées de Rennes (INSA)
Institut Universitaire de Technologie de St Denis
Institut Supérieur des Matériaux du Mans (ISMANS)
Institut Supérieur de Commerce de l'Automobile du Mans (ISCAM)

*List of schools working on TAXIA
Liste des écoles participant au projet*

IV.1. The advisory board

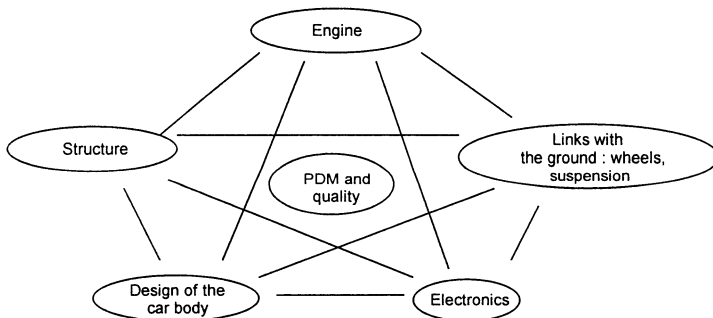
At the highest level, TAXIA is supervised by an advisory board composed of the two students who have initiated the project, a professor and the director of the SIA. The job of this board is to control the progress of the project.

IV.2. The executive board

Thus, an executive board is composed of students in charge of the different parts of the design. This board manages the project in its totality : it decides what studies must be done and what school will execute them. It gathers, controls and integrates all the results, manages the planning, and discusses the future studies to be undertaken.

IV.3. In the schools

At the working level, twelve french engineering schools or universities have been working on the project. Each school develops parts that depends on their technical skills : electronic institutes work on the development of circuitry, schools specialized in car technology, the engine and the structure... Professors supervise the work of their students, give advice and find industrial partners when needed, but all decisions are normally made by the students.



*Les 5 plateaux + le plateau SGDT qualité
The five Stages + Data management and Quality*

V. COMMUNICATION

There are two ways to communicate :

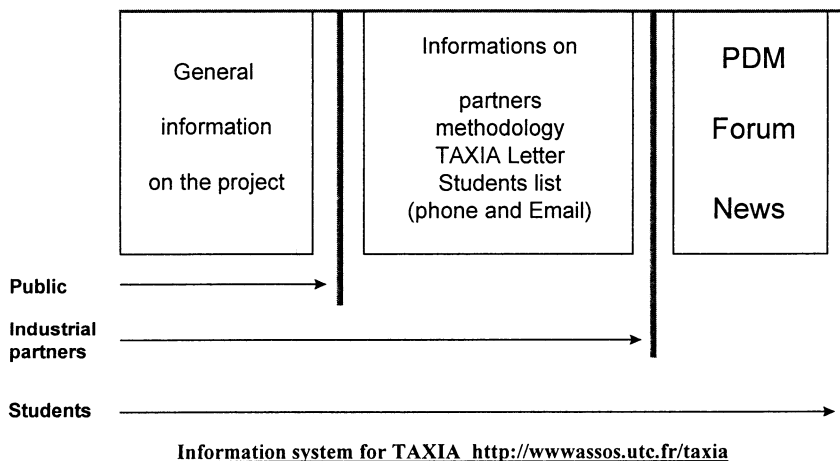
- Meetings which are held periodically to present all the results produced by the students and to study interactions. They are also the place where the students can meet each other, discuss and solve integration problems. Generally, as a lot of students attend these meetings, they are the places where the most important decisions are made. In particular, during the meeting held in Lille in July 97, the students produced the first global synthesis and decided on the modifications of the prime objectives.

- Day by day communication (certainly the most important one) is achieved in part by usual methods like phone, fax or Email. As the project is complex, the management of data structures is also complex and a new computer system has been specially designed for this purpose.

This system is based on a web server and a PDM (Product Data Management) system. It can be reached by the internet so that every school can have an access to it, at any time, thus being able to obtain the latest information very easily.

To take care of the situation where technical secrecy is important, three levels of access have been defined :

- a public access where Web pages present the project and general information. Everybody who has access to the web can read these pages
- a second level is restricted (access by password) to the students and the industrial partners. One can find a list of the partners, the methods to use, a global progress report and a list of all students working on the project.
- A third level is strictly restricted to the students working on the project. They can access all the data generated in the project : specifications, CAD models, studies, reports and meeting reports are stored and can be used when it is needed.



Other networked tools like Forums and News options have also been developed to promote asynchronous exchanges between the students.

We have noted that its use is dependant on the number of computers that a student can use in a school.

UTC students have free access to computers and internet, and they have the possibility to use CAD-CAM tools and simulation softwares. The use of this system seems rather natural. The situation is not the same in all the institutes and some schools are reticent in allowing their students to have a free access to the internet. In this case, communication is generally very difficult and slow.

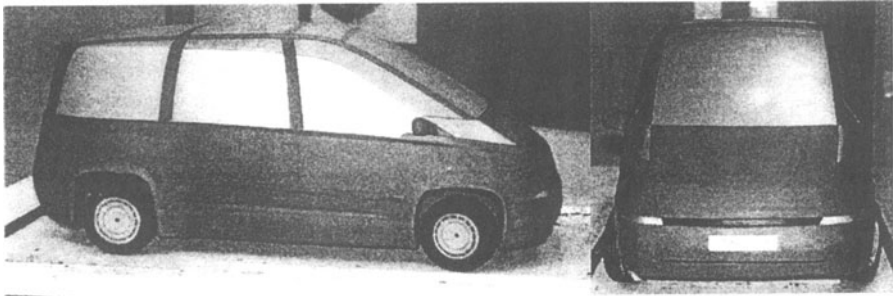
VI. TECHNICAL ASPECTS

VI.1. Description of the TAXIA car- Extracts from the specifications

The specifications have been written after sample surveys done with the taxi drivers in different towns in France. Students have also conducted some inquiries with big taxi companies (Taxis bleus, G7) to have different points of view from people in charge of taxi fleets.

Some extracts from the specification book are detailed below :

- TAXIA is a car designed for tourists visiting a town, with special services like tourist information
- It must be able to carry disabled passengers but also passengers with a large amount of luggages
- It will be comfortable for the passengers but also for a driver who spends about 8 hours a day driving the car.
- It must be distinctive from other cars in the street so that a customer can immediately recognize a TAXIA car, free for hiring.
- TAXIA will be a low emission car to preserve the air of the town where it will be used. It must respect the future european normalization on pollution.
- Price will be around 200 kF to be affordable for personal taxi drivers.



Photos du modèle TAXIA
Pictures of the TAXIA model

VII. TAXIA AT THE UNIVERSITY OF COMPIEGNE

Students at UTC have been involved in TAXIA since the beginning of the project. They have even created an association to bring together people interested in cars and particularly in developing the TAXIA concept.

UTC is in charge of the shape design of the car, the rear axle, the modeling of the structure and the communication system. Each stage is managed by a student and the whole process is supervised by one professor who controls the activity and the work of the students.

On each stage, the work is decomposed in small tasks or mini-projects (that can be done during a semester work) carried out by a group of students. Every mini-project is supervised by a teacher. If students have completed their task well, they can obtain special credits which can be credited to their personal curriculum.

VIII. DISCUSSION

The experience acquired in the first four semesters of project has been very useful not only for the students but also for the teachers.

VIII.1. Project Members

VIII.1.1.- Impact on students

Working on such a project is very appealing to the students since they like working on real objectives in the field they are interested in. It is not always so easy to control over enthusiastic involvement, and professors must guide them in their work. If not, the result can be very discouraging if a work does not progress correctly.

VIII.1.2.- Time management

Participation in the project is very time consuming for both the students and also the teachers. We have found that the work done by the students must be a part of their studies. In schools where the TAXIA project is integrated in the curriculum - by special credits for example - the work progress is very good. Students from other schools, working in free time on the project have dropped out very quickly.

VIII.1.3.- People management

As in an industrial project, it is very difficult to introduce new students once the project is under way. A special effort (in particular, meetings with presentations, progress report meetings, etc...) has been done to give them all the information they need to 'catch the running train'. It is long and it requires investment in training from the students : it is sometimes discouraging if a student works only a semester on the project.

VIII.2.Communication. Relations between partners.

Even with our communication system, we daily encounter some difficulties at the interfaces. What can be done very easily in one school can be very difficult to exchange from one school to another, especially when their agendas and curriculums are not the same. Furthermore, after all discussions, we are not always sure to talk about the same problems : do we understand the same meanings behind words and ... do we understand each other ?

VIII.3.Project management

This point is surely the most important : a strict management of the project is necessary. Every student who has worked on TAXIA has said that rules must be well established and rigorously applied. The project is managed by students and as they have no experience at this kind of job, we have encountered a lot of problems, particularly in time management and in the communication with people from the outside. These situations are

potentially very interesting, to study what has gone wrong and to establish new rules or new methods, but the objectives of the project are very tight so that we cannot spend too much time on these issues.

VIII.4. Capitalization

A lot of studies have been done during four semesters in the different schools and it has been necessary to collect all the work done to make a global synthesis. It is also a good way to put together all the data and to capitalize the knowledge. It was a very difficult task because some reports have not been prepared timely, and now with some people who have left or no longer remember all the details, some data are lost. It has been possible to save a part of the data at UTC, but we have been unable to do integrally for the whole project. More work remains to be done in this sense.

IX. CONCLUSION

TAXIA is certainly one of the most interesting "teaching" experience we have had in the last few years. It has been very fruitful for both the students and the teachers. Management of a very large project, communication with other people, modification, evolution of the teams, organization are some aspects that the students have discovered in the TAXIA project. They have also been able to test tools and methods they have learnt before and to develop their application. They have seen what should not be done, and how they can improve their work but also the work of their other partners.

More work needs to be done if we want to reach the first objectives, i.e to design and build a prototype of a standard taxi car, but even if we don't succeed, everybody has gained in skills and knowledge. Some improvements also remain to be made in order to manage correctly this kind of project, and surmount more easily the differences between the partners, the storage and the management of the knowledge, the sponsoring... This surely could not have been done only within the TAXIA project.

References

- [CUT96] CUTKOSKY et al . *MADEFAST : Collaborative Engineering over the internet*. Communications of the ACM, Sep 96, vol 39, number 9.
- [FRA97] E. Frankenberger and P. Aver. *Standardized observation of team work in design*. Research in Engineering design, Vol 9 Number 1, 1997
- [PER97] David perdriau et Bruno Ramond. *Information System for Concurrent Engineering : The TAXIA experience* , Proceedings of the international conference of the SIA, 19 et 20 nov 97.
- [TOY93] Georges Toye et al. *SHARE, A methodology and Environment for Collaborative product development*. in post proceedings of the IEEE Infrastructure for collaborative enterprises (CDR-TR # 19930507)

Chapter 9
INTEGRATED MANUFACTURING METHODOLOGY
AND APPLICATIONS

A fast and reliable cost-estimation tool for hot-forged parts.....	595
M. BERLIOZ, PH. MARIN and S. TICHKIEWITCH	
Cost-based ranking for manufacturing process selection	603
A. ESAWI and M. ASHBY	
Analytical study of multi-agent oriented manufacturing design	611
V. PATRITI, K. SCHAFER, P. CHARPENTIER and P. MARTIN	
Dynamic representation of a manufacturing process	619
B. ANSELMETTI and A. TOUMINE	
Extensions of object formalism for representing the dynamics Application to the integration of viewpoints in the design of a production system	627
M. BIGAND, D. CORBEEL, D. NDIAYE and J.P. BOUREY	
Multidimensional taguchi's model with dependent variables in quality system.....	635
C. TARCOLEA, G. DRAGOI, D. DRAGHICESCU and S. TICHKIEWITCH	
An approach to integrate safety at the design stage of numerically controlled woodworking machines	643
D. JOUFFROY, S. DEMOR, J. CICCOTELLI and P. MARTIN	
Virtual manufacturing : set up of a cooperative work in manufacturing.....	651
PH. DEPINCE, H. THOMAS, B. FURET, Y. GRATON and N. RAFII	

A FAST AND RELIABLE COST-ESTIMATION TOOL FOR HOT-FORGED PARTS.

M. BERLIOZ - P. MARIN - S. TICHKIEWITCH
*Laboratoire 3S, UJF INPG CNRS UMR 5521, Domaine Universitaire,
B.P. 53 - 38041 GRENOBLE CEDEX 9*

Abstract

This paper presents a fast cost-estimation procedure for the specific field of forging. In the first part, a description of the different available methods found in the literature and a particular company's estimation procedure are being set out. Then, tools already developed or being developed in our laboratory that could help designers in the different steps of a forging part design, are also presented. Indeed, previous forging steps have to be designed before estimating the production cost. The volume of material and the requisit energy to make the part have to be well defined. Nevertheless, the software's implementation of this method, which could be classified as a traditional approach used in the detailed design level, provides results in a few seconds.

1. Introduction

In the international marketplace, one of the industry's priorities is to be more reactive than its competitors. Nowadays, when the form of a new product has to be defined, most factories try to apply a new concept called "integrated design" [1], in which the design and the method offices work together. Indeed, approximately 80% of the final product cost is decided in the design stage, and it appears necessary to take into account the know-how of each production step to avoid mistakes. In that way, incompatibilities between the design and the method offices are avoided, time to market is decreased, quality of products is improved, and costs are reduced.

This paper deals particularly with cost-estimation in the specific field of forging. We describe, in the first chapter, different available methods to estimate costs and how a particular company proceeds to make an estimate. Then, we present several software which model each step that a hot-forged part passes through: COPEST, which deals with the transformation of a functional or machined shape representing the initial geometry, into a forgeable one; *Presto*, a preform design tool, because the transformation of a billet into a forged part is generally achieved in several steps; and *ForgeRond*, a fast simulation software which evaluates the forging load and energy required to make the part and in which a cost-estimation procedure was included. This set of tools could help the estimation office of forging companies, and the method office when successive steps have to be designed.

2. Cost-estimation: state of the art

For the continued success of a manufacturing enterprise, its cost-estimation have to be well performed, and its costing have to be accurate, to correctly determine the profitability of its various products. In the area of manufacturing, cost-estimation is the prediction of the expected cost of manufacturing a product before the actual production starts. It can be extremely harmful to an organisation: if the cost is overestimated, then the work can be lost to competitors; if the cost is underestimated, then the work will be done at loss, and a company has to make profits rather than losses [2]. Nowadays, one of the most important aspects of an industry is economics. Therefore, it is necessary to try to reduce production costs from the outset [3].

In practice, in the forging field the cost-estimation office makes hundreds of cost-estimations a month, and only three to five percent come back as orders. This very low result shows the necessity to achieve a cost-estimation tool that is fast and reliable. The current chapter of the article is sub-divided into three sections. The first one is a general method of cost-estimation based on [2]. The second one is a fast analysis of what exists in the literature for the forging process. The third paragraph is a description of the particular procedure carried out in the company observed.

2.1. GENERAL METHOD OF COST-ESTIMATION

Wierda proposed a classification system for cost estimations, according to the design level, *i.e.* on knowledge about the product* (Table 1).

Table 1. Classification for cost estimates from Wierda.

Level of design	Conceptual design	Preliminary design	Detailed design
Knowledge about the product	Materials and geometry are unknown	Materials and geometry are known	All information is known
Estimation method that could be used	<ul style="list-style-type: none"> • Factor method • Material cost method • Function method 	<ul style="list-style-type: none"> • Product comparison • Database calculation • Detailed cost function and/or parametric cost-estimation 	<ul style="list-style-type: none"> • Detailed cost-estimation • Traditional approach
Accuracy of methods	+30% -50%	-15% +30%	-5% +10%

In our case, we consider that cost-estimation of a forging part is carried out using all the information on the part and process, therefore in the detailed design level. The cost-estimation methods used for this stage are either a detailed cost function method (mathematical expression with constants and parameters derived for specific processes based upon size, alloy, weight...) or a traditional approach (for each step, cost of materials and operations are estimated, and testing, packaging, inspection, overheads, loss and yield factors, etc, are added). Forging competes with casting and/or machining in that the high tooling cost often limits the forming process to high volume. The major cost elements are the material costs (losses can be a significant amount of the total material), the direct expense costs (one of the largest expenses is the cost of the die) and the labour and overhead costs (which are very difficult to determine).

* paper from Wierda [12] cited in [2].

2.2. LITERATURE ANALYSIS

Firstly, a procedure based on a morphological shape of the part is described. This procedure was developed by W.A. Knight and C. Poli [4] in 1985 and was revised and simplified in 1992 by W.A. Knight [5]. The aim of the first method was to give a relative cost from a reference part, for configuration of different parts, instead of producing a detailed estimate for each of them. This approach was primarily used for comparing costs of different forging designs. The costs were relative to a reference forging, with a reference cost ratio for material costs (50%), operating costs (30%) and tooling costs (20%). According to the authors, two of the disadvantages of this method were the complex classification of parts, and an inconsistency with the production of big parts and unusual materials.

The revision made by Knight in 1992 takes into account the development of integrated design, and a cost-estimation is already available at the preliminary design level. This estimation is based on the main component costs of the process (material cost, facility cost, tool cost). This procedure was computerized and has the advantage of giving a cost quickly when simulations are performed, but it is still a method based on morphological shapes and cannot take into account local feature of the part.

Afterwards, an analysis of a traditional approach founded on Chamouard's heuristic and formalism [6] is made. From observations and experimental measurements, Chamouard produced a method that determines the cheapest hammer to form a part. When all characteristics of this hammer are determined, the energy expended to make the shape is known. Taking into account a relation between the energy expended on the hammer and the equivalent energy spent on a low press, or another machine, Chamouard can determine the machine able to produce the part and its production rate. The cost-estimation of a part is determined by hourly costs of machine and labour, material cost, and the cost for the time allocated to set up the tools. This method aims to integrate the knowledge of engineers, but one disadvantage is that the actual energy is not taken into account, nor are the dimensions of the initial billet.

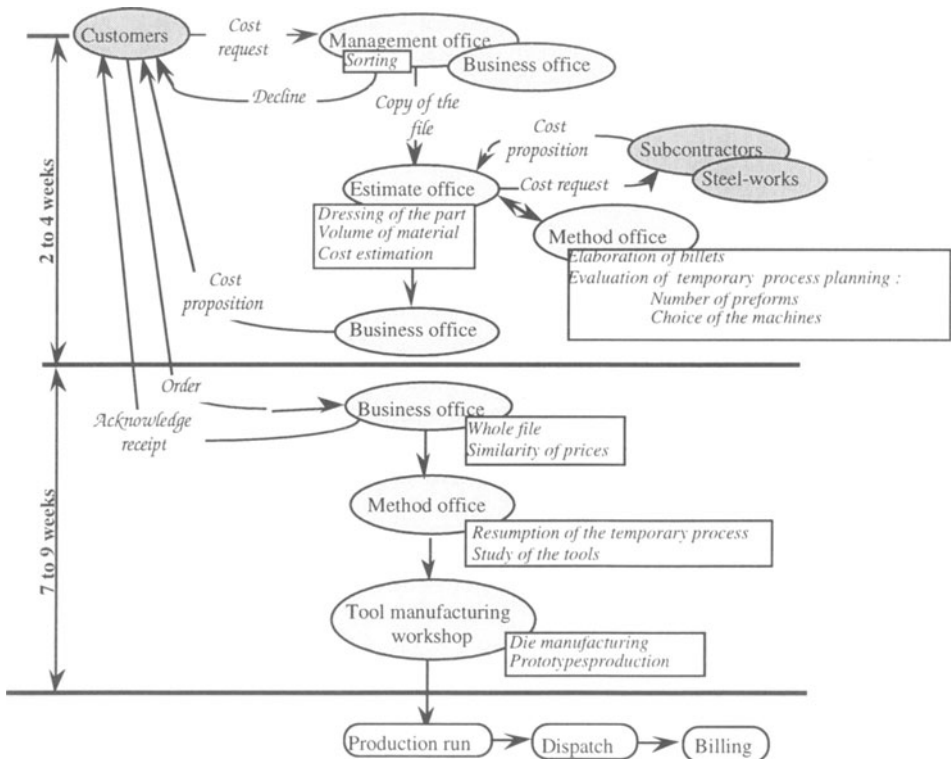
2.3. A PARTICULAR COMPANY PROCEDURE

This procedure was observed during a training period in this company. It is described in two parts : the first one is a cost-estimation from customer's letters and plans, the second one deals with what is done between the order to produce a part and the beginning of production. In forging, as perhaps in all industries, cost-estimation is a complex process and requires engineering skills to understand what happens in each step of production. To simplify the reading of the next paragraph, the readers should report to the synoptic table presented in Figure 1.

Most of the time, the business office receives letters and plans of parts from customers. A preliminary sorting is carried out to reject unproducable parts for technological or other reasons. Then the file is given to the estimate office, where the part is dressed, and the volume of material needed is evaluated. Indeed, 20 to 30% of plans sent by customers are plans of machined products, and the forgers have to add specific die features (edge fillets, draft angles...) to make the part forgeable. In the other 70 to 80% of cases, parts are already transformed, but badly, *i.e.*, they were dressed by someone unfamiliar with the rules of the art or the means of production. In all cases, parts are dressed manually to fit the company's machine capacities. The volume of the part is

then known, dimensions of the flash land are evaluated, and this volume is added to the previous one. Volume losses due to shear loss, tonghold loss, scale loss, flash loss, etc. are also added. Once the total volume is determined, dimensions of the billet can be calculated, followed by the diameter of bars to be ordered. Information on the level of production, the material to use, and the weight of material is provided to a steel-works in order to obtain the material price. Afterwards, the file is given to the method office which elaborates how the billet is cut and heated, how many preforms are needed, which machine is to be used and what is its rate, and which subcontractors to contact. Taking into account the amount of parts to produce, a compromise has to be found between the cost of a detailed die or a more powerful press and post-machining of parts. In the observed company, the different steps of production are determined by a morphological codification that was developed after years of experience. When all the information is determined, the file goes back to the estimate office which assesses the different costs of producing the part. The material costs and production costs are finally added and the total cost is sent back to the customer. From receipt of letters and plans, it takes approximately 2 to 4 weeks to make this estimation.

Figure 1. Synoptic table of the cost estimation and time to production.



When the customer accepts the proposal cost and makes an order, the business office prepares the whole file, checks that estimate and order prices match and sends back a receipt of acknowledgement. The file is then passed to the method office. The last step

resumes the temporary process planning in order to design tools and draw up the final process planning by modifying the others one already studied. The forging dies can then be manufactured and the first prototypes produced. It is only at this point that the process and geometry of dies can be validated. The production of parts can begin; the process has taken 7 to 9 weeks since the order arrived.

One can conclude that the cost-estimation and the time to produce is very long for this company, and that it involves lots of people in many different offices. Furthermore the cost-estimation is based only on temporary process, *i.e.*, on non-valid geometry of successive dies, and the order is taken with a price which is never again modified. Thus it is essential for the estimate office to be right the first time.

3. Cost-estimation and other steps in forging design

The design of a hot-forging process involves the following steps: the transformation of a functional or machined shape into a forgeable one; the proposition of preforms if the part to be obtained is complex; the simulation that checks the filling of the part and gives the forging load and energy required to make the part; and then the cost-estimation of production. This chapter of the article is separated into four sections, one for each.

3.1. A DRESSING PART TOOL: COPEST

This tool was first developed ten years ago, and the software is now being industrialized. COPEST software adds specific die-forging features, such as edge fillets, draft angles or webs, that transform the machined part into a forgeable one. Parameter values for each feature depend on the part's forging type and on its material and geometrical characteristics.

This design tool is mainly based on Chamouard's expertise. One of COPEST's specific features is how it defines radii dimensions, in order to fill up the different radii at the same time, and how it calculates the forging load necessary to obtain the desired result. This model can be used to compute plane cross-sections selected from main flowing planes of 3D parts. Then other sections are studied step by step and COPEST finally proposes a set of dressed cross-sections which ensures the coherence of pressure distribution in the part. More details concerning this software can be found under reference [7].

3.2. A PREFORM DESIGN TOOL : *Presto*

Most of the time, billets are transformed into forged parts in several steps. Intermediate shapes are obtained either in free forging, or with preforming dies, according to the number of parts to produce. Indeed, dies are estimated to represent between 15 and 20% of the production cost of a hot forged part.

The number of intermediate shapes changes according to the geometry of the part to be produced. Generally, these intermediate shapes are drawn by skilled designers, who use rules-of-thumb elaborated during their careers. These empirical guidelines depend on the material used and the machine chosen. However, most of the time, 3 consecutive blows are needed to form a part: a flattening, a preforming and a finishing one. The main task of preform dies is to ensure a good distribution of material, so as to:

- fill the finition dies without any defects,
- minimise metal losses, *i.e.* generate a flash that is as small as possible,
- reduce die wear, *i.e.* minimise metal flow in the last die so as to extend its life-time.

Our study of designing preforms is broadly based on two basic forging:

- the volume of metal is equal between two shapes; the metal loss only occurs during heating and clipping,
- each preform is deduced from the form to be obtained at the next step: that is why the forging process is generally developed from the finishing dies to the billet size.

Our double goal is to improve the existing *ForgeRond* software, presented in the next paragraph, in order to allow it to accept all kinds of billets or shapes resulting from a first flattening, and also to develop a computer preforming tool, *-Presto-*. This tool will be called on whenever a part geometry is considered to be complex.

3.3. SIMULATION AND COST-ESTIMATION TOOL: *ForgeRond*

The *ForgeRond* application performs axisymmetrical-part forging simulation [8]. This tool is based on forger's know-how. The basic models are taken from Chamouard, and new models are proposed for step-by-step simulation and take into account thermal [9] and dynamic [10] behaviour. These models describe pressure equilibrium at the interface between different sections of the shape (flash, extrusion cavities, etc.).

Up until now, most simulation software has been based on Finite Element Analysis and appears to be expensive in terms of computation time required to obtain the whole set of information from which a small part is needed in the pre-design stage. A simulation with *ForgeRond* provides information such as the evolution of the forging load and energy expended by the press, and such as the evolution of the shape during the deformation process, in only a few seconds.

In *ForgeRond*, since we assume a quasi-static evolution and negligible speeds of metal flow and deformation, results provided by simulation correlate with a slow press. Then, it is easy to obtain the global deformation energy E with the forging load F and the corresponding displacement of the moving die ΔH :

$$E = \sum \Delta E \quad \text{with} \quad \Delta E = F * \Delta H$$

The energy resulting from a simulation with *ForgeRond* and Chamouard's energy-equivalence allow us to estimate the energy whatever the machine used, for instance, a hammer. For a hammer, if several blows are needed, the kinetic energy is given by :

$$E = M_p * g * H * N$$

E : Kinetic energy (J)

M_p : falling mass (kg)

$g = 9.81 \text{ m.s}^{-2}$

H : falling height (m)

N : number of blows

The different coefficients M_p , H and N can be set to reduce global cost. Then total cost (C_{TP}) is evaluated in the following equation. Time allocated to set up tools (T_M),

hourly cost of labour (C_{HMO}), hourly cost of machine (C_{HP}), time of production (T_R), material cost (C_{MP}) and the size of production run (Q) are previously determined.

$$C_{TP} = C_{MP} + (1/Q)[(T_M + T_R) * (C_{HMO} + C_{HP})]$$

This cost-estimation method has been implemented in *ForgeRond* software [11]. Results from the estimate can now be obtained in a few seconds. This short time allows the user to look for economic solutions step by step, by shifting some parameters. Nevertheless, it's a basic tool for forgers: indeed management costs such as administration overheads, firm margins, etc, are not the direct concern of software developers. On the other hand, costs generated by complementary operations should be added (heating, die cost, flash removal, etc).

3.4. COST-ESTIMATION : EXAMPLE

The results presented in this paragraph involve the part in Figure 2.

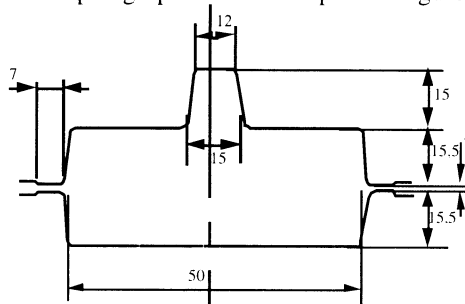


Figure 2. Axisymmetrical part with a central extrusion cavity.

Imagine that an order of 1000 parts has been taken, and that the available machine is a hammer whose characteristics are $M_p=114\text{kg}$, $H=1.2\text{m}$, rate $R=800$ parts/hour.

For a billet, which dimensions are $H=42.5\text{mm}$ and $D=44.8\text{mm}$, a simulation with *ForgeRond* (assuming a quasi-static evolution) gives the following result :

$$E_p = 1.91 \text{ kJ}$$

Energy-equivalence table from Chamouard gives the ratio $R=1.92$ for the hammer. Then, energy needed on this hammer is :

$$E_h = 1.91 * 1.92 = 3.67 \text{ kJ}$$

It is possible to determine the theoretical number of blows:

$$N = 3670 / (114 * 9.81 * 1.2) = 2.73 \text{ then } 3 \text{ blows}$$

According to the machine output, such a hammer would give the following energy distribution:

$$1\text{st blow } (114 * 9.81 * 1.2) * 0.670 = 899.15 \text{ J}$$

$$2\text{nd blow } (114 * 9.81 * 1.2) * 0.663 = 889.75 \text{ J}$$

$$3\text{rd blow } (114 * 9.81 * 1.2) * 0.656 = 880.36 \text{ J}$$

Total energy = 2669.26J, less than the required energy, so two successive blows should be added :

$$4\text{th blow } (114 * 9.81 * 1.2) * 0.649 = 870.96 \text{ J}$$

$$5\text{th blow } (114 * 9.81 * 1.2) * 0.642 = 861.57 \text{ J}$$

For the available hammer, characteristics are:

- time allocated to set up tools : $T_M = 0.5$ hour
- time of fabrication : $T_R = 6.25$ hour
- labour cost : $C_{HMO} = 52$ F/Hour
- machine cost : $C_{HP} = 116$ F/hour

The last information to be determined is the total cost of material :

$$C_{MP} = 0.92 \text{ F/part}$$

and then the total cost of the part :

$$C_{TP} = C_{MP} + (1/Q)[(T_M + T_R) * (C_{HMO} + C_{HP})] = 2.05 \text{ F}$$

4. Conclusion

In the company that has been observed, only three to five percent of cost estimates come back as orders and it commonly takes two to four weeks to establish a cost estimate, taking into account the times of subcontractor's answers. If an order is accepted then it takes about seven to nine extra weeks before the production begins. Because of this relatively long time, it appears to be important to develop tools that help the different offices implied in a cost-estimation, so as to speed up answers from forging companies.

5. References

1. TICHKIEWITCH, S., TIGER, H. : Ingénierie simultanée dans la conception de produits *La modélisation en entreprise, CIM-OSA et ingénierie simultanée, Chap.7.* 2-86601-419-7 © Hermès, Paris, 1994.
2. CREESE, R.C., ADITHAN, M., PABLA, B.S. : *Estimating and Costing for the Metal Manufacturing Industries* . Marcel Dekker, Inc. (1992).
3. GEIGER, T.S., DILTS, D.M. : Automated design-to-cost : integrating costing into the design decision *Computer-Aided Design* **28** (1996), 423-438.
4. KNIGHT, W.A., POLI, C. : A systematic approach to forging design *Machine Design* (1985).
5. KNIGHT, W.A. : Simplified early cost-estimating for hot forged parts *Int. J. Adv. Manuf. Technol.* **7** (1992), 159-167.
6. CHAMOUARD, A. : *Devis de fabrication par estampage sur presse et marteau-pilon. Choix de l'engin approprié* Adetief (1976).
7. BOUJUT, J.F., TICHKIEWITCH, S. : A step toward automatic dressing of a three dimensional stamped parts *Journal of Material Processing Technology* **34** (1992), 163-171.
8. MARIN, P., TICHKIEWITCH, S. : A step in the development of ForgeRond, a fast stamping simulation tool *Advances in Material and Processing Technologies'95*, International Conference, Dublin, 8-12 August 95, 848-856.
9. MARIN, P., LE, C., TICHKIEWITCH, S. : Taking into account thermal effects in ForgeRond, a fast hot-forging simulation tool *Advanced Technology of plasticity'96*, Proc. of the 5th ICTP, October 96, **1**, 475-478.
10. BONNAVAND, F. : Prise en compte de la viscosité dans ForgeRond : logiciel de simulation rapide d'estampage destiné à la conception intégrée *DEA de Mécanique, INPG*, (1997).
11. BERLIOZ, M. : Evaluation du coût de réalisation d'une pièce estampée *DEA de Mécanique, INPG*, (1996).
12. WIERDA, L. F. : Detailed Cost-estimation Concept and Database Structure for DIDACOE *Report IM K177, Delft University of Technology, The Netherlands*, p. 122, August 1988.

COST-BASED RANKING FOR MANUFACTURING PROCESS SELECTION

A. M. K. ESAWI and M. F. ASHBY

Engineering Design Centre

University of Cambridge

Department of Engineering

Trumpington Street

Cambridge CB2 1PZ, United Kingdom

Abstract

Manufacturing process selection involves two steps. The first involves the *screening* of all available processes to determine whether they are technically capable of making the design; the second involves the *ranking* of those which are successful, using economic criteria. The ranking step requires techniques of cost-estimation. In seeking to achieve this, two problems are encountered. The first: that the design is still in an early stage at which little information is available; the second: that conventional cost-estimation techniques require detailed information and cannot easily be applied to widely diverse processes. A simple approach for this problem is presented. It is based on the idea of a resource-consumption cost model, applicable early in the design process. The system is described and a case study is used to demonstrate how it works.

1. Background

In the early stages of designing a component, the designer is faced with many decisions among which are the selection of the most appropriate *material*, and the most appropriate *manufacturing route* - meaning one that is capable of forming the selected material to the desired shape *economically*. Both have a major impact on performance and manufacturing cost. Computer-aided design tools which help with geometry, manufacture and assembly already exist, and continue to develop. Process selection, however, has received less attention. In this paper, a systematic procedure for process selection is presented. The procedure has been implemented in the *CMS* software (1995), the features of which are illustrated below.

2. The Design Process

Typically, a product consists of *assemblies* and *components*. For example, the total system of a *car* consists of a set of assemblies, among them the *engine*, incorporating an *ignition system*, of which one unit is the *spark plug*. The spark plug, in turn is made up

of individual components such as the *body shell*, the *insulator*, the *electrodes*, etc. Process selection takes place at the component level.

It is conventional (and helpful) to think of the design process as starting with a market need and proceeding through three stages: the conceptual stage, the embodiment stage and the detailed stage. The output of these stages leads to a set of specifications and constraints which dictate how the product should be made. In the conceptual stage of design, little information is available and few constraints have been specified so all possible manufacturing processes should be considered. As the design progresses to the embodiment stage, more information on the product become available and a set of constraints are specified. These are used to determine a subset of processes which are capable of making the product. Finally, as the design reaches its final stages and becomes detailed enough to allow cost evaluation, a single process can be selected. It is helpful at each stage to know the potential processes since this influences the next level of design decisions.

3. Cost Estimating Methods

Cost estimating techniques are of several types, each serving a different stage of the design. In *Function Costing* (Wierda, 1988 and French, 1992) empirical formulae are developed for the cost of a *unit of function* - energy conversion, for example, or pumping, or control. The cost of each sub-system (performing one function) can be estimated from historical data on similar sub-systems or functional groups. These costs are then added together to give the total system costs. *Macro-scaling or "Top-Down"* estimation (Wierda, 1988 and Meisl, 1988) utilises the observation that, for families of related assemblies, the final cost is, very approximately, proportional to the weight, or (better) the cost of the material of which the assembly is made, allowing an approximate scaling for a new product. *The Meso-scaling, or Cost-scaling Method* (Allen and Swift, 1990) adds precision by scaling past costs to new requirements, allowing for change of material, for design features such as size, complexity and precision, and for production information such as batch size; it works well for families of related products. *The Micro-scaling, or "Bottom-Up"* approach starts from a set of engineering drawings for a component of an assembly, and calculates the cost of each operation involved in its manufacture, shaping and finishing. The method requires an intimately detailed description of the manufacturing process and is not a practical approach for the broad, early-stage estimates we seek here, for obvious reasons.

4. The CMS Selection Method

The *CMS* Process Selector makes use of a database which at present contains 125 processes. Each record contains data for the *attributes* of the process: physical attributes such as the materials it can handle, the tolerance, size range, section-thickness and complexity of shape; and economic attributes such as capital cost, tooling cost, and rate of production. The starting point is the idea that all processes are potential candidates until shown otherwise (Figure 1). A short-list of candidates is extracted in two steps.

The first, *screening*, eliminates processes which cannot meet the design specification. The second, *ranking*, orders the survivors by economic criteria.

4.1 SCREENING

A typical 3-stage screening takes the form of Figure 1. It shows three bar-charts, on each of which a numeric property (for example, tolerance, size) is plotted for a selected class property* (process class, material class, or shape class). The axes are chosen by the user depending on the design constraints. The processes are sorted in order of ascending value of the numeric property, which is plotted as a bar to show its range.

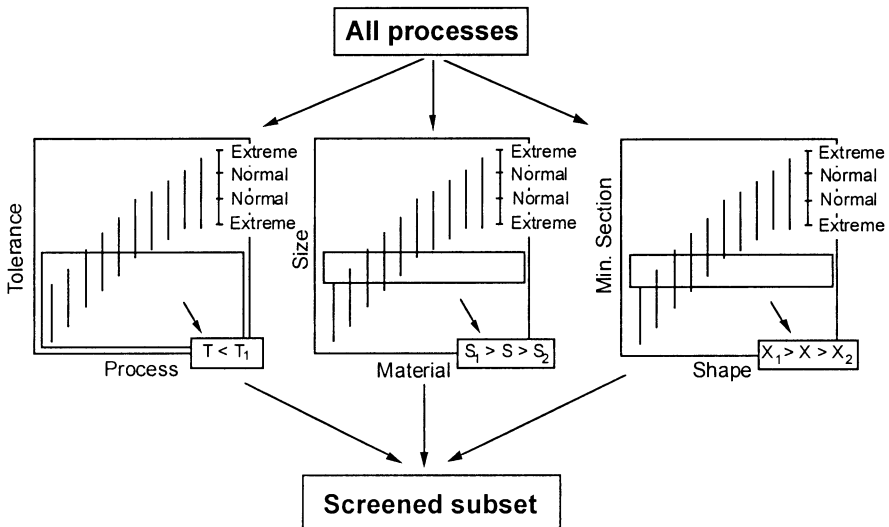


Figure 1. Stage 1: SCREENING.

The selection is made by placing a selection box onto each chart, identifying the range of tolerance, size, and so forth, specified by the design. The effect is to eliminate the processes which cannot meet the specifications.

4.2 RANKING

The second step (Figure 2) is that of *ranking*, using an estimate for the cost, C , of the product as a ranking-measure. The method uses a resource consumption approach, estimating the consumption of primary resources per unit of output and multiplying these by a cost per resource unit (Table 1). Since all processes consume resources, the method can be applied equally well to very diverse shaping methods.

* The current selector divides materials into 9 classes and shapes into 24 categories. Processes are also divided into classes: *primary*, *secondary*, and *tertiary*; with subclasses under each (Esawi and Ashby, 1997).

Table 1: Primary Resources associated with production.

Resource	Symbol	Unit
Materials and consumables	C_m	\$/kg
Capital: cost of equipment	C_c	\$
Cost of tooling	C_T	\$
Energy: power	\dot{P}	kW
cost of energy	C_E	\$/kW.hr
Time: overhead rate	\dot{C}_L	\$/hr
Space: area	A	m ²
cost of space	\dot{C}_S	\$/m ² .yr

The resulting cost-equation takes the form:

$$C = \left[\frac{mC_m}{1-f} + C_w \right] + \left[\frac{C_T}{n} \right] + \left[\frac{\dot{C}_L}{\dot{n}} \right] + \left[\frac{\dot{P}C_E}{\dot{n}} \right] + \left[\frac{A\dot{C}_S}{\dot{n}} \right] \quad (1)$$

Here C_m is the cost of the material of which it is made, m is the mass/unit of product in kg, f is the fraction of material which appears as scrap, C_w is the cost of the other consumables, C_E that of energy and \dot{C}_S that of the space associated with manufacture of the product. C_T is the cost of tooling, n the batch size (that is, the production volume), \dot{C}_L the overhead rate, and \dot{n} the rate of production. Tooling has a finite life; it may be necessary to replace it during a production run. We therefore expand the second term (the one describing the tooling costs) as follows

$$\left[\frac{C_T}{n} \right] = \left[\frac{C_{T0}}{n} \left(1 + \frac{n}{n_t} \right) \right] \quad (2)$$

in which C_{T0} is the cost of one set of tooling and n_t is the number of units which can be made before the tooling requires replacement. The tooling cost, C_{T0} includes the cost of jigs and fixtures which are uniquely associated with the manufacture of the component, but it does not include the capital cost of the equipment or plant itself. That is assigned to the overhead-rate, \dot{C}_L , which we write as

$$\left[\frac{\dot{C}_L}{\dot{n}} \right] = \left[\frac{1}{\dot{n}} \left(\dot{C}_{Lo} + \frac{C_c}{t_c L} \right) \right] \quad (3)$$

where \dot{C}_{L0} is the basic-overhead rate, C_c is the capital cost of the equipment used to make the component and the interest on that cost, t_c is the capital write-off time, and L is the load factor (the fraction of time over which the equipment is productively used).

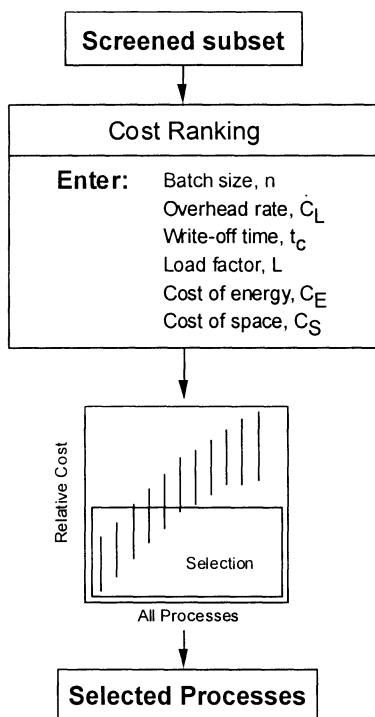


Figure 2. Stage 2: RANKING.

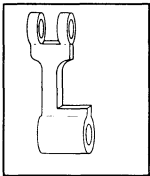
The economic attributes of each process include data for C_c , f , C_{T0} , n_t , \dot{P} and A . These are stored in the database for every process. The remaining parameters – batch size, n , the basic overhead rate, \dot{C}_{L0} , the capital write-off time, t_c , load factor, L , cost of energy, C_E and cost of space, \dot{C}_S – are entered by the user. In the present implementation, a *relative cost* is then calculated by dividing the cost estimate for each process, calculated from equation (1), by that for the cheapest one. With this information a *relative cost* bar-chart is constructed in which processes are plotted in order of increasing relative cost, as suggested in Figure 2. The order depends, of course, on the process attributes, but, importantly, it depends also on the values of the user-selected parameters, most significantly on batch size and capital write-off time. Processes offering the lowest cost are selected by superimposing a selection box onto the bar-chart, as before.

We recognise that accurate cost-estimation requires much more information than this. But accurate costing is not our aim. The software tool described here is designed

to help in the early stages of process selection, and to prompt the user not to overlook alternatives. At this stage the aim of an approximate cost-estimation is simply that of ranking. The case study that follows illustrates the method.

5. Case Study: Connecting Rod

This component, shown in Figure 3, is made of steel. Its weight is in the range 0.5 - 1 kg, and it has a minimum thickness of 25 mm. The shape can be described as a 3-D solid shape with transverse features. The designer specifies a precision of 0.25 mm. It is desired to make 10 connecting rods. Which process should be used? It is also desirable to investigate if the same process is also competitive if the batch size is increased to 1000.



Connecting rod: design requirements	
Material Class: <i>ferrous</i>	Size: <i>0.5 - 1 kg</i>
Process Class: <i>Primary, discrete</i>	Min. Section: <i>25 mm</i>
Shape Class: <i>3-D-solid-trans features</i>	Precision: <i>0.25 mm</i>
Batch Size: <i>10 or 1,000</i>	

Figure 3. The connecting rod and its design requirements.

Figure 4 shows a typical selection stage. It is a bar chart of tolerance against shape class selecting “3-D-solid-transverse features” from the shape class menu: it is this which best describes the shape of the connecting rod. The selection box imposes the tolerance requirement of 0.25 mm or better. Two more stages follow* (not shown because of space restrictions); they limit the selection to processes which (a) can shape ferrous metals; (b) can cope with the size of the connecting rod; (c) are discrete (batch-processes); and (d) are able to make the section thickness required here.

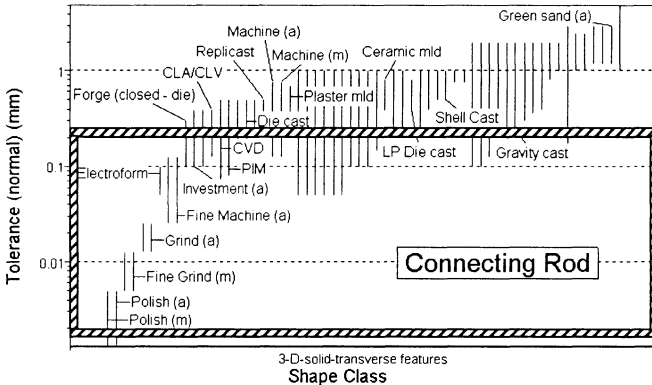


Figure 4. A chart of tolerance against shape class.

* See (Esa'wi and Ashby, 1997)

Several processes passed all the previous selection stages. They are listed in Table 2. All of them are technically capable of making the connecting rod. However, it remains to investigate which would be the cheapest process for such a component. This obviously depends on batch size. Two batch sizes were selected and a cost-based ranking step is applied. In Figure 5, a batch size of 10 units was chosen and the cost of making the connecting rod using all discrete processes in the database was calculated. The processes which passed all the previous selection stages are labelled. The same chart is plotted again in Figure 6 - this time for a batch size of 1000.

Table 2: Processes for the connecting rod.

Manual machining Automated machining Gravity casting	Investment casting Replicast Closed-die forging
--	---

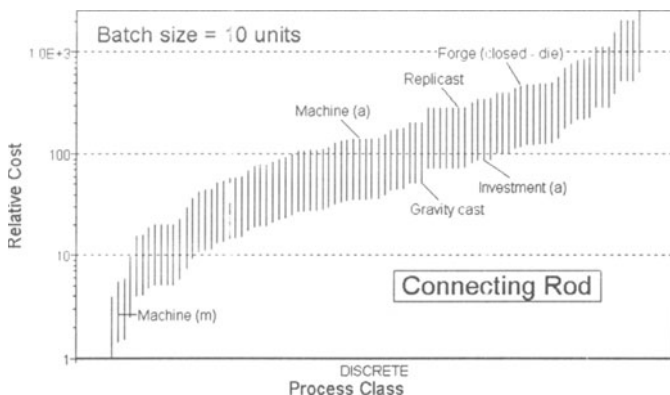


Figure 5. A chart of relative cost against process class (for 10 connecting rods).

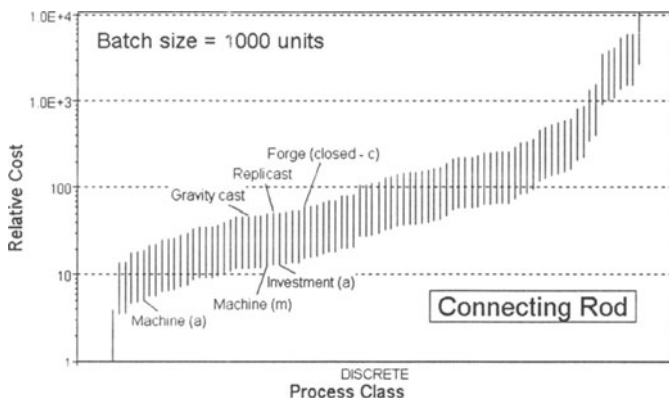


Figure 6. A chart of relative cost against process class (for 1000 connecting rods).

The cheapest process depends on the batch size. According to our cost-based ranking, the most suitable for making a batch size of 10 is *manual machining*. An alternative is *automated machining* - though more expensive for such a small batch size. This is because neither process requires a mould to be made (as for the casting and forging processes). For a batch size of 1000, *automated machining* becomes the most competitive process, followed by *gravity die-casting*.

6. Summary and Conclusions

The designer, in considering alternative choices of manufacturing-process routes for a given component, wishes to rank options by their cost. The cost must be arrived at by a technique which is applicable to all the options - that is, it should be applicable to any shape made of any material, by any process. With this breadth of scope the estimate cannot be accurate - indeed it may be only of the most approximate kind. But the goal here is that of *ranking*; and for ranking purposes an approximate estimate is good enough. Realistically, the function of the broad selector described here is to provide guidance in the early stage of design when material and process route are first under consideration; to prompt the user so that potential process routes are not overlooked; and to provide a brief description of the process and its attributes quickly and intelligibly. This, we conclude from our study, is feasible.

7. Acknowledgements

This work has been supported by the EPSRC under a research grant to the Engineering Design Centre, Engineering Department, Cambridge, UK, and by the generosity of the Körber foundation through the award of the European Prize for Science. It is a pleasure to acknowledge numerous helpful discussions with Ms Elicia Maine and Dr. David Cebon.

8. References

- Allen, A. J. and Swift, K. G. (1990) Manufacturing Process Selection and Costing, *Proceedings of the IMechE Part B - Journal of Engineering Manufacture*, **204**, 143-148.
- Ashby, M. F. (1992) *Materials Selection in Mechanical Design*, Butterworth Heinemann, London, UK.
- CMS Software, Granta Design Limited, Trumpington Mews, 40B High Street, Trumpington, Cambridge CB2 2LS, UK, 1995.
- Esawi, A. M. K. (1994) "*Systematic Process Selection in Mechanical Design*", Ph.D. thesis, Cambridge University Engineering Department, UK.
- Esawi, A. M. K. and Ashby, M. F. (1997) Computer-Based Selection of Manufacturing Processes, Cambridge University Engineering Department, Report No. TR50.
- French, M. J. Private communication, 1992.
- Meisl, C. J. (1988) Techniques for Cost-estimation in Early Program Phases, *Engineering Costs and Production Economics*, **14**, 95-106.
- Wierda, L. S. (1988) Production Cost-estimation by the Designer, *Engineering Costs and Production Economics*, **13**, 189-198.

ANALYTICAL STUDY OF MULTI-AGENT ORIENTED MANUFACTURING DESIGN

V. PATRITI*, K. SCHÄFER**, P. CHARPENTIER*, P. MARTIN**

*CRAN (Centre de Recherche en Automatique de Nancy),
Université Henri Poincaré, BP 239, F-54506 Vandœuvre Cedex, France
{vincent.patriti, patrick.charpentier}@cran.u-nancy.fr

**ENSAM Metz, 4 rue A. Fresnel, F-57070 Metz, France
{karin, patrick.martin}@metz.ensam.fr

Abstract

This research presents an analytical model of agent oriented manufacturing systems based on the notion of reliability. We use that model to study the differences between the domains of agent oriented manufacturing: workshop manufacturing and machine tool manufacturing. We examine representative examples of these domains and show that the usual hypothesis of autonomy is valid in the workshop, but not in the machine tool domain.

1. Introduction

The inherent limitations of classical centralised control architectures caused the apparition of agent oriented control paradigms. Multi-Agent [FER.95], Holonic Manufacturing [CHR.94], Heterarchical [HAT.85] and Bionic [OKI.93] Systems try to palliate the poor performance of traditional control system in very dynamic environments [DUF.87] and their difficulties with unforeseen modifications [DIL.91]. All these paradigms participate in **agent-oriented manufacturing**.

It is outside the scope of this paper to analyse the differences between these paradigms. But although these approaches are mainly used for the design of the workshop level control architecture, they propose to apply the same concepts to the design of the machine level control architecture [CHR.94], [OKI.93]. Some work has already been done with CNC controllers [TAN.95], [OVE.96], [PAT.98] and robot control [REG.95].

Fault tolerance appears to be the most important feature of agent oriented manufacturing [HAT.85]. This is obtained through full local **autonomy** [DIL.91]. Agents never make the assumption, that the other agents are operational. This gives the overall system superior fault tolerance. Not only are the agents waiting for failure, but if it happens, they try to find alternatives. But machines-tools and workshops have

specificity. Are machine tool and workshop agents **really** autonomous? In this paper we will try to validate the hypothesis, that the same ideas in multi-agent design cannot be applied without modifications to the different levels of the manufacturing process.

2. A Model of Multi-Agent Manufacturing Systems

The aim of this work is not to give the definitive solution to the questions of the design of multi-agent manufacturing systems, but to propose a possible approach with clear limits. So, we will try to clarify each step of the demonstration. The first one is the model for the basic elements of the manufacturing system:

A manufacturing system is composed of both a control system and an operational system. The operational system transforms, transports and stocks the parts, receives orders from the control system and sends back information. The elements of the operational system will be named **components**. With an agent oriented approach, the basic element of the control system is called **agent**. We suppose that:

- Each agent controls one or more components, but the control of one component cannot be shared among several agents.
- Each component or agent is defined with a state variable which equals 1, if the element is functional, and 0, if the element is not functional.

Although a degraded behaviour of the agents is not considered possible, the degraded behaviour of the system is possible with the re-organisation of the agents.

2.1. FORMAL DEFINITION

Let the 3-tuple S be the manufacturing system

$$S = \langle C, A, \Phi \rangle, \quad (1)$$

with $C = \{C_{x,y}\}$ being the set of the physical components and $\{c_{x,y}\}$ the corresponding set of state variables, $A = \{A_1, \dots, A_n\}$ being the set of the control agents and $\{a_1, \dots, a_n\}$ the corresponding set of the state variables, and Φ representing the relationships between the agents. An agent A_i controls k_i components $\{C_{i,1}, \dots, C_{i,k_i}\}$. If any of these components break down, the agent is not considered operational. The state of an agent A_i is then represented by:

$$a_i = \left(\prod_{j=1}^{j=k_i} c_{i,j} \right) \cdot \Phi_i(a_1, \dots, a_n) = \left(\prod_{j=1}^{j=k_i} c_{i,j} \right) \cdot \Phi_i(a). \quad (2)$$

$a_i = 1$ if the agent is operational.

$a_i = 0$ if the agent is not operational.

The function Φ_i is the structural function that expresses the local relationship between the agents of the system and agent A_i :

$\Phi_i(a) = 1$ if the agents needed by A_i are operational.

$\Phi_i(a) = 0$ if the agents needed by A_i are not operational.

The aim of this function is to characterise the state of the agent according to the state of the other agents. The function Φ_i is a binary model of the interaction between the agent A_i and the other agents. Φ_i can be derived from an extended reliability block diagram [VIL.88] of the system integrating both agents and associated components.

This model shows the effect of the agent oriented control system on the operational system. Although we are going to use it for a simple demonstration, it can be used for agent oriented control system design.

3. A Model for Fault Tolerance

There are a lot of definitions of the concept of autonomy. From an agent oriented manufacturing point of view it means, that the agents should be able to function when one or more of the other agents malfunction [DIL.91]. Our aim is to formally quantify autonomy for different levels of the manufacturing process. To reach that aim, we use the theory of probability and define the **operational probability** of an agent.

3.1. OPERATIONAL PROBABILITY

The reliability of a system is generally defined as the probability that the system functions [BON95]. If the state of the system can be defined with a structure function $\psi(x)$ such as

$\psi(x) = 1$ if the system is operational

$\psi(x) = 0$ if the system is not operational,

then the global reliability R of the system is the probability that this function equals to 1:

$$R = P(\psi(x) = 1). \quad (3)$$

The reliability $R_{i,j}$ of a component $C_{i,j}$ is then equal to:

$$R_{i,j} = P(c_{i,j} = 1). \quad (4)$$

This formalisation can be extended to define an **operational probability** of an agent A_i :

$$P(a_i = 1) = P\left(\left(\prod_{j=1}^{j=ki} c_{i,j}\right) \cdot \Phi_i(a) = 1\right) \quad (5)$$

Based on the study of the **process plan** we can define the global function of the system $\psi(a)$. The reliability of the global system including agents and their components is then defined as:

$$R = P(\psi(a_1, \dots, a_n) = 1) = P(\psi(a) = 1) \quad (6)$$

3.2. AUTONOMY

We based the definition of the autonomy of an agent on the probability theory given by [HAR.96].

With $P(X)$, i. e. the probability of the event X , the **stochastic independence** of two collections of events $\{E_i\}$ and $\{F_j\}$ is defined as:

$$\forall(i, j) P(E_i \cap F_j) = P(E_i) \times P(F_j) \quad (7)$$

These definitions allow us to formally define **agent autonomy**:

If the operational probability of all the agents of A are stochastically independent then the agents of A will be considered as autonomous.

For a control system $A = \{A_1, \dots, A_n\}$, the state of an agent A_i is defined by the variable a_i , with $a_i = 1$, if component A_i is operational, and $a_i = 0$ otherwise. The agents of A are considered as autonomous if :

$$P\left(\prod_{i=1}^{i=n} (a_i = 1)\right) = \prod_{i=1}^{i=n} P(a_i = 1) \quad (8)$$

Up to now we have defined the autonomy of an agent. Now we will proceed with the implications of this definition in multi-agent workshops and machine tool systems.

4. Agent Autonomy in a Workshop

Most of the work done in agent oriented manufacturing takes the hypothesis of autonomy for granted. But is it always valid? This chapter tries to demonstrate the validity of the hypothesis.

4.1. HYPOTHESIS

The machine agents in a standard workshop can be considered as autonomous.

4.2. PROOF

We will try to prove this hypothesis for a general model of job shop manufacturing, namely a workshop consisting of M machine tools of type T and with a reliability r . The resulting extended reliability block diagram is shown in Fig. 1.

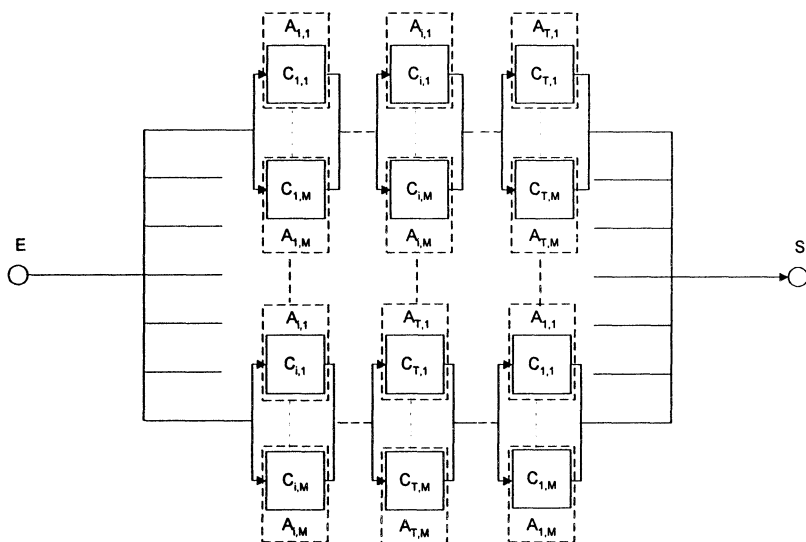


Fig. 1 : Extended reliability block diagram

In order to simplify, we make the following pessimistic suppositions:

- All types of machines participate in the manufacturing of one part.
- The number of different process plans is not defined.

Therefore, the workshop needs at least one machine of each type to be operational. Then, if we define the structural function Φ_i of the agents as the ability of the workshop to produce parts, the probability of functioning of the agent A_i is:

$$P(a_i = 1) = r \cdot \prod_{k=1}^{k=T-1} \left[1 - \prod_{j=1}^{j=M} (1-r) \right] \Leftrightarrow P(a_i = 1) = r \cdot [1 - (1-r)^M]^{T-1} \quad (9)$$

The probability of functioning of all the agents of the workshop is:

$$P\left(\prod_{i=1}^{i=M,T} (a_i = 1)\right) = r^{M \cdot T} \quad (10)$$

The agents are autonomous if:

$$P\left(\prod_{i=1}^{i=M,T} (a_i = 1)\right) = \prod_{i=1}^{i=M,T} P(a_i = 1) \Rightarrow [1 - (1-r)^M]^{M \cdot T(T-1)} \rightarrow 1 \quad (11)$$

Then the machine agents can be considered as autonomous. For example for $T = 2$ and $r = 0.95$, with $M = 2$ the value of (11) is already at 0.99.

Therefore, the autonomy decreases with an increase of the number of machine types involved in manufacturing. But we should keep in mind, that this is an approximation and other approaches are possible. For example, the same demonstration could be made with the other workshop functions (transport ...) with the same conclusion: a need for **redundancy**. In a job shop workshop this condition is easily

obtained. It led to the use of **autonomy** to improve the fault tolerance of this system type.

5. Agent Autonomy in a Machine Tool

Although we have shown, that the hypothesis of autonomy is generally valid for the workshop, nothing can yet be deduced for the machine tool level because of structural differences between machine and workshop. In fact, we claim that the autonomy hypothesis is not valid for all types of machine tools.

5.1. HYPOTHESIS

The agents composing an agent oriented machine tool system cannot be considered as autonomous.

5.2. PROOF

Here too, we can only verify or invalidate this hypothesis for a specific model. So we will try to prove it for a general machine tool model (Fig. 2). A general agent oriented machine tool could be composed of tools, parts, machining systems, transport systems, energy systems and fixture systems. Although we could practically have several instances of each of these sub-systems in a machine tool, the typical machine tool usually has only one energy, transport, fixture and machining system. The condition of high redundancy is not verified for all the machine tools. This has an important implication. The presence of a non redundant component needed by an agent A_i and controlled by an agent A_j led to:

$$\Phi_i = a_j \cdot f(a) \Rightarrow (a_i = 1 \Rightarrow a_j = 1) \Rightarrow P(a_i = 1 \wedge a_j = 1) = P(a_i = 1) \quad (12)$$

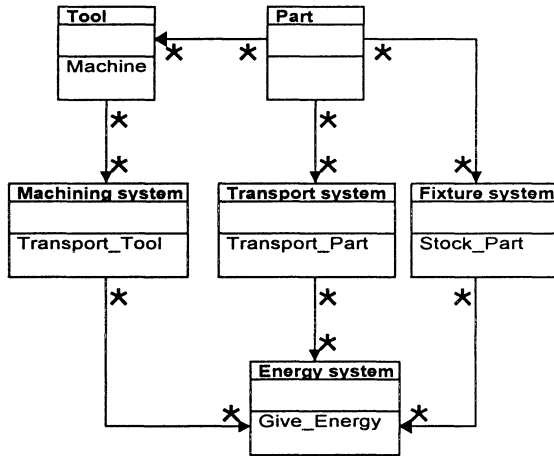


Fig. 2 : UML Model of a Machine Tool

Therefore, the hypothesis of the non-autonomy of the machine tool level agents could be considered invalid, if there is complete redundancy in the system. But this is not the usual case for most machine tools. Another solution would be to integrate the non-redundant components in the agents that need it. But this leads to a decrease in flexibility and eventually to the abandon of the agent oriented design paradigm. In fact, the only postulate would be:

The non redundant components have a very high reliability.

With that postulate, the agents would be, like the workshop machine agents, practically autonomous. But because a lot of machine tools have no redundancy for the energy, transport, fixture and machining sub-systems, we would restrict the failures to the tools and the parts, and an important part of the dynamic behaviour of the machine tool would then be occulted. Therefore, we propose to consider non-autonomy as the **specificity** of an agent oriented machine tool compared to the other levels of the manufacturing process.

6. Conclusion

The hypothesis of autonomy, taken for granted in the design of agent oriented manufacturing systems, cannot be used for all levels of the manufacturing process. We have shown, that the hypothesis is mainly tied to the redundancy of the system. Although this is generally the case at the level of the workshop, one cannot affirm its validity at the machine tool level. Therefore, the **low redundancy** and the **non-autonomy** of the agents could be considered as the specificity of the machine tool level.

However, another kind of redundancy could be found by breaking down the process plans [PAT.98]. Unfortunately, this leads to a very complex process planning,

while agent oriented design has other advantages. In fact, the use of agents accelerates the design of the control system. That leads to a faster reconfiguration of the manufacturing lines in case of a long term change in the production on the one hand, and to a faster new product design on the other hand. This is a more long-termed flexibility compared to the usual short-termed routing flexibility that we could expect from an agent oriented manufacturing system. After all, agent oriented manufacturing remains a possible solution to the problems of flexibility. However, the fault tolerance of the agents must be thought up differently, and sometimes the hypothesis of complete autonomy must be dropped.

7. References

- [BON95] J.L. Bon. "*Fiabilité des systèmes, méthodes mathématiques*", Masson, Paris, N° ISBN 2-225-84992-7, 1995.
- [CHR.94] J.H. Christensen. "*Holonic Manufacturing Systems : Initial Architecture And Standards Directions*", 1st European Conf. on Holonic Manufacturing Systems, Hannover, Germany, 1994.
- [DIL.91] D.M. Dilts. "*The Evolution of Control Architecture for Automated Control Systems*". Journal of Manufacturing Systems, Vol. 10, No 1, 1991, pp. 79-93.
- [DUF.87] N.A. Duffie, R.S. Piper. "*Non-Hierarchical Control of a Flexible Manufacturing Cell*", Robotics & Computer-Integrated Manufacturing, Vol. 3, No 2, 1987, pp. 175-179.
- [DUF.94] N.A. Duffie, V. Prabhu. "*Real-Time Distributed Scheduling of Heterarchical Manufacturing Systems*". Journal of Manufacturing Systems, Vol. 13, No 2, 1994, pp. 94-104.
- [FER.95] J. Ferber. "*Les systèmes multi-agents : Vers une intelligence collective*", InterEditions, Paris, 1995.
- [HAR.96] J. Hartong. "*Probabilités et statistiques : de l'intuition aux applications*", ISBN 2-84134-070-8, Eds. Diderot, arts et sciences, Paris, 1996.
- [HAT.85] J. Hatvany. "*Intelligence and Cooperation in Heterarchic Systems*". Robotics and Computer Integrated Manufacturing, Vol. 2, N° 2, 1985, pp. 101-104.
- [OKI.93] N. Okino. "*Bionic Manufacturing System*". Flexible Manufacturing System : Past - Present - Future, CIRP, Paris, 1993, pp. 73-95.
- [OVE.96] A. H. Overmars, D.J. Toncich. "Hybrid FMS control architectures based on holonic principles". International Journal of FMS, Vol. 8, No 3, July 1996, pp. 263-278.
- [PAT.98] V. Patriti. "Systèmes de pilotage auto-organisés et gammes distribuées : méthode de conception et application à une machine-outil". Thèse de l'UHP de Nancy I, 16 janvier 1998.
- [REG.95] S. Regnier, D. Duhaut. "*Une approche multi-agents pour la résolution de problèmes robotiques*". Troisième journées francophones sur l'IAD et les SMA, Saint bandolf, savoie, France, 15-17 March 1995, pp. 91-97.
- [TAN.95] P.I. Tanaya, J. Detand, J.P. Kruth. "*Holonic Machine Controller - a study and implementation of holonic behaviour to current NC controller*". Co-operation in Manufacturing : CIM at work, Conference Preprints, Kaatheuvel, The Netherlands, Aug 28-30, 1995, pp. 375-396.
- [VIL.88] A. Villemeur. "*Sûreté de fonctionnement des systèmes industriels*", collection de la direction des études et recherches d'EDF, ISSN 0399-4198, éditions Eyrolles, Paris, 1988.

DYNAMIC REPRESENTATION OF A MANUFACTURING PROCESS

B. ANSELMETTI, A. TOUMINE

*Laboratoire Universitaire de Recherche en Production
Automatisée,
ENS de Cachan, 61, Avenue du Président WILSON,
94235 Cachan Cedex.
email : anselm@lurpa.ens-cachan.fr*

Abstract

As a contribution to the future CAD/CAM systems, this paper proposes a procedure to take into account designer's and planner's requirements for the propagation of modifications during the industrialization step of a new product.

Every planner's choice is analyzed to define the constraints of acceptability linked to this choice. These constraints generate inequations between geometrical parameters of the workpiece. Manufacturing tolerancing is automatically calculated to detect conflicts caused by the modifications. The example presented has been obtained with CATIA and MATLAB.

1. Introduction

The industrialization of a new product requires many tests and many modifications of the product and of the manufacturing process simultaneously. The propagation of modifications is a problem because a lot of data are disturbed. The documentation cannot be easily updated. The agreement of collaborators needs many meetings.

Research works in Computer Aided Process Planning have given knowledge in manufacturing and methods for manufacturing process generation. At the present time, after every modification, CAPP systems have to analyze the part again. The generated process can be very different from the process that was originally validated.

A new approach for CAD CAM is proposed, given a common system to designers and to planners such as these by Nikos [1] and Britanik [2]. The part is represented with a parametric model. The planner describes the manufacturing process with the aid of a manufacturing expert system.

The aim of this research is the automatic propagation of modifications. The conflicts detected must be solved by the designer or the planner. This approach allows

to apply the manufacturing process of an old part to a similar new part. The application of a specific manufacturing method can then be ensured.

2. Project of A CAD/CAM architecture

The part to obtain is described with a parametric CAD model. The functional tolerancing imposed by the designer gives geometric constraints between part surfaces using the ISO tolerancing language. With maximum material conditions and least material conditions, the distances between the centers of the tolerance zones are not known.

The form feature recognition module decomposes the part into a lot of potential manufacturing features. The planner chooses the features and describes the manufacturing process, phase by phase. The ascending method uses machining features to define the intermediary shape of a workpiece and its raw shape [3].

The manufacturing process will be detailed day after day in function of choices of machines-tools, work holdings, cutting tools, cutting conditions. This problem is increased by concurrent engineering [4]. Every choice will be acceptable if most geometrical constraints are respected. So, many manufacturing constraints will be required by the planner, using surfaces of machining features. Each constraint requires geometrical relations added to an inequation system. The perennality of these requirements is given by dynamic rules. Limits are not defined by numeric values, but by functions of mechanical, physical or economical constraints.

Example in turning :

The offset for finishing operation depends on the cutting edge radius R_e and the working cutting edge angle K_r .

The minor cutting edge angle K_r' is greater than the angle of the cone of the workpiece.

Machining tolerancing can be calculated automatically [5]. Every functional or manufacturing constraint gives an inequation. The unknown values are the dimensions and the tolerances for manufacturing. The optimization maximizes the tolerances. In this step, all conflicts will be detected when there is no solution or when tolerances are too small regarding manufacturing process. In the normal situation, centered dimensions define the CAD model of the finished part and workpiece CAD models for each phase.

3. Simulation model

The machining dimensions are defined between active surfaces. In a phase, active surfaces are surfaces in contact with the set-up, surfaces machined in this phase and surfaces probed in this phase. The axis of two active surfaces in a phase is active in this phase. The intersection of two active surfaces is active. The gauge (of a cone) of an active surface is active.

Functional and manufacturing requirements must be transferred into machining dimensions for each phase. Each adjuster is in charge of producing workpieces according to these machining requirements.

Three rules give the following machining requirements. If C_{ij} is a dimension between the surfaces i and j :

- (i) Both surfaces i and j are active in the same phase: C_{ij} is the machining dimension.
- (ii) Surfaces i and j are not active in the same phase; so, the surfaces i and j are not machined in the same phase. If i is the last surface tooled and k the fixture surface in this phase, then surface i is set up with regard to k . The condition C_{ij} is decomposed in C_{ik} and a new requirement C_{kj} which has to be decomposed with the same method.
- (iii) One of the surfaces i or j is not an active surface (axis of symmetry or intersection). The requirement C_{ij} has to be decomposed into many conditions built upon active surfaces. For example, if i is the axis of both surfaces g and k , then $C_{ij} = (C_{gj} + C_{kj})/2$. Where C_{gj} and C_{kj} must be analyzed with the same method.

Manufacturing dimensions must be written with ISO language. Inequations are :

$$\sum V_{ij} + (\sum t_{if})/2 \leq C_{maxi}$$

i and j are two active surfaces of the workpiece. V_{ij} is the basic dimension, t_{ij} the location tolerance. Many requirements are looped. V_{ij} and t_{ij} are not independent.

To solve this problem, D.JIAN [6] proposes the tolerance sensitivity analysis. Here, the Δl model proposed by P.BOURDET [7] is used and developed in order to calculate V_{ij} and to take specific relations for NC machine tools into account [8].

The variables of the inequations are changed :

$$V_{ij} = L_j - L_i \text{ and } t_{ij} = \Delta l_i + \Delta l_j$$

The inequations become : $\sum L_j + (\sum \Delta l_i)/2 \leq C_{maxi}$.

Δl_i is the field which contains each surface of the machined workpieces.

L_i is the position of the axis of the field Δl_i with regard to a reference attached to the machine-tool.

The optimization of the tolerance minimizes the adjustment cost : $C = \sum k_i/\Delta l_i + C_m$ where k_i is a coefficient which depends on the manufacturing process. C_m is the cost of the raw material. If the system has no solution, conflicts can be detected accepting $\Delta l_i < 0$ and cost function $C = \sum e^{-50} \times \Delta l_i$. Surfaces with $\Delta l_i < 0$ are involved in conflicts between incompatible requirements. This method has been tested with the EXCEL solver (Microsoft) and with MATLAB toolbox.

4. Example

For A. Toumine's thesis, we programmed a prototype software in CATIA environment (Dassault Systèmes) and the optimization toolbox of MATLAB. This software had to validate the different interfaces of CATIA and test calculation procedures. After a description of the part geometry, of the process planning, of the

manufacturing requirements, the MATLAB solver optimizes all the manufacturing tolerances. So manufacturing dimensions can be obtained, along with the re-sizing of the part and the tool path in the CATIA environment.

This paragraph describes the different stages of the job. First, the designer must sketch the part with the catia sketcher. He draws the shape of the part with some geometrical constraints, such as perpendicularity or parallelism. Approximate values can be used for all dimensions. The planner draws the part in all the different phases of the process planning, from the raw shape to the part.

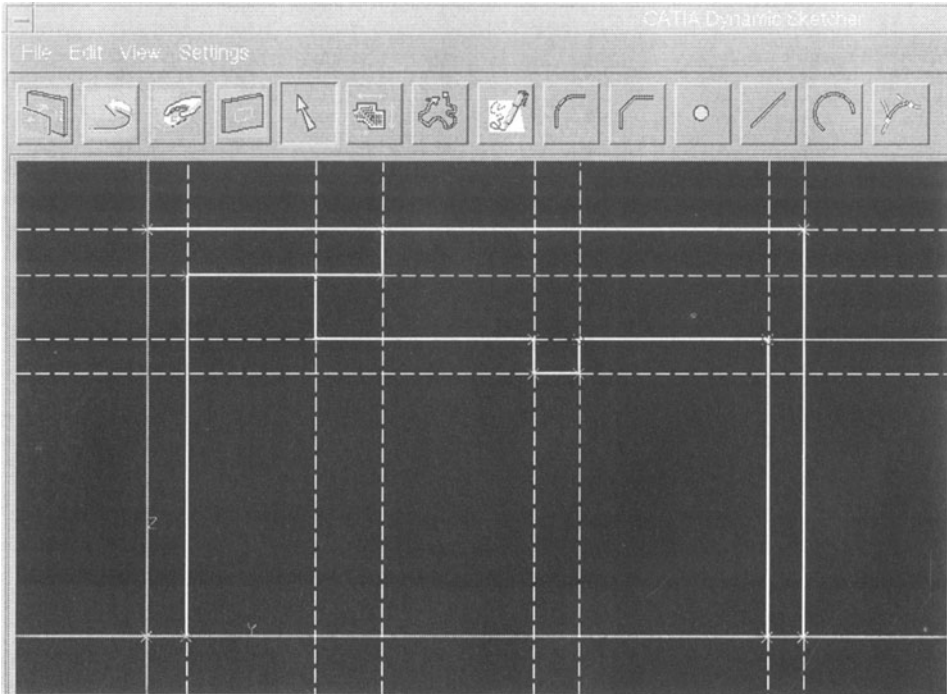


Figure 1. Drawing with sketcher

Specific IUA routines extract faces of the CAD model, particularly plans perpendicular to the directions studied. (IUA : Interactive User Applications, language of CATIA)

After this description stage, the operator have to prepare the parametrization of the part model with PARAM3D variational geometry module of CATIA. This new parametrization has to match the manufacturing dimensioning and the matrix representation in view of the MATLAB optimization.

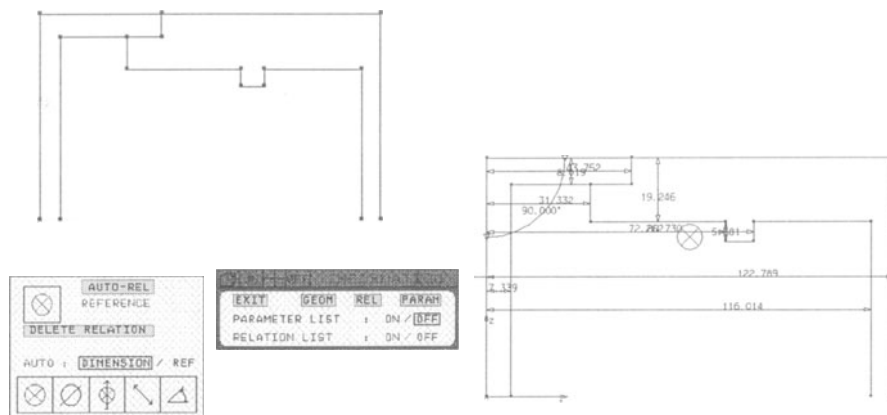


Figure 2. Parametrization

With IUA routines, the planner defines the process planning in CATIA environment. With the mouse, the operator indicates all the machining and fixture surfaces for each phase on the screen. The matrix (see table 1) contains the address of the face in CATIA, the distance between faces, the number of phase (10, 20 ...) and the type of face (1 = fixture face, 2 = machining face).

TABLE 1. Matrix of faces

	address	distance	Phase	type	Phase	type	Phase	type
11	10.0	.0000	10	1	.0	.0	.0	.0
12	34.0	7.3391	0	0	20	2.0	30	1.0
13	50.0	31.3323	0	0	.0	.0	30	2.0
14	46.0	43.7523	0	0	20	2.0	.0	.0
15	38.0	72.2619	0	0	.0	.0	30	2.0
16	26.0	80.7301	0	0	.0	.0	30	2.0
17	14.0	116.0143	0	0	.0	.0	30	2.0
18	22.0	122.7888	10	2	20	1.0	.0	.0

Then, in a different matrix (see table 2), the designer and the planner give the system all the functional and machining requirements, keeping the reference system, tolerances, mini or maxi dimensions between the surfaces.

TABLE 2. Condition matrix

first face	second face	valid	mini	valid	maxi
10 (11)	34 (12)	1	0.5	1	1.5
34 (12)	50 (13)	1	59.4	1	60.6
34 (12)	14 (17)	0	0	1	90
50 (13)	46 (14)	1	1	0	0
50 (13)	38 (15)	1	19.7	1	20.3
38 (15)	26 (16)	1	3	1	4
26 (16)	14 (17)	1	2	0	0
14 (17)	22 (18)	1	1	0	0

In table 2, columns one and two give the address of the two faces. Between these two elements, there is a minimum condition (column 4) and a maximum condition (column 6). 3 and 5 columns validate or not these conditions.

All the following steps are executed automatically by the software. With MATLAB, an algorithm determines and calculates all the machining dimensions. The convergence of the solver is compatible with a sketch drawing. The objective function and the constraints are obtained by an algorithm. The objective function is f, the constraint functions are g. CONSTR function in MATLAB optimizes this system.

$$f=1/x(9)+1/x(10)+1/x(11)+1/x(12)+1/x(13)+1/x(14)+1/x(15)+1/x(16)+1/x(17)+1/x(18)+1/x(19)+ x(8)-x(1);$$

$$g(1)=x(1);$$

$$g(2)=-x(2)+x(8)+x(10)/2+x(18)/2+0.5-x(8)+x(1)+x(16)/2+x(17)/2;$$

$$g(3)=59.4-x(3)+x(2)+x(11)/2+x(19)/2;$$

$$g(4)=-x(2)+x(3)+x(19)/2+x(11)/2+1-x(4)+x(2)+x(12)/2+x(10)/2;$$

$$g(5)=19.7-x(5)+x(3)+x(13)/2+x(11)/2;$$

$$g(6)=3-x(6)+x(5)+x(14)/2+x(13)/2;$$

$$g(7)=2-x(7)+x(6)+x(15)/2+x(14)/2;$$

$$g(8)=-x(2)+x(7)+x(19)/2+x(15)/2+1-x(8)+x(2)+x(18)/2+x(10)/2;$$

$$g(9)=x(2)-x(8)+x(10)/2+x(18)/2+1.5+x(8)-x(1)+x(16)/2+x(17)/2;$$

$$g(10)=-60.6+x(3)-x(2)+x(11)/2+x(19)/2;$$

$$g(11)=-90+x(7)-x(2)+x(15)/2+x(19)/2;$$

$$g(12)=-20.3+x(5)-x(3)+x(13)/2+x(11)/2;$$

$$g(13)=-4+x(6)-x(5)+x(14)/2+x(13)/2;$$

$$g(14)=0.001-x(9);$$

$$g(15)=0.001-x(10);$$

$$g(16)=0.001-x(11);$$

$$g(17)=0.001-x(12);$$

$$g(18)=0.001-x(13);$$

$$g(19)=0.001-x(14);$$

$$g(20)=0.001-x(15);$$

$$g(21)=0.001-x(16);$$

$$g(22)=0.001-x(17);$$

$$g(23)=0.001-x(18);$$

$$g(24)=0.001-x(19);$$

Figure 3. Objective function and constraints

The system can be initialized with initial values extracted from the part model (see table 3).

TABLE 3. Initialization matrix

L1	L2	L3	L4	L5	L6	L7	L8			
0	7.339	31.332	43.752	72.261	80.730	116.014	122.788			
ΔI1	ΔI2	ΔI3	ΔI4	ΔI5	ΔI6	ΔI7	ΔI8	Δr1	Δr2	Δr8
1	1	1	1	1	1	1	1	.5	.5	.5

The result of the optimization is in table 4.

TABLE 4. Result of the calculation

L1	L2	L3	L4	L5	L6	L7	L8
0	1.0000	61.0000	80.2542	81.0000	84.5000	87.3425	89.5274
ΔI1	ΔI2	ΔI3	ΔI4	ΔI5	ΔI6	ΔI7	ΔI8
612.803	0.248	0.305	4.844	0.294	0.705	0.979	0.252
Δr1	Δr2	Δr8					
0.251	0.247	0.894					

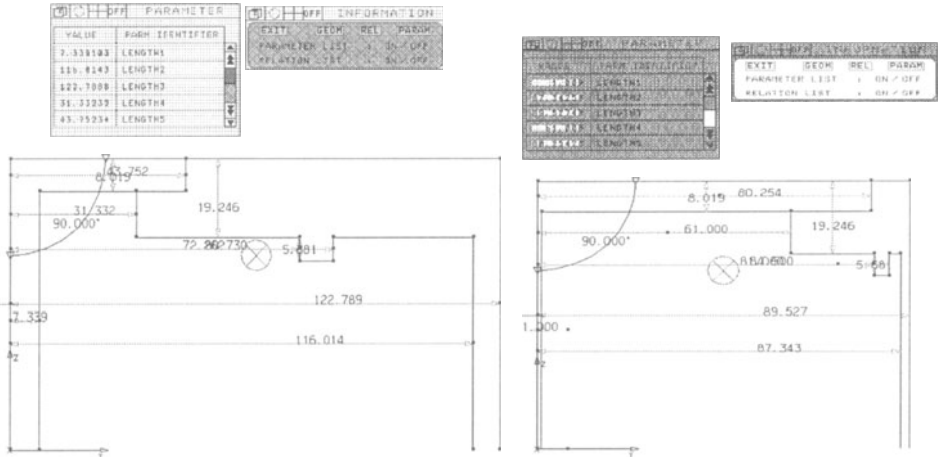


Figure 4. Original and final parts

This experimentation shows that we obtain a quick answer to resolve the mathematical system and to update all the CAD parts. The result gives the distance between faces, the tolerancing for machining operation and for setting operation and the machining dimensions.

This system can be exploited many ways. To modify a machining or a functional requirement, there is only one change in the condition matrix of the MATLAB model. Resolving this new system is not a problem, the new values are calculated. The part is updated in the CATIA environment. To modify the process planning, the operator uses the mouse, directly on the CATIA screen. He also updates some necessary conditions. There is no change for the following operations. A modification of part geometry is more elaborate. After modifications of the drawings with SKETCHER, we must extract the new faces and add them into the MATLAB model (table 1 and table 2). So lines are inserted in the matrix of faces. The PARAM3D module is used to re-initialize again all the parameters. Finally, some requirements must be added in the conditions matrix. The link between all the different parameters have to be kept. To use an existing process planning with a new part, we must recognize its faces and create the link between them and the MATLAB model. For this operation, the operator clicks on these elements on the CATIA screen. He also creates the PARAM3D parameters. So, he manually respects the consistency between the different representation models (faces, conditions, PARAM3D). Then the optimization can be carried out.

5. Limits and perspectives

Now, there are lot of limits for our software. The part is a revolution solid based on a continuous contour, there is no hole perpendicular to the revolution axis. The intermediate shape for all the phases are created manually. The only faces recognized are perpendicular to the direction of the study. The optimization with MATLAB accepts only one direction at a time. There is no interaction between these directions. The

machining conditions are static. There is no link with the machining process. Tolerancing is written without Fd&T module.

Later, our software will be easy and quick to use for an operator. It has to be developed so as to avoid some of manual operations. The part only requires to be sketched, with approximate values, and the result of a simulation gives a fast answer in the CAD-CAM environment. This system shows the incompatibility between functional or machining conditions. The operator can directly modify the sketch part or a condition.

In the future, we want to improve the system. We plan to use the manufacturing features to eliminate all limitations. Also, these manufacturing features permit the automatic creation of intermediate surfaces and the linking between elements and parameters of the CAD-CAM environment. The aim is to transfer an existing process planning on a new part, and to apply the old machining process to this new part, (compatibility of cutting tool). We also wish to update the process planning documentation.

As the system allows for modifications, it also has to stabilize the solution. The part must be stable when faces with a small modification of certain conditions. This is possible if we increase the number of constraints in the solver. So, there are different sort of constraints. Some are free, other are fixed, others can be modified in a gap.

References

1. Nikos I., Karacapilidis, Costa P., Pappis, *Production planning and control in textile industry : a case study*. Computers In industry, Vol 30, 1996, 127-144.
2. Britanik J., Marefat M., *Cased-Based Manufacturing Process Planning with Integrated Support for Knowledge Sharing*, Proceedings of ISATP'95, University of Arizona, Tucson. 1995.
3. Mognol P., *Contribution à la génération automatique de gammes en tournage : génération dirigée par évaluation progressive*. Thèse de doctorat. ENS Cachan, novembre 1994
4. Poolton J and Barclay I, *Concurrent engineering assessment : a proposed framework*, Journal of Engineering Manufacture, Vol 210, 1996, pp 321,328
5. Anselmetti B. et Bourdet P. *Optimization of a workpiece consedering production requirements*, Computers in industry (Elsevier Science Publishers) Vol 21 n°1, jan 1993, pp23-34
6. Jian Dong and Ying Shi *Variational geometry theory for tolerance sensitivity analysis*, ASME Winter Congress & Exposition San Francisco, 1995,
7. Bourdet P., *Chaînes de cotes de fabrication : le modèle*, L'ingénieur et le technicien de l'enseignement technique, décembre 1973.
8. Anselmetti B. *Simulation d'usinage bidimensionnelle sur un exemple en commande numérique*, revue Mécanique Matériaux Electricité n°398, mars 1983.

EXTENSIONS OF OBJECT FORMALISM FOR REPRESENTING THE DYNAMICS: APPLICATION TO THE INTEGRATION OF VIEWPOINTS IN THE DESIGN OF A PRODUCTION SYSTEM

M. BIGAND, D. CORBEEL, D. NDIAYE, J.P. BOUREY
Laboratoire d'Automatique et d'Informatique Industrielle de Lille (LAIL)
URA-CNRS D-1440
Ecole Centrale de Lille, B.P. 48, F-59651 Villeneuve d'Ascq Cedex
France
e-mail: bigand/corbeel/ndiayed/boureyjp@ec-lille.fr

Abstract

This paper presents the integration of the viewpoints of supervision and performance evaluation by using an object oriented modelling. The used formalism (UML) is enhanced by existential and exclusive constraints in order to ensure the data integrity of the proposed models; the dynamic aspect consists essentially here in ensuring the data consistency during linked suppressions.

1. Introduction

Our work is a part of CASPAIM project developed in the LAIL, which concerns the development of a set of methods for analysis, design and implementation of flexible production systems (FPS). Several viewpoints are simultaneously considered. Due to the diversity of the used formalisms, the integration of the multi-expert models is then impossible without a repository approach ensuring the data consistency and the exchange between the designers involved in an FPS design, [1].

We thus focus on this repository [3], which is the management system enabling different users to federate the information (data, processing, resources, events, documents, etc.) relative to one product (part, set, software, process, etc.) during its lifetime. The products we have to manage are modelled by compound objects having rich semantics, [8], which expresses the numerous dependence links between objects. But they introduce some difficulties in maintaining the information consistency, notably during some operations on the objects, as creation, modification or suppression [4].

In the most used methods and formalisms [16], [14], [6], [10], the resolution of these difficulties are postponed until the implementation. In the first section, we propose UML extensions to introduce constraints on instances as soon as the analysis starts. After, extended UML models of the data are given. Then we conclude by the integration of supervision and performance evaluation viewpoints.

2. Unified modelling language (UML) extensions

2.1. TEMPORAL EXCLUSIVENESS BETWEEN CLASSES

We wish to specify that an instance of class A ($A_1 \dots A_i \dots$) is a part of only one class B's instance ($B_1 \dots B_j \dots$) at a given instant. A class B's instance can be composed of several class A's instances. If we use the UML formalism, we obtain the diagram shown in figure 1.

We wish now to manage the history of this relationship: for example an instance A_1 is linked with B_1 between $[t_0]$ and $[t_1]$ and with B_2 between $[t_1]$ and $[t_2]$. We have thus to modify the multiplicity on the B-side as shown in figure 2. Unfortunately we lose the exclusiveness notion.



Figure 1. Class diagram for an aggregation.



Figure 2. Modified aggregation for the history management.

Thus we propose an extension depicted in figure 3. This extension emphasises the temporal exclusive ownership of a B_j instance with regard to the A_i instances and allows the history management of the aggregation.

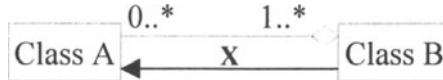


Figure 3. Exclusive constraint.

2.2. TEMPORAL EXCLUSIVENESS BETWEEN RELATIONSHIPS

Let us consider two classes A and B linked by n relationships R_1, R_2, R_n . If we use the UML formalism, we obtain diagram figure 4.

If we consider two respective instances of classes A and B, to a given moment, we wish they were not linked by more than one among the n relationships. We represent this new constraint by the symbolism in figure 5.

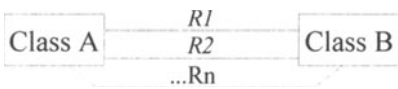


Figure 4. Relationships between two classes.

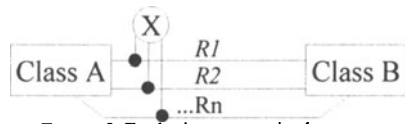


Figure 5. Exclusive constraint between relationships.

This constraint differs from the {exclusive or} constraint introduced in the UML formalism figure 6. Indeed, the {exclusive or} constraint will forbid the simultaneity of the two relationships, but definitively, with the impossibility to manage the history.

Figure 7 illustrates the use of the temporal exclusiveness:



- between relationships : a tool can be mounted on a machine (for machining a part) or be sharpened by a machine, but these two actions are not simultaneous,
- between classes: a tool can be mounted or be sharpened by several different machines during its life, but on or by one and only one machine at a given instant.

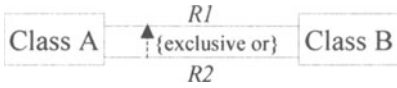


Figure 6. UML exclusive or constraint.

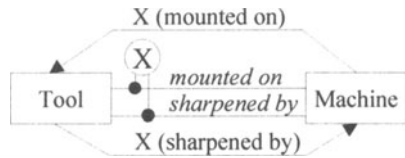


Figure 7. Exclusive constraints: example.

2.3. EXISTENTIAL CONSTRAINT

We focus now on the dynamics of suppression. Let us consider two classes A and B as the suppression of one instance of the class A entails the one of the linked instances of the class B.

We propose to enhance the UML formalism by the existential link between the two classes (cf. figure 8). In the example of figure 9, when a Programmable Logic Controller is suppressed, all the programs it contained are suppressed too.

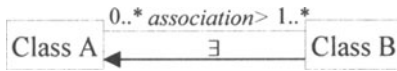


Figure 8. Existential constraint.

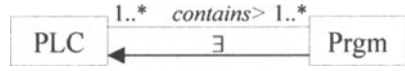


Figure 9. Example: the suppression of an instance of PLC entails the one of Prgm instances.

2.4. SCENARIO DIAGRAM FOR THE SUPPRESSION

The mechanism for the suppression of an instance of class A (cf. figure 8) can be represented by a scenario diagram. For example, figure 10 shows an instance diagram with two objects (A2 of class A and B1 of class B); if A2 is suppressed by an actor, the instance B1 of class B must be suppressed; this can be specified by the sequence diagram figure 11.



Figure 10. Example of instance diagram.

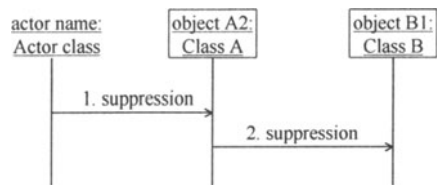


Figure 11. Scenario diagram A2 suppression.

It is also possible to develop a translation of such a constraint with the Object Constraint Language [13], as shown in [12].



2.5. PARTIAL OR TOTAL LINK

We wish now to express that the existential and exclusiveness constraints between classes are not systematic: the constraint will be applied only for some instances of the concerned classes. We thus introduce the concept of total link (the previous case), represented by a plain line, and of partial link, represented by a dotted line.

Figure 12 illustrates the use of a partial link in the case of the exclusiveness constraint between classes. A mechanical set can contain internal bolts. These bolts are not shared with another mechanical set at a given instant. If we consider the assembly of two such sets, this assembly can be made with bolts having the same features as the previous ones. These assembly bolts are shared by the two mechanical sets.

We can notice that model figure 13 seems to be valid for this problem too; but it distinguishes the "internal bolts", to which the exclusiveness constraint is applied, from the "interfacing bolts" to which it does not. This specialisation does not correspond to the reality; all the bolts have the same attributes.

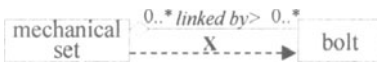


Figure 12. Example of partial exclusive constraint.

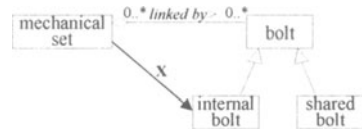


Figure 13. Bad use of exclusive constraint.

3. Viewpoint of Supervision

The supervision viewpoint is divided itself into several viewpoints described below.

3.1 VIEWPOINT OF DIAGNOSIS [15]

The goal is to obtain the automation of the diagnosis (research of fault causes). Two models have been developed: the *functional model* and the *structural model*.

The *functional model* specifies the functions of the system in terms of a hierarchical composition of elementary functions. On the object model figure 14, a reflexive aggregation allows the representation of the hierarchical composition of the *functions* executed by the *elements* of the system.

The *structural model* specifies the system components and their structural links (figure 15). The class *element* is defined as a generalisation of the classes *effective machine*, *cell* and *component*. The reflexive aggregation models the structural composition of *elements* into a more complex *element* in order to cover finally the whole studied production system.



Figure 14. Class diagram of the functional model.

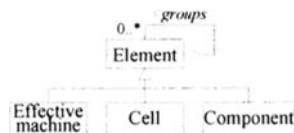


Figure 15. Class diagram for a structural decomposition of a production cell.

3.2 VIEWPOINT OF PILOTING [5]

This viewpoint concerns the effective control of the machines by managing their working modes. A structural and functional description of the cell is obtained by a bottom-up regrouping approach, which defines *effective* and *virtual machines* until the whole process is covered by a single *virtual machine*.

On the class diagram figure 16, the deletion of a *machine* entails the deletion of all the *virtual machines* of which it is the component; then an existential link between the *machine* and *virtual machine* classes is added.

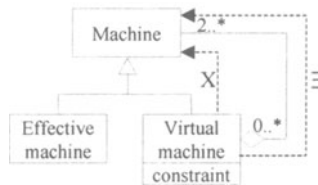


Figure 16. Class diagram for the structural and functional description of the cell.

3.3 VIEWPOINT OF CONTROL SUPERVISION [9]

An order filtering system allows the avoidance of inconsistencies between the control system and the physical system. The *Controllable Object* (CO) concept has been introduced. The decomposition of a CO leads to a set of *Elementary Controllable Objects* (ECO). The components are grouped according to functional or safety constraints and build the *Logical Functional Components* (LFC). Each elementary component is characterised by both a set of steady physical *states* and a set of performed *actions*. The *states* and *actions* of a component can be linked by *constraints*.

For this viewpoint, the object model is presented in figure 17. The deletion of the component regrouping which represents a LFC, entails the deletion of the associated constraint and reciprocally. A bi-directional existential link is added between the classes *Regrouping* and *Constraint*. In the same manner, we have added an oriented existential link between the *Component* and *Regrouping* classes.

Since a *component* can be part of only one *regrouping* at a given instant, an exclusive link is added between the corresponding classes.

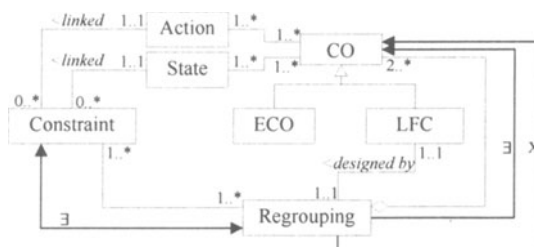


Figure 17. Class diagram for the control supervision.

3.4. INTEGRATION OF SUPERVISION'S VIEWPOINTS

The model showed figure 18 is the synthesis of the previous models.

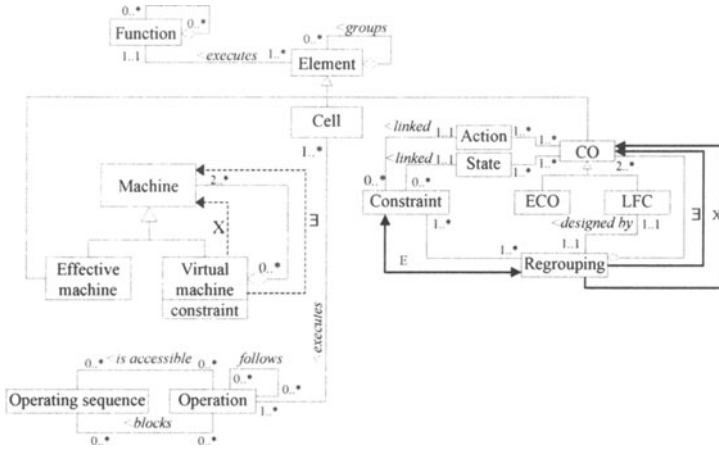


Figure 18. Supervision modelling integration.

4. Viewpoint of performance evaluation [2], [7], [11]

The performance evaluation research group works on the elaboration of the predictive deterministic and cyclic command by using Petri nets. The research of the predictive steady state command is led within two steps:

- Short term production planning: the aim is to decompose the production into one or several feasible cyclic steady states: within each steady state, a set of parts (called production horizon) is cyclically produced. A simultaneous production of part types is thus considered.
- Scheduling: a deterministic command is defined, modelled by a Marked Graph, and represented by a Gantt diagram with both resources and pallets behaviour.

The model figure 19 integrates the short-term production plan and the schedule.

A *part type* regroups a set of identical *parts*. A *linear sequence* contains a sequence of *operations* (machining, assembling...). A set of *resources* can perform one or several *operations* of the linear sequence. A *sequence* describes the set of the possible *linear sequences* for part processing. A *macro-sequence* is the cyclic ordered regrouping of *linear sequences*. A *steady state*, which results from the allocation of *resources* and *pallets*, is an aggregation of *macro-sequences*. The *steady state* describes the whole production cycle. Uses of the UML extensions:

- the existential links *part* and *resource* with *linear sequence* of the model express that the deletion of a part or a resource entails the deletion of the linear sequence,
- the deletion of a *linear sequence* or a *pallet* entails the re-scheduling of the *macro-sequence*,
- the deletion of a *part type* or a *macro-sequence* entails the re-computing of the corresponding *steady state*,



- the exclusive links express that a *linear sequence* and a *pallet* belong to a single *macro sequence* at a given time.

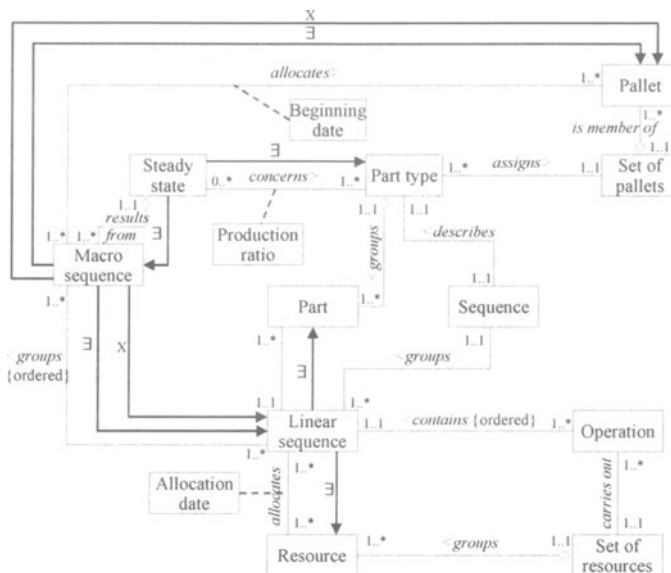


Figure 19. Extended UML model for the performance evaluation.

5. Data integration

The main difficulty of the data integration in CASPAIM project results of the multi-expert features of the approach.

The use of a common language as the extended UML constitutes a neutral description allowing the integration of the used tools and formalisms: statecharts, Petri-Nets, constraint tables...

In order to bring together the viewpoints of supervision and performance evaluation, we have searched the common objects of the two approaches. The UML diagrams have emphasised these common objects (operation, sequences...) and synonyms (effective machine = resource). The figure 20 shows the regrouping outline of the supervision and performance evaluation models (figures 18 and 19).

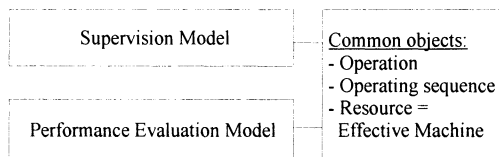


Figure 20. Regrouping of viewpoints of supervision and performance evaluation.

6. Conclusion and perspectives

The neutrality of the used formalism permitted first to each research subgroup to express the objects it manages, then to constitute the data dictionary, and at last to facilitate the integration of the viewpoints. The proposed extensions manage the dependencies among objects within the class diagram, so they improve the representation of the dynamics, which ensures better data consistency.

We are currently building a data dictionary prototype based on the Oracle database management system. The classes and associations are implemented by tables and the proposed constraints by database triggers.

The long term aim is to obtain a complete generic model. With an iterative and recursive method, an integration platform will be used to insert views progressively in our meta-model and to extract views from it.

7. References

- [1] *Representation des systèmes de contrôle et de commande des systèmes automatisés*, Norme AFNOR Z 68-901, 1996.
- [2] BERRUET P., TOGUYENI AKA, EL KHATTABI S., CRAYE E., *A process modelling for supervision in FMS : operational accessibility Graph*, CACS'D/97-IFAC, Gent, April 1997, pp225-230.
- [3] BIGAND M., BOUREY J.P., CORBEEL D., MAIK J.P., *A generalized object approach for the design of flexible manufacturing systems*, CESA'96 IMACS Multiconference, pp352-357, Lille 1996.
- [4] BIGAND M., CORBEEL D., BOUREY J.P., *The design of Flexible Manufacturing Systems by using a knowledge based system*, 15th IMACS World Congress, Berlin, August 1997, pp541-546.
- [5] BOIS S., *Intégration de la gestion des modes de marche dans le pilotage d'un système automatisé de production*, Thèse de Doctorat, Lille I, (France). 1992.
- [6] BOOCH G., *Object Oriented Design with Applications*, The Benjamin/Cummings publishing Company Inc, 1991.
- [7] CAMUS H., OHL H., KORBAA O., GENTINA J.C., *Cyclic Schedules in Flexible Manufacturing Systems with Flexibilities in operating sequences*, First International Workshop on Manufacturing and Petri Nets, 17th International Conference on Application and Theory of Petri Nets, Osaka, Japan, pages 97-116, June 1996.
- [8] COUFFIN F., *Modèle de données de référence et processus de spécialisation pour l'intégration des activités de conception en Génie Automatique*, Thèse de Doctorat de l'E.N.S de Cachan, janvier 1997.
- [9] EL KHATTABI S., CRAYE E., GENTINA J.C., *Supervision by the behavior modelling*, IEEE International Conference on Systems, Man and Cybernetics, SMC'95, Vancouver, October 95, vol. 2, pp 1416-1422.
- [10] JACOBSON I., CHRISTERSON M., JONSSON P., OVERGAARD G., *Object Oriented Software Engineering*, Addison-Wesley, ACM Press, 1992.
- [11] KORBAA O., CAMUS H., GENTINA J.C., *FMS Cyclic Scheduling with Overlapping production cycles*, 2nd International Workshop on Manufacturing and Petri Nets, 18th International Conference on Application and Theory of Petri Nets, 1997.
- [12] NDIAYE D., BIGAND M., CORBEEL D., BOUREY J.P., *Information system for production engineering: contribution to maintaining consistency of composite data using object approach*, IEPM'99, Glasgow, July 1999.
- [13] Object Constraint Language Specification version 1.1, 1 available on www.rational.com/uml, 1997.
- [14] RUMBAUGH J., BLAHA M., PREMERLANI W. EDDY F., LORENSEN W., *Object oriented Modelling and design*, Prentice-Hall 1991.
- [15] TOGUYENI AKA, EL KHATTABI S., CRAYE E., *Functional and/or structural approach for the supervision of flexible manufacturing systems*, CESA'96 IMACS, 9-13 July 1996, Symposium on discrete event and manufacturing systems, pp 716-721.
- [16] *Unified Modeling Language, Semantics and notations*, available on <http://www.rational.com>

MULTIDIMENSIONAL TAGUCHI'S MODEL WITH DEPENDENT VARIABLES IN QUALITY SYSTEM

G. DRAGOI ^{**}, C. TARCOLEA ^{*}, D. DRAGHICESCU ^{*},

^{*} Polytechnic University of Bucharest, 313, Splaiul Independentei, 77206 Bucharest, Romania

E-mail: George.Dragoi@hmg.inpg.fr

S. TICHKIEWITCH ^{**}

^{**} Laboratoire Sols, Solides, Structures de Grenoble

B.P.53 Domaine Universitaire 38401 Grenoble Cedex 9 France

E-mail: Serge.Tichkiewitch@hmg.inpg.fr

Abstract. In order to assume a production of quality, manufacturers have to adapt their processes in order to product true parts to the initial drawings. It will be more advisable for then to get a reliable process based on target points, instead of using a systematical control of each manufactured part allowing the output of the bad elements, the cost being in such case excessive. In the specialized literature, Taguchi's models are based on the use of the parabolic functions both in the mono and multidimensional cases. This paper is trying to define a Quality Loss Function (QLF) in the multidimensional case taking into consideration dependent variables. We show that the mathematical model can be considered as a positive definite quadratic form. The significant result of the paper is the decomposition of the Quality Loss Function in a sum of variances and cross products of the deviations of the arithmetical means, which are obtained from each target point for every constitutive part.

1. Introduction

The actual informational standards of manufacturing enterprises are based on methods, concepts, tools and techniques using artificial intelligence, that will permit us to adapt their activities and also their applications to continuous fluctuations of their economic environment. In fact, if we consider the enterprise not as a monolithic organization but as a set of treatment and information communication systems, we find a more dynamic organization that is necessary to the adaptation of the enterprise at the constant variability of its economic environment [2], [3].

The definition of «quality» [9] is given by ISO 8402 : "The set of properties and characteristics of a product or of a service that gives it the aptitude to satisfy the explicit and implicit needs ". The product must respond to the needs of the customer, that means what the customer wants, taking also into consideration implicit needs [5].

In the triple constraint costs /delays/performances that characterize the conduct of the enterprise, the assimilation of these requests demands the use of some specific methods [13]. In the production process there exists certain variability. We try to have no difference between the actual process means and the nominal values, and the smallest variances when the number of items is relatively big, i.e. a robust design. Taguchi defines quality as « the quality of the product is the minimum loss imparted by the product of the society from the time product is shipped » [12]. This economic loss is associated with losses due to rework, waste of resources during manufacturing, warranty cost, customer complaints and dissatisfaction, time and money spend by customers on failing products, and eventual loss of market share. When a critical quality characteristic deviates from the target value, it causes a loss. The variation from target is the antithesis of quality. “The TAGUCHI approach to robust design makes the engineer focus on reducing of variability of the process” [7] (Figure1).

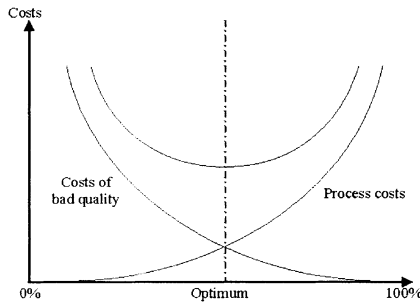


Figure 1. Cost of Quality

In the specialized literature, the Taguchi's models are based on the use of the parabolic functions both in the mono and multidimensional case [12] (Figure 2).

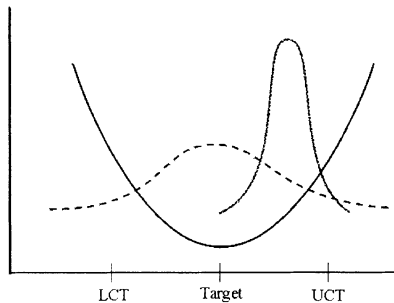


Figure 2. Quality Loss Function (QLF) and how it relates to the specification limits

2. The Quality Loss Function with dependent variables

2.1 TAYLOR DEVELOPMENT FOR QUALITY LOSS FUNCTION

Let L be a real function of n real variables (x_1, \dots, x_n) , $L : D_n \subset \mathbb{R}^n \rightarrow \mathbb{R}$, with (a_1, \dots, a_n) the target (nominal) vector. It is possible to consider that $L(x_1, \dots, x_n)$ is a continuous

function with partial derivatives up to the order of three. In these conditions the function $L(x_1, \dots, x_n)$ can be expanded by using the Taylor formula about the target value (a_1, \dots, a_n) with the rest of the second order [10]:

$$L(x_1, \dots, x_n) = L(a_1, \dots, a_n) + \frac{1}{1!} \sum_{i=1}^n \frac{\partial L}{\partial x_i}(a_1, \dots, a_n)(x_i - a_i) + \frac{1}{2!} \sum_{i=1}^n \sum_{j=1}^n \frac{\partial^2 L}{\partial x_i \partial x_j}(a_1, \dots, a_n)(x_i - a_i)(x_j - a_j) + R_2 \quad (1)$$

2.2 AN EXAMPLE: THE OVERRUNNING CLUTCH OF FORTINI

We consider as an example of the QLF problem the classical example of the overrunning clutch of Fortini [6] (see figure 3), that was studied by many authors ([1], [5], [8]) by using different methods.

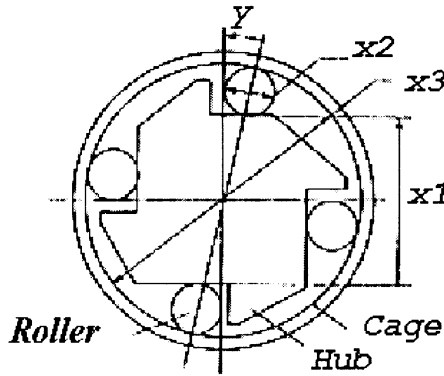


Figure 3. The overrunning clutch of Fortini

The contact angle y is the functional dimension that must be controlled and it is expressed as:

$$y = f(x_1, x_2, x_3) = \arccos\left(\frac{x_1}{x_3 - 2x_2}\right) \quad (2)$$

Therefore, we take as quality loss function the deviation of the contact angle relative to the target point:

$$L(x_1, x_2, x_3) = y - y_t \quad (3)$$

Using the Taylor development of the $L(x_1, x_2, x_3)$ we obtain the following result:

$$y - y_t = \left[\left(\frac{\partial f}{\partial x_1} \Delta_1 + \frac{\partial f}{\partial x_2} \Delta_2 + \frac{\partial f}{\partial x_3} \Delta_3 \right) + \frac{1}{2!} \left(\frac{\partial^2 f}{\partial x_1^2} \Delta_1^2 + \frac{\partial^2 f}{\partial x_2^2} \Delta_2^2 + \frac{\partial^2 f}{\partial x_3^2} \Delta_3^2 + 2 \frac{\partial^2 f}{\partial x_1 \partial x_2} \Delta_1 \Delta_2 + 2 \frac{\partial^2 f}{\partial x_1 \partial x_3} \Delta_1 \Delta_3 + 2 \frac{\partial^2 f}{\partial x_2 \partial x_3} \Delta_2 \Delta_3 \right) \right]_{(a_1, a_2, a_3)} \quad (4)$$

If we take as cost function the cost of the three elements constituting the overrunning clutch, we can evaluate these costs in regard of the used process and in regard of the obtained precision for each part (see Table 1 revised after [5]) :

TABLE 1. Cost – tolerance data for the clutch

Hub		Roller		Cage	
Tolerance [in 10 ⁻⁴ in.]	Cost [in dollars]	Tolerance [in 10 ⁻⁴ in.]	Cost [in dollars]	Tolerance [in 10 ⁻⁴ in.]	Cost [in dollars]
2	19.38	1	3.513	1	18.637
4	13.22	2	2.48	2	12.025
8	5.99	4	1.24	4	5.732
16	4.505	8	1.24	8	2.686
30	2.065	16	1.20	16	1.984
60	1.24	30	0.413	30	1.447
120	0.825	60	0.413	60	1.20
		120	0.372	120	1.033

These costs are determined as continuous curve as follows:

$$\begin{aligned}
 C_1(z) &= \frac{1}{a_1 z^2 + b_1 z + c_1} = \frac{1}{(-5.441 * z^2 + 0.01651z) * 10^{-3}}, \quad (z = \Delta_1) \\
 C_2(z) &= \frac{1}{a_2 z^2 + b_2 z + c_2} = \frac{1}{(-3.3607z^2 + 0.0595z) * 10^{-4}}, \quad (z = \Delta_2) \\
 C_3(z) &= \frac{1}{a_3 z^2 + b_3 z + c_3} = \frac{1}{(-1.1319z^2 + 0.0205z) * 10^{-4}}, \quad (z = \Delta_3)
 \end{aligned}
 \tag{5}$$

If we take as the target vector

$$(a_1, a_2, a_3) = (2.17706, 0.9000, 4.000) \text{ in inches}$$

We obtain:

$$\begin{aligned}
 y - y_t &= -3.1558\Delta_1 - 6.2458\Delta_2 + 3.1229\Delta_3 + \frac{1}{2!}[-68.4237\Delta_1^2 - 279.3729\Delta_2^2 - \\
 &69.8432\Delta_3^2 + 2 * (-69.8432)\Delta_1\Delta_2 + 2 * 69.1443\Delta_1\Delta_3 + 2 * (-138.2894)\Delta_2\Delta_3]
 \end{aligned}
 \tag{6}$$

In addition, we can resolve the following problem: What is the best manufacturing processes for the three parts of the overrunning clutch in order to minimize the global cost and to respect a specific quality?

For a given limit of the $y - y_t$, the tolerance and the manufacturing cost values are obtained in Table 2:

TABLE 2. Manufacturing cost values

Deviation (y-y _t)	Δ ₁	Δ ₂	Δ ₃	Cost [in dollars]
0.02	0.0084	0.0036	0.0107	2.6972
0.002	0.0070	0.0026	0.0117	3.0602

In this example, we saw the possibility to choose the best processes for a wanted quality of a system.

3. A new formulation for the QLF with dependant variables

Now, we propose and justify the use of the QLF with dependent variables in the multidimensional case [10]. In this paper the following assumptions are made as usual:

a) By definition, the Quality Loss Function is zero at the point (a_1, \dots, a_n) .

$$L(a_1, \dots, a_n) = 0, \quad (7)$$

b) At the target point the function L has a minimum so all its partial derivatives of the first order at this nominal value vanish,

$$\frac{\partial L}{\partial x_i}(a_1, a_2, \dots, a_n) = 0, \quad \forall i \in \overline{1, n} \quad (8)$$

c) It can also be assumed that the argument x is close enough to the target point, $x \approx a$, and consequently we can consider that the terms of orders higher than two are zero because the rest of the Taylor formula tends towards zero.

In these conditions, we get the approximate formula:

$$L(x_1, x_2, \dots, x_n) \approx \frac{1}{2!} \sum_{i=1}^n \sum_{j=1}^n \frac{\partial^2 L}{\partial x_i \partial x_j}(a_1, a_2, \dots, a_n)(x_i - a_i)(x_j - a_j) \quad (9)$$

Then it is natural to take as a model for the Quality Loss Function the following quadratic form:

$$L(x_1, \dots, x_n) = \sum_{i=1}^n \sum_{j=1}^n k_{ij}(x_i - a_i)(x_j - a_j) \quad (10)$$

Here (k_{ij}) denote the costs that can be determined for each specific case. Remarks:

- ◆ If $k_{ij} = 0$ for each pair (i, j) , $i \neq j$, we obtain the model of Multi-Component Tolerances described by Feng and Kusiak [5].
- ◆ For a given pair (i, j) the cost k_{ij} is determined by estimating the loss when x_i deviates from a_i by Δ_{x_i} and x_j deviates from a_j by Δ_j .
- ◆ It is possible that the loss caused by the deviations have unequal values for the lower and upper limits, respectively. In other words, for a given pair of indices, k_{ij} can take a single value or two values, depending on the position of the variable in regards to the target point.

Let us suppose now that m observations of identical products with multiple dimensions are taken. The expected loss given by the expression of the Quality Loss Function for a sample of m items is defined as the arithmetic mean of the losses,

$$\bar{L}(x_1, x_2, \dots, x_n) = \frac{1}{m} \sum_{\lambda=1}^m L(x_1^\lambda, \dots, x_n^\lambda) \quad (11)$$

Considering the observed values as outcomes of a random vector, we can compute the risk in terms of mathematical statistics. The arithmetical Quality Loss Function can be decomposed in the following factors: the sum of variances about the arithmetic mean value and the cross products of deviations of the empirical mean from the target value for every constitutive part:

$$\begin{aligned} \bar{L}(x_1, \dots, x_n) &= \frac{1}{m} \sum_{\lambda=1}^m \sum_{i=1}^n \sum_{j=1}^n k_{ij}(x_i^\lambda - a_i)(x_j^\lambda - a_j) = \\ &= \frac{1}{m} \sum_{\lambda=1}^m \sum_{i=1}^n \sum_{j=1}^n k_{ij} [(x_i^\lambda - \bar{x}_i) + (\bar{x}_i - a_i)] [(x_j^\lambda - \bar{x}_j) + (\bar{x}_j - a_j)] \end{aligned} \quad (12)$$

So:

$$\bar{L}(x_1, \dots, x_n) = \sum_{i=1}^n \sum_{j=1}^n k_{ij} \left[s_{ij}^2 + (\bar{x}_i - a_i)(\bar{x}_j - a_j) \right] \quad \text{with} \quad \bar{x}_i = \frac{1}{m} \sum_{\lambda=1}^m x_i^\lambda \quad (13)$$

$$\text{and} \quad s_{ij} = \frac{1}{m-1} \sum_{\lambda=1}^m (x_i^\lambda - \bar{x}_i)(x_j^\lambda - \bar{x}_j), \quad i \in \overline{1, n}; j \in \overline{1, n}$$

The value k_{ii} is determined by estimating the loss when x_i deviates from a_i by Δ_i . The value k_{ij} ($i \neq j$; $i, j = 1, 2, 3$) is determined by estimating the loss when x_i and x_j deviates from a_i and a_j by Δ_i and Δ_j .

In the bidimensional case, we found some previous result [3], [10], and [11]:

$$\begin{aligned} \bar{L}(x, y) = & k_{11} \left[s_{11}^2 + (\bar{x} - a)^2 \right] + k_{22} \left[s_{22}^2 + (\bar{y} - b)^2 \right] + \\ & k_{12} \left[s_{12}^2 + (\bar{x} - a)(\bar{y} - b) \right] + k_{21} \left[s_{21}^2 + (\bar{x} - a)(\bar{y} - b) \right] \end{aligned} \quad (14)$$

4. Examples

4.1 RECTANGLE PLACEMENT

Consider that a big fragment of iron plate has to be cut into rectangular parts. We assume that the nominal length of each part is 5 cm, the nominal width is 4 cm and that the functional limits of each dimension are of ± 0.2 mm.

If the length or width of a part is more than 0.2 mm smaller than the nominal size, the device is considered a failure.

If the length or the width of a part is more than 0.2 mm larger than the nominal size, the part may be cut again, but the exceeded material is lost.

The loss cost in proportional to the loss surface and gives for the different cases:

$$\begin{aligned} k_{11} = & \begin{cases} 4(x-5)C & \text{if } x > 5.02 \text{ and } 3.98 \leq y \leq 4.02 \\ xyC & \text{if } x < 4.98 \text{ and } 3.98 \leq y \leq 4.02 \end{cases} \\ k_{12} = & \begin{cases} (x-5)(y-4)C & \text{if } x > 5.02 \text{ and } y > 4.02 \\ xyC & \text{if } x < 4.98 \text{ and } y < 3.98 \text{ or} \\ & x < 4.98 \text{ and } y > 4.02 \end{cases} \\ k_{21} = & \begin{cases} (x-5)(y-4)C & \text{if } x > 5.02 \text{ and } y > 4.02 \\ xyC & \text{if } x < 4.98 \text{ and } y < 3.98 \text{ or} \\ & x > 5.02 \text{ and } y < 3.98 \end{cases} \quad (15) \\ k_{22} = & \begin{cases} 5(y-4)C & \text{if } 4.98 \leq x \leq 5.02 \text{ and } y > 4.02 \\ xyC & \text{if } 4.98 \leq x \leq 5.02 \text{ and } y < 3.98 \end{cases} \end{aligned}$$

4.2 THE OVERRUNNING CLUTCH OF FORTINI

We consider also the overrunning clutch of Fortini [6] (see figure 3). Now, we propose the following calculation model: let us consider the «optimal» dimensions for each component (that implies «optimal» costs). We take into consideration devices with different sizes and, implicit, different costs. Considering the observed values as

outcomes of a random vector, we can compute the risk in terms of mathematical statistics.

Given:

1^o) The target vector $(a_1, a_2, a_3) = (2.17706, 0.9000, 4.000)$ in inches

2^o) The nominal value and tolerances of angle γ are 0.144 ± 0.02 rad

3^o) The tolerance requirement for dimension i is: Δ_1 for a_1 , Δ_2 for a_2 , Δ_3 for a_3 .

The deviations around the «optimum» can be used to define k_{ij} . Obviously, there exist many other possibilities for evaluating k_{ij} .

The loss caused by unacceptable hub, unacceptable roller, unacceptable cage, respectively unacceptable hub and roller, unacceptable hub and cage, unacceptable cage and roller, is estimated $[12, 2, 10, 1, 3, 2]*C$, with C is the cost of repairing. If for given (x_1, x_2, x_3) , the value Y is not in the tolerances the devices is reject.

If for given (x_1, x_2, x_3) , the value Y is in the tolerances the values are used for the arithmetical mean.

The value k_{ii} is determined by estimating the loss when x_i deviates from a_i by Δ_i .

The value k_{ij} ($i \neq j$; $i, j = 1, 2, 3$) is determined by estimating the loss when x_i and x_j deviates from a_i and a_j by Δ_i and respectively Δ_j .

$$k_{11} = \frac{12C}{\Delta_1^2}; k_{22} = \frac{2C}{\Delta_2^2}; k_{33} = \frac{10C}{\Delta_3^2}; k_{12} = \frac{1C}{\Delta_1\Delta_2}; k_{13} = \frac{3C}{\Delta_1\Delta_3}; k_{23} = \frac{2C}{\Delta_2\Delta_3}$$

In this case the arithmetical mean of values of Quality Loss Function is:

$$\bar{L}(x_1, x_2, x_3) = \sum_{i=1}^3 k_{ij} \left[s_{ij}^2 + (\bar{x}_i - a_i)(\bar{x}_j - a_j) \right]$$

We obtain: $L(x_1, x_2, x_3) = 1.0067 * 10^{-5}$ (Table 3)

TABLE 3 *QLF for overrunning clutch of Fortini*

\bar{x}_1	2.1771	s_{11}	$7.4579 * 10^{-8}$
\bar{x}_2	0.9002	s_{22}	$9.7361 * 10^{-8}$
\bar{x}_3	4.0001	s_{33}	$8.0604 * 10^{-8}$
a_1	2.17706	s_{12}	$2.7917 * 10^{-8}$
a_2	0.9000	s_{13}	$8.6467 * 10^{-9}$
a_3	4.000	s_{23}	$1.9944 * 10^{-8}$
k_{11}	33.3333	k_{12}	3.3333
k_{22}	8.0001	k_{13}	8.3333
k_{33}	27.7778	k_{23}	6.6667
$\Delta_1 = \Delta_3$	0.0006	Δ_2	0.0005

5. Conclusion

Product/process design has a great impact on life cycle cost and quality. When a critical quality characteristic deviates from the target value, it causes a loss. An

examination of the loss function shows that variability reduction or quality improvement drives cost down.

This paper defines the Quality Loss Function in the multidimensional case taking into consideration at same time interaction. The significant result is the decomposition of the values of the Quality Loss Function in a sum of variances – covariance's and cross products of the deviations of arithmetical means, which are obtained from each target point for every constitutive part. The methods provide an efficient and systematic way to optimize designs for performance, quality, and cost. Lowest cost can only be achieved at zero variability from target. Continuously pursuing variability reduction from the target value in critical quality characteristics is the key to achieve high quality and reduce cost. The model as well as follows the approaches of achieving the quality by robust engineering design.

It allows analyzing the manufacturability cost and quality at the product design stage. Furthermore, the method can aid in integrating cost and engineering functions through the concurrent engineering approach required evaluating cost.

Principal benefits include considerable time and resource savings: determination of important factors affecting operation, performance and cost; and quantitative recommendations for design which achieve lowest cost, high quality solutions. It is the systematic and efficient approach for determining the optimum configuration of design parameters for performance, quality and cost.

6. References

1. Chase, K., Green W., *Design Issues in Mechanical Tolerance Analysis*, Manufacturing Review 1, 1988, 50-59.
2. Dragoi, G., Guran, M., *Sisteme integrate de productie asistate de calculator*, Ed. Tehnica., Bucharest, 1997.
3. Dragoi, G., *"Bazele proiectarii si productiei asistate de calculator"*, UPB, Bucharest, 1997.
4. Ealey, L. A., *"Les methodes de Taguchi dans l'industrie occidentale"*. Les Editions Organisations, Paris, 1990.
5. Feng, C., X., Kusiak, A., *"Robust Tolerance Design with the Integer Programming Approach"*, Journal of Manufacturing Science and Engineering, vol.119, November 1997, 603-610.
6. Fortini, E., *"Dimensioning for Interchangeable Manufacture"*, Industrial Press, New York, 1967.
7. John, W., M., P., *"Statistical Methods in Engineering and Quality Assurance"*, Wiley Series in Probability and Mathematical Statistics, 1990.
8. Krisnaswanu, M. Mayne, R., *"Optimising Tolerance Allocation Based of Manufacturing Cost and Quality Loss"*, Advanced in Design Automation, DE-Vol. 69-1, ASME New York, 1994.
9. Ross, P., *"Taguchi Techniques for Quality Control"*, Edition Mc. Graw Hill, Book Company, New York, 1988.
10. Tarcolea, C., Paris, A., Dragoi, G., *"Etude de la qualité dans la phase de conception. Modèle de type Taguchi multidimensionnel"*, Université d'automne "Conception Intégrée des systèmes mécatroniques intelligents", deuxième édition, Bucarest, 13 – 17 octobre 1997, vol. "Conception Intégrée des systèmes mécatroniques intelligents, UPB, oct. 1997, 124-131.
11. Tarcolea, C., Paris, A., *"Modele bidimensionale de tip Taguchi"*, Rev. Management industrial, nr.1-2, 1995.
12. Taguchi, G., Elsayed A., E., Hsiang, C., T., *"Quality Engineering in Production Systems"*, Mc.Graw – Hill Book Company, International Edition, 1989.
13. Yagou, P., *"L'Ingenierie Simultanée"*, Edition Hermès, Paris, 1994.

AN APPROACH TO INTEGRATE SAFETY AT THE DESIGN STAGE OF NUMERICALLY CONTROLLED WOODWORKING MACHINES

D. JOUFFROY*, S. DEMOR*, J. CICCOTELLI*, P. MARTIN**

**Institut National de Recherche et de Sécurité (INRS),
Av. de Bourgogne, BP 27, F-54501 VANDOEUVRE Cedex*

***Centre de Recherche en Automatique de Nancy (CRAN/CNRS),
BP 239, F-54506 VANDOEUVRE Cedex*

Abstract

This paper presents the research work undertaken in the domain of the safety of numerically controlled woodworking machines. It begins with an overview of the legislative and safety framework in which manufacturers design new machines. Then it proposes a hazards identification and analysis aimed at integrating safety principles in the design of numerically controlled woodworking machines. A real working situation is then analysed an approach that combines an ergonomic approach with a functional analysis, and that places the emphasis on the man/machine system. The results of this analysis are used to enrich a distributed design model applied in an experiment aimed to improving the wood-particles extraction system of these machines.

1. Introduction

Operators have long been subject to multiple and numerous accidents while working on woodworking machines. Automation has led to reducing the hazards run but not fully eradicated them, and has in certain cases even introduced new ones. Thus, accidents still occur (amputations, perforations, death) all too often (Statistiques CNAMTS, 1997).

This remark applies to the numerically controlled routing machines, the particular subject of interest in this study (Fig. 1).

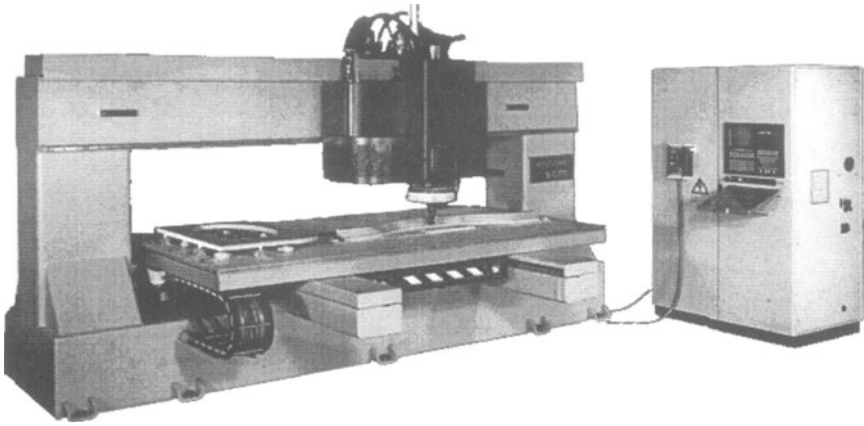


Figure 1. Numerically controlled woodworking machine (or router)

This paper provides a review of the legislative and normative framework in which manufacturers design new machines, before going on to present the approach adopted to identify and analyse hazards in order to integrate safety regulations in the design of numerically controlled woodworking machines.

To reduce the hazards linked to routing machines, a real work situation was analysed using a process employing both ergonomic approach and functional analysis, that places the emphasis on the activity of the man/machine system. The results were used to enrich a distributed design model employed in a design experiment on the wood-particles extraction system of these machines.

2. Legislative framework

On a legislative level, designers have had an obligation to satisfy essential safety requirements since European directives came into force (Directive 89/392/CEE, 1989).

To help manufacturers design machines that meet the requirements of these directives, numerous groups (composed of representatives of manufacturers, end users, and research and prevention centres) working within standardisation bodies, have been drafting texts laying down technical specifications. In addition to the basic standards applicable to all types of machines, there are also product-family and product-specific standards for particular categories of machines (Fig. 2).

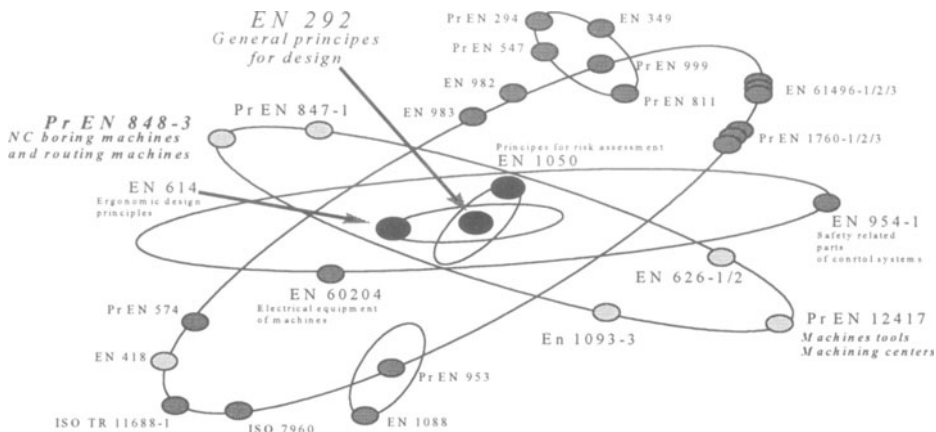


Figure.2. European standards relative to NC router safety (Standard project Pr EN 848-3, 1996)

In the case of numerically controlled woodworking machines, the range of machined items (in terms of both species and inherent characteristics) means that full automation of these machines is difficult to foresee. As a result, the operator must work closely with the machine to achieve a common objective, namely to machine items of wood in accordance with the specification drawing.

It would therefore appear necessary to take account of the operator in any analysis process aiming to reduce the hazards on these machines.

3. Towards intrinsic safety

3.1. CHAIN OF EVENTS

Machines are still considered dangerous ; we speak of "*dangerous entities*" in the chain of events leading to an accident on a machine and injury to man (Fig. 3). In certain circumstances, this situation can be considered as "*potentially dangerous*" and can end up in an accident unless specific measures are taken to interrupt the chain of events.

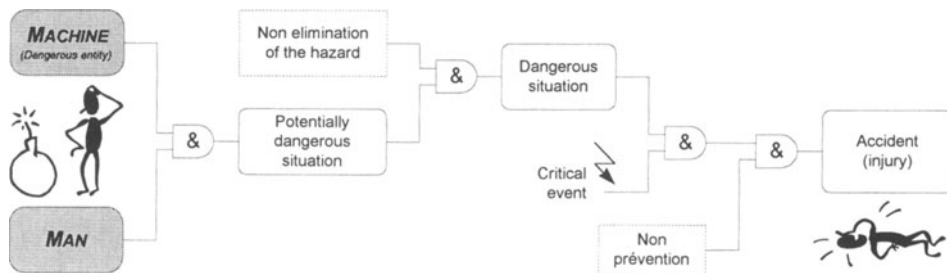


Figure.3. Chain of events leading to an accident (Ciccotelli, 1997)

The measures taken will be all the more effective the earlier they occur in the chain. Thus, it is advised to give priority to reducing the dangerous features of the machine and to anticipating the critical events, before going on to predict prevention possibilities. This is termed *intrinsic safety*.

3.2. CONTRIBUTION OF AN ERGONOMIC APPROACH AND A FUNCTIONAL ANALYSIS

To apply this principle, it is necessary both to identify and assess the future activity of the operators on the machine at the design stage. With this in mind, certain ergonomic approaches propose analysing a reference operating situation in order to identify elements of variability, sources of incident, factors of complexity, and "*typical activities*" linked to these elements (Daniellou, 1989). This process can highlight probable characteristics of the future activity of the new work situation; characteristics that can then be considered in the design project of a new system.

These methods are often entirely distinct from the functional analysis approach currently undertaken during the design of a new product or system of production. To overcome this drawback, a methodological process (MAFERGO [Fadier, 1994]) is employed, together with operation, malfunction and structural-functional analyses, through a general methodological diagram grouping both the functional and ergonomic approach. The functional analysis can describe the manufacturing process and assess the technical malfunctions of the system. The ergonomic analysis provides knowledge of the real activity of the man/machine system while assessing the impact of malfunctions on the activities of the operator. The subsequently carried out causal analysis, integrating all the technical, human and organisational events, can describe ways of improvement validated by simulations based on modelling the man/machine system.

4. Application to a real operating situation

Using this process, we identified and analysed the hazards and difficulties linked to using routing machines in a real operating situation.

This six-day intervention in a furniture making factory provided an analysis of five operators working on two types of routers.

4.1. ERGONOMIC APPROACH

The analysis is based on the video recorded observations of the activities of the various operators on the two machines. These observations were followed up by interviews with the operators to obtain justifications for their actions and to elicit explanations of how malfunctions were corrected (Demor, 1997).

Through these observations, three different activity phases were identified :

- running production cycles,

- changing over product series,
- entering and setting new programmes.

The collected data was used with three main aims in mind :

- analysing both the malfunctions and incidents, and their management,
- analysing the regulations carried out by the operators during the three phases,
- analysing the hazards linked to working on these machines and the way they are handled by the operators.

The malfunctions and incidents observed can generally be put down to the characteristics of the raw materials, to difficulties in altering the programme or to technical failures of the system. A number of similarities between these incidents and the two accidents declared over the eight years that these machine have been used in the firm, were highlighted. The dangerous nature of some incidents was also pointed.

Two main problems linked to the design of the machine liable to be a source of hazards were identified :

- problems in the presentation of information on the control screen,
- difficulties in getting information related to the tool movements despite the fact that it is important during setting phases (this problem is primarily linked to the characteristics of the wood-particles extraction system).

The routing machines studied had moving parts during operation that could lead to risks of projection of the item or tool, and to risks of contact between the operator and parts of the machine. These risks may have direct consequences such as cuts, crushing, ... The observations demonstrate that they are even greater as the operator works directly in the movement zone of the machine head, particularly :

- during setting, when he carries out a tactile check of machining quality and a visual check of both the tool movement and its contact with the item.
- during machining, when he positions an item or removes chips of wood, even though the unit is machining another item on the same bed (pendulum work).

However, the operators would appear to apply safety practices, that prevent the appearance of certain incidents :

- when changing series, the programme (trajectories, speeds, ...) and tools are checked,
- when carrying out setting, numerous visual, tactile and sound checks are performed while running the programme gradually, several times if necessary,
- positioning and fixing the primary items are consciously checked, to avoid items and chips of wood projecting. Machine stops are programmed to ensure that any chips are cleared before the machining of woodpieces.

4.2. FUNCTIONAL ANALYSIS

The man/machine pair was modelled from this analysis through its co-operating, functional and operational activity (Jouffroy *et al.*, 1998).

This model (Fig 4) of the interaction between man and machine was designed from both the operating and malfunction point of views (Ortiz-Hernandez, 1995). The software tool employed allows the consequences of machine and operator malfunctions

to be predicted during the entering, setting and machining phases, and various analyses to be carried out (FMEA, fault tree) that highlight the points critical to the safety of the operator.

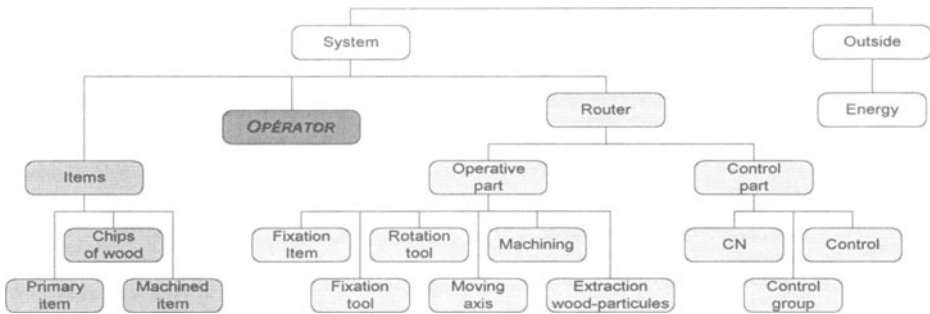


Figure 4. Summarised hierarchical decomposition of the man/machine system

Propositions of improvements and/or modifications, allow existing machines to be modified and safety regulations to be integrated during the design of new machines.

5. Integrating a distributed design method

It is not enough to integrate the regulations stemming from these analysis into the specification, for them to be taken into account automatically in the development cycle of the machine (Tichkiewitch *et al.*, 1993). In the same way as consideration is given to production costs during the product design stage, equal consideration must be given to the specific safety aspects, that encompass the entire life cycle of the product from the preliminary phases of design through to the final product stage, namely destruction and recycling (Standard NF EN 292, 1991).

With the appearance of concurrent engineering at the onset of the 90's (Sohlenius, 1992 ; Cerezuela, 1996), new concepts emerged that allow better integration of the safety regulations in the life cycle, in the same way as for manufacturing, maintenance or marketing.

5.1. PROPOSED DESIGN METHOD

To achieve this, a method was employed proposing that, with respect to design, a product emerges gradually from the different points of view encountered throughout the product life cycle (Garro, 1995). The model defined by a network of actors able to exchange and interact mutually is founded on connectionist principles (Fig 5). Each actor has its own objective and contributes to the emergence of a product meeting a global objective. Emergence is aided by the properties of the network (heterogeneity, non closure, non atom-like cell structure [Salau, 1995]), and communications between actors to develop coherent proposals.

Adding H.S.E. (Health, Safety and Ergonomics) actors contributes to a better integration of safety principles, the multi-disciplinary know-how and knowledge of these actors allowing a reduction in risks without the introduction of new hazards.

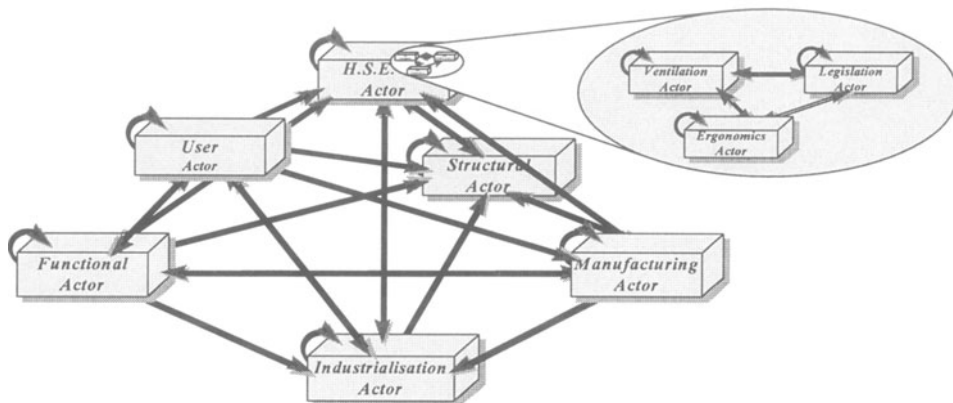


Figure 5. Distributed design model

5.2. APPLICATION TO AN ELEMENT OF A MACHINE

This distributed design model was employed within the context of an experiment undertaken by INRS and CRAN focused on improving the system for extracting the wood particles produced by machining.

This part of the machine causes the operators a great deal of discomfort as :

- the existing extraction system makes getting visual information from the tool difficult during machining, despite these information are important during the setting phase,
- and when the extraction system is not effective :
- the operators have to clean the machine regularly to prevent failure of the item keeping system and the result is significant loss of productivity,
- they are permanently exposed to wood dust likely to cause pulmonary irritation and even cancer of the ethmoid.

To be in a position to quantify the improvements, ventilation measurements were taken that provided the efficiencies and the dust concentrations at the work station of both the old and new systems.

6. Conclusion

Through a viewpoint integrated approach (ergonomics approach, functional modelling, and "safety profession" integration), a process is proposed that contributes to the safety of machinery. The distributed design method remains to be validated on an part of a machine, and thus the relevance of such a process still has to be demonstrated to the manufacturers.

7. Références

- Cerezuela, C.(1996) "*Contribution à l'élaboration de méthodes et d'outils d'aide à la conception et à la fabrication dans une perspective d'ingénierie concurrente : le cas du câblage électrique*", University of Aix-Marseille III, Ph. D in automation and computer science, 10/1996, 176p.
- Ciccotelli, J. (1997) "*Vers des machines et systèmes plus sûrs. Quelques perspectives de recherche et de développement*", in "CND - Hygiène et sécurité du travail 166", 1er trim. 1997, pp. 189-200.
- Daniellou, F. (1989) "*Méthodes d'introduction de l'ergonomie dans la conception des postes de travail*", in "L'ergonomie de conception", De Keyser V. et Van Daele A., Ed. De Boeck University, 1989, pp. 81-89.
- Demor, S. (1997) "*Etude ergonomique préliminaire des activités de conduite des "Défonceuses" dans une ébénisterie*", private communication, n° 97/10, INRS, 11/97, 25p.
- Directive 89/392/CEE (1989) Directive Européenne du 14 juin 1989 concernant le rapprochement des législations des Etats membres relatives aux machines, modifiée par les directives 91/368/CEE du 20/06/1991 et 93/44/CEE du 14/06/1993, J.O.C.E. n° L 183 du 29/06/1989, pp. 9-32 ; n° L 198 du 22/07/1991, pp. 16-32 ; n° L 175 du 19/07/1993, pp. 12-20.
- Fadier, E. (1994) "*M.A.F.E.R.G.O. : Méthode d'Analyse de Fiabilité et ERGonomie Opérationnelle*", AFTIM, Paris, 1993, in "Sécurité et Médecine du Travail", n°101, 1994, pp. 40-46
- Garro, O., Salau I. and Martin, P. (1995) "*Distributed Design Theory and Methodology*", Concurrent Engineering Revue, Vol. 3, n°1, 1995, pp. 43-54.
- Jouffroy, D., Ciccotelli, J. and Martin, P. (1998) "*Apport d'une méthode de conception à la sécurité des machines à bois à commande numérique*", IMS-EUROPE 1998, to be published, 15-17/04/98, Lausanne, 10p.
- Standard NF EN 292 (1991) *Sécurité des machines - Notions fondamentales. Principes généraux de conception. Partie 1: Terminologie de base, méthodologie*", Paris-La-Défense, AFNOR, 12/1991, 33p.
- Standard project Pr EN 848-3 (1996) *Safety of woodworking machines - NC boring machines and routing machines*", Paris-La-Défense, AFNOR, 3/1996, 49p.
- Ortiz-Hernandez, J. (1995) "*Les systèmes de production automatisés : une approche socio-technique*", University of Franche-Comté, Ph. D in automation and computer science, 11/1995, 117p.
- Salau, I. (1995) "*La conception distribuée : théorie et méthodologie*", University Henri Poincaré Nancy I, Ph. D in automatization, 03/1995, 128p.
- Sohlenius, G. (1992) "*Concurrent Engineering*", Annals of CIRP 41, 1992, 11p.
- Statistiques CNAMTS (1997) "*Statistiques financières et technologiques des accidents du travail : années 1993 - 1994 - 1995*", CNAMTS, 1997, 405 p.
- Tichkiewitch, S. et al. (1993) "*Ingénierie simultanée dans la conception de produits*", in "Compte-rendu des Universités d'été du pôle productique Rhône-Alpes", 1993.

VIRTUAL MANUFACTURING : SET UP OF A COOPERATIVE WORK IN MANUFACTURING

Ph. DÉPINCÉ *, H. THOMAS *, B. FURET *, Y. GRATON, N. RAFII **

Atelier InterÉtablissements de Productique de Nantes

3, rue du Maréchal Joffre BP 34103 - 44041 Nantes Cédex 01

**Institut de Recherche en Cybernétique de Nantes (IRCyN)*

1 rue de la Noë, 44321 Nantes, France

*** Institut Universitaire de Technologie de Nantes, France*

Abstract

The setting of a production is a complex task which involves heterogeneous agents, systems and activities. Nowadays hardware and software materials exist which make easier the work of the different agents (network, modular fixture, database, loading and unloading NC programs). In the case of a multisite activity, these tools are not sufficient and we have to reorganize the whole process. Taking into account the two sites of the Atelier InterÉtablissements de Productique (A.I.P) of Nantes, we have implemented communications tools and a data management system in order to use the tools (hardware and software) available on the two sites on the same project. In this paper we describe the different tools we have used and our approach to create a product data management system.

1. INTRODUCTION

The setting up of a new product, from its design to its distribution, requires a great number of resources stemming from multiple and various disciplines which are generally not grouped together only one place. Usually, due to communication and availability problems, this setting up takes a long time which can be prejudicial to the enterprise's productivity. In order to cope with this problem, a solution consists in selecting the resources involved in the creation project and in synthesizing them together in a all-in-one and communicating feature : a virtual enterprise.

Our goal, in the A.I.P. of Nantes, is to achieve the setting of an educational and research platform developed in the context of industrial (SME) integration. We want to show up the processes and the means required for the creation and management of the whole product data : from its design to its commercialization including supplying, production,

measurement, assembly,

This platform will allow the training of students for a global approach of the enterprise according to a project-based structure. This structure allows to break down the divisions between functions and tools (CAD, CAM, CAPP, ...) in a context of virtual enterprise and to integrate cooperation thanks to modern communication tools (Furet 96).

As the A.I.P. of Nantes has a multisite structure and as our common activity is oriented towards mechanical production, our work deals with the preparation and the setting of the production. The different software and hardware used in the two sites underline the difficulties linked to data exchange (CAD, CAM, ...) we have to deal with. Before tackling the problem of data management we have to know what the nature of the exchange is (what are the data?, how do they progress ?, ...).

Setting up the production is complex because it includes several proceedings and this is a wonderful example of groupwork. We must reorganize those proceedings since we can't manage a voluntary approach of the agents involved in the preparation stage of the production. This is all the more necessary since we are in the context of virtual manufacturing.

In this paper, we explain the processes we have adopted for the manufacturing of a part - from the geometric, technologic and economic data- in a virtual enterprise context. The aim of this project is the setting of tools allowing the process's analysis, the tasks and data modelization and, finally, the optimization of their time organization. Moreover we have underlined the needs for communication : not only between machines or software but also between humans. In this study we have classified these exchanges in two categories : technical data and cooperation data.

2. PREPARATION AND SETTING OF THE PRODUCTION

2.1. PROCESSES

We are in the context of small business or small industrial companies fitted out with NC Machine-Tools producing manufactured mechanical parts. This enterprise is organized according to the virtual manufacturing concept:

- either a multisite enterprise which produces where resources are available,
- or a partnership between the customer, producer, subcontractor and supplier,
- or a consortium of enterprises working together on a shared project (AIP, 1996).

Here we only deal with the preparation and the setting of the production. This step is part and parcel of the life-cycle of a product : from its design to its marketing.

Here is our approach on the preparation and the setting of the production:

First we deal with the geometry of a part, with its technical (material, quality ...) and economical (aim, cost, expected rate) data to obtain the manufactured product. Figure 1 shows the evolution of the different steps from the file definition of the geometry of the part coming from a CAD software to its manufacturing, gradually enlarging what is called the "manufacturing files" (Bregeon, 1995).

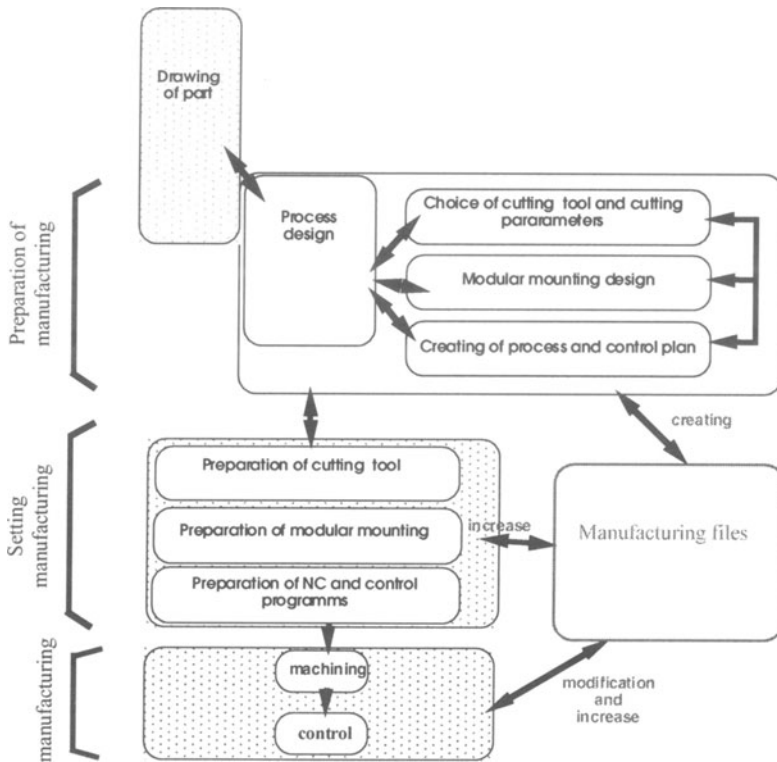


Fig. 1: Preparation and setting of the production

2.2. MEANS AND AGENTS

During the preparation, several tasks are required. Those tasks involve different means : manufacturing and control machines, computers and software which are often heterogeneous, as well as agents whose competencies are various and multiple. All those means and agents can be distributed on two or more sites. As far as material and software means are concerned all the followings are available in the A.I.P.:

- NC Machine Tool 3,4 and 5 axis and Co-ordinate Measuring System (CMS),
- Tool-Gage, Modular Fixture,
- Heterogeneous CAM software to create the process plan and the CN programs, prepare the cutting tools and the modular mounting, and load NC programs into the machine tool.

Moreover, we must notice the abilities and the various concerns of agents working on the manufacturing process (production engineers, CN program engineers, operators, ...).

3. ANALYSIS OF THE PREPARATION AND SETTING OF THE PRODUCTION

In order to determine the different tools, an analysis of the manufacturing of a standard part was undertaken. Four steps were necessary:

- Analysis of the already existing process,
- Modeling of activities and their associated data,
- Optimization of those activities (scheduling),
- Management of the process with the agents, the tools and the different means.

3.1. ANALYSIS OF THE EXISTING PROCESS

Firstly, we have analyzed the process of the preparation and manufacturing of the part. In order to achieve this first step, we have gathered manufacturing data and activities linked to the achievement of their tasks from all the agents dealing with the preparation and setting of the production. This analysis leads to :

- a list of the input data which are needed in order to achieve in good conditions each activity,
- a list of the output data for all activities,
- the description of all basic activities,
- registration of the necessary resources, so that the activities can be successfully carried out.

3.2. ACTIVITIES AND DATA MODELISATION

This modelization has been done thanks to the SADT methodology. This methodology (Structured Analysis Design Technique) was developed in 1972 by Softech (Ross IGL). This methodology is based on graphic representation by boxes. The box represents the activity and the arrows represent the input, output, mechanisms, and controls of the activity. A mechanism or resource is the means that performs the activity, for example, a person or an equipment. A constraint is something which influences or controls how

an activity will be carried out. Unlike inputs, mechanisms and controls are generally not transformed or consumed by the activity. An input is the result of the activity. Each box describing an activity can be split into sub-activities. This methodology is considered as general and can be applied to any case or problem. It can be used in the multidisciplinary teams which concerned our study (Calvez, 1990).

Thanks to the analysis of the already existing process, the modeling enabled us to collect all the tasks that need to be fulfilled and the necessary associated data (Lepeltier, 1998). The SADT modeling is known for its powerful expression. However its lack of a temporal semantic forced us to combine it with the PERT/GANTT methods (Lesage and al., 1995).

3.3. ACTIVITIES OPTIMISATION

The PERT method describes the interactions between the different steps of the project as a network of activities and events. In this method, we describe activities which are essential and events which begin and end each activity. Those activities are determined by a preceding relation specifying the sequence of tasks. PERT diagrams together with GANTT diagrams bring into relief the duration of the project and the necessary time for each task.

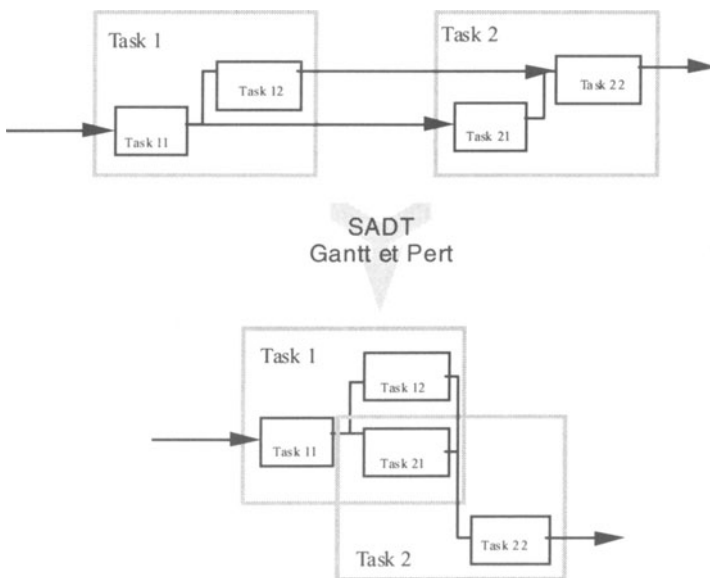


Fig. 2 : Task optimization by SADT and PERT methods combination

Those two approaches, SADT method with PERT/GANTT methods enabled us to optimize the whole process according to the definition of simultaneous activities (Figure 2) instead of sequential ones (Cavaliere, 1996).

3.4. PROCESS MANAGEMENT

The SADT and PERT/GANTT approaches allow us to analyze and optimize, with the notion of time, the process of preparation and the setting of the production. However, it is necessary, in order to optimize the data exchange, to add a step consisting in analyzing, modeling and automating the flow of the documents and in general the information about the process of production (David and al., 1996). This part of the study, which is in progress, consists in more or less important automation of the process.

4. MODEL IMPLEMENTATION

As a consequence of the previous stage of analysis and transcription of data, several means seem to be necessary to set this groupwork in the virtual manufacturing context (Jacquet and al., 1996). We noticed among other things :

- Representation and conversion of data,
- Management of those data (integration of data, filing, creation, validation, broadcasting),
- Management of the process,
- Setting of the communication function.

In our study we deal with the management of the data and the process within the context of the groupwork and the setting of the communication function as far as the virtual manufacturing is concerned. Figure 3 shows the simplified platform of tests.

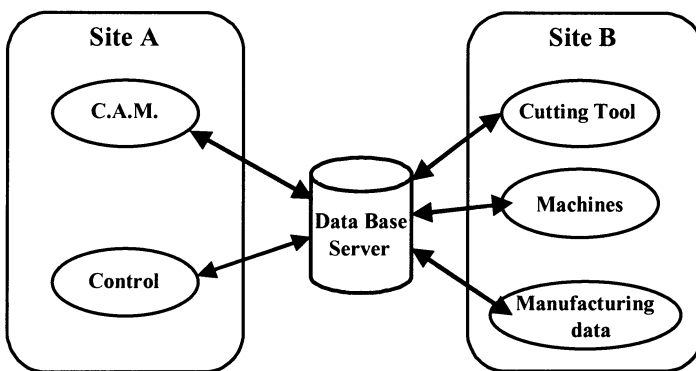


Fig. 3 : Simplified diagram for groupwork validation

4.1. SETTING OF THE PDMS

At this stage, we deal with the setting of the Product Data Management Systems (Radoing, 1995). The setting of the PDMS allows us to solve the problem of data management (integration of data, files, creation, validation, broadcasting). This database contains all the necessary information for the preparation of the production. It can be shared from a distance and be used and filled in by all the agents working in the stage of the preparation of the production.

The carrying out of the database consists in determining the table, defining the request, creating the data capture forms and the output states, managing the database according to the function of the agents. This management was conducted thanks to the Access software from Microsoft Co.

4.2. COMMUNICATION MEANS

At the same time we shared some resources on an FTP server and set means of communication between the different agents working in the groupwork towards preparing and setting the production. The electronic mailing improved the groupwork thanks to the notion of asynchronous cooperation that is to say the different agents can interact on their activities, exchanging data without co-temporality.

5. CONCLUSION

The originality of our work doesn't lie in the use of already existing methods but in a structured approach. In fact, the combination of the SADT and PERT/GANTT methods permitted to reveal, on the one hand, activities and associated data and, on the other hand, their synchronization. Our approach in the analysis stage has been all the more necessary since the setting of the groupwork must be carried out in the context of a virtual manufacturing because the organization of the activities and data becomes more important compared in to a monosite structure.

The precise analysis i.e. the activities split up in hierarchical sub-activities of the preparation, the setting of the production and the use of the project management as far as temporal aspects are concerned, allowed us to determine simultaneous functions instead of sequential ones.

The management of the process thanks to a Product Data Management Systems improves the duration of preparation reducing the mistakes in data capture and allowing to give a particular context for each agent. Moreover, the application of the method and the rule is easier thanks to Product Data Management Systems and it provides us with a

better knowledge about the future process of manufacturing. The setting of the communication tools (email, FTP Server,...) improves the exchange between the agents working on several sites.

In our study, for the manufacturing of the standard part, the time saved is about 50% compared to a conventional preparation.

The next step will be the setting, on the one hand, of videoconferencing tools, whiteboard, agenda and, on the other hand, the integration of software around the concepts of GroupWare and Workflow to improve the groupwork.

6. REFERENCES

- AIP (1996) : "*Rapport d'activité et de prospective*", Comité National de Coordination des A.I.P..
- D. Bregeon (1995) : "*Utilisation de la méthode SADT pour formaliser la démarche de mise en oeuvre de la production dans le cadre d'une PME/PMI sous-traitante en usinage et équipée de MOCN*", examen probatoire CNAM Fabrication Mécanique.
- J.-P. Calvez (1990) : "*Spécification et conception des systèmes - Une méthodologie*". Edition Masson.
- S. Cavaliere (1996) : "*Etude de la mise en place d'un système de gestion de projet*". Memoire Ingénieur – Ecole Centrale de Nantes/ IUT de Nantes - Erasmus.
- T. David , M. Zellouf (1996) : "*Organisation des activités, des acteurs et des flux d'informations dans une entreprise virtuelle avec Process Weaver*", Projet des AIPs.
- B. Furet (1996) : "*Une mode ou de véritables enjeux stratégiques pour les entreprises.*" Conférence PRIMECA'96 : La réorganisation de la conception dans un contexte concourant. 23 mai 1996 – AIP Lorrain – France.
- L. Jacquet, J.F. Petiot, J.L. Sommer, Y. Koyama (1996) : "*Analyse de la mise en place d'un scénario d'ingénierie communicantes*" - IDMME'96, Nantes, Vol. 2, pp. 623-632.
- B. Lepeltier, (1998). "*La préparation et la mise en oeuvre de la production: Mise en place d'un système de gestion de données techniques*" - Mémoire Ingénieur CNAM Production automatisée.
- J.J Lesage, B.Denis (1995) : "*Un panorama de la recherche en conception de la conduite des systèmes de production*". Congrès International de Génie Industriel de Montréal.
- Radoing (1995) : " Les SGDT", Collection HERMES.

AUTHORS INDEX

ABISROR.....77	BRAIBANT.....291	DESSEIN.....423	GUO.....307
ANGELES.....225	BRAIBANT.....331	DESSEIN.....439	HABBAL.....133
ANGELES.....265	BREITKOPF.....151	DESSEIN.....463	HAMEL.....275
ANSELMETTI.....619	BRISSAUD.....471	DI PASQUALE.....291	HOCHARD.....27
ARNOULT.....35	CAENEN.....207	DJENI.....331	HUBERT.....27
ASHBY.....505	CAMPION.....3	DOMASZEWSKI.....51	JOUFFROY.....643
ASHBY.....603	CASTELAIN.....207	DORNFELD.....471	KNOPF-LENOIR.....109
AVALLE.....85	CHABLAT.....225	DOUMEINGTS.....537	KNOPF-LENOIR.....159
BALLOT.....389	CHAMPANEY.....43	DRAGHICESCU.....635	KNOPF-LENOIR.....307
BARLET.....307	CHARPENTIER.....611	DRAGOI.....635	KOO JEONG SEO.....51
BATOZ.....109	CHEDMAIL.....241	DRAZETIC.....19	LAFON.....93
BATOZ.....307	CHENG GENDONG.....101	ESAWI.....603	LAFOND.....381
BAUD.....561	CHEROUAT.....323	ESCAIG.....151	LAGARRIGUE.....423
BELHOUS.....323	CHTOUROU.....283	EYNARD.....537	LAGARRIGUE.....439
BELINGARDI.....85	CICCOTELLI.....643	FALKENAUER.....415	LAGARRIGUE.....463
BEN CHAABANE.....291	CLEMENT.....199	FAUROUX.....257	LANGE.....521
BENNIS.....365	CLOZEL.....249	FEAUTRIER.....349	LAPERRIERE.....381
BENNIS.....373	CONGOURDEAU.....77	FENG ZHIGIANG.....51	LARTIGUE.....349
BERLIOZ.....595	CONSTANT.....249	FINE.....167	LE CARDINAL.....569
BERTHILLIER.....35	CORBEEL.....627	FONTANILI.....431	LEBOUVIER.....27
BEUZIT.....133	CORNETTE.....19	FORTIN.....373	LEBRUN.....405
BIGAND.....627	COUTELLIER.....67	FURET.....651	LEGOFF.....455
BILLEREY.....249	CUBELES-VALADE.....357	GACEL.....275	LENGUIN.....513
BILLOET.....3	D'ACUNTO.....405	GAKWAYA.....283	LEON (Coordin.).....553
BILLOET.....323	DAMAY.....241	GELIN.....299	LEON.....167
BLANQUET.....67	DANIEL.....365	GHOUATI.....299	LEON.....191
BLANZE.....43	DARCOVITCH.....265	GILBERT.....497	LIMAYEM.....489
BLONDAZ.....471	DE FONSECA.....217	GIORDANO.....397	LIU SHUTIAN.....101
BOCQUET.....561	DE LIT.....415	GIRARD.....537	MALLON.....545
BOGARD.....11	DELACOURT.....67	GIRAUD.....93	MARIN G.....77
BOMME.....143	DELCHAMBRE.....415	GOGU.....545	MARIN PH.....595
BONNAFE.....315	DELCROIX.....125	GOUSKOV.....341	MARKIEWICZ.....19
BOUABDALAH.....307	DELEBARRE.....67	GRATON.....651	MARTIN P.....611
BOULHARTS.....3	DELMOTTE.....315	GROSJEAN.....315	MARTIN P.....643
BOURDET.....389	DEMARQUILLY.....545	GU YUANXIAN.....101	MARTIN P.....405
BOURDIN.....315	DEMOL.....67	GUERRY.....233	MARTINS.....257
BOURDON.....59	DEMOR.....643	GUEURY.....405	MAZA.....191
BOUREY.....627	DENG XIO-LING.....27	GUILLOT.....283	MCMAHON.....481
BRAIBANT.....125	DEPINCE.....651	GUILLOTEAU.....35	MEKHILEF.....561

MERCIER.....307	POLIT.....3	RUBIO.....463	TICHKIEWITCH.....635
MERROUCHE.....159	PONSONNET.....431	RUIZ OSCAR.....183	TIMON.....349
MG-IT (COLLECT.) 553	POSADA JORGE.....183	RYCKELYNCK.....175	TOLLENAERE.....529
MINEUR.....207	POURROY.....529	SAMPER.....397	TOUMINE.....619
MONTAGNIER.....265	PRADES.....207	SANCHEZ.....257	TREBUCQ.....529
NACEUR.....109	RAFIL.....651	SARTOR.....257	TRIKI.....109
NACEUR.....307	RAMOND.....585	SAS.....217	TROUSSIER.....529
NDIAYE.....627	RAVALARD.....19	SCHAFFER.....611	VALLINO.....77
NIGROWSKY.....545	RAY.....545	SCHMIT.....275	VAN BRUSSEL.....217
NOËL.....167	REDONNET.....423	SEO YOONHO.....577	VEDRINE.....43
NOËL.....191	REDONNET.....439	SERRE.....199	VERON.....167
OUDSHOORN.....125	REDONNET.....463	SHAKOURZADEH...331	VILLENEUVE.....447
QUEZDOU.....233	REGNIER.....233	SILLION.....191	VILLENEUVE.....455
PAGNACCO.....117	RENAUDIN.....51	SORIANO.....431	VINCENT.....431
PATOU.....331	REVEL.....11	SOUZA DE CURSI...117	WEGST.....505
PATRITL.....611	RIVIERE A.....199	TARCOLEA.....635	WENGER.....225
PAVIE.....291	RIVIERE A.....357	TASSEL.....455	WU CHU-JEN.....265
PECOT.....3	RIVIERRE L.....3	THIEBAUT.....349	YAKHOU.....59
PELLE.....175	ROËLANDT.....275	THIEBAUT.....389	YANNOU.....241
PESEUX.....35	ROËLANDT.....315	THIRION.....19	YANNOU.....489
PETIOT.....497	ROËLANDT.....77	THOMAS.....651	YVARIS.....513
PINO.....373	RUBIO.....423	TICHKIEWITCH.....341	ZIMMERMANN.....143
PLAY.....59	RUBIO.....439	TICHKIEWITCH.....595	